SAND79-8176
Unlimited Release

Final Report Conceptual Design of An Advanced Water/Steam Central Solar Receiver Volume I

FOSSIL POWER SYSTEMS

RESEARCH & DEVELOPMENT

POWER SYSTEMS
COMBUSTION ENGINEERING, INC.

Contract 18-6879B
for Sandia National Laboratories

Issued by Sandia National Laboratories, operated for the United States Department of Energy by Sandia Corporation.

FINAL REPORT

Conceptual Design of An Advanced Water/Steam

Central Solar Receiver

Volume I

Prepared by

Combustion Engineering, Inc.
Power Systems Group
Windsor, CT 06095

Contract 17078

Prepared for

Sandia Laboratories
Livermore, CA 94550

Under Contract 18-6879B

Project Manager: F. T. Matthews

Principal Contributors: H. M. Payne, Project Engineer
B. C. Jones
T. K. Snyder
M. J. Davidson

June, 1980

NOTICE

Acknowledgement

The contributions of the test personnel of the Kreisinger Development Laboratory in behalf of Task 10, are hereby acknowledged.

TABLE OF CONTENTS

Volume I

TABLE OF CONTENTS

(Continued)

Volume I

TABLE OF CONTENTS

(Continued)

Volume I

TABLE OF CONTENTS

(Continued)

Volume I

TABLE OF CONTENTS

(Continued)

Volume I

APPENDICES

Volume I

Volume II

Volume II consists of a listing of the reduced test data from Task 10--Rifled Tubing Tests. Results and sample data appear in Section 7 of Volume I.

LIST OF FIGURES

Volume I

LIST OF FIGURES

(Continued)

LIST OF FIGURES

(Continued)

LIST OF FIGURES

(Continued)

LIST OF FIGURES

(Continued)

LIST OF FIGURES

(Continued)

List of Tables

Volume I

List of Tables

Volume I (Continued)

I. Introduction and Executive Summary

1.1 Objective

The objective of this project was to develop a conceptual design of an advanced water/steam solar central receiver, which would be more cost effective than the present design employed in the Barstow 10MWe pilot plant. Studies[(1)] have shown that the major cost in a solar thermal central receiver plant is the collector sub-system (heliostats). The number of heliostats required for a given electrical power output is a function of, among other things, the efficiency of the conversion of heat energy to electrical energy (cycle efficiency). This fact justifies the search for improvements in the receiver/storage/electrical generation systems of the plant, with the potential for an overall cost benefit via a reduction of collector sub-system size. This project is directed to an advanced receiver sub-system primarily, and is limited to water/steam substance as the heat absorbing medium.

An experimental program was included in the project to determine the feasibility of using rifled tubing in the high heat flux environment of the proposed solar receiver evaporator section. Rifled tubing has been shown to enhance the boiling heat transfer mechanism at lower heat flux levels in conventional boilers.

1.2 Summary and Conclusions

Conceptual designs of four* external water/steam receivers were developed, which consist of drum type boilers, with forced circulation evaporators using rifled tubing to maintain efficient nucleate boiling. Evaporator, Preheater, and Superheater panels are arranged to take advantage of the flux distribution from a biased North field collector sub-system. Final steam temperature is 866K (1100F), to be compatible with a high temperature storage sub-system.

---

(1) Numbers in parenthesis refer to references at end of report.

* One receiver was designed for two pressures at the same nominal power level. (640 MWt).

Reheaters are located low on the receiver tower, and are powered by a dedicated portion of the North field. Table 1.1 lists the estimated cost of three receivers and Table 1.2 lists separate reheater costs. Figure 1.1 shows the relative physical sizes of these units. These receivers will serve a range of turbine sizes from 100MWe to 300MWe and Solar Multiple from 1.3 to 1.7.

Major conclusions from this project are:

1. A drum-type boiler with forced circulation evaporator using rifled tubing can be designed for the high heat flux of a North field collector without the porblems associated with DNB (departure of nucleate boiling).
2. Existing boiler technology and materials can be used to design an advanced water/steam receiver.
3. Rifled tubing has been shown by test data to provide protection to evaporator panels at peak heat flux levels 30% greater than the design point of these receivers.
4. Estimated budgetary type costs of these receivers vary from $10 per pound of steam, for the large receiver to $13 per pound of steam for the smaller unit.
5. Fatigue life has been conservatively calculated to be 30,000 full strain range cycles. This is adequate for the diurnal cycling, plus some cloud cycling over a 30-year period.
6. It is possible that the allowable creep-fatigue cycles may be increased to 40,000-50,000 by an inelastic stress analysis. This analysis has been recommended for future work and will be required to resolve the cyclic lifetime of these receivers.
7. Additional analysis is also needed to resolve receiver and plant control systems.

Table 1.1

Advanced W/S Receiver Costs* (thousand$)
Delivered and Erected

Steam Flow	Thermal Power	Cost
126 kg/s(1×10^6 lb/hr)	321 MWt	$13,900
252 " (2×10^6 lb/hr)	640 "	23,380
378 " (3×10^6 lb/hr)	933 "	31,600

* 1979 dollars

Table 1.2

Estimated Reheater Costs* (Thousand$)
Delivered and Erected+

Turbine Power MWe/Press.	Reheater Steam Flow kg/s (lb/hr$\times10^{-6}$)	Reheater Cost
100/12.4 (1800)	73.1 (.58)	2,400
200/12.4 (1800)	171.3 (1.36)	5,200
200/16.5 (2400)	142.4 (1.13)	4,500
300/16.5 (2400)	228.0 (1.81)	7,000

+Does not include reheat steam leads.

*1979 Dollars

I. Introduction and Executive Summary

1.1 Objective

The objective of this project was to develop a conceptual design of an advanced water/steam solar central receiver, which would be more cost effective than the present design employed in the Barstow 10MWe pilot plant. Studies[1] have shown that the major cost in a solar thermal central receiver plant is the collector sub-system (heliostats). The number of heliostats required for a given electrical power output is a function of, among other things, the efficiency of the conversion of heat energy to electrical energy (cycle efficiency). This fact justifies the search for improvements in the receiver/storage/electrical generation systems of the plant, with the potential for an overall cost benefit via a reduction of collector sub-system size. This project is directed to an advanced receiver sub-system primarily, and is limited to water/steam substance as the heat absorbing medium.

An experimental program was included in the project to determine the feasibility of using rifled tubing in the high heat flux environment of the proposed solar receiver evaporator section. Rifled tubing has been shown to enhance the boiling heat transfer mechanism at lower heat flux levels in conventional boilers.

1.2 Summary and Conclusions

Conceptual designs of four* external water/steam receivers were developed, which consist of drum type boilers, with forced circulation evaporators using rifled tubing to maintain efficient nucleate boiling. Evaporator, Preheater, and Superheater panels are arranged to take advantage of the flux distribution from a biased North field collector sub-system. Final steam temperature is 866K (1100F), to be compatible with a high temperature storage sub-system.

---

(1) Numbers in parenthesis refer to references at end of report.

* One receiver was designed for two pressures at the same nominal power level. (640 MWt).

Reheaters are located low on the receiver tower, and are powered by a dedicated portion of the North field. Table 1.1 lists the estimated cost of three receivers and Table 1.2 lists separate reheater costs. Figure 1.1 shows the relative physical sizes of these units. These receivers will serve a range of turbine sizes from 100MWe to 300MWe and Solar Multiple from 1.3 to 1.7.

Major conclusions from this project are:

1. A drum-type boiler with forced circulation evaporator using rifled tubing can be designed for the high heat flux of a North field collector without the porblems associated with DNB (departure of nucleate boiling).
2. Existing boiler technology and materials can be used to design an advanced water/steam receiver.
3. Rifled tubing has been shown by test data to provide protection to evaporator panels at peak heat flux levels 30% greater than the design point of these receivers.
4. Estimated budgetary type costs of these receivers vary from \$10 per pound of steam, for the large receiver to \$13 per pound of steam for the smaller unit.
5. Fatigue life has been conservatively calculated to be 30,000 full strain range cycles. This is adequate for the diurnal cycling, plus some cloud cycling over a 30-year period.
6. It is possible that the allowable creep-fatigue cycles may be increased to 40,000-50,000 by an inelastic stress analysis. This analysis has been recommended for future work and will be required to resolve the cyclic lifetime of these receivers.
7. Additional analysis is also needed to resolve receiver and plant control systems.

Table 1.1

Advanced W/S Receiver Costs* (thousand$)
Delivered and Erected

Steam Flow	Thermal Power	Cost
126 kg/s($1x10^6$ lb/hr)	321 MWt	$13,900
252 " ($2x10^6$ lb/hr)	640 "	23,380
378 " ($3x10^6$ lb/hr)	933 "	31,600

* 1979 dollars

Table 1.2

Estimated Reheater Costs* (Thousand$)
Delivered and Erected+

Turbine Power MWe/Press.	Reheater Steam Flow kg/s ($lb/hr x10^{-6}$)	Reheater Cost
100/12.4 (1800)	73.1 (.58)	2,400
200/12.4 (1800)	171.3 (1.36)	5,200
200/16.5 (2400)	142.4 (1.13)	4,500
300/16.5 (2400)	228.0 (1.81)	7,000

+Does not include reheat steam leads.

*1979 Dollars

Figure 1.1

DESIGN RECEIVER AND TOWER ARRANGEMENTS

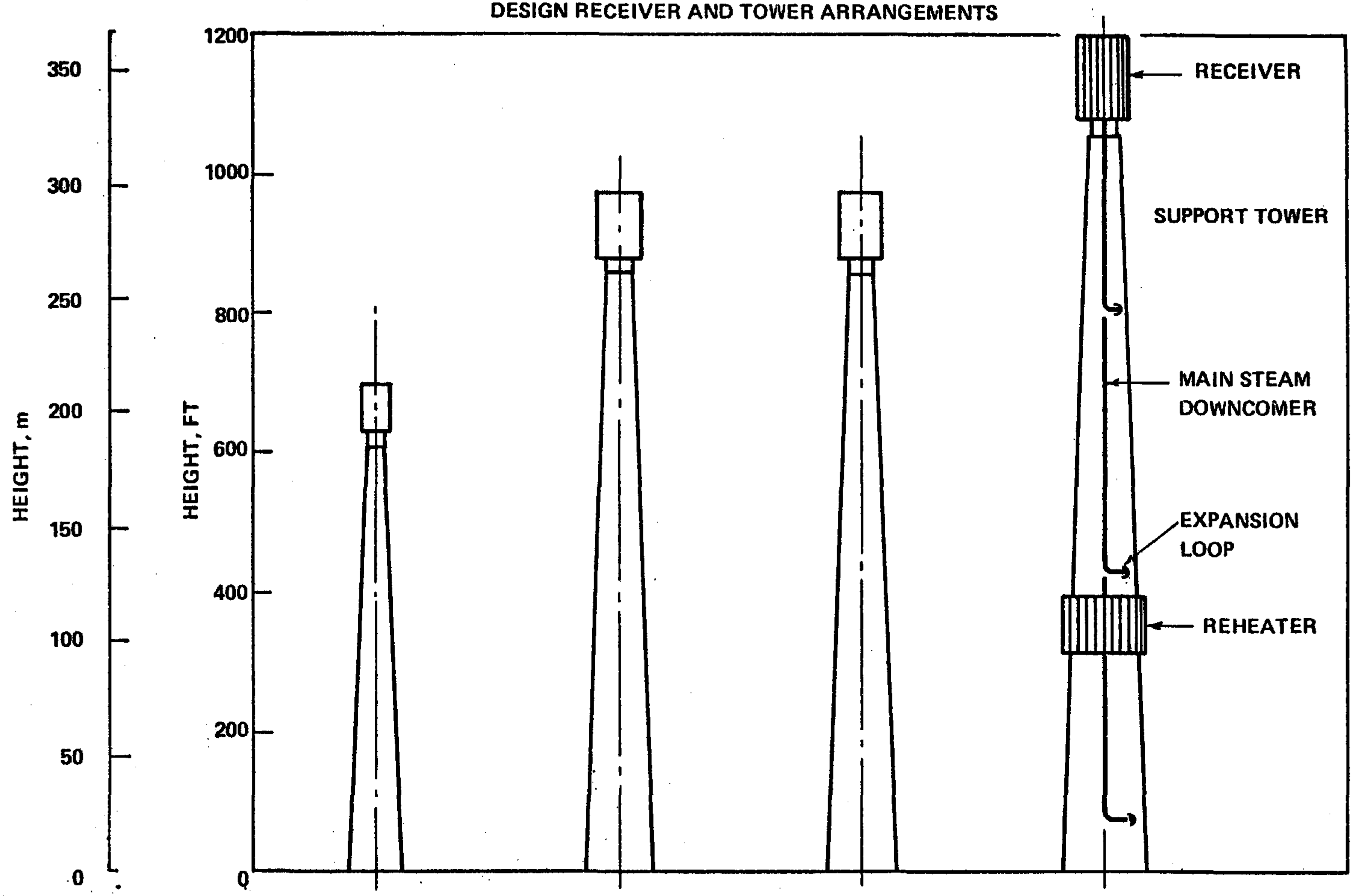

STM. FLOW, Kg/HR (LB/HR)	$.45 \times 10^6$ (1×10^6)	$.91 \times 10^6$ (2×10^6)	$.91 \times 10^6$ (2×10^6)	1.4×10^6 (3×10^6)
CYCLE PRESS., MPa (PSIA)	12.4 (1800)	12.4 (1800)	16.5 (2400)	16.5 (2400)

1.3 Background

The central receiver design for the 100MWe Pilot Plant at Barstow, and the proposed 100MWe commercial plant design, consist of an external receiver producing 515°C (960°F) steam temperature at 10.3 MPa (1500 psia) turbine throttle pressure. The flow path through the receiver is once-through, from feedwater to final superheat in a single-pass, up-flow circuit. The turbine is a single expansion, non-reheat machine. Estimated net turbine cycle efficiency is 33.6% for the 100MWe[2]. The receiver thermal efficiency at design point, is estimated at 90%, based on the incident power at the receiver, including the estimated convective and radiation losses to the atmosphere.

A design review of the above receiver was conducted in 1978 by C-E[3]. The significant result from that study showed that the proposed once-through design of the 100MWe commercial plant was subjected to severe thermal stress due to a critical heat flux condition (DNB) followed by a stable film boiling condition with a highly degraded heat transfer. The result is a large increase in tube crown temperature at the stable film boiling location.

Due to the asymmetrical heating of the external receiver panels, this temperature gradient (heated side to non-heated side), causes thermal stresses in the panels at the points where the panels are constrained by guides and supports. This stressed condition is a maximum at rated operating conditions of the receiver, and is independent of the time rate of heating and cooling. Since it is presumed that rated conditions will be achieved almost on a daily basis, from a cold start, stress now becomes cyclic. Anlaysis[3] of the 100MWe plant showed that the proposed design, in the high heat flux environment, would have a fatigue life of the order of a few years, instead of the 30-year design objective. The result is independent of any other contributory factor in fatigue life analysis.

1.4 Technical Approach

The selection of the preferred advanced water-steam receiver design was made by considering the following options:

I. Boiler Types (Table 1.3)

  a. Once-through (single pass to superheat)

  b. Drum-type

    1. Natural circulation

    2. Pumped circulation

II. Turbine Cycle Parameters (Table 1.4)

  a. Category I

    1. Throttle Pressure.

    2. Main steam temperature

    3. Non-reheat

  b. Category II

    1. Throttle pressure

    2. Main Steam Temperature

    3. Reheat temperature

III. Reheat/Storage Options (Table 1.5)

  a. Low temperature storage "live steam" reheater.

  b. High temperature storage

    1. Solar reheater

    2. Partial pass-through storage reheat

    3. Supercritical primary receiver--100% power pass through storage.

IV. Receiver/Turbine/Storage Sizes Combinations (Table 1.6)

  a. Turbine size range (100MWe-300MWe)

  b. Turbine throttle pressure (1800-2400)

  c. Storage Multiple (1.3-1.7)

The above options are discussed below:

1.4.1 Boiler Options--A drum-type forced-circulation boiler design was chosen from the various boiler options available in Table 1.3. The selection of this boiler configuration was made to avoid problems of DNB and instability which can occur in once-through (single pass to superheat) units. Density-wave instabilities are not likely to occur where the liquid and vapor phases are separated.

By providing pumped circulation, protection of the evaporator circuits under high heat flux conditions can be assured through the use of rifled tubing and by orificing the flow circuits according to the heat flux requirements. Rifled tubing allows optimization of the circulation system for minimum pump costs by reducing the circulation ratio required.

A test program (Task 10) was designed to both obtain rifled tubing performance data at the high heat flux levels associated with the north side receiver evaporator section, and to verify the selected design circulation ratio.

An external receiver configuration was chosen for this project. Previous studies indicate that the external arrangement is lighter weight and easier to erect than a cavity type, due to its modular panel construction.[1]

1.4.2 Turbine Parameters--A receiver operating with RFP Category II steam conditions was selected. Category II defines final steam temperatures and pressures as those greater than 10.3 MPa (1500 psi) and 515°C (960°F). Higher pressure, higher temperature, reheat cycles, inherently have better heat rates; thus, for a given electrical power output, fewer heliostats would be required. For example, a 16.5 MPa (2400 psia), 538°C (1000°F) turbine cycle with reheat to 538°C (1000°F), and a gross cycle efficiency of 43%, would theoretically require a collector field size 20% less than a Category I plant.

Turbine cycle parameters for various options are listed in Table 1.4. The final selection of turbine cycles (nos. 2 and 3) included both the 12.4 MPa and

Table 1.3

Receiver Boiler Options

No.		Description
1.	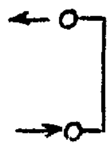	Once-through (single pass) sub-cooled liquid to superheated steam. Can be used for sub-critical steam pressures, but required for supercritical (continuous phase) pressures.
2.	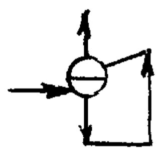	Drum-type boilers. These separate the steam/water phases in a drum. Saturated steam is collected and passed through a separate superheater.
2a.	(see above)	Natural circulation. Depends on density gradients between down comers and risers to provide circulation in boiling circuits.
2b.	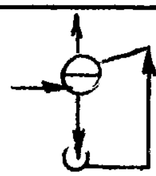	Forced circulation. Uses pumps to provide circulation in boiling circuits. Independent of density gradients.

Table 1.4

Turbine Cycle Parameters

Cycle No.	RFP Category	Pressure MPA(psia)	Main Steam Temp. ^{o}K (^{o}F)	RH Temp. ^{o}K (^{o}F)
1	I	10.34 (1500)	789 (960)	none
2	II	12.4 (1800)	811 (1000)	811(1000)
3	II	16.5 (2400)	811 (1000)	811 (1000)
4	II	24. (3500)	811 (1000)	811 (1000)

16.5 MPa (1800 & 2400 psia) pressures, as turbines operating at these pressures are generally available in the plant power size range contemplated (100-300MWe). The gain in cycle efficiency between the 16.5 MPa (2400 psia) reheat cycle, over the 10.3 MPa (1500 psia) cycle is 15%.

1.4.3 Reheat/Storage Options--Table 1.5 lists the various reheat options considered, and their relationship to the storage and electrical generation sub-systems. These are described in detail in Section 2. The first three options involve a sub-critical pressure receiver, while the fourth one employs a supercritical pressure receiver in a separate, primary loop. In this unique arrangement, 100% receiver power passes through the storage sub-system, which acts as a buffer between the receiver and the electrical generation sub-system.

Each option was evaluated on the following operation scenario: 1) eight hours operation at full power plus changing of storage at specified multiples, then, 2) operation from storage until the storage energy was exhausted.

A daily average plant efficiency was calculated for each option listed. Results indicated that Option Nos. 2 and 4 gave the highest efficiencies, each option having about the same efficiency, (table 1.6). Before a preferred selection was made between these two, a supercritical receiver primary loop was analyzed thermally. These analyses are described in Section 4. Results showed Option No. 4 to be more complex and larger than Option No. 2--Solar Reheater, for the same power rating. Option 2--Solar Reheater, was therefore chosen as the preferred arrangement.

High temperature storage units were included in most of the options in Table 1.5. In order to generate rated steam temperature from the storage operating mode, the charging side steam temperature must be 55.6% (100°F) higher than 538C (1000F). This required 593C (1100F) steam from the receiver. It will be shown later that this temperature requirement impacts the material selection and fatigue life of the absorber panels.

Table 1.5

Reheat/Storage Options

No.	Description	Reference Fig. Nos.
1	Live steam reheater with low temperature storage	Fig. 2.1, 2.4, 2.4A 2.5, 2.5A
2	Solar reheater with high temperature and low temperature storage units.	Fig. 2.2, 2.7, 2.7A, 2.8, 2.8A
3	High temperature and low temperature storage units. A portion of the high temperature storage unit dedicated to reheat.	Fig. 2.9, 2.9A, 2.10, 2.10A
4	Supercritical receiver primary loop--100% power pass-through storage to sub-critical steam cycle w/reheat.	Fig. 2.11, 2.11A

Table 1.6 - Comparison of Daily Efficiency - 8 hr Charging

	No.1(Fig.2.4)			No.2(Fig.2.7)			No.3(Fig.2.9)			No.4(Fig.2.11)		
Arrangement Description	Live Steam Reheat/LT Storage			Solar Reheat HT/LT Storage			Hi Temp Reheat Pass-Thru (HT/LT)			Supercritical Receiver - 100% Pass Thru		
Solar Multiple	1.3	1.5	1.7	1.3	1.5	1.7	1.3	1.5	1.7	1.3	1.5	1.7
1. Electrical Power Generated, MW	192.8	192.8	192.8	192.8	192.8	192.8	Not Applicable	192.8	192.8	174.3+	174.3+	174.3+
2. Energy Collected by Receiver, MW-hr	4633	5362	6077	4647	5361	6076		5367	6086	4456	5142	5828
3. Energy to Turbine, MW-hr	3574	3574	3574	3574	3574	3574		3580	3580	3428	3428	3428
4. Energy Stored, MW-hr	1058.6	1787	2502	1072	1787	2502		~~271.5~~ 1516	~~381~~ 2126	1036	1713	2398
5. Electrical Energy Generated (RealTime) MW-hr	1543	1543	1543	1543	1543	1543		1543	1543	1394	1394	1394
6. Real Time Efficiency, %	43	43	43	43	43	43		43	43	41	41	41
7. Electrical Power Generated from Storage, MW	73	73	73	138	138	138		138	138	192.8	192.8	192.8
8. Thermal Power Requried from Storage, MW	327	327	327	389	389	389		~~89.1~~ 299	~~89.1~~ 299	447	447	447
9. Hours of Operation from Storage	3.24	5.46	7.65	2.76	4.6	6.43		3.1*	4.27*	2.3	3.8	5.36
10. Storage Operation Efficiency,%	22	22	22	35.6	35.6	35.6		35.6	35.6	43	43	43
11. Electrical ENERGY Generated from Storage, MW-hr	237	399	559	381	634	887		428	589	443	733	1033
12. Overall Efficiency,%	38	36	34.6	41	40.6	39.9		36.7	35.0	41	41	41

*Based on exhaustion of high temp. storage unit before lo temp. unit.
+Corrected for supercritical pump power.

1.4.4 Receiver/Turbine/Storage Size Selection

The last step in the receiver design selection process was to determine the receiver power rating (MWt) for a "commercial" plant size. For Reheat/Storage Option No. 2, the daily "average" efficiency does not vary significantly with the solar multiple. See Table 1.6. Typical turbine heat balances were used to obtain the required steam flows for plants with 100 to 250 MWe output. A table was constructed of receiver steam flow requirements for these typical turbine cycles with solar multiples of 1.3, 1.5, and 1.7. Results are shown in Table 1.7. From this table, four receivers were selected, two for a pressure of 12.4 MPa (1800 psia) and two for 16.5 (2400 psia) having steam flow capacities of 126, 252, and 378 kg/s (1×10^6, 2×10^6, 3×10^6 lb/hr). These four receivers are capable of covering the entire power/solar multiple design range. The 252 kg/s steam flow receiver includes both 12.4 and 16.5 MPa (1800 and 2400 psia) pressure levels.

Table 1.8 summarizes the receiver parameters for the four receivers selected for conceptual design and cost estimating. The receiver steam flow ratings listed, include the main receiver, (main steam plus storage), but do not include the reheat requirements. The reheater is independent of the solar multiple and is sized for the selected turbine requirements. The physical location of the reheater in Reheat Option No. 2, is conceived to be located on the main receiver tower at approximately one third the tower height, and powered by a dedicated position of the North field heliostats.

1.4.5 Conceptual Design Summary

The external receivers were designed for an asymmetrical flux distribution, with a North side peak flux of 0.85 MW/M^2 and a South flux of 0.3 MW/M^2. Parametric analyses of the receiver thermal and hydraulic performance indicated that the evaporator should be located on the North side, with the finishing superheater on the South side. By matching of heat flux with heat transfer rates,

TABLE 1.7

Steam Flows Required from Receiver Kg/s (lb/hr)

ID No.	Turbine Nominal Power (MW)			Solar Multiple		
	100	200	250	1.3	1.5	1.7
3	10.1 MPa 811/811K (1465 psia 1000/1000 F)	Delete for reasons of less efficient than 12.4 MPa (1800 psia.)				
4A		12.5 MPa 811/811K (1815 psia 1000/1000 F)		(1,774,240) 223.55	(2,047,200) 257.9	(2,320,000) 292.3
4B	12.5 MPa 811/811K (1815 psia 1000/1000 F)			(873,600) 110.07	(1,008,000) 127.0	(1,142,400) 143.94
5B		16.6 MPa 811/811K (2415 psia 1000/1000 F)		(1,706,000) 214.95	(1,968,000) 247.96	(2,231,000) 281.1
5C			16.6 MPa 811/811K (2415 psia 1000/1000 F)	(2,070,000) 260.8	(2,389,000) 301.0	(2,707,000) 341.07

Table 1.8

Summary of Selected Receiver Parameters

Design No.	Turbine Cycle No.	Steam Flow kg/s(lb/hr)	Rec. Power MW(t)	Reheat Option No.	Boiler Option No.
1	2	126 ($1x10^6$)	320.8	2	2b
2	2	252 ($2x10^6$)	641.7	2	2b
3	3	252 ($2x10^6$)	621.7	2	2b
4	3	378 ($3x10^6$)	932.6	2	2b

materials selection were made to minimize metal temperatures.

Table 1.9 lists the materials selected for the various components of the receivers. Maximum mid-wall temperatures are listed for an allowable stress of 700MPa (10,000 psi).

The rifled tubing test program (Task 10) results showed that the proposed rifled tubing performed satisfactorily with a good reserve margin, from DNB relative to the design point selected for the evaporator. Figure 1.2 shows the test points marking the DNB threshold for the parameters indicated. The design point for the receiver evaporator is seen to lie in the "safe" zone. Pressure drop for the rifled tubing was found to be as predicted. Although rifled tubing pressure drop is approximately twice that of smooth tubing, this is offset by the advantages resulting from the prevention of DNB at the design conditions. Rifled tubing allows optimization of the circulation system for minimum pumping costs.

1.4.6 Creep Fatigue Life

The receiver developed in this project was designed to avoid the high frequency temperature oscillations due to DNB and dynamic instability phenomena, plus the diurnal stresses due to film boiling in the evaporator. The critical areas relative to creep fatigue life involve: 1) superheater panel thermal stresses due to one-sided heating; which became cyclic stresses due to daily start up and shut down, plus effects of clouds, and 2) transient thermal stresses due to the rates of heating and cooling thick metal sections. These two phenomena were analyzed for critical areas in the receiver. These areas included a finishing stage superheater panel for 1) above, and a superheater outlet header for 2) above. Details of the analyses are presented in Appendix G. The panel creep-fatigue analysis was conducted on that portion of the finishing stage superheater which indicated the highest metal temperature from the thermal analysis. Section 3 describes the parametric analyses performed to reduce

Table 1.9

RECEIVER TUBE PANEL MATERIAL SELECTIONS

Panel	ASME Spec. No.	Nominal Composition	Midwall Temperature @ 700MPa (10,000 psi)
Evaporator	SA-213 T11	1¼ Cr-½Mo-.75Si	516C (960F)
1st Stage Superheater	SA-213 T22	2¼ Cr-1Mo	518C (965F)
2nd Stage Superheater	SA-213 TP-316H	16Cr-1Ni-2Mo	618C (1145F)
Preheater	SA-192	0.12C	410C (770F)
Reheater	SA-213 TP-316H	16Cr-1Ni-2Mo	618C (1145F)

Figure 1.2

RIFLED TUBE DESIGN PERFORMANCE CURVE

TUBE O.D. = 2.86 cm (1.125 in)
TUBE I.D. = 2.17 cm (0.854 in)

INSIDE FLUX = 945,000 W/M^2 (300,000 BTU/HR FT^2)

PRESSURE = 19.65 MPa (2850 PSIA)

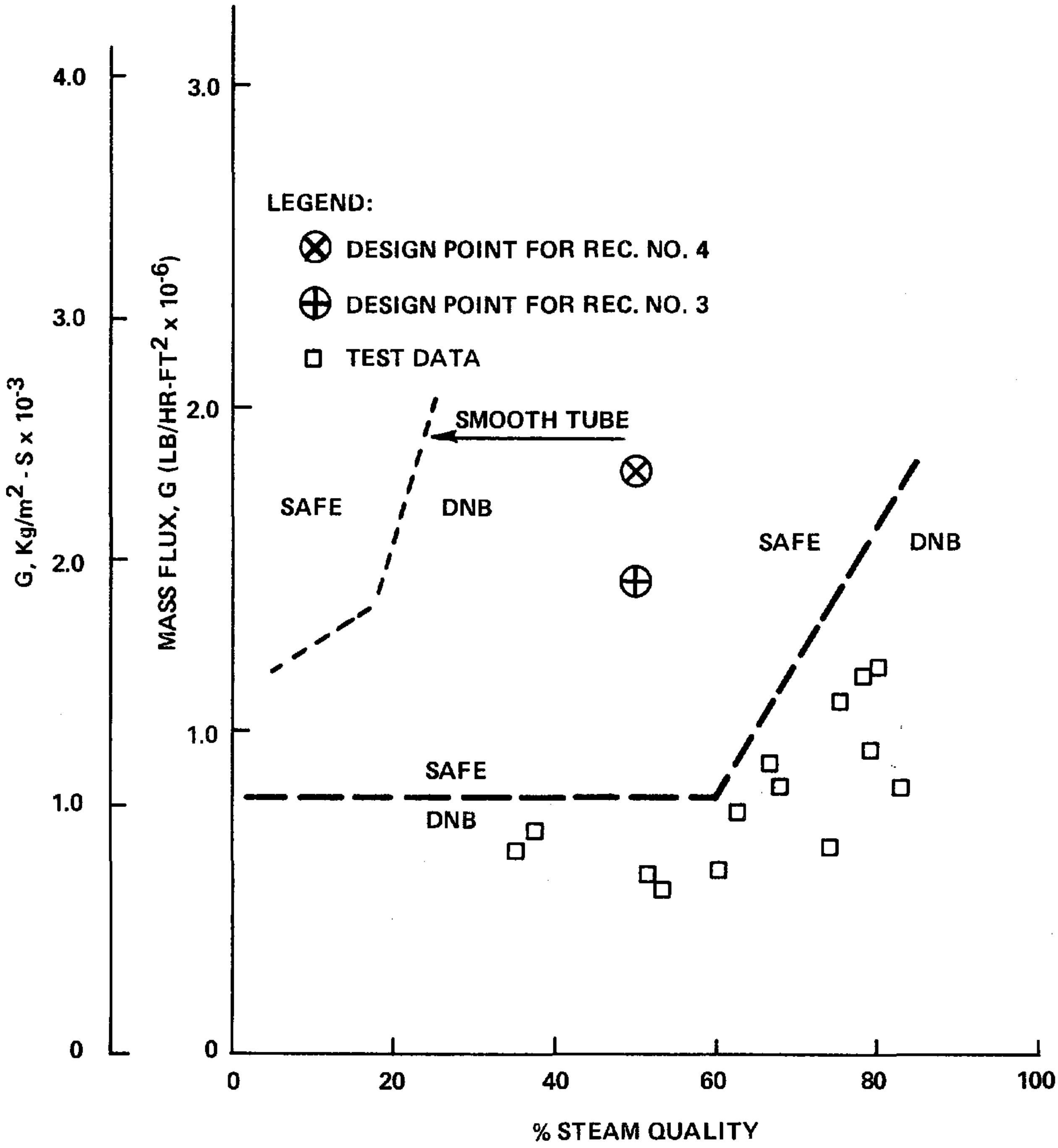

the peak temperature to a minimum, consistent with 593C (1100F) outlet steam temperature. The analysis procedure involved an elastic analysis simulation of an inelastic problem. As such, the results are conservative, because relaxation of the stresses was not considered. With this procedure, 30,000 life-cycles were predicted for the panel using Stainless 316 material, which in this case, was better than Incoloy 800. Since this is a conservative approach, it is probable that an inelastic analysis would increase the allowable cycles to 40,000. The transient problem was analyzed using an average rate of steam temperature charge of 222^{o}C (400^{o}F) per hour. The result of this analysis was also 30,000 cycles. Higher rates would reduce this value.

The assessment of these results in terms of achieving a 30 year lifetime is subject to unknown cloud effects. The calculated allowable fatigue cycles above are more than enough to satisfy the diurnal cycles for a 30-year period, which are estimated as 10,000. The remaining 20,000 cycles are allocated to various cloud effects, which are difficult to assess, in terms of fatigue life cycles. There are unknown aspects such as, the magnitude of strain range caused by various cloud intensities and their frequency of occurance. A specification of life cycle performance is needed in order to certify a design for meeting the life time requirement.

2. Systems Analysis and Selection of Preferred System

2.1 Preliminary Analysis

This section describes the preliminary analysis and baseline assumptions used in the beginning of the conceptual design development of an advanced water/steam receiver. The analysis consisted of a preliminary steam cycle evaluation involving several proposed arrangements of a recirculation receiver. Initially, two ways of incorporating reheat into the system were considered. One was the live steam reheater, and the other was the solar reheater. Both arrangements involved only low temperature 316°C (600°F) storage. Latter arrangements incorporated high temperature storage. Results of these preliminary analyses indicated that the 16.6 MPa (2400 psia) cycle with reheat gave a 15% heat rate improvement over the 10.3 MPa (1500 psia) non-reheat cycle. The receiver arrangement presented in this section was the base starting point. Further analyses resulted in modification to the original concept. These will be discussed in subsequent sections.

2.1.1 Receiver Concept Arrangement

Figure 2.1 shows the arrangement of the 16.5 MPa (2400 psia) receiver, with a "live steam" reheater, and Figure 2.2 shows the same receiver with a solar heated reheater.

The baseline concept for the receiver configuration consists of an external unit with the North side maximum heat flux equal to 0.85 MW/m^2, and a 3:1 flux profile, North to South. With essentially the same heat input as the 100 MWe commercial plant, the electrical power output in this case will be approximately 120 MWe. By starting with a known incident energy and working toward the electrical output, the interface requirements with the heliostat field should be minimized. The panels are arranged in a manner similar to that recommended, as a means to avoid the DNB problems in the 100MWe commercial plant.(3)

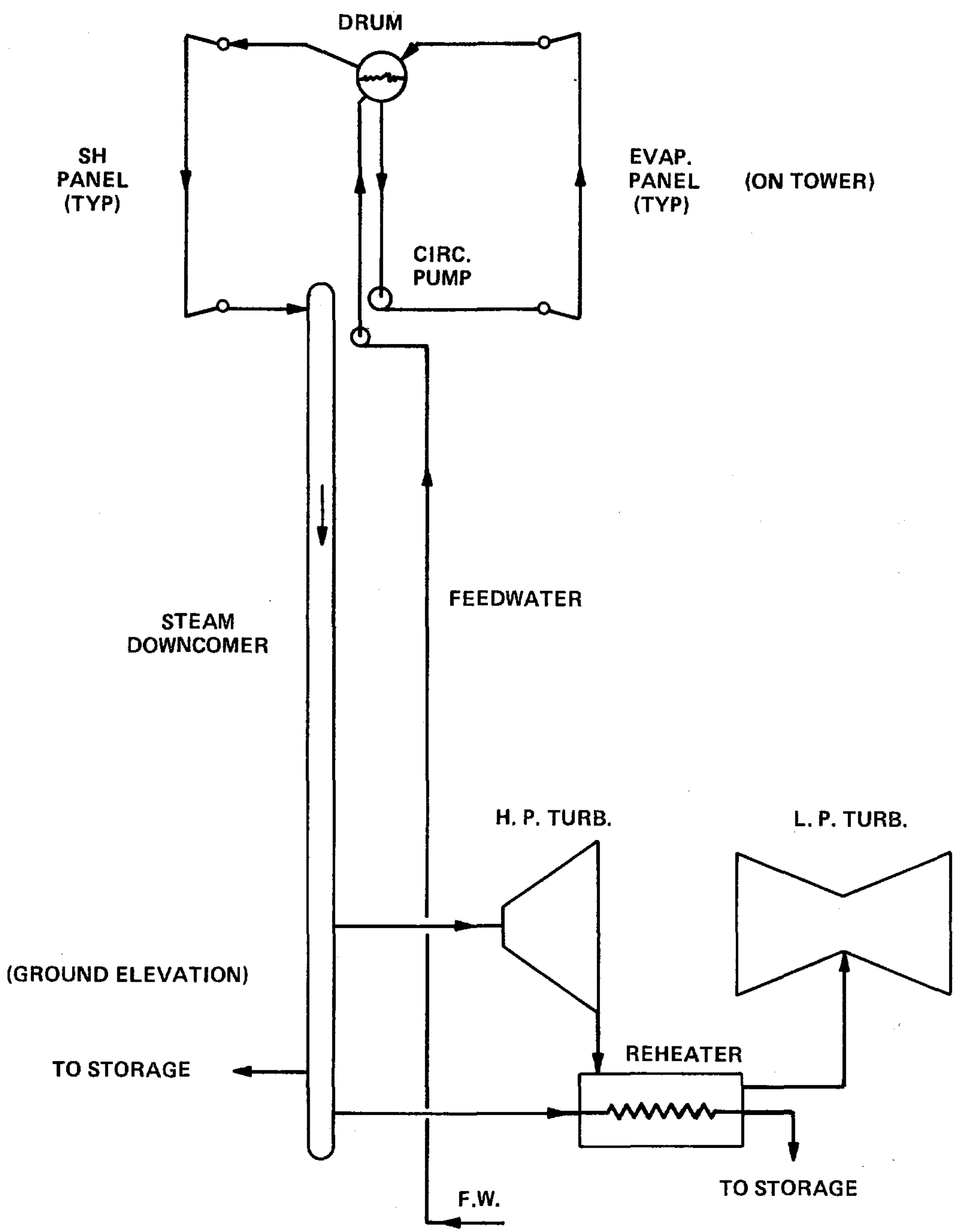

Figure 2.1
CIRCUIT ARRANGEMENT FOR SOLAR RECEIVER – "LIVE" STEAM REHEATER

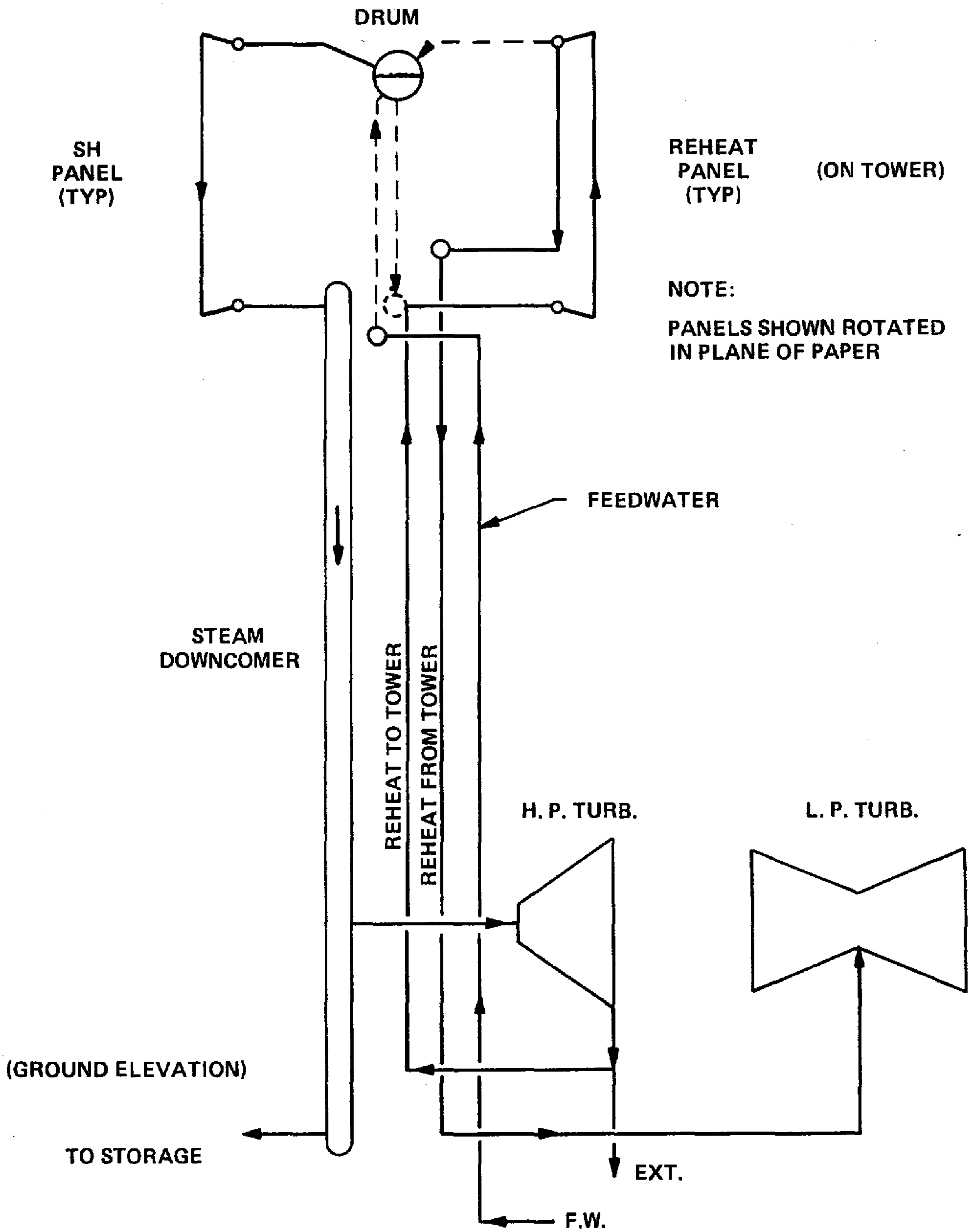

Figure 2.2
CIRCUIT ARRANGEMENT FOR SOLAR RECEIVER–
SOLAR REHEATER

In this concept, the individual panels are arranged to absorb the highest heat flux in the evaporator, which is designed with rifled tubing to eliminate the DNB. Superheater and reheater panels are then placed in regions of lower heat flux. This type of arrangement was shown to cause no significant loss in receiver efficiency, while retaining the high incident flux levels on the north side[3].

The baseline assumption for fatigue life includes 50,000 full temperature range cycles, consisting of 10,000 diurnal cycles, and 40,000 cloud cycles over a period of 30 years. The convective and radiant heat loss model assumes natural convection coefficient based on existing data from the literature[3]. This model probably predicts low convective losses. The accelerations used in the seismic loading of the receivers atop their respective towers were calculated from a tower formula developed for Sandia by Stearns-Rogers. A linear extrapolation was made for the taller towers above 180 m. In the area of controls, it was assumed that the recirculation receiver requirements for control purpose would be feasible, although different from those required for control of a once-through unit.

Figure 2.3 shows a preliminary distribution of the panels based on their calculated heat absorption profiles. The matching of panels with the various regions of heat absorption is not exact, and some adjustments may be necessary to balance the heat absorption to discrete panels. This graph gives an idea of the concept employed in this receiver study.

KEY PLAN

EXTERNAL CENTRAL RECEIVER

Symmetrical about N-S Axis

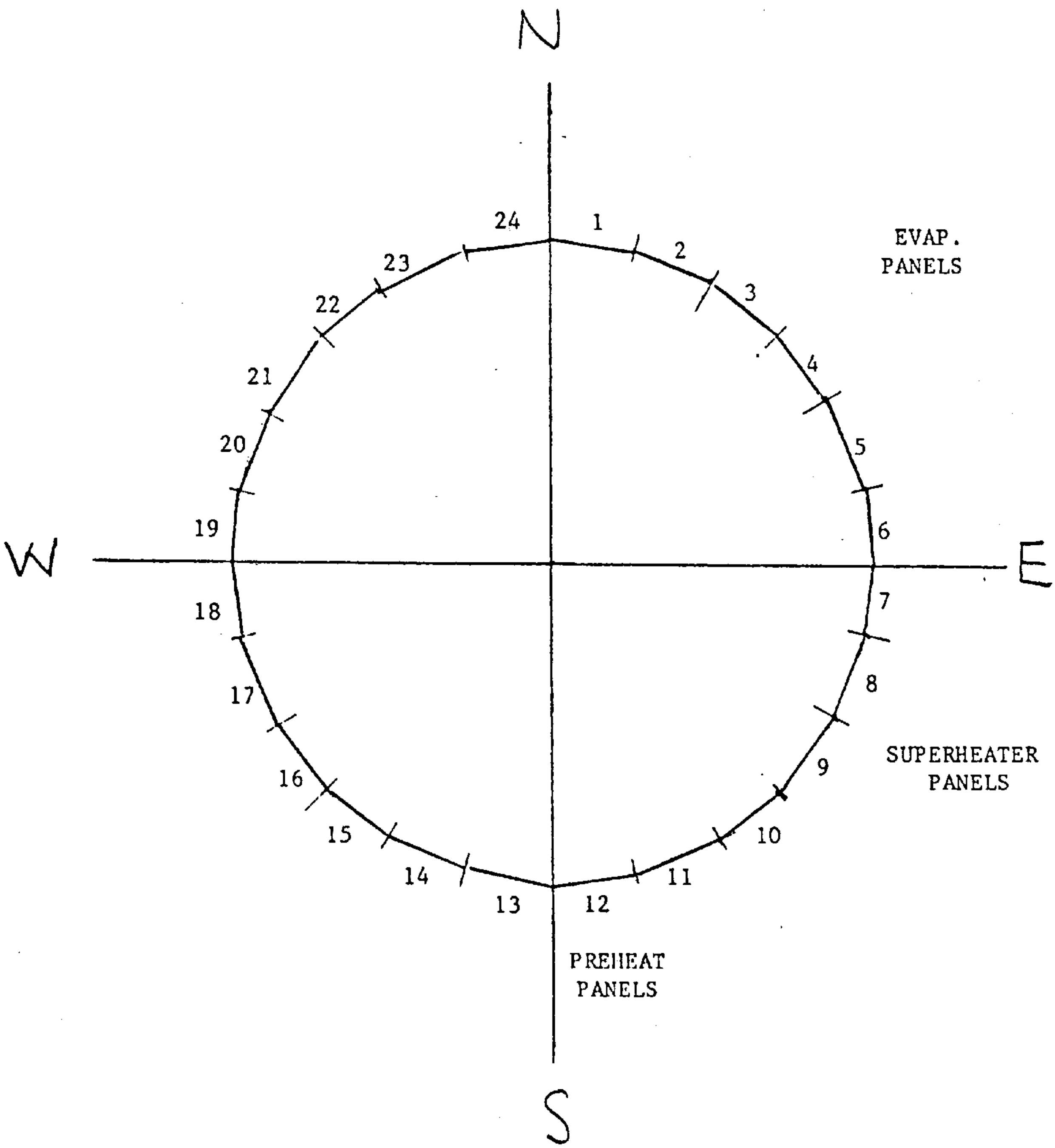

FIGURE 2.3

2.2 Selection of Preferred System

2.2.1 Selection Criteria

The selection process for the preferred system involves selecting the preferred cycle arrangement from the four different arrangements presented below. The selection was based on a calculation of a daily overall efficiency taking into account the power generated from storage in each of the four arrangements presented below. The absolute values of the efficiencies reported are turbine cycle efficiencies and do not include what would be feed pump power and boiler losses. In the case of the supercritical primary receiver, the supercritical circulating pump power was subtracted from the net electrical generation when operating in real time. The turbine cycle is still calculated on the same basis for all arrangements. As shown below, two arrangements were about equal in performance under this scenario. The preferred selection of the subcritical receiver vs. the supercritical was made on the basis of a study of the supercritical receiver presented in Section 4. This indicated problems with the coupling and the heat transfer analysis resulted in a larger receiver (lower flux).

The selection of the preferred power rating of the receiver was not made in this project. Rather, a selected range of receiver power ratings (sizes) was conceptually designed and costed. This information will be input for others who will conduct overall plant follow-on system analyses. Four receivers sizes were picked from a matrix of plant power level and solar multiple combinations as being representative of the range of sizes required. One receiver size satisfies several different combinations of power and solar multiple.

2.2.2 System Analyses

The receiver designs for this analysis are all in Category II, i.e., the steam temperatures and pressures are higher than those for the first generation Barstow plant; 10.34 MPa/789K (1500 psia/960°F/non-reheat). The original C-E proposal was for the 16.55 MPa/811K/811K (2400 psia/1000°F/1000°F) reheat cycle, covering the power range of 100 MWe to 300 MWe. Two separate component arrangements were originally proposed: 1) a "live steam reheater" coupled to a low temperature 315°C (600°F) Storage Sub-system, Figure 2.1, and, 2) a separate solar reheater mounted on the receiver tower, with a low temperature storage sub-system, Figure 2.2. The proposed "live steam reheater" consisted of a heat exchanger to transfer heat to the reheat steam from the receiver steam. In this arrangement, the receiver would be sized to include the reheater thermal power requirements. Reject heat from the "live steam reheater" would be utilized to charge the low temperature storage unit. The solar reheater would be equivalent to a separately fired reheater in a boiler.

Shortly after the beginning of the program, it was decided to investigate high temperature storage sub-systems as a means of improving the steam cycle efficiency when operating from storage (Table 2.1). In addition, a high temperature molten salt storage unit might allow steam to be reheated in the storage unit, without the requirements of a separate "live steam reheater." This concept appeared to be initially beneficial, and two additional cycles were proposed in addition to the original two cycles described above. Also, a supercritical receiver with 100% pass-through of energy through a high temperature storage was proposed for study. In this arrangement, the supercritical receiver (single phase) would become a primary loop, discharging the entire heat pick-up to a high temperature storage unit. The entire plant would then operate from the high temperature storage unit, including the reheat. This arrangement would provide a thermal buffer between the cyclic nature of the solar heat flux and the constant steam temperature requirements of a steam turbine cycle in the storage mode would suffer no

Table 2.1

Reheat/Storage Options

No.	Description	Reference Fig. Nos.
1	Live steam reheater with low temperature storage	Fig. 2.1, 2.4, 2.4A 2.5, 2.5A
2	Solar reheater with high temperature and low temperature storage units.	Fig. 2.2, 2.7, 2.7A, 2.8, 2.8A
3	High temperature and low temperature storage units. A portion of the high temperature storage unit dedicated to reheat.	Fig. 2.9, 2.9A, 2.10, 2.10A
4	Supercritical receiver primary loop--100% power pass-through storage to sub-critical steam cycle w/reheat.	Fig. 2.11, 2.11A

loss of efficiency which would otherwise occur if other storage arrangements were selected. In this context, the supercritical receiver is more in line with other advanced receivers using other heat absorbing substances (molten salt and liquid metals). It thus appeared that two possible arrangements employing high temperature storage could be utilized in conjunction with an advanced Category II receiver.

A simplifeid analysis procedure, based on an 8-hour changing time, was applied to each of the above four cycle arrangement. The objective was to determine their relative daily efficiencies. Although not an actual operational scenario, it serves as a comparison tool. This scenario consisted of full power operation for 8 hours, then storage operation for the time required to exhaust the energy stored during the first eight hoours. Calculations were made for several values of the solar multiple. This parameter is the ratio of the receiver thermal power to the thermal power required to operate the turbine at full load on the "best" solar day. This ratio represents the amount of power put into storage. Thus, with a S.M.=1.3, the receiver and heliostat field are approximately 30% larger than those required to supply only the turbine thermal power. The balance of the excess power generally is used to charge storage.

Figure 2.4 to 2.11 include the heat and mass balances for the four arrangements described above. For clarity, separate balances are shown for solar operation and storage operation. Figure 2.6 shows the turbine expansion line for the 16.5 MPa (2400 psia) cycle. Turbine operation from the low temperature storage unit would require steam admission at the point indicated on Figure 2.6. This is near the end of the turbine expansion line and is responsible for the very low turbine cycle efficiency when operating in this mode.

FIGURE 2. 4 LIVE STEAM REHEATER
(RECEIVER POWERED)
SM = 1.3

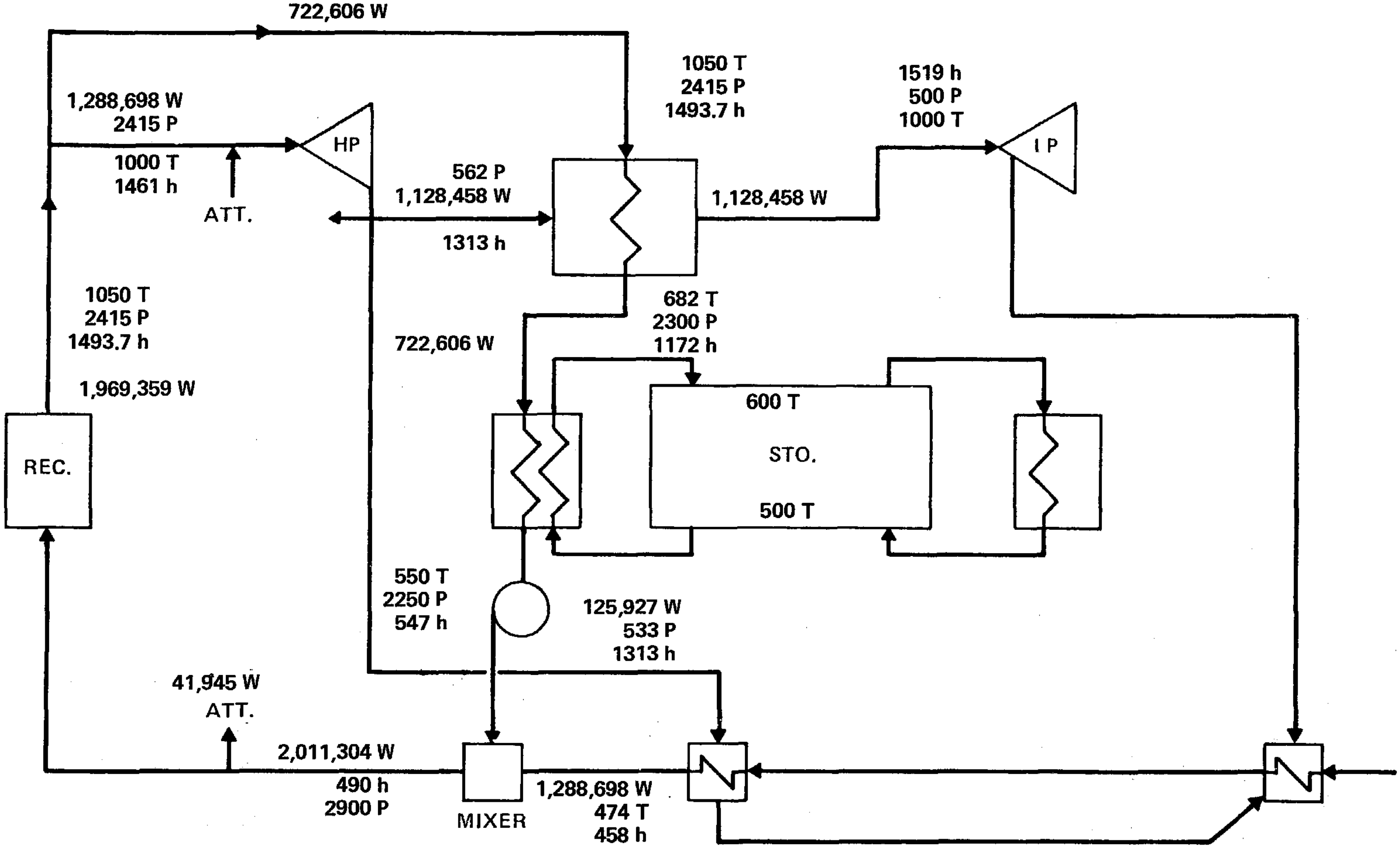

FIGURE 2.4A
(S.I. Units)

LIVE STEAM REHEATER
(RECEIVER POWERED)
SM = 1.3

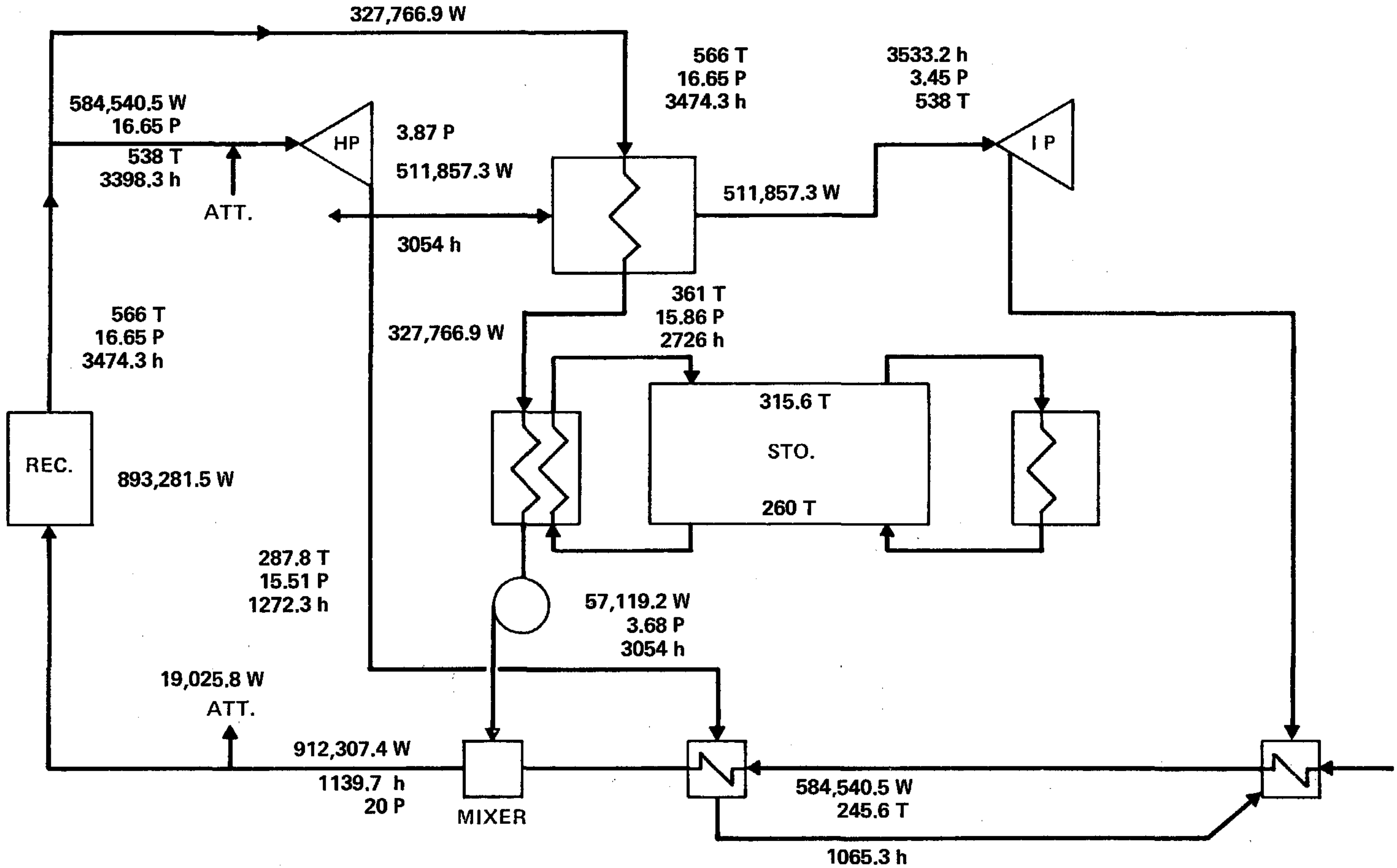

FIGURE 2.5 LIVE STEAM REHEATER (STORAGE POWERED) SM = 1.3

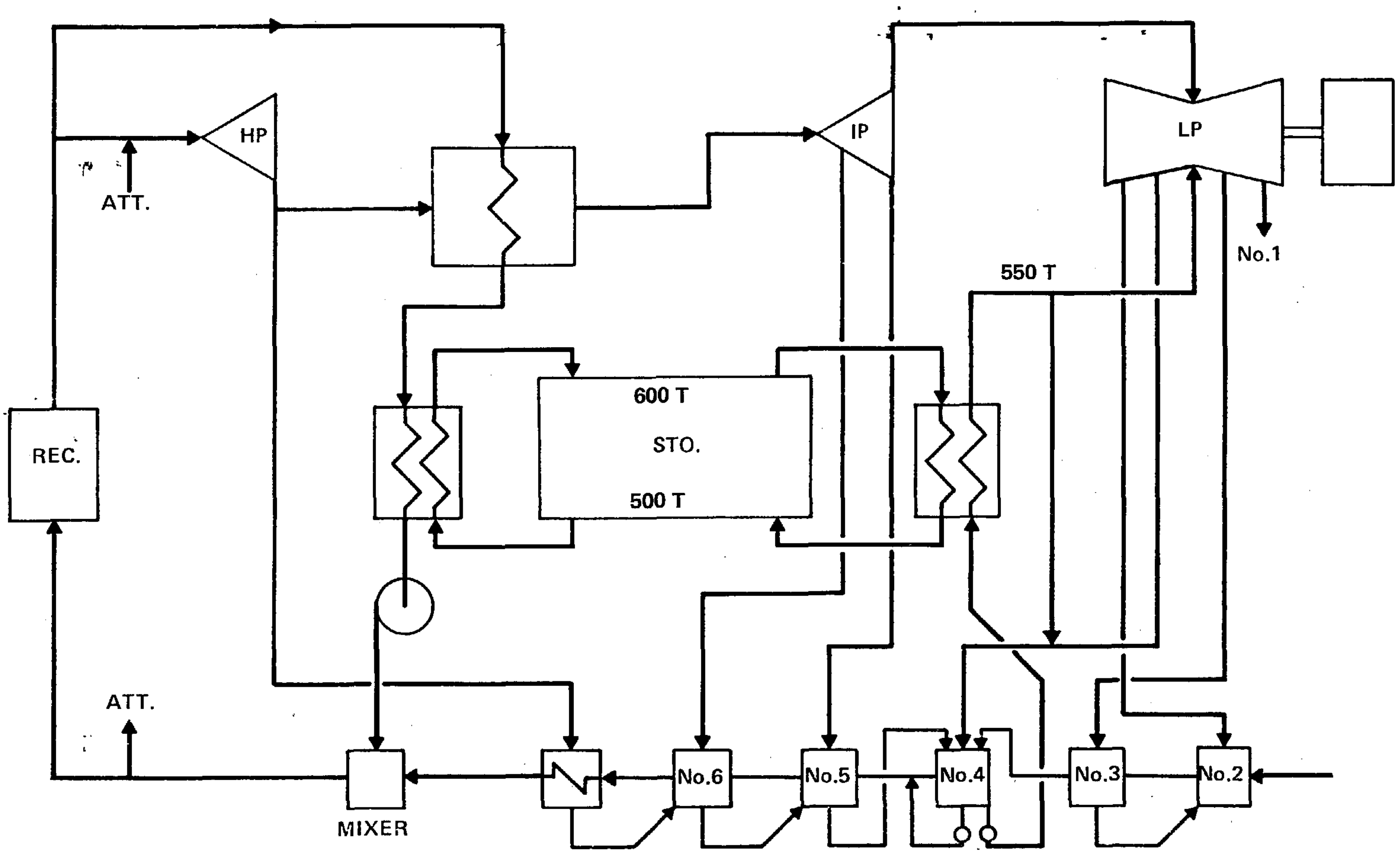

FIGURE 2.5A
(S.I. Units)

LIVE STEAM REHEATER
(STORAGE POWERED)
SM = 1.3

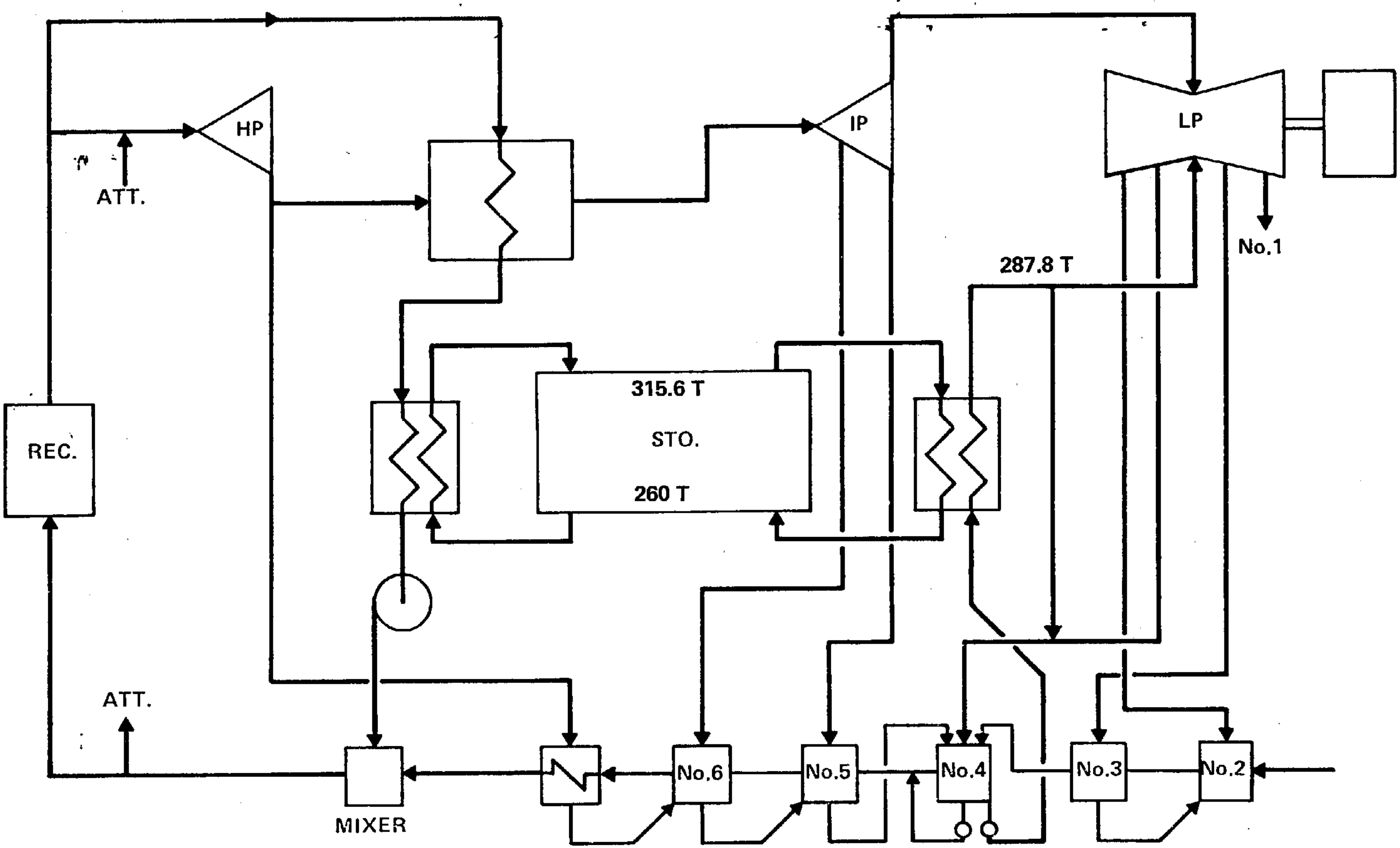

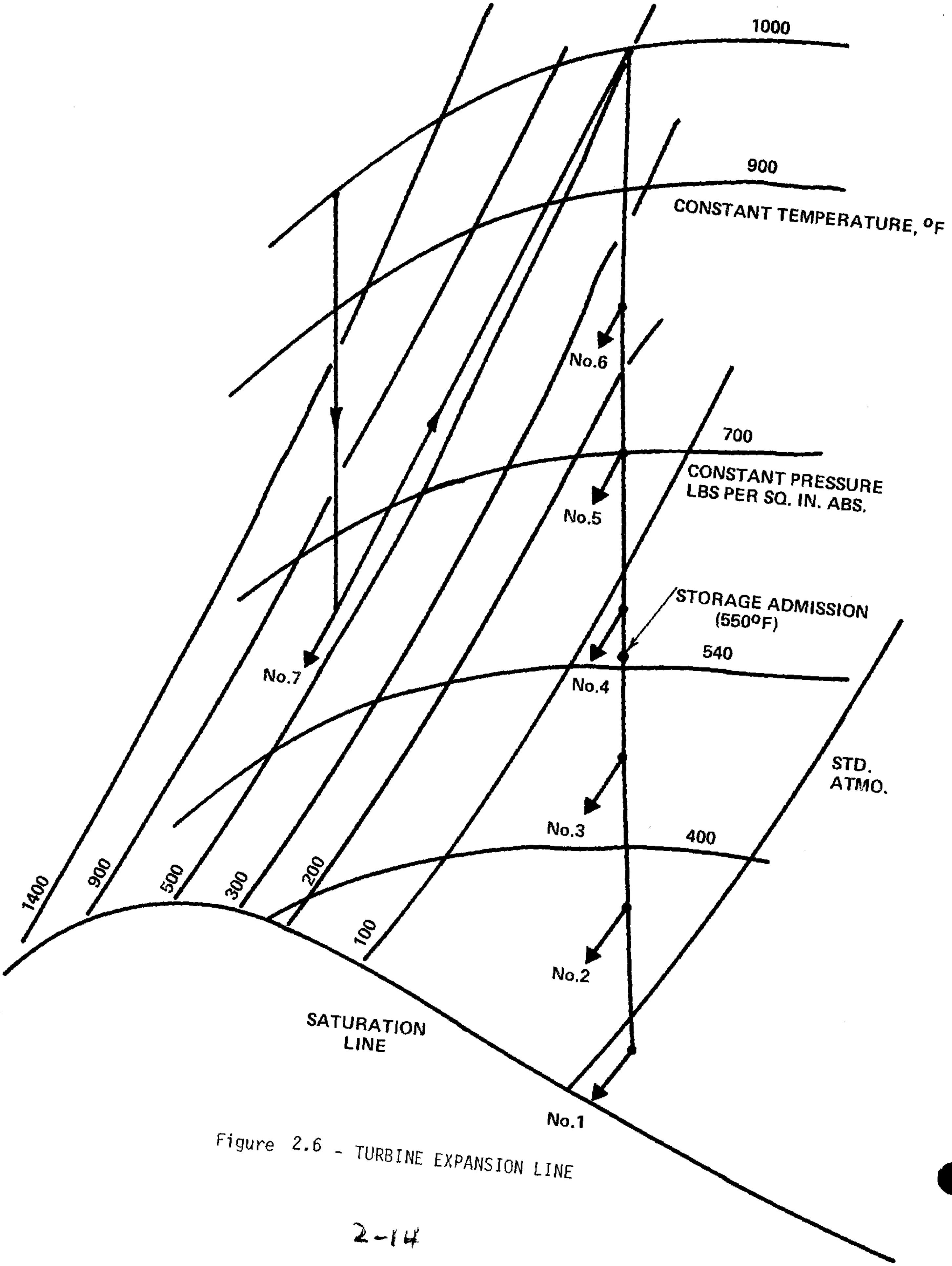

Figure 2.6 - TURBINE EXPANSION LINE

HIGH TEMPERATURE STORAGE/SOLAR REHEAT

FIGURE 2.7 (RECEIVER POWERED)

SM = 1.3

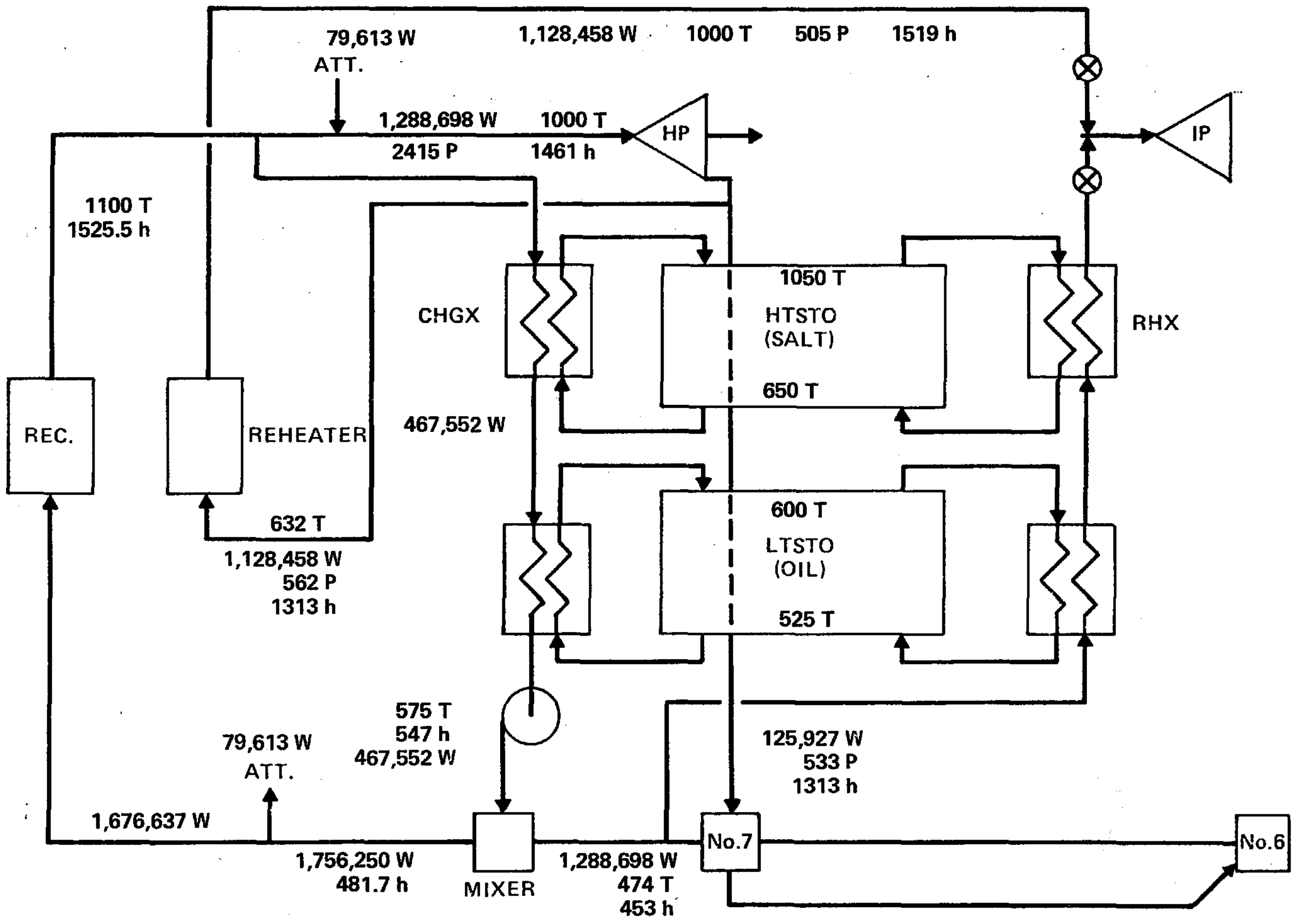

HIGH TEMPERATURE STORAGE/SOLAR REHEAT

FIGURE 2.7A
(S.I. Units)

RECEIVER POWERED

SM = 1.3

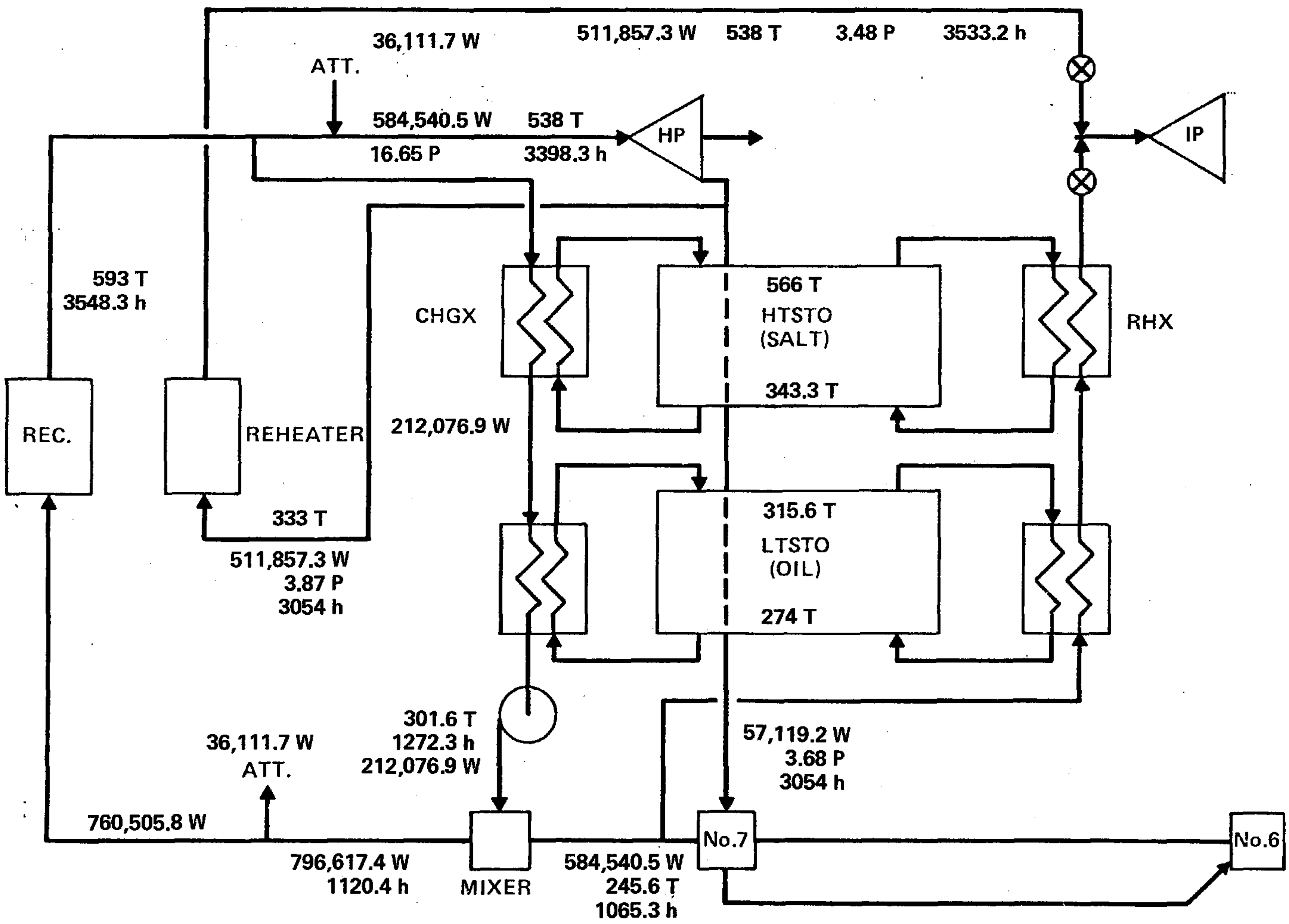

HIGH TEMPERATURE STORAGE/SOLAR REHEAT

FIGURE 2.8 (STORAGE POWERED)

SM = 1.3

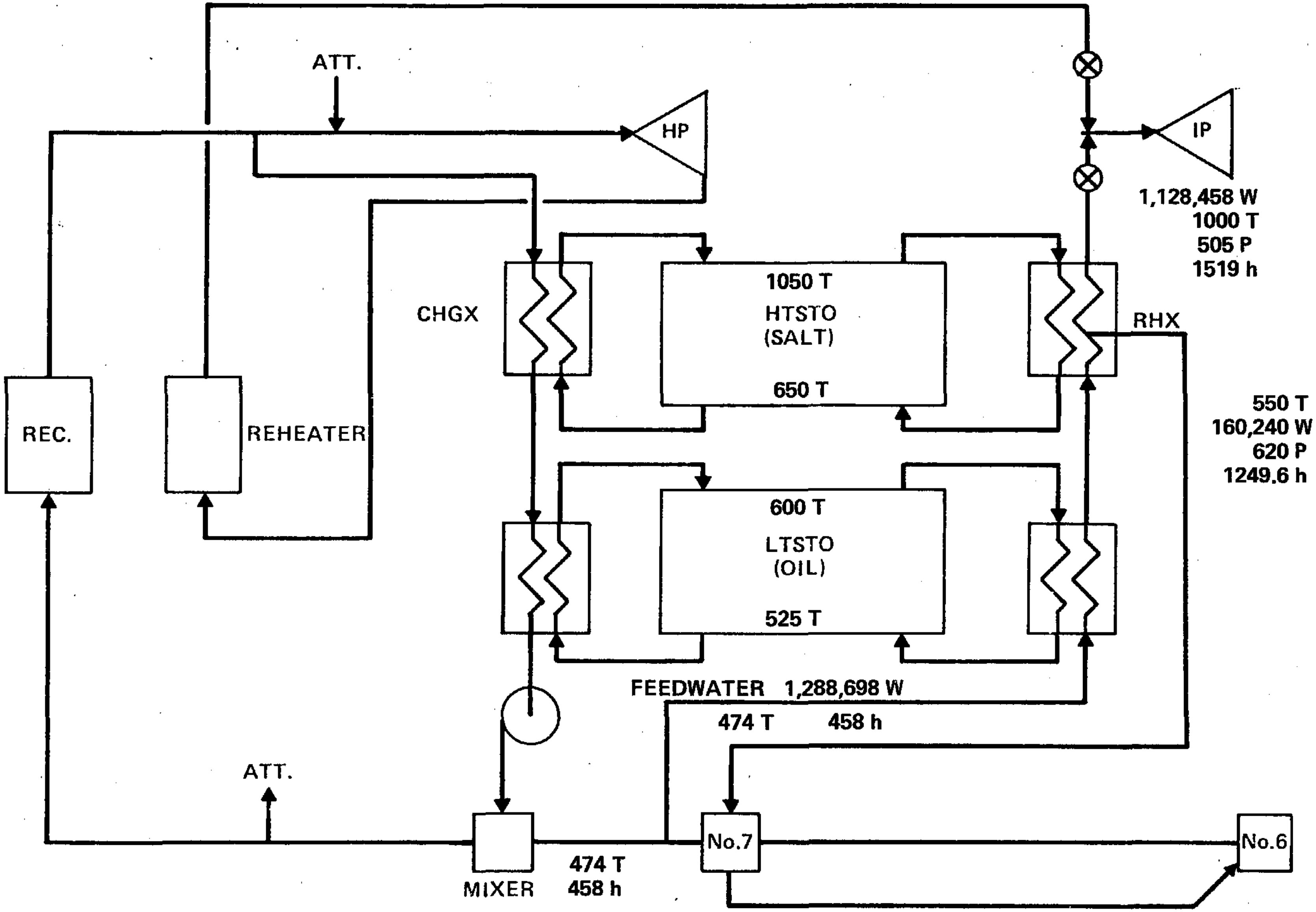

HIGH TEMPERATURE STORAGE/SOLAR REHEAT

FIGURE 2.8A (S.I. Units) (STORAGE POWERED)

SM = 1.3

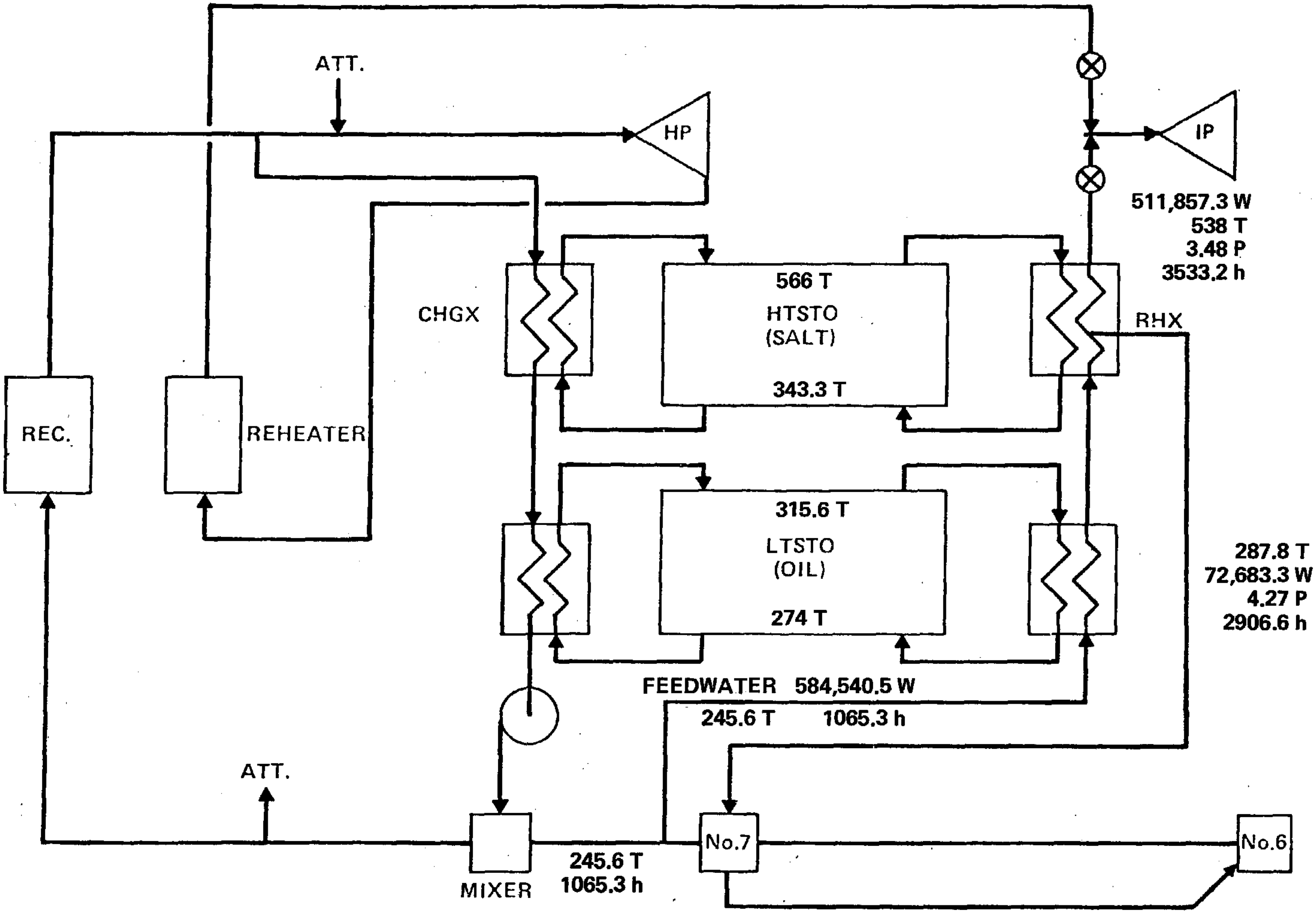

2-18

HIGH TEMPERATURE STORAGE/REHEAT

FIGURE 2.9 (RECEIVER POWERED)

SM = 1.5

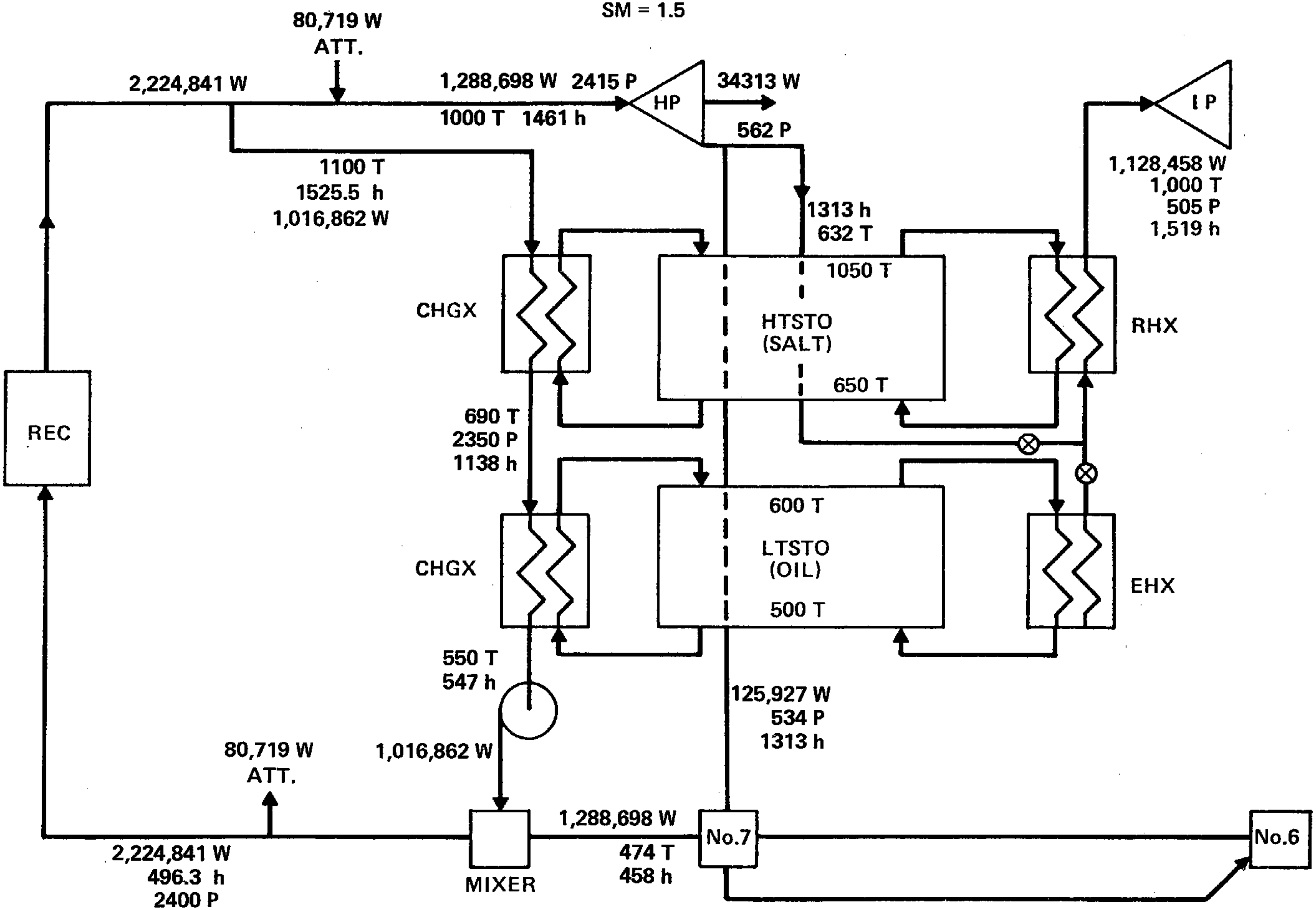

HIGH TEMPERATURE STORAGE/REHEAT

(RECEIVER POWERED)

SM = 1.5

FIGURE 2.9A
(S.I. Units)

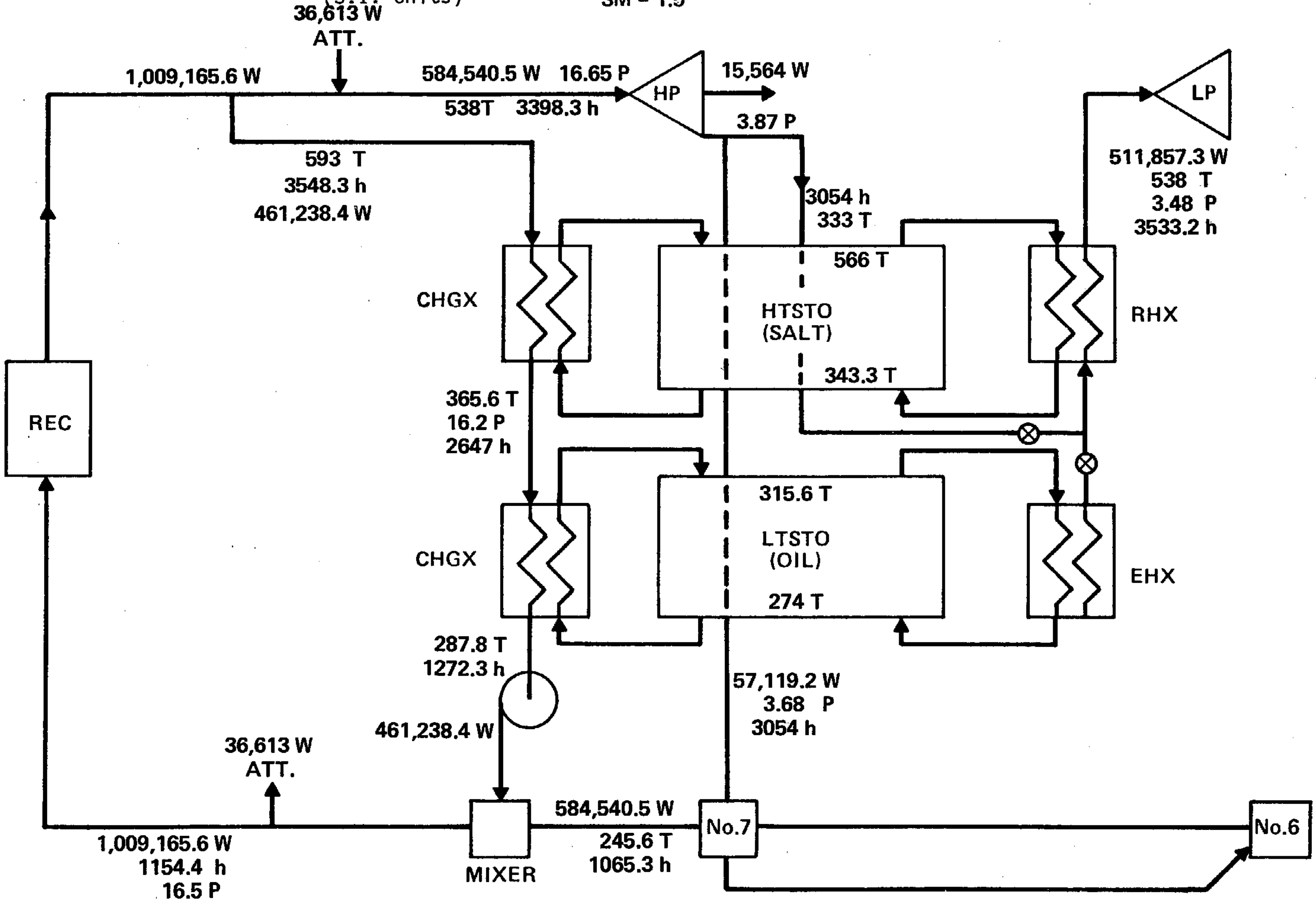

HIGH TEMPERATURE STORAGE/REHEAT

FIGURE 2.10 (STORAGE POWERED)

SM = 1.5

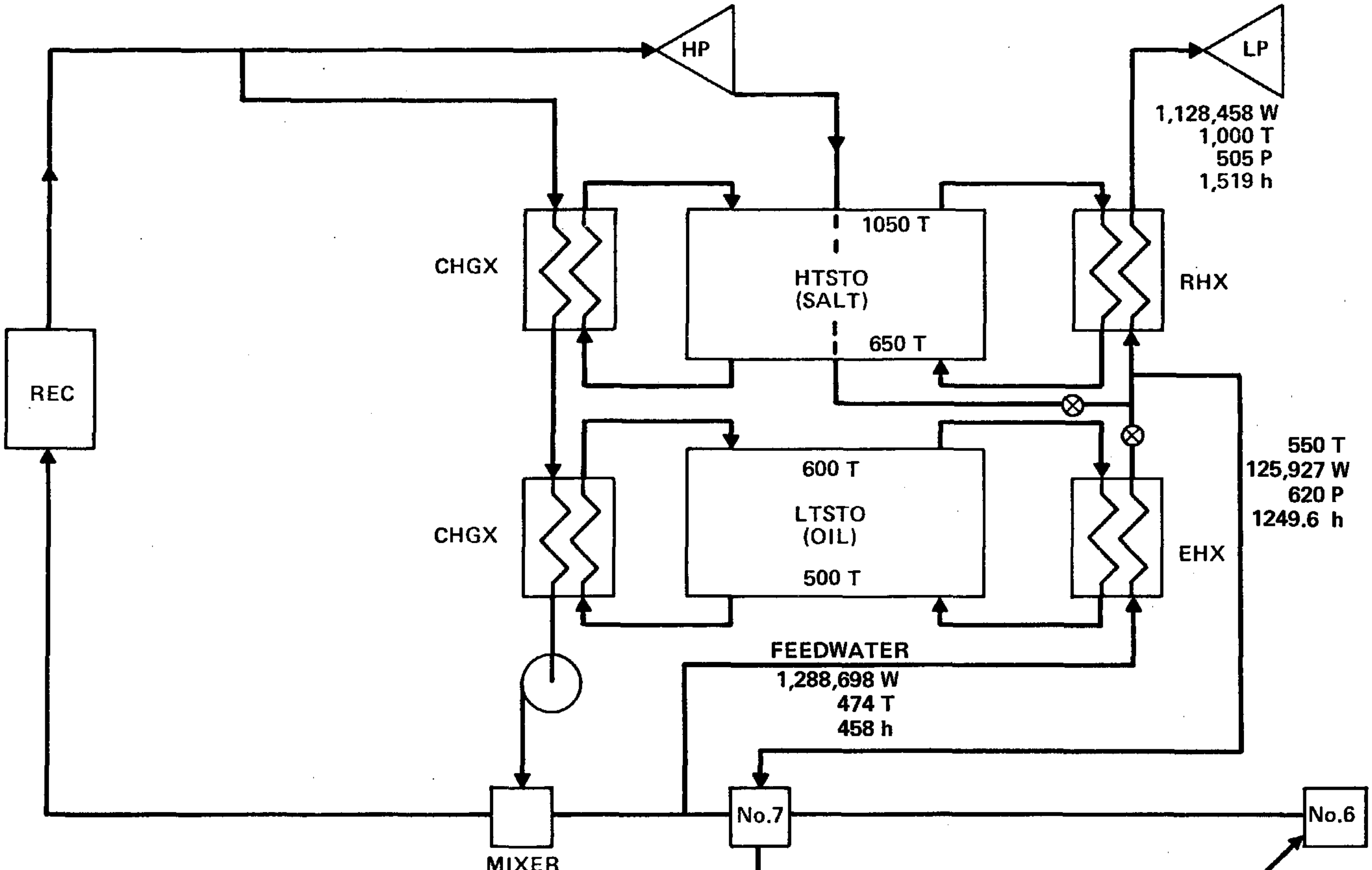

HIGH TEMPERATURE STORAGE/REHEAT

FIGURE 2.10A (S.I. Units) (STORAGE POWERED)

SM = 1.5

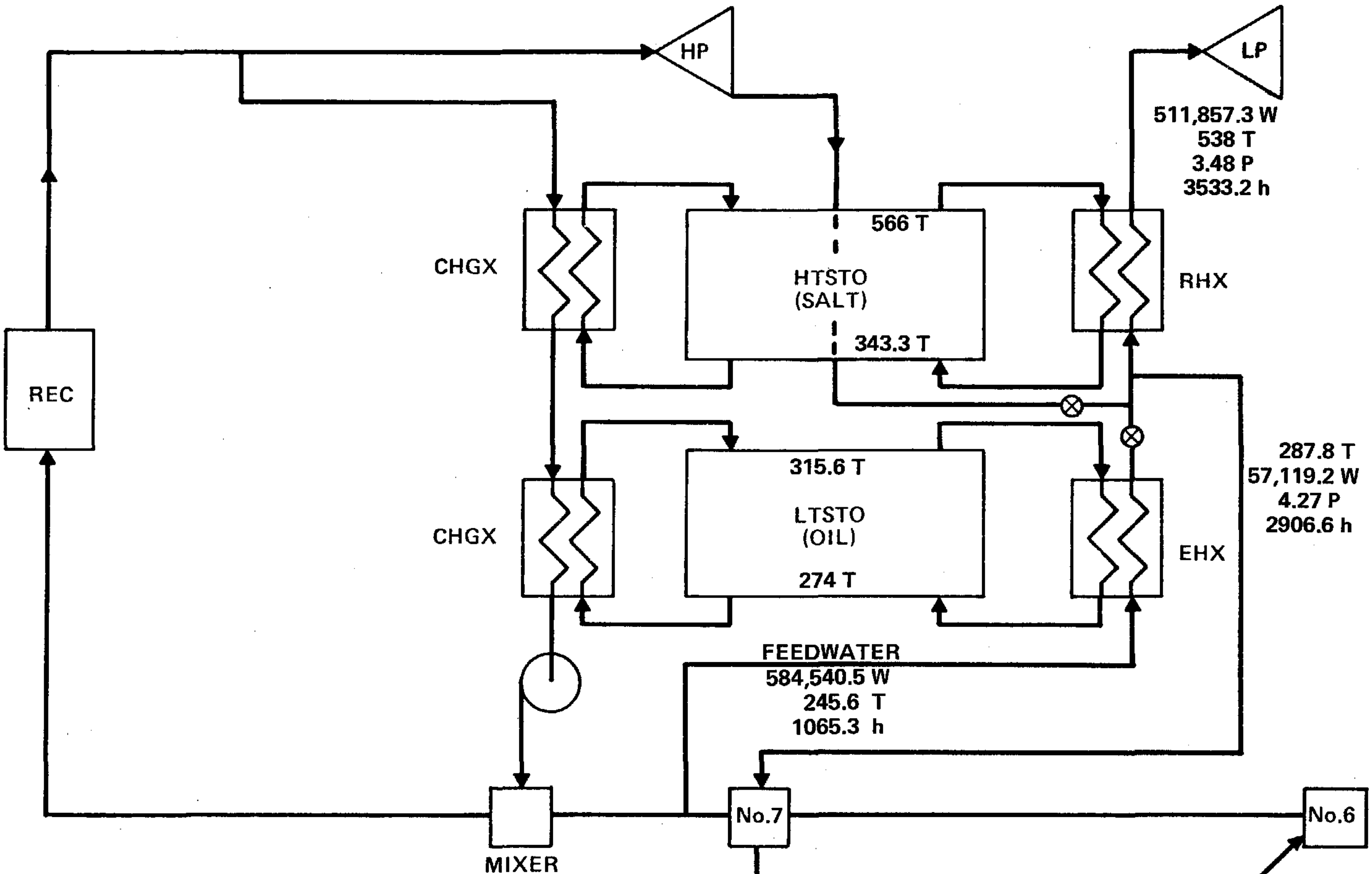

FIGURE 2.11 SUPERCRITICAL RECEIVER – ONE STORAGE TANK
100% PASS - THRU STORAGE
SM = 1.3

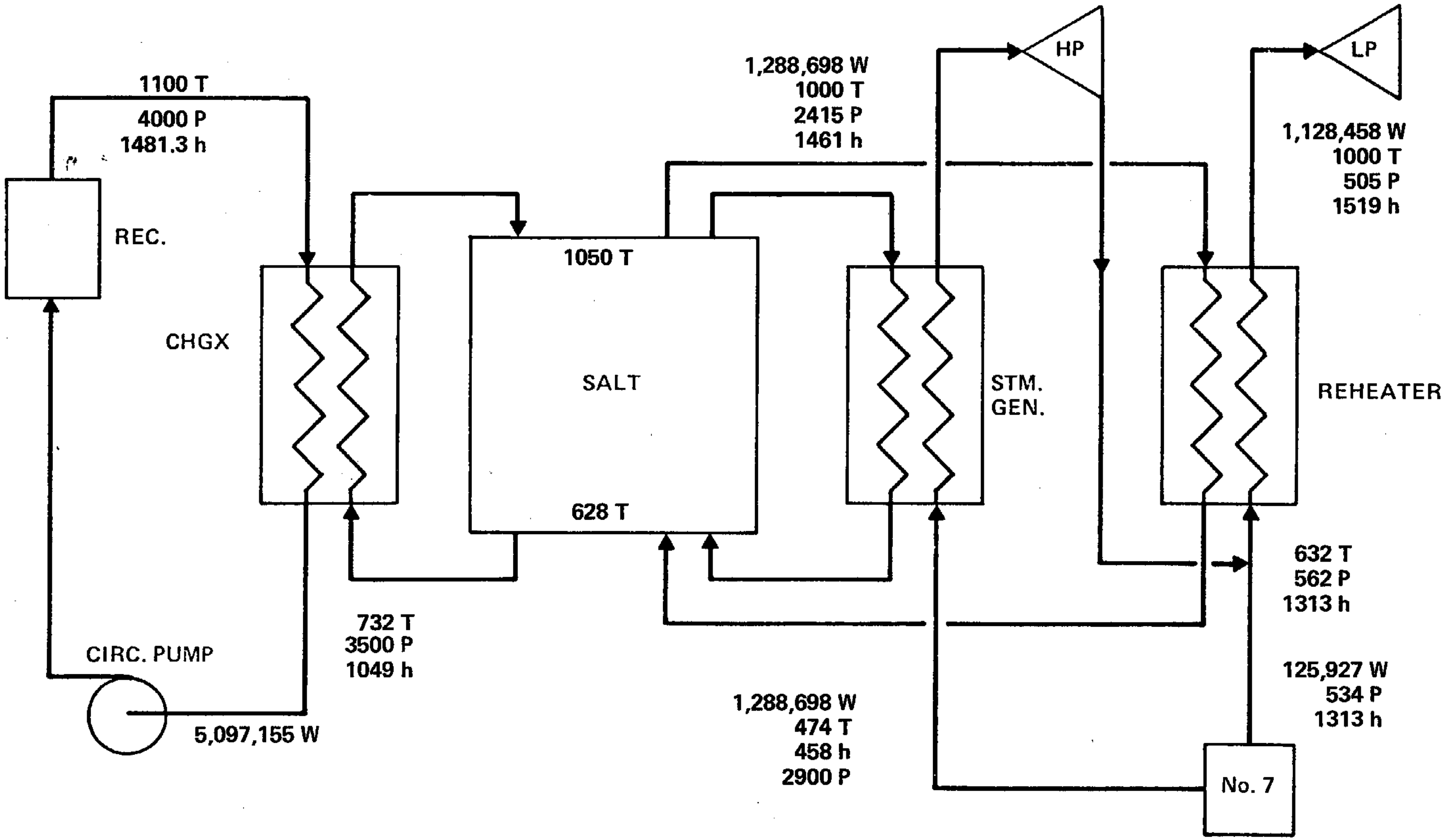

2-23

SUPERCRITICAL RECEIVER – ONE STORAGE TANK

FIGURE 2.11A 100% PASS - THRU STORAGE
(S.I. Units)
SM = 1.3

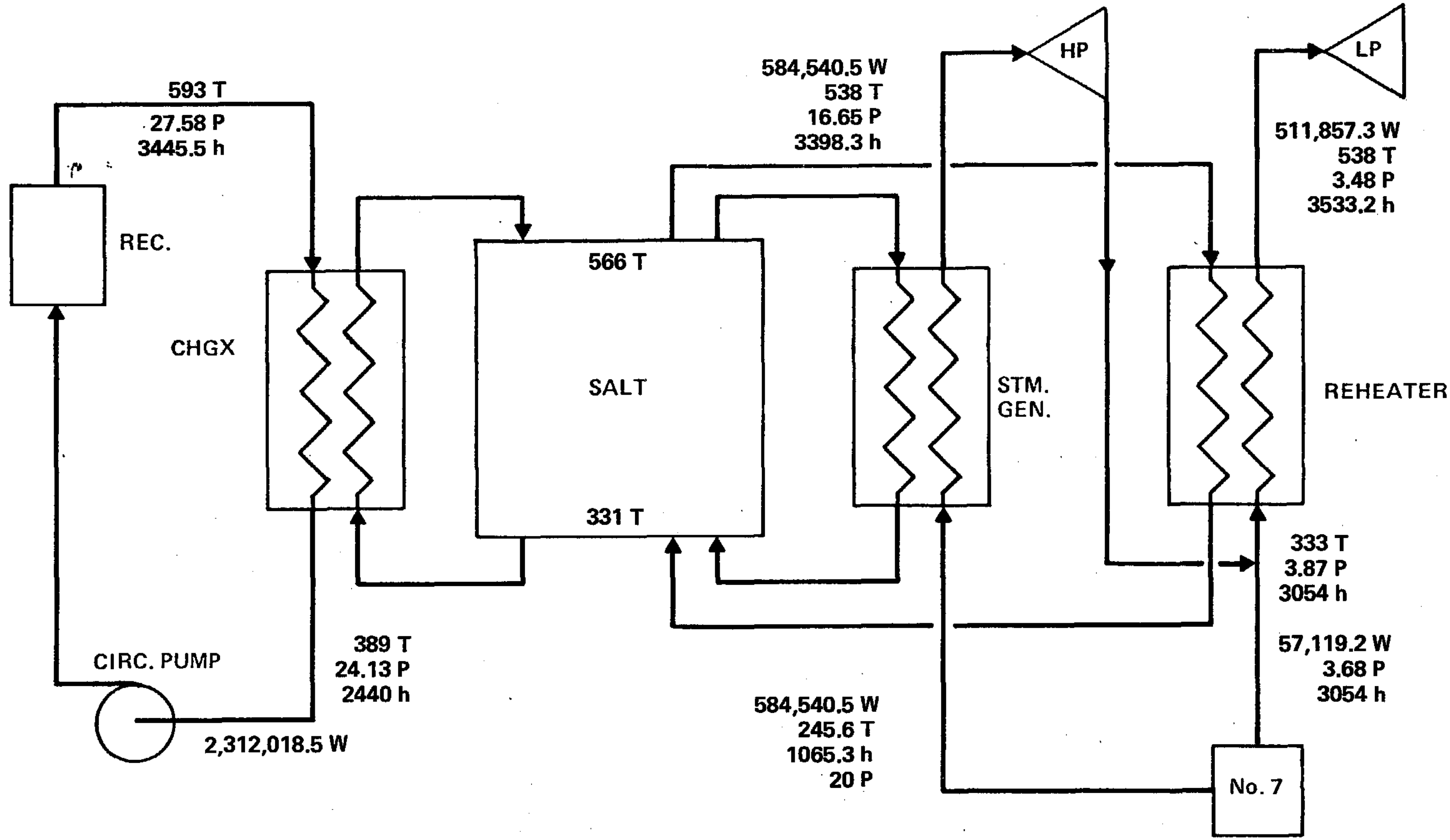

Table 2.2 summarizes the results of the efficiency calculations described above. The quoted values of the efficiencies are the turbine cycle values, without consideration for feed pump power and boiler losses. These are values to be used for comparison purposes. Item 6, the real time efficiency, is the same for all cases except the super-critical, since the same turbine cycle is used. In that case, the supercritical pump power is subtracted. Item 10, storage operation efficiency, is a function of the way the storage is connected to the turbine cycle. These efficiencies vary from 22% to 43%. The lowest value, 22% is a result of the low temperature storage. When high temperature storage is incorporated, the efficiency goes up to 35.6%. The supercritical primary loop cycle has the best efficiency because of the 100% pass-through. In the storage mode, the cycle efficiency is not reduced by the supercritical pump power. Storage efficiency is better than the real-time efficiency. The bottom line, 12, shows the "daily integrated" efficiencies according to the assumed scenario. These also are a function of solar multiple, as well as cycle arrangement. Note that the overall efficiency decreases with increasing solar multiple (except for the supercritical primary receiver). The magnitude of this decrease depends on the storage operation efficiency. This is logical, because a large SM means more time running from storage. If a larger time is spent operating at a lower efficiency, it follows that the overall integrated efficiency will be reduced. The high temperature reheat pass-through cycle (No. 3) is a special case. Although employing high temperature storage, the daily efficiencies are not much better than the low temperature storage (No. 1). This is due to the mis-match between the high temperature and low temperature storage modules. Note that the high temperature unit exhausts before the low temperature unit. This in effect, wastes the low temperature energy, resulting in degradation in efficiency. This reduced efficiency is reflected in Table 2.3. Due to the reheat pass-through in No. 3, a S.M.=1.3 is not possible. A potential solution to this problem would be to transfer this heat into the feedwater heating train, or reject the heat to the condenser. This would require extensive revision of the standard turbine extractions and feed heaters, or a substantial increase in the size of the final heat rejection system.

It is therefore concluded that (excluding No. 4 - supercritical primary loop) Option No. 2 - Solar Reheat with HT/LT Storage produces the best overall efficiency. The remainder of this project was directed toward receiver design with separate solar reheaters.

2.2.3 Receiver Size Determination

Due to the large number of potential sizes and solar multiples, interfacing requirements with the storage and plant electrical generation sub-systems, it was decided to concentrate on a few receiver designs that would satisfy a range of possible combinations of electrical power and storage sub-systems. Since the simple scenario described in the previous section may not adequately represent the true annual energy cost picture, for all plant conditions, optimization of these sub-systems would not be required in this program. Instead, four basic receivers are to be conceptually designed. These were developed from the matrix of Table 2.3 and are listed in Table 2.4. Three basic power levels were selected represented by three steam flows, and two pressure cycles. Information from the General Electric Co. indicated that standard turbines in the 100 MWe range were 12.4 MPa (1800 psia) throttle pressure, vs. 16.5 MPa (2400 psia) for the larger sizes. Both pressures are available in the 200 MWe range. The receiver power ratings (steam flow) were selected to cover the range of electrical output and solar multiple of Table 2.3.

Table 2.2 - Comparison of Daily Efficiency - 8 hr Charging

	No.1(Fig.2.4)			No.2(Fig.2.7)			No.3(Fig.2.9)			No.4(Fig.2.11)		
Arrangement Description	Live Steam Reheat/LT Storage			Solar Reheat HT/LT Storage			Hi Temp Reheat Pass-Thru (HT/LT)			Supercritical Receiver - 100% Pass Thru		
Solar Multiple	1.3	1.5	1.7	1.3	1.5	1.7	1.3	1.5	1.7	1.3	1.5	1.7
1. Electrical Power Generated, MW	192.8	192.8	192.8	192.8	192.8	192.8		192.8	192.8	174.3+	174.3+	174.3+
2. Energy Collected by Receiver, MW-hr	4633	5362	6077	4647	5361	6076		5367	6086	4456	5142	5828
3. Energy to Turbine, MW-hr	3574	3574	3574	3574	3574	3574		3580	3580	3428	3428	3428
4. Energy Stored, MW-hr	1058.6	1787	2502	1072	1787	2502		~~271.5~~ 1516	~~381~~ 2126	1036	1713	2398
5. Electrical Energy Generated (RealTime) MW-hr	1543	1543	1543	1543	1543	1543		1543	1543	1394	1394	1394
6. Real Time Efficiency, %	43	43	43	43	43	43		43	43	41	41	41
7. Electrical Power Generated from Storage, MW	73	73	73	138	138	138	Not Applicable	138	138	192.8	192.8	192.8
8. Thermal Power Requried from Storage, MW	327	327	327	389	389	389		~~89.1~~ 299	~~89.1~~ 299	447	447	447
9. Hours of Operation from Storage	3.24	5.46	7.65	2.76	4.6	6.43		3.1*	4.27*	2.3	3.8	5.36
10. Storage Operation Efficiency,%	22	22	22	35.6	35.6	35.6		35.6	35.6	43	43	43
11. Electrical ENERGY Generated from Storage, MW-hr	237	399	559	381	634	887		428	589	443	733	1033
12. Overall Efficiency,%	38	36	34.6	41	40.6	39.9		36.7	35.0	41	41	41

*Based on exhaustion of high temp. storage unit before lo temp. unit.
+Corrected for supercritical pump power.

TABLE 2.3

Steam Flows Required from Receiver Kg/s (lb/hr)

ID No.	Turbine Nominal Power (MWe)			Solar Multiple		
	100	200	250	1.3	1.5	1.7
3	10.1 MPa 811/811K (1465 psia 1000/1000 F)	Delete for reasons of less efficient than 12.4 MPa (1800 psia.)				
4A		12.5 MPa 811/811K (1815 psia 1000/1000 F)		(1,774,240) 223.55	(2,047,200) 257.9	(2,320,000) 292.3
4B	12.5 MPa 811/811K (1815 psia 1000/1000 F)			(873,600) 110.07	(1,008,000) 127.0	(1,142,400) 143.94
5B		16.6 MPa 811/811K (2415 psia 1000/1000 F)		(1,706,000) 214.95	(1,968,000) 247.96	(2,231,000) 281.1
5C			16.6 MPa 811/811K (2415 psia 1000/1000 F)	(2,070,000) 260.8	(2,389,000) 301.0	(2,707,000) 341.07

Table 2.4

Summary of Selected Receiver Parameters

Design No.	Turbine Cycle No.	Steam Flow kg/s(lb/hr)	Rec. Power MW(t)	Reheat Option No.	Boiler Option No.
1	2	126 (1×10^6)	320.8	2	2b
2	2	252 (2×10^6)	641.7	2	2b
3	3	252 (2×10^6)	621.7	2	2b
4	3	378 (3×10^6)	932.6	2	2b

3. Parametric Analyses

3.1 Introduction

This section documents certain parametric analyses conducted with baseline assumptions regarding flux distribution. Results reported herein led to a change in superheater design which is reported in Section 5. The receiver outlet temperature is 593°C (1100°F), based on 538°C (1000°F) superheat and reheat temperatures in the turbine steam cycle, and 55.6°C (100°F) terminal temperature difference in the storage sub-system. The receiver design parametrics are based on four conceptual water/steam cycles which are summarized in Table 3.1. These were selected as a result of the system analysis presented in Section 2.

The study includes a parametric evaluation of advanced water/steam superheater, evaporator, and reheat tube panels. Design variables such as aspect ratio (L/D), flux distribution, superheater location, tube material, tube size, pressure drop, tube crown temperature, and absorption efficiency were explored.

Lateral flux gradients across tube panels were also studied as they affect fluid outlet and tube crown temperatures. Panel orificing requirements were developed.

Tube crown temperature and pressure drop studies were also done to optimize pressure drop and tube crown temperature.

The primary analytic tool used in the parametric analysis is a computer program referred to as the STPP Code (Solar Thermal Performance Program). The STPP Code is a C-E developed computer program for analyzing the thermal performance of tube panels in an external cyclindrical receiver. The program can evaluate preheat, evaporator, superheater, and reheat tube panels. It can also evaluate a once-through steam generator configuration. Details of the STPP Code are reported in Appendix A. Sample STPP computer outputs for different panel sections are presented in Appendix B.

TABLE 3.1

CONCEPTUAL ADVANCED WATER/STEAM CYCLES

Receiver Outlet Temp. = 593°C (1100°F)

Cycle No.	Steam Flow Kg/hr (lb/hr)	Turbine Throttle Pressure MPa (psia)
1	$.45 \times 10^6$ (1×10^6)	12.4 (1800)
2	$.91 \times 10^6$ (2×10^6)	12.4 (1800)
3	$.91 \times 10^6$ (2×10^6)	16.5 (2400)
4	1.4×10^6 (3×10^6)	16.5 (2400)

3.2 Water/Steam Receiver Subsystems

3.2.1 Receiver Design Criteria

3.2.1.1 Heat and Mass Balances

The parametric study is based on an analysis of tube panels in a cylindrical external central receiver. The final steam temperature of 593°C (1100°F) was determined by adding 56°C (100°F) total terminal temperature difference to the required turbine throttle temperature of 538°C (1000°F). The 56°C (100°F) includes 28°C (50°F) on each side of the high temperature storage unit.

Figures 3.1 through 3.4 show the baseline receiver heat and mass balances for the 4 advanced water/steam cycles outlined in Table 3.1. Steam generation is based on controlled recirculation water/steam circuitry. The feedwater input conditions to the preheater (or economizer) are dictated by the turbine cycle. The temperature at the exit of the preheater is set at 56°C (100°F) less than the drum saturation temperature. This gives about 28°C (50°F) subcooling at the circulation pump suction to satisfy NPSH requirements. The drum pressure is set at 3.10 MPa (450 psi) above the turbine throttle pressure to allow sufficient superheater and steam downcomer pressure drop.

3.2.1.2 Incident Flux Distribution--There are both radial (on receiver circumference) and vertical (along tube panel length) incident flux distributions to be applied in the receiver design. The assumed radial incident flux profile is shown in Figure 3.5. The distribution results from a non-symmetrical heliostat field, creating a north side maximum flux of .85 MW/m^2 (270,000 $BTU/hr\text{-}ft^2$) and a south side minimum of .28 MW/m^2 (90,000 $BTU/hr\text{-}ft^2$). The north to south side flux ratio is 3:1

Figure 3.1
RECEIVER HEAT AND MASS BALANCE
CYCLE No. 1

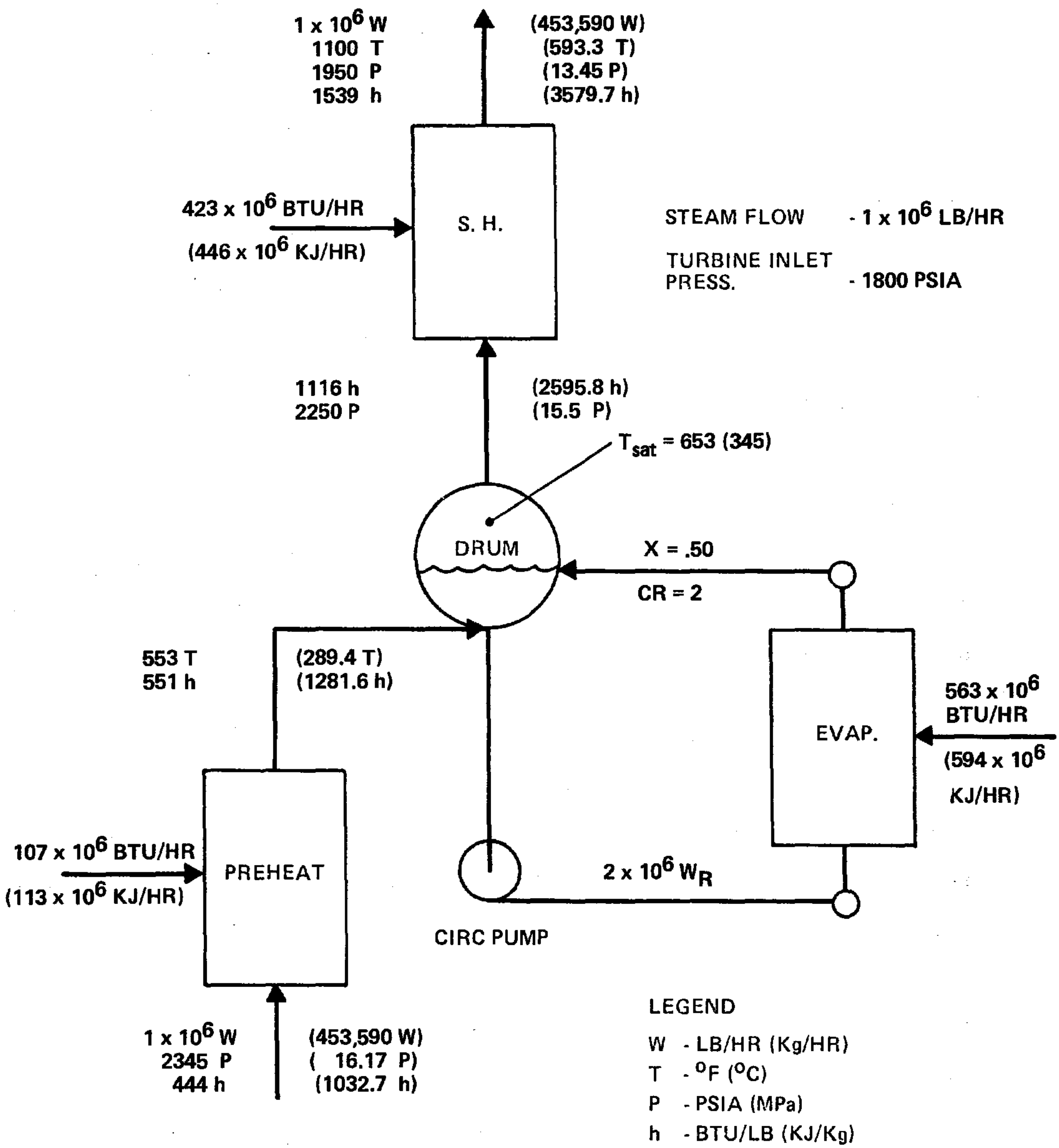

Figure 3.2
RECEIVER HEAT AND MASS BALANCE
CYCLE No. 2

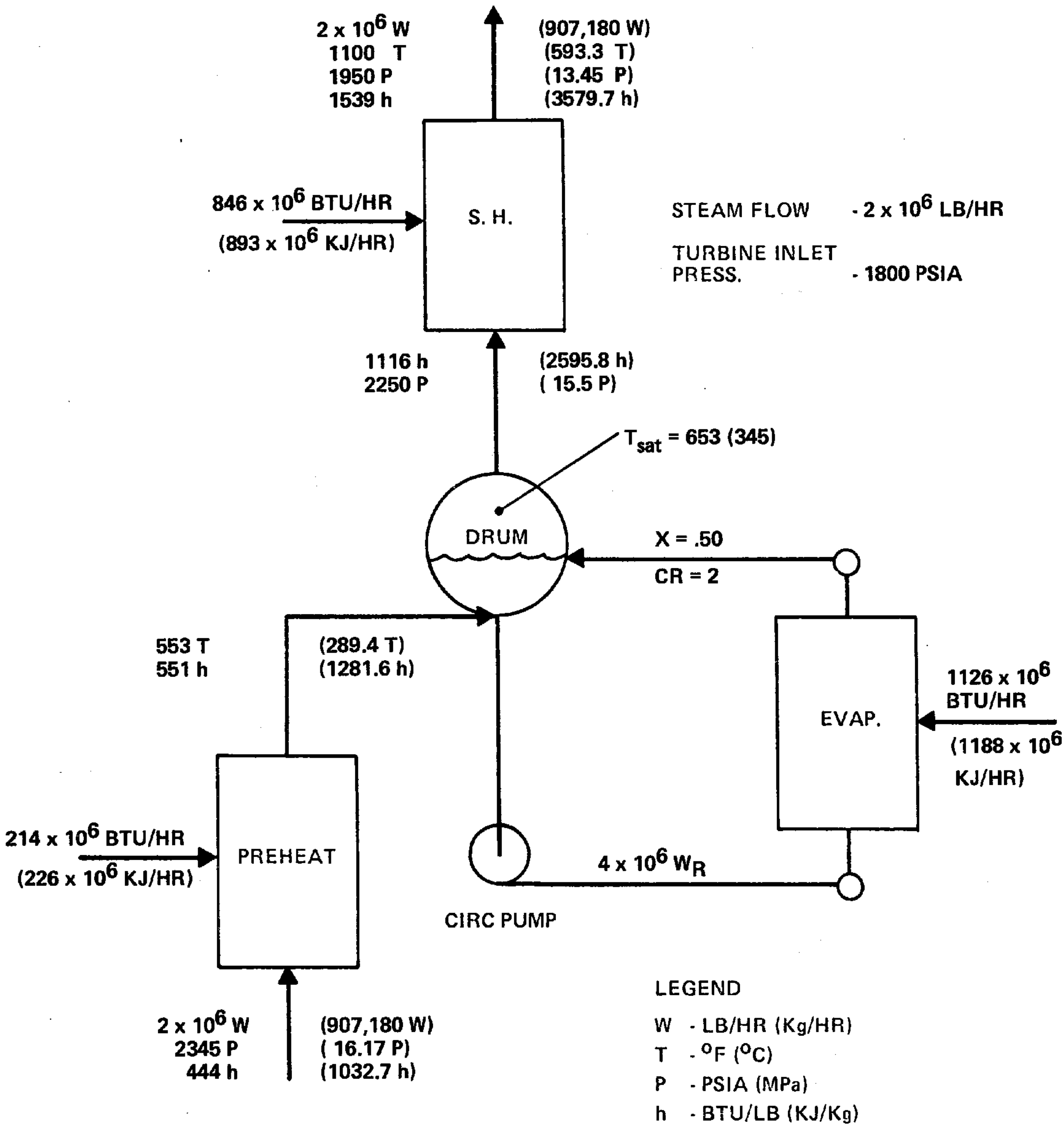

Figure 3.3
RECEIVER HEAT AND MASS BALANCE
CYCLE No. 3

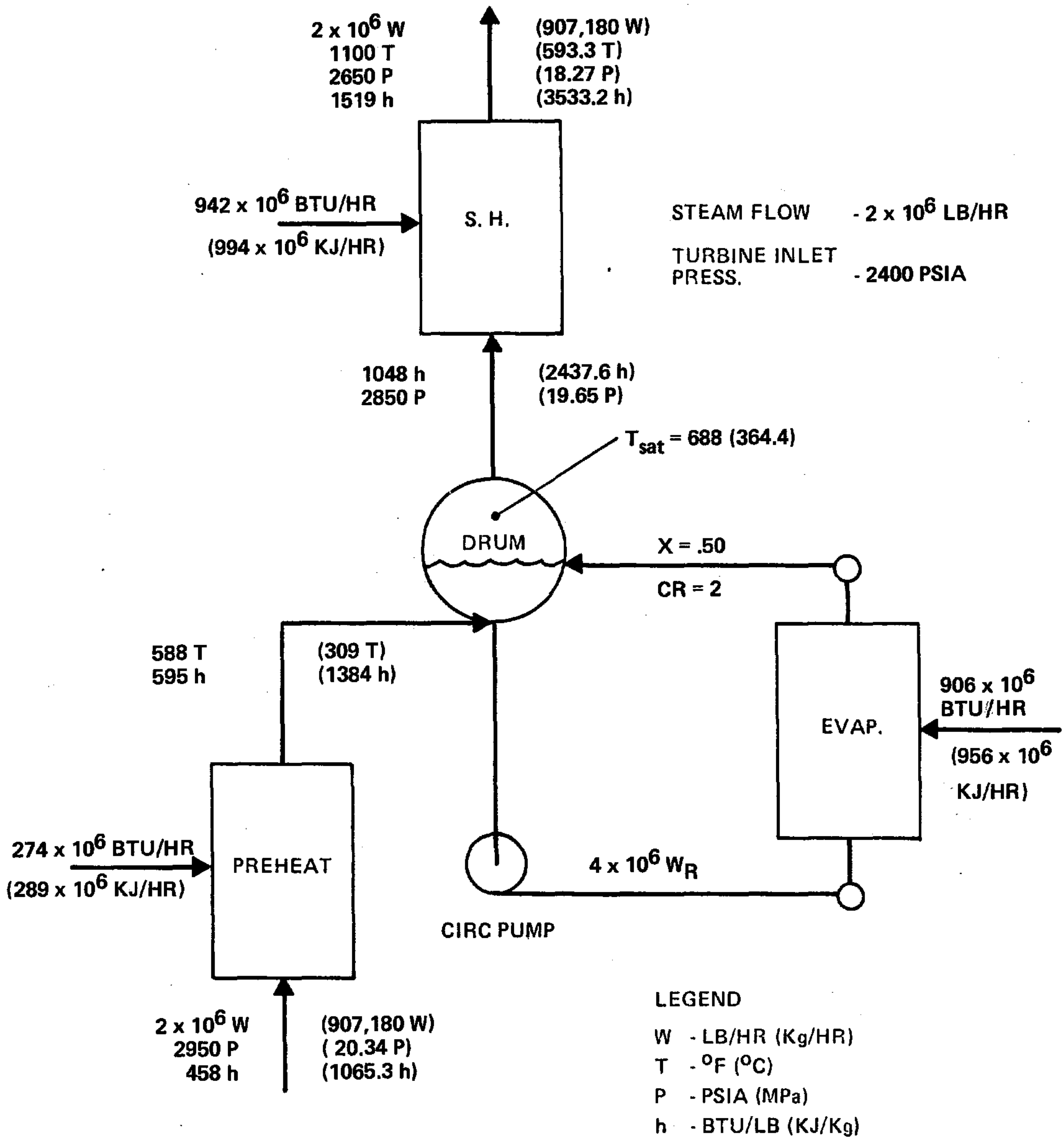

Figure 3.4

RECEIVER HEAT AND MASS BALANCE

CYCLE No. 4

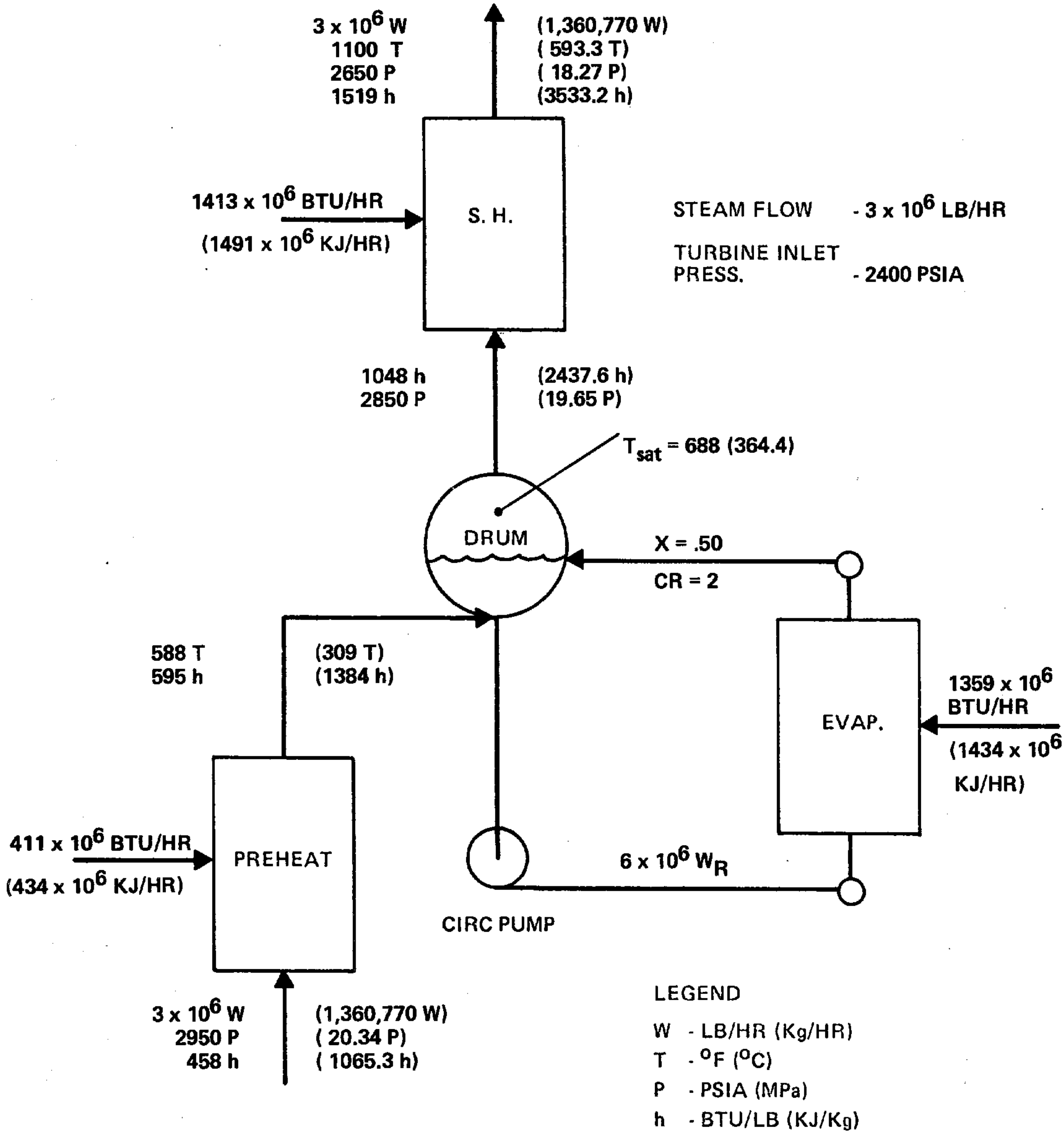

Figure 3.5
RADIAL FLUX PROFILE

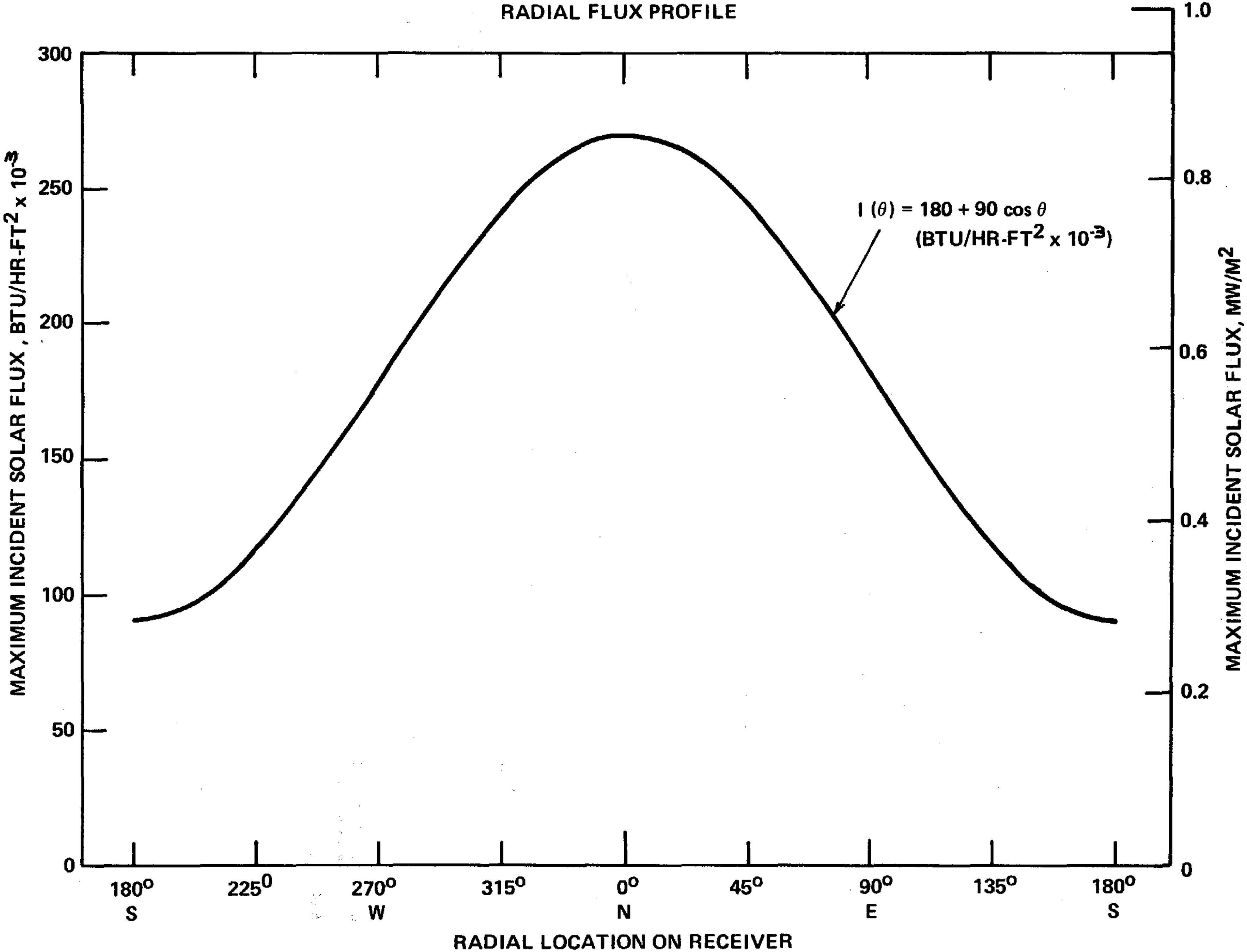

Several vertical flux profiles shown in Figure 3.6 were developed for parametric investigations. The baseline vertical flux profile, indicated as profile B, results from a 5-point aim strategy. The peak flux, I_{max}, corresponds to the radial flux values in Figure 3.5. The radial integrated average of I_{max} in Figure 3.5 is .57 MW/m^2 (190,000 BTU/hr-ft^2). The average of the vertical profiles in Figure 3.6 is .735 I_{max}, giving an overall receiver average incident flux of .42 MW/m^2 (140,000 BTU/hr-ft^2).

The vertical flux profiles A and C are alternate flux profiles used in the parametric study. These profiles were derived from the baseline profile B such that the averaged flux values of the profiles are equivalent. Due to uncertainty in heliostat field limitations, profiles A and C may not be reproducible by the heliostat field.

3.2.1.3 Aspect Ratio--The baseline receiver aspect ratio (L/D) for the design was chosen to be 1.5. This selection is based on indications that the heliostat field can provide optimum focusing on a receiver with an L/D of about 1.5.

Figure 3.7 shows pressure drop and mass velocity scaling parameters based on total steam flow for receivers with constant L/D. The approximate dimensions shown are for receivers with an aspect ratio of 1.5. Pressure drop through the tube panels varys proportionately to the square root of the total steam flow.

If a constant pressure drop were desired, the receiver aspect ratio would vary. Figure 3.8 shows relative variations in L/D required of the receivers. The receiver aspect ratio decreases linearly with increasing steam flow to maintain the same pressure drop in the different receivers.

3.2.1.4 Receiver Size--The heat loads indicated in Figures 3.1 through 3.4 divided by the average incident flux, after correcting for an assumed receiver efficiency, gives the total receiver surface area required. The overall

Figure 3.6
VERTICAL FLUX PROFILES

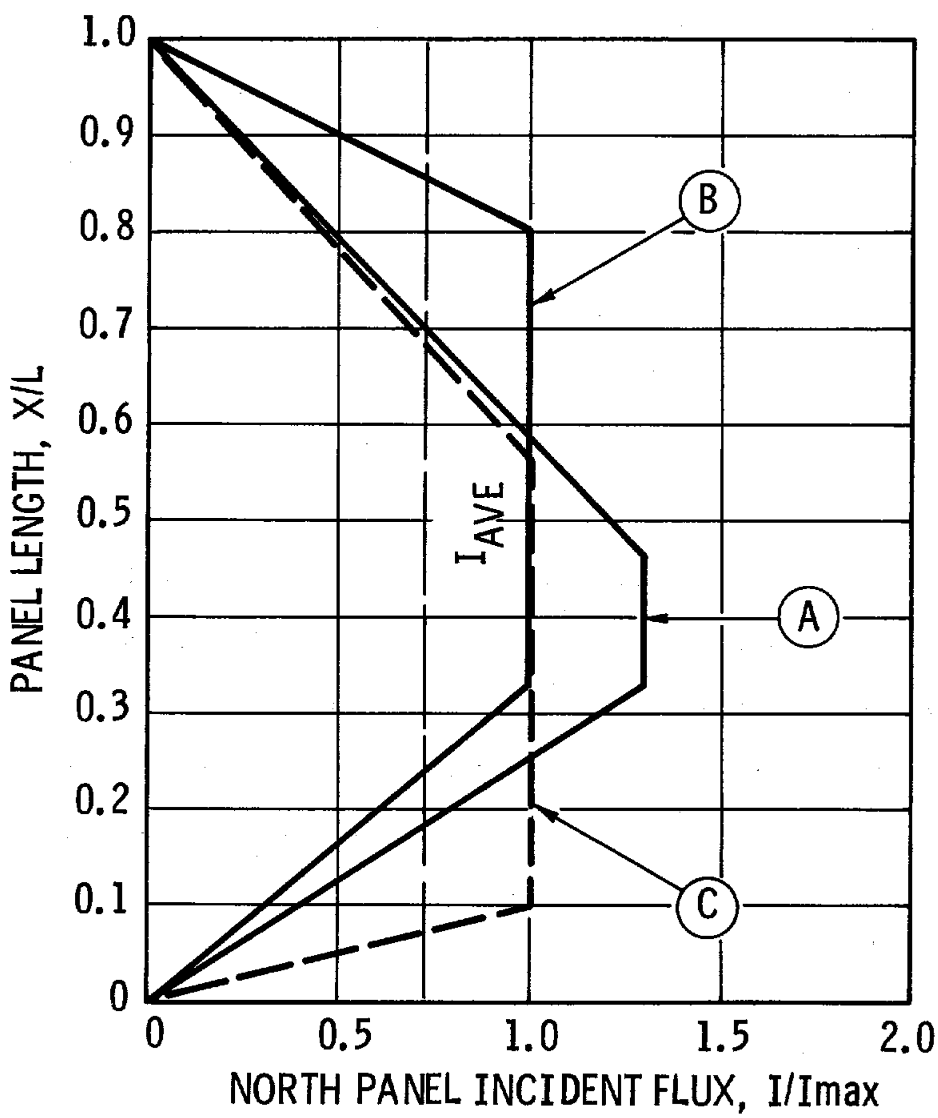

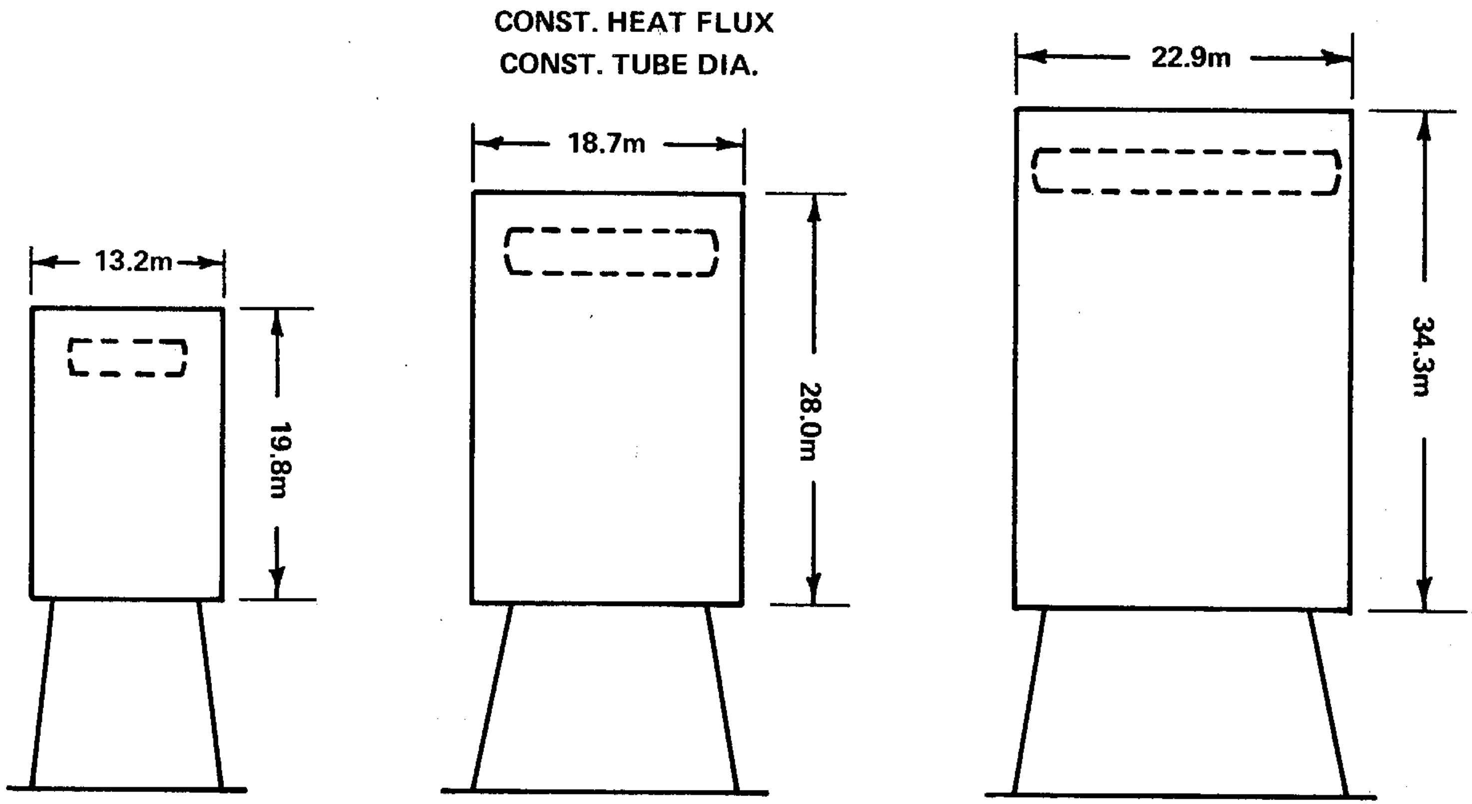

STEAM FLOW (Kg/hr)	$.45 \times 10^6$	$.9 \times 10^6$	1.4×10^6
MASS VELOCITY	1.0	$\sqrt{2}$	$\sqrt{3}$
ΔP FACTOR	1.0	$2 \sqrt{2}$	$3 \sqrt{3}$
SURFACE (M^2)	821	1,643	2,465

Figure 3.7
RECEIVER SCALING PARAMETERS FOR L/D = 1.5

CONST. HEAT FLUX
CONST. TUBE DIA.

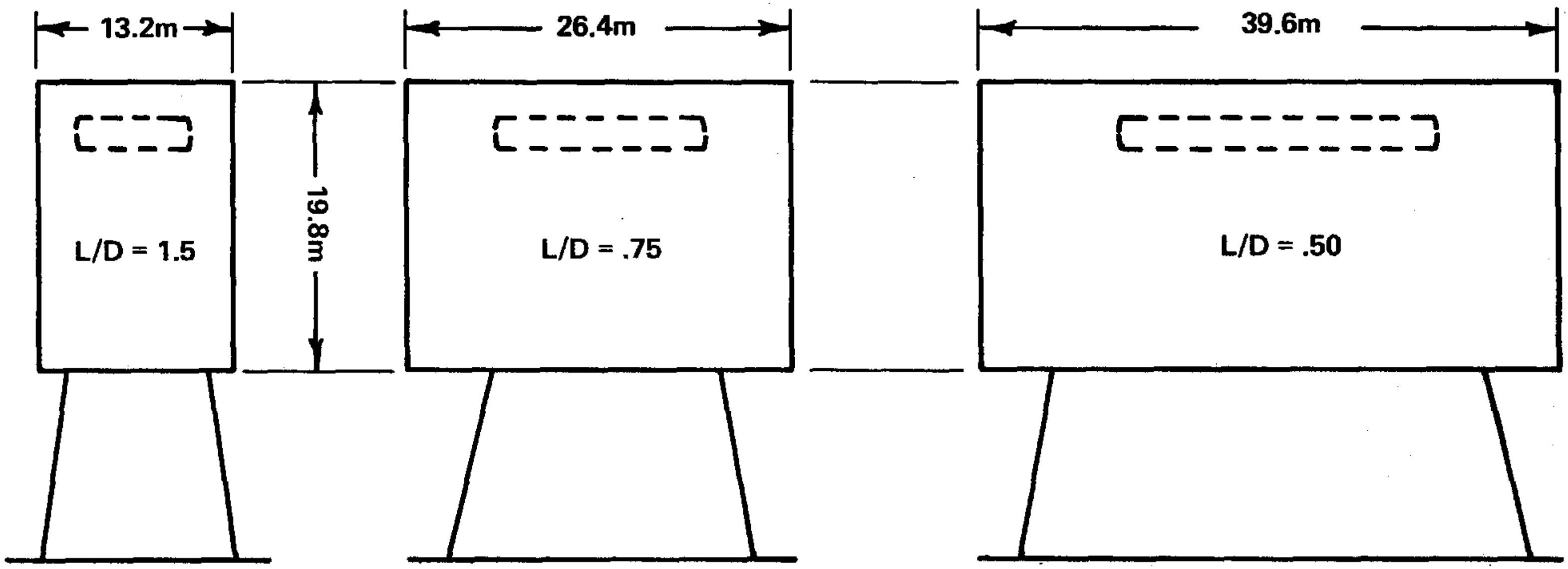

STEAM FLOW (Kg/hr)	$.45 \times 10^6$	$.9 \times 10^6$	1.4×10^6
MASS VELOCITY	1.0	1.0	1.0
ΔP FACTOR	1.0	1.0	1.0
SURFACE (M^2)	821	1,643	2,465

Figure 3.8
RECEIVER SCALING PARAMETERS FOR CONSTANT HEIGHT

receiver efficiency is assumed to be 90 percent for parametric design purposes. The total surface is proportioned so that each receiver component has the correct amount of heat absorption. Panel widths are based on a constraint that the maximum panel width not exceed 3.6 m (12 feet). This conforms to current manufacturing standards for shop assembled welded wall panels.

3.2.1.5 Tube Panel Locations--The recirculation evaporator is located on the north side of the receiver in the high incident flux region. The evaporator can maintain a high nucleate boiling film coefficient with rifled tubing, thereby minimizing tube metal temperatures in the high heat flux region. Test results of the rifled tubing test program (Task 10) are presented in Section 7.

The superheater was initially located adjacent to the evaporator in an intermediate flux region, and the preheater located on the south side of the receiver in the lowest flux region. Results of subsequent metal temperature and creep fatigue analysis required placement of the preheat panels in the intermediate flux region and the superheater on the south side in order to achieve reasonable cycle lifetime.

3.2.2 Receiver Materials Selection--Tube material selection is based on metal temperature ranges developed in the different tube panel sections. An allowable stress level of 70 MPa (10,000 psi) has been chosen as the criteria for sizing the tubes based on A.S.M.E. Pressure Vessel Code, Section 1. The maximum allowable midwall temperature for a given tube material is the temperature corresponding to the allowable stress level of 70 MPa (10,000 psi). Tube material selections for the different tube panel actions are presented in Table 3.2.

Table 3.2

RECEIVER TUBE PANEL MATERIAL SELECTIONS

Panel	ASME Spec. No.	Nominal Composition	Midwall Temperature @ 700MPa (10,000 psi)
Evaporator	SA-213 T11	1¼ Cr-½Mo-.75Si	516C (960F)
1st Stage Superheater	SA-213 T22	2¼ Cr-1Mo	518C (965F)
2nd Stage Superheater	SA-213 TP-316H	16Cr-1Ni-2Mo	618C (1145F)
Preheater	SA-192	0.12C	410C (770F)
Reheater	SA-213 TP-316H	16Cr-1Ni-2Mo	618C (1145F)

3.2.3 Receiver Thermal Performance

3.2.3.1 Recirculation Evaporator Study--The objective of this series of analyses is to determine the relationships between the major parameters involved in a recirculation evaporator, (in contrast to a once-through type). Pressure drop therefore is critical for the selection of circulation pumps and pumping power.

The size of pumps (capacity and head) and the power required, are influenced directly by the circulation ratio of the evaporator. This is defined as the ratio of mass flow in the evaporator circuits divided by the mass flow of steam desired as output. By this definition a once-through system would have a circulation ratio (CR) of 1. Bulk quality theoretically generated is the reciprocal of the circulation ratio. The circulation ratio is selected to avoid departure from nucleate boiling (DNB) in the evaporator panels.

In common boiler practice, a CR of 4:1 is used. Due to the high heat flux of this solar receiver application, this circulation ratio would be prohibitive from either the large pressure drop of small tubing, or the excessive metal temperatures of larger, thick walled tubing.

For this application, rifled tubing is being considered for the high heat flux environment of the evaporator section. In some lower heat flux environments, rifled tubing has been shown capable of eliminating the DNB critical quality throughout the entire quality region to saturated steam. Data was not available, however, for the high heat flux of this application and a test program(Task 10) was conducted to develop the required data. Rifled tubing test results are presented in Section 7. It was initially estimated, by linear extrapolation of existing data, that a CR of 2:1 might be sufficient for this application using properly sized rifled tubing.

Figure 3.9 shows the effect of varying tube size on the mass velocity and panel exit quality. The STPP code was run with constant heat flux and a constant absorption. The baseline vertical flux profile B was used. For a given tube size, the mass velocity shown is that required to obtain a desired bulk quality at the panel outlet. The influence of tube size is quite large. As tube size is increased, a point is reached where wall thickness is too large to maintain the tube crown metal temperature within limits for the selected material. The 3.91 cm (1.5 in.) OD tube size produced excessive metal temperatures at mass velocities below approximately 2.44×10^3 Kg/m^2-S (1.8×10^6 lb/hr-ft^2). All tube sizes are quoted on the OD but each curve shown implies an ID based on the ASME Pressure Vessel Code, Section I formula for boiler tubing.

Figure 3.10 shows the variation of pump power and mass velocity with tube size at various outlet qualities. This plot is based on the same runs made for Figure 3.9 above. Pump power rises significantly at tube sizes less than 2.54 cm (1 in. OD). Not much improvement results in tube sizes greater than 3.81 cm (1.5 in.) OD. This limits the tube size selection to between 2.54 cm (1 in.) and 3.81 cm. (1.5 in.) OD.

Figure 3.11 is another plot of the data showing the maximum tube crown temperature as a function of tube size and outlet quality. This graph shows 2.81 cm. (1.5 in.) OD to be an upper limit from the temperature aspect. The above runs were made with the assumption that nucleate boiling prevailed in all cases.

Figure 3.12 shows the effect of varying the heat flux in the evaporator with a constant tube size. Again mass velocity is plotted against outlet quality with q/A as the parameter. In these runs, the STPP code was run with the C-E correlation for DNB. All data points to the right of the dashed line

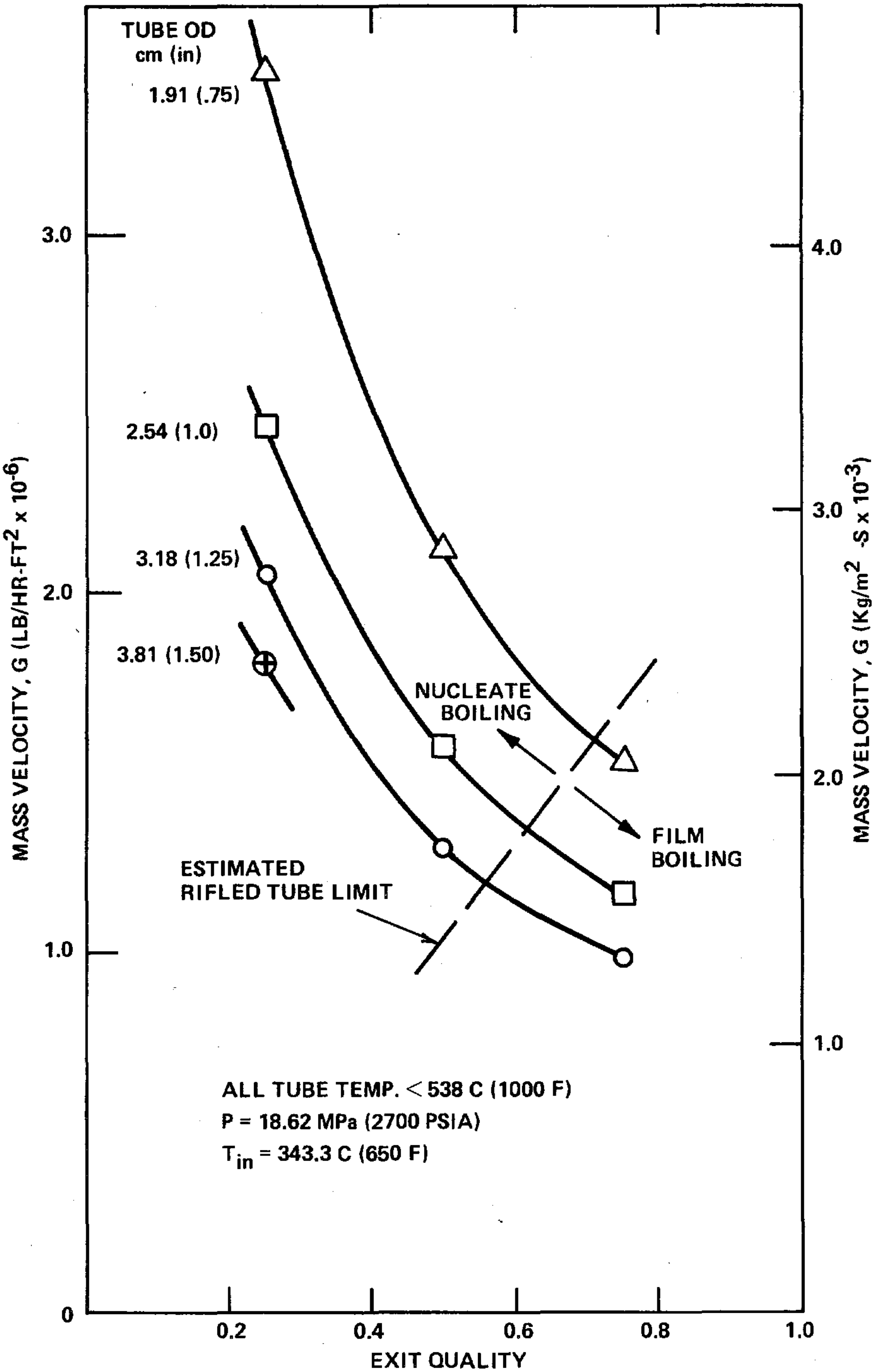

Figure 3.9
EFFECT OF TUBE SIZE ON FLOW AND QUALITY FOR CONST. HEAT ABS. AND HEAT FLUX

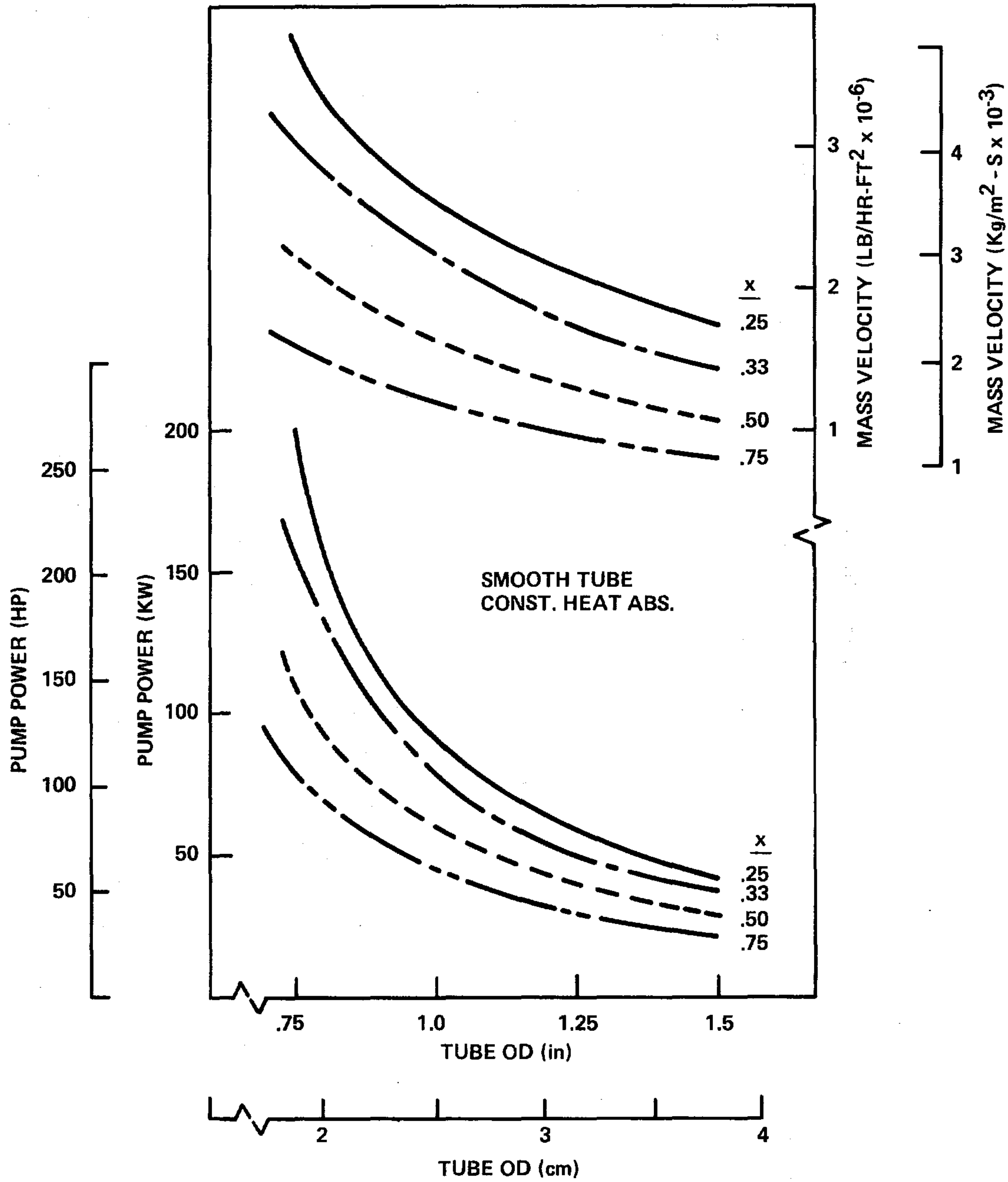

Figure 3.10
RECIRCULATION EVAPORATOR FLOW AND PUMP POWER
vs QUALITY AND TUBE SIZE

Figure 3.11

RECIRCULATION EVAPORATOR TUBE METAL TEMP. vs TUBE SIZE

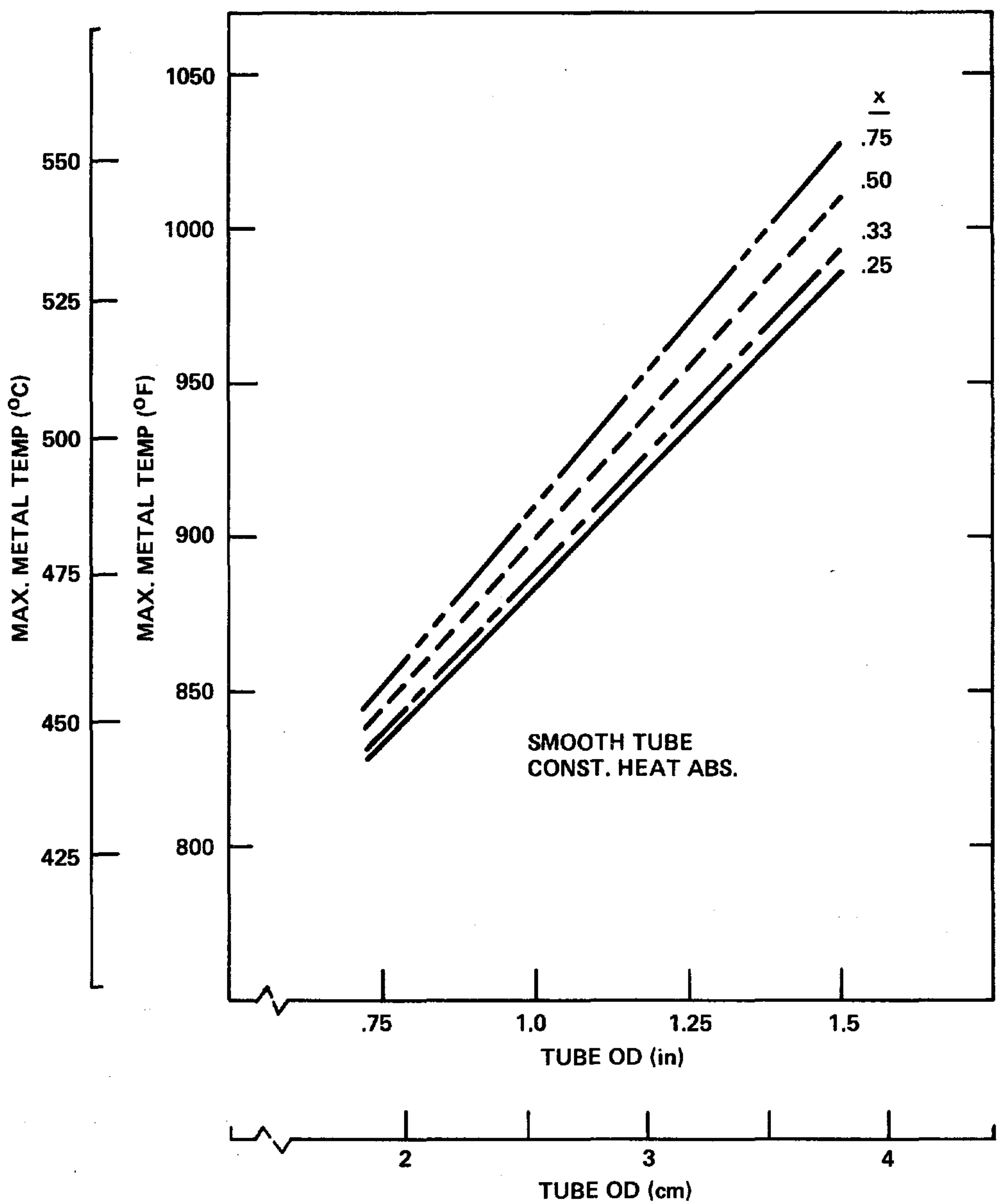

Figure 3.12
EFFECT OF HEAT FLUX ON CRITICAL QUALITY

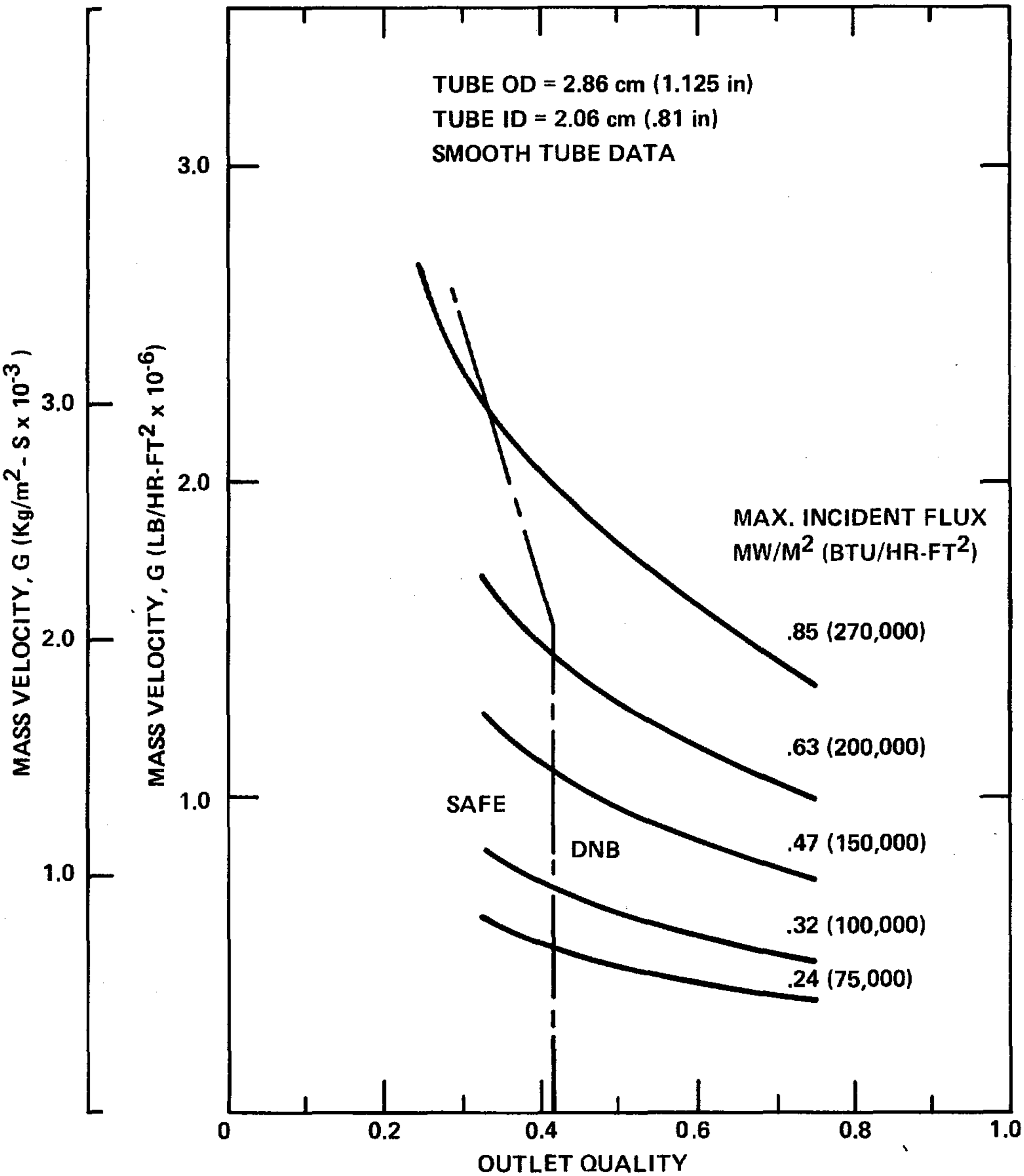

represent runs that exhibited DNB at some quality point in the panel. The runs to the left of the dashed line showed no DNB. These are smooth tube data. It is obvious that the high flux in the smooth tube would require a very large circulation ratio in order to allow sufficient margin for preventing DNB. This curve demonstrates the need for rifled tubing, where it is anticipated that a quality of at least 50% will be obtained without DNB at the 0.85 MW/M^2 (270,000 $BTU/hr\text{-}ft^2$) incident flux.

Figure 3.13 shows the tube crown temperature for an evaporator panel with 0.85 MW/M^2 incident flux, assuming a rifled tube and 50% outlet quality. Table 3.3 lists panel thermal efficiency for various flux levels and circulation ratios. Subsequent results of Task 10 testings confirmed the selection of a 2:1 circulation ratio.

3.2.3.2 Superheater Study

3.2.3.2.1 Tube Crown Temperature--A range of heat flux values was applied to superheater panels, employing various tubing sizes. The assumed baseline parametric configuration for the superheater is a two-stage unit with parallel flow panels within each stage. The baseline vertical flux profile B is assumed. The resultant metal temperatures are plotted in Figures 3.14 and 3.15 for the first and second stage superheaters, respectively.

The second stage superheater tubes are TP-316 stainless steel. An absolute metal temperature limit of 1200^{o}F is superimposed on Figure 3.16. This selected limit is less than a 1300^{o}F limit for 316 stainless based on corrosion and metalurgical considerations. The selected limit of 1200^{o}F is intended for bracketing design parameters.

Lowering the tube size decreases the maximum tube crown temperature because of a reduction in tube wall thickness and an increase in the inside film coefficient. The results indicate that a tube size of 1.91 cm. (.75 in) OD or less is required in the finishing superheater stage at flux levels up to .50 MW/m^2 (160,000 $BTU/hr\text{-}ft^2$). Even at the lowest flux level of

Figure 3.13
EVAPORATOR TEMPERATURE PROFILE

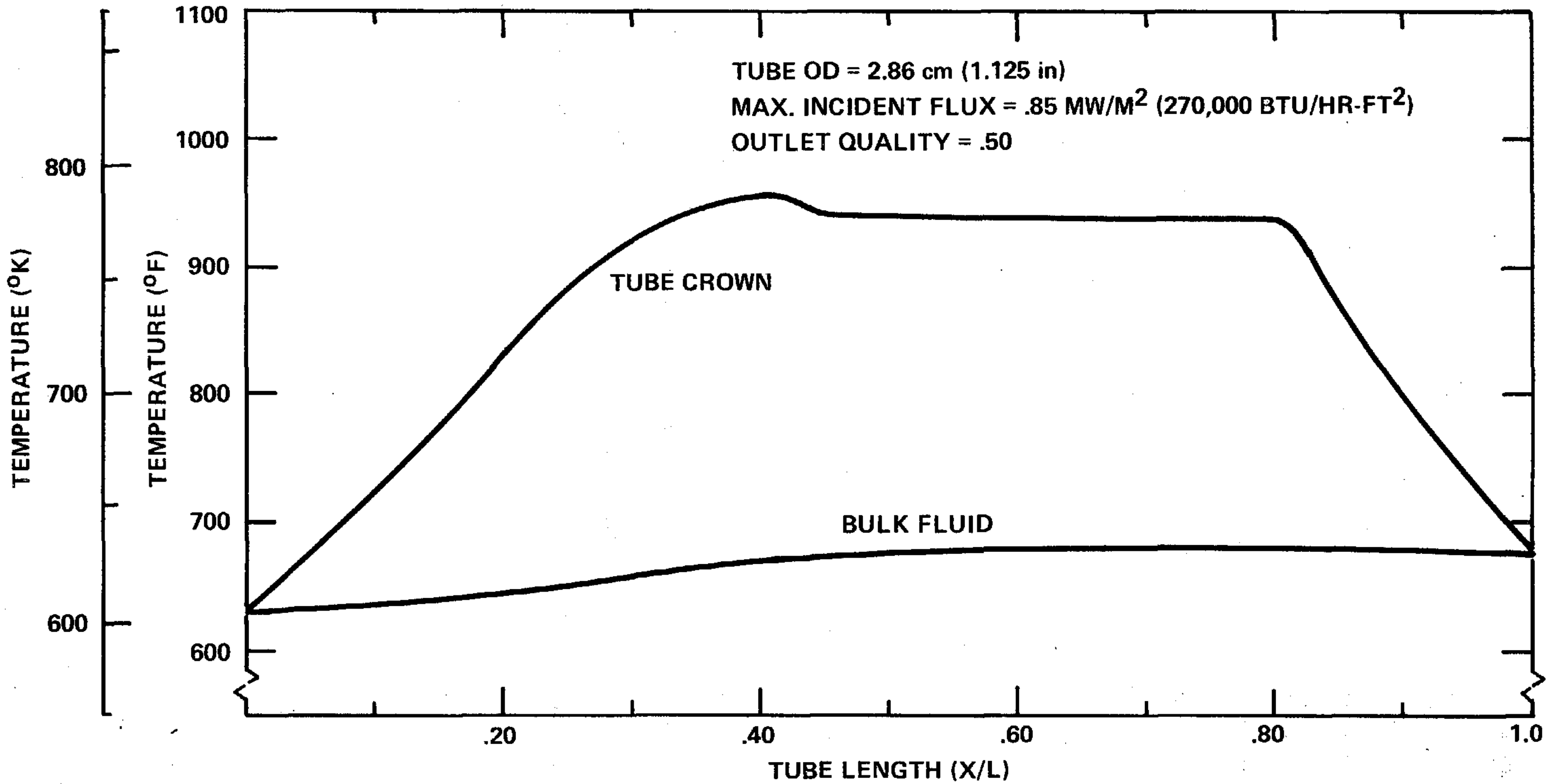

TABLE 3.3

EVAPORATOR THERMAL EFFICIENCIES

Outlet Quality	Incident Flux, MW/m^2 (BTU/hr-ft^2) .85 (269,500)	.63 (200,000)	.47 (150,000)	.32 (100,000)	.24 (75,000)
33%	.91	.93	.92	.90	.88
50%	.95	.92	.91	.90	.89
75%	.92	.92	.91	.89	.88

Figure 3.14

FIRST STAGE SUPERHEATER MAX. TUBE CROWN TEMP. vs HEAT FLUX

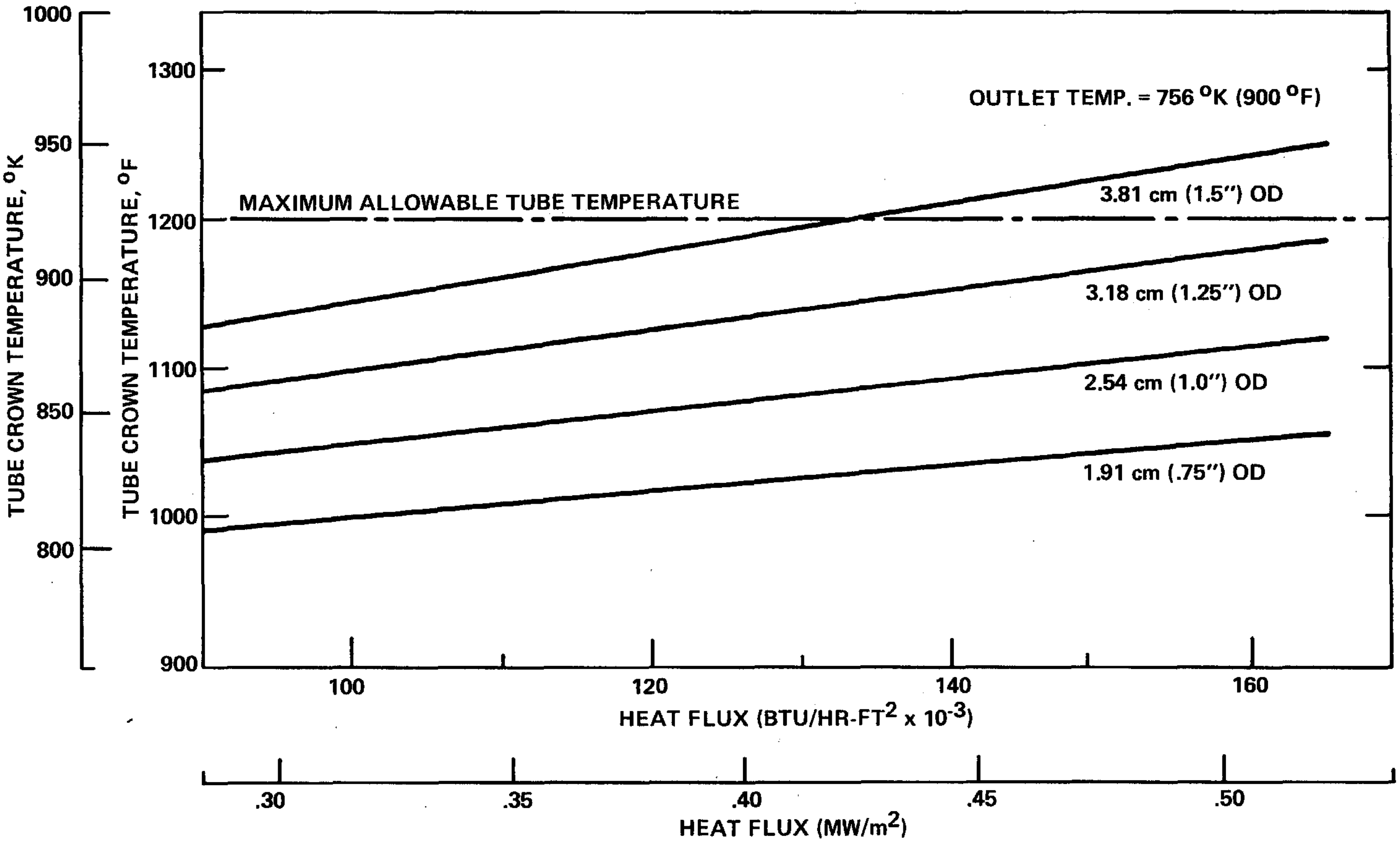

Figure 3.15
SECOND STAGE SUPERHEATER MAX. TUBE CROWN TEMP. vs HEAT FLUX

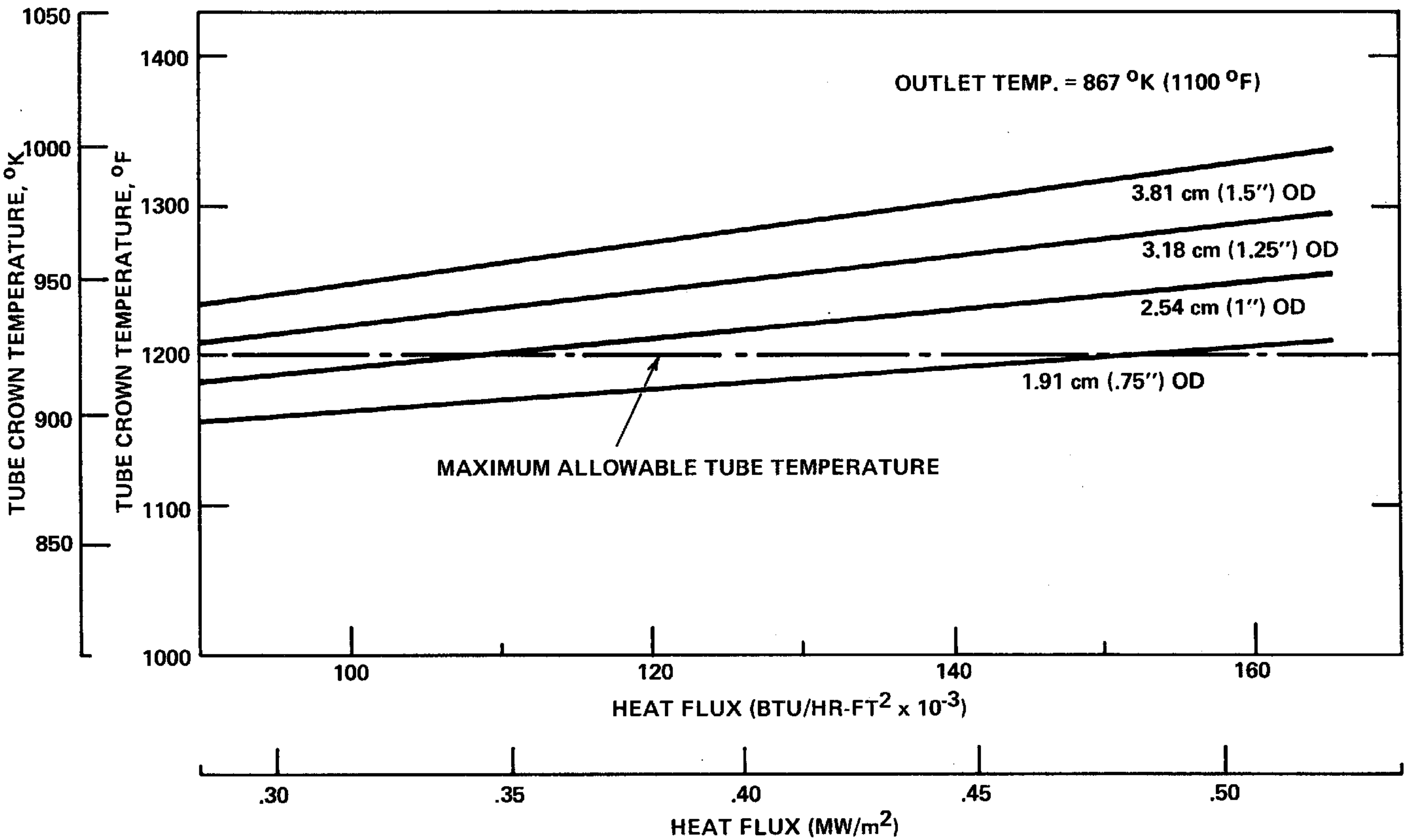

Figure 3.16

FIRST STAGE SUPERHEATER TEMPERATURE PROFILE
(HIGH FLUX ZONE)

NOTE: NOT FINAL DESIGN SEE SECTION 5.

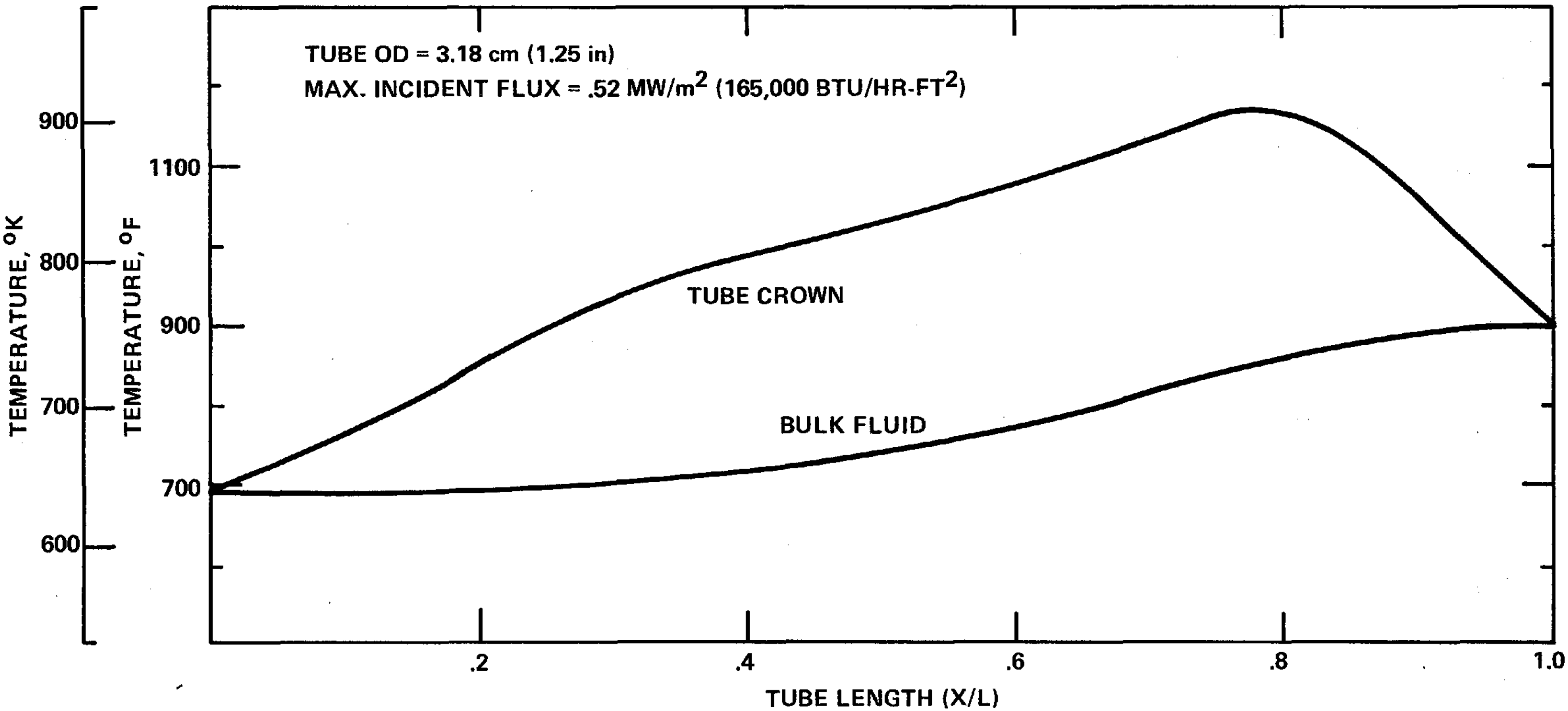

.28 MW/m^2 (90,000 $BTU/hr\text{-}ft^2$) on the south side of the receiver, tube crown temperature will reach nearly 626°C (1160°F) using 1.91 cm. (.75 in.) OD tubes.

Figures 3.16 and 3.17 show typical tube crown and bulk fluid temperature profiles in the first and second superheater stages respectively, with baseline vertical flux profile B. The important characteristic of these curves is the relationship between the tube crown temperature and changes in incident flux. Near the tube entrance, crown temperature increases rapidly with increasing incident flux level. In the middle of the tube length, the crown temperature rises more slowly because the incident flux level reaches a constant value. Tube crown temperature drops off rapidly near the tube exit as incident flux decreases.

The point of maximum tube crown temperature is reached where incident flux starts to decrease from I_{max} in the constant flux region. This observation implies that if the transition to decreasing flux were shifted away from the tube exit, maximum tube crown temperatures might be reduced. Vertical flux profiles A and C were developed to investigate the anticipated temperature reductions.

Figure 3.18 compares the second stage superheater tube crown temperatures of the vertical flux profiles A, B, and C. The results indicate the profile C is the best vertical distribution, showing a reduction in crown temperature of almost 28°C (50°F) compared to the baseline profile B. Profile A shows no reduction in crown temperature mainly because the maximum flux in this distribution is higher than in profiles B and C. An optimum vertical flux profile is concluded to be one which exhibits a flux distribution biased towards the tube entrance, where bulk steam temperatures in the tube are lowest.

The bulk fluid/tube crown temperature differential creates axial stresses in the tube which affect the tube fatigue life. Figures 3.19 and 3.20 show the effect of tube size and flux level on the tube temperature differential in first and second stage superheater panels.

Figure 3.17

SECOND STAGE SUPERHEATER TEMPERATURE PROFILE

(HIGH FLUX ZONE)

NOTE: NOT FINAL DESIGN. SEE SECTION 5.

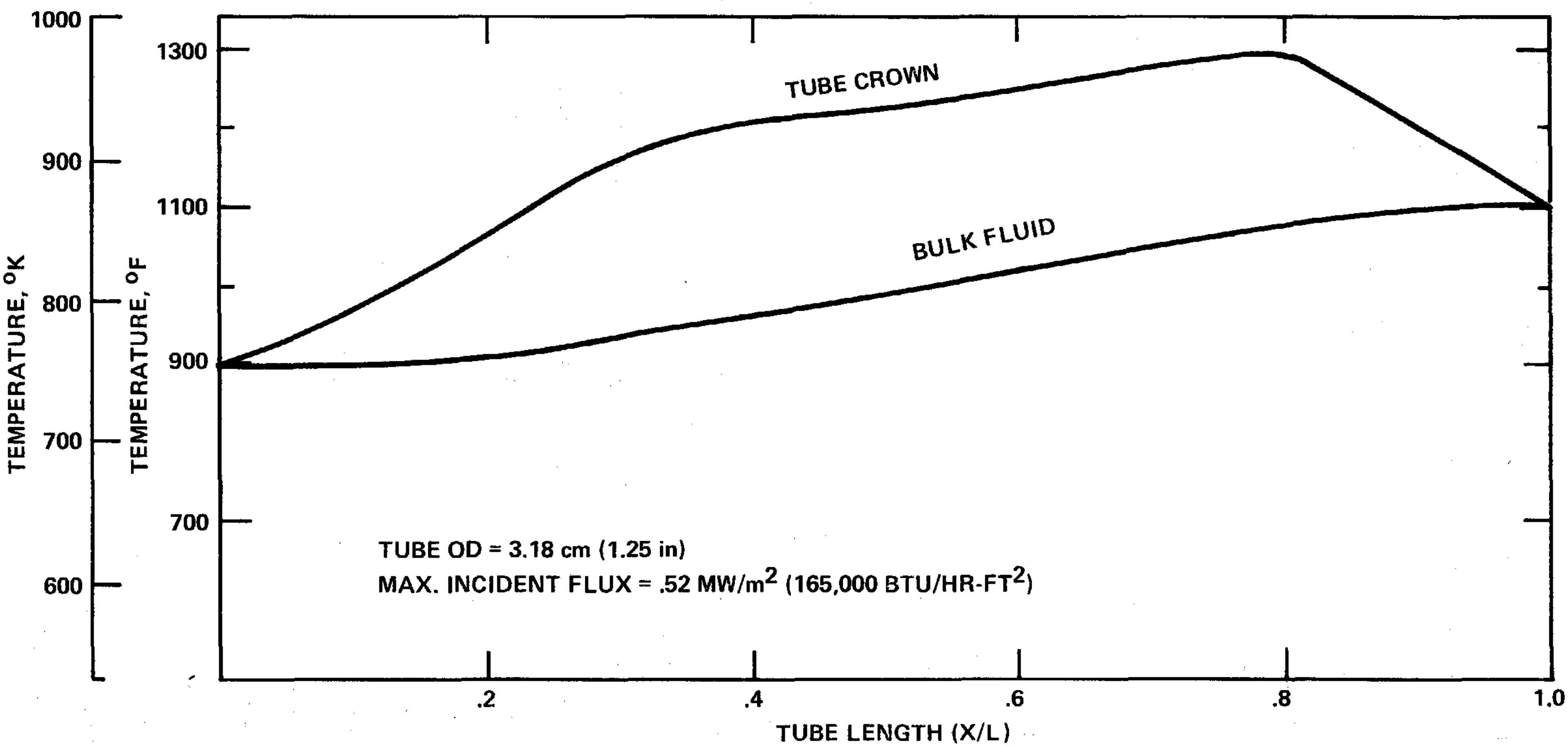

Figure 3.18
COMPARISON OF TEMPERATURE PROFILES IN SECOND STAGE SUPERHEATER
(HIGH FLUX ZONE)

NOTE: NOT FINAL DESIGN. SEE SECTION 5.

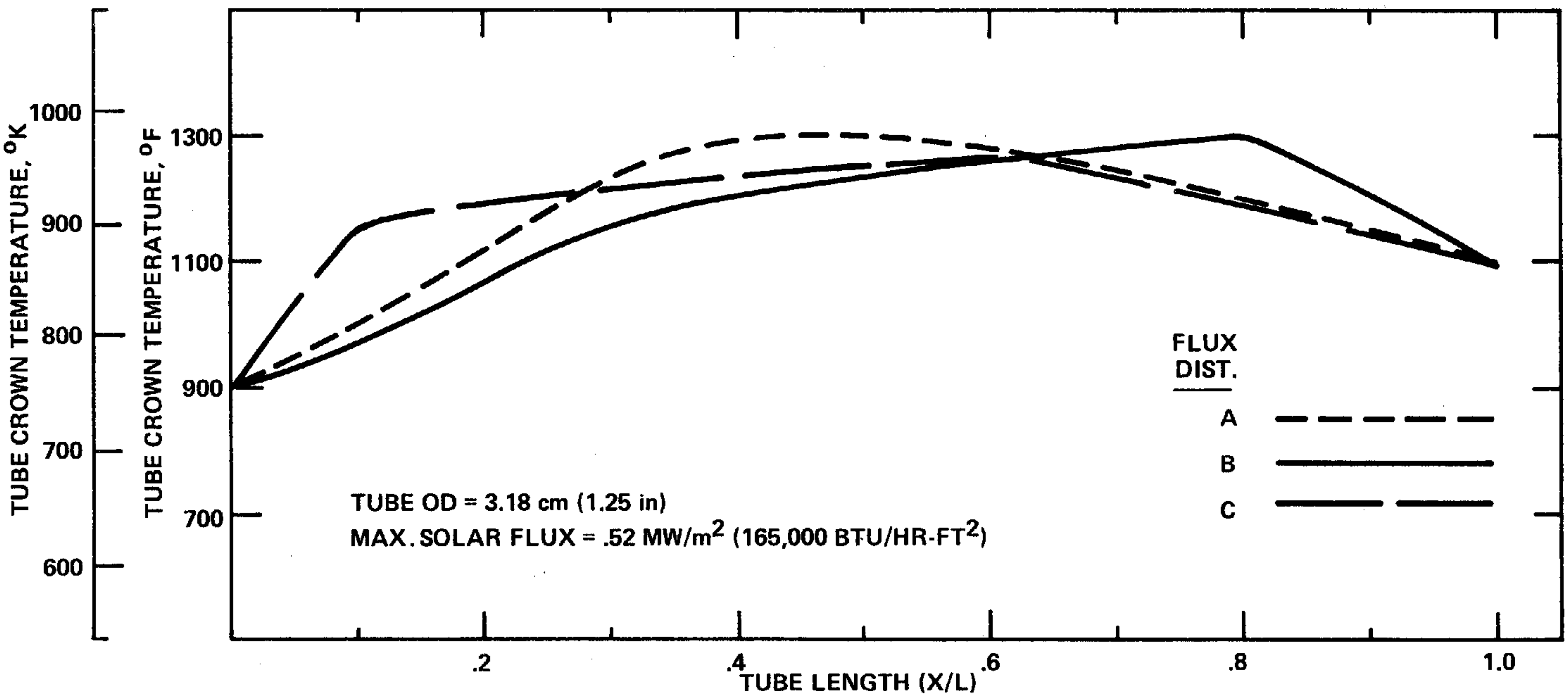

Figure 3.19

FIRST STAGE SUPERHEATER MAXIMUM TUBE TEMPERATURE DIFFERENCE

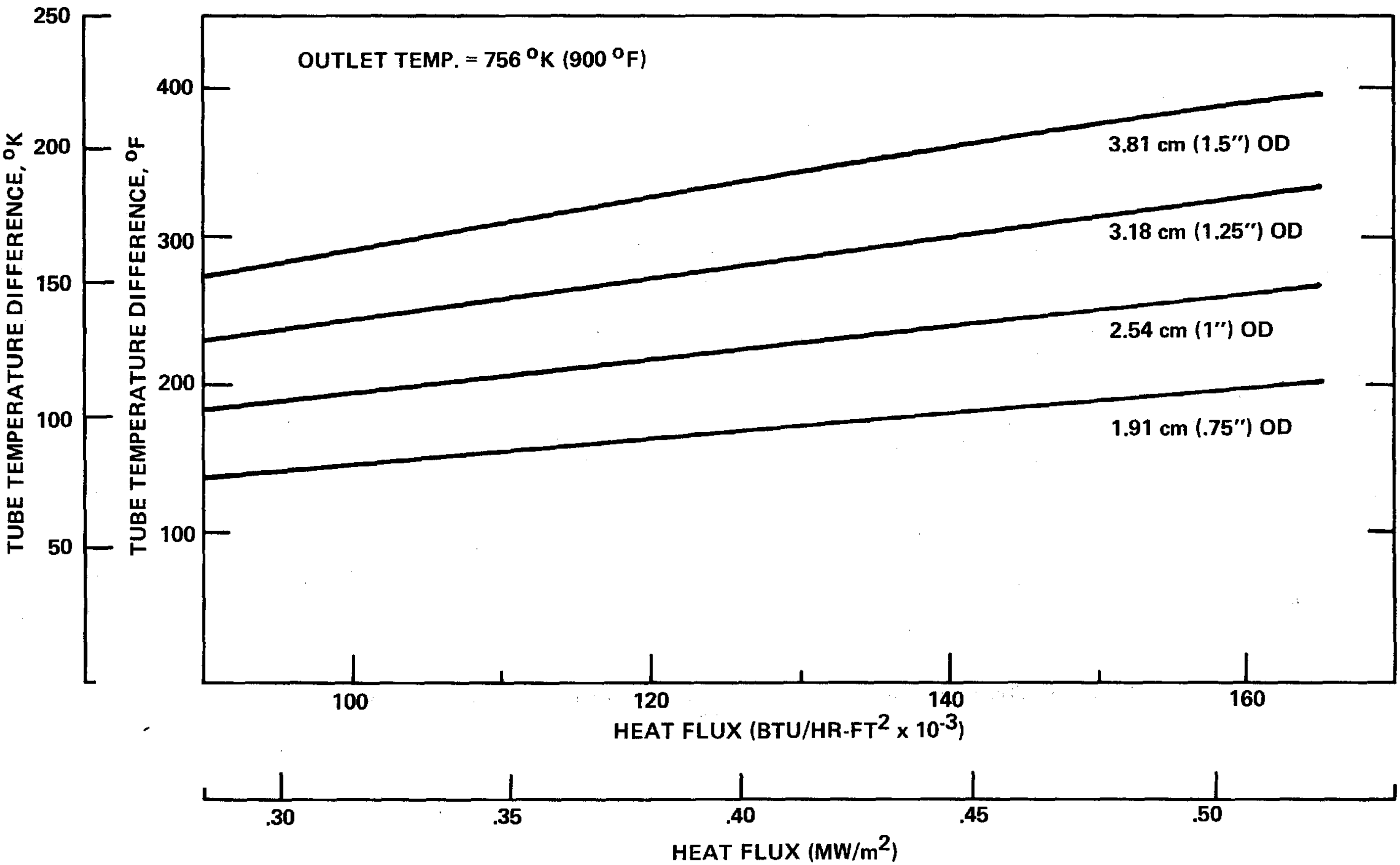

Figure 3.20

SECOND STAGE SUPERHEATER MAXIMUM TUBE TEMPERATURE DIFFERENCE

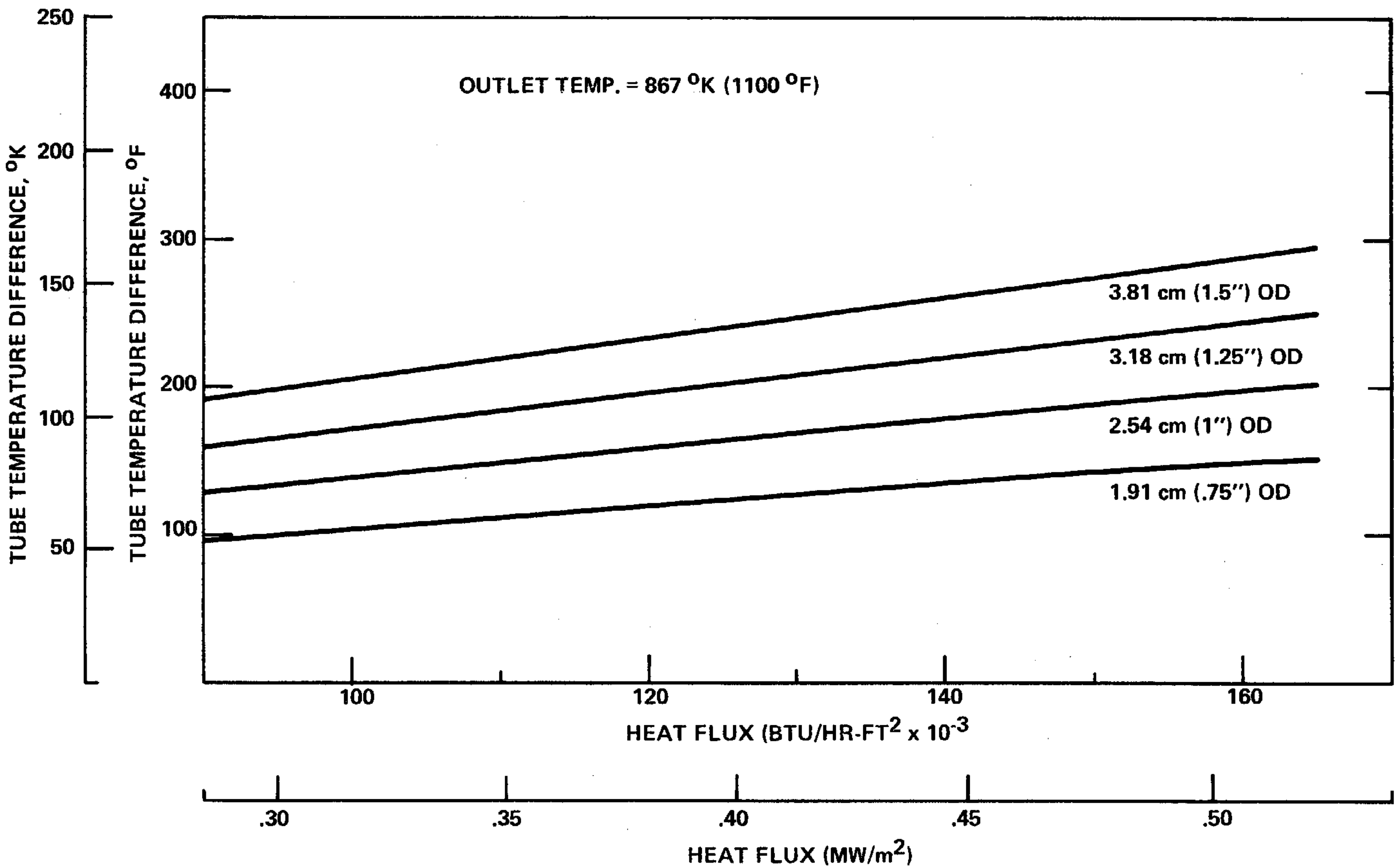

Thermal efficiency in superheater tubes is dependent on the tube crown temperature profile, which is itself a function of tube size and incident flux. Table 3.4 shows the variations in absorption efficiency as a function of both tube size and incident flux. Superheater panel efficiencies can vary between approximately 80 and 90 percent.

3.2.3.2.2 Pressure Drop--There is a trade off between minimizing tube crown temperature and minimizing pressure drop in the superheater. Lowering the tube size decreases tube crown temperature. However, pressure drop increases due to an increased mass velocity. The momentum and elevation components of pressure drop are insignificant in superheater panels. Figures 3.21 and 3.22 show the effect of tube size and mass velocity on the smooth tube frictional pressure drop in first and second stage superheater panels.

A total pressure drop of 3.10 MPa (450 psia) is available between the steam drum and the turbine throttle based on the heat and mass balances developed in Figures 3.1 through 3.4. The tube size and superheater staging arrangement must be selected so that the overall pressure drop is within the above limit.

3.2.3.2.3 Staging Configuration--Superheater staging configurations were explored to determine an optimum design. Based on the tube crown temperature data shown in Figure 3.15, a tube size of 1.91 cm (.75 in) OD or less is required for the finishing superheat stage. This tube size range would apply even if the finishing superheater were located in the lower flux region on the south side of the receiver.

The small tubes however greatly increase pressure drop as seen in Figures 3.21 and 3.22. In order to minimize the pressure drop while using small tubes, the mass velocity must be minimized. This can be done by providing parallel flow staging in the superheater.

TABLE 3.4

SUPERHEATER THEMERAL EFFICIENCIES

Tube Size cm (inches)	Stage	Incident Flux MW/m^2 ($BTU/hr\text{-}ft^2$) .52 (165,000)	.44 (140,000)	.38 (120,000)	.28 (90,000)
1.91 (.75)	First	.90	.89	.88	.86
	Second	.86	.86	.85	.83
2.54 (1.00)	First	.89	.88	.87	.85
	Second	.86	.87	.86	.82
3.12 (1.25)	First	.88	.87	.87	.84
	Second	.86	.86	.85	.81
3.81 (1.50)	First	.88	.87	.86	.84
	Second	.86	.86	.85	.81

Figure 3.21
FIRST STAGE SUPERHEATER PRESSURE DROP

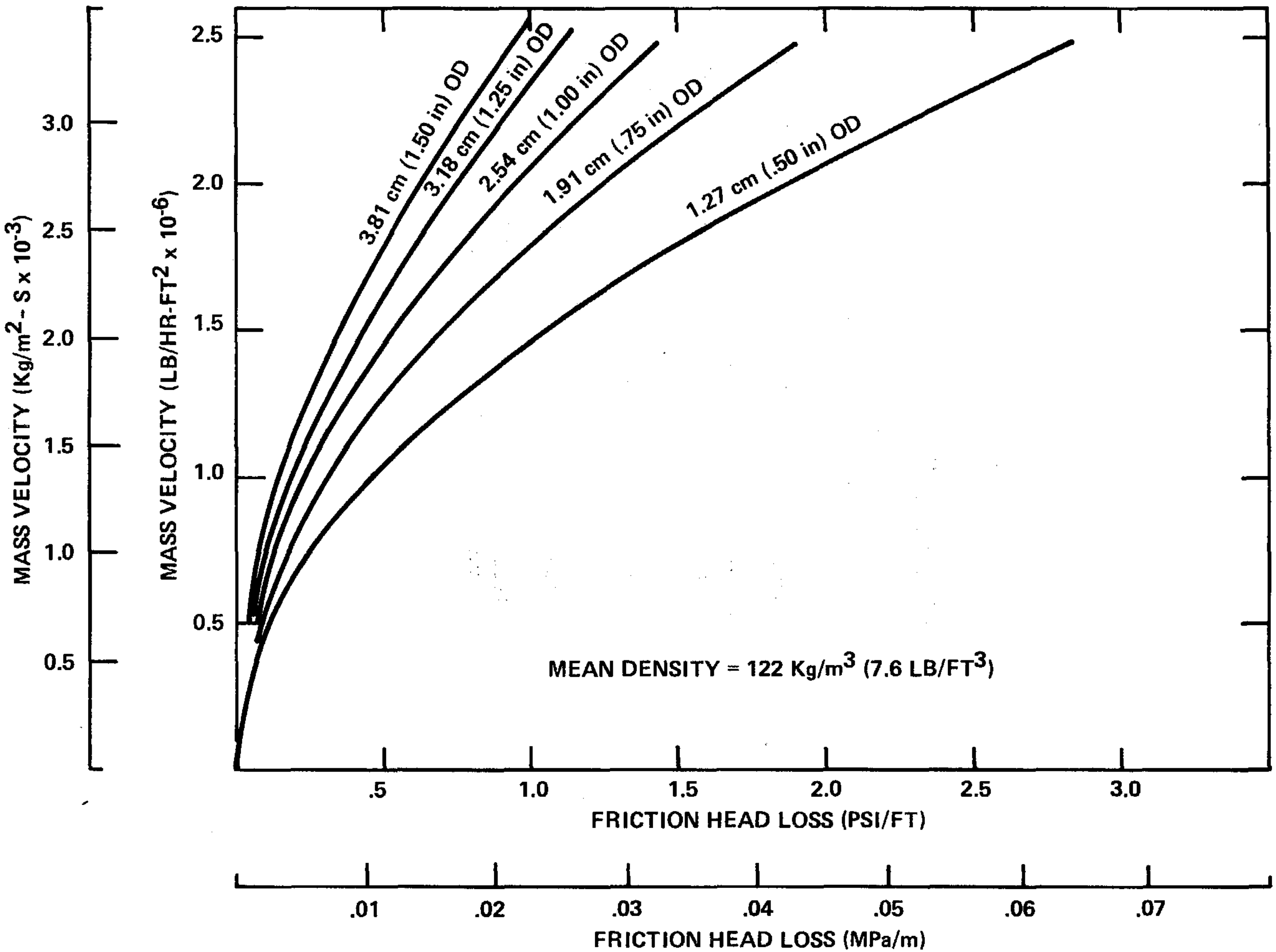

Figure 3.22
SECOND STAGE SUPERHEATER PRESSURE DROP

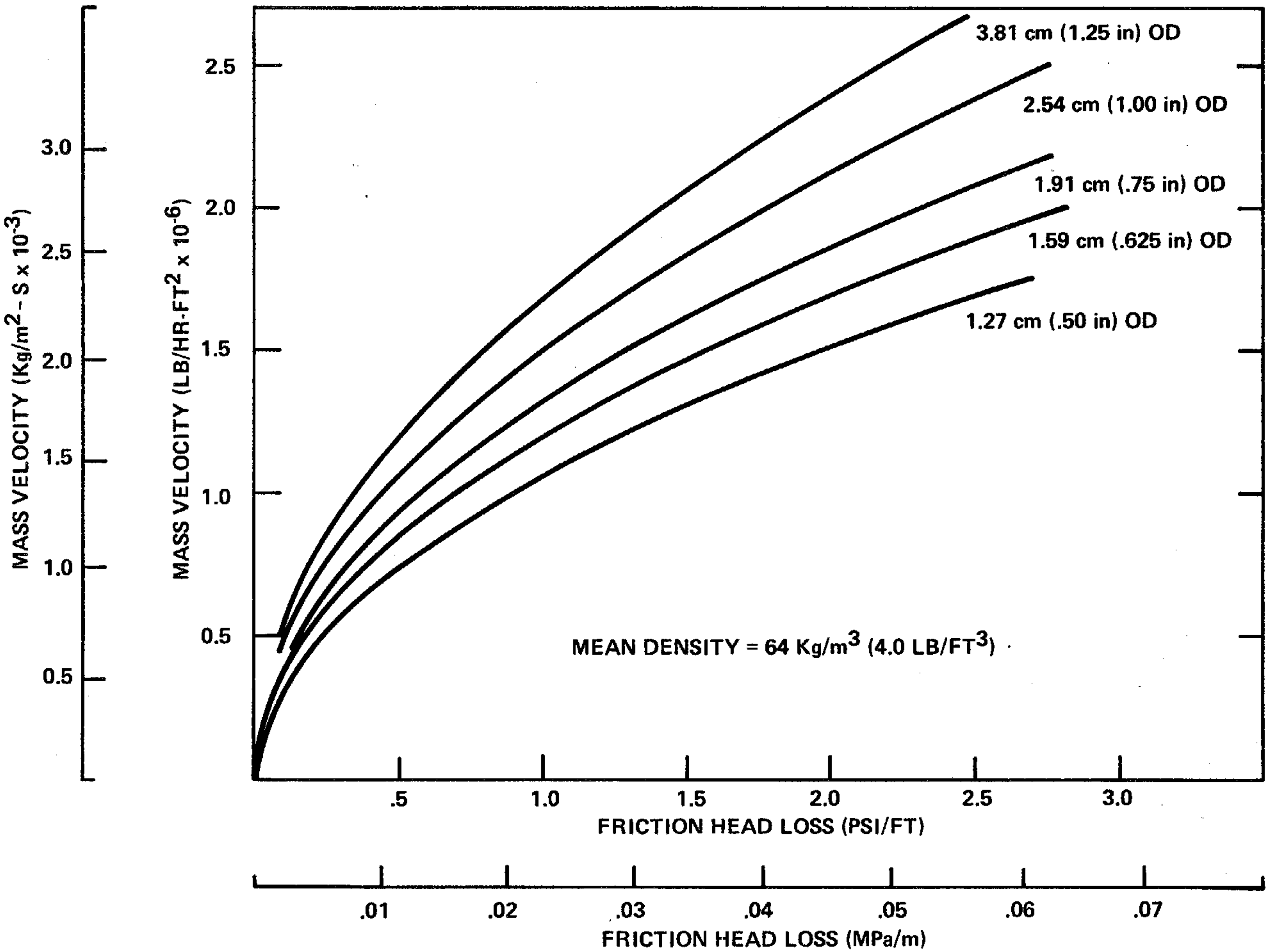

Figure 3.23 presents what is considered an optimal superheater staging arrangement using small tubes ($\geq$ 1.91 cm. or .75 in.) in the finishing stage. The superheater consists of 2 stages. For illustration the superheater is comprised of a total of 6 equal width panels. The second stage consists of the small tube/parallel flow configuration in order to minimize both pressure drop and tube crown temperature.

The first stage consists of a single panel with larger tubes. This is a conservative design which minimizes the effects of any deposits due to carryover during abnormal operation. Superheated steam entering the small tubes of the second stage is thereby ensured to be free of any carryover deposits.

3.2.3.2.4 Superheater Location--The most desirable location for the superheater is in the lower flux region of the south side of the receiver. Figures 3.24 and 3.25 show a 1.4 x 10^6 Kg/hr (3x10^6 lb/hr) receiver layout with the superheater located next to the evaporator, and with the superheater located on the south side, respectively.

With the superheater located on the south side, the maximum incident flux on the second stage is about.46 MW/m^2 (145,000 BTU/hr-ft^2). Based on results in Figure 3.15, small tubes ($\leq$ 1.91 cm. or .75 in.) limit the maximum tube crown temperatures to less than 1200^{o}F.

3.2.3.2.5 Lateral Flux Gradients--The effect of lateral flux gradients is most severe in the finishing superheater stage due to high metal temperatures. A study was done to determine the effect of such gradients in a second stage superheater panel of the 1.4 x 10^6 Kg/hr (3x10^6 lb/hr) receiver with a tube size of 1.59 cm (.625 in.).

Figure 3.23
PROPOSED SUPERHEATER STAGING

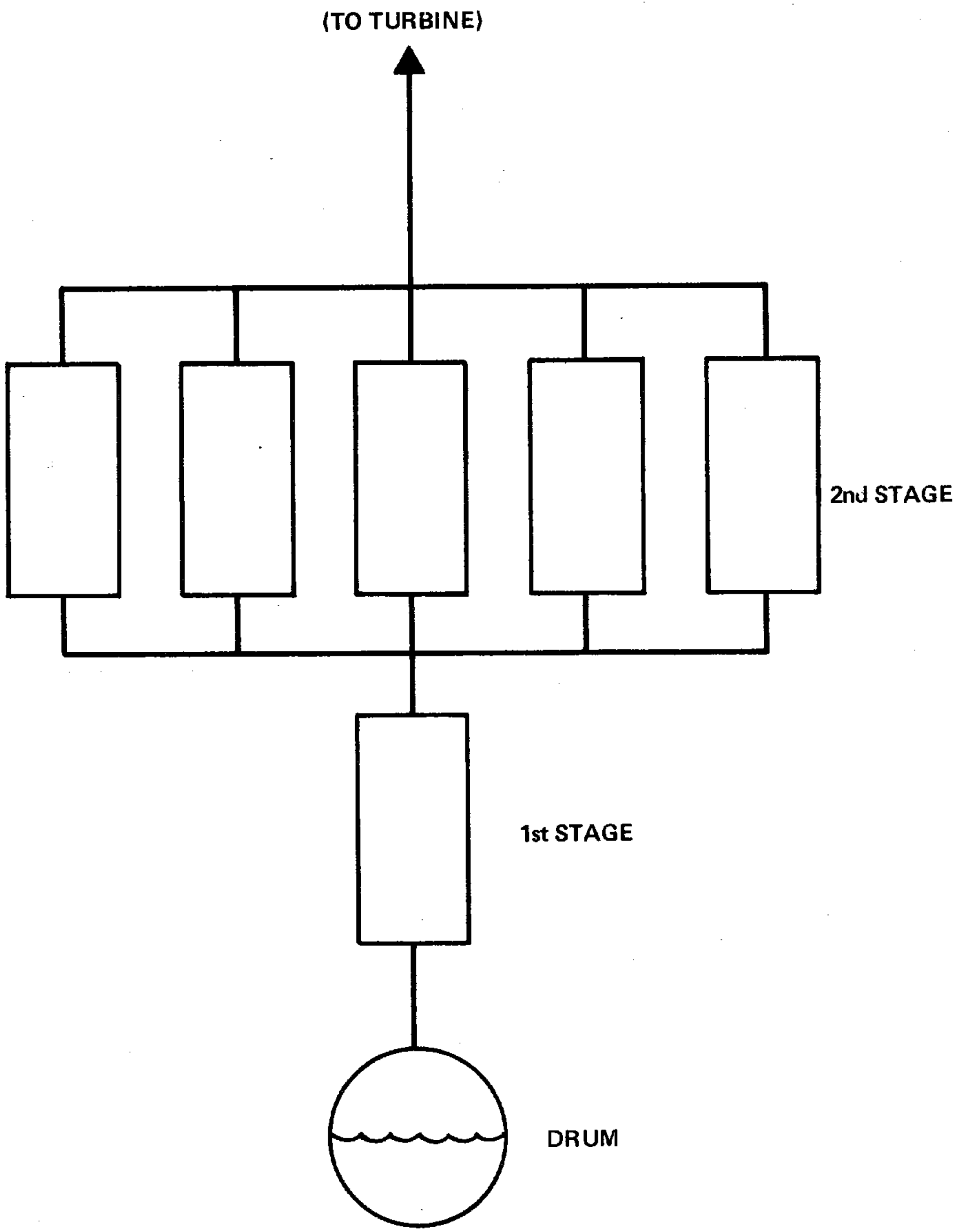

Figure 3.24

RECEIVER LAYOUT WITH SUPERHEATER IN LOW FLUX REGION

STEAM FLOW = 1.4×10^6 Kg/HR (3×10^6 LB/HR)
DIAMETER = 22.9m (75.0 FT)
LENGTH = 34.3m (112.6 FT)

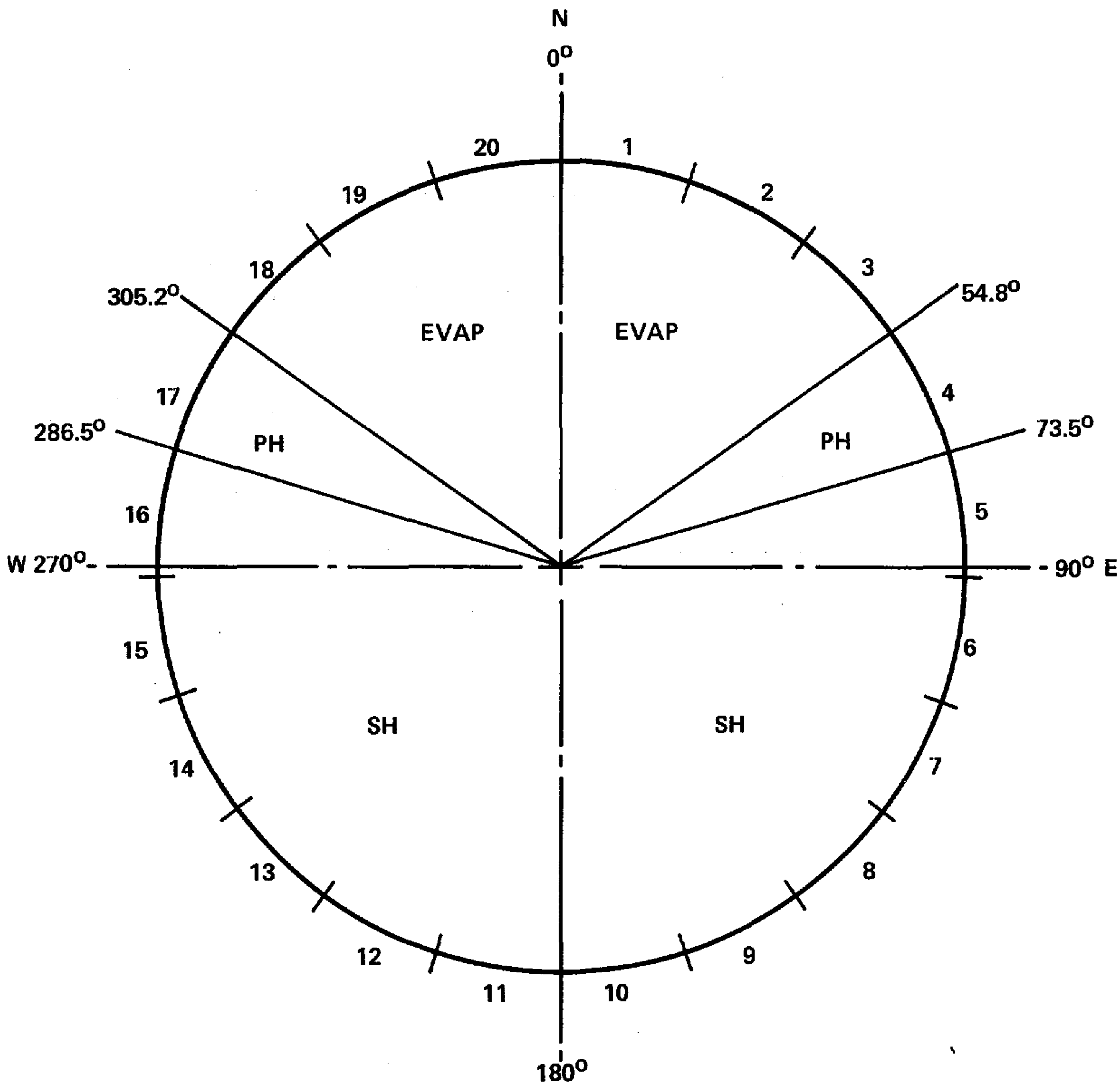

TOP VIEW

Figure 3.25

RECEIVER LAYOUT WITH SUPERHEATER IN HIGH FLUX REGION

STEAM FLOW = 1.4×10^6 Kg/HR (3×10^6 LB/HR)
DIAMETER = 22.9m (75.0 FT)
LENGTH = 34.3m (112.6 FT)

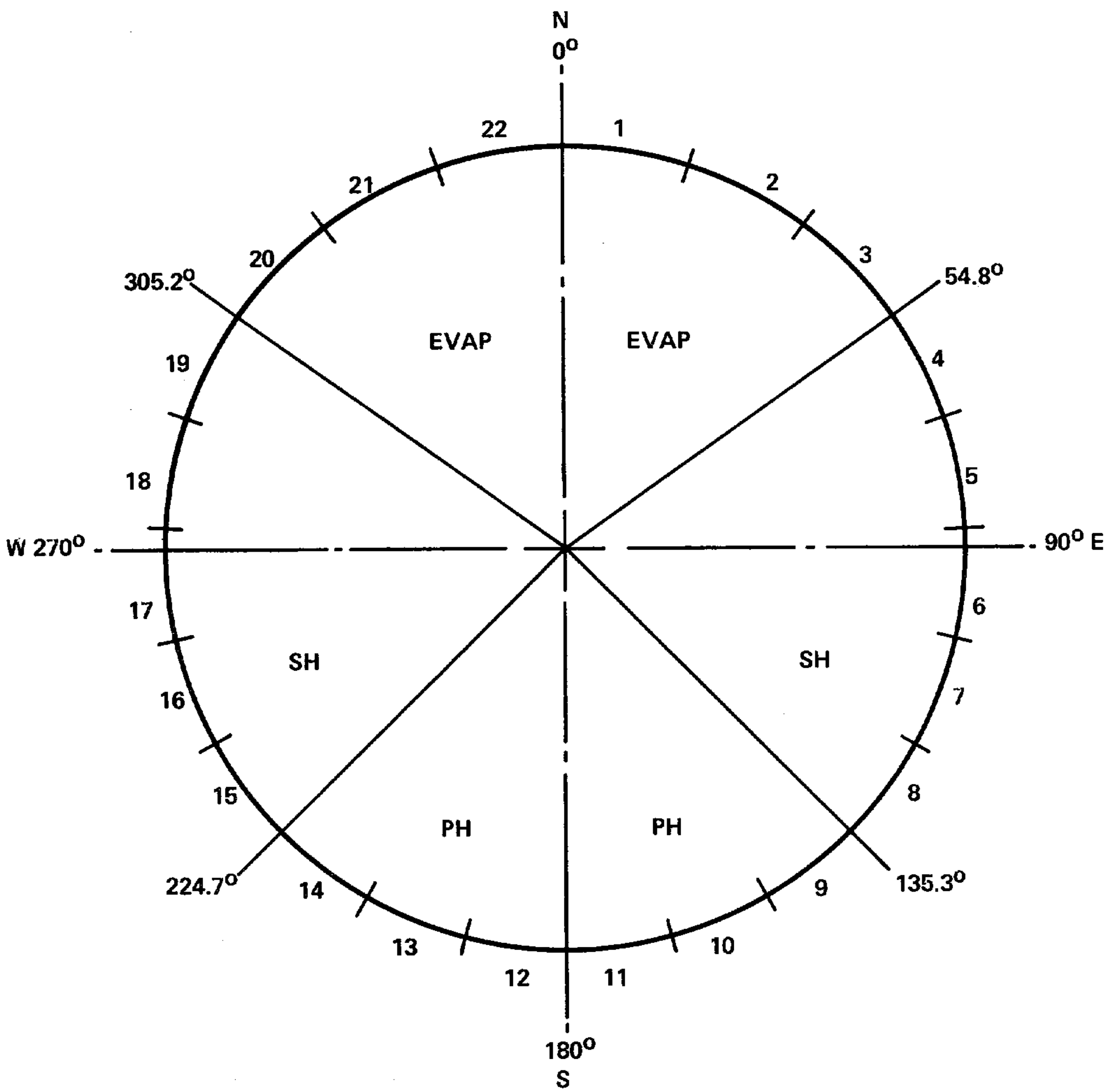

TOP VIEW

The selected tube panel has an average incident flux of .55 MW/m^2 (173,000 $BTU/hr\text{-}ft^2$). On the northern most tube of the panel however, the lateral flux gradient increases the incident flux to .60 MW/m^2 (190,000 $BTU/hr\text{-}ft^2$). The average steam outlet temperature in the tube panel is 593°C (1100°F).

Results of the study indicate that without orificing individual tubes, the bulk steam temperature on the northern tube would be approximately 641°C (1185°F). The southern most tube in the panel would subsequently exhibit an outlet temperature of about 546°C (1015°F).

An outlet steam temperature of 641°C (1185°F) is unacceptable because the corresponding increase in tube crown temperature would ultimately result in premature tube failure. Therefore, individual tubes located in the second stage superheater must be orificed to maintain an outlet temperature of 1100°F in all the tubes in the panel. Figure 3.26 shows orificing requirements to control steam flow to the individual tubes and thereby maintain a uniform 593°C (1100°F) outlet temperature.

3.2.4 Reheater Study

The analysis for the solar reheater parallels that for the superheater. The concept for the solar reheater involves a separate unit, located at some point on the tower below the receiver proper. A portion of the north field would be dedicated to reheater duty exclusively.

Recognizing that reheat piping up and down the tower could be a major cost item, it is desirable to locate the reheater as low as possible to the ground. An additional constraint is the low pressure drop dictated by the turbine cycle. The allowable reheater panel pressure losses and piping losses are much less than in the superheater.

Figure 3.26
TYPICAL SUPERHEATER ORIFICING REQUIREMENTS

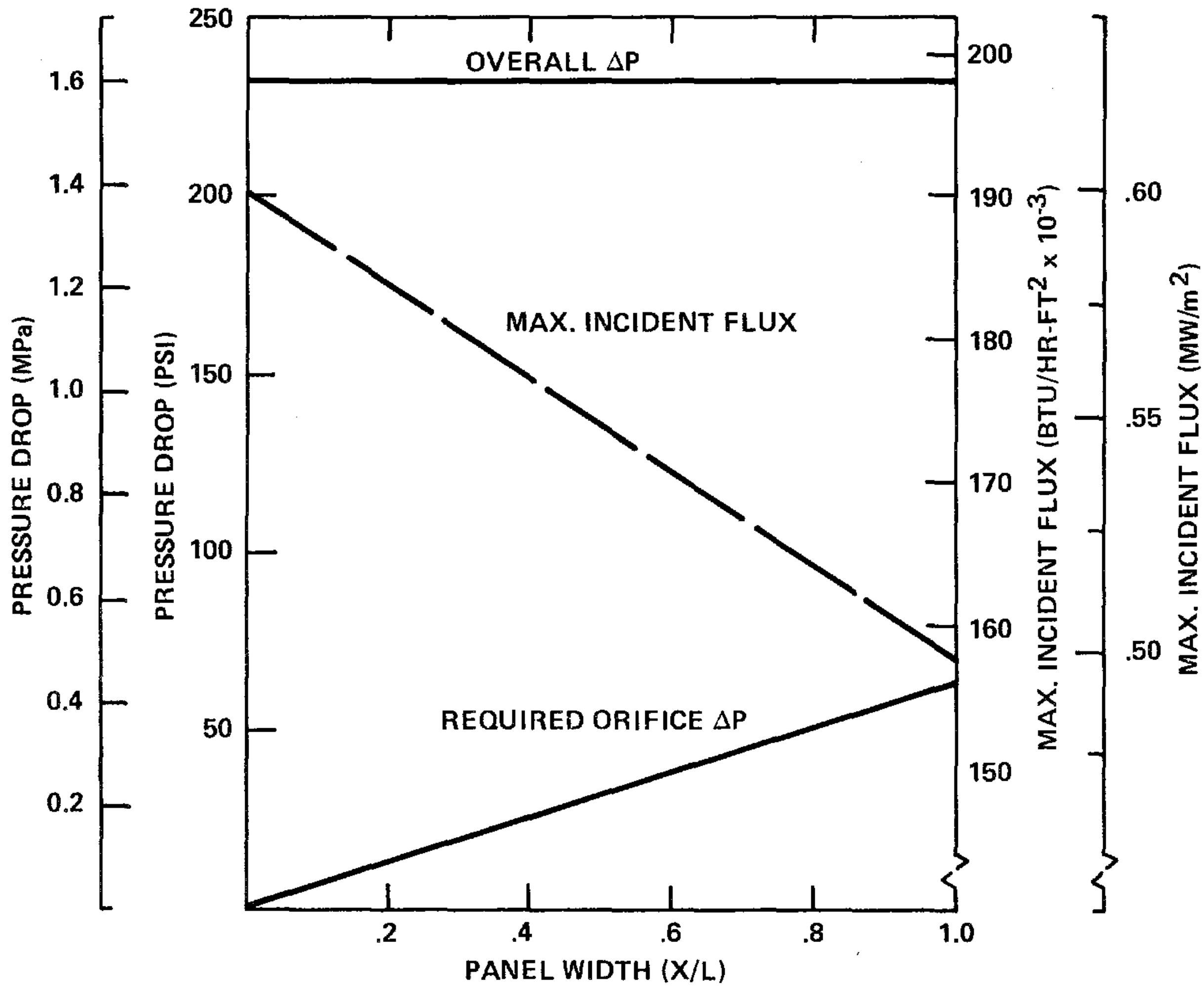

The proposed circuit arrangement is single stage with individual panels in parallel flow. The reheater is directly coupled to the turbine steam cycle. The reheater outlet temperature is 538°C (1000°F) as required by the turbine cycle.

The primary consideration in the reheater design is the trade off between maximum tube crown temperature and pressure drop when varying the tube size. The reheater outlet temperature of 538°C (1000°F) is less than the 539°C (1100°F) required in the superheater. On this basis, tube temperature constraints are somewhat reduced relative to the superheater.

Figure 3.27 shows reheater pressure drop as a function of both tube size and mass velocity. Pressure drop in the reheater is higher than in the superheater for a given mass velocity, because the lower operating pressure results in lower steam density and higher steam velocity.

Pressure drop in the reheater can be minimized by designing the reheater at a reduced aspect ratio. Heliostat field limitations imposed on the reheater aspect ratio are unknown. Preferably the reheater aspect ratio should be less than unity to reduce pressure drop.

Figure 3.28 shows the effect of aspect ratio on maximum tube crown temperature in the reheater. Reducing the reheater aspect ratio increases the maximum tube crown temperature. This is caused by a reduction in mass velocity which decreases the inside film coefficient. There is a trade off between decreased pressure drop and increased metal temperature when the reheater aspect ratio is reduced.

Based on flux profile parametrics developed under the superheater study, the vertical flux profile C is the best profile for the reheater design. In order to maintain maximum tube crown temperatures to less than 649°C (1200°F), the maximum peak flux should be approximately .20 MW/m^2 (65,000 $BTU/hr\text{-}ft^2$)

Figure 3.27
REHEATER PRESSURE DROP

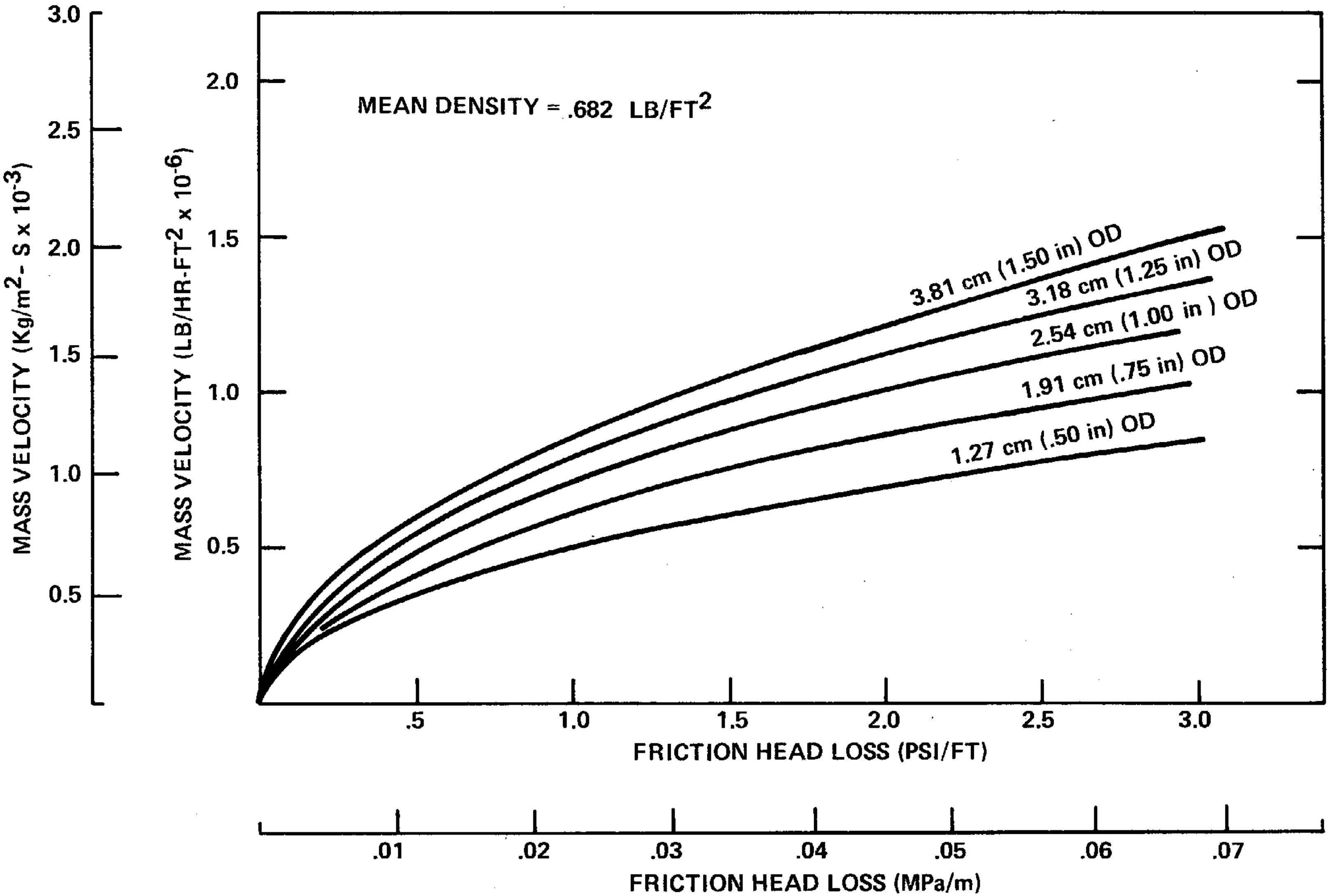

3-43

Figure 3.28
MAXIMUM CROWN TEMPERATURE vs REHEATER ASPECT RATIO

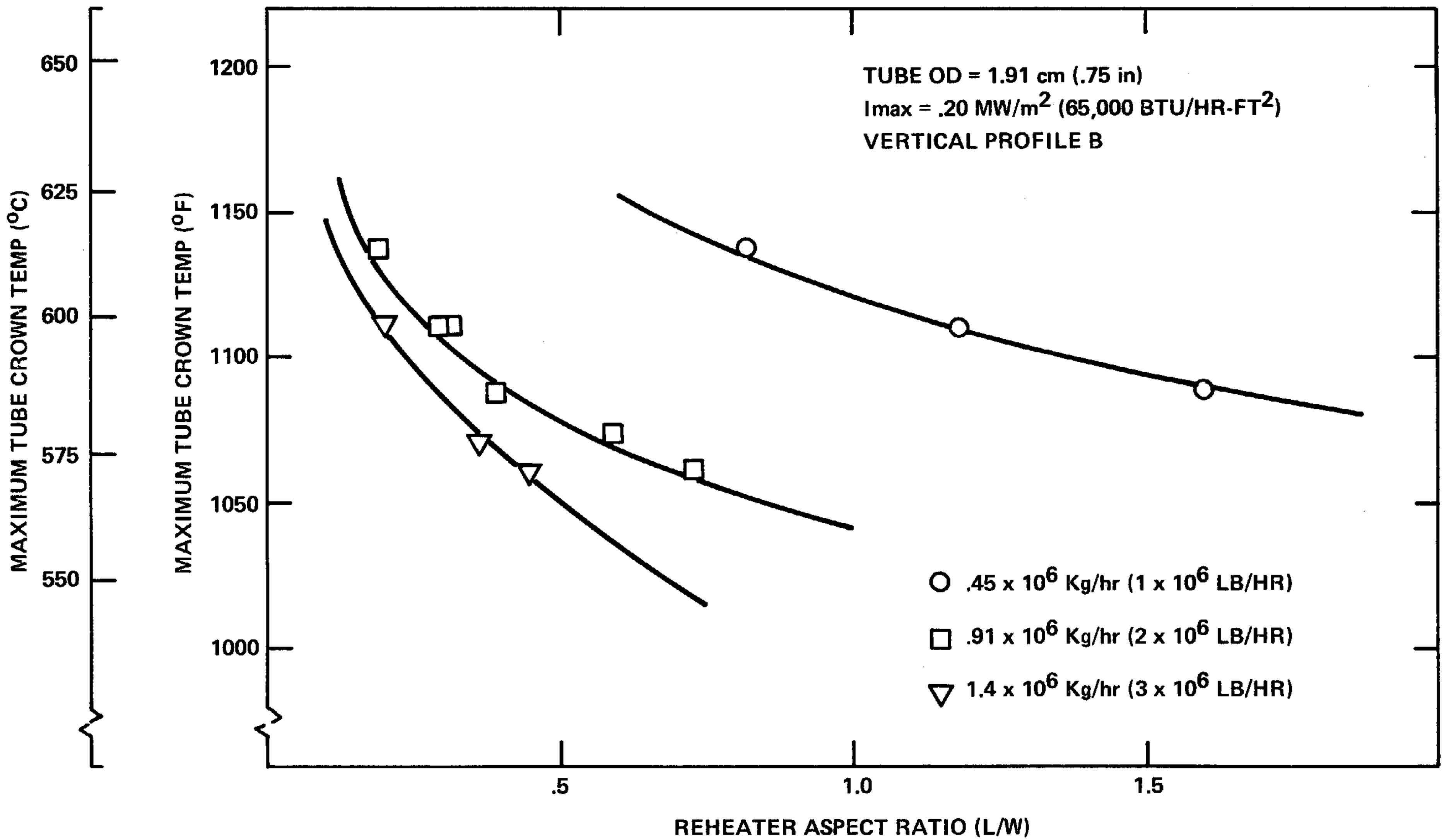

4. Supercritical Receiver Parametric Study and Conceptual Design

4.1 Introduction

This section presents an analysis of a supercritical solar central receiver. This is Reheat/Storage Option No. 4 from Table 1.5. Daily "average" efficiency of this option was equal to that of Option No. 2--Solar Reheater, which was the final design selection. The purpose of this section is to document the analysis of the supercritical receiver and to discuss some of the potential problem areas which led to the ultimate rejection of this option. The steam conditions at the outlet of the receiver are 593^{o}C (1100^{o}F) and 24.1 MPa (3500 psia). The receiver outlet steam is passed through thermal storage and then recirculated to the receiver through a closed loop circuit.

The baseline thermal storage system is assumed to consist of a high temperature molten salt which stores sensible heat. The turbine cycle operates directly from thermal storage at all times. Energy can be supplied continuously during evening operation or during periods of intermittent cloud cover. An important advantage of the supercritical cycle is its ability to provide continuous steam to the turbine generator.

A parametric study of the cycle layout and receiver configuration is presented, and critical design areas identified. The critical design areas relate to 1) high tube crown temperatures on north facing panels, 2) heat exchange limitations in thermal storage, and 3) pump limitations in the receiver circulation loop.

Two conceptual cycle arrangements are presented. The receiver parametrics are based on steam conditions dictated by the cycles. Limitations imposed by heat transfer to and from thermal storage, and by circulation pump requirements are also detailed. Receiver design parametrics including flux distribution, metal temperature, pressure drop, aspect ratio, and tube size are explored with regard to optimum design.

4.2 Combined Cycle Analysis

4.2.1 Overview--An outlet temperature of 593°C (1100°F) was chosen based on superheat and reheat temperatures in the turbine cycle. The molten salt temperature is 566°C (1050°F) allowing a 28°C(50°F) temperature differential on the charging and discharging heat exchangers. Figure 4.1 is a schematic of the cycle requirements.

Tube wall thickness is a concern with regard to metal temperatures. In order to minimize the tube wall thickness, the system design pressure was specified no higher than necessary to maintain the system in the supercritical region. The specified receiver outlet pressure is 24.1 MPa (3500 psia).

The above restrictions provide the basis for the supercritical cycle analyses. Primary areas of concern in the cycle investigations are heat transfer limitations in the storage heat exchangers, and pumping requirements for the receiver circulation pump.

4.2.2 Thermal Storage Limitations--Energy collected in the receiver is stored as sensible energy in the molten salt. A temperature gradient called a thermocline is developed between the inlet and outlet of the molten salt tank. Molten salt at 566°C (1050°F) is extracted from the top of the tank, and passed through a discharging heat exchanger, whereby heat is transferred into the turbine cycle steam. Relatively cooler molten salt is extracted from the bottom of the storage tank to be heated to 566°C (1050°F) in a charging exchanger. The molten salt transfers sensible energy in a linear temperature-enthalpy regime (i.e. constant specific heat).

Figure 4.1
SUPERCRITICAL RECEIVER CYCLE REQUIREMENTS

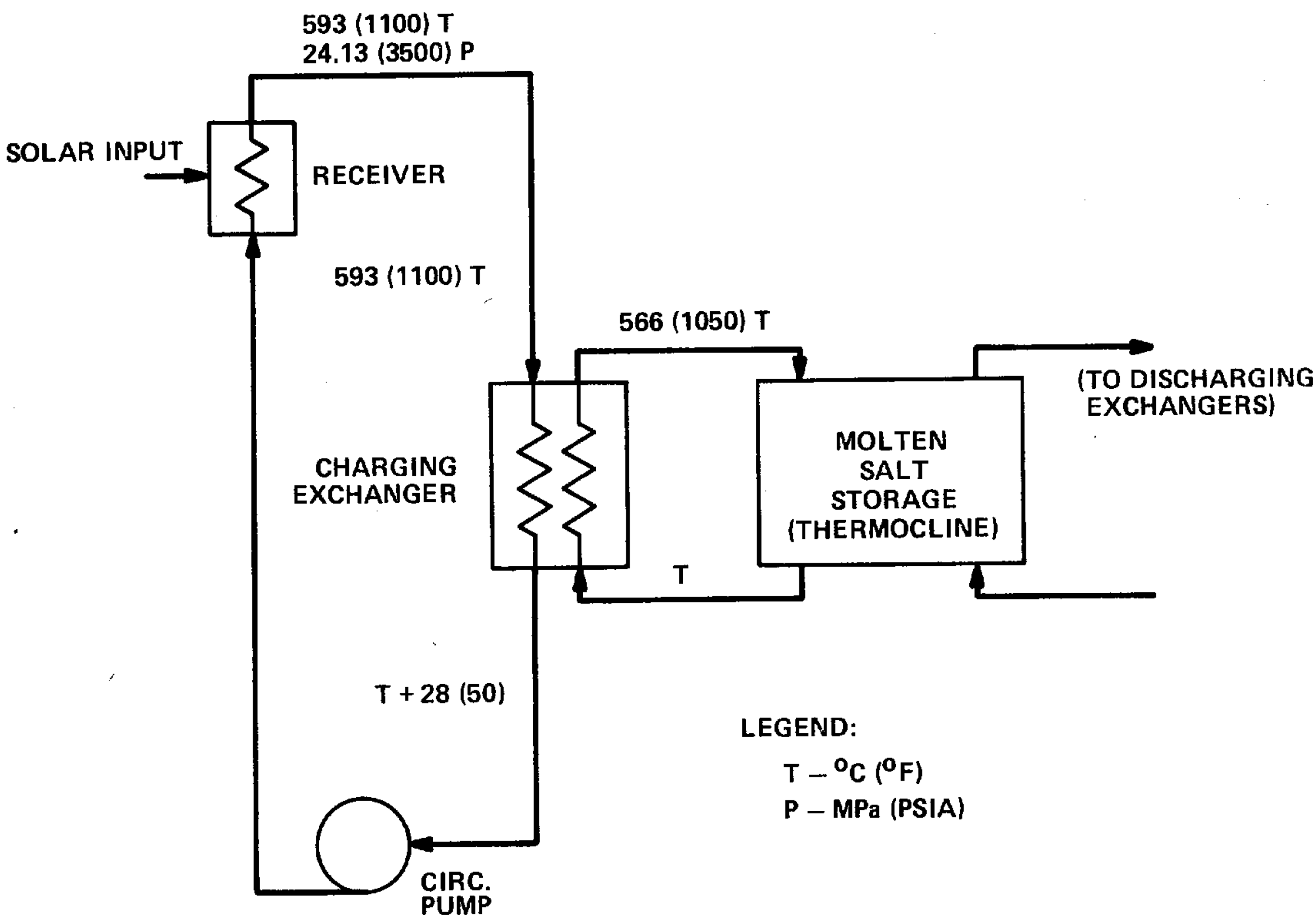

In the turbine cycle, feedwater is heated to superheated steam in the discharging exchanger. Much of the heat transfer occurs at constant steam temperature during evaporation.

A similar relationship is exhibited in the charging exchanger because the supercritical steam passes through a quasi phase change as it is cooled from 593^{o}C (1100^{o}F). The non-linear heat transfer characteristics in both the charging and discharging heat exchangers create pinch points with the molten salt.

Figure 4.2 shows the non-linear temperature relationship which exists as supercritical steam at 593^{o}C (1100^{o}F) is cooled to varying temperatures leaving the charging heat exchanger. The non-linearities become more severe as the outlet temperature is lowered to below 371^{o}C (700^{o}F).

Figure 4.3 illustrates the temperature relationships for a single thermal storage tank operating between 360^{o}C (680^{o}F) and 566^{o}C (1050^{o}F). The turbine cycle is based on 538^{o}C (1000^{o}F) superheat and reheat temperatures, and a pressure of 16.5 MPa (2400 psia) at the turbine throttle. The hot and cold salt temperatures are set by the restriction of a minimum 28^{o}C (50^{o}F) temperature differential at the inlet and outlet of the charging and discharging exchangers.

Referring to Figure 4.3, there is a pinch point of 11^{o}C (20^{o}F) between the salt and the supercritical steam. A lowering of the steam outlet temperature to below 404^{o}C (760^{o}F) would further reduce the pinch point differential resulting in more inefficient heat transfer. The supercritical steam temperature leaving the charging exchanger is thus limited to a minimum of about 404^{o}C (760^{o}F).

Figure 4.2
SUPERCRITICAL TEMPERATURE PROFILES

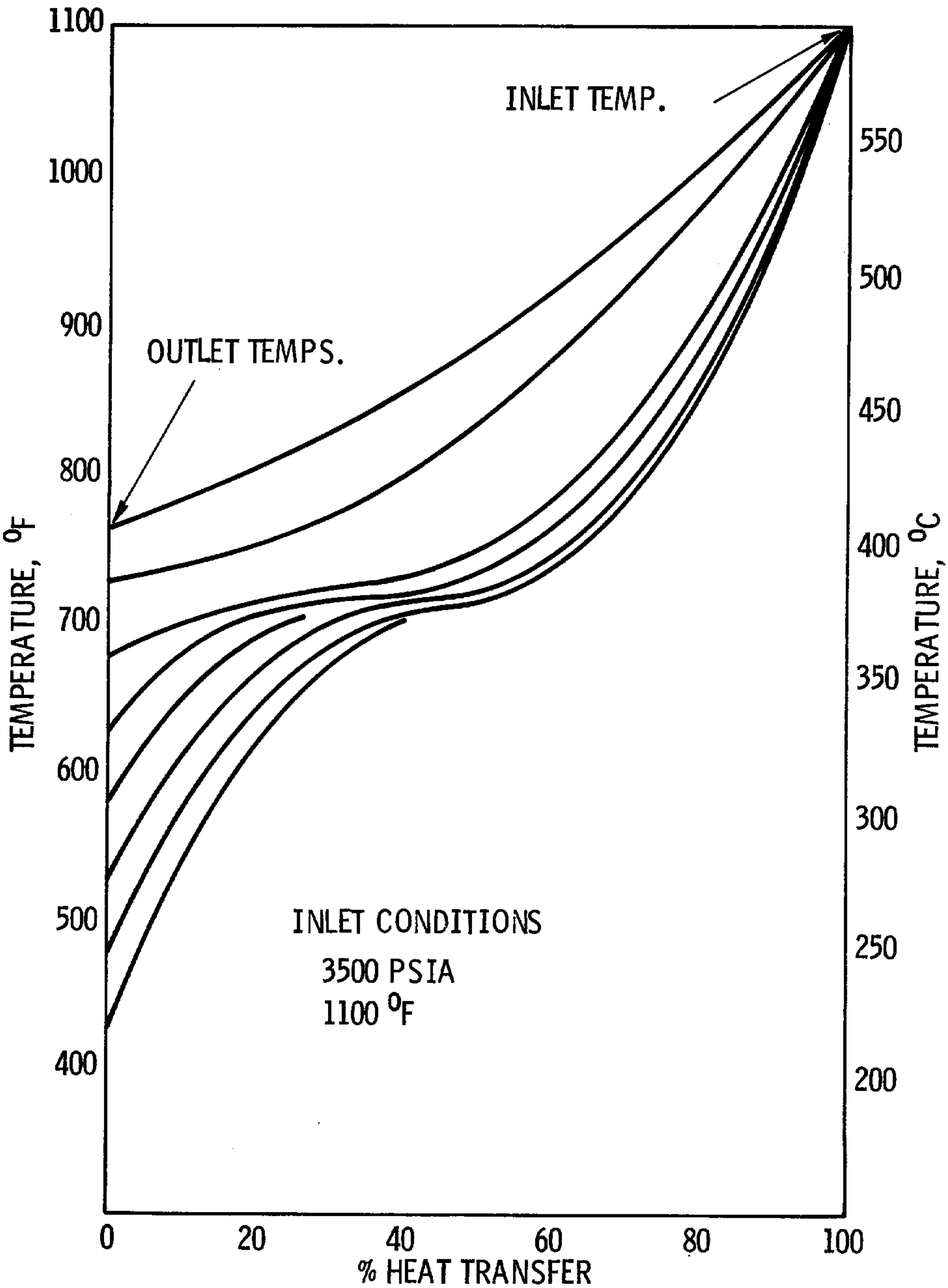

Figure 4.3
CYCLE A HEAT EXCHANGE CHARACTERISTICS

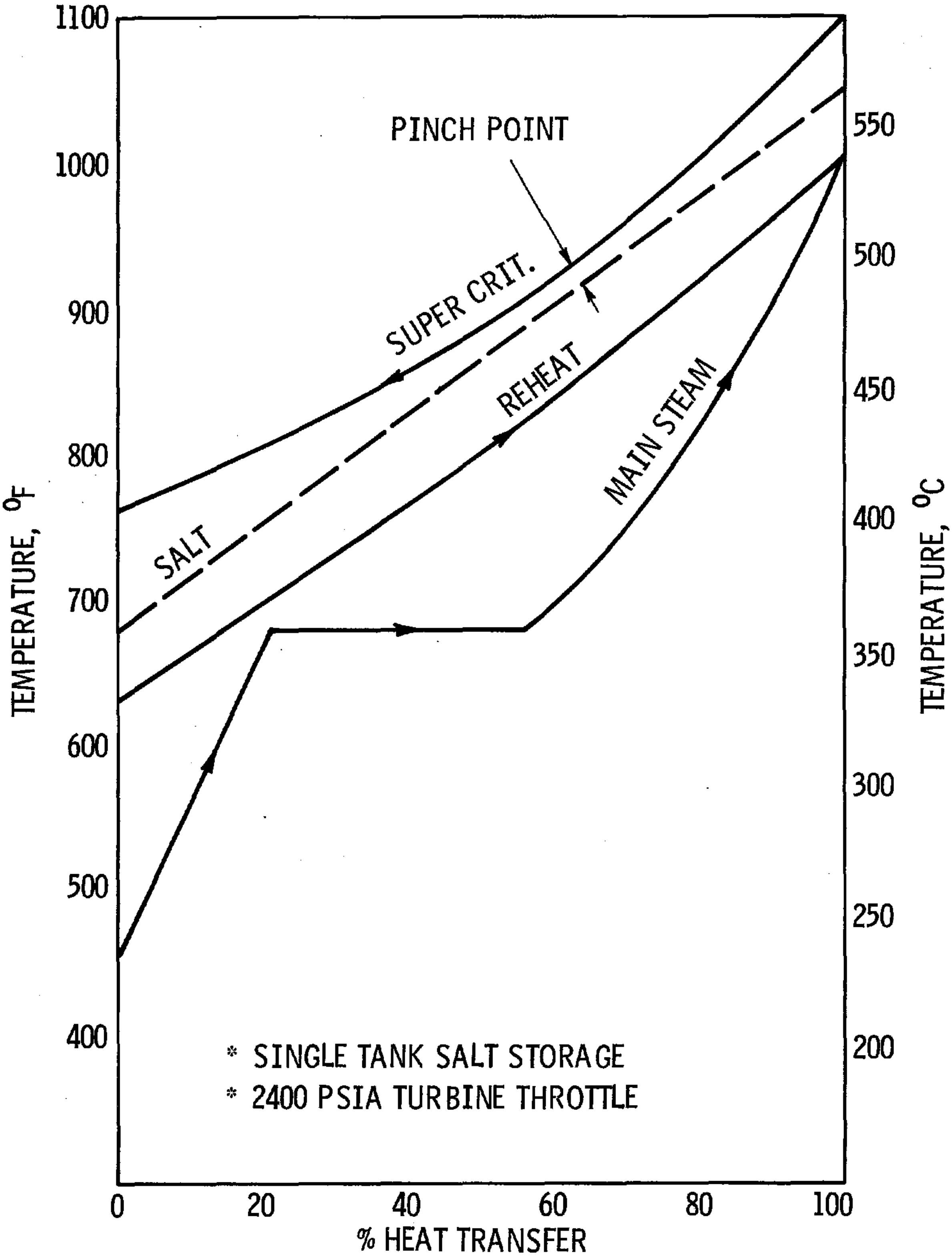

As the steam temperature is lowered to less than 404°C (760°F), the enthalpy drop per degree of steam temperature increases rapidly. The supercritical steam shows an effective phase change in this temperature range. Corresponding to the increased drop off in enthalpy is a rapid decrease in specific volume. The decrease in specific volume indicates a quasi phase change from vapor to liquid. Figure 4.4 is a pressure-enthalpy diagram which shows the quasi phase change process in the region above the steam dome. It is desirable to lower the supercritical steam temperature to less than 404°C (760°F) to increase the enthalpy drop, and consequently lower the circulation mass and volume flow rates.

Figure 4.5 shows an alternate arrangement for lowering the steam outlet temperature to 357°C (675°F) and to effectively bring the steam into a liquid phase. The arrangement utilizes high and low temperature salt storage tanks, and a steam cycle with the turbine throttle pressure reduced from 16.5 MPa (2400 psia) to 12.4 MPa (1800 psia). There is a pinch point to 14°C (25°F) between both the low temperature salt and the main steam, and between the high temperature salt and supercritical steam. Re-heat steam is generated entirely in the high temperature storage.

The turbine throttle pressure was lowered to decrease the steam saturation temperature, thereby allowing a greater temperature differential between the molten salt and the steam. A further lowering of supercritical steam outlet temperature to less than 357°C (675°F) would require lowering turbine throttle pressure to less than 12.4 MPa (1800 psia).

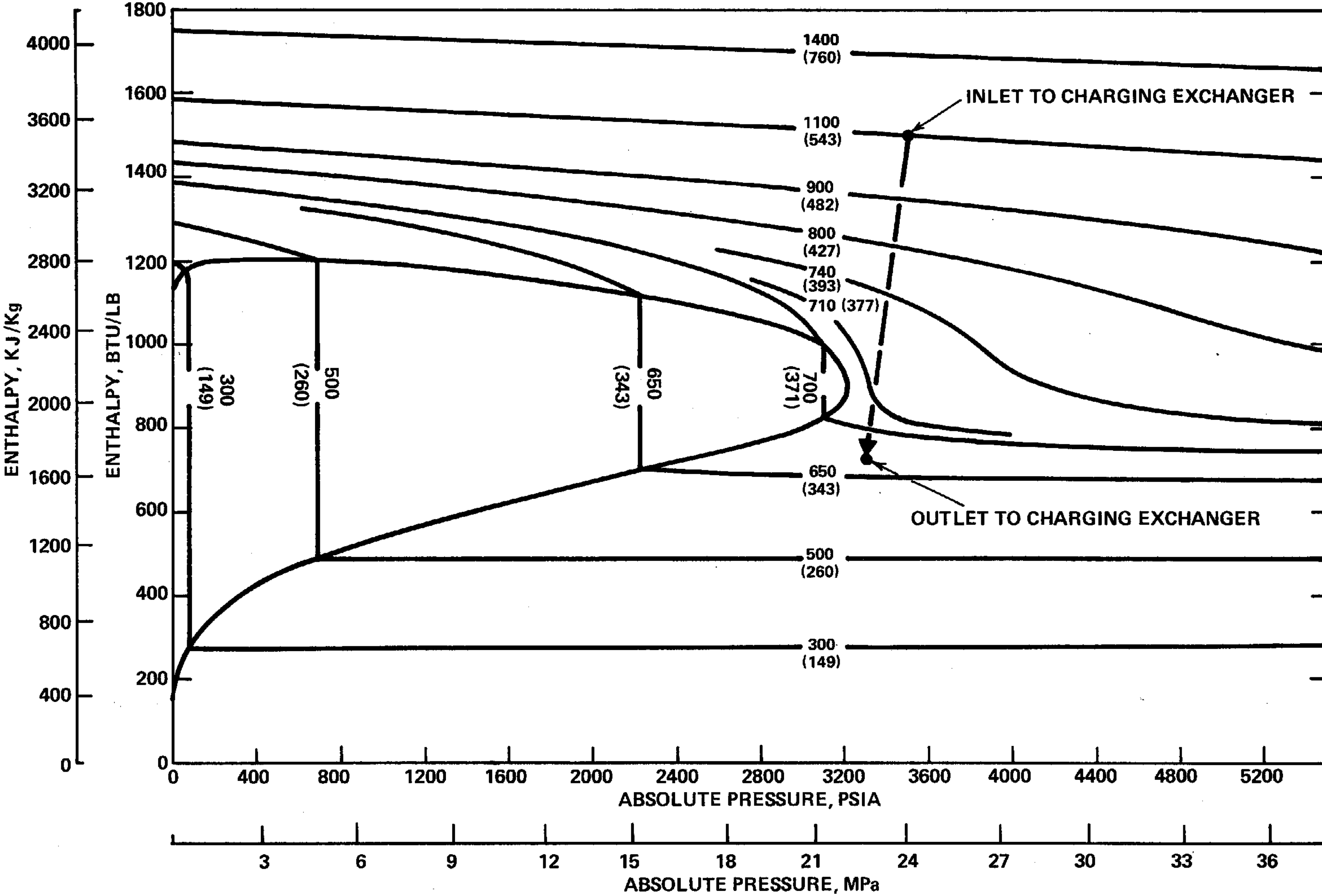

Figure 4.4
QUASI PHASE CHANGE IN SUPERCRITICAL REGION

Figure 4.5
CYCLE B HEAT EXCHANGE CHARACTERISTICS

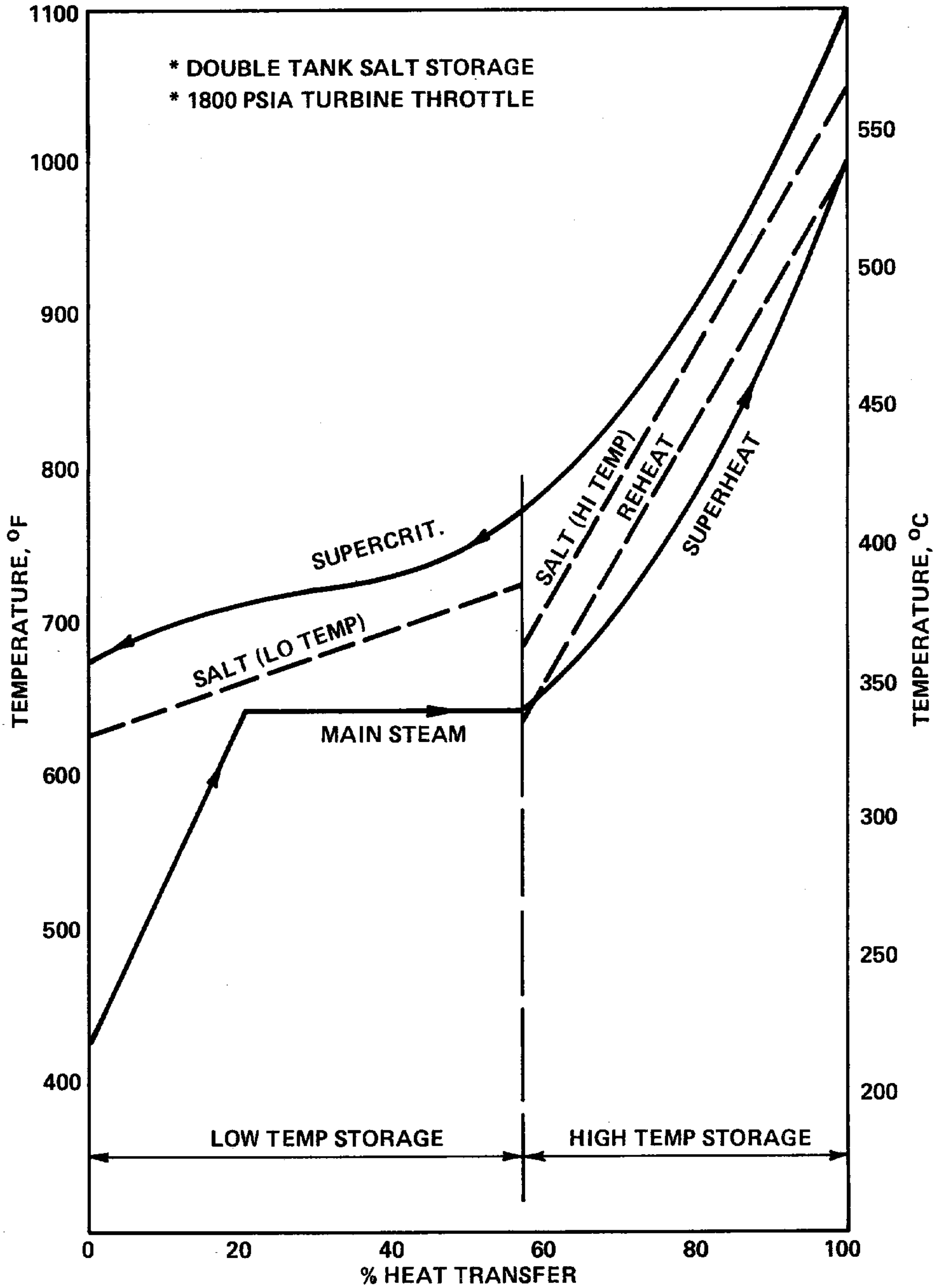

4.2.3 Circulation Pump Requirements--A receiver circulation pump is required to pump feedwater or steam up the tower to the receiver. The pump must be capable of providing sufficient head at the high flow rates encountered in the receiver circulation loop.

Standardized boiler circulation pumps generally provide only several hundred feet of head at flow rates typically encountered in circulation boilers.

The overall circulation loop pressure drop is estimated to range up to a maximum of about 2.76 MPa (400 psi) depending on the design specifications. The steam conditions at the suction of the pump determine the head required to satisfy the overall pressure drop in the circulation loop. The pump suction conditions are approximately the steam properties on the outlet of the charging exchanger.

The circulation pump can generally supply a greater head at lower volumetric flow rates. Ideally, the steam should be sub-cooled at the pump suction to attain the maximum pump head. On the other hand it is desirable to circulate the fluid up the tower in a low density state to minimize elevation head loss.

Two conceptual cycles have been arranged based on the heat transfer configurations shown in Figures 4.3 and 4.5. Pump requirements are respectively based on both the "low" density and "high" density steam conditions at the pump suction. Cycle details are explored in the following sections.

4.2.4 Conceptual Cycle A--Figure 4.6 presents a schematic of a super critical receiver plant utilizing the single salt tank storage system. The nominal plant rating is 200 MWe with a solar multiple of 1.5. Heat exchanger characteristics are presented in Figure 4.3. The turbine cycle is based on throttle conditions of 16.5 MPa (2400 psia) and 538°C (1000°F).

Figure 4.6

SUPERCRITICAL RECEIVER – ONE STORAGE TANK (2400 PSIA STEAM CYCLE)
100% PASS-THRU STORAGE
SM = 1.5 (NOMINAL)
PLANT RATING = 200 MW (NOMINAL)
(ENGLISH UNITS)

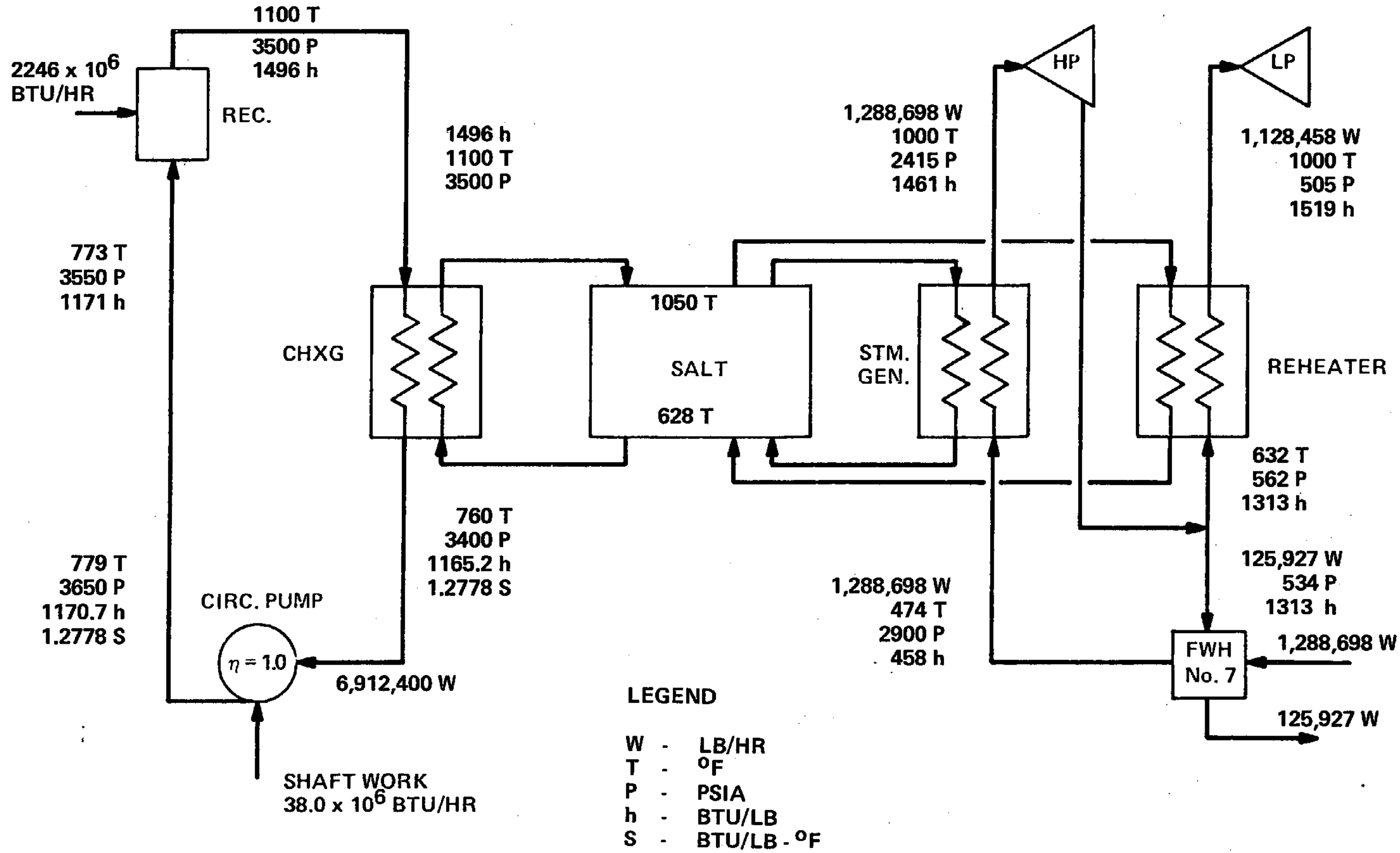

Figure 4.6a
SUPERCRITICAL RECEIVER – ONE STORAGE TANK (2400 PSIA STEAM CYCLE)
100% PASS-THRU STORAGE
SM = 1.5 (NOMINAL)
PLANT RATING = 200 MW (NOMINAL)
(SI UNITS)

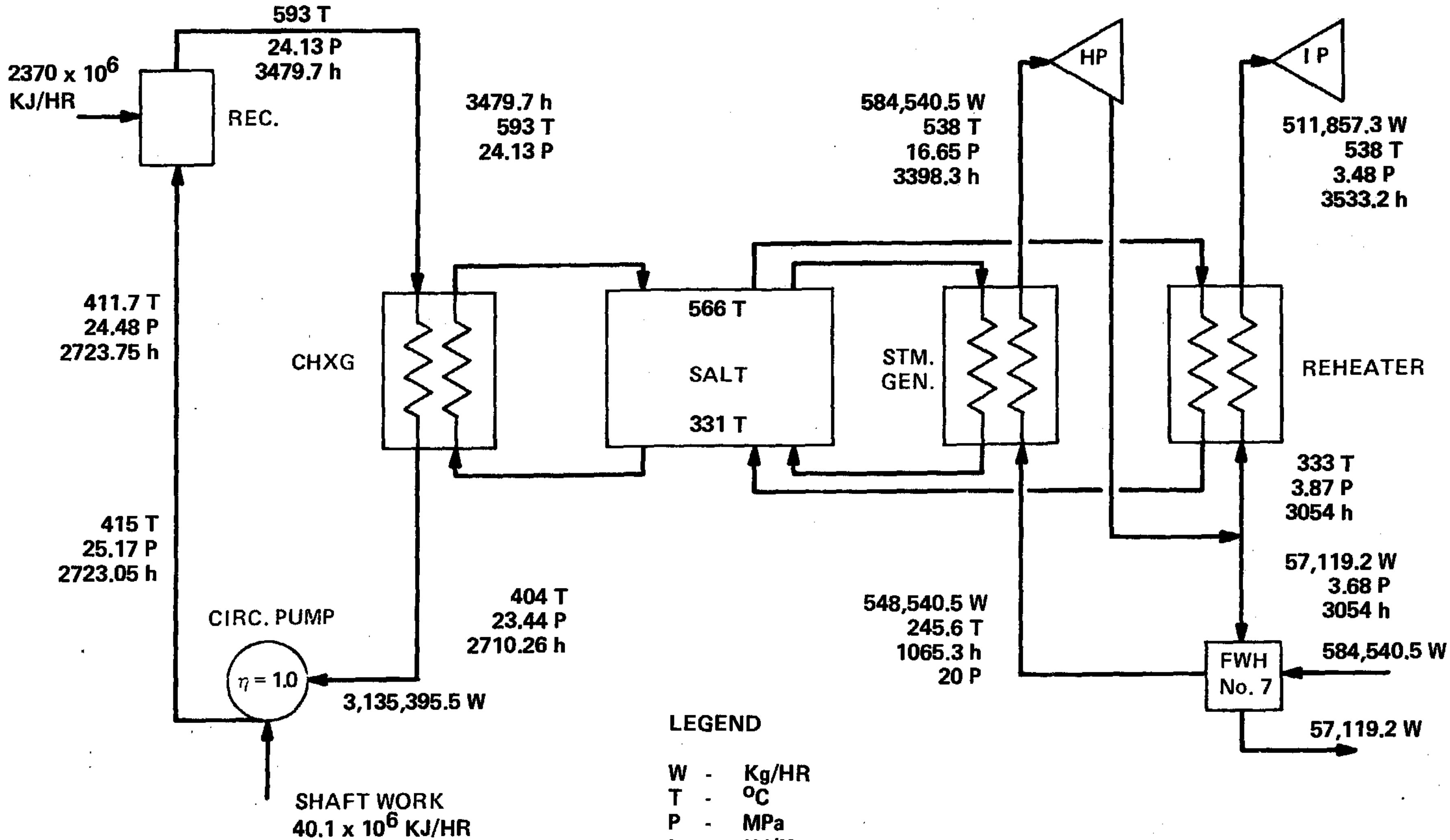

LEGEND

W - Kg/HR
T - °C
P - MPa
h - KJ/Kg
S - KJ/Kg - °C

The steam density leaving the charging exchanger is about 128 kg/m^3 (8.31 lb/ft^3). The supercritical steam is effectively in a vapor state. The steam is re-circulated up the tower resulting in an elevation head loss of about .41 MPa (60 psi). The total pressure drop in the circulation loop is about 1.72 MPa (250 psi).

A major problem with this configuration is the capability of the circulation pump to provide a required 1,311m (4300 ft) of head at a volumetric flow rate of 6.3 m^3/s ($1x10^5$ GPM). The capacity and head required of the pump are out of the range of present commercial circulation pump capability. Significant pump technology development would be required to satisfy the specific requirements for this particular supercritical application.

4.2.5 <u>Conceptual Cycle B</u>--The alternate cycle configuration shown in Figure 4.7 is intended to minimize circulation pump limitations. Two salt storage tanks (high and low temperature) are utilized to reduce the outlet steam temperature to 357°C (675°F). The heat exchanger characteristics are those presented in Figure 4.5. The turbine throttle pressure is subsequently derated from 16.5 MPa (2400 psia) to 12.4 MPa (1800 psia).

The steam density at the outlet of the second charging exchanger is 591 kg/m^3 (36.9 lb/ft^3). The steam is pumped directly up the tower creating an elevation head loss of about 1.72 MPa (250 psi). The total circulation loop pressure drop is approximately 2.76 MPa (400 psi).

The overall circulation flow rate however is less than half of the circulation flow rate in Cycle A, while the volumetric flow has been reduced by nearly an order of magnitude to .63 m^3/s ($1x10^4$ GPM). The required pump head is about 488m (1600 ft). Table 4.1 shows a comparison of circulation pump requirements in Cycles A and B. The isentropic pump power required in Cycle B is less than 25 percent of that required in Cycle A.

Figure 4.7

SUPERCRITICAL RECEIVER — TWO STORAGE TANKS (1800 PSIA STEAM CYCLE)
100% PASS-THRU STORAGE
SM = 1.5 (NOMINAL)
PLANT RATING = 200 MW (NOMINAL)
(ENGLISH UNITS)

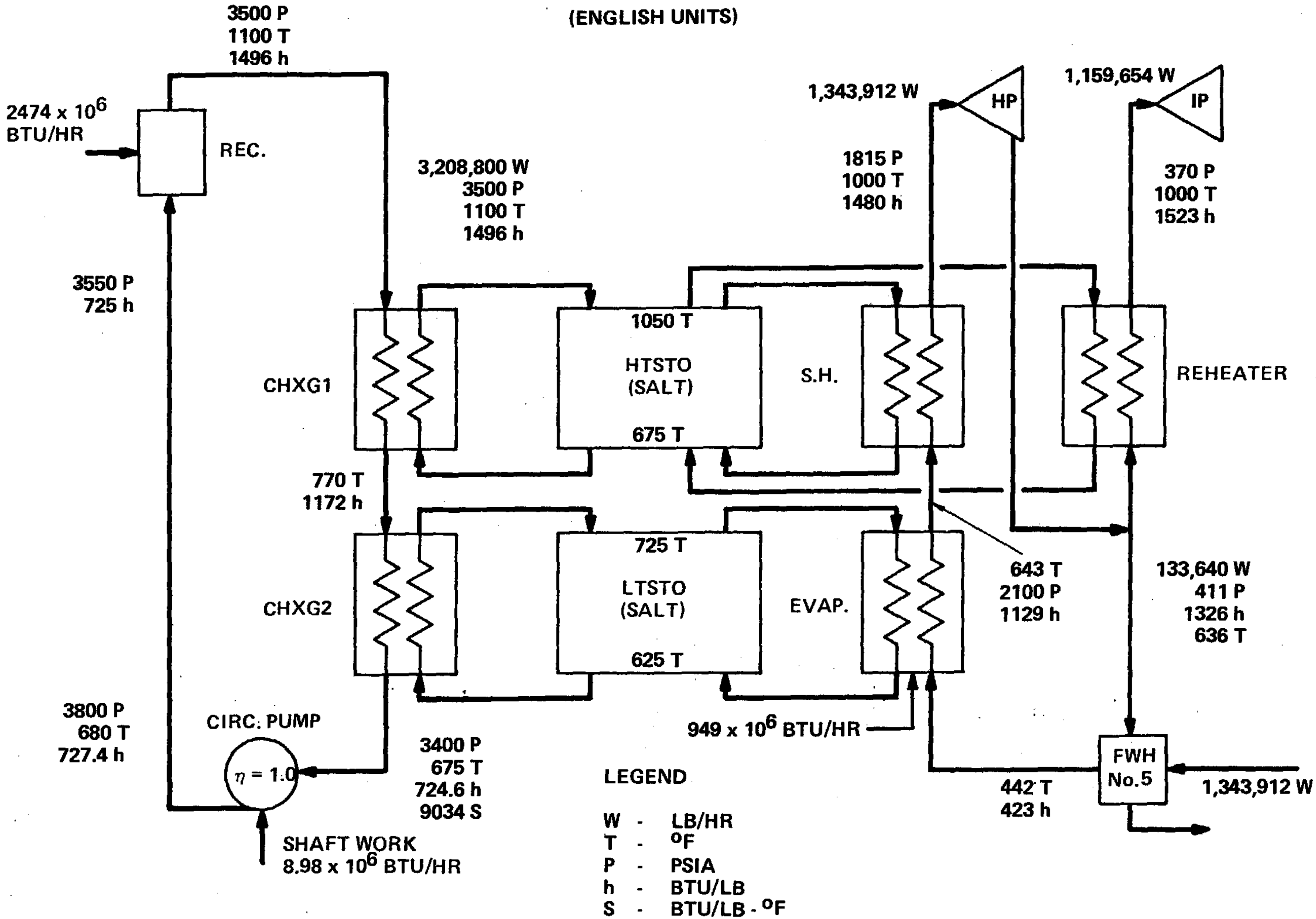

Figure 4.7a

SUPERCRITICAL RECEIVER — TWO STORAGE TANKS (1800 PSIA STEAM CYCLE)

100% PASS-THRU STORAGE

SM = 1.5 (NOMINAL)

PLANT RATING = 200 MW (NOMINAL)

(SI UNITS)

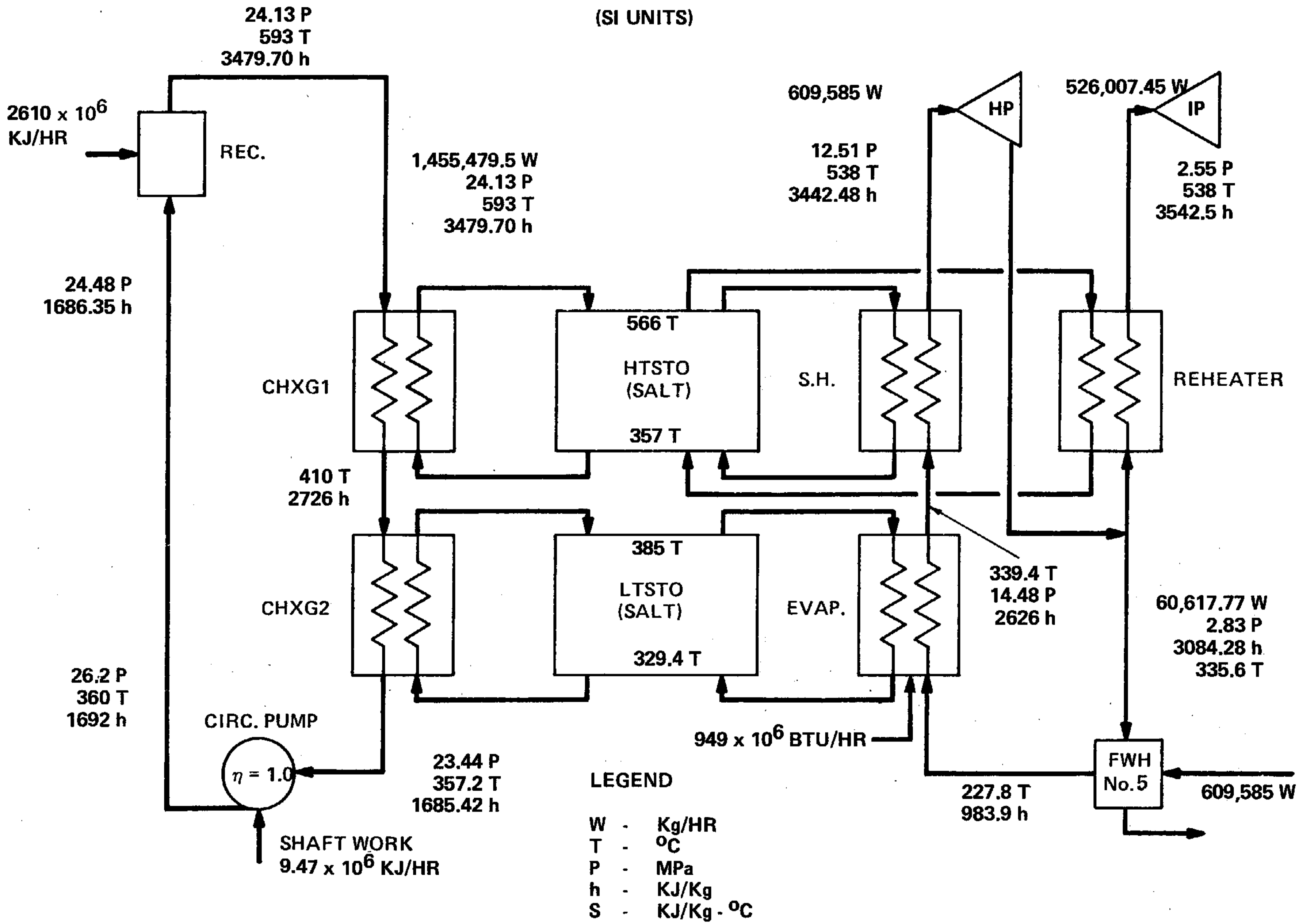

4-15

TABLE 4.1

Comparison of
Circulation Pump Requirements
For Cycles A and B

	Cycle A	Cycle B
Suction Press., MPa (psia)	23.4 (3400)	23.4 (3400)
Suction Temp., ^oC (^oF)	404 (760)	357 (675)
Steam Density, kg/m^3 (lb/ft^3)	133 (8.31)	591 (36.9)
Mass Flow, kg/hr (lb/hr) x 10^{-6}	3.135 (6.912)	1.145 (3.209)
Volume Flow, m^3/s (GPM x 10^{-3})	6.54 (103.6)	.681 (10.3)
Pump ΔP, MPa (psi)	1.72 (250)	2.76 (400)
Required Head, m (ft)	1,320 (4,330)	475 (1,560)
Isentropic Pump Power, KW/Hp	11,100 (14,900)	2,630 (3,530)

Tentative discussions with pump manufacturers indicate that a modified boiler feed pump could supply the required capacity and head in Cycle B. The pump would require a thicker suction casing to compensate for higher operating pressure. However, the modifications can be readily adapted to the present standardized pumps without major pump development.

4.2.5.1 Supercritical Re-heat Option--An alternate configuration utilizing a supercritical re-heat exchanger was explored for minimizing the elevation head loss in the tower. Figure 4.8 shows this concept incorporated into the supercritical circulation loop.

The supercritical steam is effectively pumped in the liquid phase as shown previously. However, it is re-heated to a higher temperature before being re-circulated up the receiver tower. The required reheat energy is provided by 593°C (1100°F) extraction steam from the receiver. Reheating the steam lowers steam density thereby reducing elevation head loss in the tower. The overall pressure drop in the circulation loop is reduced by approximately 25 percent from 2.76 to 2.07 MPa (400-300 psi).

However, the required flow rate in the circulation loop more than doubles to accommodate reheating. There is a trade-off between the lowered pressure drop in the loop and the increased circulation flow rate. The advantages gained by lowering the pressure drop in the loop are offset by the increased circulation flow rate and additional heat exchanger hardware.

4.2.6 Alternate Configurations

4.2.6.1 Multiple Salt Tank Storage--Additional salt storage tanks over different temperature ranges could be employed to provide better heat exchanger characteristics and provide a further lowering of supercritical steam temperature at the outlet of the charging exchanger. The storage system cost and complexity would however increase with additional storage tanks. Cost parametrics must be developed to show the cost effectiveness of a multiple tank energy storage system.

Figure 4.8

EXTRACTION STEAM REHEAT OPTION

(ENGLISH UNITS)

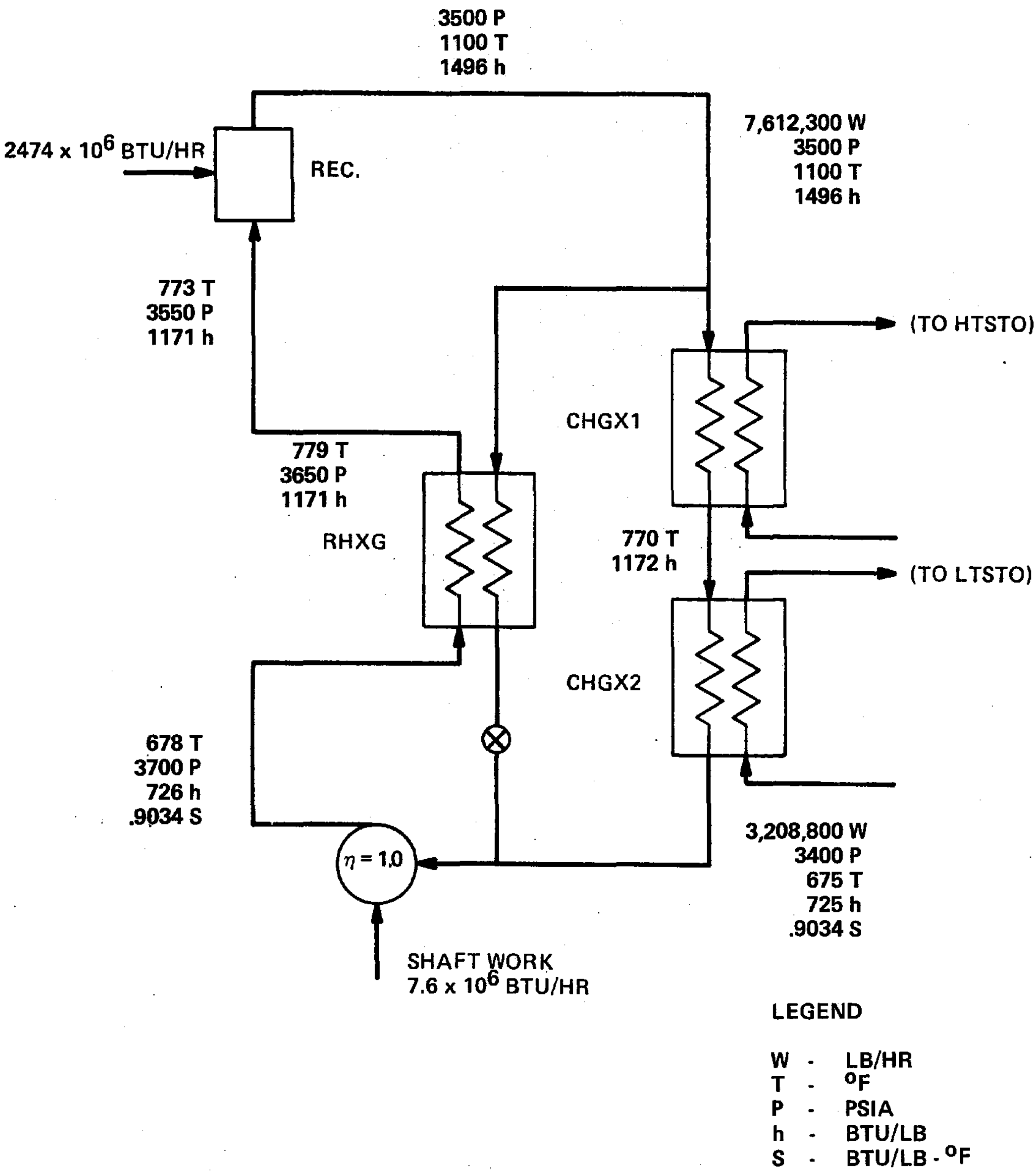

Figure 4.8a
EXTRACTION STEAM REHEAT OPTION
(SI UNITS)

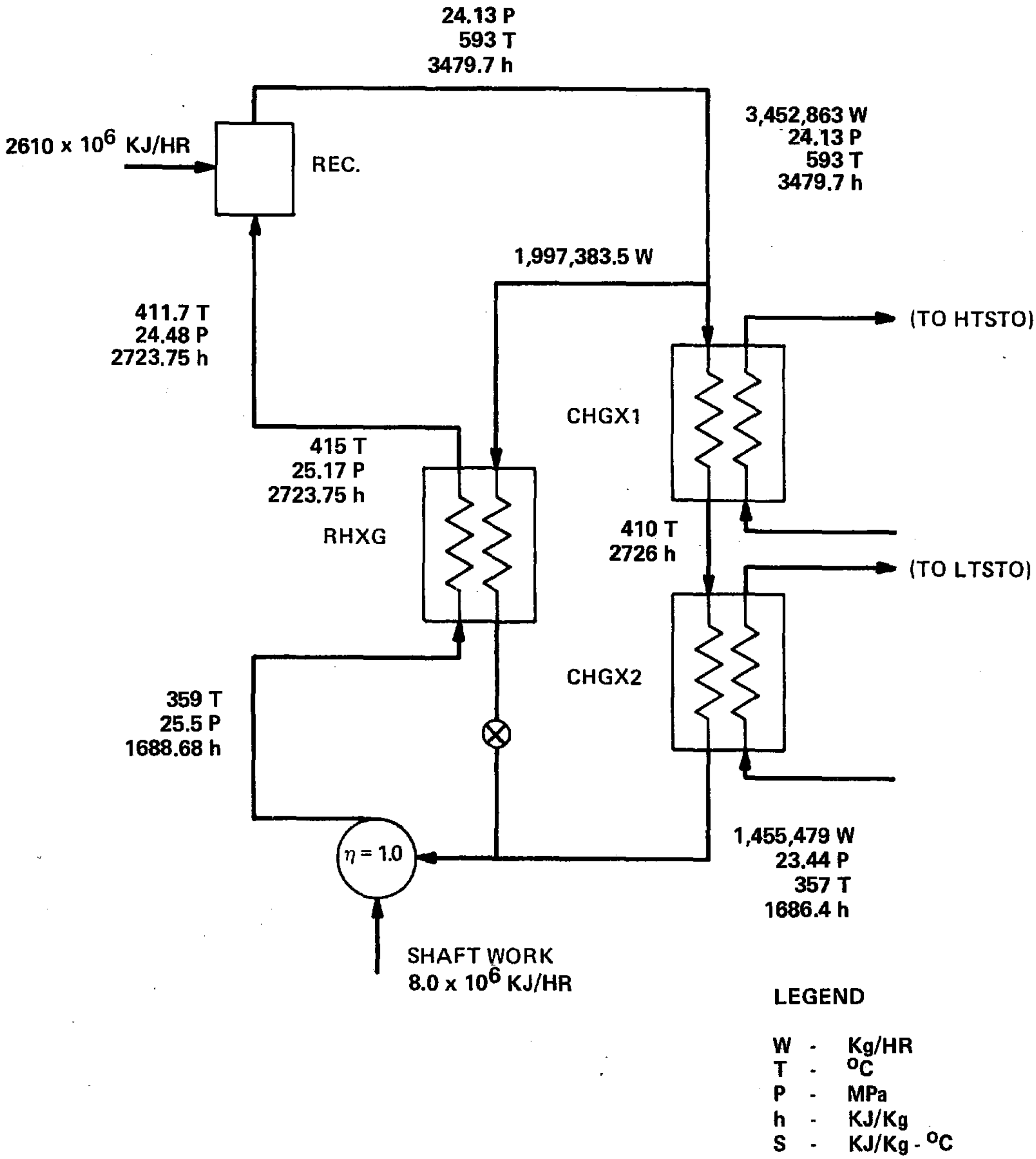

4.2.6.2 De-rated Turbine Throttle Temperature--The turbine throttle temperature could be de-rated to provide better temperature characteristics in the heat exchangers. Figure 4.9 shows the combined effects of lowering turbine throttle temperature to 510°C (950°F), while using a 3-salt tank storage system. The turbine throttle pressure is 16.5 MPa (2400 psi). Re-heat is accomplished in the high temperature storage.

Lowering the throttle temperature decreases the cycle efficiency, while increasing the throttle pressure increases efficiency. The net efficiency gain in this configuration must be compared against the additional cost of a third storage tank.

4.2.6.3 Eutectic Salt Storage--A eutectic salt could be used to take advantage of phase change temperature characteristics. The turbine main steam as well as the supercritical steam exhibit change of phase temperature profiles. A eutectic salt might be developed to follow the steam temperature during phase change. A single molten salt storage system could then be used to lower the supercritical steam in the circulation loop to a desired temperature. Eutectic salts should be considered as a development item in the supercritical receiver cycle.

4.2.6.4 Increased Supercritical Operating Pressure--The temperature-enthalpy relationship of supercritical steam should theoretically become more linear at higher operating pressures. Figure 4.10shows the storage heat exchanger profiles for a 34.5 MPa (5000 psia) supercritical receiver cycle. The configuration consists of only one salt storage tank combined with a 12.4 MPa (1800 psia) turbine cycle and a derated turbine throttle temperature of 510°C (950°F). The outlet supercritical steam temperature is 357°C (675°F).

Figure 4.9
PROPOSED ALTERNATE CYCLE

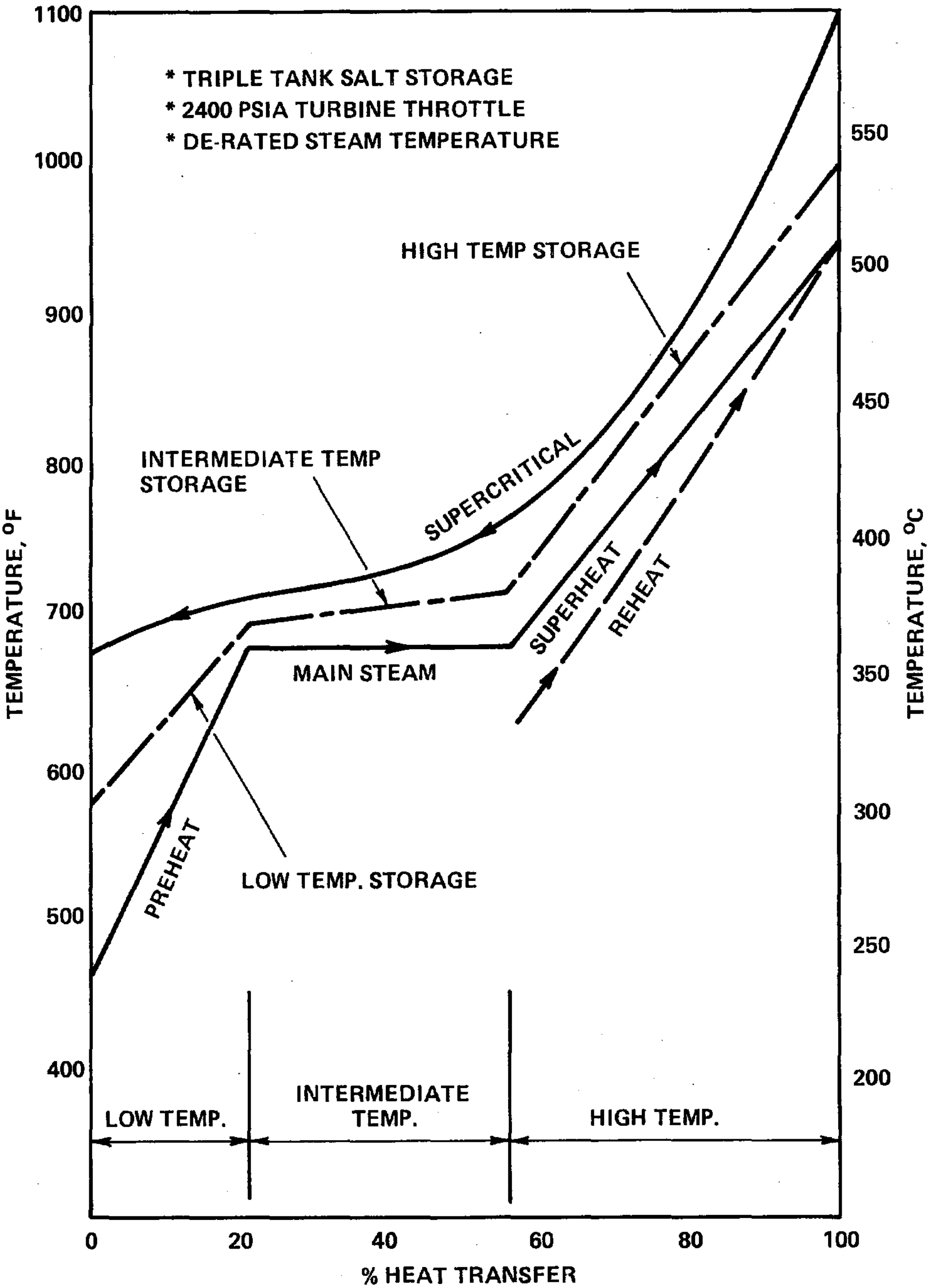

Figure 4.10
5000 PSIA SUPERCRITICAL CYCLE

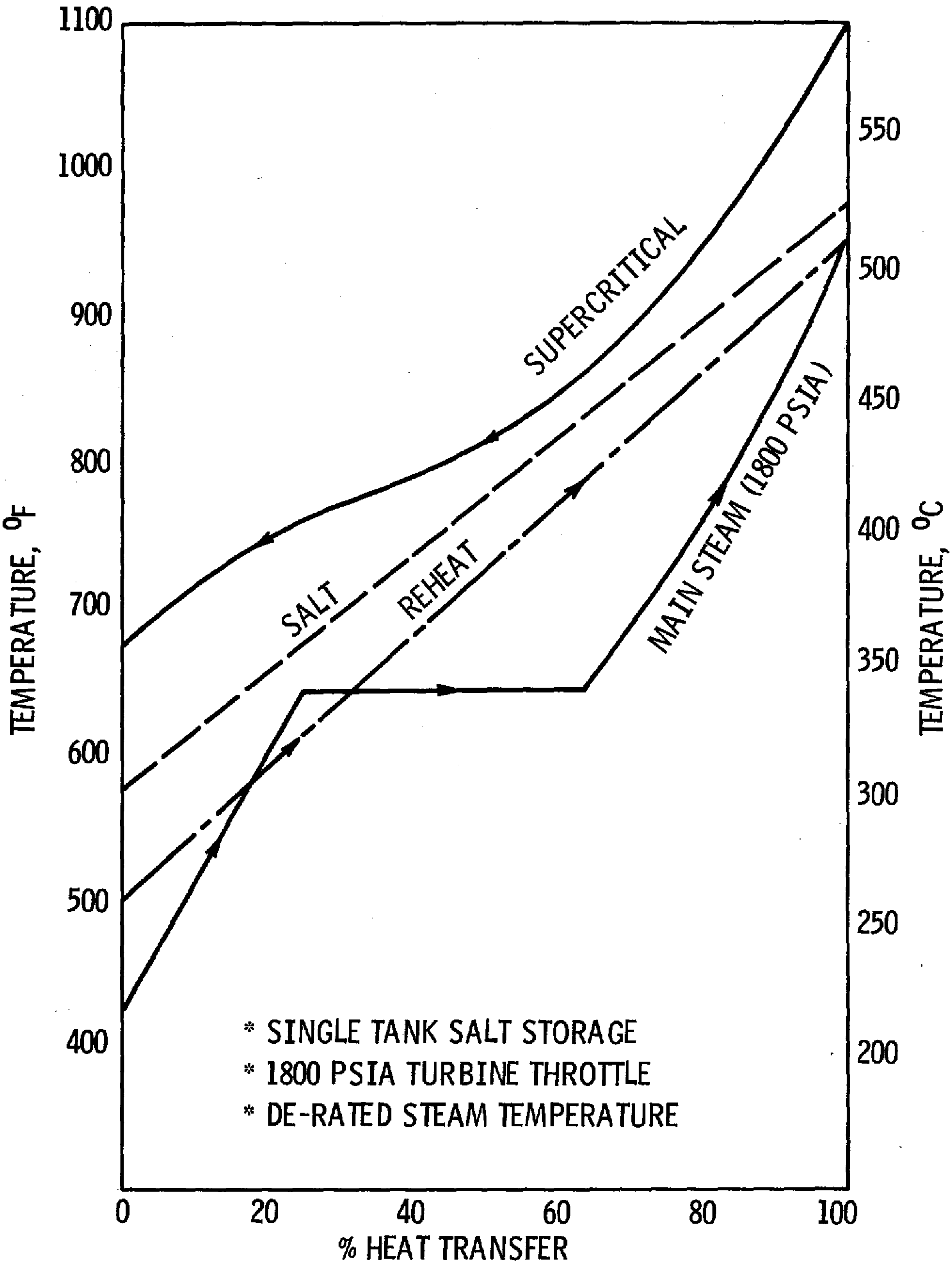

The re-heat inlet temperature has been lowered from 332^{o}C (630^{o}F) to 260^{o}C (500^{o}F) to minimize the pinch point between the re-heat and the molten salt. The reheat could be cooled in a feedwater heater before entering the re-heat exchanger.

The temperature profiles shown in Figure 4.10 are acceptable for efficient heat exchange. However, due to the higher operating pressure greater wall thickness in the receiver tube panels would promote higher tube crown temperatures. The design problems associated with higher metal temperatures must be weighed against the operational savings derived out of a single salt tank storage system.

4.3 Receiver Parametric Study

4.3.1 Overview--The supercritical receiver parametric study is based on the inlet and outlet conditions of the receiver in Cycle A. Cycle A is considered more conservative with regard to receiver parametrics than Cycle B, since the inlet receiver steam temperature in Cycle A is higher. The parametric curves presented in this section show where design limitations exist in the receiver.

The basic receiver configuration is presented in Figure 4.11. An external panel receiver is assumed. The receiver shape is cylindrical with the tube panels located around the circumference. A symmetric flux profile is assumed to exist radially around the north-south axis of the receiver. A trapezoidal flux profile is assumed to exist vertically along the tube panels.

Tube crown temperatures are sensitive to the flux intensity on the tube panels. The highest flux intensities encountered are on the north facing panel of the receiver. The north panel is thus the limiting panel with regard to tube crown temperature. The north panel also has the smallest diameter tubes (to minimize metal temperature) and the greatest steam flow. To this extent the north tube panel is also limiting with regard to overall receiver pressure drop. The receiver parametrics which show relationships between tube crown temperature, flux intensity, and pressure drop are subsequently based on analyses of the north facing panel.

Figure 4.11
SUPERCRITICAL RECEIVER LAYOUT

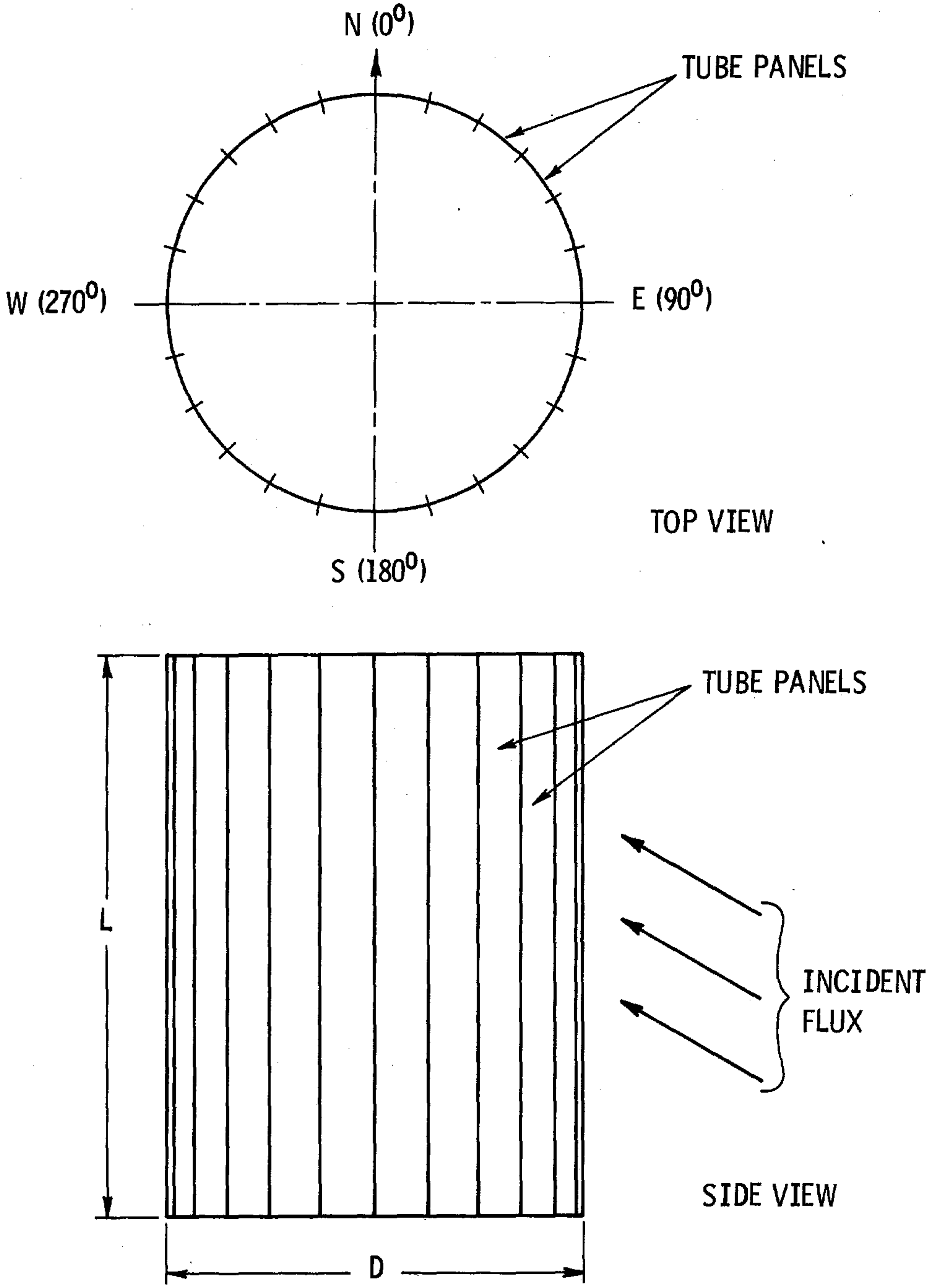

4.3.2 Flux Distributions--Several combinations of radial flux distribution and trapezoidal flux profiles were investigated. Due to the uncertainty in heliostat filed limitations, these flux profiles may not be reproducible.

The radial flux distributions investigated are shown in Figure 4.12. Distribution 1 is the base profile used in the subcritical parametric study (Section 3). Distribution 2 has the same integrated average flux. However, the maximum peak flux has been reduced from .85 to .72 MW/m^2 (270,000 to 230,000 $BTU/hr\text{-}ft^2$) on the north panel. Distribution 3 was derived from Distribution 1 by reducing the flux levels by half. The integrated average flux is .28 MW/m^2 (90,000 $BTU/hr\text{-}ft^2$). The lower average flux level requires increased receiver surface area for a given receiver thermal output.

The vertical flux profiles were investigated in Section 3 and are presented in Figure 3.6. Combinations of the radial and trapezoidal flux profiles were investigated to determine parametric effects on the receiver design.

Temperature and pressure drop analyses were performed using the STPP code developed previously and summarized in Appendix A. Table 4.2 presents the thermal analysis matrix and results summary for the north facing panel of the receivers designed using various combinations of flux profiles. This matrix is the basis of the supercritical receiver parametric study.

4.3.3 Metal Temperatures--Maximum metal temperatures occur on the tube outer surface at the tube crown. High tube crown temperatures promote metalurgical instability and a reduction in the creep resistance and fatigue life of the tube panel. Creep/fatigue interactions are not considered in this preliminary analysis.

Figure 4.12
RADIAL FLUX PROFILES

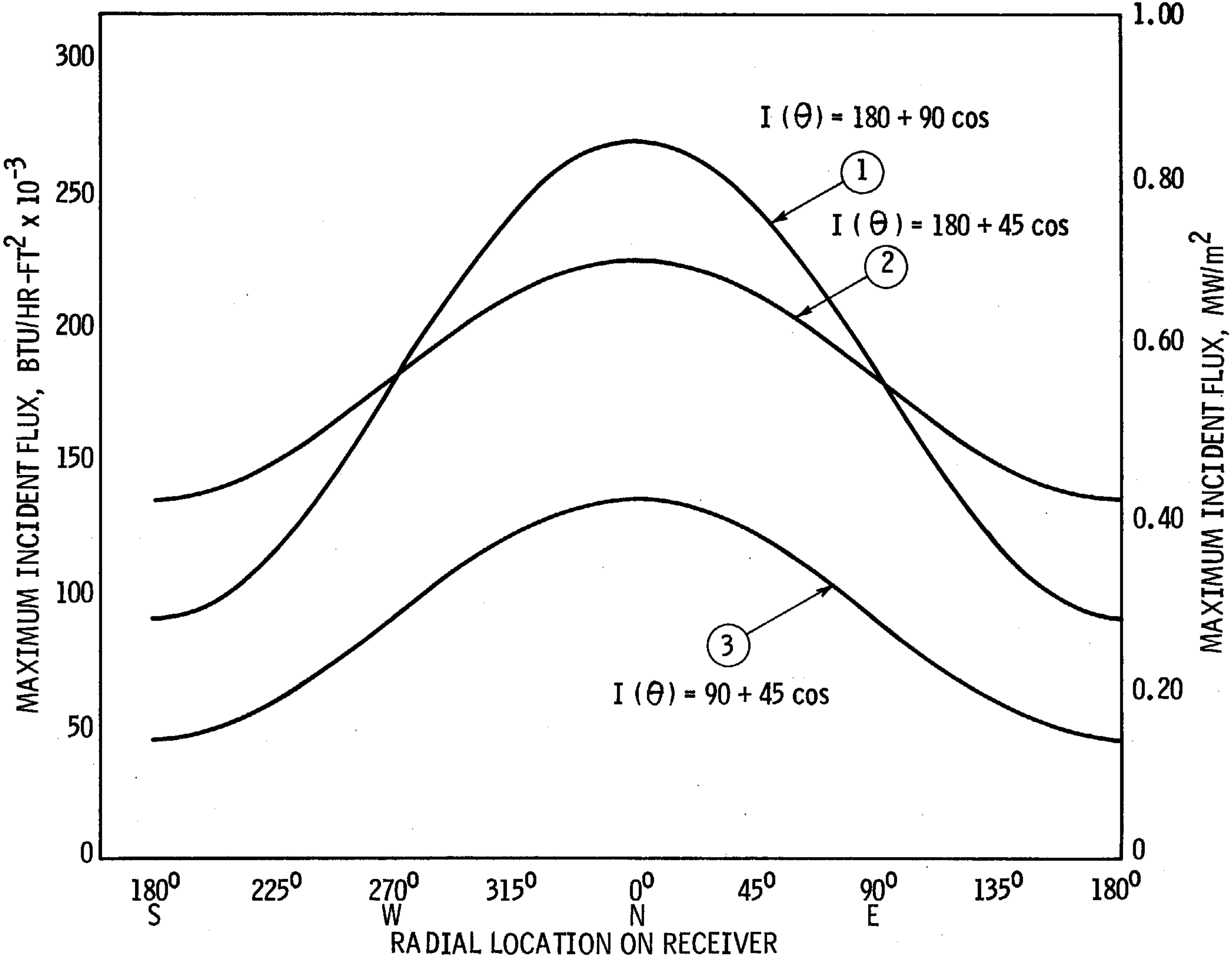

4-26

TABLE 4.2

MATRIX OF THERMAL ANALYSIS RUNS
AND RESULTS SUMMARY

Run No.	Flux Distribution	L/D Ratio	Tube OD cm (in)	Maximum Tube Crown Temp. °C (°F)	Overall Pressure Drop, MPa (psi)
1	1-A	1.5	3.81 (1.50)	895 (1643)	.255 (37.0)
2	1-B	1.5	3.81 (1.50)	884 (1623)	.248 (35.9)
3	1-C	1.5	3.81 (1.50)	844 (1552)	.259 (37.6)
4	1-C	1.0	3.18 (1.25)	808 (1487)	.245 (35.6)
5	2-C	2.0	1.91 (.75)	663 (1225)	1.585 (229.9)
6	2-C	1.5	3.81 (1.50)	800 (1472)	.194 (28.2)
7	2-C	1.5	1.91 (.75)	669 (1236)	1.074 (155.8)
8	2-C	1.0	1.91 (.75)	674 (1246)	.610 (88.5)
9	2-C	.5	1.91 (.75)	692 (1277)	.242 (35.1)
10	3-C	2.0	3.81 (1.50)	687 (1268)	.294 (42.7)
11	3-C	2.0	3.18 (1.25)	663 (1225)	.470 (68.1)
12	3-C	2.0	2.54 (1.00)	634 (1174)	.709 (102.9)
13	3-C	2.0	1.91 (.75)	614 (1138)	1.652 (239.6)
14	3-C	1.5	3.18 (1.25)	667 (1233)	.328 (47.5)
15	3-C	1.5	1.91 (.75)	619 (1147)	1.107 (160.6)
16	3-C	1.0	2.54 (1.00)	644 (1192)	.285 (41.4)
17	3-C	1.0	1.91 (.75)	624 (1155)	.632 (91.7)
18	3-C	.5	1.91 (.75)	632 (1170)	.250 (36.2)

Tube crown temperature is strongly dependent on the local incident heat flux at the tube surface. Figure 4.13 illustrates a typical relationship between flux level and tube crown temperature along the tube length. Crown temperature increases most rapidly in the increasing flux region of the vertical flux trapezoid. The crown temperature continues to rise in the constant flux region, and then falls off as the flux decreases towards the tube outlet.

There is a strong relationship between the tube crown temperature and the flux level in the increasing flux region of the trapezoid. Figure 4.14 shows test results from a variety of runs with different flux profile combinations. Tube crown temperature increases linearly with the incident flux level. The larger O.D. tubes show a greater slope due to larger tube wall thickness.

Figure 4.14 can be used to approximate flux limitations in the supercritical receiver. A maximum temperature line of 510°C (950°F) is super-imposed in Figure 4.14. This is the highest temperature allowed at the point where the maximum incident flux is attained on the tube. The point of maximum flux corresponds to the onset of the constant flux region on the vertical flux profile. An additional 139°C (250°F) temperature rise occurs along the tube in the constant flux region (approximately), to reach a limiting tube crown temperature of 649°C (1200°F). This temperature limit is somewhat arbitrary since it does not guarantee the fatigue life of the tube.

Figure 4.13
TYPICAL INCIDENT FLUX AND CROWN TEMPERATURE vs TUBE LENGTH

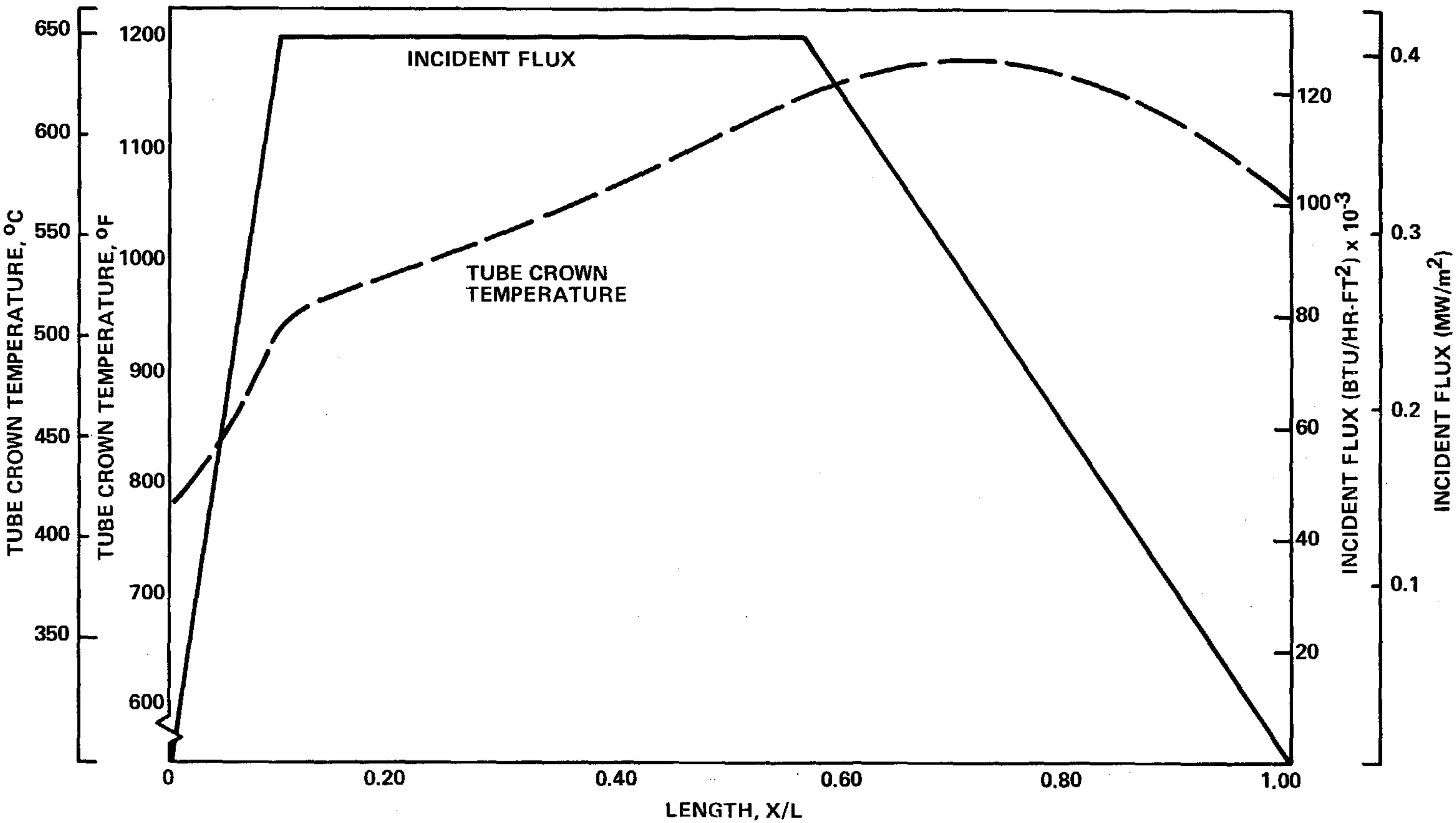

Figure 4.14
TUBE CROWN TEMPERATURE vs INCIDENT FLUX*

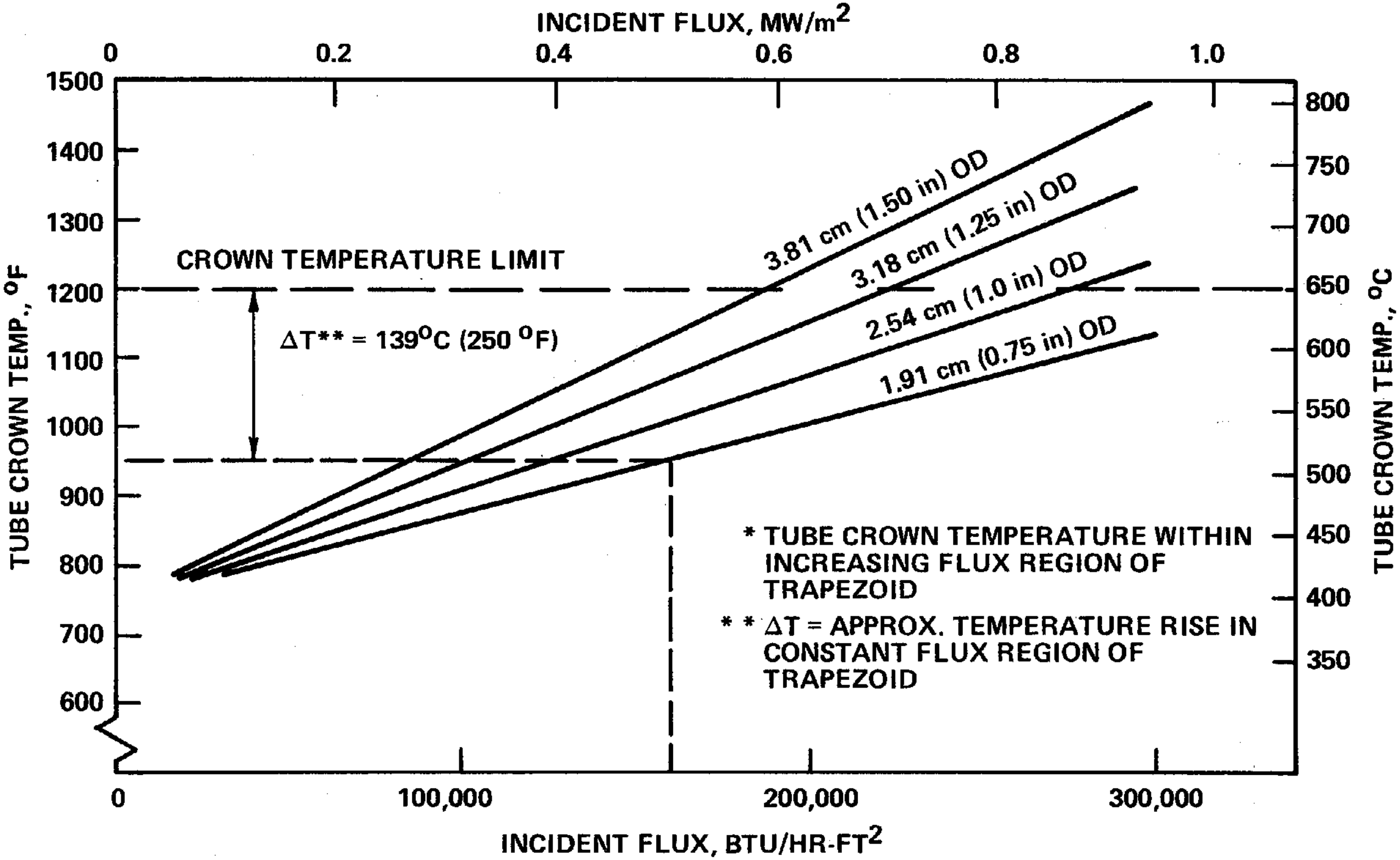

Each curve corresponding to a different tube size intercepts the limiting temperature of 510°C (950°F) at different incident flux levels. Figure 4.15 shows the intercept points plotted as the maximum allowable flux vs. tube diameter.

A design range is shown for the maximum peak heat flux and tube diameter. Boiler operating experience indicates that receiver tube sizes should not be less than 1.91 cm (.75 in) OD in a once through system. Smaller tubes could ultimately pose a problem with tube and orifice fouling.

From a design standpoint, Figure 4.15 can be used to match tube sizes with an allowable maximum incident flux. Smaller tubes can withstand higher incident flux. With the smallest recommended tube size of 1.91 cm. (.75 in.) OD tubes, the supercritical receiver would be limited to a maximum peak flux of about .52 MW/m^2 (165,000 $BTU/hr\text{-}ft^2$).

4.3.4 Pressure Drop--Minimizing the receiver pressure drop is important for lowering the required circulation pump head. Figure 4.16 shows friction head loss vs. mass velocity for various tube sizes in the supercritical receiver panels.

The overall tube panel pressure drop is dependent on the panel length. For a receiver of given thermal output, the panel length is a function of the receiver aspect ratio (L/D). Figure 4.17 presents overall pressure drop vs. aspect ratio for different size tubes. The pressure drop results shown in Figure 4.17 are for the flux distribution profiles 2-C and 3-C. There appears to be little effect of flux distribution on the panel pressure drop.

A generalized single phase pressure drop analysis was performed to calculate the pressure drop through any tube panel in the receiver. The resultant pressure drop relation is shown as Equation 4.1. A complete derivation of Equation 1 and the implied assumptions are presented in Appendix A.

Figure 4.15
MAXIMUM ALLOWABLE PEAK FLUX vs TUBE DIAMETER
IN THE SUPERCRITICAL RECEIVER

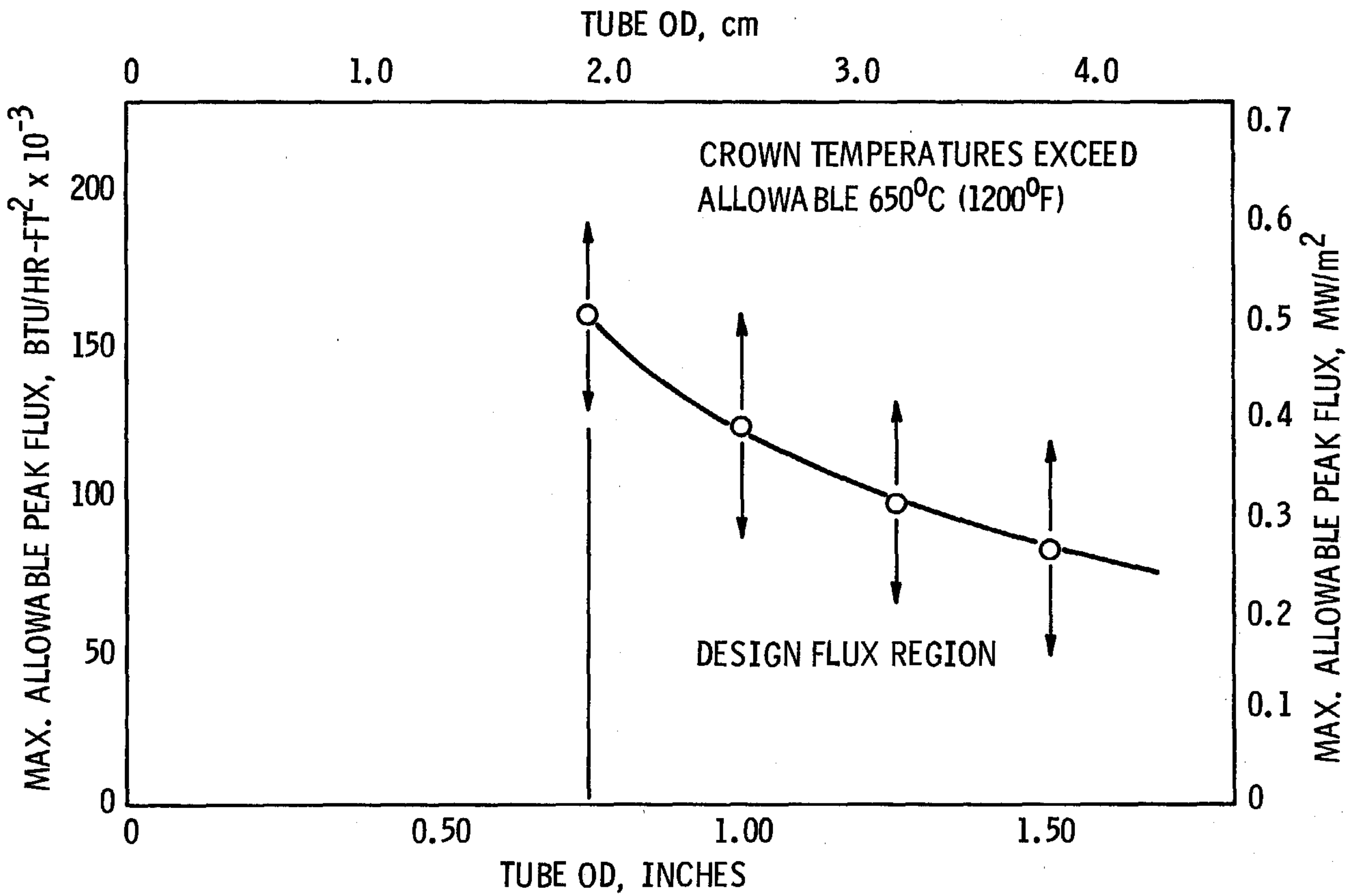

Figure 4.16
PRESSURE DROP vs MASS VELOCITY

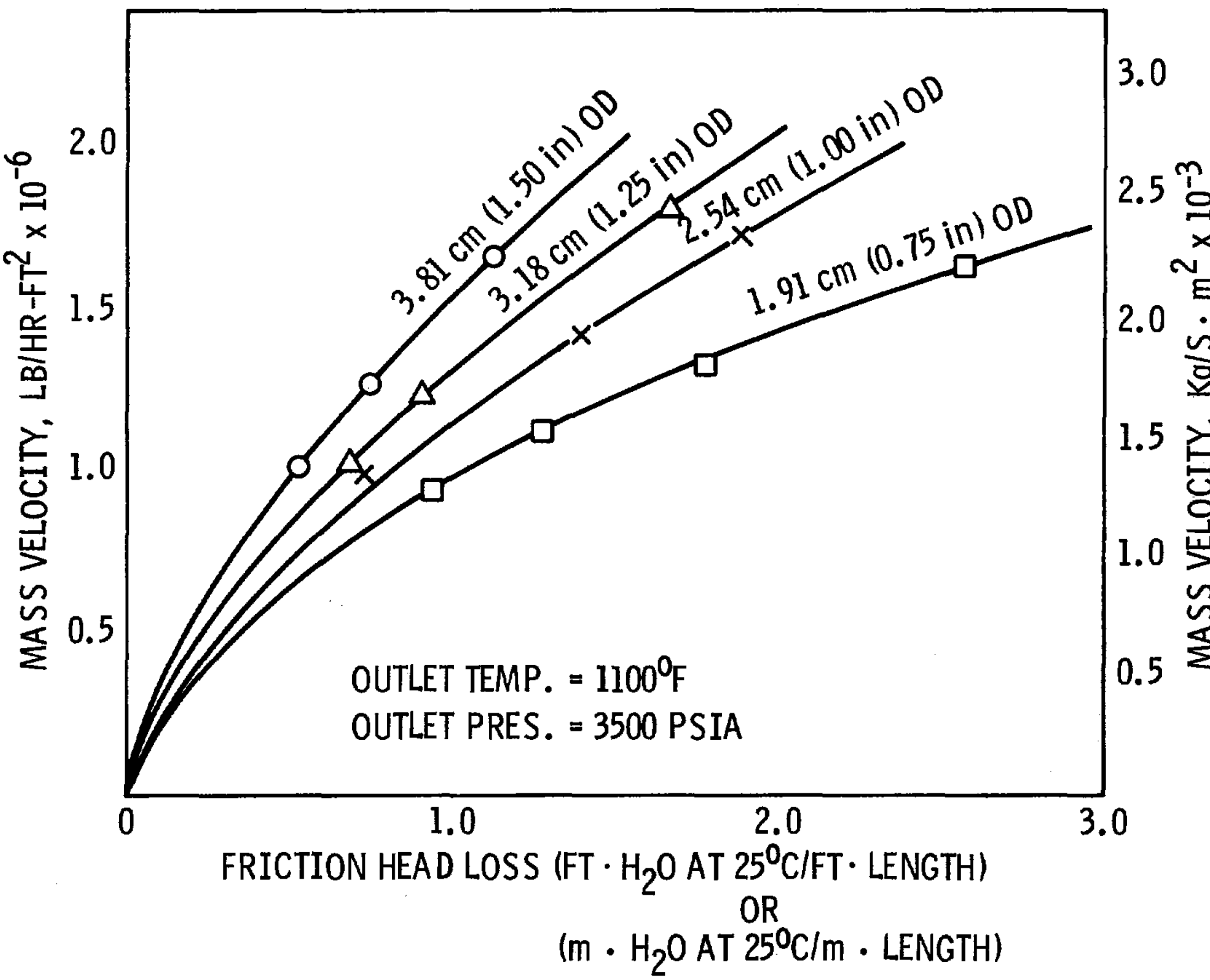

Figure 4.17
PRESSURE DROP vs L/D RATIO (NORTH PANEL)

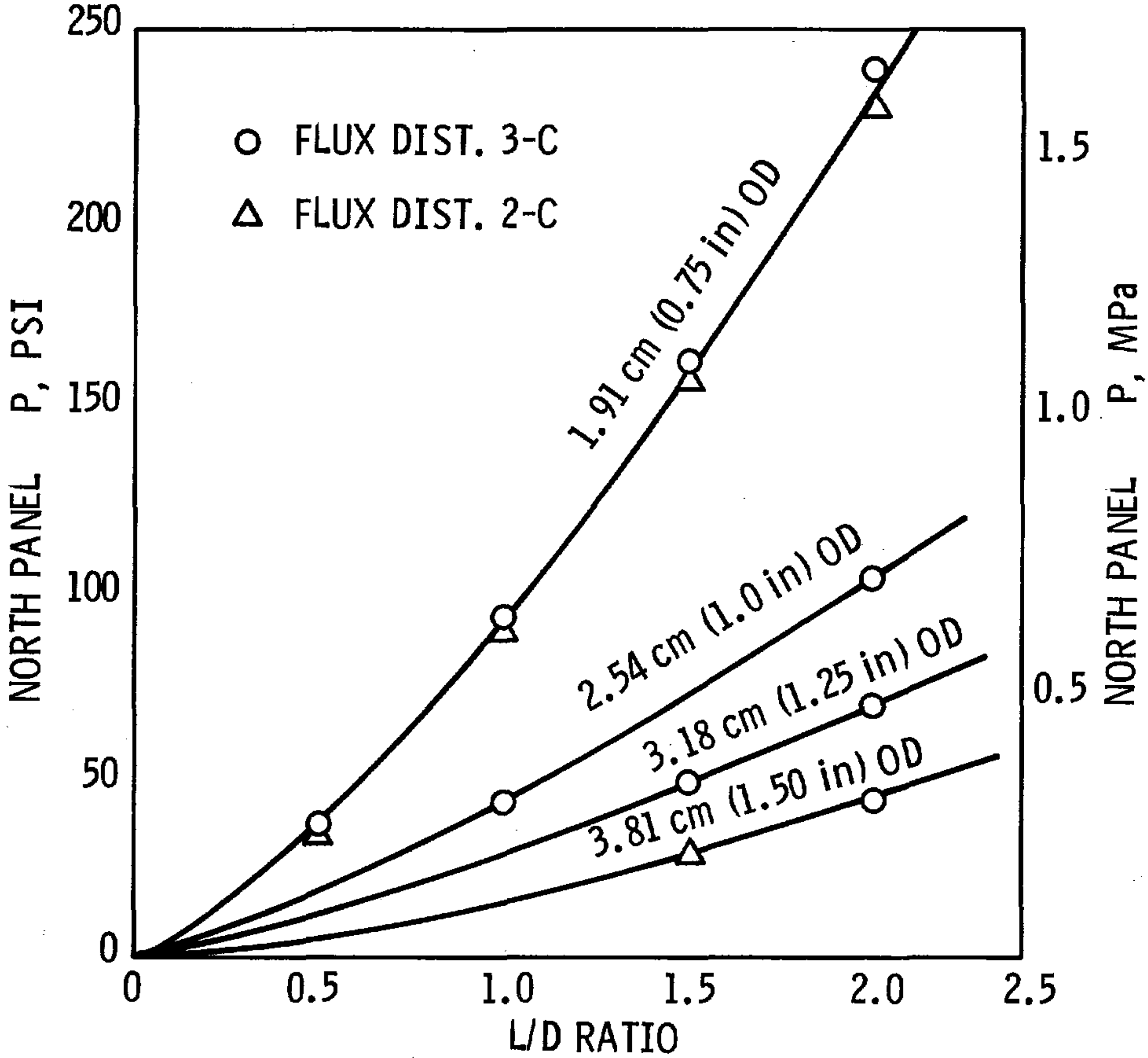

$$\Delta P_f = \frac{16\ f}{\alpha^2 \pi^4} \left(\frac{\bar{\eta}}{\eta}\right)^2 \left(\frac{d_o}{d_i}\right)^2 \left(\frac{D}{d_i}\right)^3 \left(\frac{L}{D}\right) \left(\frac{Q}{\Delta h\ D^2}\right) \left(\frac{1}{2g\rho}\right) \qquad (4.1)$$

The frictional pressure drop in any tube panel can be calculated in terms of the thermal and dimensionsl characteristics of the receiver, and in terms of the local flux intensity on the panel. Figure 4.18 shows Equation 4.1 in non-dimensional form for estimating the north panel pressure drop in a receiver with flux distributions 2-C and 3-C.

The relationship between the receiver aspect ratio and overall diameter can be expressed as:

$$\frac{L}{D} = \frac{1}{D^2} \times \left(\frac{Q}{\alpha \bar{\eta} \pi I}\right)^2 \qquad (4.2)$$

The non-dimensional curves shown in Figure 4.18 are intended for estimating frictional pressure drop in the north panel for various design conditions. Pressure drop estimations outside of the range of assumptions used in Figure 4.18 should be calculated directly from Equations 4.1 and 4.2.

4.3.5 Optimized Flux Profile Combination--The maximum allowable peak flux estimations shown in Figure 4.15 constrains the supercritical receiver design to a maximum north panel flux of somewhere near .52 MW/m^2 (165,000 $BTU/hr\text{-}ft^2$). On this basis the flux distributions 1-A, 1-B, 1-C, 2-A, 2-B, and 2-C are out of the range for design consideration in the supercritical receiver.

Table 4.3 shows the effect of the vertical flux profile on the maximum tube crown temperature. Profiles A and B result in the highest tube crown temperature. Profile C yields a maximum tube crown temperature about 75° less than Profiles A and B.

Figure 4.18
NON-DIMENSIONALIZED FRICTION PRESSURE DROP

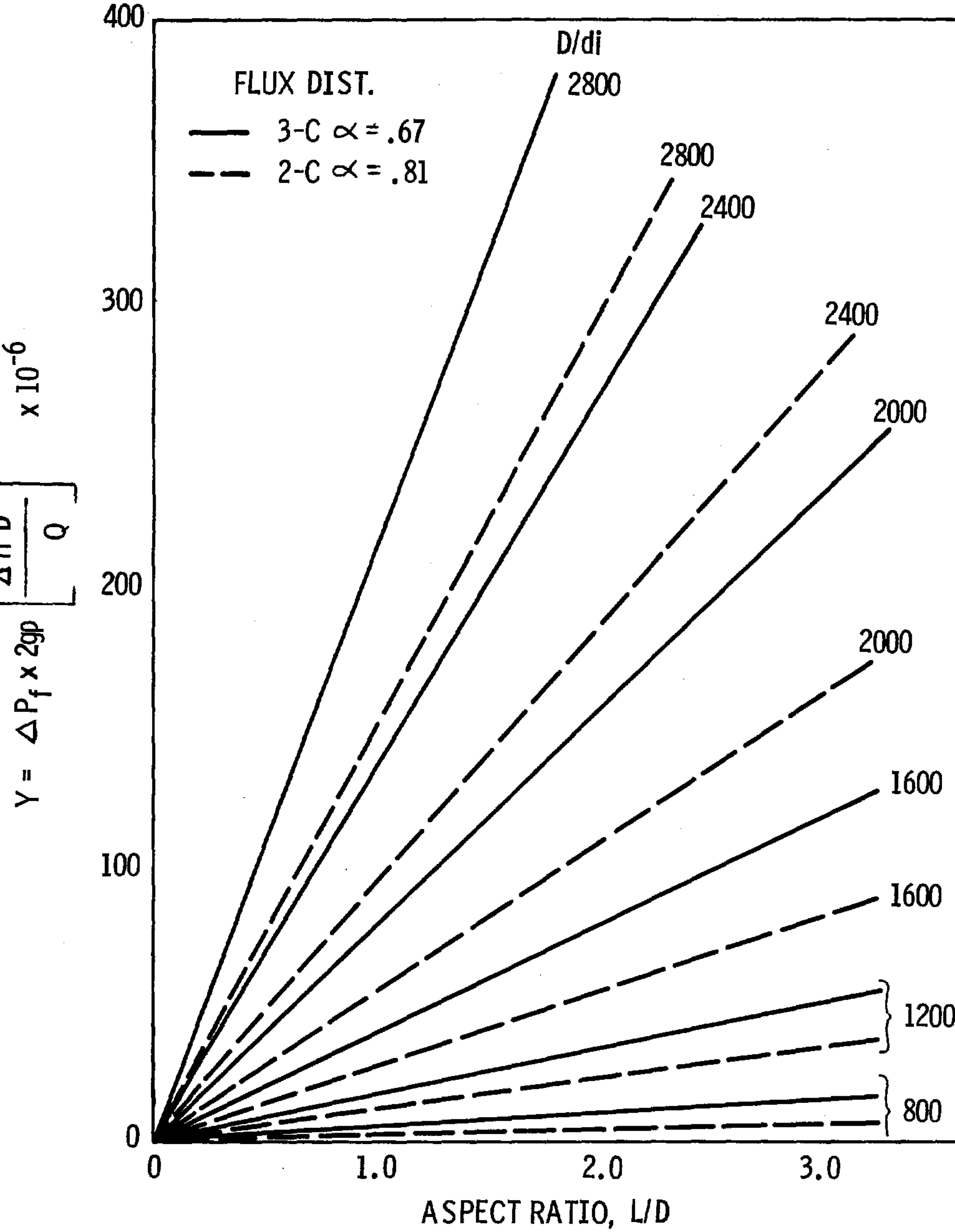

TABLE 4.3

COMPARISON OF
MAXIMUM TUBE CROWN TEMPERATURES*

Run No.	Flux Distribution	T_{CROWN} °C (°F)
1	1-A	895 (1643)
2	1-B	884 (1623)
3	1-C	844 (1552)

*L/D = 1.5-2.0
Tube OD = 3.81 cm (1.50 in.)
Panel ΔP < .276 MPa (40 psi)
Outlet Temp. = 593°C (1100°F)

Profile C is the best vertical profile for minimizing tube crown temperature. Based on this result it appears that an optimum vertical flux profile is one which exhibits rapidly increasing flux near the panel entrance. The incident flux should begin decreasing from the maximum flux somewhere near the tube panel mid-point. Effectively the normalized flux profile should be shifted away from the tube panel exit and towards the entrance where bulk steam temperatures are the lowest.

Based on the results of parametric analyses, flux profile 3-C may be satisfactory for supercritical receiver design within the specified metal temperature limitations.

Figure 4.19 shows panel absorption efficiency vs. length for flux profile 3-C. An average absorption efficiency of 85.1 percent is indicated.

Variations of tube crown temperature with length along the tube is shown in Figure 4.20. Tube crown temperature increases most rapidly in the increasing flux region, and then increases more slowly in the constant flux region. A maximum tube crown temperature of 624°C (1155°F) is shown.

Figure 4.21 shows variations in temperature differentials between the tube crown and bulk steam temperatures. Thermal stresses developed in the tube are a function of crown/fluid temperature differentials. The maximum differential along the tube length is nearly 111°C (200°F).

4.4 Conceptual Receiver Design

A preliminary conceptual receiver design has been developed based on the Cycle B design conditions (Figure 4.7), and flux profile 3-C. This design is preliminary since additional analyses in the areas of creep resistance and fatigue life of the tube panels need to be performed.

Figure 4.19
ABSORPTION EFFICIENCY vs PANEL LENGTH

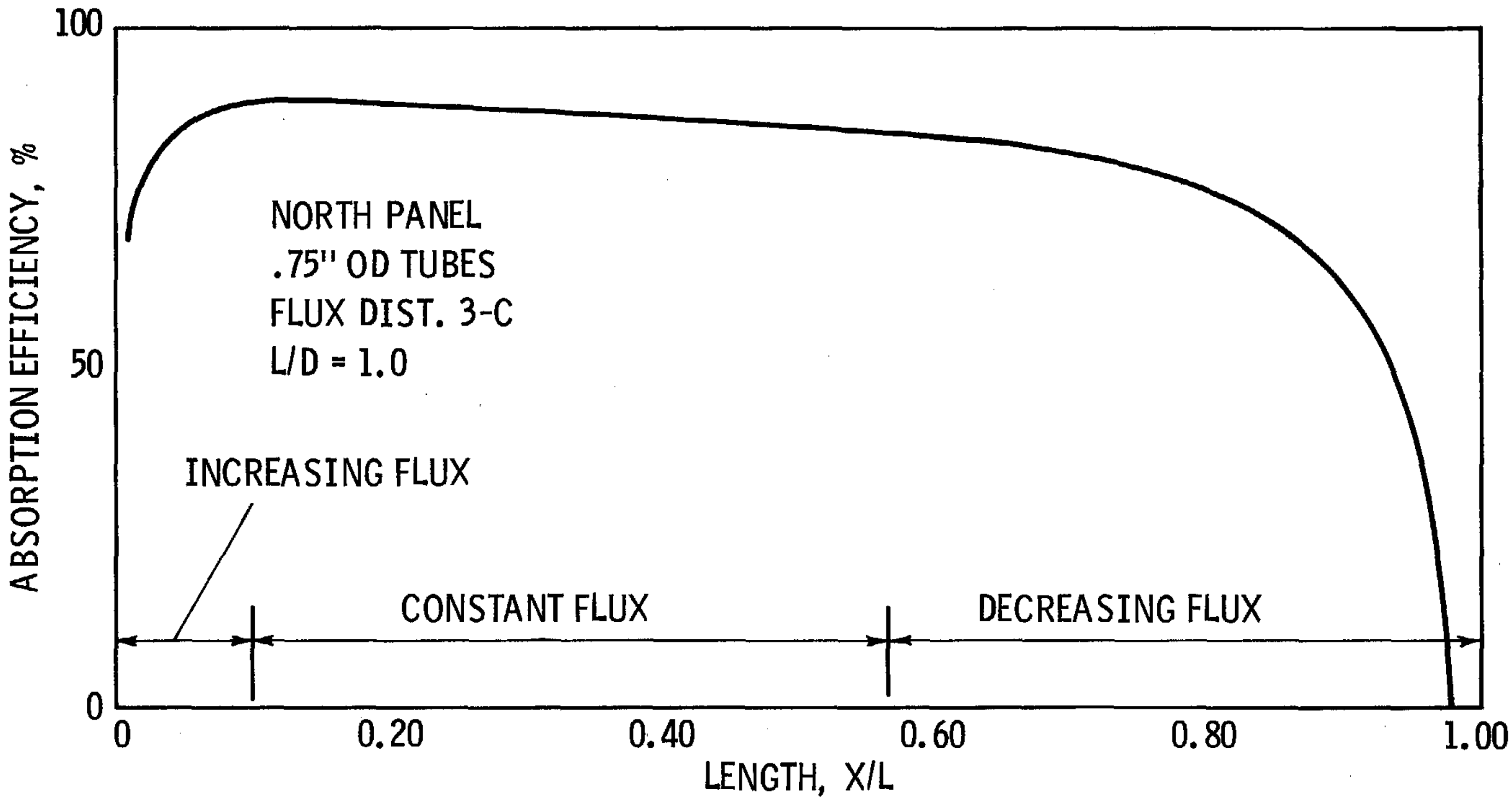

Figure 4.20
TUBE CROWN TEMPERATURE vs PANEL LENGTH

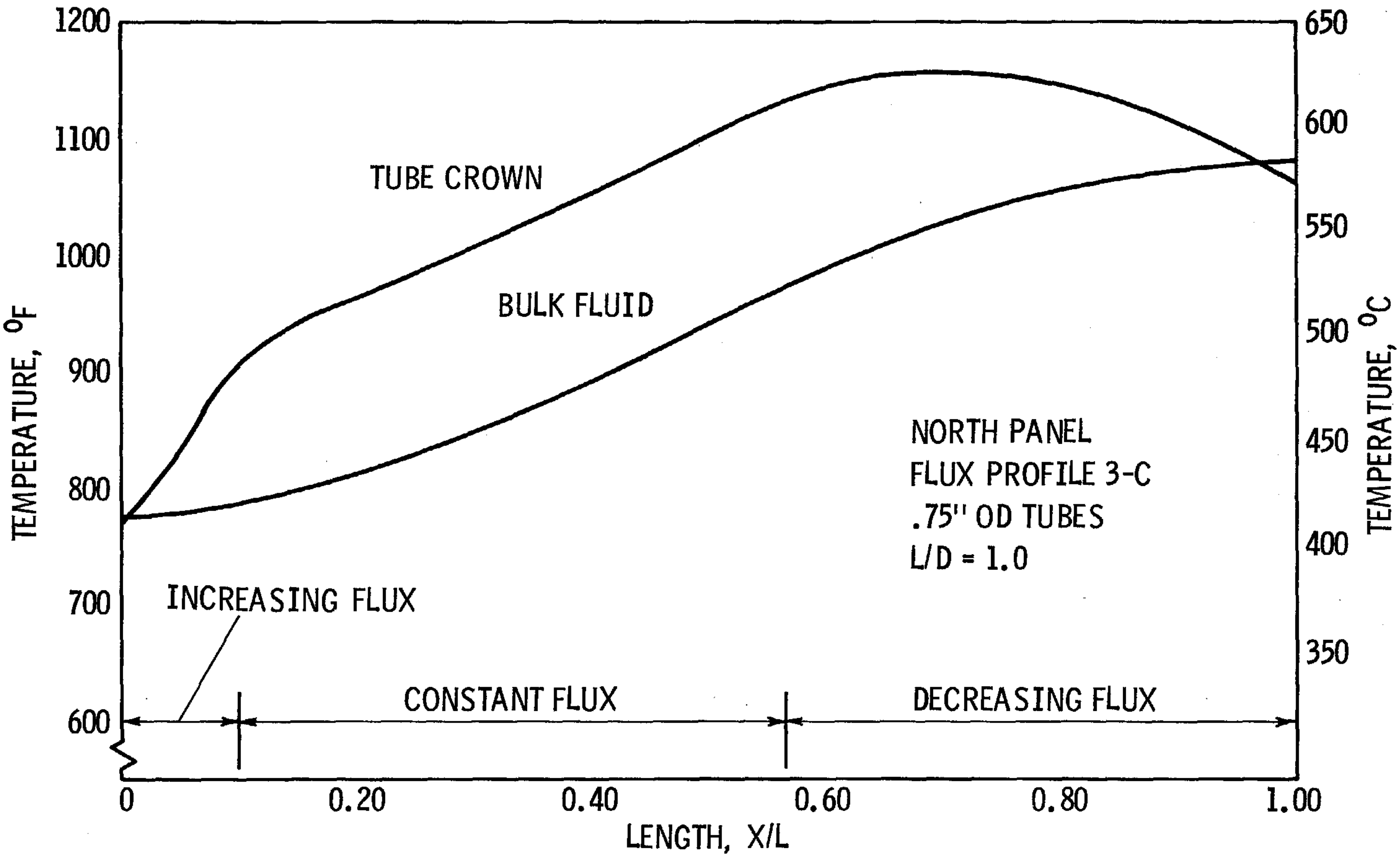

Figure 4.21
TUBE TEMPERATURE DIFFERENTIAL vs PANEL LENGTH

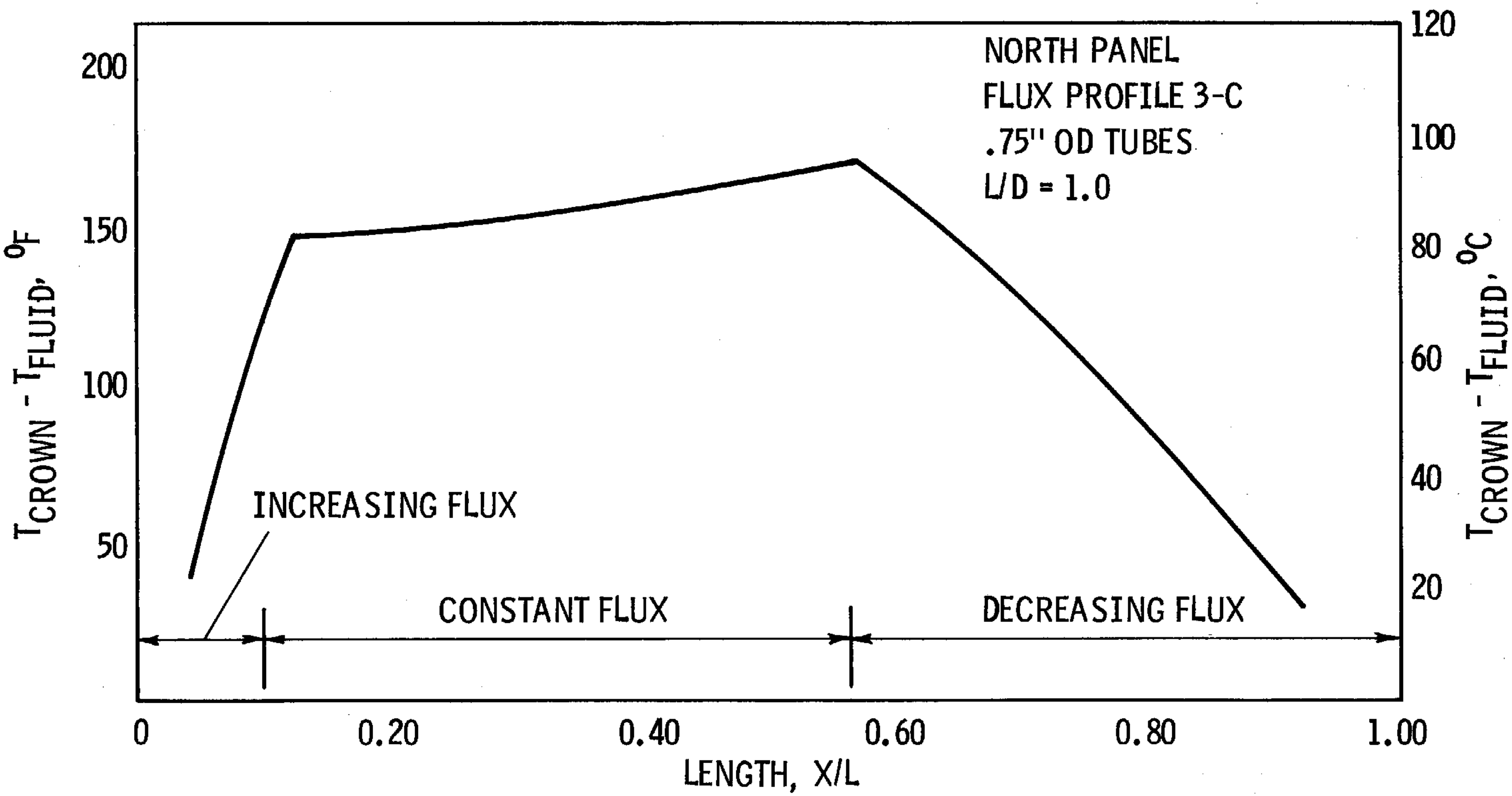

A receiver aspect ratio (L/D) of unity was chosen for a design basis. The primary concern with selecting an L/D is the overall receiver pressure drop, which should be minimized. A larger L/D increases the receiver pressure drop. However, the inside film coefficient also increases with an increasing L/D, and subsequently maximum tube crown temperatures are reduced. Figure 4.22 shows the trade-off between pressure drop and tube crown temperature as the L/D is varied.

The conceptual supercritical receiver has a length and diameter equal to 33.28m (109.2 ft). There would be 30 parallel panels located on the circumference of the cylindrical receiver. Each panel would have a width of 3.99m (11.44 ft). Table 4.4 presents a summary of the preliminary conceptual design characteristics.

The tube size chosen is 1.91 cm. (.75 in.) OD which is the minimum recommended size based on fouling and corrosion considerations in a once through receiver. The tube material would be TP-316H stainless steel. It is emphasized that the creep resistance and fatigue life of this material at maximum tube crown temperatures approaching 1160^{o}F requires further analysis.

The receiver circulation pump for the receiver design can be supplied by a standard boiler feed pump with some modifications to the suction casing. The pump requirements were outlined in Table 4.1.

The overall absorption efficiency of the supercritical receiver ranges near 84-85 percent. Relative to a sub-critical water/steam receiver of similar thermal output the supercritical receiver exhibits lower overall absorption efficiency for several reasons. The most important effect on absorption efficiency is the average flux level on the receiver. The receiver size is effectively doubled by designing the receiver for flux profile 3-C as opposed to flux profile 1-C. By designing for a lower flux level, absorption efficiency is sacrificed.

Figure 4.22

TUBE CROWN TEMPERATURE AND RECEIVER PRESSURE DROP vs RECEIVER ASPECT RATIO

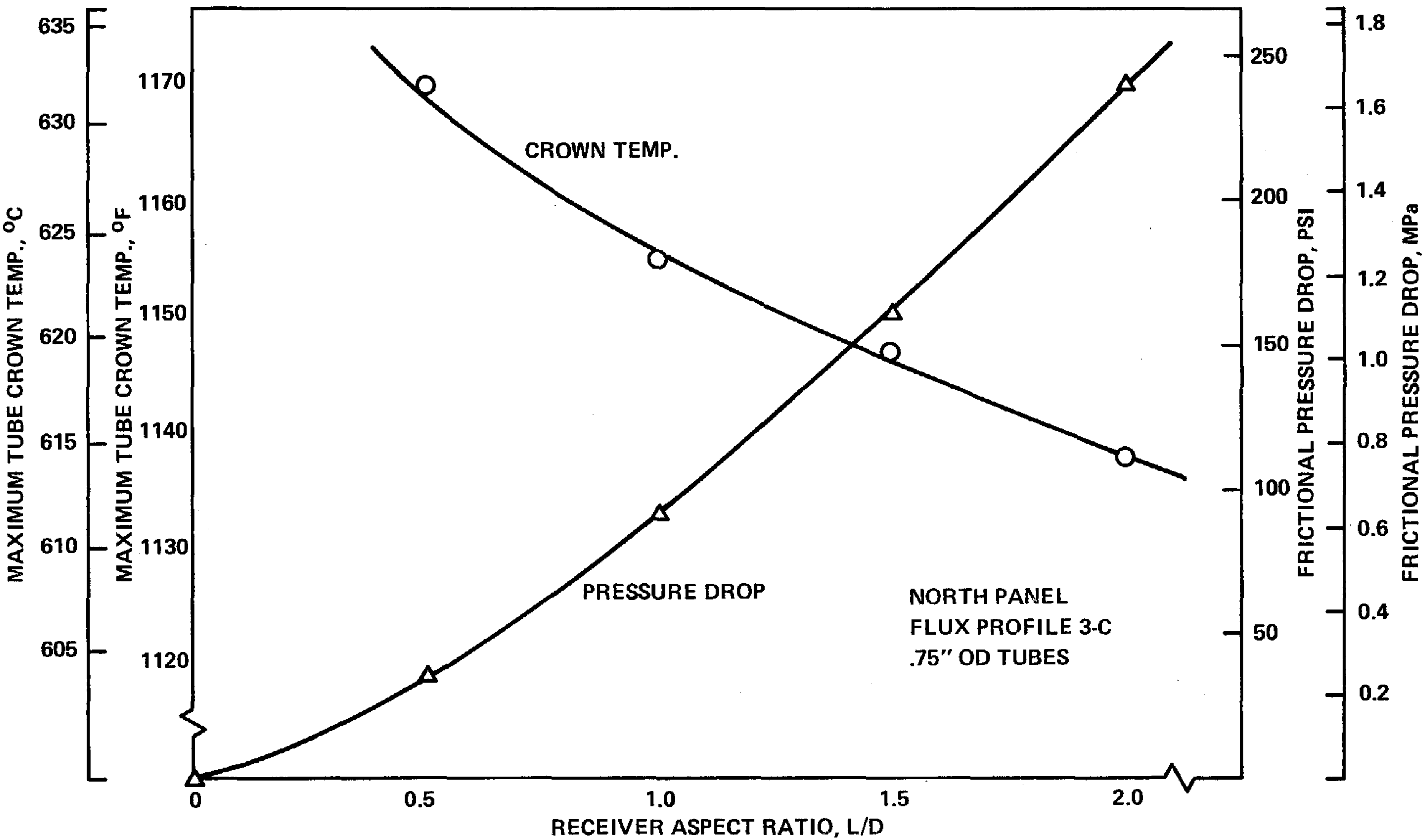

TABLE 4.4

Preliminary Design Characteristics of a Supercritical Receiver

Nominal Plant Rating, MW	200
Solar Multiple	1.5
Supercritical Steam Flow, kg/hr (lb/hr)x10^{-6}	1.456 (3.209)
Outlet Temperature, ^{o}C (^{o}F)	593 (1100)
Outlet Pressure, MPa (psia)	24.1 (3500)
Heat Absorbed, KJ/hr (BTU/hr)x10^{-6}	2610 (2474)
Flux Distribution	3-C
Maximum Incident Flux, MW/m^2 (BTU/hr-ft^2)	.43 (135,000)
Overall Surface Area, m^2 (ft^2)	3,480 (37,460)
Receiver Height, m (ft)	33.3 (109.2)
Receiver Diameter, m (ft)	33.3 (109.2)
Aspect Ratio	1.0
Approx. Tower Height, m(ft)	268 (880)
No. of Panels	30
Overall Absorption Eff., %	85
Tube OD, cm (in)	1.91 (.75)
Tube ID, cm (in)	1.30 (.59)
Number Tubes/Panel	183
Panel Width, m (ft)	3.49 (11.44)
Tube Material	TP-316H (stainless)
Nominal Pressure Drop, MPA (psi)	.689 (100)
Maximum Tube Crown Temp., ^{o}C (^{o}F)	624 (1155)

Another important factor relating to overall absorption efficiency is the once through nature of the receiver. Each once through parallel panel in the receiver will see an 593°C (1100°F) outlet steam temperature. Compared to a water/steam receiver, the supercritical receiver will exhibit significantly higher average metal temperatures resulting in greater back radiation and convection losses.

4.5 Summary and Conclusions

A preliminary cycle evaluation and parametric analysis was performed to scope out the feasibility of a supercritical solar central receiver. The following is a summary of the major results and conclusions of the study:

a) Two conceptual supercritical cycles were presented. Cycle A utilizes a single salt storage tank coupled to at 16.5 MPa (2400 psia) and 538°C (1000°F) turbine cycle. The circulation pump requirements in Cycle A are out of the range of present standardized pump design.

   Cycle B is a high and low temperature salt storage system coupled to an 12.4 MPa (1800 psia) and 538°C (1000°F) turbine cycle. Discussions with pump manufacturers indicate that a standard design boiler feed pump could fill the pump requirements dictated by this cycle.

b) The thermal storage heat exchangers are limited by pinch points developed from non-linear temperature/enthalpy characteristics in both the main turbine steam and supercritical receiver steam.

c) Several alternatives were presented to explore options in the cycle layout. These alternatives included 1) supercritical re-heat after the circulation pump, 2) multiple salt tank storage, 3) derated turbine throttle temperature, 4) eutectic salt storage, and 5) increased supercritical operating pressure.

d) A parametric study was performed based on the receiver operating conditions in Cycle A. Flux distributions, tube crown temperature and pressure drop were explored in detail for different receiver designs. Tube crown temperature and pressure drop data were generated using an in-house computer program designed to perform tube panel thermal analyses.

e) Results of computer analyses were used to generate incident flux and tube size limitations in the receiver design based on a maximum allowable tube crown temperature of 648°C (1200°F). At a tube size of 1.91 cm. (.75 in.) OD the maximum allowable peak flux is about .52 MW/m^2 (165,000 $BTU/hr\text{-}ft^2$).

f) The minimum recommended tube size for the supercritical receiver is 1.91 cm (.75 in) OD based on limitations imposed by tube corrosion and fouling in a once through unit.

g) It is desirable to shift the incident flux under the vertical profile towards the lower half of the tube panel where bulk steam temperature is the lowest. This reduces the maximum crown temperature on the tubes.

h) Flux distribution 3-C is the only combination of radial and trapezoidal profiles which limits maximum tube crown temperature to less than 648°C (1200°F).

i) A generalized receiver pressure drop correlation was presented. The correlation can be used to develop the relationship between the frictional pressure drop in the tube panels and variables such as flux level, receiver aspect ratio, tube size, etc.

j) It is desirable to design the supercritical receiver at an aspect ratio (L/D) of greater than unity to effectively increase the inside film coefficient thereby reducing tube crown temperatures. Increasing the L/D however increases the pressure drop in the receiver and thus a higher L/D can become limited by circulation pump head and capacity. The preliminary conceptual receiver design is for an L/D equal to unity due to pressure drop limitations.

k) A fatigue life assessment must be performed to evaluate tube panel life expectancy in the preliminary conceptual design.

5. Conceptual Design and Cost/Performance Estimates

5.1 Introduction

5.1.1 System Requirements

This project has been limited to the receiver sub-system design. The preferred design is a Category II, subcritical, recirculation, drum-type electric generation, and master control, sub-systems are somewhat different in detail from the once-through single pass design. These requirements are identified below:

1) Steam Turbine--A reheat turbine requires the appropriate flow of steam at the particular temperature and pressure of the selected steam cycle, plus the required reheat flow and steam conditions. Turbines usually require constant steam temperature over the upper half of the load range. Steam must be supplied from either the receiver, storage, or a combination of the two. When operating from storage alone, the high pressure turbine stage is idle, as steam pressure generated from storage is not high enough to be admitted to the high pressure unit.

2) Receiver Sub-System--Basically, a boiler requiring a design that accepts solar heat flux from the collector field and transfers it to the steam in an efficient manner, with a 30-year lifetime based on creep-fatigue damage due to the transient and cyclic nature of the solar insolation. This requirement is based on 10,000 diurnal cycles plus some undefined cloud cycles.

The high temperature portions of the superheater and reheater are critical areas for the creep-fatigue damage. Materials and designs of these sections have been selected to minimize the thermal stresses due to the one-sided heat flux. Allowable creep-fatigue cycles due to this phenomena were calculated to be 30,000 based on a conservative analysis. Start-up and shut-down transients can be controlled so that the critical areas identified throughout the plant do not exceed a calculated temperature change rate. In addition, this boiler must be mounted atop a tower and survive dynamic loads including wind and seismic at the particular site.

This receiver design requires a control system which, in addition to its own internal loops, must regulate the heliostat field under certain conditions, to satisfy the receiver requirements. The receiver design requires some control of the collector sub-system as a conventional boiler requires a control of the fuel firing system to meet the requirements of the boiler. The control system will be described conceptually in the next section.

3) Collector Sub-System--For this design of Advanced water/steam receiver, the collector field is required to assist the receiver in its function, rather than merely accept and concentrate whatever insolation is available. Due to the reheat requirements of the system, a portion of the collector field is required to be solely dedicated to the reheater as if it were a separate receiver. In addition, under certain conditions during start-up the distribution of heat required by the receiver is different than that needed at full operating power. Receiver integrity requries selective control of portions of the collector field during this time, and also during certain cloud transients and emergency conditions.

4) Master Control Sub-System--This system integrates the operation of various sub-systems above to achieve the required overall plant performance objectives. The receiver loop control system must react to and provide inputs to the master control sub-system. A definition of the proposed receiver control requirements is contained in the next section.

5.1.2 System Performance and Control Requirements

The receivers designed under this project were sized to provide design point (full load) conditions to meet the proposed steam cycle conditions of temperature and pressure. The power ratings were selected to cover a range of power ratings to meet a combination of turbine-generators and solar storage requirements. Extensive partial load performance calculations were not deemed necessary. The receiver controls requirements will be defined in a general way.

Some performance requirements are unique for this application, and differ significantly from those of a once-through design. Solar plants, in general operate differently from conventional plants because of the transient nature of solar insolation. As an example, most fossil-fired plants require that the boiler follow the turbine load demand, and maintain constant steam temperature over the upper half of the load range. The boiler, in turn demands the required power input from the fuel firing system.

In a solar plant, this may be the requirement part of the time, but during other times, in order to gain the maximum benefit from the available insolation, the system must respond primarily to the input power (solar insolation) and not the electrical generation demand. The optimization of these control modes is beyond the scope of this project.

In order to meet the receiver performance requirements, the controls for the receiver are shown schematically in Figure 5.1. These sub-loop control systems are as follows:

Figure 5.1
CONTROL SYSTEM

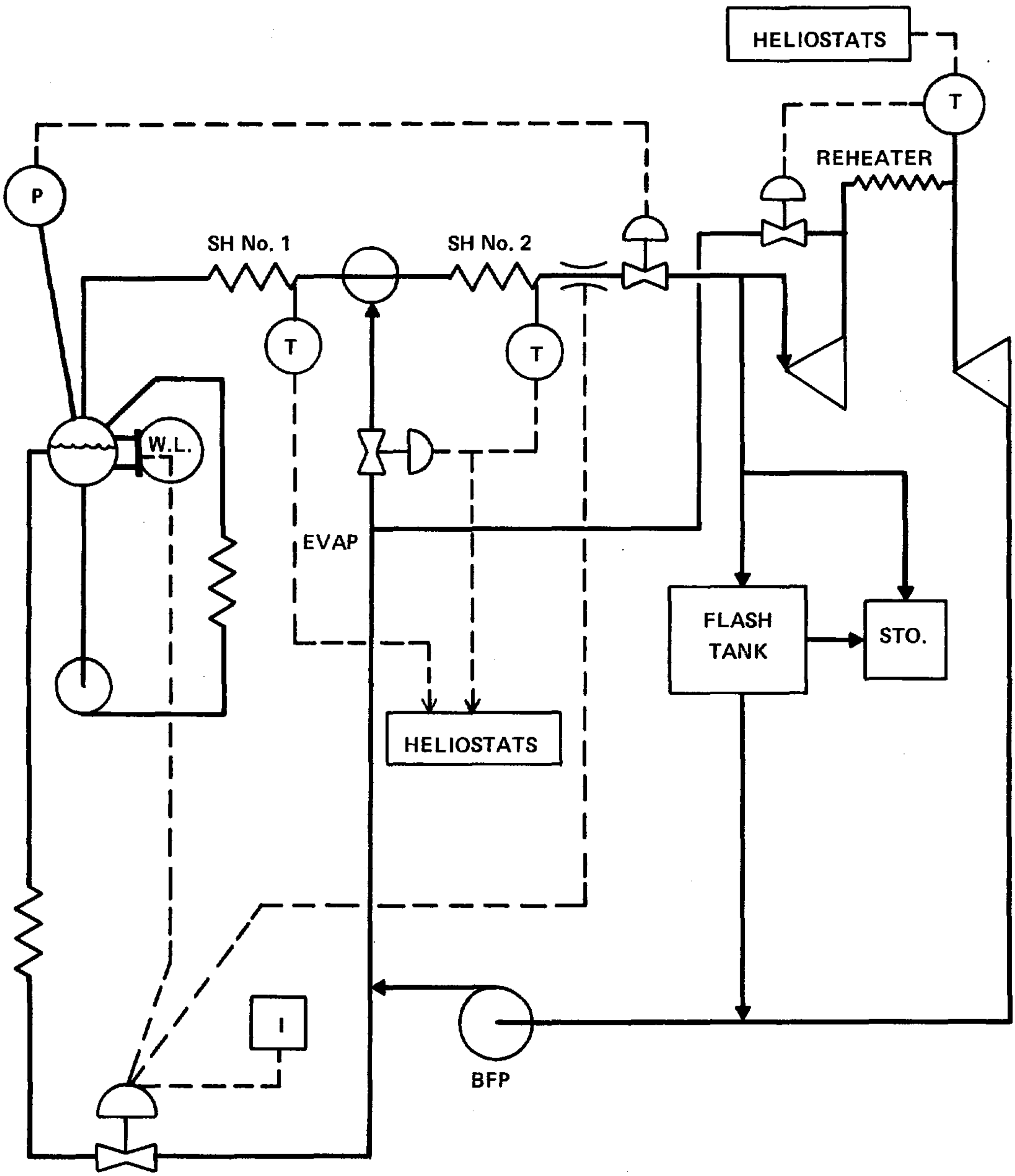

5.1.2.1 Receiver Pressure Control--In the solar plant, insolation must be used when available and is not always available on demand, or is wasted if modulated as in a conventional firing system. In this case, the drum pressure control is revised. It is proposed to modulate the steam flow to match the output energy to that coming from the collector field. This system requires a steam control valve at the superheater outlet, which responds to a pressure signal from the drum. This valve defines the limit of the receiver sub-system. Beyond this valve, steam is delivered either to the turbine or the storage, or both, by proportioning valves. Although not a part of the control system, the required safety valves on the drum and superheater, as dictated by the ASME Boiler Code, will be available to protect the pressure parts from over-pressure during an upset condition.

5.1.2.2 Receiver Steam Temperature Control--At the design point, the final superheat outlet temperature is obtained by the superheater surface if the insolation is as assumed. Interstage spray desuperheaters are provided to control final superheat temperature if the heat absorption is too high. It is not planned to utilize spray water continuously at the full load design point. The spray is intended to be a trimming operation. In addition to spray desuperheating, it will be necessary to have some control over a portion of the collector field. It may be necessary to slew certain heliostats to protect the superheater panels under conditions of cloud transients and when operating at lower pressures. Start-up conditions will be described later. As shown in Figure 5.1 the first stage superheater will require a metal temperature control to slew heliostats for over-temperature protection.

5.1.2.3 <u>Drum Water Level Control</u>--This sub-loop is similar to a conventional plant, and will probably consist of a 3-element controller. The feedwater control valve responds to the drum water level as a primary signal, plus it will require a signal from the steam flow and from the feedwater flow rate measurements as a feed-forward anticipatory type of control function.

5.1.2.4 <u>Start-up and Shut-down Transients</u>--During start-up, the receiver pressure will be increased along with the final temperature along lines indicated on Figure 5.2, which shows the steam state points on a pressure vs. enthalpy diagram. It becomes apparent that at pressures less than the design point, the balance between the heat absorption for the economizers, evaporator, and superheater changes. At low pressures, the evaporator requires a larger percentage of the total absorption. In drum-type units, fixed state points are required. Thus, during start-up, the collector field must be biased to adjust the heat absorption distribution as needed. This may not be matched, so certain heliostats will have to be slewed to accommodate the start-up. Similar actions are needed during a regular shut-down.

The rate of start-up/shud-down will be controlled by the critical component in the system regarding thermal stresses, varying with time. The superheater outlet lead was checked to determine the maximum rate of temperature rise. This is the heaviest wall pipe in the superheater, and appears to be the component which would limit the start-up rate. An initial guess of 400°F/hr. produced approximately 30,000 cycles which is adequate for normal diurnal cycles. A 222°C (400°F/hr) average rate requires 3 hours to achieve full temperature. No problem with the evaporator is forseen due to the forced re-circulation design.

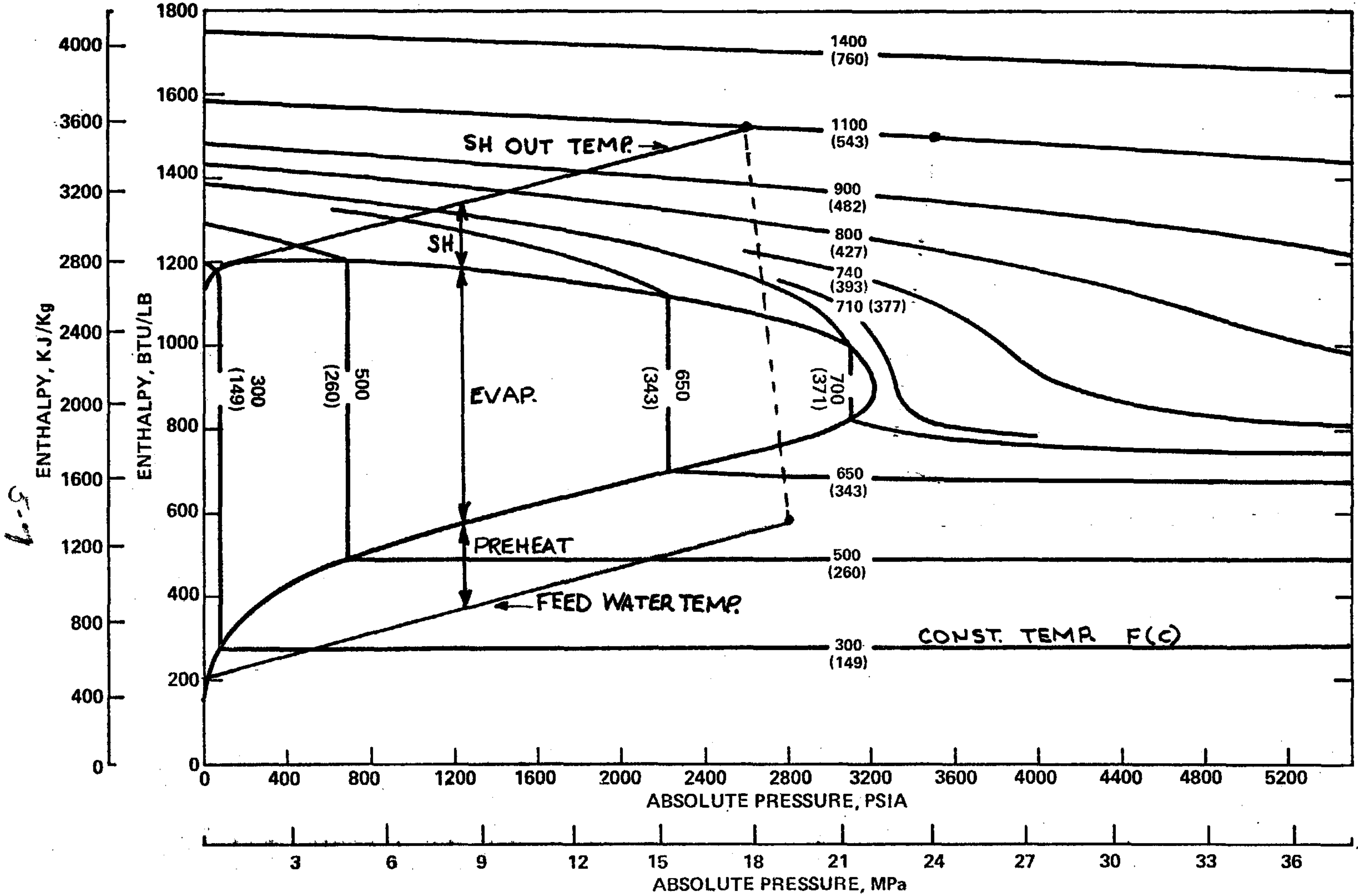
ENTHALPY, KJ/Kg
ENTHALPY, BTU/LB
ABSOLUTE PRESSURE, PSIA
ABSOLUTE PRESSURE, MPa
SH OUT TEMP.
SH
EVAP.
PREHEAT
FEED WATER TEMP.
CONST. TEMP. F(C)
1400 (760)
1100 (543)
900 (482)
800 (427)
740 (393)
710 (377)
700 (371)
650 (343)
500 (260)
300 (149)
0
400
800
1200
1600
2000
2400
2800
3200
3600
4000
200
600
1000
1400
1800
4400
4800
5200
3
6
9
12
15
18
21
24
27
30
33
36

Figure 5.2

5.1.2.5 Reheater Control--Reheat steam temperature controls are separate and function in the same manner as the superheat control. Since the reheater has a dedicated field, this should be no problem during normal start-up and shut-down. The entire reheater field must remain slewed until reheat flow has been established after starting the turbine. These requirements will have to be further studied and incorporated into the master control system functions.

5.1.2.6 Cloud Transients--Response to cloud transients is difficult to analyze due to a lack of a definitive input. In some respects, a re-circulation receiver may be more difficult to control during a cloud transient than a once-through receiver. This is due to the segregated nature of the heat absorbing components located around the circumference of the receiver. As an example, a sharp-edge cloud approaching west to east will first shut off insolation to a portion of the superheater, economizer, and evaporator. The east side will still be receiving heat. The receiver designs are split along a N to S axis, to allow some mixing to occur due to such a situation. The economizer and superheaters are divided but join a single evaporator at the drum interface. A N to S cloud would be worse as it would selectively imbalance the evaporator and superheater during the time requried to transverse the collector field. A quick-look analysis was made to determine the magnitude of the time consultants under certain assumed conditions. Results are reported in the Appendix. Further analysis needs to be done in this area.

5.2 Water Steam Receiver Subsystems

5.2.1 Receiver Subsystems Requirements

The receiver designs are based on results generated in the parametric study. The primary design requirement is to minimize tube crown temperatures on the high temperature superheater and reheater surfaces. Tube panel fatigue life and creep resistance are increased by minimizing tube crown temperatures.

The conceptual designs for four advanced water/steam receivers have been developed based on the nominal cycle conditions shown in Table 3.1. The receiver heat and material balances are presented in Figures 3.1 through 3.4. The receiver outlet temperature of 593°C (1100°F) is the basis of the advanced water/steam receiver design.

The radial flux profile assumed for the design is presented in Figure 3.5. Trapezoidal profile C, shown in Figure 3.6, is the assumed vertical flux distribution along the tube panel length.

An overall receiver absorption efficiency of 90 percent was assumed in sizing the receiver. This efficiency was also assumed for calculating the required evaporator, superheater and preheater surface areas. The actual efficiencies developed from STPP computer runs vary slightly from the assumed 90 percent efficiency. The correction for actual efficiencies would result in a minor correction in surface area calculations. Actual efficiencies developed from computer runs can be used in a final receiver design.

5.2.2 Receiver Design--Figures 5.3 and 5.4 show plan views of panel geometry for the 12.4 MPa (1800 psia) and 16.5 MPa (2400 psia) cycles, respectively. The relative evaporator surface area is greater in the 12.4 MPa (1800 psia) steam cycles because the phase change enthalpy (h_{fg}) is greater at lower saturation

Figure 5.3

RECEIVER PLAN VIEW
12.4 MPa (1800 PSIA) STEAM CYCLES

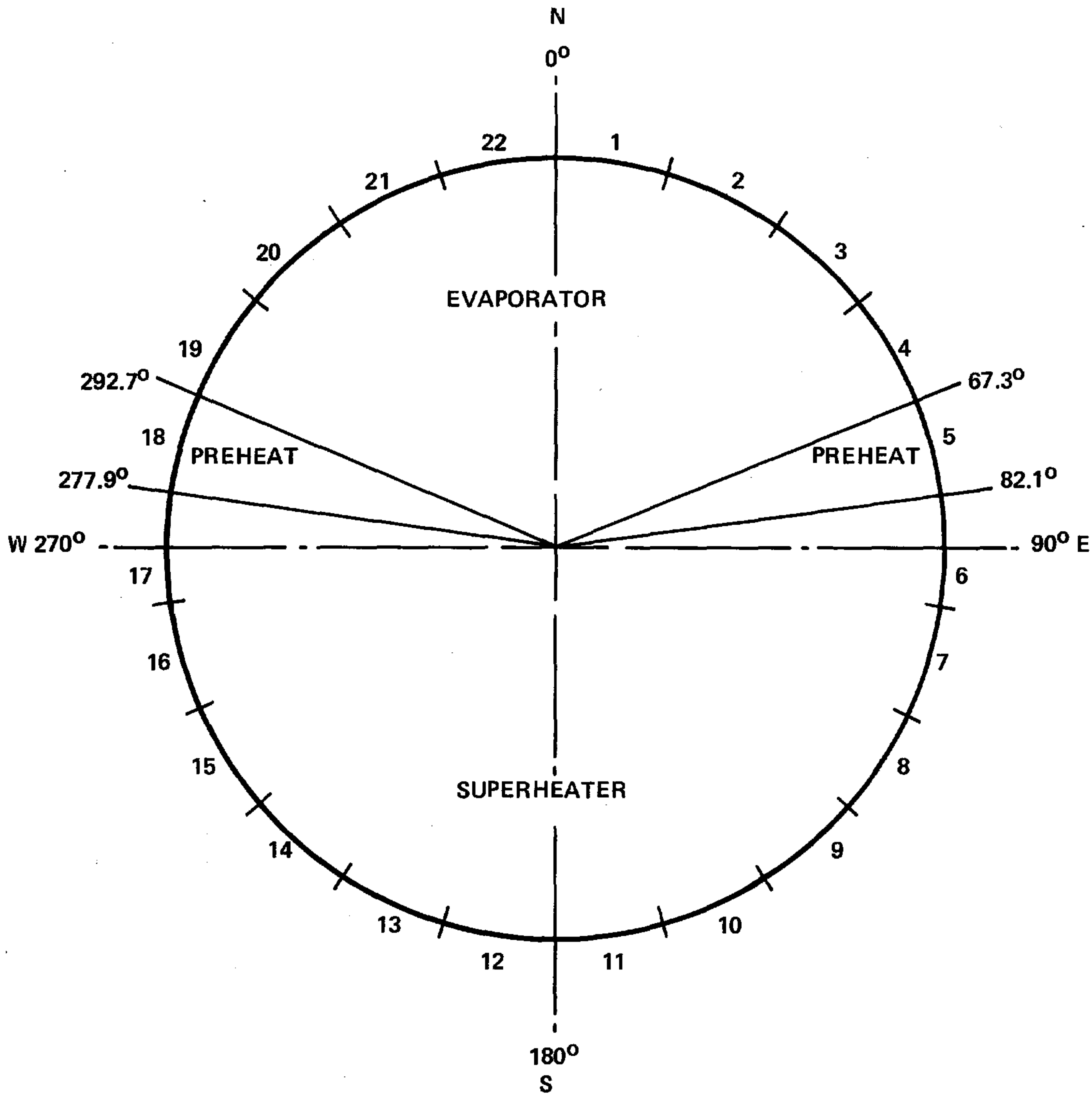

Figure 5.4
RECEIVER PLAN VIEW
16.5 MPa (2400 PSIA) STEAM CYCLES

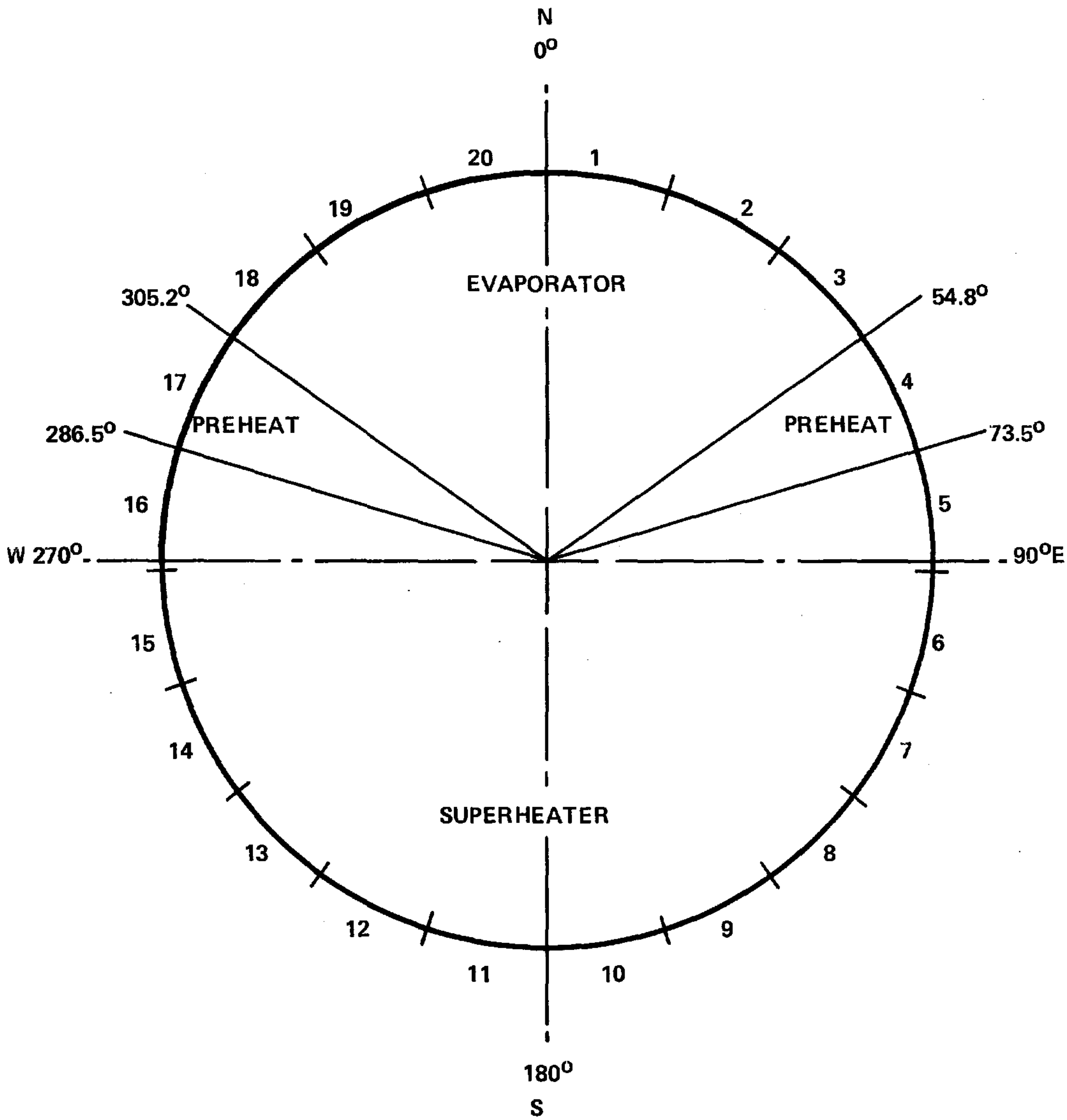

pressure. The receivers are symmetric about the north/south axis. Description of receiver designs herein will be for the symmetric half of the receiver defined by the north/south axis.

The evaporator section is located on the north side of the receiver in the highest incident flux region. The preheat panel is located adjacent to the evaporator. The superheater is located on the south side of the receiver in the low flux region, to promote low tube crown temperatures.

The evaporator and preheat panel sections are single stage, parallel flow panels. The superheater is 2-stage with a single panel first stage. The second superheater stage consists of small tube, parallel flow panels. Figures 5.5 and 5.6 show details of the superheater staging for the 12.4 MPa (1800 psia) and 16.5 MPa (2400 psia) receivers, respectively.

Steam flow to individual panels in the second stage superheater would be orificed to provide 593^{o}C (1100^{o}F) steam at the outlet header of each panel. In addition, steam flow to individual tubes in the second stage superheater panels would be orificed to ensure uniform steam temperatures at the outlet of each tube. Tube orificing requirements are based on results of the lateral flux gradient analysis presented under Section 3.2.3.

A tabulation of design parameters of the overall receiver, as well as for evaporator, superheater, and preheat panel sections are presented in Tables 5.1 through 5.5. Figures 5.7 and 5.8 show detailed plan views and side views of the 1.45x10^{6} Kg/hr (3x10^{6} lb/hr) receiver. Figure 5.9 shows the exploded panel arrangement for the same receiver. Physical configurations for the .91x10^{6} Kg/hr (2x10^{6} lb/hr) and .5 x 10^{6} Kg/hr (1x10^{6} lb/hr) receivers are similar to those in Figures 5.7 through 5.9.

Figure 5.5

SUPERHEATER STAGING

12.4 MPa (1800 PSIA) STEAM CYCLES

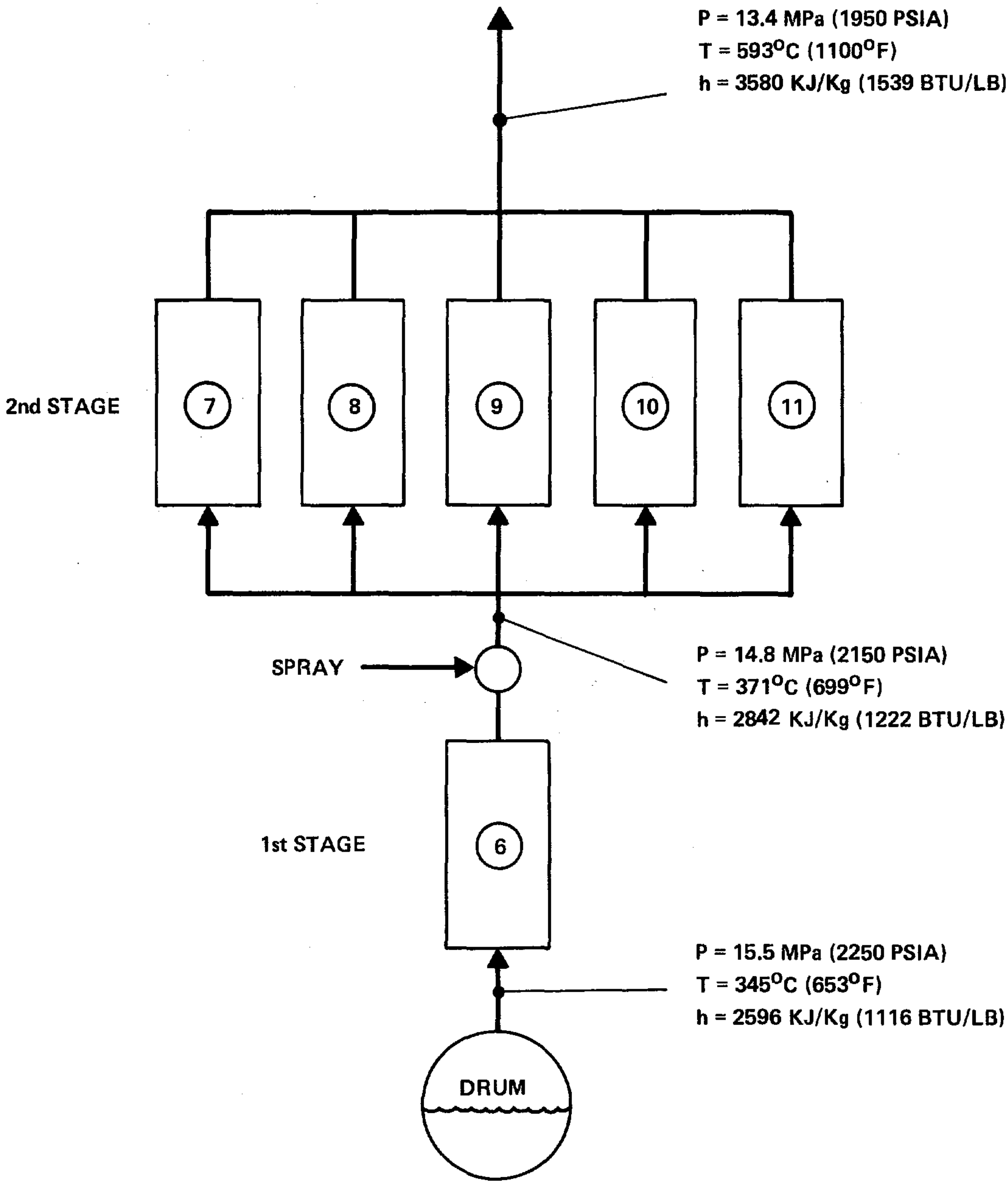

Figure 5.6
SUPERHEATER STAGING
16.5 MPa (2400 PSIA) STEAM CYCLES

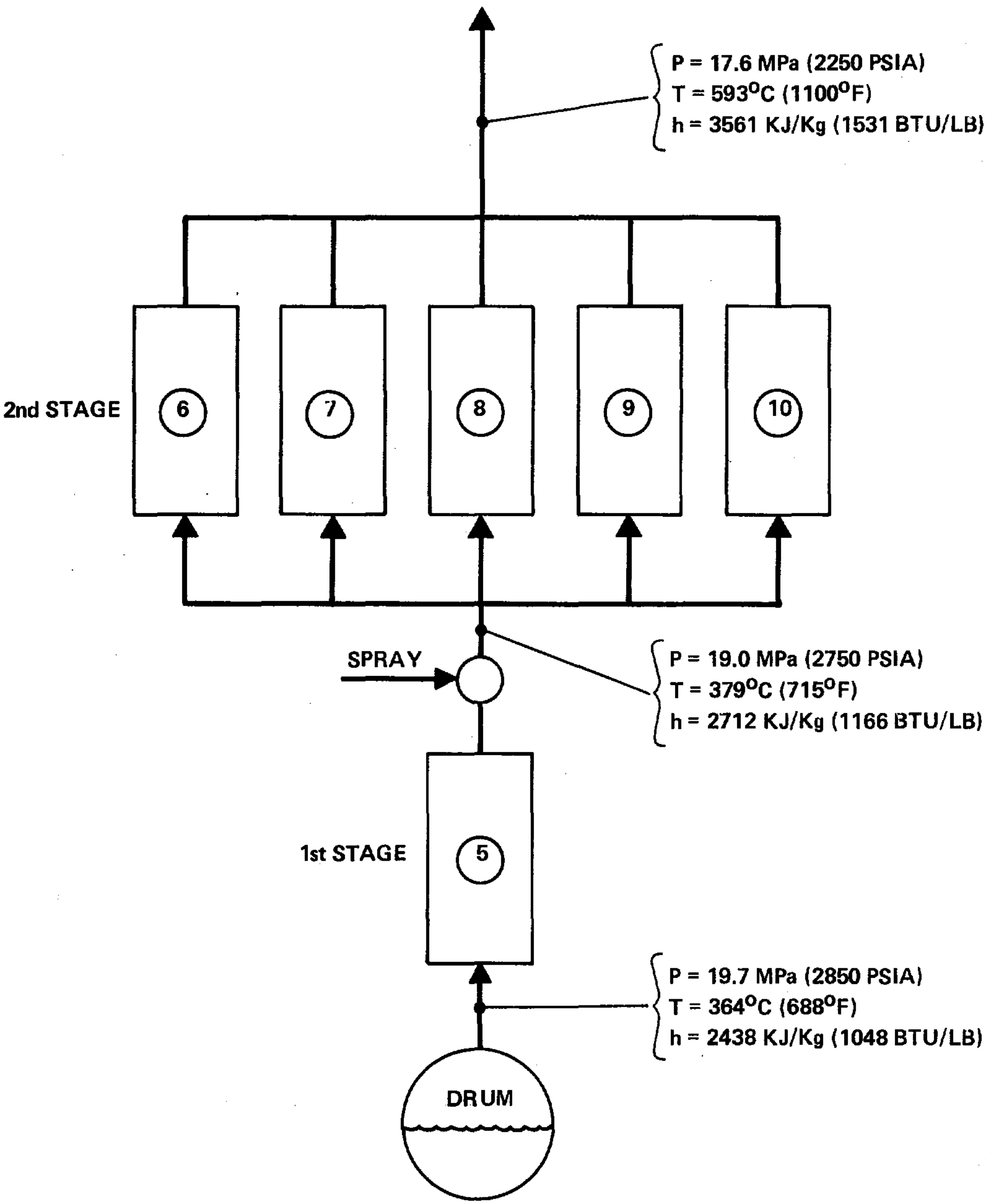

TABLE 5.1

Overall Receiver Conceptual Design Data

Cycle No.	1	2	3	4
Steam Flow, kg/hr (lb/hr) x 10^{-6}	.45 (1.0)	.91 (2.0)	.91 (2.0)	1.4 (3.0)
Final Steam Temp., ^{o}C (^{o}F)	593 (1100)	593 (1100)	593 (1100)	593 (1100)
S.H. Outlet Pressure, MPa (psia)	13.4 (1950)	13.4 (1950)	17.6 (2550)	17.6 (2550)
F.W. Inlet Temp., ^{o}C (^{o}F)	239 (462)	239 (462)	246 (474)	246 (474)
F.W. Inlet Press., MPa (psia)	16.2 (2345)	16.2 (2345)	20.3 (2950)	20.3 (2950)
Heat Absorbed, KJ/hr (BTU/hr) x 10^{-6}	1153 (1093)	2306 (2186)	2239 (2122)	3358 (3183)
Flux Distribution	1-C	1-C	1-C	1-C
Overall Surface Area, m^2/ft^2	846.3 (9110)	1696 (18,255)	1643 (17,690)	2465 (26,535)
Receiver Height, m (ft)	20.1 (65.96)	28.5 (93.37	28.0 (19.91)	34.3 (112.56)
Receiver Diameter, m (ft)	13.4 (43.97)	19.0 (62.24)	18.7 (61.27)	22.9 (75.04)
Receiver Circumference, m (ft)	42.1 (138.1)	59.6 (195.5)	58.7 (192.5)	71.8 (235.7)
Aspect Ratio	1.5	1.5	1.5	1.5
Number of Panels	22	22	20	20
Drum Diameter, m (ft)	18.3 (60)	18.3 (60)	20.1 (66)	20.1 (66)
Drum Length, m (ft)	12.2 (40)	17.7 (58)	14.0 (46)	18.7 (61.5)
Drum Pressure, MPa (psia)	15.5 (2250)	15.5 (2250)	19.7 (2850)	19.7 (2850)

TABLE 5.2

Evaporator Design Data

Cycle No.	1	2	3	4
Circulation Flow, kg/hr (lb/hr)x10^{-6}	.91 (2.0)	1.8 (4.0)	1.8 (4.0)	2.7 (6.0)
Circulation Ratio	2 : 1	2 : 1	2 : 1	2 : 1
Exit Quality, %	50	50	50	50
No. of Parallel Panels	8	8	6	6
Panel Width, m (ft)	1.97 (6.46)	2.79 (9.14)	2.98 (9.77)	3.65 (11.96)
No. Tubes/Panel	62	88	94	115
Tube OD, cm (in)	3.18 (1.25)	3.18 (1.25)	3.18 (1.25)	3.18 (1.25)
Tube ID, cm (in)	2.49 (.98)	2.49 (.98)	2.34 (.92)	2.34 (.92)
Tube Material	SA-213 T11	SA-213 T11	SA-213 T11	SA-213 T11
Ave. Mass Flux, kg/m^2s (lb/hr-ft^2x10^{-6})	1130 (.837)	1600 (1.18)	1990 (1.47)	2440 (1.80)
Heat Absorbed, KJ/hr (lb/hr) x 10^{-6}	594 (563)	1188 (1126)	956 (906)	1434 (1359)
Overall Surface Area, m^2 (ft^2)	316.6 (3408)	634.2 (6827)	500.6 (5388)	750.3 (8076)
Max. Tube Crown Temp., ^{o}C (^{o}F)	474 (886)	468 (875)	513 (956)	510 (950)

TABLE 5.3

1st Stage Superheater Design Data

Cycle No.	1	2	3	4
Flow Arrangement	Parallel Panel Upflow	Parallel Panel Upflow	Parallel Panel Upflow	Parallel Panel Upflow
Steam Flow, kg/hr (lb/hr) x 10^{-6}	.45 (1.0)	.91 (2.0)	.91 (2.0)	1.4 (3.0)
Inlet Temp., ^{o}C (^{o}F)	345 (653)	345 (653)	364 (688)	364 (688)
Outlet Temp., ^{o}C (^{o}F)	371 (699)	371 (699)	379 (715)	379 (715)
Inlet Press., MPa (psia)	15.5 (2250)	15.5 (2250)	19.7 (2850)	19.7 (2850)
Outlet Press., MPa (psia)	14.8 (2150)	14.8 (2150)	19.0 (2750)	19.0 (2750)
Heat Absorbed, KJ/hr (BTU/hr) x 10^{-6}	112 (106)	224 (212)	249 (236)	373 (354)
Overall Surface Area, m^2 (ft^2)	76.7 (826)	153.7 (1654)	162.0 (1744)	243.0 (2616)
No. of Parallel Panels	2	2	2	2
Panel Width, m (ft)	1.91 (6.26)	2.70 (8.86)	2.89 (9.49)	3.54 (11.62)
No. of Tubes/Panel	75	85	76	93
Tube OD, cm (in.)	2.54 (1.00)	3.18 (1.25)	3.81 (1.50)	3.81 (1.50)
Tube ID, cm (in.)	2.01 (.79)	2.41 (.95)	2.69 (1.06)	2.69 (1.06)
Tube Material	SA-213-T22	SA-213-T22	SA-213-T22	SA-213-T22
Ave. Mass Flux, kg/m^2-s (BTU/hr-ft^2x10^{-6})	2660 (1.96)	3240 (2.39)	2916 (2.15)	3570 (2.63)
Max. Tube Crown Temp., ^{o}C (^{o}F)	448 (838)	469 (877)	527 (980)	522 (971)

TABLE 5.4

<u>2nd Stage Superheater Design Data</u>

Cycle No.	1	2	3	4
Flow Arrangement	Parallel Panel Upflow	Parallel Panel Upflow	Parallel Panel Upflow	Parallel Panel Upflow
Steam Flow, kg/hr (lb/hr) x 10^{-6}	.45 (1.0)	.91 (2.0)	.91 (2.0)	1.4 (3.0)
Inlet Temp., ^{o}C (^{o}F)	371 (699)	371 (699)	379 (715)	379 (715)
Outlet Temp., ^{o}C (^{o}F)	593 (1100)	593 (1100)	593 (1100)	593 (1100)
Inlet Press., MPa (psia)	14.8 (2150)	14.8 (2150)	19.0 (2750)	19.0 (2750)
Outlet Press., MPa (psia)	13.4 (1950)	13.4 (1950)	17.6 (2550)	17.6 (2550)
Heat Absorbed, KJ/hr (BTU/hr) x 10^{-6}	334 (317)	669 (634)	770 (730)	1155 (1095)
Overall Surface Area, m^2 (ft^2)	383.7 (4130)	768.3 (8270)	810.1 (8720)	1215 (13,080)
No. of Parallel Panels	10	10	10	10
Panel Width, m (ft)	1.91 (6.26)	270 (8.86)	2.89 (9.49)	3.54 (11.62)
No. Tube/Panel	150	189	202	223
Tube OD, cm (in)	1.27 (.500)	1.43 (.563)	1.43 (.563)	1.59 (.625)
Tube ID, cm (in)	.99 (.39)	1.12 (.44)	1.07 (.42)	1.17 (.46)
Tube Material	TP-316H	TP-316H	TP-316H	TP-316H
Ave. Mass Flux, kg/m^2-s (lb/hr-ft^2 x 10^{-6})	1090 (.804)	1360 (1.00)	1400 (1.03)	1590 (1.17)
Max. Tube Crown Temp., ^{o}C (^{o}F)	619 (1146)	617 (1143)	612 (1133)	614 (1138

TABLE 5.5

Preheat Panel Design Data

Cycle No.	1	2	3	4
Flow Arrangement	Single Stage Upflow	Single Stage Upflow	Single Stage Upflow	Single Stage Upflow
F.W. Flow, kg/hr (lb/hr) x 10^{-6}	.45 (1.0)	.91 (2.0)	.91 (2.0)	1.4 (3.0)
Inlet Temp., ^{o}C (^{o}F)	239 (462)	239 (462)	246 (474)	246 (474)
Outlet Temp., ^{o}C (^{o}F)	289 (553)	289 (553)	309 (588)	309 (588)
Inlet Press., MPa (psia)	16.2 (2345)	16.2 (2345)	20.3 (2950)	20.3 (2950)
Outlet Press., MPa (psia)	15.6 (2260)	15.6 (2260)	19.7 (2860)	19.7 (2860)
Heat Absorbed, KJ/hr (BTU/hr) x 10^{-6}	113 (107)	226 (214)	289 (274)	434 (411)
Overall Surface Area, m^2 (ft^2)	69.6 (749)	139.4 (1501)	170.8 (1838)	256.0 (2756)
No. of Parallel Panels	2	2	2	2
Panel Width, m (ft)	1.73 (5.68)	2.45 (8.04)	3.05 (10.0)	3.73 (12.24)
No. Tube/Panel	68	77	96	98
Tube OD, cm (in)	2.54 (1.0)	3.18 (1.25)	3.18 (1.25)	3.81 (1.50)
Tube ID, cm (in)	2.01 (.79)	2.41 (.95)	2.26 (.89)	2.69 (1.06)
Tube Material	SA-192	SA-192	SA-192	SA-192
Ave. Mass Flux, kg/m^2-s (BTU/hr-ft^2 x 10^{-6})	2,930 (2.16)	3,580 (2.64)	3,270 (2.41)	3,390 (2.50)
Max. Tube Crown Temp., ^{o}C (^{o}F)	337 (638)	353 (668)	367 (692)	383 (721)

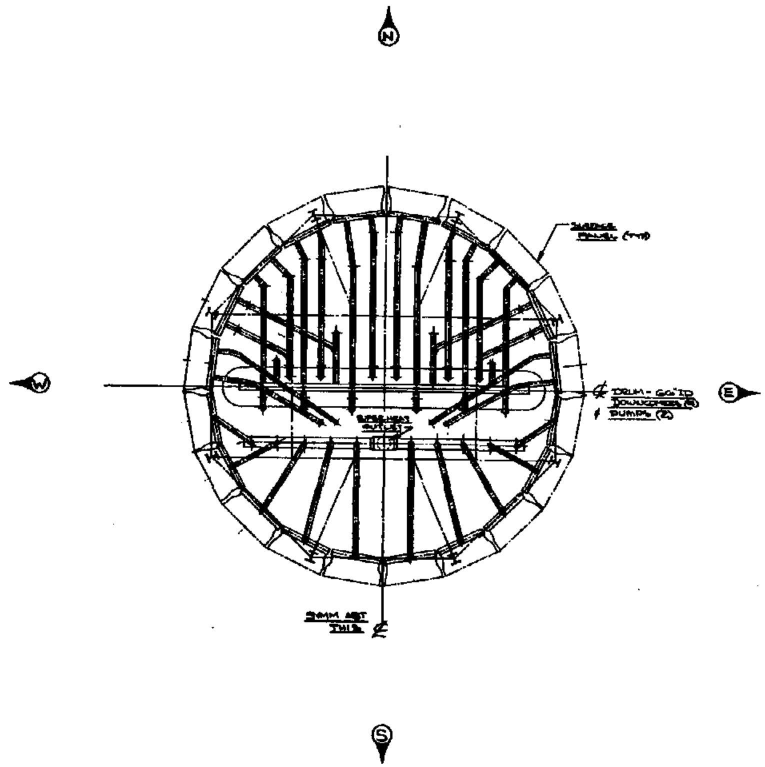

—UPPER PLAN VIEW—
—SECTION "C-C"—

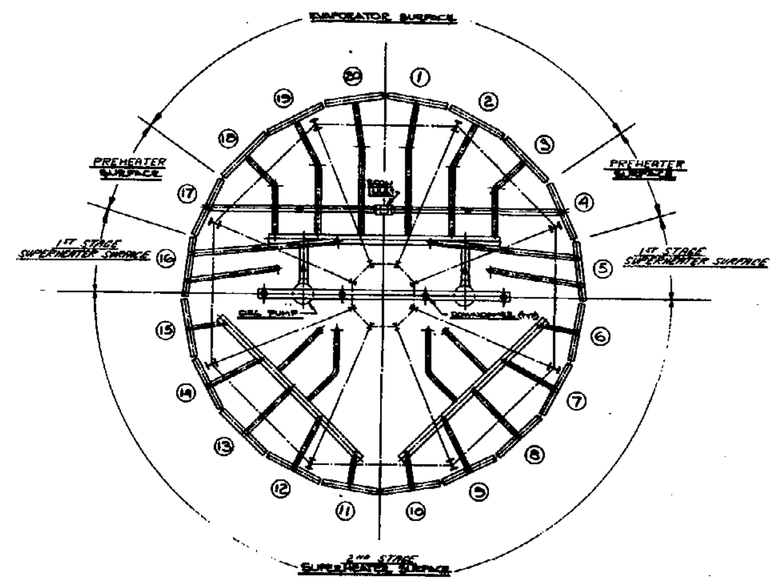

—LOWER PLAN VIEW—
—SECTION "D-D"—

NOTE:
1) SURFACE DESIGNATIONS APPLY TO BOTH VIEWS.
2) SECTION DESIGNATIONS APPLY TO BOTH VIEWS.
3) COMPASS ORIENTATION APPLIES TO BOTH VIEWS.
4) SURFACE PANELS ARE LOCATED TANGENT TO A 75-0 DIAMETER.
5) NUMBERS CIRCLED ARE PANEL REFERENCE NUMBERS AND APPLY TO BOTH VIEWS.

1.4 x 10⁶ Kg/Hr (3.0 x 10⁶ Lb/Hr) ADVANCED WATER STEAM SOLAR RECEIVER
NOTE: DESIGN GEOMETRIES FOR .91 x 10⁶ Kg/Hr (2.0 x 10⁶ Lb/Hr)
AND .45 x 10⁶ Kg/Hr (1.0 x 10⁶ Lb/Hr) RECEIVERS ARE SIMILAR

REF DWGS.
SIDE VIEWS — NE794 648
PANEL ARRGT — NE794 650

FIG. 5.7

This proprietary drawing is the property of C-E POWER SYSTEMS, COMBUSTION ENGINEERING, INC. WINDSOR, CONNECTICUT	C-E POWER SYSTEMS	PLAN VIEWS ADVANCED WATER/STEAM SOLAR RECEIVER FOR SANDIA LABORATORIES
DRAWN BY Wiwze CHECKED EKR		SCALE 6"=1'-0"
DATE 12-19-79 APPROVED		DWG NO. NE794 619-0

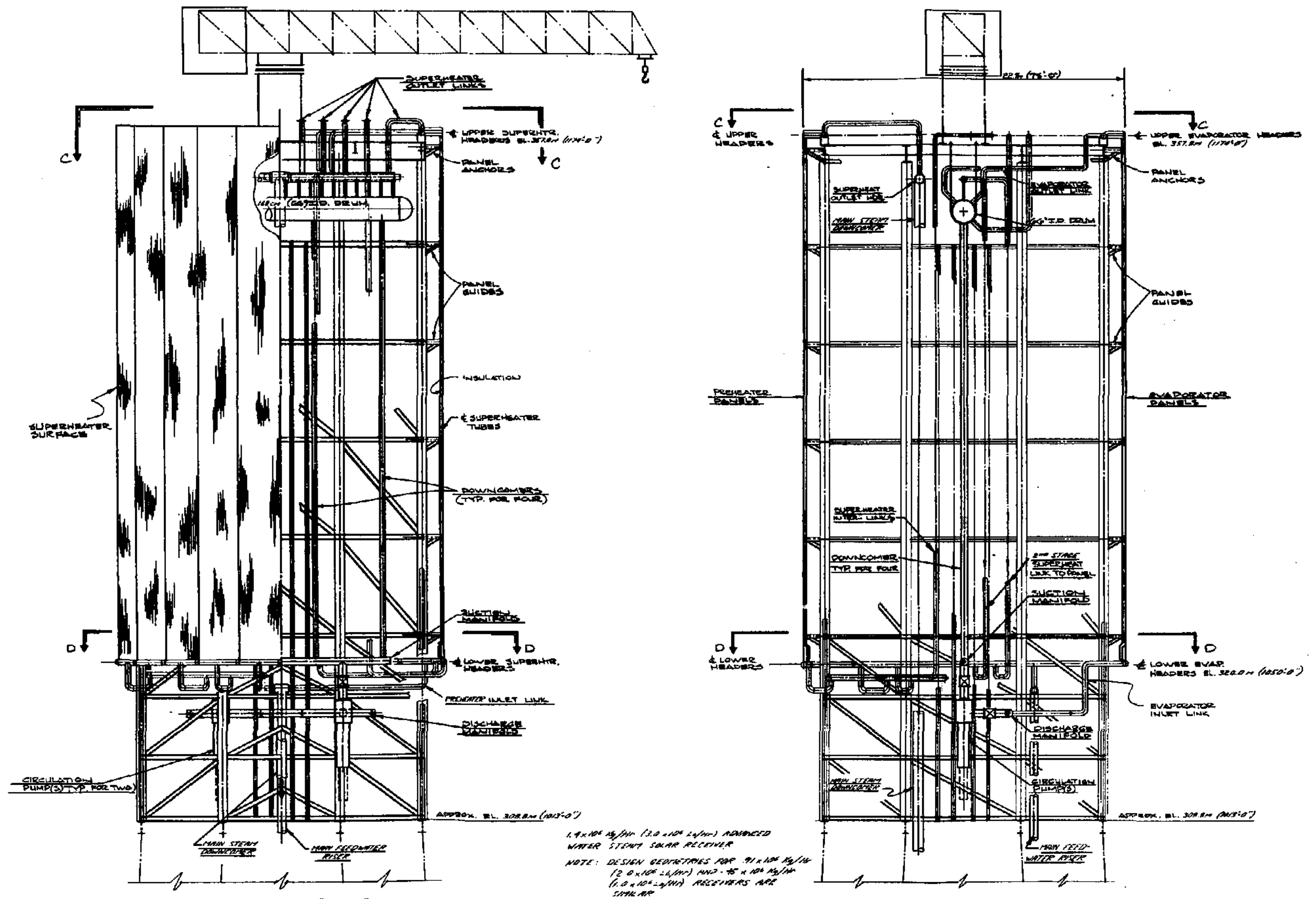

SECTION "B-B"
SUPERHEATER ASSEMBLIES
(NOTE: THIS SECTION SYMMETRICAL ABOUT ℄)

1.4 x 10⁶ Kg/Hr (3.0 x 10⁶ Lb/Hr) ADVANCED WATER STEAM SOLAR RECEIVER

NOTE: DESIGN GEOMETRIES FOR .91 x 10⁶ Kg/Hr (2.0 x 10⁶ Lb/Hr) AND .45 x 10⁶ Kg/Hr (1.0 x 10⁶ Lb/Hr) RECEIVERS ARE SIMILAR

-REFERENCE DWGS.-
PLAN VIEWS NE 794649
PANEL ARRGT. NE 794650

SECTION A-A
ECONOMIZER & EVAPORATOR ASSEMBLIES

FIG. 5.8

3 x 10⁶ LB STEAM/HOUR
SIDE VIEWS
ADVANCED WATER/STEAM SOLAR RECEIVER
FOR
SANDIA LABORATORIES

C-E POWER SYSTEMS
DRAWN BY G.M. FRANCHI CHECKED EKR
DATE 12-10-79 APPROVED R.C.
SCALE 1/16" = 1'0" DWG NO. NE 794648 0

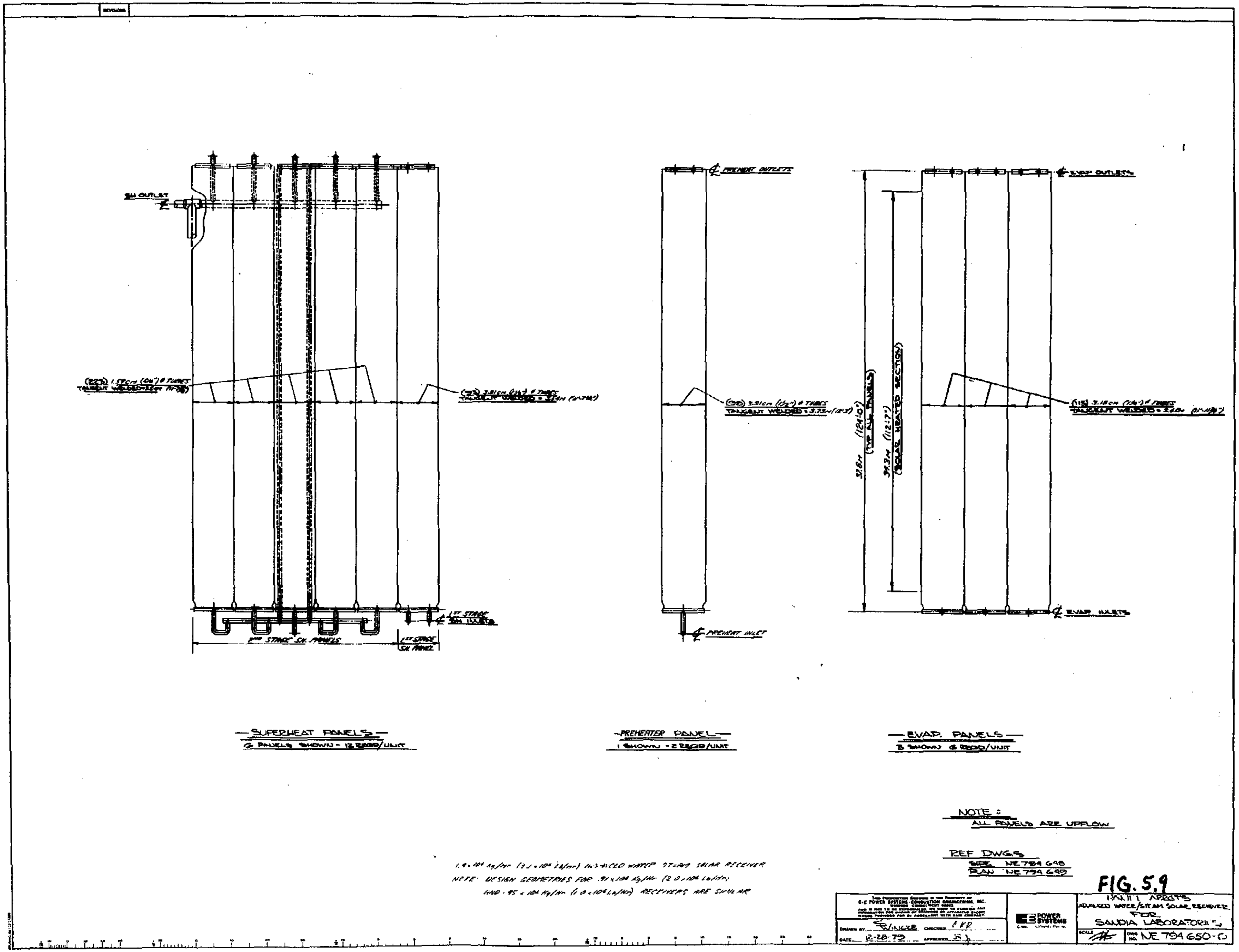
SH OUTLET
(223) 1.59cm (5/8") ∅ TUBES TANGENT WELDED
(73) 3.81cm (1 1/2") ∅ TUBES TANGENT WELDED
1ST STAGE SH INLETS
2ND STAGE SH PANELS
1ST STAGE SH PANEL
SUPERHEAT PANELS
6 PANELS SHOWN - 12 REQD/UNIT
℄ PREHEAT OUTLETS
(98) 3.81cm (1 1/2") ∅ TUBES TANGENT WELDED • 3.73m (12'3")
℄ PREHEAT INLET
PREHEATER PANEL
1 SHOWN - 2 REQD/UNIT
37.8m (124'-0") (TYP ALL PANELS)
34.3m (112'7") (SOLAR HEATED SECTION)
℄ EVAP OUTLETS
(115) 3.18cm (1 1/4") ∅ TUBES TANGENT WELDED
℄ EVAP INLETS
EVAP. PANELS
3 SHOWN 6 REQD/UNIT
NOTE:
ALL PANELS ARE UPFLOW
REF DWGS
SIDE NE 794 648
PLAN NE 794 649
NOTE: DESIGN GEOMETRIES FOR .91 x 10⁶ Kg/Hr (2.0 x 10⁶ Lb/Hr)
AND .45 x 10⁶ Kg/Hr (1.0 x 10⁶ Lb/Hr) RECEIVERS ARE SIMILAR
C-E POWER SYSTEMS
DRAWN BY Wincze
CHECKED EVR
DATE 12-28-79
PANEL ARRGTS
ADVANCED WATER/STEAM SOLAR RECEIVER
FOR
SANDIA LABORATORIES
DWG NO. NE 794 650-0

FIG. 5.9

The primary objective in the four conceptual designs was to limit tube crown temperatures in the superheater while limiting pressure drop. Table 5.6 presents a summary of maximum tube crown temperature

in the final superheater designs. By utilizing small tubes and parallel flow panels in the second stage, maximum tube crown temperatures are limited to less than 621°C (1150°F) in all superheater tube panels. Superheater pressure drops are within design limits.

Another design objective was to prevent DNB in the evaporator tube panels. This objective has been confirmed in rifled tube testing. Figures 5.10 and 5.11 show DNB test points plotted against steam quality and mass flux. The design evaporator mass flux ranges for the 12.4 MPa (1800 psia) and 16.5 MPa (2400 psia) receiver cycles are respectively superimposed on Figures 5.10 and 5.11. Results show that mass fluxes are in the safe region and DNB will not occur.

5.2.3 Receiver Losses

Thermal absorption efficiencies in the design receiver tube panels have been calculated with the STPP computer code. Receiver losses are a function of ambient back radiation and convection losses. Back radiation losses are calculated in the computer code by assuming a panel solar absorptivity (α) of .95 and infared emissivity (ε) of .89. An assumed outside film coefficient of 17 W/m^2 - ^oC(3.0 $BTU/hr\text{-}ft^2\text{-}^oF$) was used for calculating convection losses.

Table 5.7 presents thermal absorption efficiencies tabulated for the conceptual designs. Overall receiver absorption efficiencies are approximately 92 percent.

Figure 5.10

EFFECT OF MASS FLUX ON DNB QUALITY

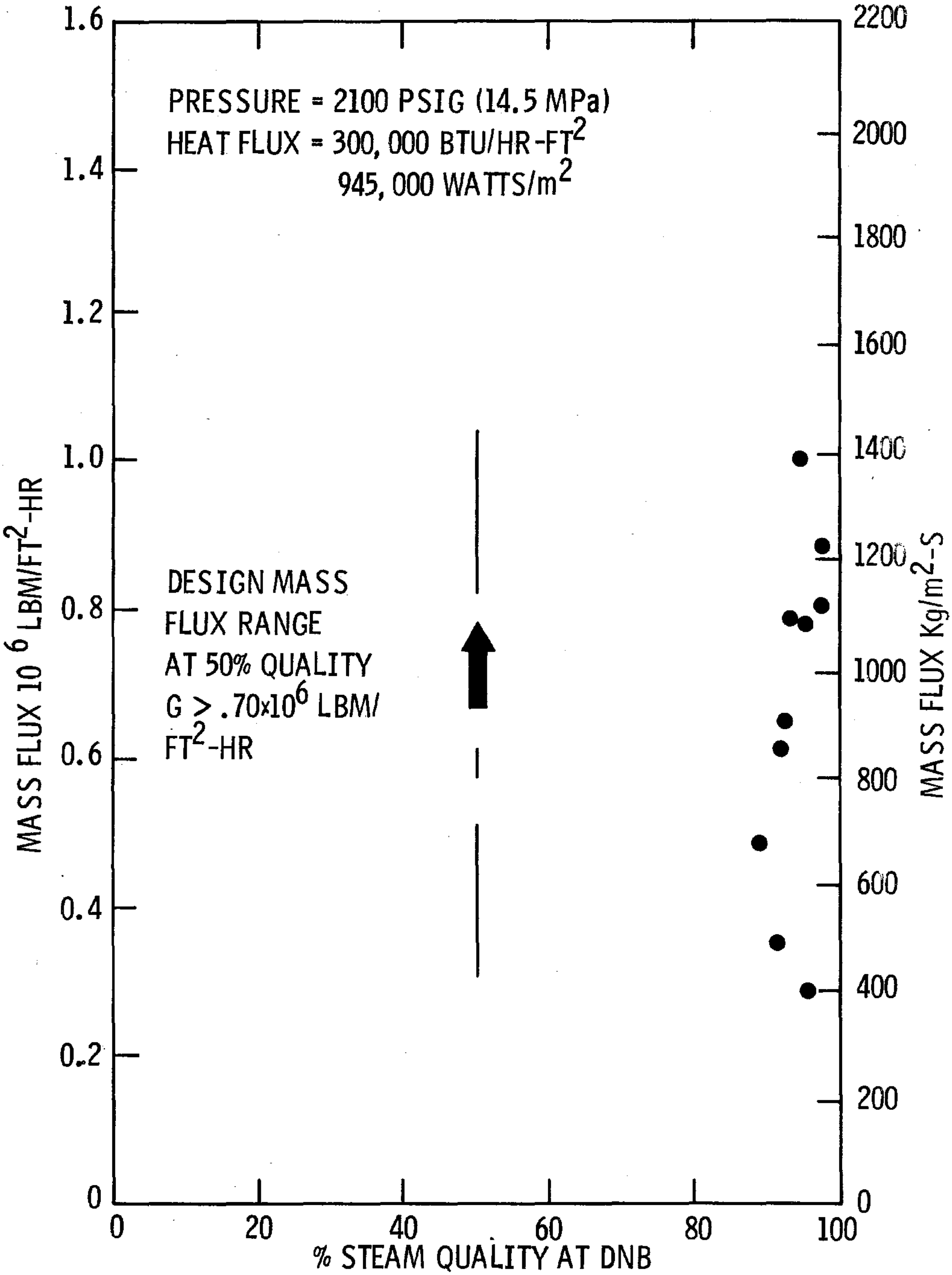

Figure 5.11
EFFECT OF MASS FLUX ON DNB QUALITY

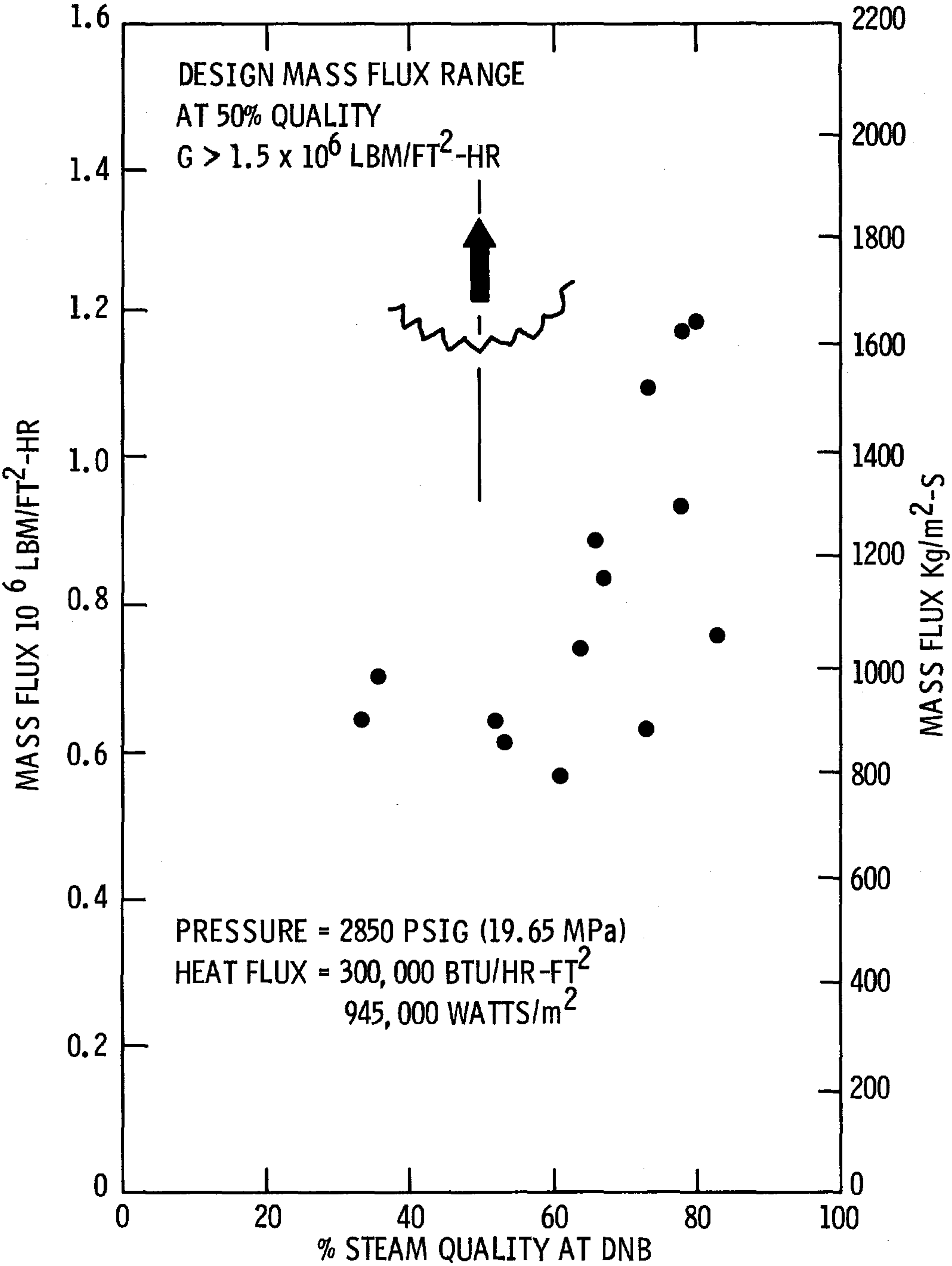

TABLE 5.6

2nd Stage Superheater - Maximum Tube Crown Temperatures and Tube Temperature Differentials

Receiver No.	Panel No.	Max. Crown Temp. °C (°F)	Temp. Differential* °C (°F)
1	7	619 (1146)	49 (88)
	8	614 (1137)	38 (73)
	9	610 (1130)	26 (59)
	10	609 (1128)	29 (52)
	11	607 (1124)	28 (51)
2	7	617 (1143)	41 (74)
	8	613 (1135)	38 (68)
	9	609 (1128)	31 (56)
	10	606 (1122)	24 (43)
	11	605 (1121)	26 (47)
3	6	612 (1133)	34 (61)
	7	607 (1124)	25 (45)
	8	603 (1118)	20 (36)
	9	600 (1112)	13 (23)
	10	599 (1111)	12 (22)
4	6	614 (1138)	38 (69)
	7	606 (1123)	28 (51)
	8	604 (1120)	21 (37)
	9	601 (1113)	14 (26)
	10	600 (1112)	14 (26)

* Tube temp differential = $T_{CROWN} - T_{FLUID}$ @ max. crown temp.

TABLE 5.7

TUBE PANEL EFFICIENCIES

Panel No.		Receiver No. 1	2		3	4
1	Evap.	.934	.932	Evap.	.925	.925
2	Evap.	.933	.932	Evap.	.925	.924
3	Evap.	.932	.931	Evap.	.924	.924
4	Evap.	.931	.930	Preheat	.942	.938
5	Preheat	.950	.944	S.H.	.914	.908
6	S.H.	.926	.919	S.H.	.883	.881
7	S.H.	.877	.876	S.H.	.870	.868
8	S.H.	.862	.862	S.H.	.850	.850
9	S.H.	.842	.842	S.H.	.825	.824
10	S.H.	.816	.818	S.H.	.820	.818
11	S.H.	.814	.815			
*Ave. Evap.		.93	.93		.92	.92
*Ave. Preheat		.95	.94		.94	.94
*Ave. S.H.		.87	.87		.87	.87
*Overall Receiver		.92	.92		.92	.92

*Averages are flux weighted.

5.2.4 Circulation Pumps

The evaporator recirculation loop configuration is shown in Figure 5.12. Evaporator circulation is maintained by 2 parallel circulation pumps, each pump supplying one-half of the design flow. In the event of a single pump outage, sufficient flow would be maintained by the other parallel pump to provide evaporator cooling.

The design point circulation pump requirements are presented in Table 5.8. Circulation pumps selected for the receiver designs are presented in Appendix D. The pumps selected are standard wet motor boiler circulation pumps with a 1.15 service factor.

It is noted that pump specitifications for the $.45 \times 10^6$ Kg/hr (1×10^6 lb/hr) receiver are omitted from Appendix D. This is because the head and capacity requirements for the small receiver are slightly below the standard range for boiler circulation pumps. Discussions with the pump manufacturer indicate that a similar but modified boiler circulation pump could be supplied for the small receiver.

5.2.5 Riser/Downcomer Design

The main feedwater riser and steam downcomer design specifications are presented in Table 5.9. Due to the low feedwater temperature, the main feedwater riser is SA-106B carbon steel. The steam downcomer however must be SA-312 stainless due to the 593°C (1100°F) final steam temperature. Both main riser and downcomer sections would be constructed of seamless welded pipe. Expansion sections would be incorporated into the design to account for thermal elongation.

Figure 5.13 shows approximate tower heights for the 4 conceptual receiver designs. Corresponding main riser and downcomer lengths range between

Figure 5.12

EVAPORATOR RECIRCULATION LOOP

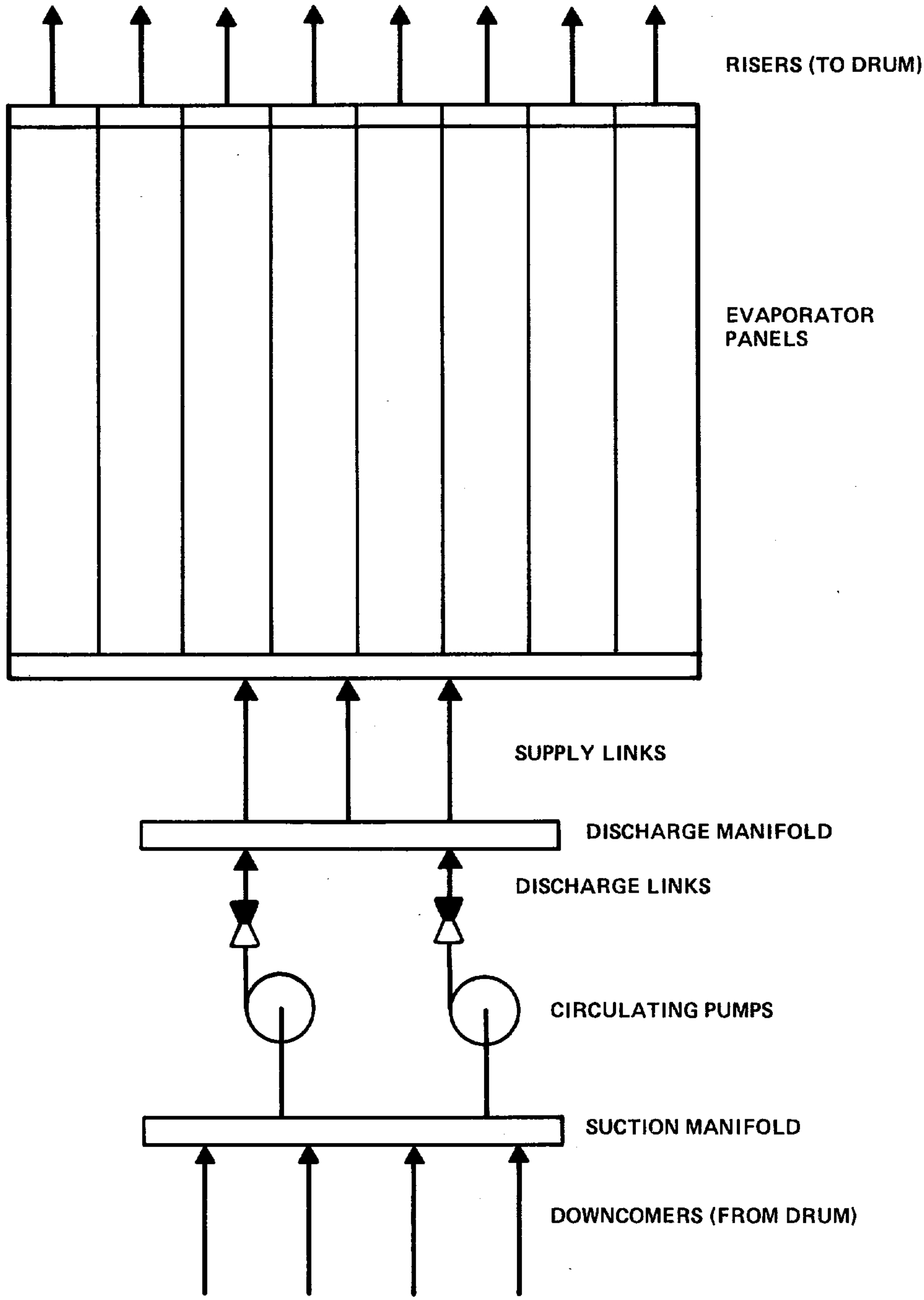

TABLE 5.8

Circulation Pump Requirements at Full Load

Receiver No.	1	2	3	4
Receiver Steam Flow, Kg/hr (lb/hr)	$.45 \times 10^6$ (1×10^6)	$.91 \times 10^6$ (2×10^6)	$.91 \times 10^6$ (2×10^6)	1.4×10^6 (3×10^6)
Turbine Throttle Pressure, MPa (psia)	12.4 (1800)	12.4 (1800)	16.5 (2400)	16.5 (2400)
Pump Suction Pressure, MPa (psia)	19.86 (2880)	19.79 (2870)	15.65 (2270)	15.58 (2260)
Pump Suction Temperature, ^oC (^oF)	343 (650)	343 (650)	321 (610)	321 (610)
Required Head, m (ft)	155 (508)	95.1 (312)	47.2 (155)	20.1 (66)
Total Volumetric Flow, m^3/hr (GPM)	4,379 (19,280)	2919 (12,850)	2716 (11,960)	1358 (5,980)
Available NPSH, m (ft)	735 (2410)	725 (2380)	628 (2060)	622 (2040)

Figure 5.13
DESIGN RECEIVER AND TOWER ARRANGEMENTS

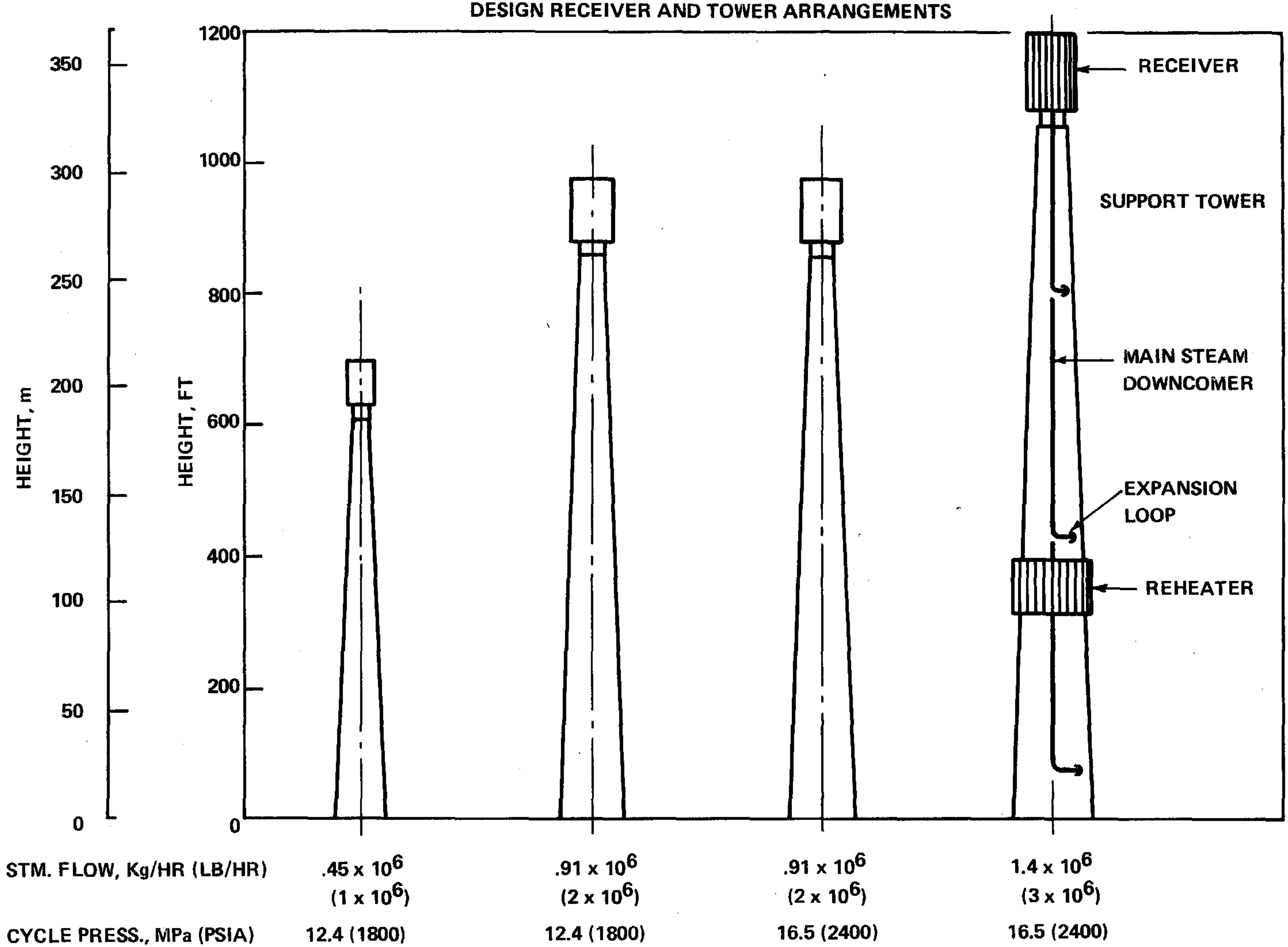

TABLE 5.9

Main Riser/Downcomer Design Specifications

	Receiver Steam Flow kg/hr (lb/hr)	Turbine Throttle Pressure MPa (psia)	Outer Dia. cm (in)	Inner Dia. cm (in)	ASME Spec.
MAIN FEEDWATER RISER	$.45 \times 10^6$ (1×10^6)	12.4 (1800)	32.4 (12-3/4)	25.7 (10.1)	SA-106B (carbon)
	$.91 \times 10^6$ (2×10^6)	12.4 (1800)	45.7 (18)	38.9 (15.3)	"
	$.91 \times 10^6$ (2×10^6)	16.5 (2400)	45.7(18)	37.3 (14.7)	"
	1.4×10^6 (3×10^6)	16.5 (2400)	50.8 (20)	41.4 (16.3)	"
MAIN STEAM DOWNCOMER	$.45 \times 10^6$ (1×10^6)	12.4 (1800)	45.7 (18)	38.4 (15.1)	TP-316H (stainless)
	$.91 \times 10^6$ (2×10^6)	12.4 (1800)	61.0 (24)	51.3 (20.2)	"
	$.91 \times 10^6$ (2×10^6)	16.5 (2400)	61.0 (24)	49.0 (19.3)	"
	1.4×10^6 (3×10^6)	16.5 (2400)	66.0 (26)	53.1 (20.9)	"

TABLE 5.10

Reheater Riser/Downcomer Design Specifications

	Nominal Plant Rating (MW)	Turbine Throttle Pressure MPa (psia)	Outer Dia. cm (in)	Inner Dia. cm (in)	ASME Spec.
REHEATER RISER	100	12.4 (1800)	50.8 (20)	48.4 (19.2)	SA-106B (carbon)
	200	12.4 (1800)	66.0 (26)	63.2 (24.9)	"
	200	16.5 (2400)	61.0 (24)	57.7 (22.7)	"
	300	16.5 (2400)	71.1 (28)	67.1 (26.4)	"
REHEATER DOWNCOMER	100	12.4 (1800)	50.8 (20)	48.8 (19.2)	SA-335 P22 (ferritic)
	200	12.4 (1800)	71.1 (28)	68.1 (26.8)	"
	200	16.5 (2400)	66.0 (26)	62.2 (24.5)	"
	300	16.5 (2400)	81.3 (32)	76.7 (30.2)	"

approximately 183m (600 ft) and 335m (1100 ft). Reheater locations are also shown in Figure 5.24 based on the reheater being located 1/3 of the way up the main tower. The corresponding reheater riser and downcomer sections range between approximately 61m (200 ft) and 113m (370 ft).

The reheater riser and downcomer design specifications are shown in Table 5.10. The pipe sizing is based on pressure drop limitations imposed in the reheat cycle. Section 5.2.7 contains additional details of reheater design. The main reheat riser is made from carbon steel. The selection of a ferritic steel for the steam downcomer is based on the 538°C (1000°F) reheat steam temperature. Pipe sections would be constructed of seamless welded pipe. Expansion sections would also be located in the reheat riser and downcomer to account for thermal elongation.

5.2.6 Receiver Structural Support Design and Analysis

5.2.6.1 Introduction--A design study was performed for the solar receiver support structure. Support structures were designed based on receiver steam flows of .45 x 10^6 kg/hr (1.0 x 10^6 lb/hr), .77 x 10^6 kg/hr (1.7 x 10^6 lb/hr), and 1.4 x 10^6 kg/hr (3.0 x 10^6 lb/hr). The .77 x 10^6 kg/hr (1.7 x 10^6 lb/hr) receiver was analyzed prior to the final selection of receiver size based on steam flow for receiver conceptual designs. The structures were designed based on static and dynamic loads to meet the requirements of the 1969 American Institute of Steel Construction (AISC) code for W-type members.

5.2.6.2 Design Procedure

The solar receiver is located on top of a support tower (Figure 5.14). Table 5.11 shows the assumed receiver dimensions used in the support structure design and analysis.

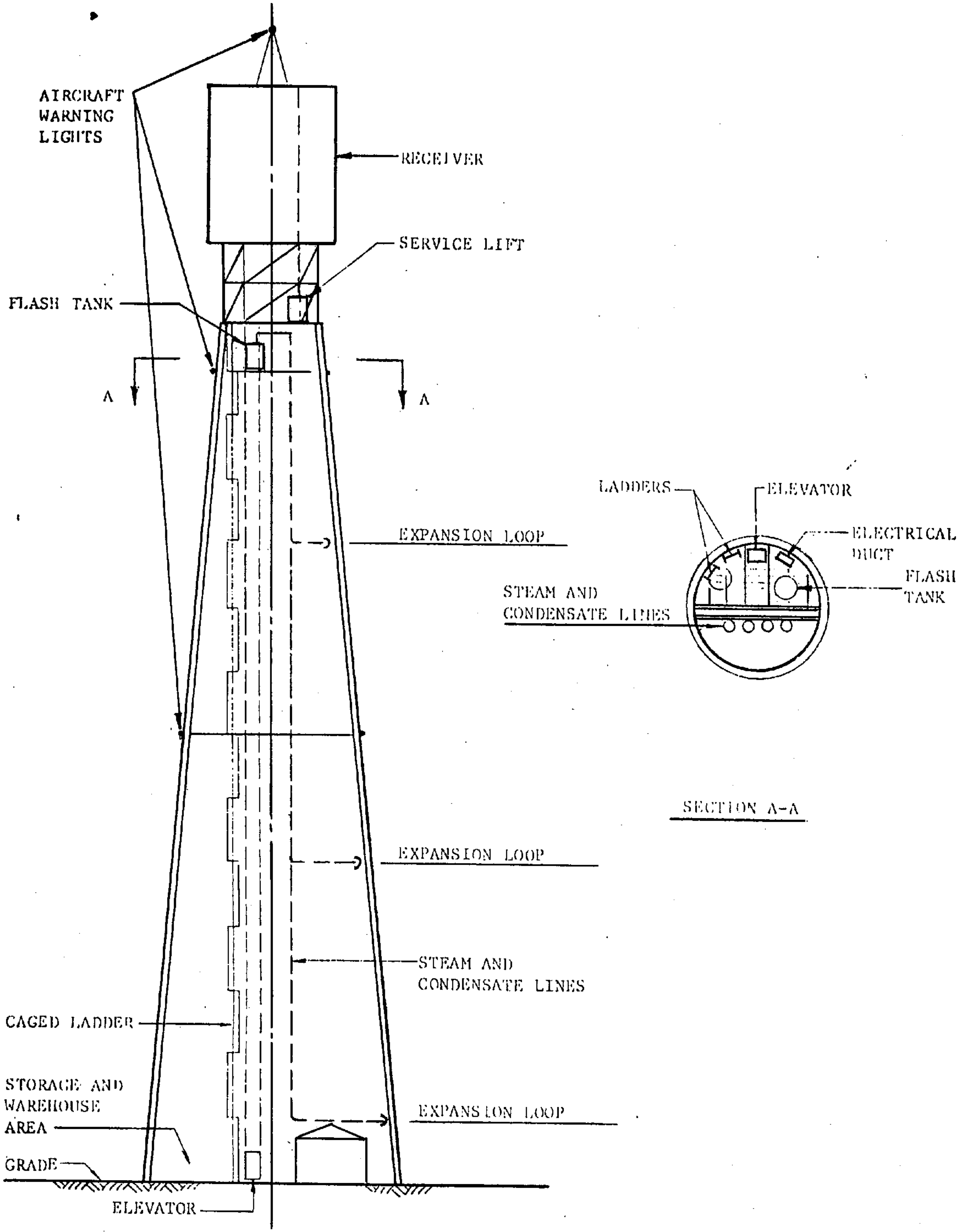

Figure 5.14 - Typical Receiver and Tower Arrangement

TABLE 5.11

Overall Receiver Dimensions

Steam Flow kg/hr (lb/hr)	Receiver Height m (ft)	Receiver Diameter m (ft)	Support Tower Height m (ft)
$.45 \times 10^6$ (1.0×10^6)	19.8 (65)	13.3 (43.5)	185 (607)
$.77 \times 10^6$ (1.7×10^6)	38.7 (127)	17.1 (56)	242 (794)
1.4×10^6 (3.0×10^6)	34.3 (112.6)	22.9 (75)	321 (1052)

The basic structural configuration for each receiver support tower was kept constant with the number of support levels being varied. An octagonal symmetric structure was chosen (see Figure 5.15). This shape minimizes the amount of secondary steel bracing from the solar tube panels to the main support structure, while minimizing the complexity of the structure.

Most of the dead weight loading is concentrated on the top level. The drum and downcomers are supported from the top level by two large members. The tube panels are hung from the outside members of the top octagon (Figure 5.15a). Intermediate levels have radial members connecting the outer octagon to a smaller inner octagon. (Figure 5.15b). Eight main outside columns transmit the load to the base of the structure. These are diagonally braced (Figure 5.15c).

The complexity of the structure depends upon the number of levels needed to support the panels. The horizontal buckstay spacing determines this. The distance between buckstays is a function of the panel flexibility, and panel tube size determines this flexibility. Table 5.12 shows the assumed receiver sizes and corresponding panel tube sizes. These selected tube sizes may not necessarily agree with the final design tube sizes.

Flexibility was determined by calculating an equivalent plate thickness based on moment of inertias. From the Uniform Building Code (UBC) the panel wind loading is 1.47 KPa (.213 psi) at 290m (950 ft.). The buckstay spacing was based on maximum panel deflection of 1.27 cm. (.50 in.) in the most flexible panel due to this wind loading. Calculated stresses due to these deflections are well below the allowable stress. Figure 5.16 shows the calculated buckstay spacings.

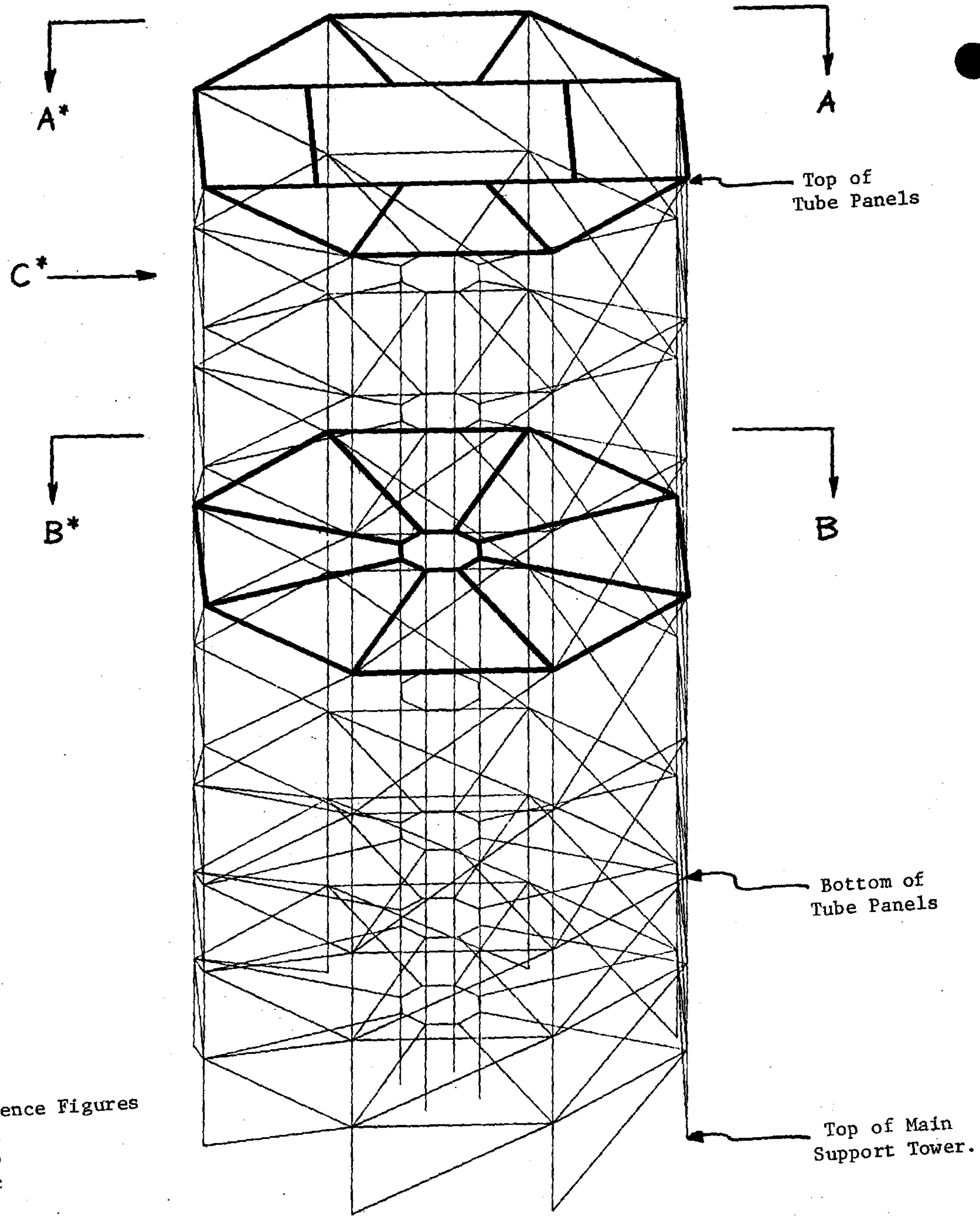

*Reference Figures
5.14a
5.14b
5.14c

Figure 5.15 Octagonal Support Structure

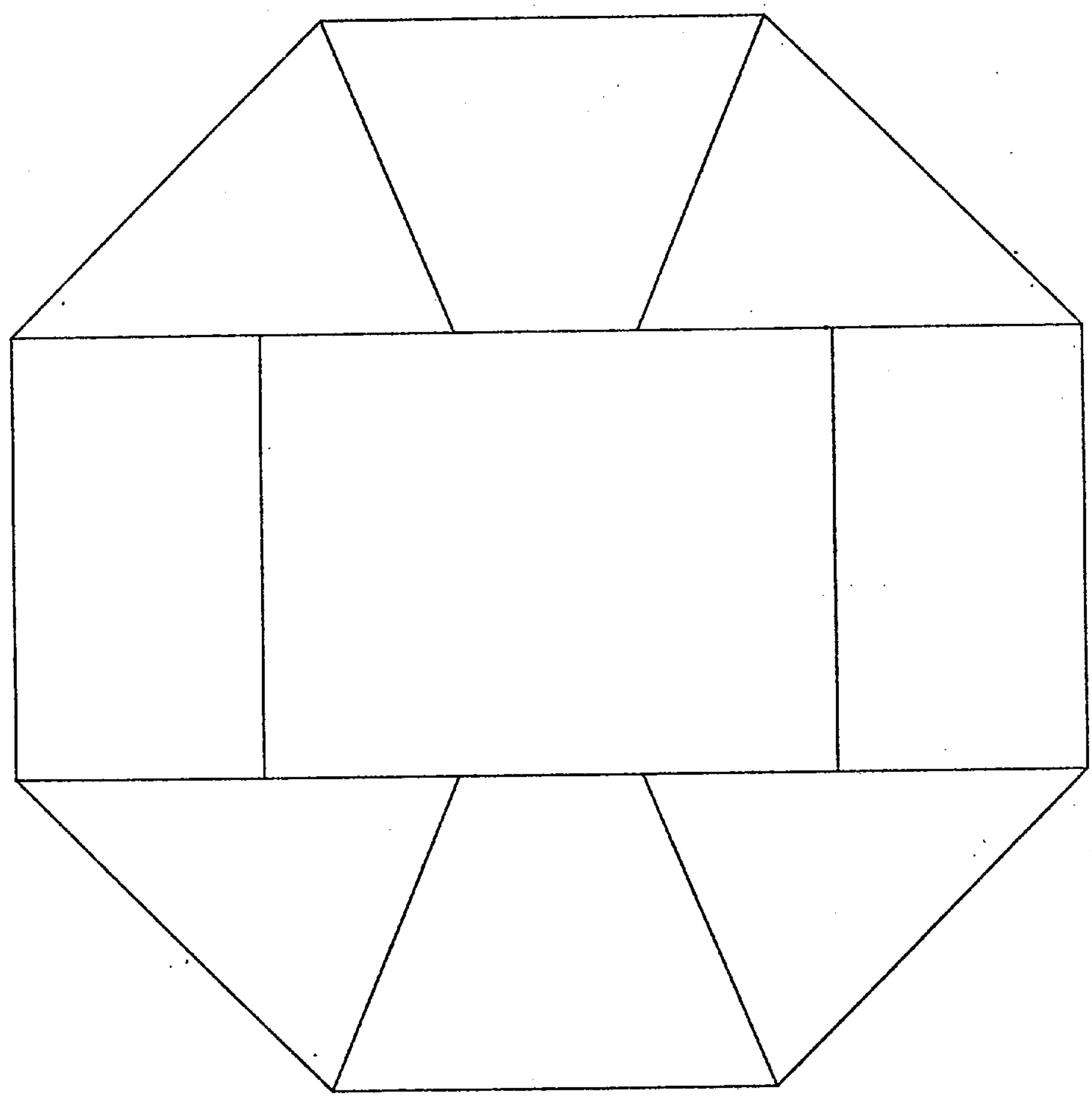

Figure 5.15a Top Support, Section A-A

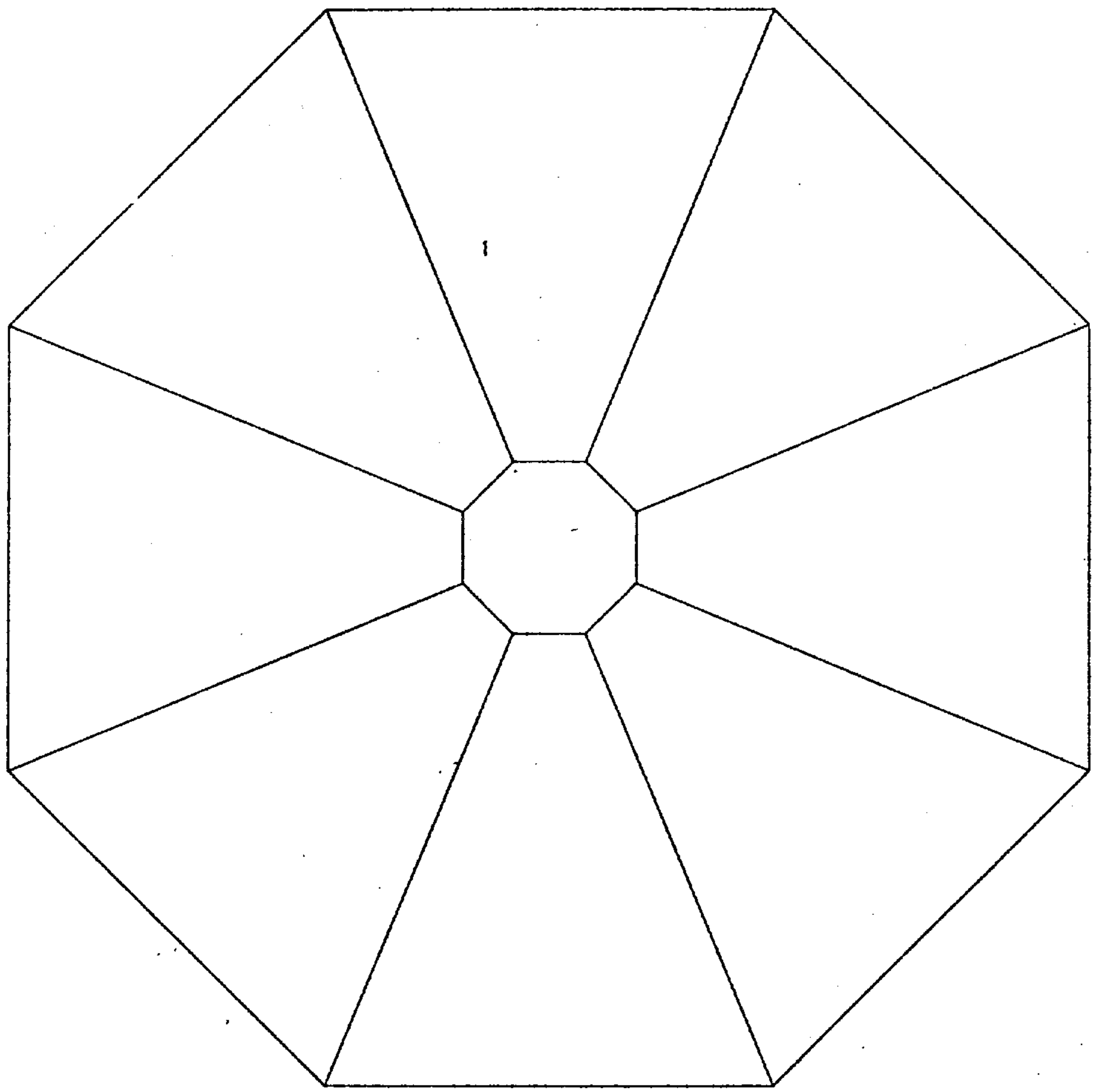

Figure 5.15b Intermediate Support Level, Section B-B

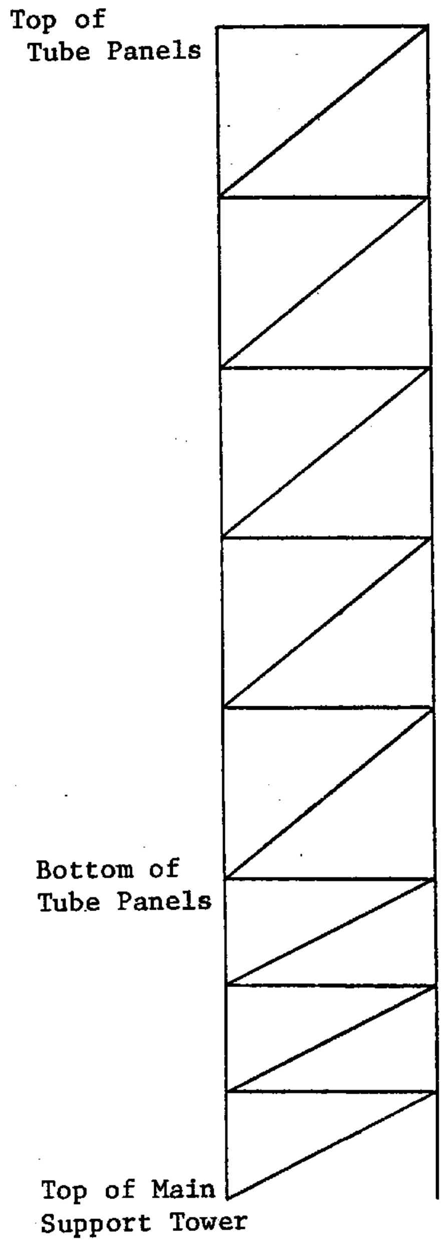

Figure 5.15c Columns and Diagonal Bracing, View C

Figure 5.16 Level Spacing and Horizontal Buckstay Spacing

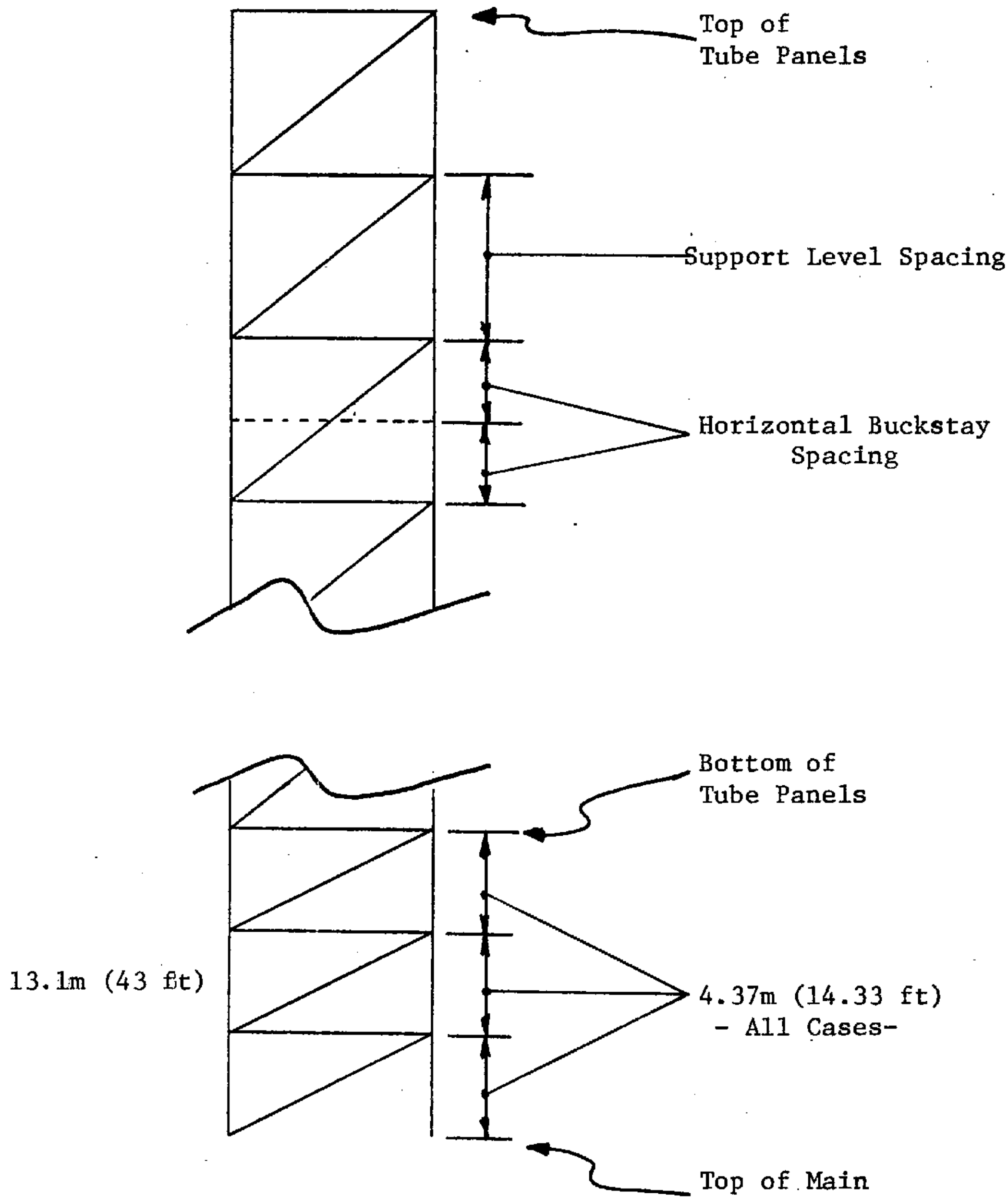

Steam Flow kg/hr (lb/hr)	Horizontal Buckstay Spacing m (ft)	Support Level Spacing m (ft)
$.45 \times 10^6$ (1.0×10^6)	2.51 (8.25)	5.03 (16.5)
$.77 \times 10^6$ (1.7×10^6)	1.83 (6.00)	3.66 (12.0)
1.4×10^6 (3.0×10^6)	3.49 (11.46)	6.99 (22.92)

TABLE 5.12

Panel Tube Sizes

Steam Flow kg/hr (lb/hr)	Tube Size, cm (in) Economizer OD	Economizer ID	Evaporator OD	Evaporator ID	Superheater OD	Superheater ID
$.45 \times 10^6$ (1.0×10^6)	3.18 (1.25)	2.44 (0.96)	3.18 (1.25)	2.51 (0.99)	3.18 (1.25) 1.91 (0.75)	2.42 (0.953) 1.50 (0.59)
$.77 \times 10^6$ (1.7×10^6)	1.27 (0.50)	.76 (0.30)	1.27 (0.50)	.76 (0.30)	1.27 (0.50)	.76 (0.30)
1.4×10^6 (3.0×10^6)	3.81 (1.50)	2.69 (1.06)	3.18 (1.25)	2.36 (0.93)	4.45 (1.75) 2.54 (1.0)	3.18 (1.25) 1.88 (0.74)

A height of 13.1m (43 ft.) was maintained from the bottom of the panels to the top of the main support tower to accommodate the circulation pumps (see Figure 5.16).

The design of the basic structure for each receiver is similar to the structure presented in Figure 5.15. For each design, the member sizes for each case were determined using the member selection feature of the STRUDL computer program.[2]

Static and dynamic loads were applied to the structure and the individual structural member sizes were selected. The selected members were then code checked. The selection of member sizes is an iterative process. After the individual members are selected, based on one of the defined loadings, a new stiffness analysis of the entire sturcture is performed. The loads are then redistributed within the structure, and a code check usually reveals some failed or undersized members. These members are changed and a new stiffness analysis is performed. This process is repeated until the members of the structure pass the code.

5.2.6.3 Loading Conditions--The structure was designed based on static loads (dead weight, component weights, wind and ice) and dynamic loads (earthquake).

Static component weights applied to the structure for each design are shown in Tables 5.13, 5.14, and 5.15. The two largest loadings were the drum weight and the panel weights. Figures 5.17, 5.18, and 5.19 show the drum and panel loading, and point of load application for each size solar receiver.

TABLE 5.13

Component Weights
$.45 \times 10^6$ kg/hr (1.0×10^6 lb/hr) Steam Flow

	KN (kips)
Drum, Water and Downcomers	1,370 (308.1)
Panels, Headers and Extensions	1,997 (449.0)
Horizontal and Vertical Buckstays, Bracing	286 (64.2)
Circulation Pumps	273 (61.3)
Piping and Valves	266 (59.7)
Platforms	141 (31.7)
Connections	155 (34.8)
Crane	445 (100)
Stairways	50.3 (11.3)

TABLE 5.14

Component Weights
$.77 \times 10^6$ kg/hr (1.7×10^6 lb/hr) Steam Flow

	KN (kips)
Drum, Water in Drum	1,922 (432)
Panels, Headers and Extensions	2,037 (458)
Horizontal and Vertical Buckstays, Bracing	534 (120)
Circulation Pumps	289 (65)
Piping and Valves	311 (70)
Platforms	334 (75)
Connections	222 (50)
Crane	445 (100)
Stairways	133 (30)

TABLE 5.15

Component Weights
1.4×10^6 kg/hr (3.0×10^6 lb/hr) Steam Flow

	KN (kips)
Drum, Water and Downcomers	2,522 (567.1)
Panels, Headers and Extensions	6,260 (1407.4)
Horizontal and Vertical Buckstays, Bracing	568 (127.6)
Circulation Pumps	273 (61.3)
Piping and Valves	467 (105.0)
Platforms	489 (110.0)
Connections	374 (84.0)
Crane	445 (100.0)
Stairways	148 (33.2)

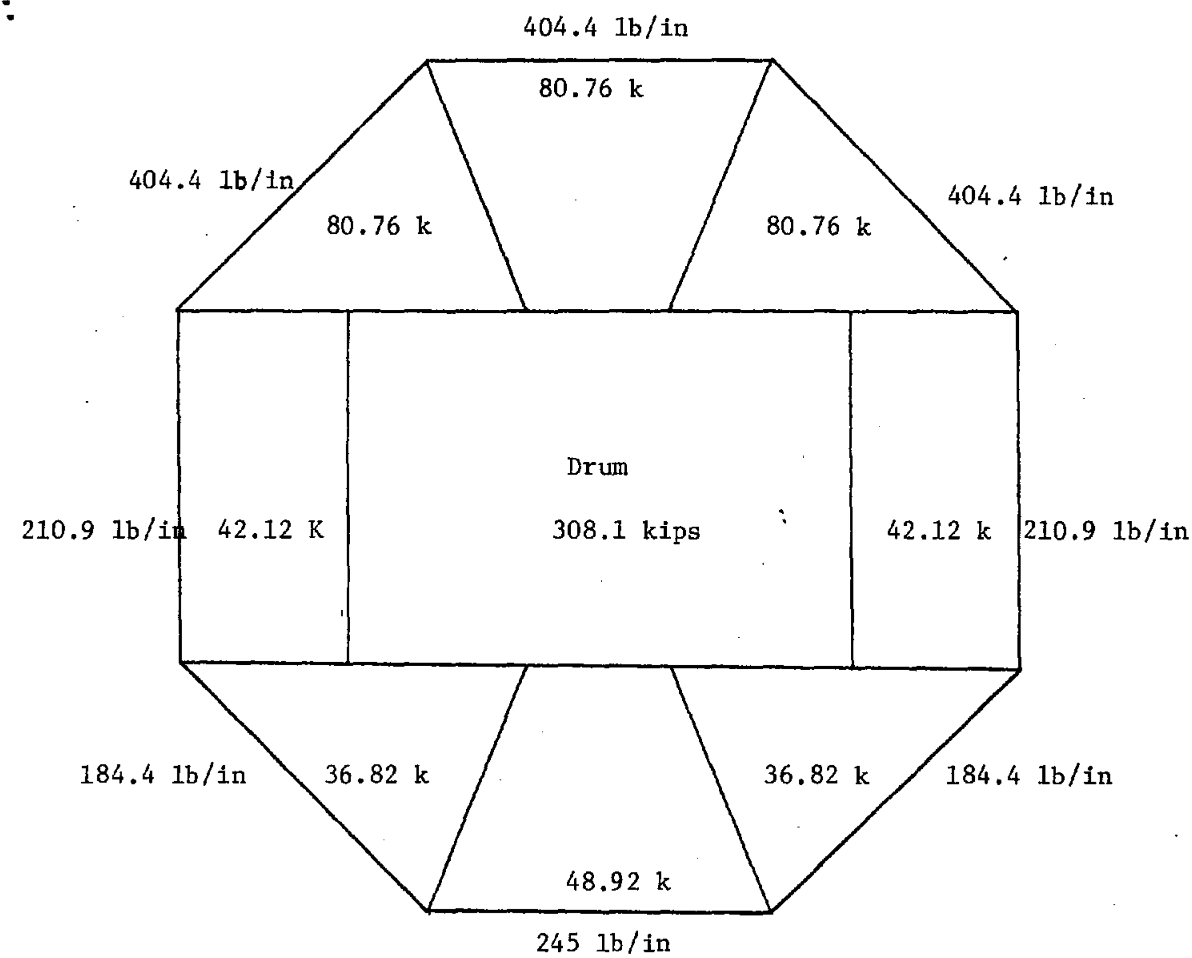

S.I. Conversion:

lb/in x 1.216 = N/m

KIP x 4.448 = KN

Figure 5.17

Panel Weights and Applied Loading to Structure

$.45 \times 10^6$ kg/hr (1.0×10^6 lb/hr) Steam Flow

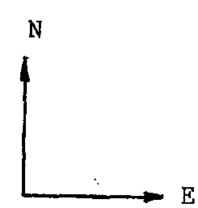

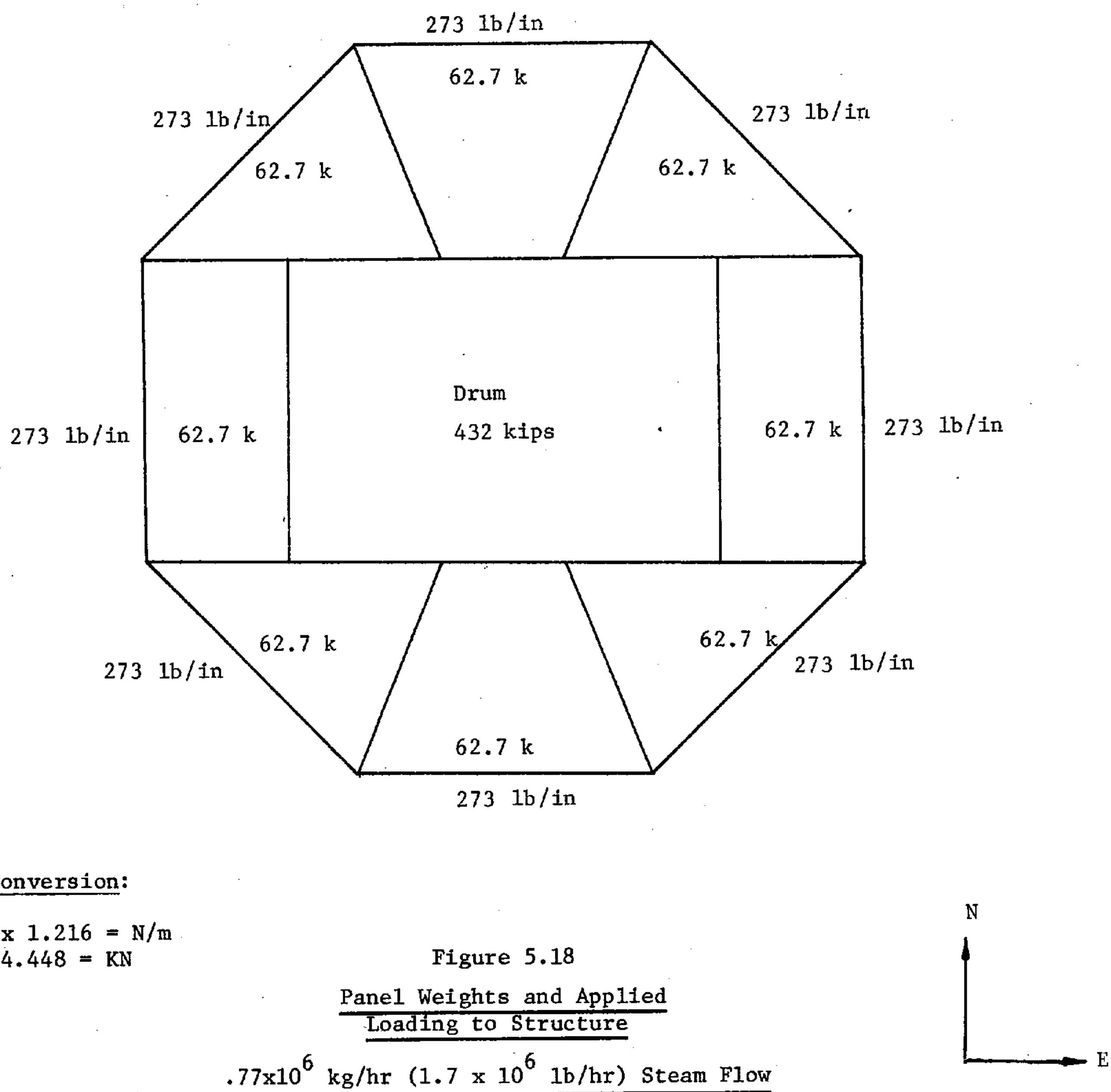

S.I. Conversion:

lb/in x 1.216 = N/m
KIP x 4.448 = KN

Figure 5.18

Panel Weights and Applied Loading to Structure

$.77 \times 10^6$ kg/hr (1.7×10^6 lb/hr) Steam Flow

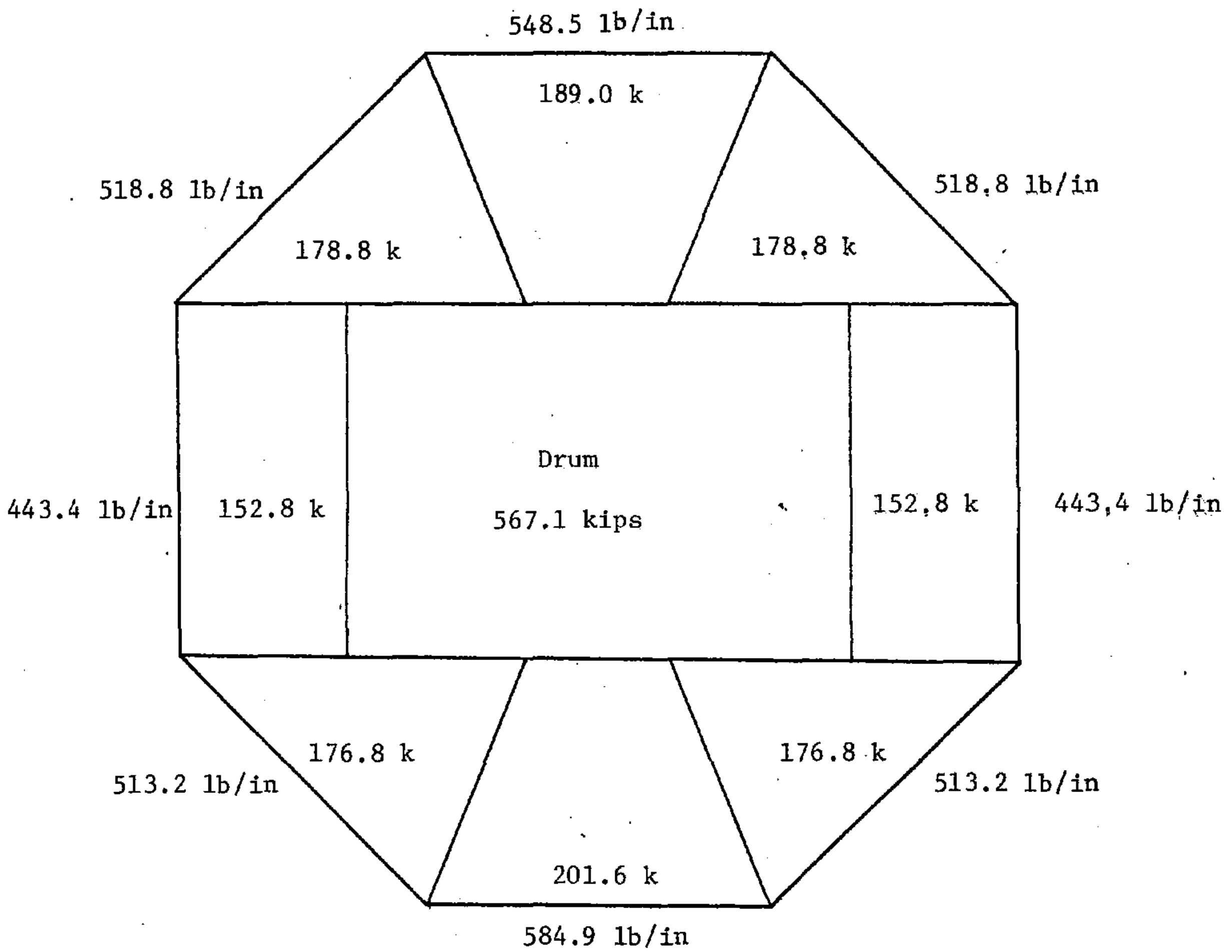

<u>S.I. Conversion</u>

lb/in x 1.216 = N/M
KIP x 4.448 = KN

Figure 5.19

Panel Weights and Applied
Loading to Structure
1.4×10^6 kg/hr (3.0×10^6 lb/hr) Steam Flow

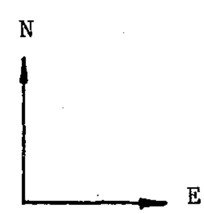

Static ice and wind 'live' loads were applied in conjunction with the component weights to the structure. The ice loading was assumed to be 5.1 cm. (2.0 in.) of ice on all the panels and top platform. The wind loadings were based on UBC pressure load due to wind at an elevation of 290m (950 ft). The winds were applied in the North-South and East-West directions. Table 5.16 shows the calculated loads applied in each case due to ice and wind.

The static dead and live loads were combined as per normal design procedure. The following static loads and loading combinations were applied to the structure:

1. Dead weight (structure and component)
2. Dead weight plus ice load
3. Dead weight plus ice plus wind North-South
4. Dead weight plus ice plus wind East-West
5. Dead weight plus ice plus wind South-North
6. Dead weight plus ice plus wind West-East

Dynamic earthquake loads were applied to the structure. The applied accelerations were determined from the following equations provided by Sandia Laboratories. For lateral acceleration:

$$X_{TT} = 1.05\ X_g + \frac{1}{25} \quad H_T \quad \frac{X_g}{W_R} - 4.4$$

where

H_T = height of support tower, ft

W_R = weight of receiver, kips

For vertical acceleration:

$$X_{TT} = 0.75 \text{ for } x_g = 0.25g$$

TABLE 5.16

Ice and Wind Loading Conditions

Steam Flow kg/hr (lb/hr)	Ice Load KN (kips)		Wind Load* N/m (lb/in)
$.45 \times 10^6$ (1.0×10^6)	421 (94.6)	59.2 (13.3)	76.2 (62.7)
$.77 \times 10^6$ (1.7×10^6)	667 (150)	116 (26.0)	69.3 (57)
1.4×10^6 (3.0×10^6)	1,240 (278.7)	207 (46.5)	133 (109.2

*Wind load along outside of horizontal octagonal member.

The .45 x 10^6 kg/hr (1.0 x 10^6 lb/hr) and the 1.40 x 10^6 kg/hr (3 x 10^6 lb/hr) receiver base accelerations were based on the 'survival' ground acceleration, x_g, of .25g. Using the equation for lateral acceleration, the calculated accelerations based on final receiver weights are:

.45 x 10^6 lb/hr (1.0 x 10^6 lb/hr) x_{TT} = .43g
1.4 x 10^6 lb/hr (3.0 x 10^6 lb/hr) x_{TT} = .46g

Because each receiver tower weight was estimated for the dynamic analysis, a base lateral acceleration of .5g was applied to the structures. The vertical acceleration applied to each structure was .75g.

The .77 x 10^6 kg/hr (1.7 x 10^6 lb/hr) receiver was designed based on the 'operational' ground acceleration of .15g. Using the lateral acceleration equation, the calculated acceleration was .315g. This acceleration was applied in the lateral and vertical directions.

The horizontal and vertical design response spectra are taken from the Atomic Energy Commission (AEC) Regulatory Guide 1.60 (for seismic design of nuclear power plants). Figures 5.20 and 5.21 are plots of the response spectra scaled to 1g accelerations.

A modal analysis using the Householder-Ortega-Weilandt method was performed for the first ten modes using the appropriate accelerations and response spectra. Table 5.17 lists the modal frequencies for the three designs. Equivalent pseudo static loads in the x, y, and z directions were calculated based on combining the modal results using the RMS (root mean square) method. These 'static' loads were then applied to the structure in combination with the real static loads. Additional loading combinations applied to the structure were (continuing from the previous loading conditions):

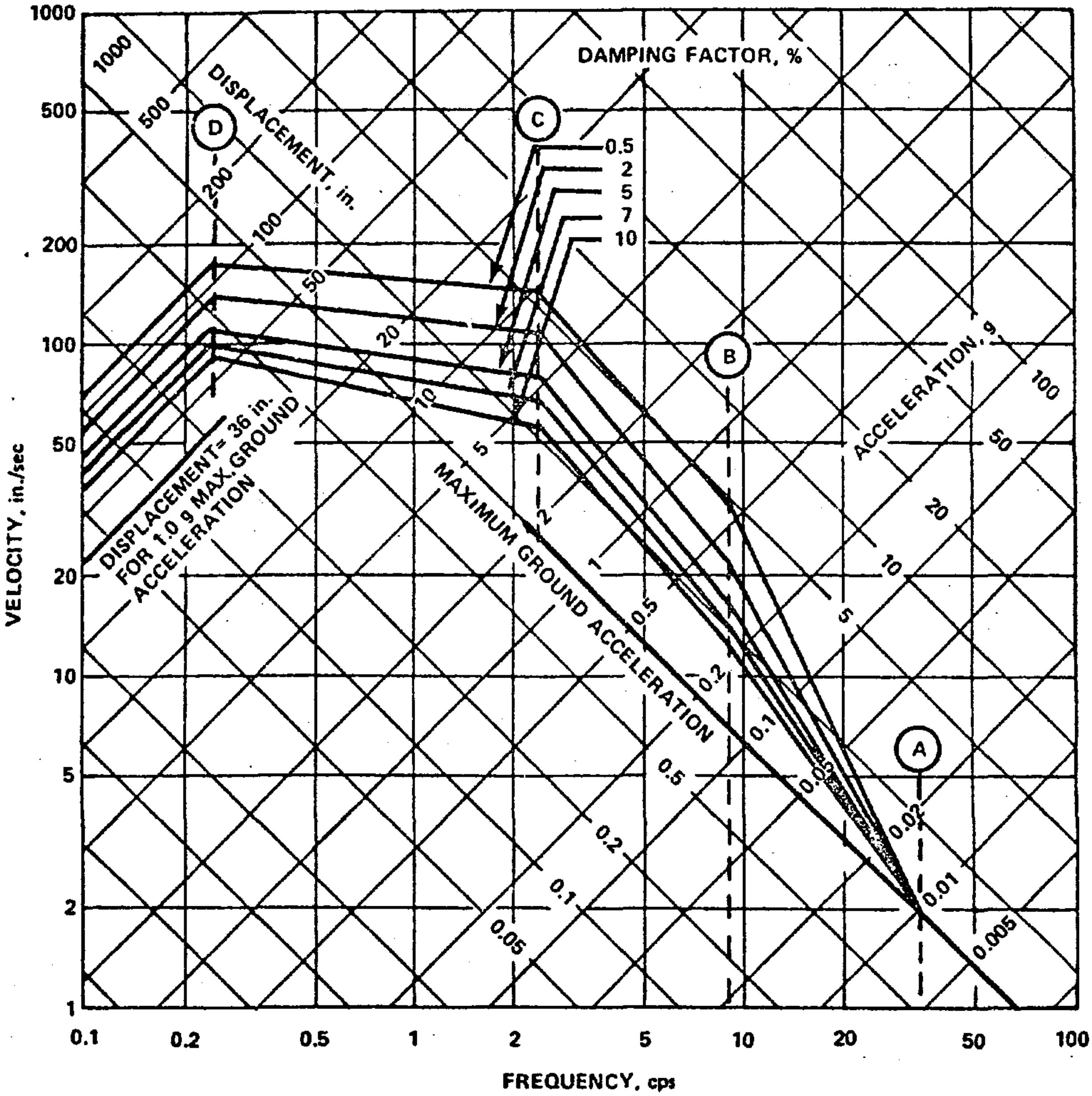

FIGURE 20 HORIZONTAL DESIGN RESPONSE SPECTRA - SCALED TO 1g HORIZONTAL GROUND ACCELERATION

S.I. Conversion

in/sec x 39.4 = m/s
in. x 254 = cm.

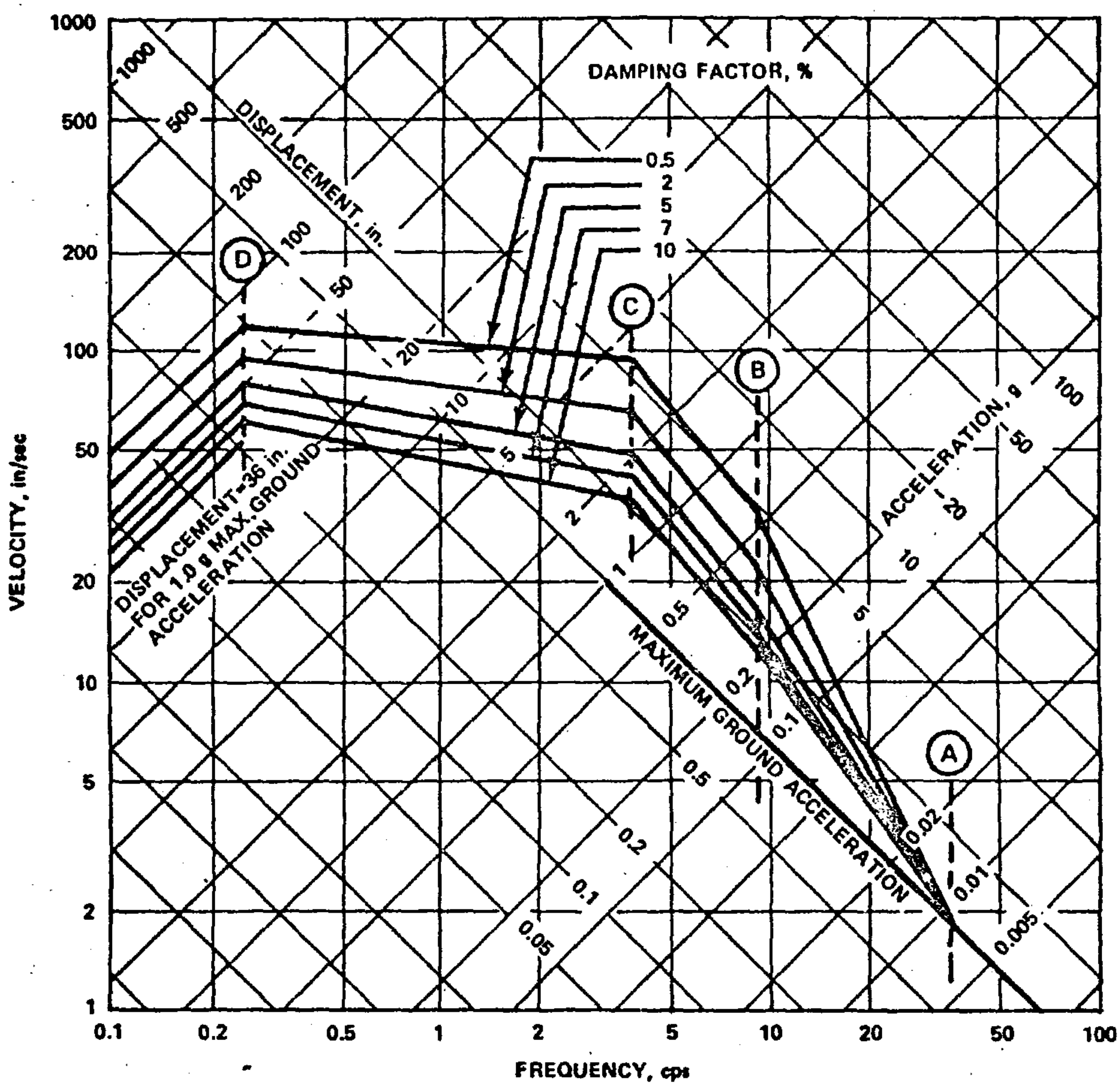

FIGURE 5.21 VERTICAL DESIGN RESPONSE SPECTRA - SCALED TO 1g HORIZONTAL GROUND ACCELERATION

<u>S.I. Conversion:</u>

in./sec. x 39.4 = m/s
in. x 2.54 = cm.

TABLE 5.17

Modal Frequencies (cycles/sec)

Mode	.45 x 10^6 kg/hr (1.0 x 10^6 lb/hr)	.77 x 10^6 kg/hr (1.7 x 10^6 lb/hr)	1.4 x 10^6 kg/hr (3.0 x 10^6 lb/hr)
1	.397	.506	.261
2	1.23	1.61	.728
3	2.03	2.74	1.08
4	2.71	2.75	1.51
5	3.31	2.76	1.91
6	3.75	3.89	2.24
7	3.78	5.19	2.28
8	3.86	5.78	2.71
9	5.94	6.31	3.44
10	6.42	7.36	3.5

7. Dead weight plus 'pseudo-x' earthquake load

8. Dead weight plus 'pseudo-y' earthquake load

9. Dead weight plus 'pseudo-z' earthquake load

10. Dead weight plus 'negative pseudo-x' earthquake load

11. Dead weight plus 'negative pseudo-y' earthquake load

12. Dead weight plus 'negative psuedo-z' earthquake load

5.2.6.4 Boundary Conditions

The receiver support structure was analyzed as a space frame (this allows arbitrary three dimensional deformations). The column diagonal bracing and the horizontal radial bracing were assumed to be pin connected (this allows only axial loading in the member and no moments will be transmitted). The main drum support girders and the secondary drum support steel were also pin connected. The eight outside vertical columns were assumed to be fixed supports.

5.2.6.5 Results

The 12 static and dynamic loads were applied to the structures and the member sizes were selected.

The sizes of every member is not presented, however for each boiler, a representative member size is presented in Figures 5.22, 5.23, and 5.24 for the basic components of the structure. Table 5.18 shows the final weights of the structure and components that were calculated.

5.2.7 Reheater Design

The solar reheater is an independent tube panel section located on the main tower at some distance below the main receiver. A portion of the north heliostat field would be reserved exclusively for reheat duty.

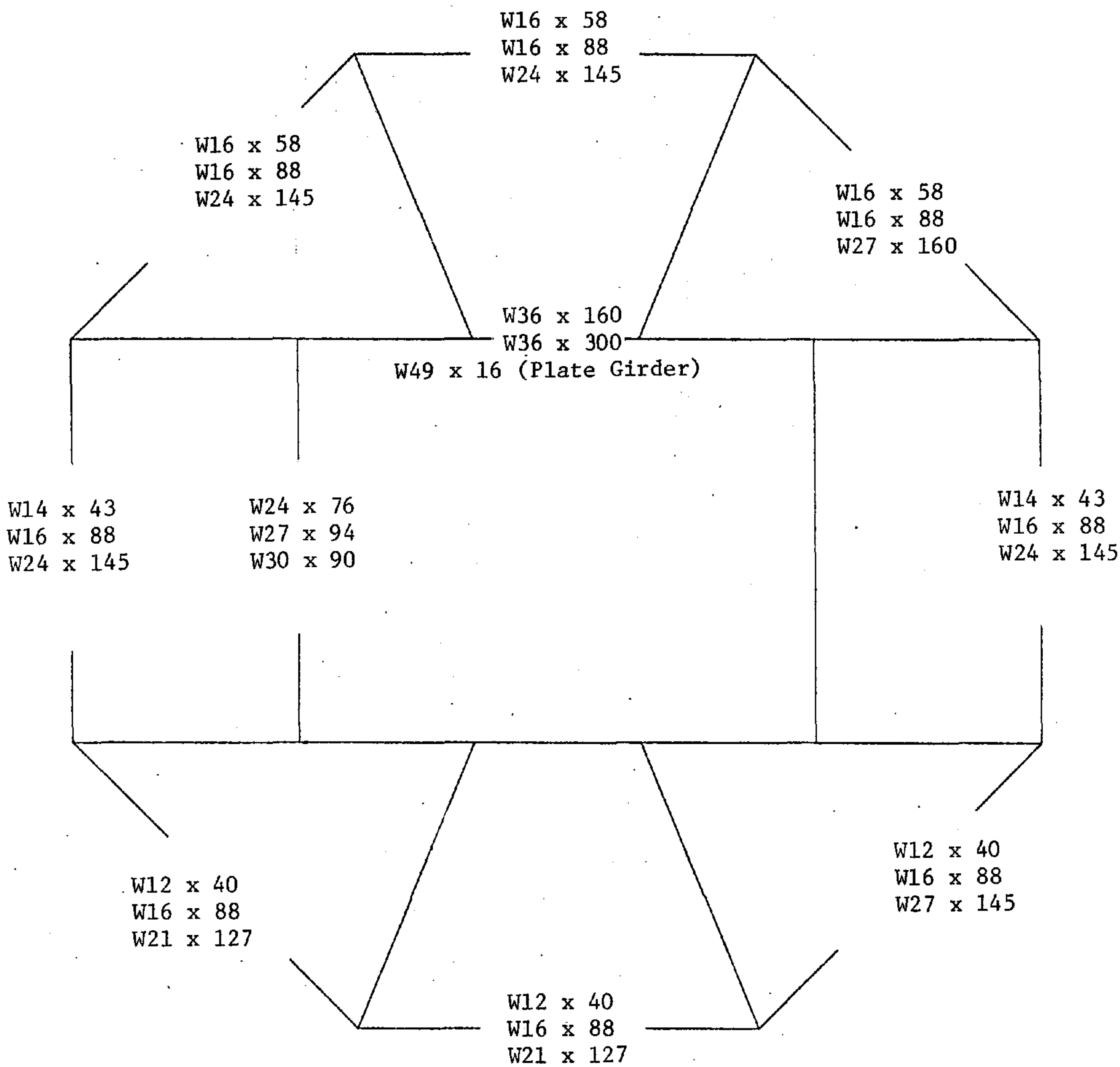

Order, kg/hr (lb/hr):

$.45 \times 10^6$ (1.0×10^6)
$.77 \times 10^6$ (1.7×10^6)
1.9×10^6 (3.0×10^6)

S.I. Conversion:

in. x 2.54 = cm.
lb/in. x 1.216 = N/m

Figure 5.22 Member Sizes Top

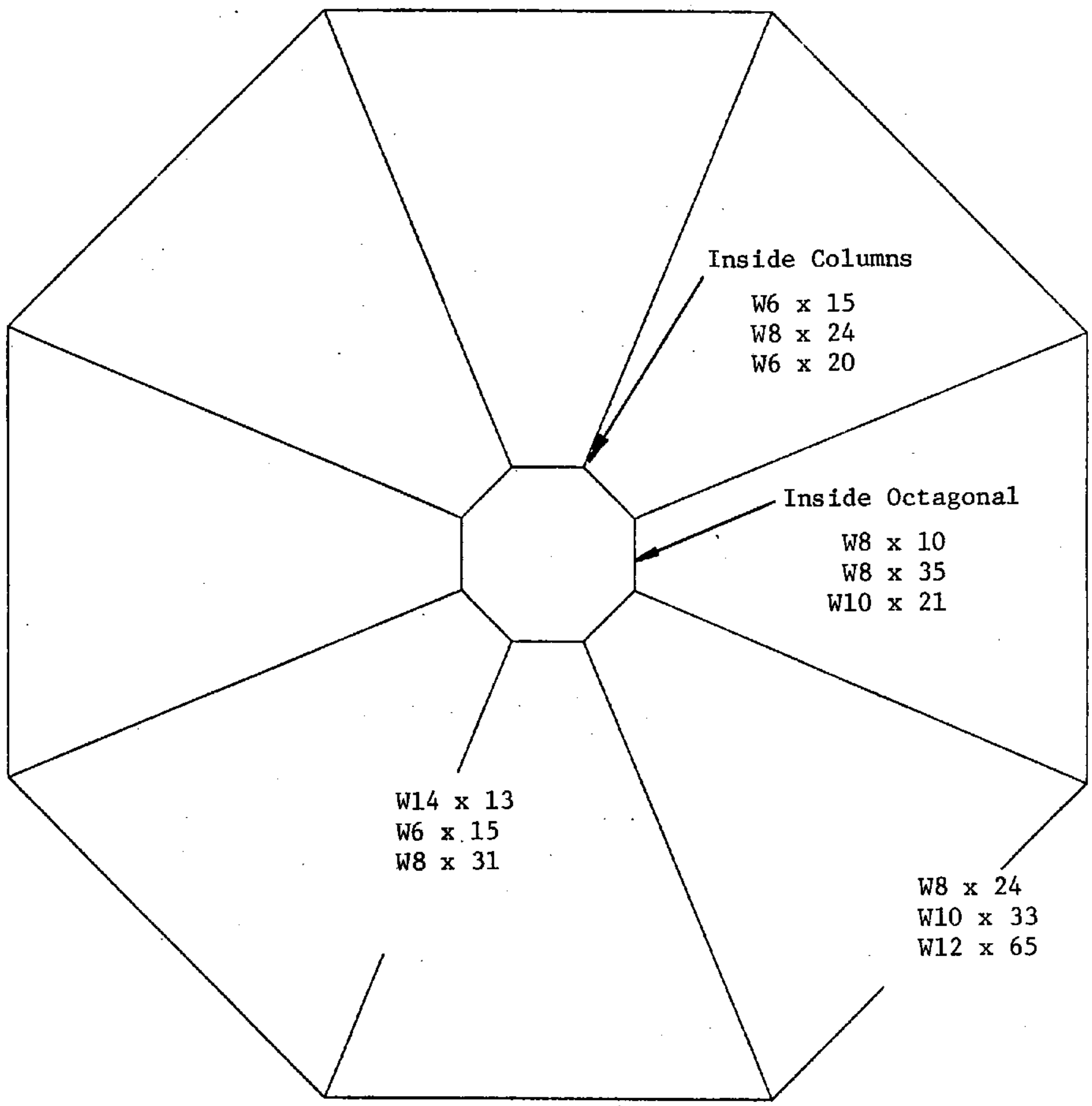

<u>Order, kg/hr (lb/hr):</u>

$.45 \times 10^6$ (1.0×10^6)
$.77 \times 10^6$ (1.7×10^6)
1.4×10^6 (3.0×10^6)

<u>S.I. Conversion:</u>

in. x 2.54 = cm.
lb/in. x 1.216 = N/m

Figure 5.23
Typical Member Sizes
Intermediate Support Level

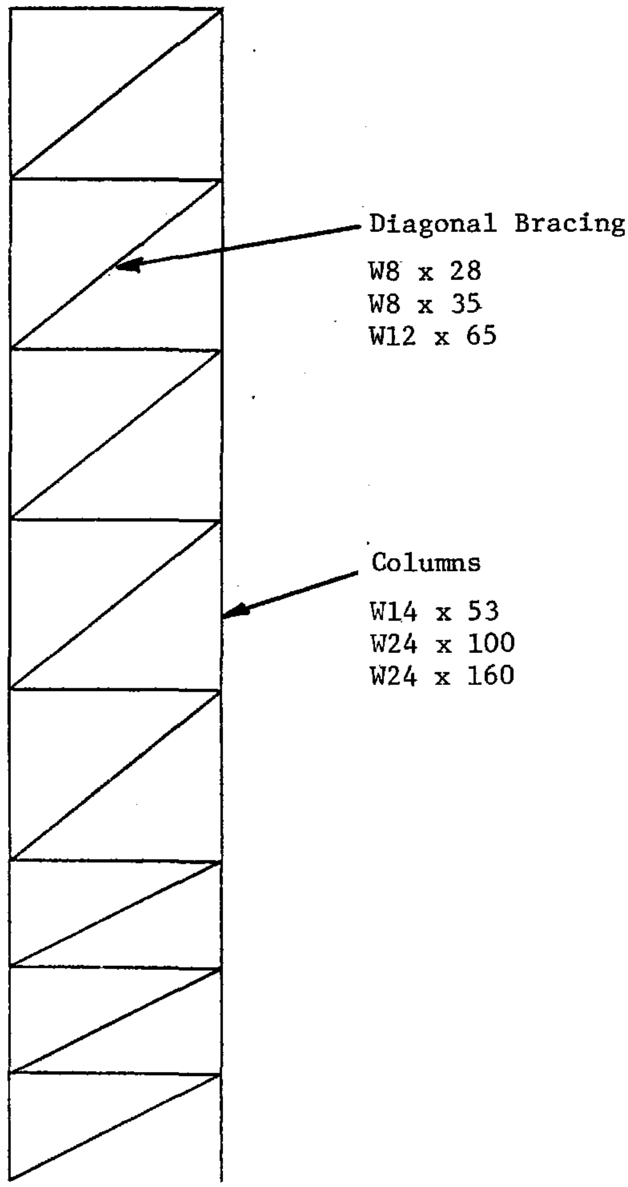

Order, kg/hr (lb/hr):

$.45 \times 10^6$ (1.0×10^6)
$.77 \times 10^6$ (1.7×10^6)
1.4×10^6 (3.0×10^6)

S.I. Conversion:

in. x 2.54 = cm.
lb/in x 1.216 = N/M

Figure 5.24
Typical Member Sizes

TABLE 5.18

Structural and Total Dead Weight

Steam Flow kg/hr (lb/hr)	Structure Weight KN (kips)	Component Weight KN (kips)	Total Weight KN (kips)
$.45 \times 10^6$ (1.0×10^6)	623 (140)	4,982 (1,120)	5,604 (1,260)
$.77 \times 10^6$ (1.7×10^6)	1,401 (315)	6,227 (1,400)	7,628 (1,715)
1.4×10^6 (3.0×10^6)	2,980 (670)	11,324 (2,546)	14,304 (3,216)

The reheater consists of multiple, single pass, parallel tube panels. Final reheat steam temperature is controlled with spray de-superheating prior to the reheat inlet header. Reheater layout is presented in Figure 5.25.

Reheater conceptual design specifications are presented in Table 5.19. The conceptual design selection is based on reheater parameters such that maximum tube crown temperatures and pressure drop developed in the reheater are within acceptable limits. A maximum incident flux of 65,000 BTU/hr-ft^2 is the basis of reheater design. Trapezoidal profile C is the vertical flux profile along the tube panel length.

Several points should be made about the conceptual design. First, the reheaters are sized for the respective turbine cycle requirements on a MWe basis. The reheater requirements are independent of the four receiver sizes which are on a Kg/hr (lb/hr) of steam basis, because the reheater does not carry a solar multiple.

The second point concerns reheater pressure drop. The turbine cycle fixes the available pressure drop to 10% of the extraction pressure, which must include the reheater tubes, headers, piping, valves, etc. A guide-line used in boiler practice recommends that 50-60% of the total pressure drop be in the reheater panels, with the remainder in the piping, etc. Calculations have shown that the pressure drop available for the steam piping from the turbine up the tower, and back, is adequate, and poses no physical restriction on the maximum height from the ground. The cost will be affected by the height, however, and it is suggested that the minimum height which will satisfy the field be selected, and then the piping can be optimized for minimum cost. Reheater steam piping size selections are presented in Section 5.2.5 based on the reheater located 1/3 of the way up the main tower.

Figure 5.25

REHEATER STAGING

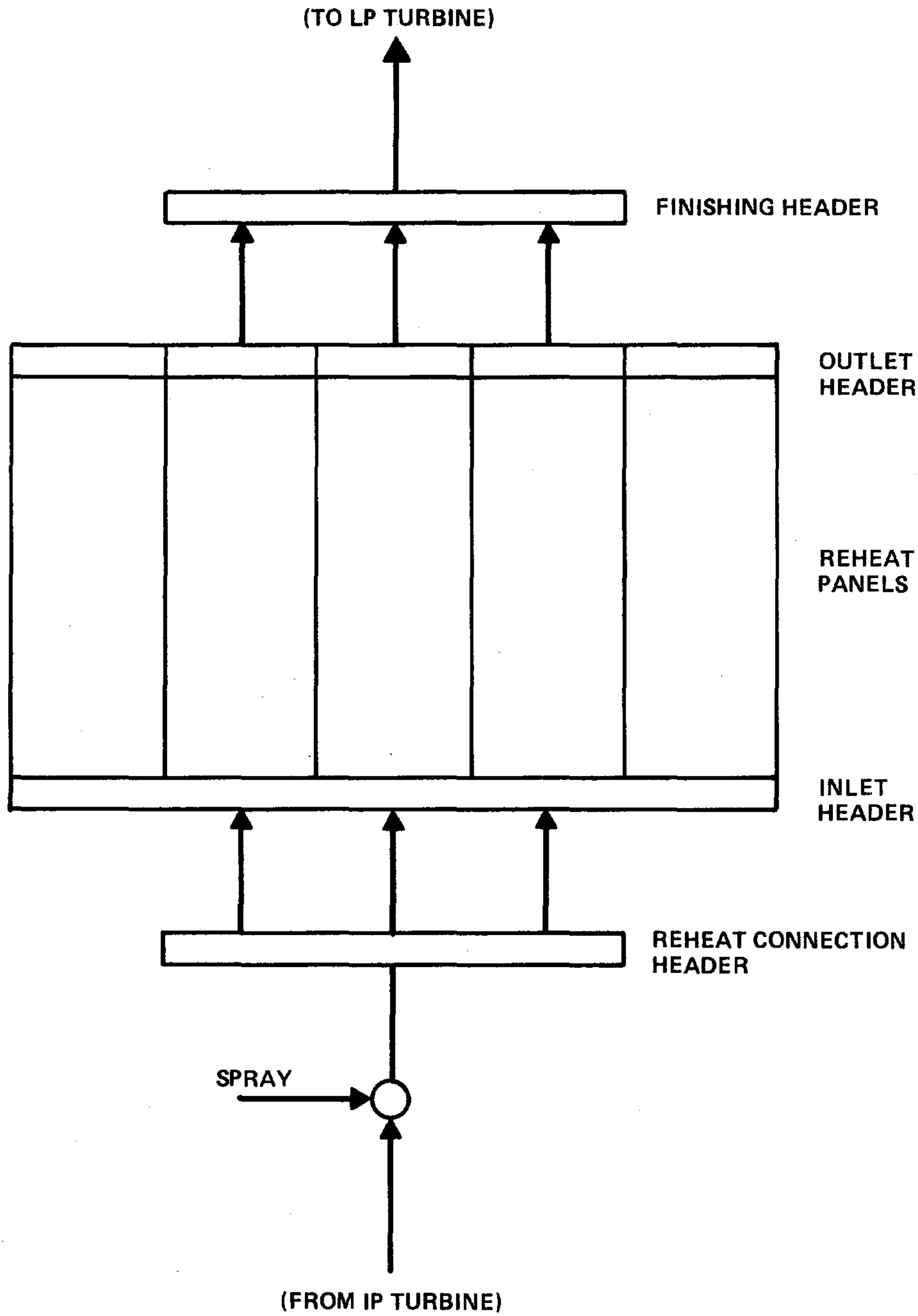

TABLE 5.19

Solar Reheater Design Parameters

Nominal Plant Rating, MWe	100	200	300	400
Turbine Throttle Press., MPa (psia)	12.4 (1800)	12.4 (1800)	16.5 (2400)	16.5 (2400)
Flow Arrangement	Single Stage Upflow	Single Stage Upflow	Single Stage Upflow	Single Stage Upflow
Reheat Steam Flow, kg/hr (lb/hr) x 10^{-3}	263 (580)	617 (1360)	513 (1130)	821 (1810)
Inlet Temp., ^oC (^oF)	336 (636)	331 (628)	333 (632)	333 (631)
Outlet Temp., ^oC (^oF)	538 (1000)	538 (1000)	538 (1000)	538 (1000)
Inlet Press., MPa (psia)	2.83 (411)	2.83 (411)	3.87 (562)	3.86 (560
Outlet Press., MPa (psia)	2.70 (392)	2.70 (392)	3.68 (533)	3.66 (531)
Total ΔP Avail., MPa (psi)	.282 (41)	.282 (41)	.386 (56)	.386 (56)
Heat Absorbed, KJ/hr (BTU/hr) x 10^{-6}	120.3 (114.0)	286.3 (271.3)	244.9 (232.1)	396.2 (375.5)
Max. Incident Flux, MW/m^2 ($BTU/hr\text{-}ft^2$)	.20 (65,000)	.20 (65,000)	.20 (65,000	.20 (75,000)
No. of Parallel Panels	5	11	7	11
Steam Flow/Panel, kg/hr (lb/hr) x 10^{-3}	52.6 (116)	56.2 (124)	73.0 (161)	74.8 (165)
Panel Length, m (ft)	18.3 (60)	18.3 (60)	24.4 (80)	24.4 (80)
Panel Width, m (ft)	3.11 (10.2)	3.35 (11.0)	3.38 (11.1)	3.51 (11.5)
Overall Width, m (ft)	15.5 (51.0)	37.0 (121.3)	23.7 (77.9)	38.4 (126.0)
No. Tubes/Panel	163	176	178	184
Tube OD, cm (in)	1.91 (.75)	1.91 (.75)	1.91 (.75)	1.91 (.75)
Tube ID, cm (in)	1.75 (.69)	1.75 (.69)	1.75 (.69)	1.75 (.69)
Tube Cond., $W/M^2\text{-}^oK$ ($BTU/hr\text{-}ft^2\text{-}^oF$)	277 (160)	277 (160)	277 (160)	277 (160)
Mass Flux, $kg/m^2\text{-}s$ ($lb/hr\text{-}ft^2$ x 10^{-6})	352 (.26)	352 (.26)	461 (.34)	461 (.34)
Panel Header OD, cm (in)	35.6 (14)	35.6 (14)	40.6 (16)	40.6 (16)
Panel Header ID, cm (in)	31.8 (12.5)	31.8 (12.5)	36.3 (14.3)	36.3 (14.3)
Header Length, m (ft)	3.11 (10.2)	3.35 (11.0)	3.38 (11.1)	3.51 (11.5)
Max. Tube Crown Temp., ^oC (^oF)	599 (1110)	593 (1100)	579 (1075)	579 (1075)

The reheater aspect ratio (H/W) affects pressure losses in the tube panels. The 12.4 MPa (1800 psia) and 16.5 MPa (2400 psia) turbine cycles limit reheater loop pressure drop to .284 MPa (41.2 psi) and .387 MPa (56.2 psi) respectively. Panel lengths were selected to limit pressure drop based on turbine cycle operating pressure. The reheater panel widths were then selected based on the required reheater heat load. Resultant reheater aspect rates vary between .5 and 1.2 in the four reheater designs. The selected tube size for all the reheaters is a nominal 1.91 cm. (.75 in.) OD. The maximum tube crown temperature developed in the reheater designs is near 593°C (1100°F). Thermal absorption efficiency in the reheater designs is approximately 78 percent.

5.2.8 Tube Panel Life Analysis--An elastic fatigue analysis was performed on the second stage superheater panel No. 6 in the 1.4×10^6 kg/hr (3.0×10^6 lb/hr) receiver. This tube panel is considered the most critical panel in the receiver because it exhibits the highest tube crown temperature - 615°C (1139°F).

The fatigue analysis is based on the following conditions:

Tube OD, cm (in.)	1.59 (.625)
Tube ID, cm (in.)	1.17 (.46)
Maximum Heat Flux, MW/m^2 ($BTU/hr\text{-}ft^2$)	.242 (76,760)
Internal Tube Pressure, MPa (psia)	19.0 (2750)
Bulk Steam Temp., °C (°F)	576 (1069)
Inside Film Coefficient, $KW/m^2\text{-}°C$ ($BTU/hr\text{-}ft^2\text{-}°F$)	15.0 (2642)

A complete cycle in this analysis is considered a single startup and shutdown sequence from cold conditions, 21°C (70°F). This is not representative of actual receiver operating conditions. Most thermal cycling will be over a partial load excursion as clouds temporarily block portions of the heliostat field. The complete analysis procedure has been outlined in Appendix G.

The maximum elastic effective stress was calculated to be 252MPa (36,600 psi). The 'pseudo' plastic strain range was calculated to be 1.8×10^{-3}, producing an estimated fatigue life of 30,000 cycles. This is a first cycle strain range, and relaxation of this stress with time has not been accounted for. Therefore 30,000 cycles is a very conservative fatigue life. A more representative plastic analysis would result in a greater calculated fatigue life.

5.3 Cost Estimates

Cost estimates for the main receivers are listed in Table 5.20. Costs were estimated in detail for the $.45\times10^6$ kg/hr (1×10^6 lb/hr) and the 1.4×10^6 kg/hr (3×10^6 lb/hr) receivers. The costs for the $.91\times10^6$ kg/hr (2×10^6 lb/hr) receivers are interpolated according to an average power law scaling factor developed from the detailed cost estimates of the other receivers and listed in Table 5.20J. There are actually two receivers for $.91\times10^6$ kg/hr (2×10^6 lb/hr). One was sized for 16.5 MPa (2400 psia) and one for a 12.4 MPa (1,800 psia) steam cycles. The dimension of these two receivers are close, and no great error is introduced by this method.

In Table 5.20, the steam downcomer and water riser piping are listed separately. These costs are a significant part of the total receiver costs. In the large unit, these leads amount to 26% of the total cost. These costs are for carbon steel feed water risers and 316H stainless steam downcomers.

Table 5.21 lists the estimated replacement costs for various panels, with and without headers, for the large and the small receiver. These costs are on a delivered, but not erected basis. Panel attachments are included, but no structural attachments. Reheater costs are listed in Table 5.22. The reheater does not store energy. There is no solar multiple involved. As such, each reheater in Table 5.22 is sized for the particular steam cycle listed. The steam flows, pressures, and temperatures were taken from the four cycles listed. This means that a given reheater cannot be associated one-to-one with a given main receiver and tower. As an example, consider the selection for a 100 MWe plant with a solar multiple of 1.3. The turbine steam flow would be 84.7 kg/s (671,956 lb/hr), with a reheat flow of 73.1 kg/s (579,832 lb/hr). For a solar multiple of 1.3, the receiver would be sized 30% larger, 110 kg/s (873,543 lb/hr). If, for the same turbine cycle, a solar multiple of 1.7 was desired, the main receiver would be sized for 143.9 kg/s (1,142,325 lb/hr), a 70% increase. The reheater size for these two cases would not change. The reheater location on the tower would be a function of the plant rating and the collector field requirements. The interface with the collectors field was not investigated in this study. Consequently, the costs quoted in Table 5.22 does not include reheat steam leads.

TABLE 5.20

Advanced Water/Steam Receiver Costs* (thousands$)

(Delivered and erected)

Receiver Steam Flow	Receiver Only	Water Riser/Steam Downcomer	Total
126 kg/s (1 x 10^6) lb/hr	11,650	2,250	13,900
252 " (2 x 10^6) "	19,600)	5,100	23,380
378 " (3 x 10^6) "	23,450	8,150	31,600

+Scope of Equipment:

1. Evaporator System
2. Superheater
3. Economizer (Preheater)
4. Pressure Parts Support Steel
5. Casing and Buckstays
6. Setting, Insulation, Lagging
7. Circulation Pumps, Valves and Drives
8. Platforms and Stairways
9. Complete Structural Steel
10. Valves and Accessories
11. Solar State Steam Temperature Controls
12. Shop sub assembly

* 1979 Dollars

TABLE 5.21

Estimated Replacement Panel Costs+
(in thousands)

Panel	Receiver Steam Flow	
	126 kg/s ($1x10^6$ lb/hr)	378 kg/s ($3x10^6$ lb/hr)
Preheater Panels w/ Headers (SA-192)	119	219
" " w/o "	93	187
Evaporator Panel w/ Headers (T-11 (rifled tubes)	132	380
" w/o " "	114	348
Superheater Panel w/ Headers (T-22)	128	284
" " w/o "	95	235
Superheater Panel w/ Headers (316H-SS)	303	838
" " w/o "	266	586

* Delivered, but not erected.
Includes panel mountings and buckstay supports.

+ 1979 Dollars

TABLE 5.22

Estimated Reheater Costs (thousand$)+
(Delivered and Erected)

Turbine Power MWe/Press.	Reheater Steam Flow kg/s ($lb/hr x 10^{-6}$)	Reheater Cost
100/12.4 (1800)	73.1 (.58)	2,400
200/12.4 (1800)	171.3 (1.36)	5,200
200/16.5 (2400)	142.4 (1.13)	4,500
300/16.5 (2400)	228.0 (1.81)	7,000

* Does not include reheat steam leads.

+ 1979 Dollars

6. Assessment of Commercial Scale Advanced Water/Steam System, and Recommendations for Future Work

6.1 Potential Improvements

The receivers designed in this study were selected to power a high temperature/high pressure stand alone solar plant with high temperature storage capability. Receiver outlet steam temperature was selected as $593^{o}C$ ($1100^{o}F$) to charge high temperature storage. Based on a 16.5 MPa (2400 psia) $538^{o}C/538^{o}C$ ($1000^{o}F/1000^{o}F$) reheat cycle, a 15% reduction in collector-field requirements would be expected, over that in the Barstow low pressure plant. This is based on the differences in turbine and receiver cycle efficiencies between the two systems. Costs of these high performance receivers varies from $10.53 per pound of steam for the larger unit, to $13.90 per pound of steam for the smaller unit. Since this study not relate a given receiver power to a specified turbine power, a comparison on a KW basis is not possible without taking into account storage multiple. If it is assumed that the $.454 \times 10^{6}$ kg/hr (1×10^{6} lb/hr) receiver could power a buffer only storage plant, approximately 157 MWe could be generated. The unit installed cost for the receiver, including steam and water leads, but exclusive of tower, would be $88.55/kwe.

It is noted that the preferred system is a sub-critical receiver feeding a sub-critical turbine. A study was done to develop the requirements for a "primary loop" supercritical receiver feeding a sub-critical cycle. Results discussed in Section 4 show that this arrangement has serious problems with the heat transfer equipment and requires a larger receiver, with practically all stainless surface to produce the same power. In essence the supercritical receiver requirements are more like those for a superheater than an evaporator.

6.2 Potential Limitations

There are two major areas of uncertainty inherent in the designs of these high temperature receivers, which may impose limitations on operation efficiency and/or lifetime.

There is presently no design data for convective heat losses from these larger external receivers. Since a large amount of surface in the superheater and reheater operates at high temperatures, convective and radiation losses may be significant, especially at lower loads (power level). At some point in the load range, the convective and radiant losses may be greater than the heat absorption, and , power level would be curtailed. Radiation losses can be calculated with some degree of assurance, but the degree of confidence in the convective determination is lacking. A research program and/or test data from Barstow will help solve this problem.

For external receivers, some method of minimizing wind circulation and vertical natural circulation over the face of external receivers should be explored.

The other major design uncertainty of the high temperature receivers is meeting the anticipated 30-year plant life time based on creep-fatigue interactions. Results of an elastic-'pseudo' plastic stress analysis indicated that the high temperature superheater would have a fatigue life of 30,000 full strain range cycles. This value is conservative. It is probable that with a full inelastic analysis, where the stresses are allowed to relax, would produce 50,000 cycles or more. Even so, the question of lifetime is still open. If only diurnel cycles were considered, 10,000 would be sufficient for 30 years. The open ended question is how to assess cloud effects. In the original requirements for this study, it was thought that 50,000 full range cycles would be sufficient. This was based on 10,000 diurnal and 40,000 clouds (4 full shut-downs a day), which is purely arbitrary.

The other unknown is how various clouds, their shading intensity, and frequency, will affect operation. For some, controls will be able to handle operation with minimum cycling of the receiver. How much damage these "smaller" clouds will do is presently unknown. It seems that a large number of operating scenarios would have to be investigated to assess this effect. The solar industry needs a detail specification in this area so that designers can work from the same base point.

As an example, by considering the following scenario, it may be argued that 30,000 full range cycles is sufficient for 30 year's life. If it is assumed that plant maintenance (scheduled) outages, and the fact that some days are too low in insolation to start up, only 75% of the year is available for operation. This accounts for 274 days/year, or 8,213 diurnal cycles in 30 years. If it requires 222 $^{\circ}$C/hr (400°F/hr) assumed start up and shutdown rate, and a dense cloud shut down operation by noon, it would take 2 hours minimum to regain full temperature, and depending on the time of year, shutdown would have to be initiated around 4 p.m. This drastically reduces generation. It would appear that a mid-afternoon re-start would be impractical, even during summer solstice. Hence, 2 full cycles due to clouds would be a maximum tollerated during an operating day. Adding these to 8213 diurnal gives 24,639 cycles, which meets the 30,000 available cycles determined by the above analysis.

Of course, the above scenario is not 100% representative of all conditions. There will be days when operation at derated steam conditions will be possible for either running or charging storage. Hence, the metal is not working at the high temperatures, and a different analysis is required.

6.3 Recommendations for Future Work

Fatigue Analysis: It may be concluded that the only way to assure 30 years' life of the receiver is to show 10^6 cycles or greater in analysis. Certainly this would include most all types of operation. However, until a more definitive design criteria for cloud effects is established, 30,000 full range cycles might also be sufficient for 30 years' life.

With respect to this fatigue life study, it is recommended that: 1. Further stress analysis be undertaken to more accurately define the cyclic lifetime. This would involve an elastic-plastic analysis, which allows stresses to relax; 2. A study be conducted to determine the amount of lifetime gained by lowering the final outlet steam temperature. This should be traded off against the decrease in cycle efficiency.

There are other areas requiring further analysis to more completely define the advanced water/steam system begun here. Under the present contract, approximately 50% of the funds were allocated and expended in Task 10--Rifled Tubing Test Program. This allocation reduced the amount of funds available for the analysis/design tasks. In addition to the stress analysis requirements mentioned above, the following items are identified:

Test Data Analysis: Results of these tests are included in Volume II of this report. The data was plotted for the DNB tests, and listed for all runs. No analysis was included due to time constraints. Analysis should be completed to develop a correlation suitable for computer application to predict DNB performance of the rifled tubing. Pressure drop data should be analyzed to develop an equivalent roughness factor to be applied to the subject rifled tubing pressure loss calibration.

With the above design information, the circulation system could be further optimized.

Other Analyses:

1. Part-load and Transient Analysis. Performance of the subject receivers under part-load operation and during transients should be studied to define control requirements and establish detailed operating procedures. This requires development of a transient model of the system.

2. Stability Analysis. This design should not be prone to either dynamic or static stability but a low load analysis should be performed to verify this and to aid in selection of orificing for matching flows to heat flux.

3. An investigation of the effect of receiver L/D on the collector field requirements and on tower designs should help optimize the interface between these sub-systems.

4. Institutional restraints should be investigated for specific sites, as their effects may be different from site-to-site.

7.0 Rifled Tubing Test Program - Task 10

7.1 Introduction and Summary

The test program described here was included in the conceptual design phase in order to assess the feasibility of designing a high heat flux solar water/steam receiver without the attendant problems associated with DNB and film boiling heat transfer. The objective of these tests was to determine the DNB limits (critical quality and mass flux) for the high peak heat flux associated with the solar receiver. The circulation ratio would then be selected to avoid the DNB and film boiling regions. Test data on the performance of rifled tubing was not available at the 0.85 Mw/m^2 maximum north-panel flux levels. At lower flux levels, rifled tubing has been shown to eliminate DNB and film boiling in evaporators. In some tests nearly 100% saturated steam was obtained before experiencing a DNB temperature excursion. In other cases, evaporators may still be operated with lower circulation ratios (CR) than would be possible with smooth tubing. This has the effect of significantly reducing pump size and pumping power required. Successful performance of rifled tubing in this solar receiver application will hopefully result in an evaporator with a maximum CR = 2:1. Retention of the high heat flux allows a smaller, more efficient receiver for the same output power.

The test program described in this section was developed utilizing an existing heat transfer loop at C-E's Kreisinger Development Laboratory. One unique feature of the KDL test loop is the ability to apply heat to the test tubing over 180^{o} of tube surface. By applying heat to only one side of the tube, the test results are felt to more accurately represent tube behavior under actual operating conditions.

A two-dimensional finite-element heat transfer analysis was also conducted. Temperature profile and heat flux were modeled for the selected rifled tube in order to gage the effect of the rifling geometry on the tube crown temperature measurement. The model was solved with computer program MARC Heat, and the results used to determine thermocouple placement on the tested rifled tube.

The following sections describe the test loop, test matrix, loop operation, final results and finite element analysis. A discussion of the data reduction program is included in Appendix F. A complete collection of the reduced test data is included in Volume II.

Final DNB test data show DNB critical steam qualities to be over 80% for heat flux levels of up to 1.26 Mw/m^2 (measured at the tube interior) for the general range of mass flows expected in this design. Low pressure, low heat flux tests were able to achieve 95+% steam quality over a broad range of mass flow.

The test results in general show critical qualities in excess of 70%. For recirculation (subcritical) boiler, a circulation ratio of 2:1 is desirable for control purposes. This circulation ratio yields a maximum quality of 50%. At the high flux levels encountered in the solar receiver, the rifled tubing increases the critical quality for DNB by a factor of almost 2 over a smooth tube and reaches a critical quality well above that which will be obtained at the design circulation ratio.

7.2 Test Facility Description

The test program under Task 10 was carried out at Combustion Engineering's Kreisinger Development Laboratory. The Heat Transfer and Corrosion Test Loop (HTCTL) was modified specifically for high heat flux--high mass flow testing.

The test loop is in effect an electrically heated, forced circulation boiler designed for sub- and super-critical steam generation. It is a closed loop, (Figure 7.1) with heat rejection to a pair of three-stage condensers. Two different tube segments may be set up at the same time and loop operation

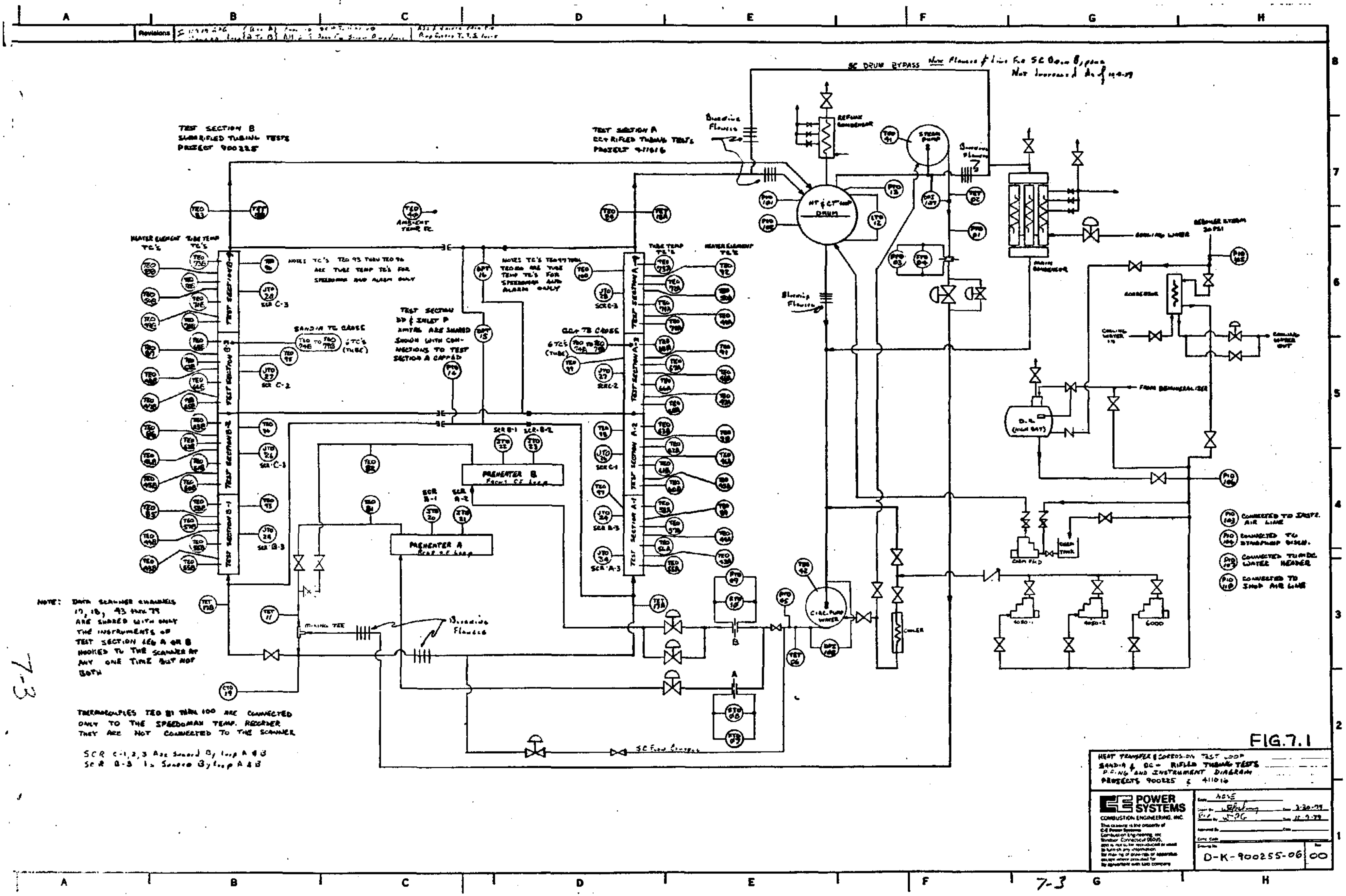

SC DRUM BYPASS
TEST SECTION B
SANDIA RIFLED TUBING TESTS
PROJECT 900225
TEST SECTION A
CE RIFLED TUBING TESTS
PROJECT 411016
HT & CT DRUM
STEAM PUMP
REFLUX CONDENSER
MAIN CONDENSER
COOLING WATER
PREHEATER A
PREHEATER B
CIRC. PUMP
COOLER
CONDENSER
FROM DEMINERALIZER
D.R. (HIGH BAY)
CHEM FEED
MIXING TEE
Bleeding Flanges
SC Flow Control
NOTE: DATA SCANNER CHANNELS 17, 18, 43 THRU 79 ARE SHARED WITH ONLY THE INSTRUMENTS OF TEST SECTION LEG A OR B HOOKED TO THE SCANNER AT ANY ONE TIME BUT NOT BOTH
THERMOCOUPLES TEO 81 THRU 100 ARE CONNECTED ONLY TO THE SPEEDOMAX TEMP. RECORDER THEY ARE NOT CONNECTED TO THE SCANNER
SCR C-1,2,3 Are Shared By Loop A & B
SCR B-3 Is Shared By Loop A & B
HEAT TRANSFER & CORROSION TEST LOOP
SANDIA & CE RIFLED TUBING TESTS
PIPING AND INSTRUMENT DIAGRAM
PROJECTS 900225 & 411016
POWER SYSTEMS
COMBUSTION ENGINEERING, INC.
D-K-900255-06
00

FIG.7.1

can be switched quickly from one to the other by means of blocking flanges. The test loop has approximately 1MWe connected power capability, including power for preheat and the test sections. The steam pump, (Figure 7.1) which recirculates saturated steam from the drum to the test section inlet, provides the equivalent of 2MW additional connected power. Test section and preheater power is provided by resistance heating elements operating at 480 volts a.c.

The rifled tube test element is divided into five sections, the first an unheated entrance section, followed by four heated test sections. The total tube sections are 6.55m (21.5 ft) long, consisting of 2.858cm. (1.125)in. O.D. rifled tubing as shown in Figure 7.2. Each individual section is approximately 1.22m (4 feet) long, separately controlled for heat input. The heat is applied over 180° of circumference of the tube as shown in Figure 7.2. Heater rods are arranged around half the tube with dummy rods on the remaining half. The heater rods contain high flux density heater wire on a central core, surrounded by highly packed boron nitride material. The units are swaged into the shape shown in the figure. Power leads exit from each end of the heater.

Figure 7.3 shows the tube thermocouple detail for one test section. The basic tube thermocouple pattern includes one tube crown temperature measurement at 30.5cm (12 in.) axial intervals with an additional set of radial thermocouples at elevation 378cm (149 in.). Pressure taps are provided at the entrance, exit, and center of the test segments to measure the pressure drop during testing.

A flow diagram including loop instrumentation is shown in Figure 7.1. Saturated water from the drum is pumped into the preheaters by the circulation pump located below the test section. Flow is measured by means of orifices in the flow lines and two pairs of differential pressure cells for high and

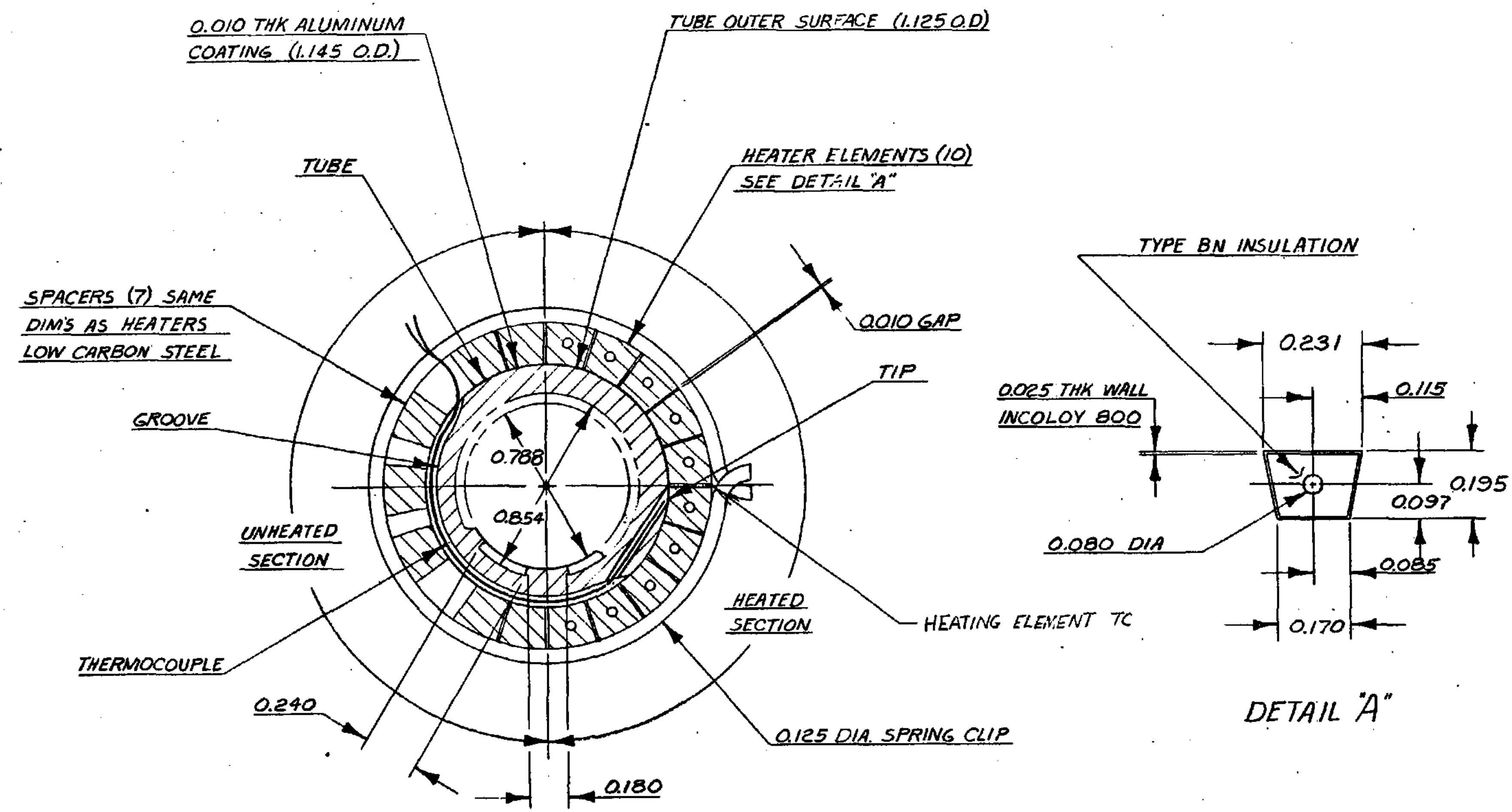

FIG. 7.2

FIGURE 3 SANDIA

TEST SECTION, HEATER ELEMENTS, SPRING CLIPS & SPACERS

PROJECT NO. 900255 DATE 4/2/79

DRAWN BY GJ DWG NO. 900255-2

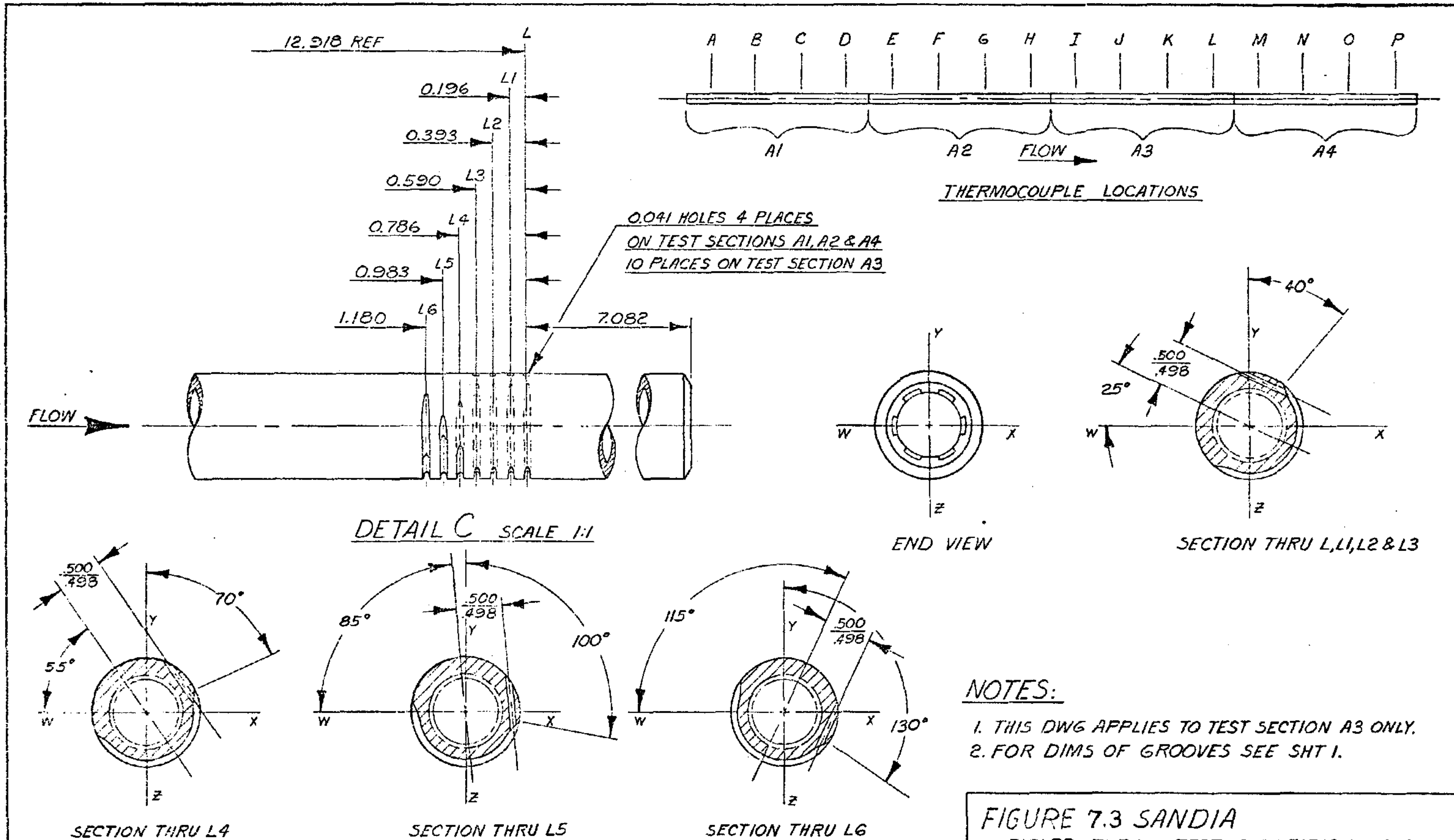

NOTES:

1. THIS DWG APPLIES TO TEST SECTION A3 ONLY.
2. FOR DIMS OF GROOVES SEE SHT 1.

FIGURE 7.3 SANDIA
RIFLED TUBING TEST SUBSECTIONS AND TC LOCATIONS

PROJECT NO 900255 DATE 4/24/79

DRAWN BY GW DWG NO 900255-5 SH 2

low-range pressure drop. Flow through each preheater is controlled by individual control valves. Steam from the drum is routed to the condensers (one reflux) or to the steam pump. Use of the steam pump to deliver saturated steam to the test segment inlet allows higher steam qualities and mass flows than would be possible with the electric preheaters alone. Steam flow is regulated by pneumatically actuated control valves and measured by an orifice as in the case of the water flows. Mixing of the streams takes place in a mixing tee before the test segment inlet.

All control valves are pneumatically actuated from the operator's console. Loop pressure is automatically controlled by regulation of the flow of cooling water to the condensers. A small feedwater pump provides makeup water to the system for any loss which may occur during operation, and a chemical feed pump is available to provide for water treatment.

Instrumentation

The HTCTL is fully instrumented for the departure from nucleate boiling (DNB) and pressure drop testing that is part of the Sandia program. Test section tube wall metal temperatures are measured at 12 inch intervals as are the exterior surface temperatures of the electric heater elements. Absolute pressures and temperatures at each flow orifice are measured by pressure cells and a platinum resistance thermal device (RTD). Input electrical power is measured by watt transducers attached to the silicon controlled rectifier (SCR) power controllers which are used to set individual test section and preheater power input.

Some of these instruments, plus others (drum water level, circulation and pump motor winding temperatures, etc.) are connected to the loop safety system which functions to protect the loop whould an unsafe situation occur. A complete instrumentation list follows (Table 7.1) showing the data scanner channel number, a brief description of the measuring instrument and its range. The "Instrument Tag Number" in Table 7.1 corresponds to the circled instrument numbers on the

TABLE 7.1

INSTRUMENT LIST
Heat Transfer & Corrosion Test Loop
Sandia & CC-Rifled Tubing Tests
Projects 900255

Page 1
Date: October 8, 1979
Rev: 0

Instrument Tag No.	Description	Scanner No.	Transducer Range	Transducer Output	Signal Conditioning
	Short	00			
PTO 01	Steam Orifice Pressure Transmitter	01	0-3000 psig	4-20 ma	I/V 0.7-3.5 VDC
TET 02	Steam Orifice Temp. RTD	02	0-1000^{o}F	4-20 ma	I/V 0.7-3.5 VDC
FTO 03	Steam Orifice DP Hi	03	0-300 in H_2O	4-20 ma	I/V 0.7-3.5 VDC
FTO 04	Steam Orifice DP Lo	04	0-30 in H_2O	4-20 ma	I/V 0.7-3.5 VDC
PTO 05	Water Circ. Pump Discharge Pressure	05	0-4000 psig	4-20 ma	I/V 0.7-3.5 VDC
TET 06	Water Cir. Pump Discharge Temp. RTD	06	0-1000^{o}F	4-20 ma	I/V 0.7-3.5 VDC
FTO 07	Water Orifice A DP Hi	07	0-3000 in H_2O	4-20 ma	I/V 0.7-3.5 VDC
FTO 08	Water Orifice A DP Lo	08	0-30 in H_2O	4-20 ma	I/V 0.7-3.5 VDC
FTO 09	Water Orifice B DP Hi	09	0-300 in H_2O	4-20 ma	I/V 0.7-3.5 VDC
FTO 10	Water Orifice B DP Lo	10	0-30 in H_2O	4-20 ma	I/V 0.7-3.5 VDC
TET 11	Mix TEE Water Inlet Temp. RTD	11	0-1000^{o}F	4-20 ma	I/V 0.7-3.5 VDC
LTO 12	Drum Water Level DP	12	0-50 in H_2O	4-20 ma	I/V 0.7-3.5 VDC
PTO 13	Drum Pressure Transmitter	13	0-3000 psig	4-20 ma	I/V 0.7-3.5 VDC
PTO 14	Test Section Outlet Pressure	14	0-4000 psig	4-20 ma	I/V 0.7-3.5 VDC
PDT 15	Full Test Section Pressure Drop (DP)	15	0-20 psid	4-20 ma	I/V 0.7-3.5 VDC
PDT 16	Half Test Section Pressure Drop (DP)	16	0-10 psid	4-20 ma	I/V 0.7-3.5 VDC
TET 17A & TET 17B	Test Sections A & B Inlet RTD	17	0-1000^{o}F	4-20 ma	I/V 0.7-3.5 VDC

TABLE 7.1 continued

INSTRUMENT LIST
Heat Transfer & Corrosion Test Loop
Sandia & CC-Rifled Tubing Tests
Projects 900255

Page 2
Date: October 8, 1979
Rev: 00

Instrument Tag No.	Description	Scanner No.	Transducer		Signal Conditioning
			Range	Output	
TET 18A & TET 18B	Test Sections A & B Outlet RTD	18	0-1000°F	4-20 ma	I/V 0.7-3.5 VDC
CTO 19	Circ. Water Conductivity Transmitter	19	0-10 Mhos	20-100 mv	
JTO 20	SCR A-1 Power Preheat A	20	0-120 kw	0-24 mv	
JTO 21	SCR A-2 Power Preheat A	21	0-120 kw	0-24 mv	
JTO 22	SCR B-1 Power Preheat B	22	0-120 kw	0-24 mv	
JTO 23	SCR B-2 Power Preheat B	23	0-120 kw	0-24 mv	
JTO 24	SCR B-3 Power Test Section B1 or ½ A1	24	0-120 kw	0-24 mv	
JTO 25	SCR NM6 Power Test Section B-1	25	0-40 kw	0-40 mv	
JTO 26	SCR C-1 Power Test Section B-2 or A-2	26	0-250 kw	0-5v	
JTO 27	SCR C-2 Power Test Section B-3 or A-3	27	0-250 kw	0-5v	
JTO 28	SCR C-3 Power Test Section B-4 or A-4	28	0-250 kw	0-5v	
JTO 29	SCR NM-7 Power Test Section A-1	29	0-40 kw	0-40 mv	
JTO 30	SCR NM-8 Power Test Section A-2	30	0-40 kw	0-40 mv	
JTO 31	SCR NM-9 Power Test Section A-3	31	0-60 kw	0-5 v	
JTO 32	SCR NM-10 Power Test Section A-4	32	0-60 kw	0-5 v	
JTO 33	SCR NM-5 Power Spare	33	0-40 kw	0-40 mv	
JTO 34	SCR A-3 Power Test Section ½ A-1	34	0-120 kw	0-24 mv	

TABLE 7.1 continued

INSTRUMENT LIST
Heat Transfer & Corrosion Test Loop
Sandia & CC-Rifled Tubing Tests
Projects 900255

Instrument Tag No.	Description	Scanner No.	Transducer Range	Transducer Output	Signal Conditioning
--	Short	35			
--	Short	36			
--	Short	37			
--	Short	38			
--	Short	39			
TEO 40	Ambient Temp TC	40			
TEO 41	Steam Pump Winding TC	41	Type K	mv	
TEO 42	Water Circ. Pump Winding TC	42	Type K	mv	
TEO 43	Test Section 1 Heater TC 1	43	Type K	mv	
TEO 44	Test Section 1 Heater TC 2	44	Type K	mv	
TEO 45	Test Section 2 Heater TC 1	45	Type K	mv	
TEO 46	Test Section 2 Heater TC 2	46	Type K	mv	
TEO 47	Test Section 3 Heater TC 1	47	Type K	mv	
TEO 48	Test Section 3 Heater TC 2	48	Type K	mv	
TEO 49	Test Section 4 Heater TC 1	49	Type K	mv	
TEO 50	Test Section 4 Heater TC 2	50	Type K	mv	
--	Short	51			
--	Short	52			

TABLE 7.1 continued

INSTRUMENT LIST
Heat Transfer & Corrosion Test Loop
Sandia & CC-Rifled Tubing Tests
Projects 900255

Page 4
Date: October 8, 1979
Rev: 00

Instrument Tag No.	Description	Scanner No.	Transducer Range	Transducer Output	Signal Conditioning
--	Short	53			
--	Short	54			
TEO 55	Test Section 1 Tube TC 1	55	Type K	mv	
TEO 56	Test Section 1 Tube TC 2	56	Type K	mv	
TEO 57	Test Section 1 Tube TC 3	57	Type K	mv	
TEO 58	Test Section 1 Tube TC 4	58	Type K	mv	
--	Short	59	--	--	
TEO 60	Test Section 2 Tube TC 1	60	Type K	mv	
TEO 61	Test Section 2 Tube TC 2	61	Type K	mv	
TEO 62	Test Section 2 Tube TC 3	62	Type K	mv	
TEO 63	Test Section 2 Tube TC 4	63	Type K	mv	
--	Short	64	--	--	
TEO 65	Test Section 3 Tube TC 1	65	Type K	mv	
TEO 66	Test Section 3 Tube TC 2	66	Type K	mv	
TEO 67	Test Section 3 Tube TC 3	67	Type K	mv	
TEO 68	Test Section 3 Tube TC 4	68	Type K	mv	
--	Short	69	--	--	
TEO 70	Test Section 4 Tube TC 1	70	Type K	mv	

TABLE 7.1 continued

INSTRUMENT LIST
Heat Transfer & Corrosion Test Loop
Sandia & CC-Rifled Tubing Tests
Projects 900255

Instrument No.	Description	Scanner No.	Transducer Range	Transducer Output	Signal Conditioning
TEO 71	Test Section 4 Tube TC 2	71	Type K	mv	
TEO 72	Test Section 4 Tube TC 3	72	Type K	mv	
TEO 73	Test Section 4 Tube TC 4	73	Type K	mv	
TEO 74	Tube TC Cross TC 1	74	Type K	mv	
TEO 75	Tube TC Cross TC 2	75	Type K	mv	
TEO 76	Tube TC Cross TC 3	76	Type K	mv	
TEO 77	Tube TC Cross TC 4	77	Type K	mv	
TEO 78	Tube TC Cross TC 5	78	Type K	mv	
TEO 79	Tube TC Cross TC 6	79	Type K	mv	
--	Short	80			
TEO 81	Preheat A Discharge Fluid Temp. TC	--	Type K	mv	
TEO 82	Preheat B Discharge Fluid Temp. TC	--	Type K	mv	
TEO 83	Test Section Leg B Discharge Fluid Temp. TC	--	Type K	mv	
TEO 84	Test Section Leg A Discharge Fluid Temp. TC	--	Type K	mv	
TEO 85	Test Section B-1 Heater TC 3	--	Type K	mv	
TEO 86	Test Section B-2 Heater TC 3	--	Type K	mv	
TEO 87	Test Section B-3 Heater TC 3	--	Type K	mv	

TABLE 7.1 continued

INSTRUMENT LIST
Heat Transfer & Corrosion Test Loop
Sandia & CC-Rifled Tubing Tests
Projects 900255

Instrument Tag No.	Description	Scanner No.	Transducer		Signal Conditioning
			Range	Output	
TEO 88	Test Section B-4 Heater TC 3		Type K	mv	
TEO 89	Test Section A-1 Heater TC 3		Type K	mv	
TEO 90	Test Section A-2 Heater TC 3		Type K	mv	
TEO 91	Test Section A-3 Heater TC 3		Type K	mv	
TEO 92	Test Section A-4 Heater TC 3		Type K	mv	
TEO 93	Test Section B-1 Tube TC 5		Type K	mv	
TEO 94	Test Section B-2 Tube TC 5		Type K	mv	
TEO 95	Test Section B-3 Tube TC 5		Type K	mv	
TEO 96	Test Section B-4 Tube TC 5		Type K	mv	
TEO 97	Test Section A-1 Tube TC 5		Type K	mv	
TEO 98	Test Section A-2 Tube TC 5		Type K	mv	
TEO 99	Test Section A-3 Tube TC 5		Type K	mv	
TEO 100	Test Section A-4 Tube TC 5		Type K	mv	
PIO 101	Drum Pressure Gauge		0-5000 psig	visual	
PIO 102	Loop Hydrostatic Test Pressure Gauge		0-10,000 psig	visual	
PIO 103	Instrument Air Pressure Gauge		0-200 psig	visual	
PIO 104	Dynapump Discharge Pressure Gauge		0-100 psig	visual	
PIO 105	Reboiler Pressure Gauge		0-60 psig	visual	

TABLE 7.1 continued

INSTRUMENT LIST
Heat Transfer & Corrosion Test Loop
Sandia & CC-Rifled Tubing Tests
Projects 900255

Instrument Tag No.	Description	Scanner No.	Transducers Range	Transducers Output	Signal Conditioning
PIO 106	Dyna Pump Inset Pressure Gauge		0-60 psig	visual	
PIO 107	MDC Water Pressure Gauge		0-100 psig	visual	
PIO 108	Water Circ. Pump DP Gauge		0-300 psid	visual	
PIO 109	Steam Pump DP Gauge		0-50 psid	visual	

flow/instrumentation diagram, Figure 7.1.

7.3 Data Acquisition/Reduction

7.3.1 Data Acquisition--When a selected test condition is attained the data acquisition system is activated to record the loop condition for subsequent reduction by the HTCTL computer code. Most instrument signals from the measuring transducers are in the form of a varying amperage output. These signals are conditioned to a variable voltage output by a signal conditioning device and then recorded by an automatic data scanner. Data from the loop are simultaneously recorded on punched paper tape in the C-E central computer system. There are 80 channels of data recorded five times at one minute intervals during each complete data scan. Some information (test number, observed DNB elevations, time-of-day, barometer, etc.) are entered manually by the operators.

Individual channel voltages may be monitored by the operator at the console or at the data scanner. A schematic of the data acquisition/reduction process is shown in Figure 7.4.

7.3.2 Data Reduction Procedure--The data reduction procedure used to reduce raw data from the data scanner file to engineering terms is described below. Most data reduction was performed on C-E's CDC Cyber 172 computer using the NOS time sharing system.

After the data scan was completed at the test loop a procedure is initiated by the loop operator at the timesharing terminal located near the test loop. The data reduction computer program is used to reduce the stored raw inputs to usable form. An output printout showing instrument outputs, errors and results of flow and temperature calculations is printed out at the terminal for immediate reference. The entire process, from completion of the automatic data scan to completion of the output printing requires about four minutes. All raw data was saved on disk memory in the CDC system for future use or reference, a copy on

Data Acquisition/Reduction Schematic
Sandia DNB Test
Figure 7.4

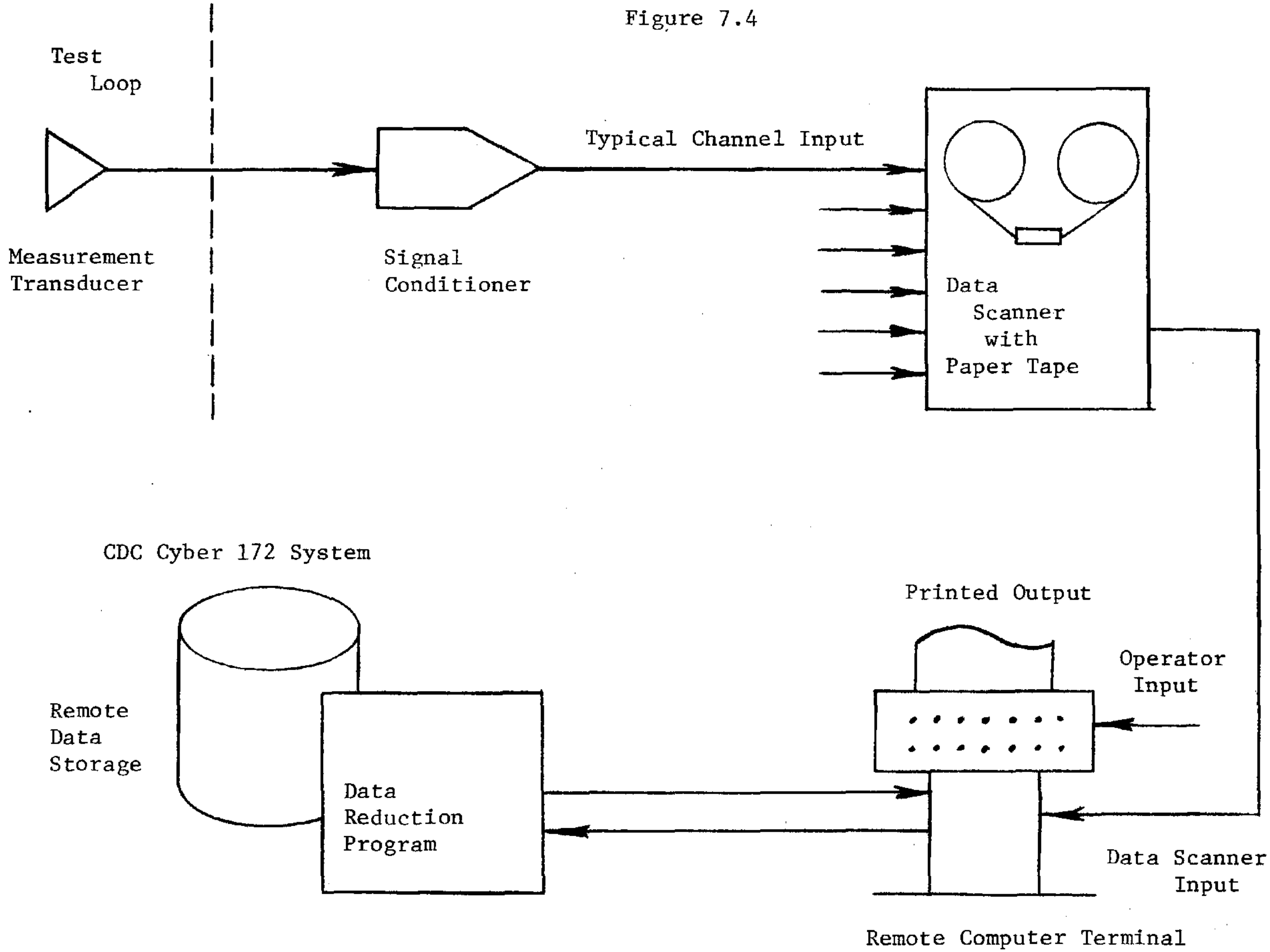

paper tape was also retained as a further backup.

7.3.3 <u>Data Reduction Program (HTLRED1)</u>--The data reduction program HTLRED1 uses the above data files to produce a data output sheet for each test point. A sample output appears in Figure 7.5.

<u>Reduced Data Output</u>

Heading

The top two lines characterize the test by identifying the laboratory doing the work, the project number, and the type of test.

The next line gives the test number of that particular test, the time, and date of the test. This test date should correspond to the constant file date listed at the bottom of the page to assure that the proper instrument conversion constants were used to reduce the data.

The test section conditions are listed for each test as follows:

Test section outlet pressure is given in psia. Total flow (A, B circulating flows and steam flow) is given in lb/hr. Rifled tube mass flow is given in lbm/hr/ft^2. This is the flow per unit cross sectional area in the tube. For rifled tube, major (root) diameter is used as a representative diameter.

The test section temperatures are next given with thermocouple numbers, heat flux to the test section at the location of each thermocouple, quality at same location and indication of DNB. Heat flux is calculated at the root diameter based on 180^o of heat input to the fluid.

Pressure drops at various test section locations are given with corresponding inlet and outlet qualities.

Also given is the test section quality at the inlet and outlet of each pressure drop measurement zone.

FIGURE 7.5
REDUCED DATA OUTPUT SHEET

C E KREISINGER DEVELOPMENT LABORATORY
PROJECT #900255 SANDIA SOLAR RECEIVER RIFLED TUBE DNB TEST
TEST # 127 TIME 1020 DATE 11/20/79

TEST SECTION CONDITIONS

OUTLET PRESSURE	2105.4	+/-	5.4	PSIA
TOTAL FLOW	.4343E+04	+/-	.38E+02	LB/HR
RIFLED MASS FLOW	.1092E+07	+/-	.95E+04	LB/HR-FT2

TC#	ELEV (IN)	TEMP	HEAT FLUX AT TC (1000 BTU/HR-FT2)	QUALITY AT TC (PCT)	DNB
73	200.	769.	303.6 +/- 5.1	51.7 +/- 2.3	
72	188.	772.	303.6 +/- 5.1	49.9 +/- 2.3	
71	176.	766.	303.6 +/- 5.1	48.2 +/- 2.3	
70	164.	771.	303.6 +/- 5.1	46.4 +/- 2.3	
68	148.	768.	301.1 +/- 5.1	45.3 +/- 2.3	
67	136.	778.	301.1 +/- 5.1	43.5 +/- 2.3	
66	124.	772.	301.1 +/- 5.1	41.8 +/- 2.3	
65	112.	784.	301.1 +/- 5.1	40.0 +/- 2.3	
63	96.	750.	295.2 +/- 5.1	38.9 +/- 2.2	
62	84.	736.	295.2 +/- 5.1	37.2 +/- 2.2	
61	72.	759.	295.2 +/- 5.1	35.5 +/- 2.2	
60	60.	753.	295.2 +/- 5.1	33.8 +/- 2.2	
58	44.	767.	290.6 +/- 5.2	32.6 +/- 2.2	
57	32.	752.	290.6 +/- 5.2	31.0 +/- 2.2	
56	20.	784.	290.6 +/- 5.2	29.3 +/- 2.2	
55	8.	787.	290.6 +/- 5.2	27.6 +/- 2.2	

PRESSURE DROPS

LOCATION	INLET QUALITY (PCT)	OUTLET QUALITY (PCT)	PRESSURE DROP (PSID)
TOTAL TEST SECTION	27.1 +/- 2.2	52.3 +/- 2.3	8.13 +/- .16
UPPER TEST SECTION	39.5 +/- 2.3	52.3 +/- 2.3	4.95 +/- .08

RIB TEMPERATURE PROFILE

768.2 689.6 783.8 789.2 779.7 772.1 763.3

TEST SECTION OUTLET FLUID PROPERTIES

SAT TEMPERATURE	643.1	+/-	.4	F
STEAM SPEC VOL	.17431	+/-	.00069	FT3/LB
WATER SPEC VOL	.02618	+/-	.00003	FT3/LB
STEAM VISCOSITY	.05437	+/-	.00005	LB/FT-HR
WATER VISCOSITY	.17039	+/-	.00021	LB/FT-HR
SURFACE TENSION	.000398	+/-	.000003	LB/FT
STEAM THERM CONDUCTIVITY	.0651	+/-	.0002	BTU/HR-FT-F
WATER THERM CONDUCTIVITY	.2666	+/-	.0003	BTU/HR-FT-F
STEAM SAT ENTHALPY	1130.10	+/-	.44	BTU/LB
WATER SAT ENTHALPY	684.43	+/-	.63	BTU/LB

CONST FILE DATE 12/14/79 K DATA REDUCED 09.38.33. 80/01/24.

KDL PROJ LEADER . . . . DATE . ./ . /. .

Test Section Outlet Fluid Properties

With test section outlet pressure and temperature, fluid properties were obtained through 1967 ASME steam table subroutines and functions. Listed properties are shown below:

Fluid Property	Subroutine or Function	Unit
Saturation Temperature	TSL	^oF
Steam Specific Volume	SRSORT	Ft^3/lb
Water Specific Volume	SRSORT	Ft^3/lb
Steam Viscosity	VISV	lb/ft-hr
Water Viscosity	VISL	lb/ft-hr
Surface Tension	TENS	lb/ft
Steam Thermal Conductivity	CONDV	BTU/hr-ft-F
Water Thermal Conductivity	CONDL	BTU/hr-ft-F
Steam Saturated Enthalpy	SATUR	BTU/lb
Water Saturated Enthalpy	SATUR	BTU/lb

The constant file (TAPE88) used to reduce the data is also included. This date would ordinarily correspond with the date of the test data listed at the top of the page. Also given are the time and date when the data was reduced.

7.4 Test Matrix

The test matrix for DNB and pressure drop data was developed to take the maximum advantage of the heat transfer test loop capabilities. In general, set-up points were developed to allow measurements of pressure drop at various flows and test section outlet steam qualities. During the course of the test program, as the DNB curves became obvious, additional starting points were added to "fill in" gaps in the DNB data and to extend the DNB testing to the maximum mass flux available. For the Sandia test program the range of loop parameters were as follows:

Pressure	2100 psig and 2850 psig
Test Section Heat Flux	100,000 to 400,000 $BTU/hr/ft^2$
Test Section Outlet Steam Quality	0 to 100+%
Test Section Mass Flux	0.2 to 1.9×10^6 $lbm/hr/ft^2$

Loop pressure and test section heat flux were held constant for each individual test run. Mass flow was then varied manually to determine the DNB flow rate (see section 7.5.3).

The combined use of the electric preheaters and the steam pump allowed considerable variation of the test section inlet (and therefore outlet) steam conditions. Steam quality at any point in the test section is calculated by the data reduction program.

The loop performed within design and safety parameters set up prior to the test program. The 400,000 $BTU/hr/ft^2$ heat flux level is the highest heat flux level run to date on the HTCTL and is believed to be the upper limit for the present configuration and materials.

7.5 Loop Operation

7.5.1 Calibration--Two complete calibrations of loop instrumentation were done during the Sandia test program--one at the start of testing and one at the completion of the test plan. Individual instruments were calibrated as follows:

Platinum resistance temperature devices-(RTD) were calibrated in a heated fluidized bed and checked against a laboratory standard RTD. Ice points were taken during the test program to check for any drift which may have occurred with time.

Pressure cells were calibrated by a dead weight cylinder for pressures in the range of the test plan.

Differential Pressure cells were calibrated against simple manometers while both were subjected to static pressures in the range of loop operating conditions.

The watt transducers were removed from the test loop and bench-calibrated at reduced voltages and loads.

Thermocouples were not separately calibrated, but the tube T.C.'s were checked during shakedown for uniformity and good contact.

The results of each individual instrument calibration were correlated by regression analysis which resulted in the constants used in data file TAPE88 and in the uncertainties discussed in Appendix F. For the most part, very little change was seen in the individual correlation constants over the course of the test program. The one exception was the differential pressure cell which measured low flow on the B water line.

7.5.2 Shakedown--Loop shakedown for the Sandia test program included heat loss tests, operator training, and a general checkout of loop operation. The heat loss tests were conducted to determine the relationship between heater element temperature and test section heat loss, as well as preheater bulk fluid temperature and preheater heat loss. The coefficients determined by these tests were included in the constant file (TAPE88) and used throughout the test program.

Heat loss testing was performed by first filling the loop and steam drum with water and pumping up to a hydrostatic pressure of 2500 psig. The preheaters and test section power controllers were then turned on to supply heat to the circulating water. Since sub-cooled liquid was used for all heat loss testing, the amount of heat transferred to the fluid may be measured by comparing test section and preheater inlet and outlet temperatures and mass flow rates. Heat input is determined from the watt transducers and the difference is the heat loss to the test loop surroundings. Heat losses for the total test section and the preheaters were plotted against heater element surface temperature and bulk fluid temperature, respectively (Figures 7.6a and 7.6b). The heat loss tests were repeated at the end of this Sandia test program.

7.5.3 Test Procedure--Testing was carried out on a 24-hour basis with weekend and holiday shutdowns. The test program went smoothly, with only minor equipment failures, none of which warranted curtailment or delay of the test program.

The following procedure was used for all test points. First, the loop is stabilized at the set up or starting point. Heat flux and mass flow are checked by running the data reduction program for a series of data scans taken at that point. Once the set up point has been established, the operator then begins to search for DNB.

The top test section tube metal temperature thermocouples are connected to a strip chart recoder as well as the automatic data scanner. To establish a DNB test condition, the operator reduces water mass flow rate while monitoring the strip chart recorder output. Test Section Heat flux and preheater power is normally kept constant. When a DNB point is reached, tube metal temperatures at that point rise and this is visible on the strip recorder. After allowing the condition to stabilize, another data scan is taken with the operator inputting the observed DNB elevations. As DNB is a function of steam quality and mass flow at a given temperature, pressure, and heat flux, this method establishes one such condition under which DNB will occur. Since the highest steam qualities occur in the top of the test segment, DNB will usually be observed there first and not occur in the lower three test sections. For data analysis purposes, however, the temperature profile of the entire tube is examined and the onset of DNB defined as the conditions existing at that

TOTAL TEST SECTION HEAT LOSS vs TEMPERATURE DIFFERENCE

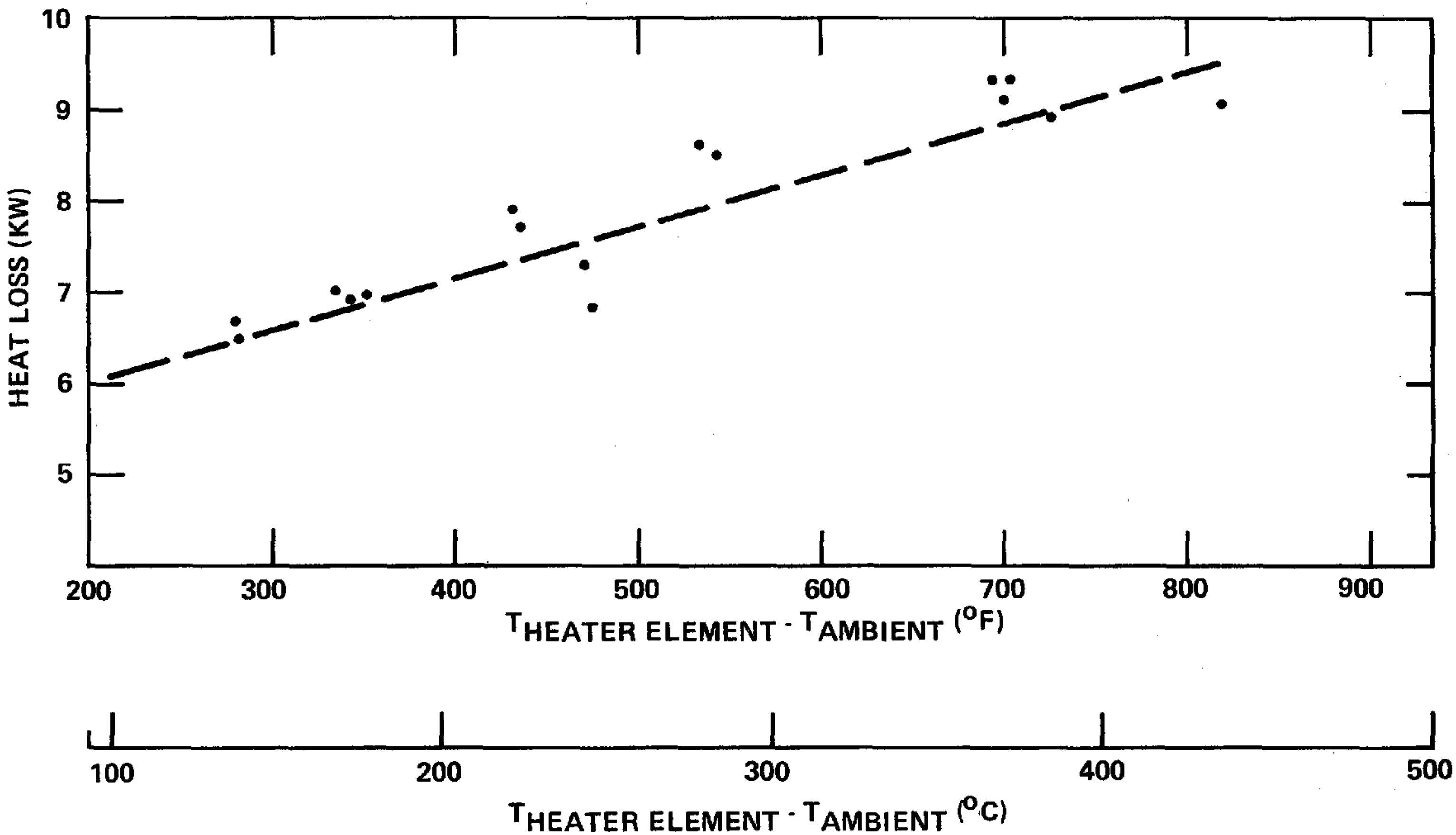

FIGURE 7.6a

PREHEATER HEAT LOSS vs TEMPERATURE DIFFERENCE

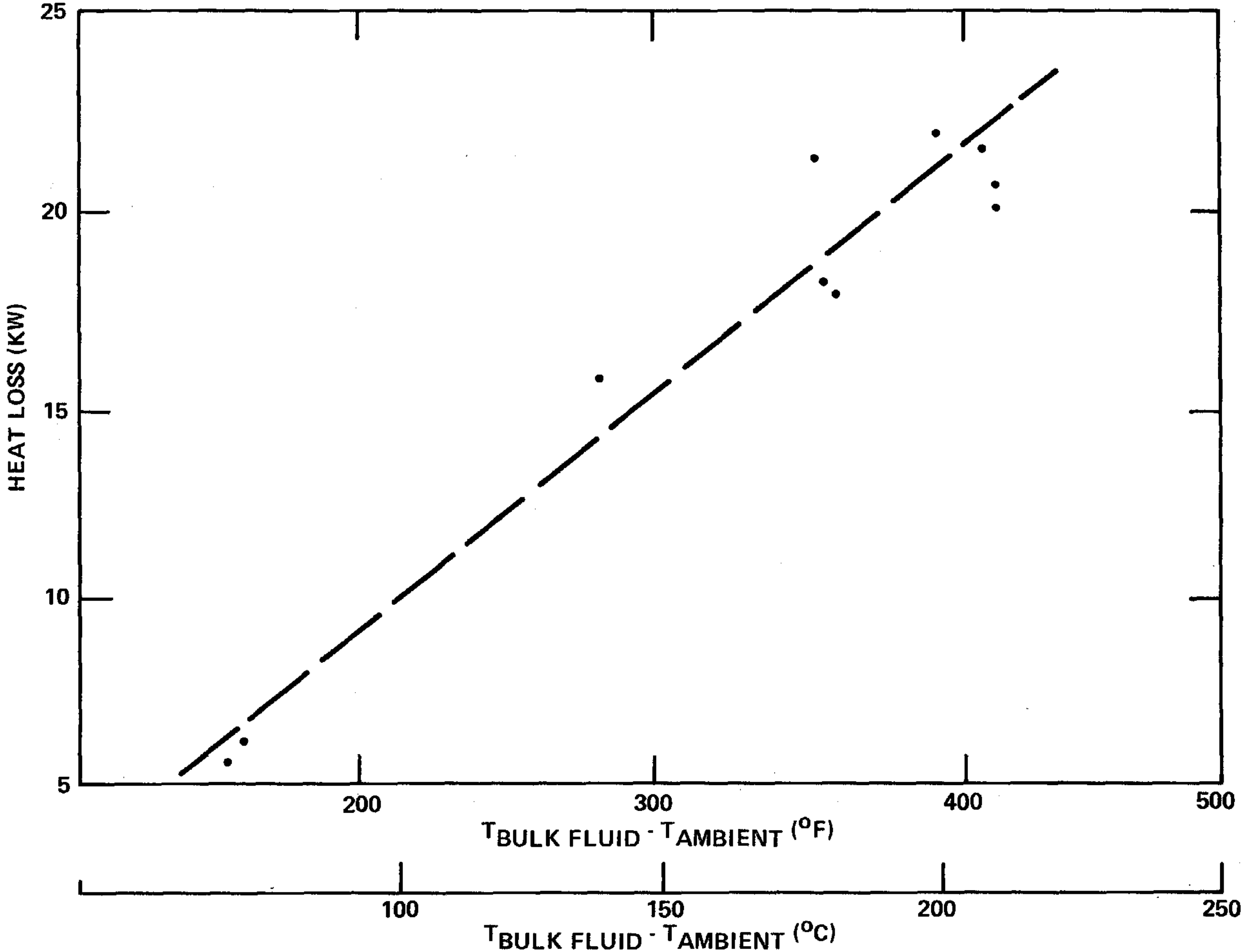

FIGURE 7.6b

elevation which first exhibits a $2.8^{o}C$ ($5^{o}F$) temperature departure from the nucleate boiling level. Using this basis provides a consistant operator-independent criteria for evaluating the test data. A sample of the strip chart during two DNB test points are shown in Figure 7.7, 7.8 and listings of the reduced data printout follow.

The tube metal temperatures that appear on these reduced output pages are uncorrected outputs from the chromel-alumel thermocouples installed on the rifled tubes. Due to small variations in the placement and contact of the individual thermocouple beads, the listed temperatures show variation over the length of the tube. For this reason the printed tube temperatures should not be used for boiling heat transfer coefficient calculations unless corrected to a common basis. The temperature at a given elevation does not vary significantly for fixed pressure and heat flux levels unless the tubing at that elevation is experiencing DNB during the data scan as can be seen in the upper elevations of runs 149B and 151B. The accuracy of the individual thermocouples used here is $\pm 2.22C$ ($4^{o}F$).

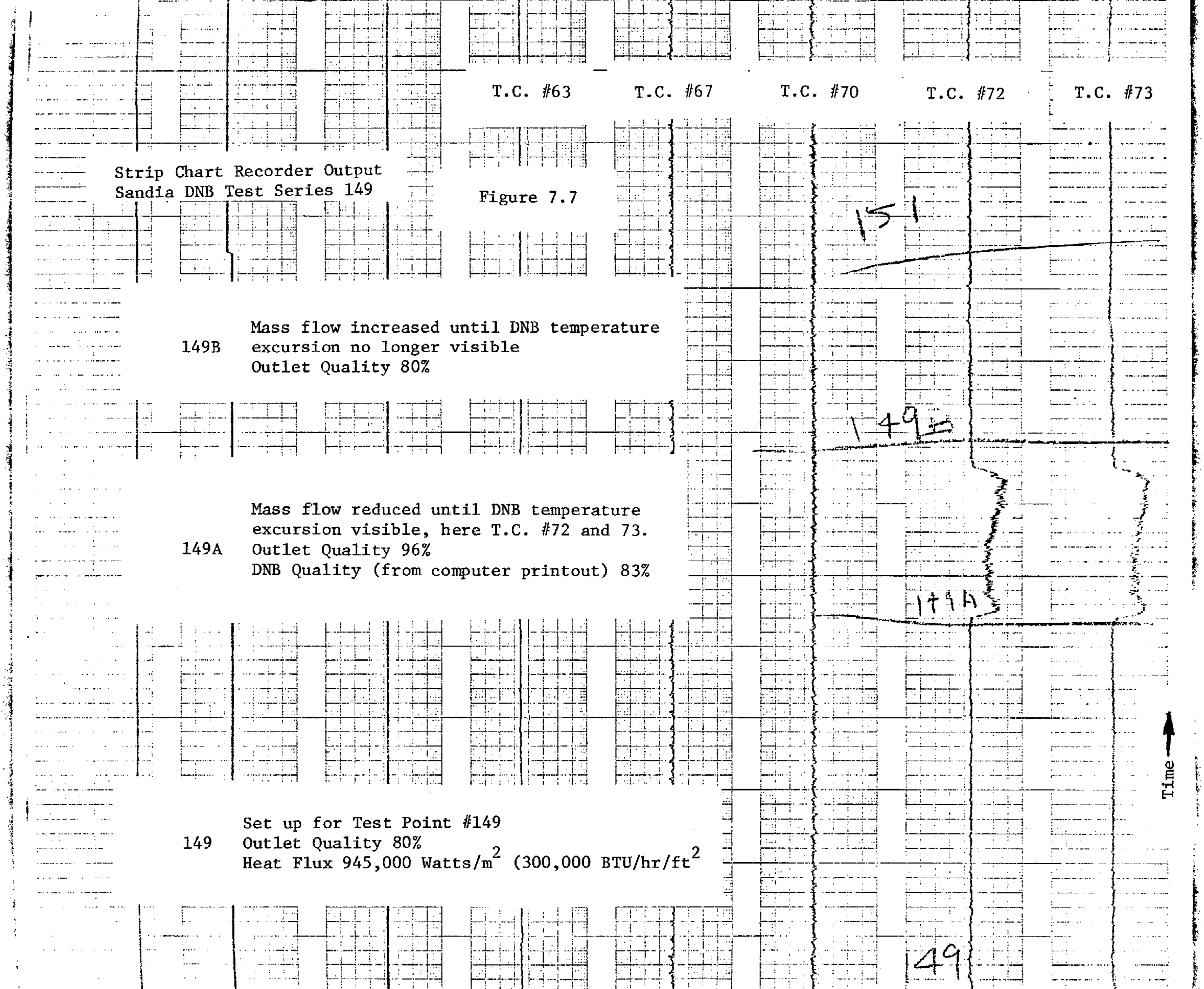

Figure 7.7 Strip Chart Recorder Output Sandia DNB Test Series 149

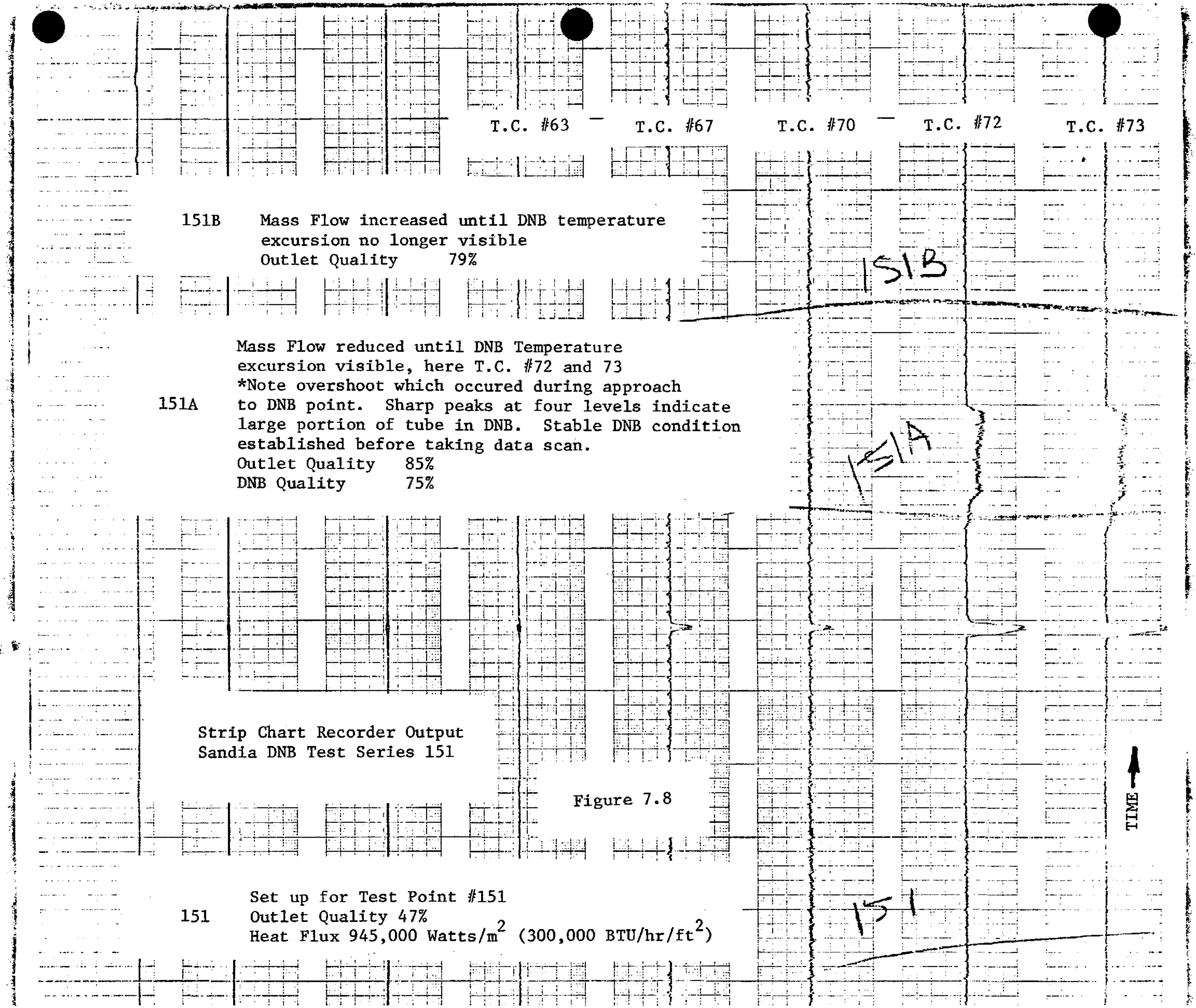
T.C. #63
T.C. #67
T.C. #70
T.C. #72
T.C. #73
151B Mass Flow increased until DNB temperature excursion no longer visible
Outlet Quality 79%
151B
151A Mass Flow reduced until DNB Temperature excursion visible, here T.C. #72 and 73
*Note overshoot which occured during approach to DNB point. Sharp peaks at four levels indicate large portion of tube in DNB. Stable DNB condition established before taking data scan.
Outlet Quality 85%
DNB Quality 75%
151A
Strip Chart Recorder Output
Sandia DNB Test Series 151
TIME
151 Set up for Test Point #151
Outlet Quality 47%
Heat Flux 945,000 Watts/m2 (300,000 BTU/hr/ft2)
151

Figure 7.8

C-E KREISINGER DEVELOPMENT LABORATORY
PROJECT #900255 SANDIA SOLAR RECEIVER RIFLED TUBE DNB TEST
TEST # 149   TIME 1230   DATE 11/26/79

TEST SECTION CONDITIONS

OUTLET PRESSURE	2821.5	+/-	2.0	PSIA
TOTAL FLOW	.3692E+04	+/-	.33E+02	LB/HR
RIFLED MASS FLOW	.9281E+06	+/-	.82E+04	LB/HR-FT2

TC#	ELEV (IN)	TEMP	HEAT FLUX AT TC (1000 BTU/HR-FT2)	QUALITY AT TC (PCT)	DNB
73	200.	811.	297.7 +/- 5.6	79.1 +/- 3.9	
72	188.	816.	297.7 +/- 5.6	75.9 +/- 3.9	
71	176.	806.	297.7 +/- 5.6	72.7 +/- 3.9	
70	164.	807.	297.7 +/- 5.6	69.4 +/- 3.9	
68	148.	807.	300.8 +/- 5.5	67.3 +/- 3.9	
67	136.	819.	300.8 +/- 5.5	64.0 +/- 3.9	
66	124.	812.	300.8 +/- 5.5	60.7 +/- 3.9	
65	112.	828.	300.8 +/- 5.5	57.5 +/- 3.9	
63	96.	791.	290.8 +/- 5.1	55.3 +/- 3.9	
62	84.	779.	290.8 +/- 5.1	52.2 +/- 3.9	
61	72.	800.	290.8 +/- 5.1	49.0 +/- 3.9	
60	60.	789.	290.8 +/- 5.1	45.8 +/- 3.9	
58	44.	813.	292.8 +/- 5.1	43.7 +/- 3.9	
57	32.	796.	292.8 +/- 5.1	40.6 +/- 3.9	
56	20.	829.	292.8 +/- 5.1	37.4 +/- 3.9	
55	8.	832.	292.8 +/- 5.1	34.2 +/- 3.9	

PRESSURE DROPS

LOCATION	INLET QUALITY (PCT)	OUTLET QUALITY (PCT)	PRESSURE DROP (PSID)
TOTAL TEST SECTION	33.1 +/- 3.9	80.2 +/- 3.9	0.00 +/- .02
UPPER TEST SECTION	56.4 +/- 3.9	80.2 +/- 3.9	0.00 +/- .08

RIB TEMPERATURE PROFILE

806.6   732.1   822.6   823.5   812.5   809.2   799.9

TEST SECTION OUTLET FLUID PROPERTIES

SAT TEMPERATURE	686.1	+/-	.1	F
STEAM SPEC VOL	.10115	+/-	.00018	FT3/LB
WATER SPEC VOL	.03159	+/-	.00002	FT3/LB
STEAM VISCOSITY	.06400	+/-	.00004	LB/FT-HR
WATER VISCOSITY	.13982	+/-	.00011	LB/FT-HR
SURFACE TENSION	.000101	+/-	.000001	LB/FT
STEAM THERM CONDUCTIVITY	.1020	+/-	.0001	BTU/HR-FT-F
WATER THERM CONDUCTIVITY	.2299	+/-	.0001	BTU/HR-FT-F
STEAM SAT ENTHALPY	1052.61	+/-	.31	BTU/LB
WATER SAT ENTHALPY	773.67	+/-	.28	BTU/LB

CONST FILE DATE 12/14/79 M   DATA REDUCED 10.33.59.   80/01/15.

KDL PROJ LEADER . . . . DATE . ./ . /. .

7.28

C-E KREISINGER DEVELOPMENT LABORATORY
PROJECT #900255 SANDIA SOLAR RECEIVER RIFLED TUBE DNB TEST
TEST # 149A TIME 1255 DATE 11/26/79

TEST SECTION CONDITIONS

OUTLET PRESSURE	2836.2	+/-	1.7	PSIA
TOTAL FLOW	.3121E+04	+/-	.44E+02	LB/HR
RIFLED MASS FLOW	.7846E+06	+/-	.11E+05	LB/HR-FT2

TC#	ELEV (IN)	TEMP	HEAT FLUX AT TC (1000 BTU/HR-FT2)	QUALITY AT TC (PCT)	DNB
73	200.	857.	296.7 +/- 5.1	95.1 +/- 6.5	DNB
72	188.	859.	296.7 +/- 5.1	91.2 +/- 6.5	DNB
71	176.	867.	296.7 +/- 5.1	87.3 +/- 6.5	DNB
70	164.	823.	296.7 +/- 5.1	83.5 +/- 6.5	DNB
68	148.	807.	300.0 +/- 5.1	80.9 +/- 6.5	
67	136.	820.	300.0 +/- 5.1	76.9 +/- 6.5	
66	124.	813.	300.0 +/- 5.1	73.0 +/- 6.5	
65	112.	829.	300.0 +/- 5.1	69.1 +/- 6.5	
63	96.	792.	290.5 +/- 5.0	66.6 +/- 6.5	
62	84.	780.	290.5 +/- 5.0	62.8 +/- 6.5	
61	72.	801.	290.5 +/- 5.0	59.0 +/- 6.5	
60	60.	790.	290.5 +/- 5.0	55.2 +/- 6.5	
58	44.	814.	293.6 +/- 5.1	52.6 +/- 6.5	
57	32.	797.	293.6 +/- 5.1	48.8 +/- 6.5	
56	20.	830.	293.6 +/- 5.1	45.0 +/- 6.5	
55	8.	833.	293.6 +/- 5.1	41.2 +/- 6.5	

PRESSURE DROPS

LOCATION	INLET QUALITY (PCT)	OUTLET QUALITY (PCT)	PRESSURE DROP (PSID)
TOTAL TEST SECTION	39.9 +/- 6.4	96.4 +/- 6.5	0.00 +/- .02
UPPER TEST SECTION	67.8 +/- 6.5	96.4 +/- 6.5	0.00 +/- .01

RIB TEMPERATURE PROFILE
807.4 732.9 823.4 824.2 813.5 810.1 800.8

TEST SECTION OUTLET FLUID PROPERTIES

SAT TEMPERATURE	686.9	+/-	.1	F
STEAM SPEC VOL	.09985	+/-	.00015	FT3/LB
WATER SPEC VOL	.03177	+/-	.00002	FT3/LB
STEAM VISCOSITY	.06431	+/-	.00004	LB/FT-HR
WATER VISCOSITY	.13905	+/-	.00009	LB/FT-HR
SURFACE TENSION	.000096	+/-	.000001	LB/FT
STEAM THERM CONDUCTIVITY	.1029	+/-	.0001	BTU/HR-FT-F
WATER THERM CONDUCTIVITY	.2292	+/-	.0001	BTU/HR-FT-F
STEAM SAT ENTHALPY	1050.34	+/-	.26	BTU/LB
WATER SAT ENTHALPY	775.75	+/-	.24	BTU/LB

CONST FILE DATE 12/14/79 M DATA REDUCED 10.34.01. 80/01/15.

KDL PROJ LEADER . . . . DATE . ./ . /. .

C-E KREISINGER DEVELOPMENT LABORATORY
PROJECT #900255 SANDIA SOLAR RECEIVER RIFLED TUBE DNB TEST
TEST # 1498 TIME 1310 DATE 11/26/79

TEST SECTION CONDITIONS

OUTLET PRESSURE	2835.5	+/-	1.3	PSIA
TOTAL FLOW	.3705E+04	+/-	.40E+02	LB/HR
RIFLED MASS FLOW	.9315E+06	+/-	.10E+05	LB/HR-FT2

TC#	ELEV (IN)	TEMP	HEAT FLUX AT TC (1000 BTU/HR-FT2)	QUALITY AT TC (PCT)	DNB
73	200.	812.	296.7 +/- 5.1	79.4 +/- 4.9	
72	188.	817.	296.7 +/- 5.1	76.1 +/- 4.9	
71	176.	808.	296.7 +/- 5.1	72.9 +/- 4.9	
70	164.	808.	296.7 +/- 5.1	69.6 +/- 4.9	
68	148.	807.	300.0 +/- 5.1	67.4 +/- 4.8	
67	136.	820.	300.0 +/- 5.1	64.2 +/- 4.8	
66	124.	813.	300.0 +/- 5.1	60.9 +/- 4.8	
65	112.	829.	300.0 +/- 5.1	57.6 +/- 4.8	
63	96.	791.	290.3 +/- 5.0	55.4 +/- 4.8	
62	84.	780.	290.3 +/- 5.0	52.2 +/- 4.8	
61	72.	801.	290.3 +/- 5.0	49.0 +/- 4.8	
60	60.	790.	290.3 +/- 5.0	45.8 +/- 4.8	
58	44.	814.	292.8 +/- 5.1	43.7 +/- 4.8	
57	32.	797.	292.8 +/- 5.1	40.5 +/- 4.8	
56	20.	830.	292.8 +/- 5.1	37.3 +/- 4.8	
55	8.	833.	292.8 +/- 5.1	34.1 +/- 4.8	

PRESSURE DROPS

LOCATION	INLET QUALITY (PCT)	OUTLET QUALITY (PCT)	PRESSURE DROP (PSID)
TOTAL TEST SECTION	33.0 +/- 4.8	80.5 +/- 4.9	0.00 +/- .02
UPPER TEST SECTION	56.5 +/- 4.8	80.5 +/- 4.9	0.00 +/- .06

RIB TEMPERATURE PROFILE
807.1 732.8 823.2 824.0 813.1 809.8 800.6

TEST SECTION OUTLET FLUID PROPERTIES

SAT TEMPERATURE	686.8	+/-	.1	F
STEAM SPEC VOL	.09991	+/-	.00011	FT3/LB
WATER SPEC VOL	.03177	+/-	.00002	FT3/LB
STEAM VISCOSITY	.06430	+/-	.00003	LB/FT-HR
WATER VISCOSITY	.13908	+/-	.00007	LB/FT-HR
SURFACE TENSION	.000097	+/-	.000000	LB/FT
STEAM THERM CONDUCTIVITY	.1029	+/-	.0001	BTU/HR-FT-F
WATER THERM CONDUCTIVITY	.2293	+/-	.0001	BTU/HR-FT-F
STEAM SAT ENTHALPY	1050.45	+/-	.20	BTU/LB
WATER SAT ENTHALPY	775.65	+/-	.18	BTU/LB

CONST FILE DATE 12/14/79 M DATA REDUCED 10.34.02. 80/01/15.

KDL PROJ LEADER . . . . DATE . ./ . /. .

C-E KREISINGER DEVELOPMENT LABORATORY
PROJECT #900255 SANDIA SOLAR RECEIVER RIFLED TUBE DNB TEST
TEST # 151 TIME 1320 DATE 11/26/79

TEST SECTION CONDITIONS

OUTLET PRESSURE	2843.8	+/-	2.4	PSIA
TOTAL FLOW	.7149E+04	+/-	.82E+02	LB/HR
RIFLED MASS FLOW	.1797E+07	+/-	.21E+05	LB/HR-FT2

TC#	ELEV (IN)	TEMP	HEAT FLUX AT TC (1000 BTU/HR-FT2)	QUALITY AT TC (PCT)	DNB
73	200.	810.	297.1 +/- 5.1	45.9 +/- 5.0	
72	188.	817.	297.1 +/- 5.1	44.2 +/- 5.0	
71	176.	806.	297.1 +/- 5.1	42.5 +/- 5.0	
70	164.	808.	297.1 +/- 5.1	40.8 +/- 5.0	
68	148.	807.	298.6 +/- 5.1	39.7 +/- 5.0	
67	136.	820.	298.6 +/- 5.1	38.0 +/- 5.0	
66	124.	813.	298.6 +/- 5.1	36.3 +/- 5.0	
65	112.	829.	298.6 +/- 5.1	34.5 +/- 5.0	
63	96.	792.	290.9 +/- 5.0	33.4 +/- 5.0	
62	84.	781.	290.9 +/- 5.0	31.7 +/- 5.0	
61	72.	801.	290.9 +/- 5.0	30.1 +/- 5.0	
60	60.	790.	290.9 +/- 5.0	28.4 +/- 5.0	
58	44.	816.	296.8 +/- 5.1	27.3 +/- 5.0	
57	32.	799.	296.8 +/- 5.1	25.6 +/- 5.0	
56	20.	832.	296.8 +/- 5.1	23.9 +/- 5.0	
55	8.	836.	296.8 +/- 5.1	22.2 +/- 5.0	

PRESSURE DROPS

LOCATION	INLET QUALITY (PCT)	OUTLET QUALITY (PCT)	PRESSURE DROP (PSID)
TOTAL TEST SECTION	21.6 +/- 5.0	46.5 +/- 5.0	11.24 +/- .07
UPPER TEST SECTION	34.0 +/- 5.0	46.5 +/- 5.0	6.54 +/- .06

RIB TEMPERATURE PROFILE
807.3 733.1 823.3 824.1 813.2 809.9 800.7

TEST SECTION OUTLET FLUID PROPERTIES

SAT TEMPERATURE	687.3	+/-	.1	F
STEAM SPEC VOL	.09919	+/-	.00021	FT3/LB
WATER SPEC VOL	.03187	+/-	.00003	FT3/LB
STEAM VISCOSITY	.06448	+/-	.00005	LB/FT-HR
WATER VISCOSITY	.13865	+/-	.00013	LB/FT-HR
SURFACE TENSION	.000094	+/-	.000001	LB/FT
STEAM THERM CONDUCTIVITY	.1034	+/-	.0002	BTU/HR-FT-F
WATER THERM CONDUCTIVITY	.2289	+/-	.0001	BTU/HR-FT-F
STEAM SAT ENTHALPY	1049.16	+/-	.38	BTU/LB
WATER SAT ENTHALPY	776.82	+/-	.35	BTU/LB

CONST FILE DATE 12/14/79 M DATA REDUCED 10.34.04. 80/01/15.

KDL PROJ LEADER . . . . DATE . ./ . /. .

C-E KREISINGER DEVELOPMENT LABORATORY
PROJECT #900255 SANDIA SOLAR RECEIVER RIFLED TUBE DNB TEST
TEST # 151A TIME 1350 DATE 11/26/79

TEST SECTION CONDITIONS

OUTLET PRESSURE	2835.7	+/-	1.9	PSIA
TOTAL FLOW	.3822E+04	+/-	.37E+02	LB/HR
RIFLED MASS FLOW	.9607E+06	+/-	.94E+04	LB/HR-FT2

TC#	ELEV (IN)	TEMP	HEAT FLUX AT TC (1000 BTU/HR-FT2)	QUALITY AT TC (PCT)	DNB
73	200.	837.	296.8 +/- 5.1	84.4 +/- 4.5	DNB
72	188.	839.	296.8 +/- 5.1	81.2 +/- 4.5	DNB
71	176.	841.	296.8 +/- 5.1	78.0 +/- 4.5	DNB
70	164.	812.	296.8 +/- 5.1	74.9 +/- 4.5	DNB
68	148.	807.	298.3 +/- 5.1	72.8 +/- 4.5	
67	136.	819.	298.3 +/- 5.1	69.6 +/- 4.5	
66	124.	812.	298.3 +/- 5.1	66.4 +/- 4.5	
65	112.	828.	298.3 +/- 5.1	63.2 +/- 4.5	
63	96.	791.	290.7 +/- 5.0	61.1 +/- 4.5	
62	84.	780.	290.7 +/- 5.0	58.0 +/- 4.5	
61	72.	801.	290.7 +/- 5.0	55.0 +/- 4.5	
60	60.	790.	290.7 +/- 5.0	51.9 +/- 4.5	
58	44.	816.	298.4 +/- 5.1	49.8 +/- 4.5	
57	32.	799.	298.4 +/- 5.1	46.6 +/- 4.5	
56	20.	833.	298.4 +/- 5.1	43.4 +/- 4.5	
55	8.	836.	298.4 +/- 5.1	40.2 +/- 4.5	

PRESSURE DROPS

LOCATION	INLET QUALITY (PCT)	OUTLET QUALITY (PCT)	PRESSURE DROP (PSID)
TOTAL TEST SECTION	39.2 +/- 4.5	85.4 +/- 4.5	0.00 +/- .02
UPPER TEST SECTION	62.2 +/- 4.5	85.4 +/- 4.5	0.00 +/- .07

RIB TEMPERATURE PROFILE
806.6 732.4 822.4 823.4 812.6 809.3 800.0

TEST SECTION OUTLET FLUID PROPERTIES

SAT TEMPERATURE	686.9	+/-	.1	F
STEAM SPEC VOL	.09990	+/-	.00017	FT3/LB
WATER SPEC VOL	.03177	+/-	.00002	FT3/LB
STEAM VISCOSITY	.06430	+/-	.00004	LB/FT-HR
WATER VISCOSITY	.13908	+/-	.00010	LB/FT-HR
SURFACE TENSION	.000097	+/-	.000001	LB/FT
STEAM THERM CONDUCTIVITY	.1029	+/-	.0001	BTU/HR-FT-F
WATER THERM CONDUCTIVITY	.2293	+/-	.0001	BTU/HR-FT-F
STEAM SAT ENTHALPY	1050.42	+/-	.29	BTU/LB
WATER SAT ENTHALPY	775.67	+/-	.27	BTU/LB

CONST FILE DATE 12/14/79 M DATA REDUCED 10.34.05. 80/01/15.

KDL PROJ LEADER . . . . DATE . ./ . /. .

C-E KREISINGER DEVELOPMENT LABORATORY
PROJECT #900255 SANDIA SOLAR RECEIVER RIFLED TUBE DNB TEST
TEST # 151B TIME 1415 DATE 11/26/79

TEST SECTION CONDITIONS

OUTLET PRESSURE	2835.1	+/-	2.1	PSIA
TOTAL FLOW	.4186E+04	+/-	.37E+02	LB/HR
RIFLED MASS FLOW	.1052E+07	+/-	.93E+04	LB/HR-FT2

TC#	ELEV (IN)	TEMP	HEAT FLUX AT TC (1000 BTU/HR-FT2)	QUALITY AT TC (PCT)	DNB
73	200.	813.	298.4 +/- 5.1	77.9 +/- 4.0	
72	188.	818.	298.4 +/- 5.1	75.0 +/- 4.0	
71	176.	808.	298.4 +/- 5.1	72.1 +/- 4.0	
70	164.	808.	298.4 +/- 5.1	69.2 +/- 4.0	
68	148.	807.	299.4 +/- 5.1	67.3 +/- 4.0	
67	136.	819.	299.4 +/- 5.1	64.4 +/- 4.0	
66	124.	812.	299.4 +/- 5.1	61.5 +/- 4.0	
65	112.	828.	299.4 +/- 5.1	58.5 +/- 4.0	
63	96.	791.	291.0 +/- 5.0	56.6 +/- 4.0	
62	84.	780.	291.0 +/- 5.0	53.8 +/- 4.0	
61	72.	801.	291.0 +/- 5.0	51.0 +/- 4.0	
60	60.	789.	291.0 +/- 5.0	48.2 +/- 4.0	
58	44.	816.	298.6 +/- 5.1	46.2 +/- 4.0	
57	32.	799.	298.6 +/- 5.1	43.3 +/- 4.0	
56	20.	833.	298.6 +/- 5.1	40.4 +/- 4.0	
55	8.	836.	298.6 +/- 5.1	37.5 +/- 4.0	

PRESSURE DROPS

LOCATION	INLET QUALITY (PCT)	OUTLET QUALITY (PCT)	PRESSURE DROP (PSID)
TOTAL TEST SECTION	36.6 +/- 4.0	78.9 +/- 4.0	0.00 +/- .05
UPPER TEST SECTION	57.6 +/- 4.0	78.9 +/- 4.0	0.00 +/- .07

RIB TEMPERATURE PROFILE
806.9 732.5 823.0 823.8 812.9 809.6 800.3

TEST SECTION OUTLET FLUID PROPERTIES

SAT TEMPERATURE	686.8	+/-	.1	F
STEAM SPEC VOL	.09995	+/-	.00019	FT3/LB
WATER SPEC VOL	.03176	+/-	.00003	FT3/LB
STEAM VISCOSITY	.06429	+/-	.00005	LB/FT-HR
WATER VISCOSITY	.13911	+/-	.00011	LB/FT-HR
SURFACE TENSION	.000097	+/-	.000001	LB/FT
STEAM THERM CONDUCTIVITY	.1028	+/-	.0001	BTU/HR-FT-F
WATER THERM CONDUCTIVITY	.2293	+/-	.0001	BTU/HR-FT-F
STEAM SAT ENTHALPY	1050.51	+/-	.33	BTU/LB
WATER SAT ENTHALPY	775.59	+/-	.30	BTU/LB

CONST FILE DATE 12/14/79 M DATA REDUCED 10.34.06. 80/01/15.

KDL PROJ LEADER . . . . DATE . ./ . /. .

After scanning and reducing the DNB data point, the water mass flow rate is increased slightly until the DNB temperature excursions are not visible on the strip recorder. A data scan is then taken to verify the status of the loop at the DNB point and to provide a check against which to compare the tube metal temperatures for evaluating DNB conditions. Set up is then begun for the next starting point.

During the course of testing it was determined that 400,000 BTU/hr-ft^2 heat flux would be attainable with the Sandia loop configuration. Additional test points were established for this heat flux level and made up the final series of tests for the Sandia test segment. After the completion of the Sandia test program and post-test calibrations, the HTCTL was reconfigured for post-critical heat flux testing on a slightly different tube segment.

7.5.4 Problems--Although the physical operation of the test loop went very well, several inconsistancies in the reduced data were cause for concern.

One problem described in the weekly progress reports was discovered in the low heat flux DNB testing. Many data runs were indicating steam qualities at the onset of DNB in excess of 100% (i.e. superheated steam). This is a physical impossibility due to the nature of boiling heat transfer and prompted an investigation of the steam quality calculation.

From the post-test instrument calibration, it was determined that the low-flow differential pressure cell on B line (FTO 10, Figure 7.1) had experienced a drift in the zero pressure output. When this drift was plotted against loop operating time, (Figure 7.9) it was found to be linear with time through the test program. By comparing the pre and post-test calibrations the drift has been found to affect only the zero pressure reading of that cell and not the overall cell calibration correlation. All raw data was therefore reduced again after the completion of the test program using new constant files updated for each day of loop operation. The check of the watt transducers

FIGURE 7.9

ZERO DRIFT OF DIFFERENTIAL PRESSURE CELL No. 10
vs HTCTL OPERATING TIME

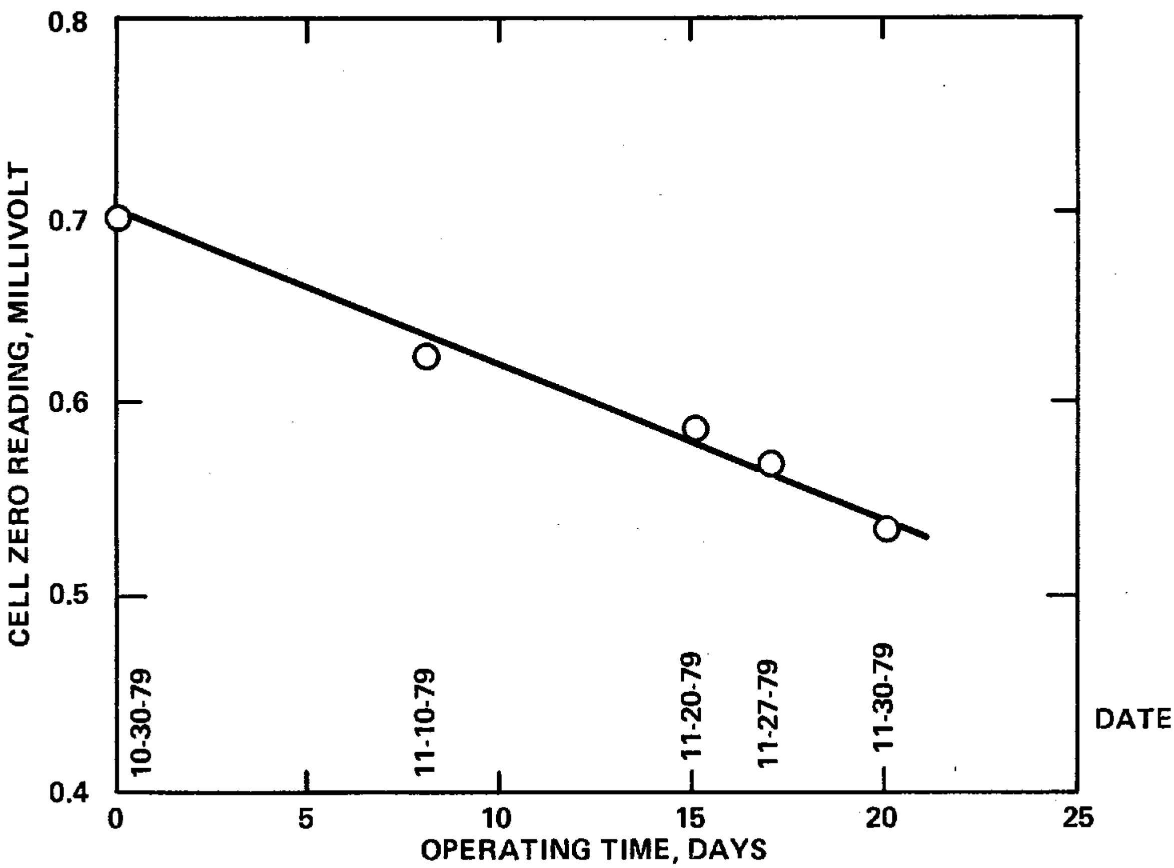

and heat loss correlations provided small changes from the pre-test values and thus minimal impact on the calculated steam quality. The re-run test points fell more in line with the expected values.

After the completion of the Sandia program a problem was noted in the pressure drop measurements which are printed out on the data reduction program output sheet. Investigation showed that the differential pressure cells (DPT 15 and DPT 16 Figure 7.1) used to measure pressure drop within the test segment were incorrectly spanned at the start of the test program. Under certain test conditions (primarily low heat flux and low mass flow) the cells would reach the end of their measurement range and "peg" at one particular reading. This error does not affect the DNB data collected during the test program and is confined only to those tests where the total test segment pressure drop is less than approximately 7 psi. Pressure drop measurements in this range have been deleted from the final output presented in Appendix G.

7.6 Test Results/Conclusions

The effect of mass flux and steam quality on the DNB point at various pressures and heat fluxes is presented in Figures 7.10 to 7.17. There are four heat fluxes for each of two pressure levels.

At the lower pressure, 14.5 MPa (2100 psig) DNB qualities range in excess of 90% at the higher mass fluxes for all tested levels of heat input. Figure 7.10 is representative of the classic DNB curve showing a "plateau" at a mass flux of 271 $kg/m^2/s$ (0.2 $lbm/hr/ft^2$) at which DNB is seen to occur over a wide range of steam quality and a sharp vertical slope at higher mass flux levels where quantity is independent of mass flux. This trend was observed in all tests, becoming less defined at the higher fluxes and pressure. The plateau is not obtained in all tests because at low rates of mass flow instabilities prevented achieving accurate DNB determinations in these cases.

At the higher pressure 19.7 MPa (2850 psig) DNB is seen to occur at lower steam qualities and high mass fluxes for similar tube heat input. Data taken during the Sandia testing is comparable to previous results from HTCTL testing in similar heat and mass flux ranges. The DNB behavior for rifled tubing subjected to 180^{o} heat input had not been investigated for heat fluxes in excess of $0.63 MW/m^2$ (200,000 $BTU/hr/ft^2$). The Sandia testing has significantly extended the available data in this area.

The test data confirms that the selected circulation ratio (2:1) yielding an exit quality of 50% will not result in DNB over the range of flux levels anticipated for this design. An analysis has shown the measured pressure drop to fall very closely to that of previous testing and experimental correlation. Those pressure measurements taken outside the calibration range of the pressure drop DP cells have been removed from the final output as described in Section 7.3.4

A complete listing of the Sandia test program reduced data is presented in Appendix G.

FIGURE 7.10

EFFECT OF MASS FLUX ON DNB QUALITY

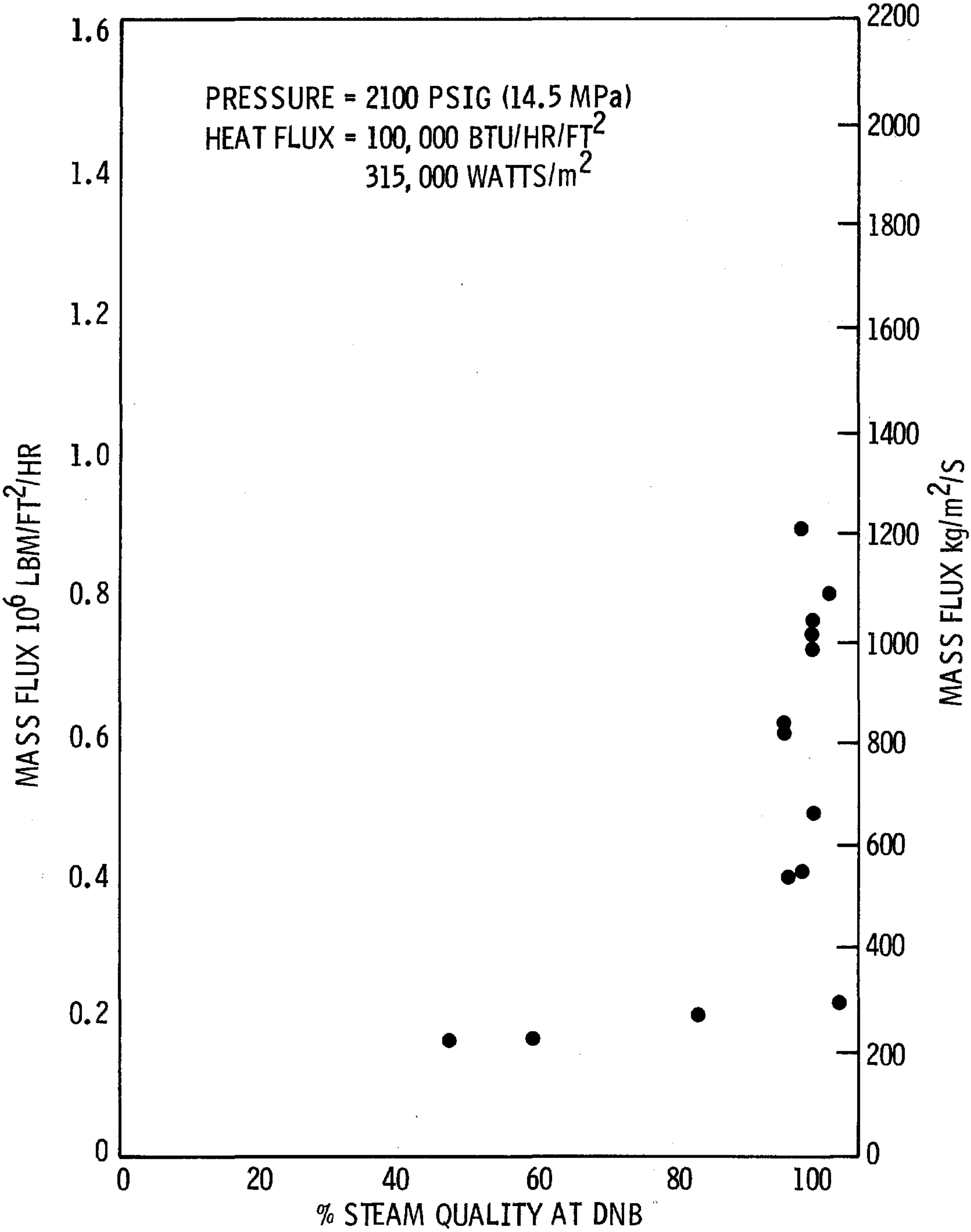

FIGURE 7.11

EFFECT OF MASS FLUX ON DNB QUALITY

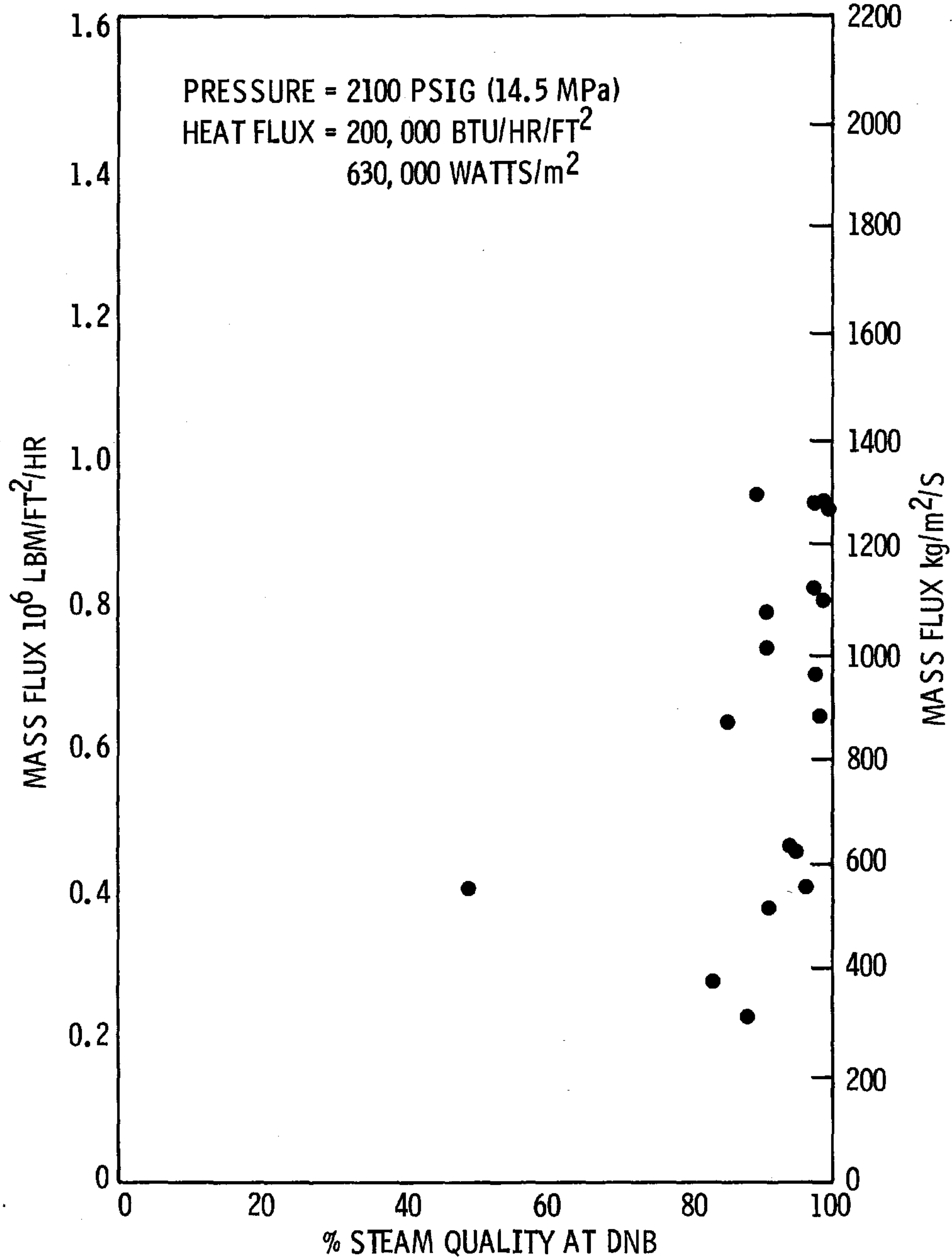

FIGURE 7.12

EFFECT OF MASS FLUX ON DNB QUALITY

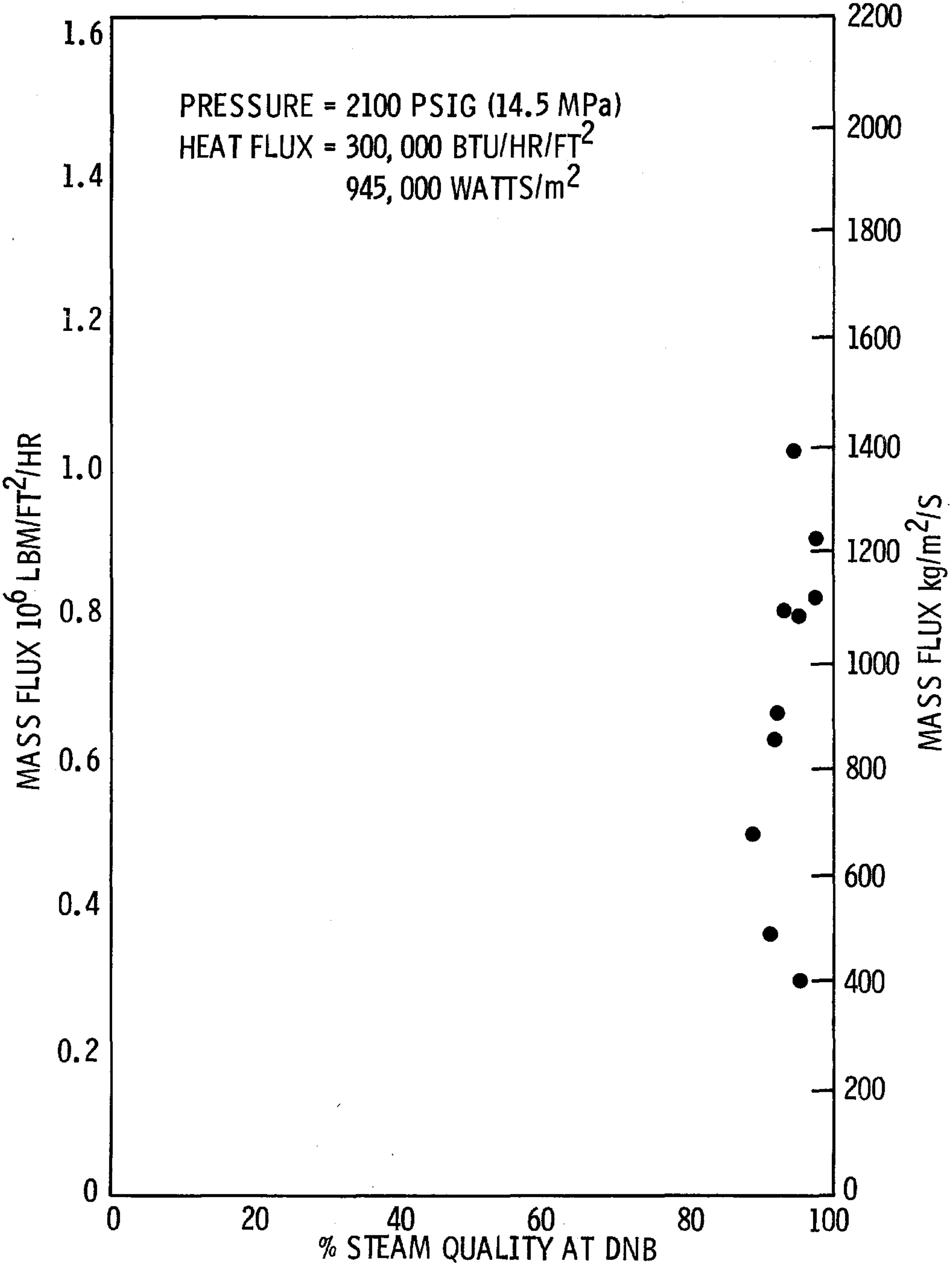

FIGURE 7.13

EFFECT OF MASS FLUX ON DNB QUALITY

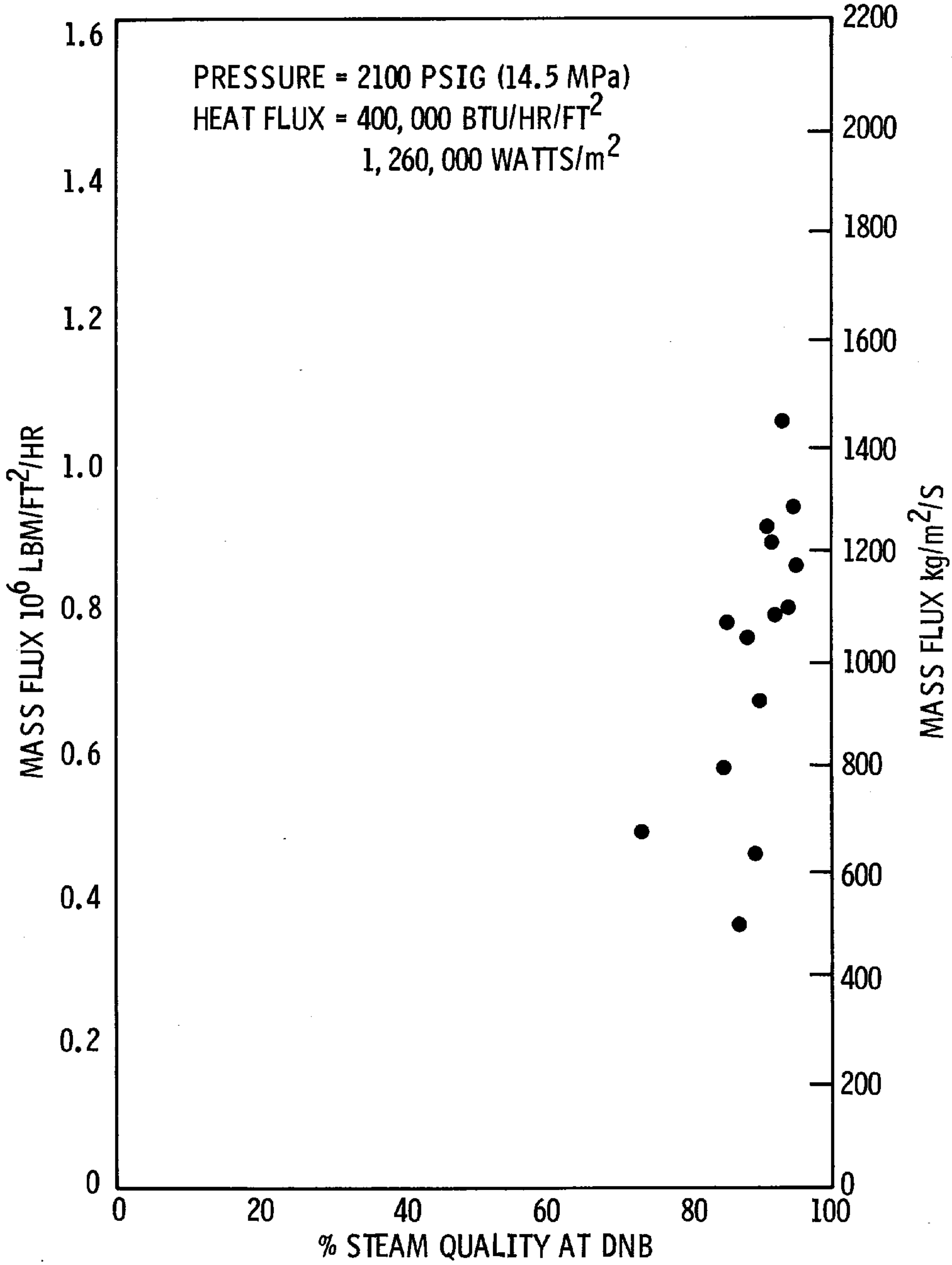

FIGURE 7.14

EFFECT OF MASS FLUX ON DNB QUALITY

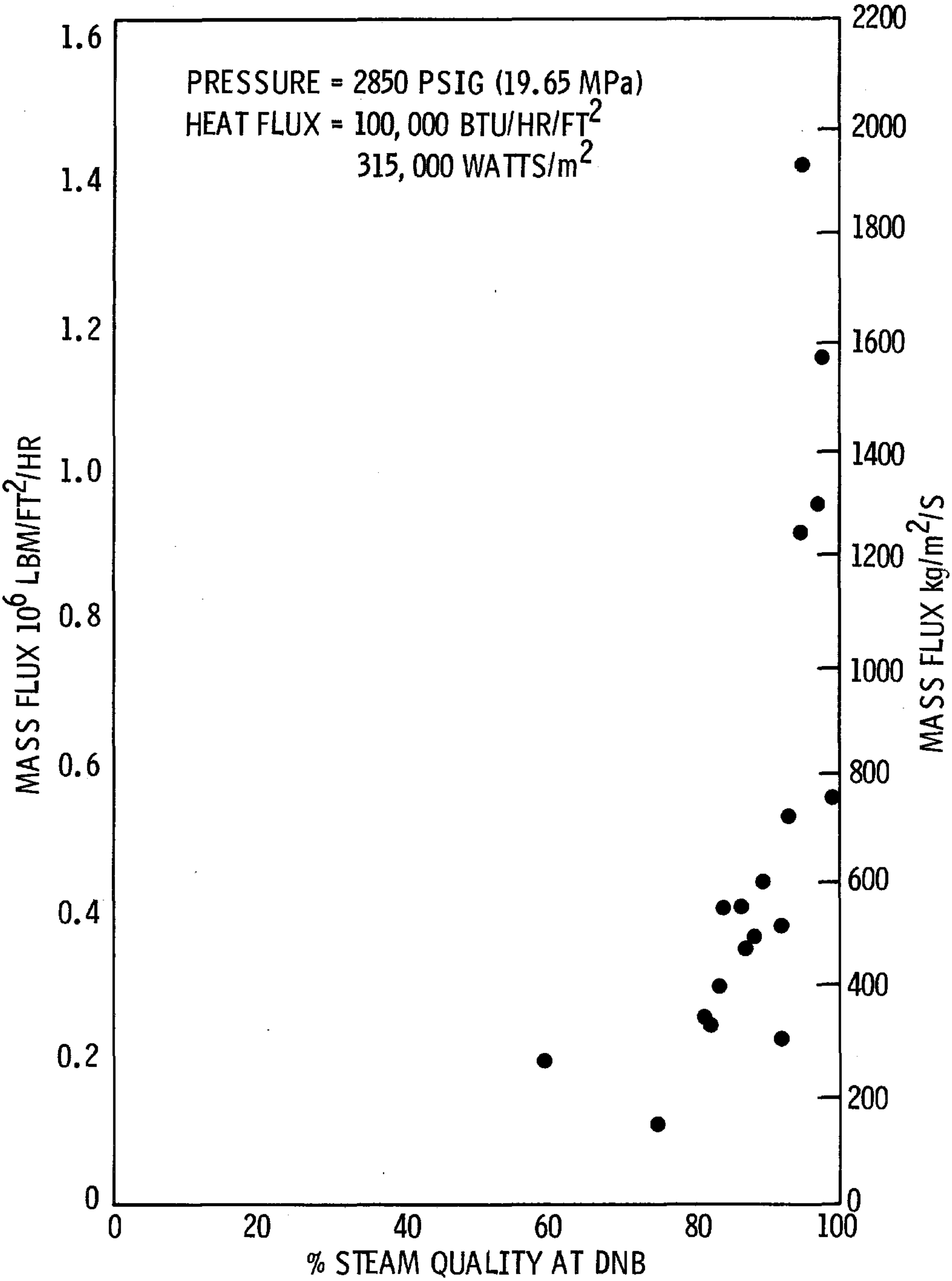

FIGURE 7.15

EFFECT OF MASS FLUX ON DNB QUALITY

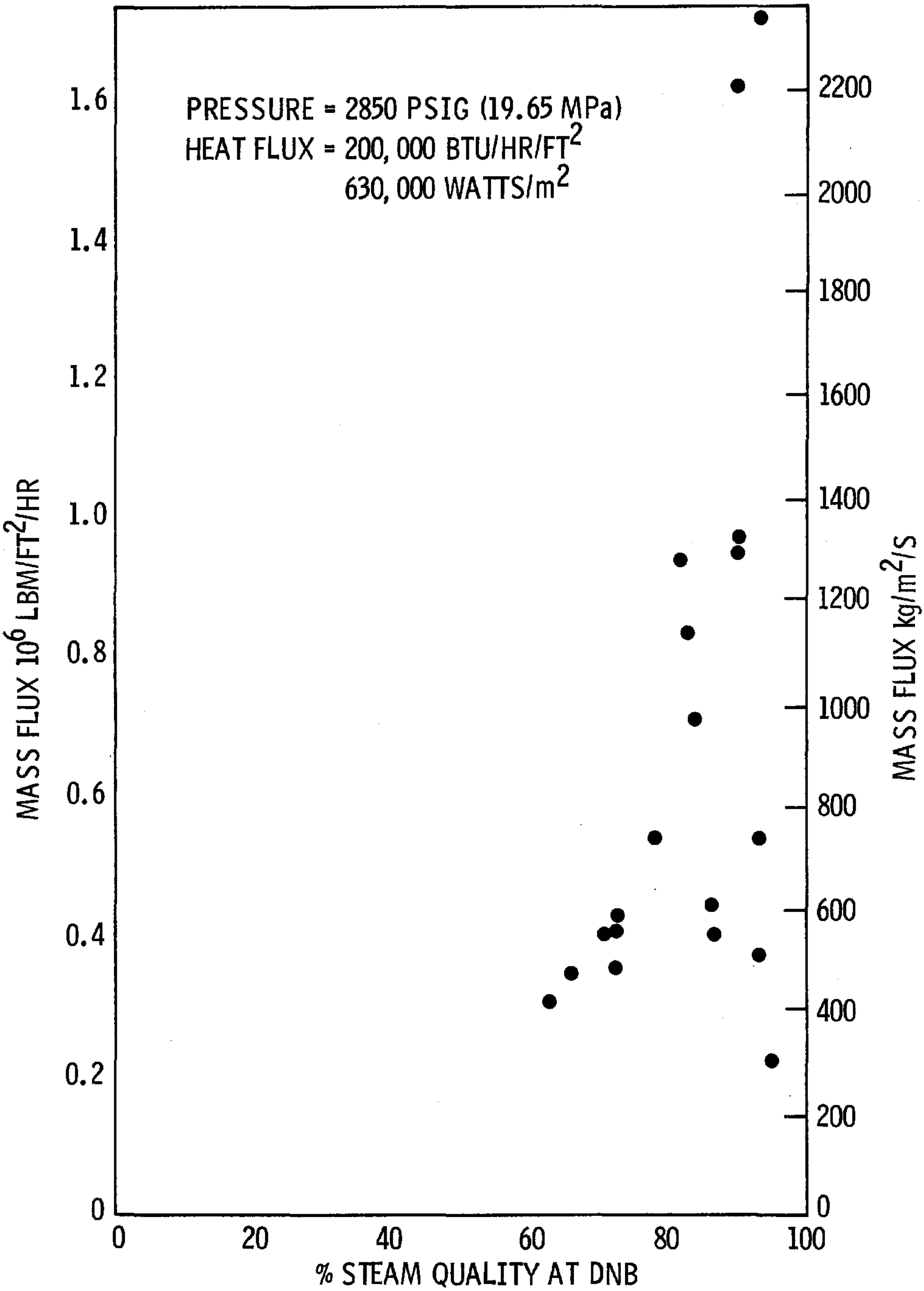

FIGURE 7.16

EFFECT OF MASS FLUX ON DNB QUALITY

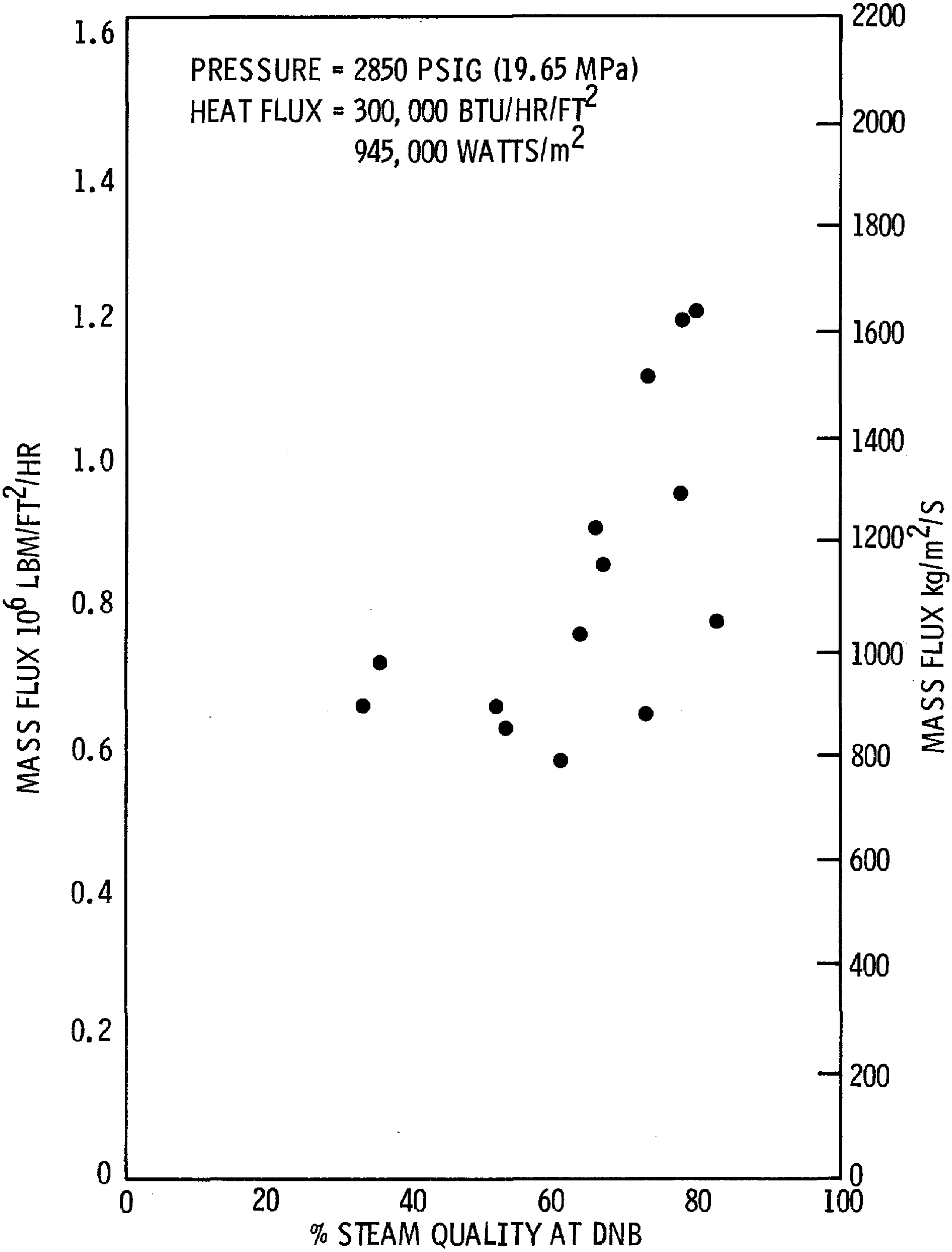

FIGURE 7.17

EFFECT OF MASS FLUX ON DNB QUALITY

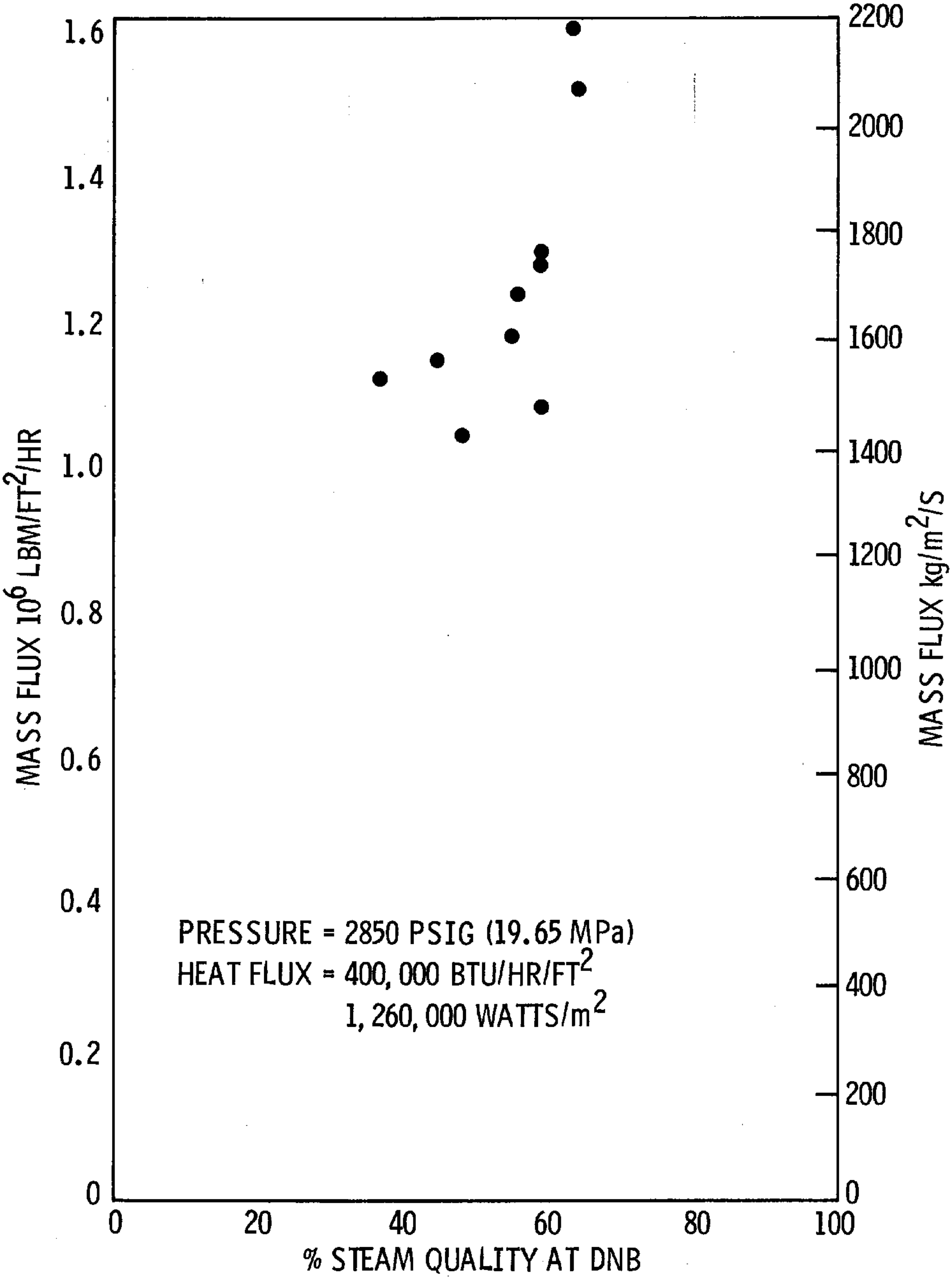

7.7 Heat Flux Analysis of Rifled Tubing

A two-dimensional heat conduction analysis was done to determine the sensitivity of the tube crown temperature to an orientation over a land or groove of the rifling and to operating conditions that might exist during the test. Since it was not practical to exactly orient the tube thermocouples with respect to the lands and grooves of the rifling, a knowledge of the difference in readings was desired in order to interpret the data. It was also desirable to know how the tube crown thermocouple would respond to a loss of a single heater rod in the vicinity of the thermocouple. The test rig flux input is uniform over 180° of circumference, whereas the radiant distribution is a Cosine function. Both input flux distributions were modeled in this sub-task. Various assumed distributions of inside film coefficients were run to simulate the physical condition of either water or steam films in the rifling grooves. The thermocouple location for this case was directly over the interface between a land a groove.

The heating element was modeled using triangular finite elements on MARC Heat computer program (see Figure 7.18). Due to symmetry, only half of the heating element was modeled. The boundary condition on the tube contact surface of the heating element was a combined or effective film coefficient, which included the thermal resistances of the actual film and of the tube material below the heater, and a bulk fluid temperature of $685^{\circ}F$. The remaining three surfaces of the heater were insulated. A plot of the isotherms through the heating element is shown in Figure 7.19.

The rifled tube was modeled using quadrilateral finite elements on MARC, both with the aluminum coating (Figure 7.20) and without (Figure 7.21). Several cases were run for comparative purposes: (1) all heaters on and (2) one heater off, (3) all heaters on, w/Al coating and crown located at the interface of the thick and thin tube wall sections, (4) all heaters on, w/Al coating and the crown located at the center of the thick tube wall section,

FIGURE 7.18: HEATER ELEMENT MODEL

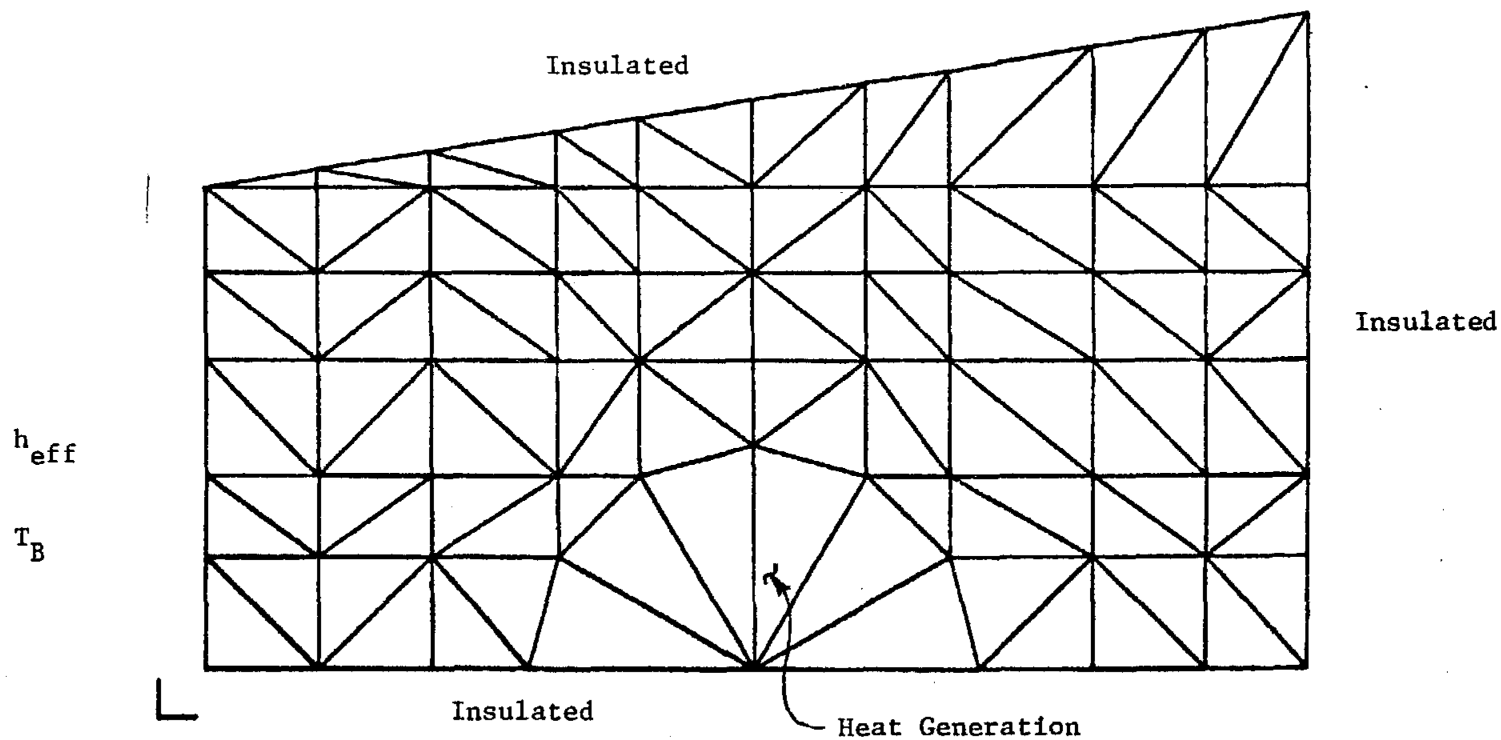

FIGURE 7.19: HEATER ELEMENT ISOTHERMS

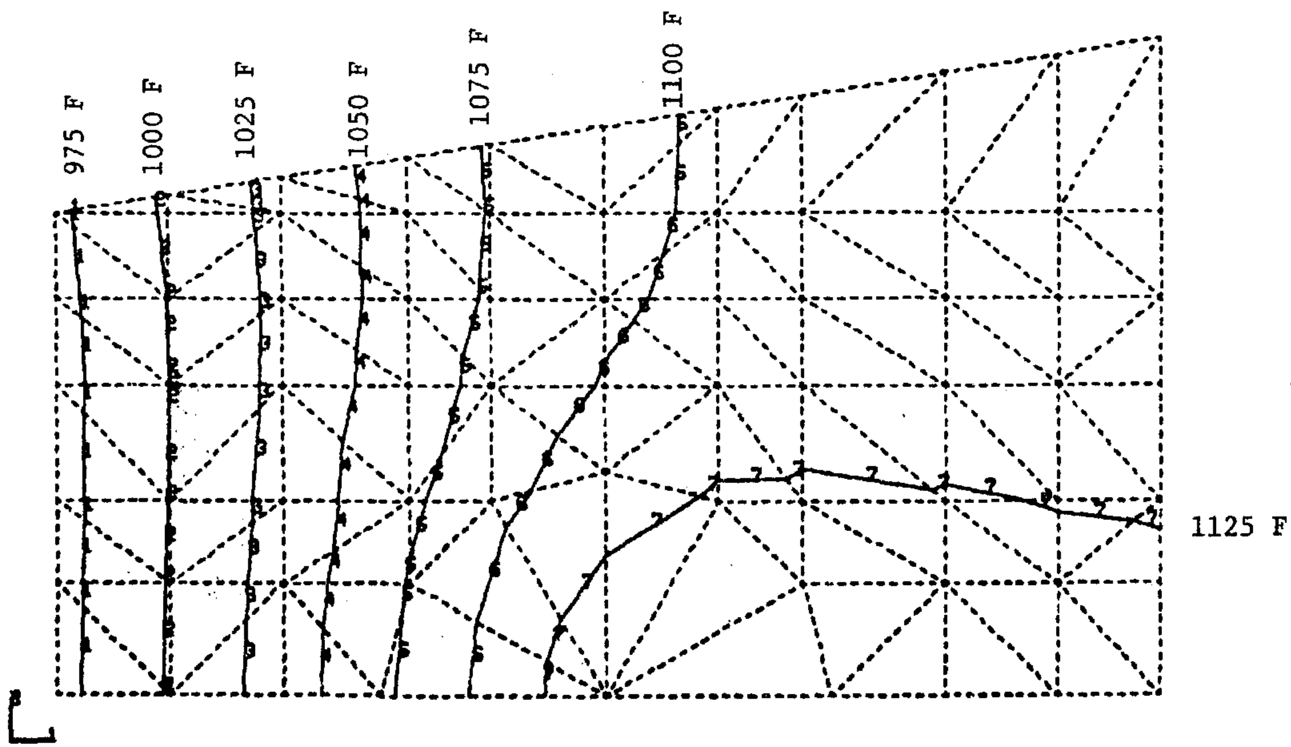

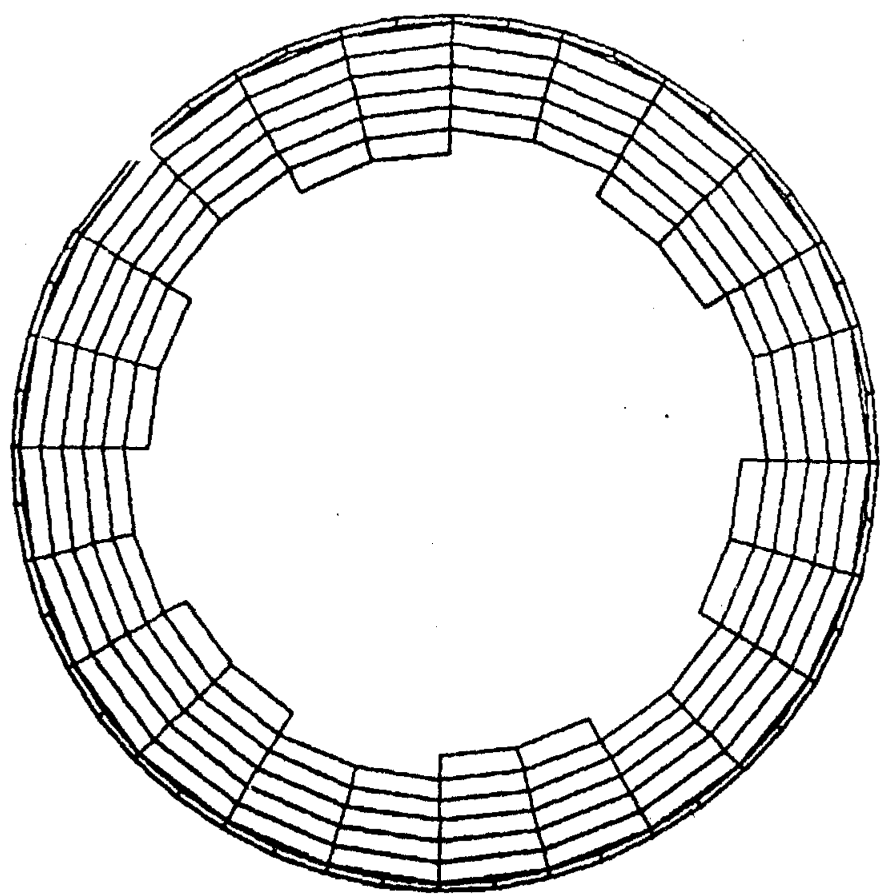

FIGURE 7.20: TUBE MODEL WITH ALUMINUM COATING

FIGURE 7.21: TUBE MODEL WITHOUT ALUMINUM COATING

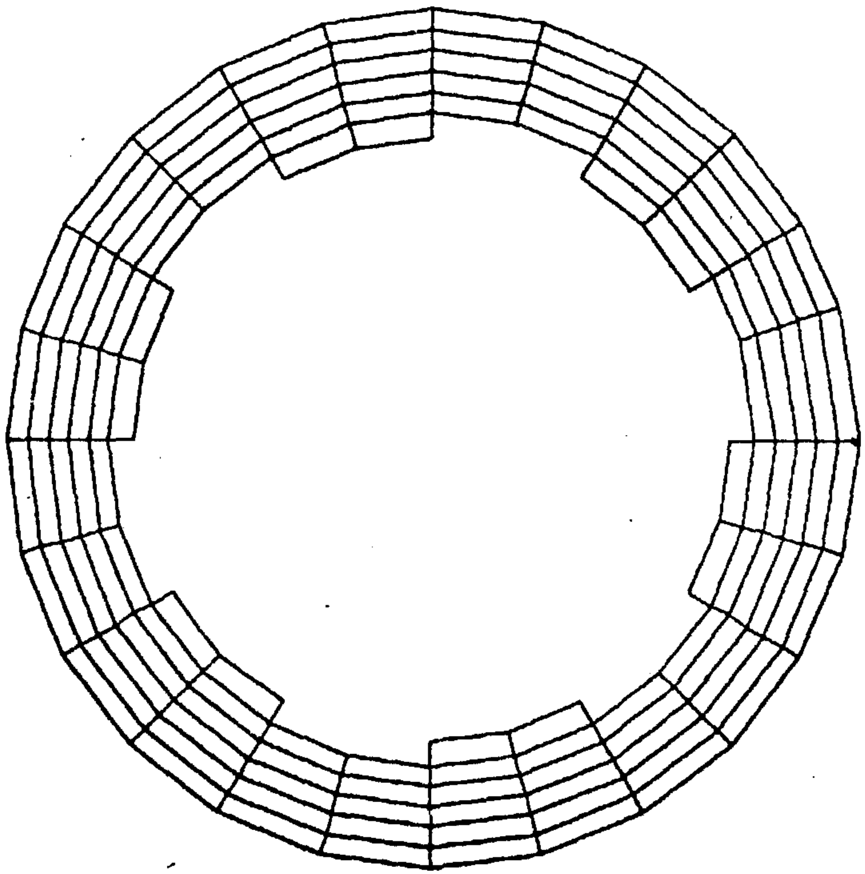

7.50

(5) all heaters on, w/Al coating and the crown located at the center of the thin wall tube section, and (6) a cosine distributed flux input to the tube.

Cases 1 and 2 provide a comparison of the inside flux distribution and how it is effected by the loss of a heater (see Figures 7.22 and 7.23). Figure 7.24 is a plot of the inside heat flux distribution for case 6, the cosine distributed applied flux.

The crown temperature varied from 500°C (931°F) to 496°C (925°F) depending on whether the thermocouple was over the thick section (land) or the thin section (groove). The significant difference was due to the loss of an adjacent heater rod. In this case, the crown temperature varied from 496°C (924°F) to 439°C (823°F). Isotherm plots for cases 1 through 6 are shown in Figures 7.25 through 7.30.

Three additional cases were modeled for the rifled tube of the subject contract. The three cases modeled differ in the film coefficient distribution on the inside surface; a uniform film of 500 BTU/(hr-f^2-°F) (steam contact with tube) on all inner surfaces, a film of 500 in the grooves and 5000 on the ribs and rib sides and a film of 500 on the ribs and 5000 on the rib sides and grooves.

Figure 7.31 is a plot of the inside heat flux distributions for these three cases. The peaks that occur at the crown and at thirty degree increments in each direction from the crown for the case of steam in the grooves are due to water contact with the sides of the ribs. The unconnected triangular data points are the result of applying the low film to the sides of the ribs instead.

Figures 7.32 to 7.34 are isotherm plots with the outside crown temperature indicated for each of the three cases.

TABLE 7.2

Variation of Thermocouple Measurement

Case #	Thermocouple Measurement ^{o}F	Description
1	924.31	T/C located at interface of thick and thin tube wall sections; no Al coating
2	823.39	Same as Case 1 but with adjacent heater turned off
3	928.05	Same as Case 1 but with Al coating
4	931.61	T/C located at center of thick tube wall section; with Al coating
5	925.11	T/C located at center of thin tube wall section; with Al coating
6	920.0	Cosine Fluid Distribution

Figure 7.22
INSIDE HEAT FLUX DISTRIBUTION – ALL HEATERS OPERATING
TOTAL FLUX INPUT = 0.715 MW/M^2

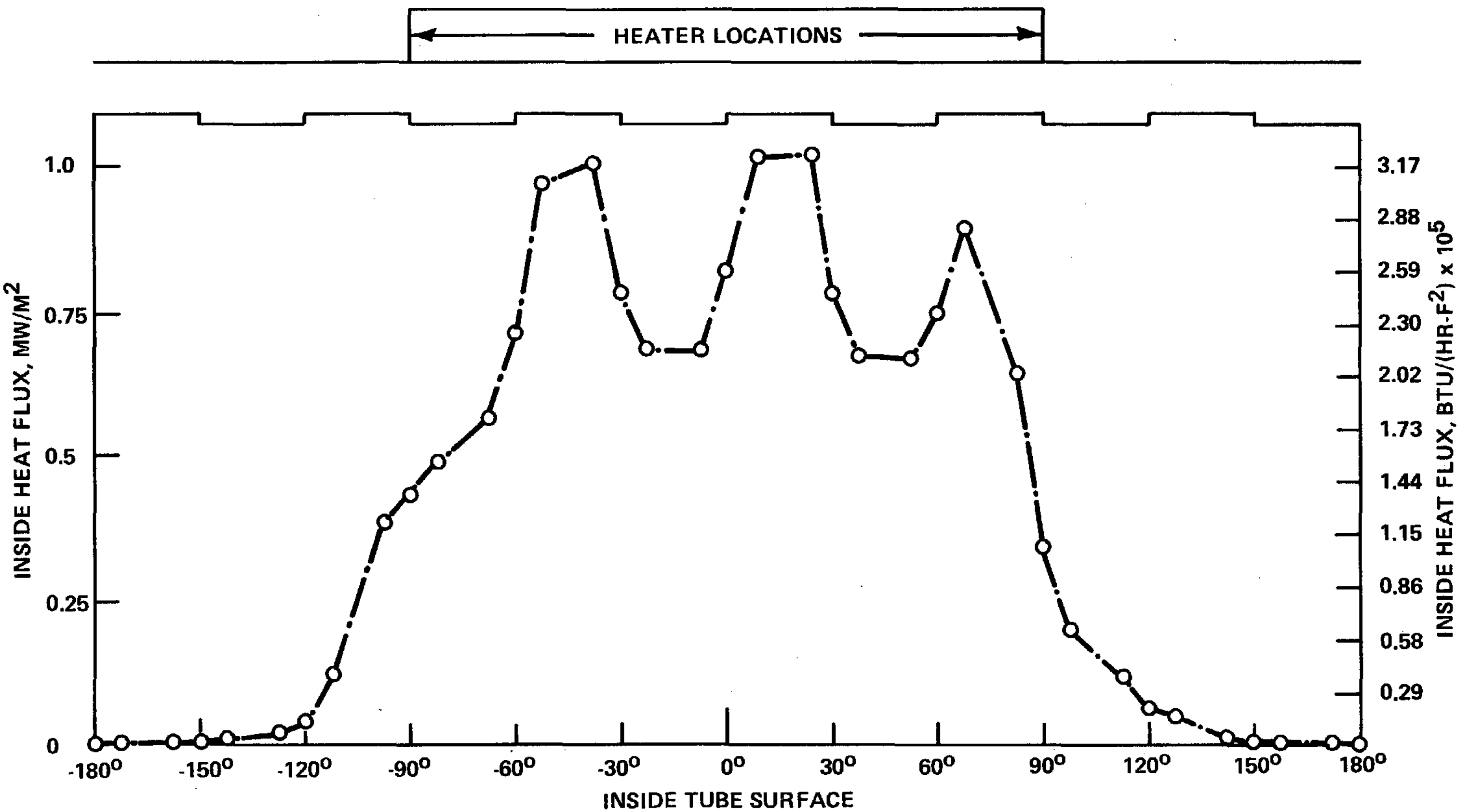

7.53

Figure 7.23

INSIDE HEAT FLUX DISTRIBUTION – ONE HEATER OFF

TOTAL FLUX INPUT = 0.715 MW/M^2

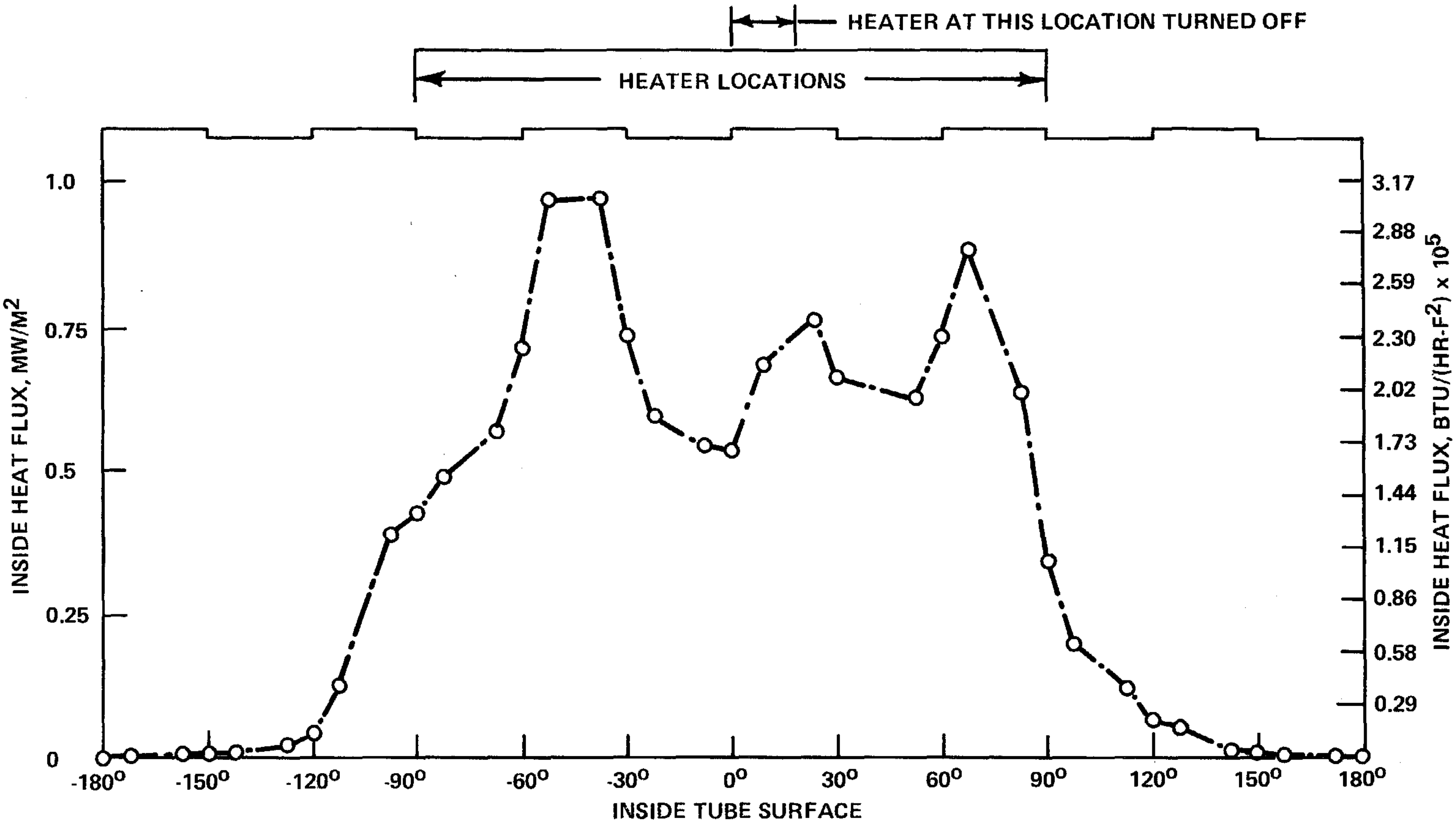

7.54

Figure 7.24
(REVISED) INSIDE HEAT FLUX DISTRIBUTION – COSINE APPLIED FLUX

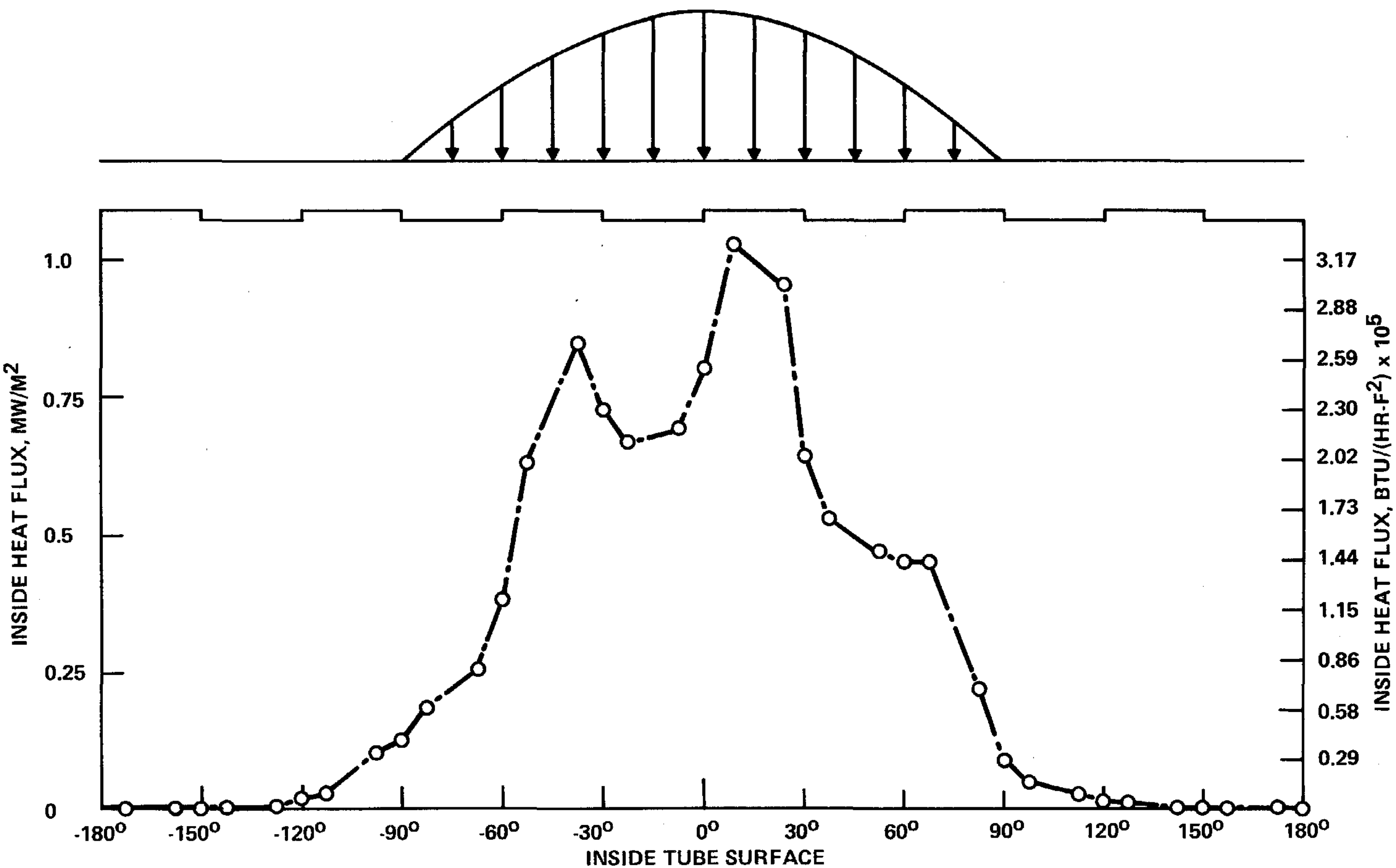

7.55

FIGURE 7.25 ISOTHERMS FOR CASE I

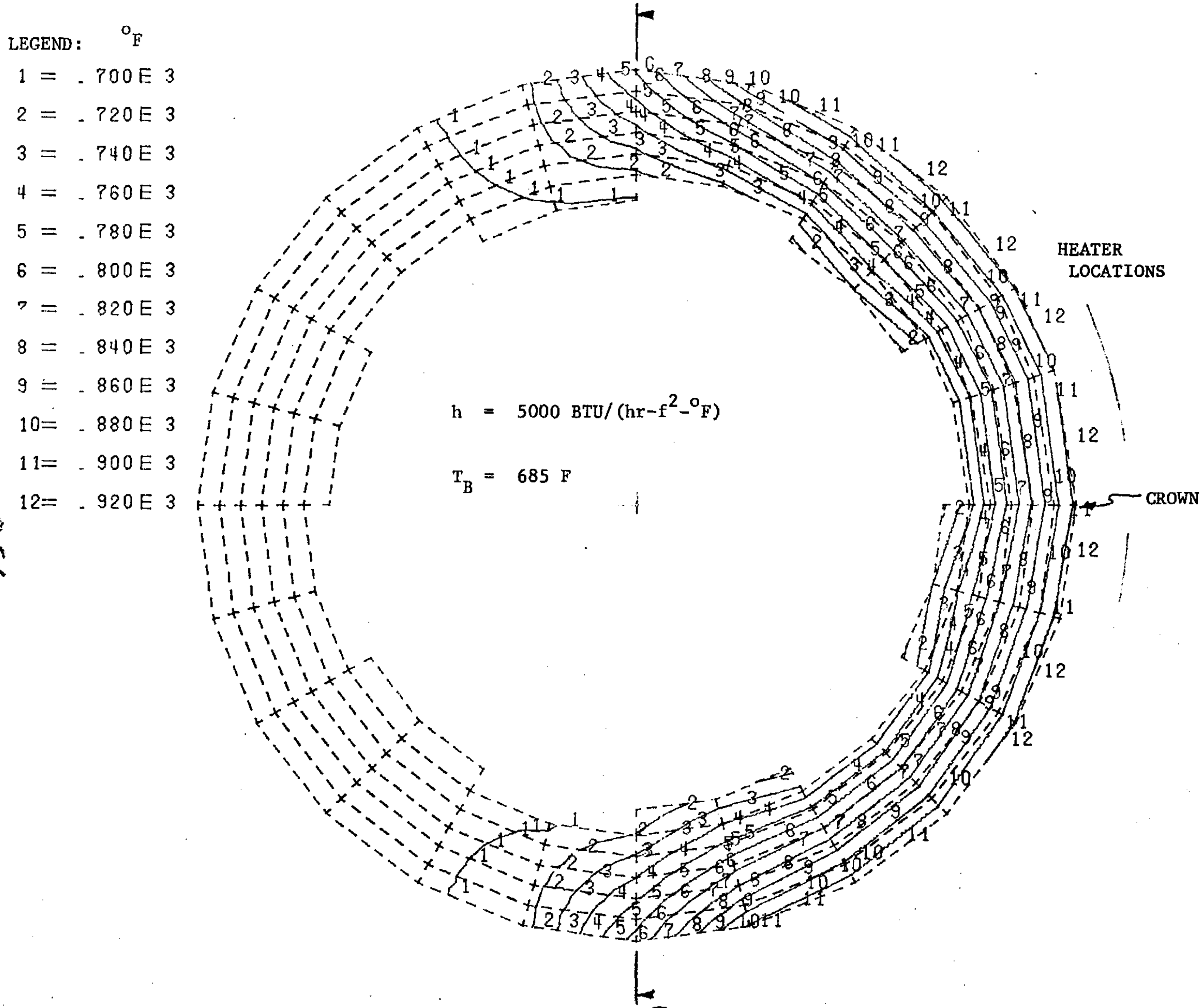

FIGURE 7.26 ISOTHERMS FOR CASE II

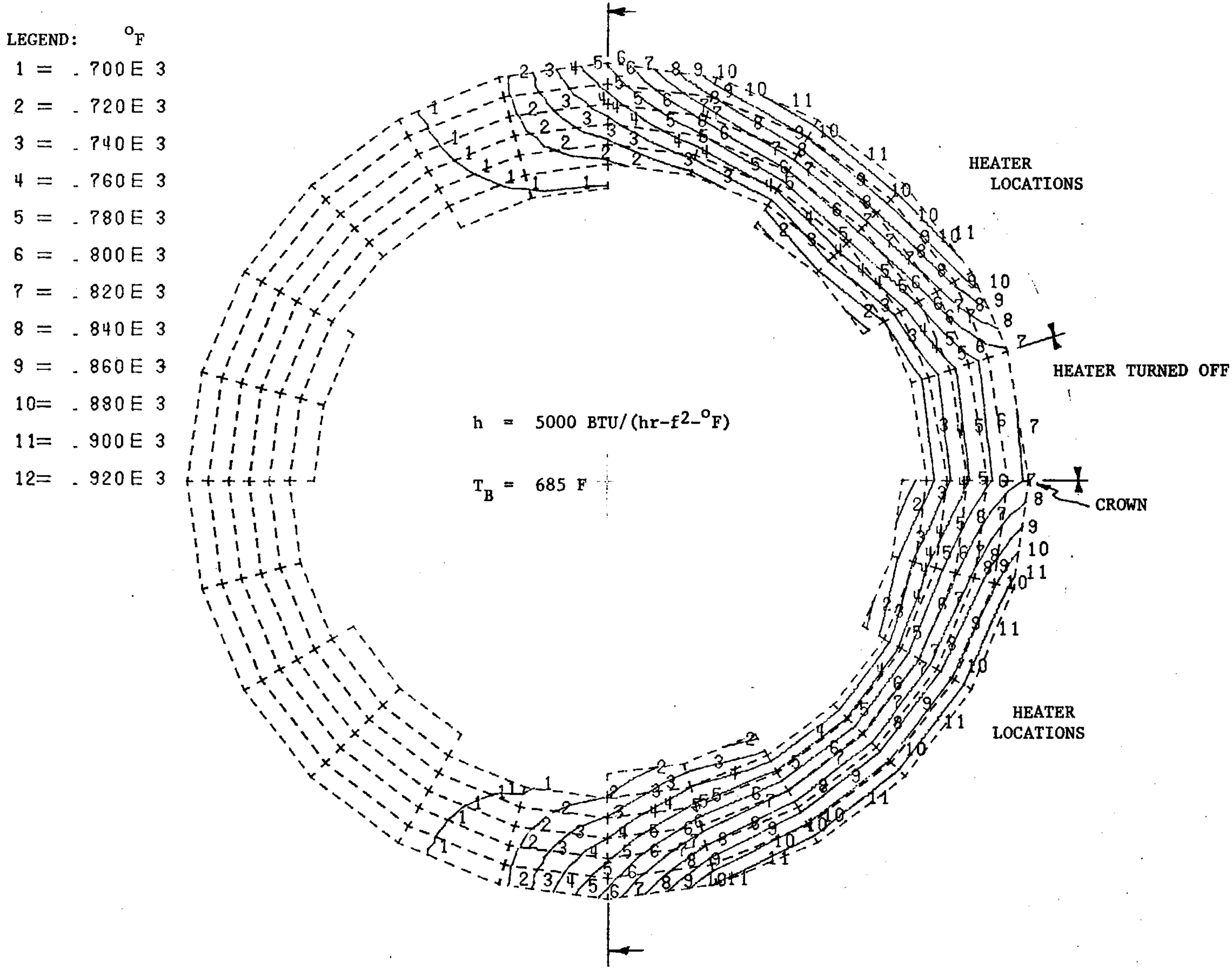

FIGURE 7.27 ISOTHERMS FOR CASE 3

LEGEND: ^{o}F

1 = .700E 3
2 = .720E 3
3 = .740E 3
4 = .760E 3
5 = .780E 3
6 = .800E 3
7 = .820E 3
8 = .840E 3
9 = .860E 3
10= .880E 3
11= .900E 3
12= .920E 3

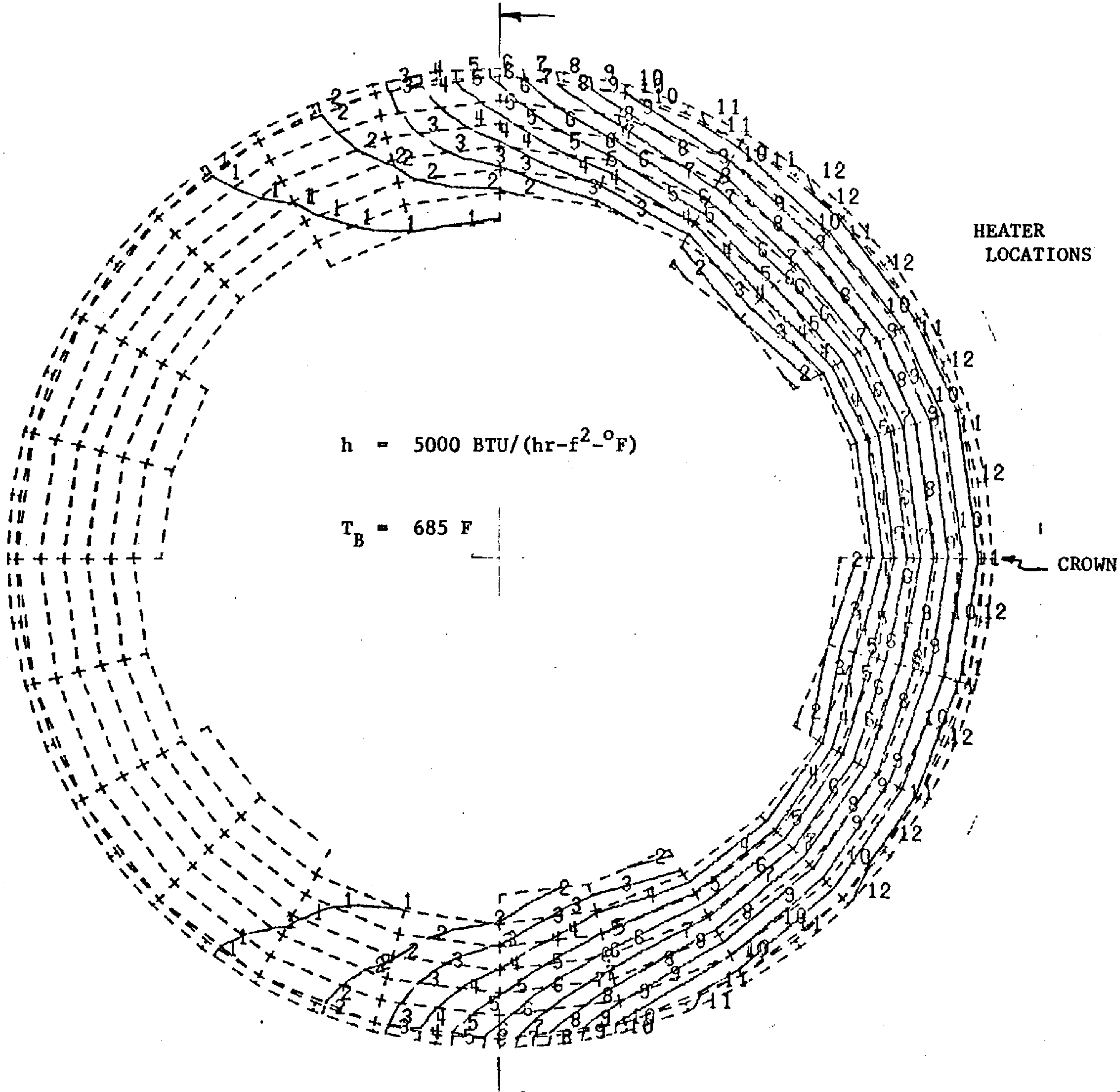

FIGURE 7.28 ISOTHERMS FOR CASE 4

LEGEND: °F

1 = .700E 3
2 = .720E 3
3 = .740E 3
4 = .760E 3
5 = .780E 3
6 = .800E 3
7 = .820E 3
8 = .840E 3
9 = .860E 3
10= .880E 3
11= .900E 3
12= .920E 3

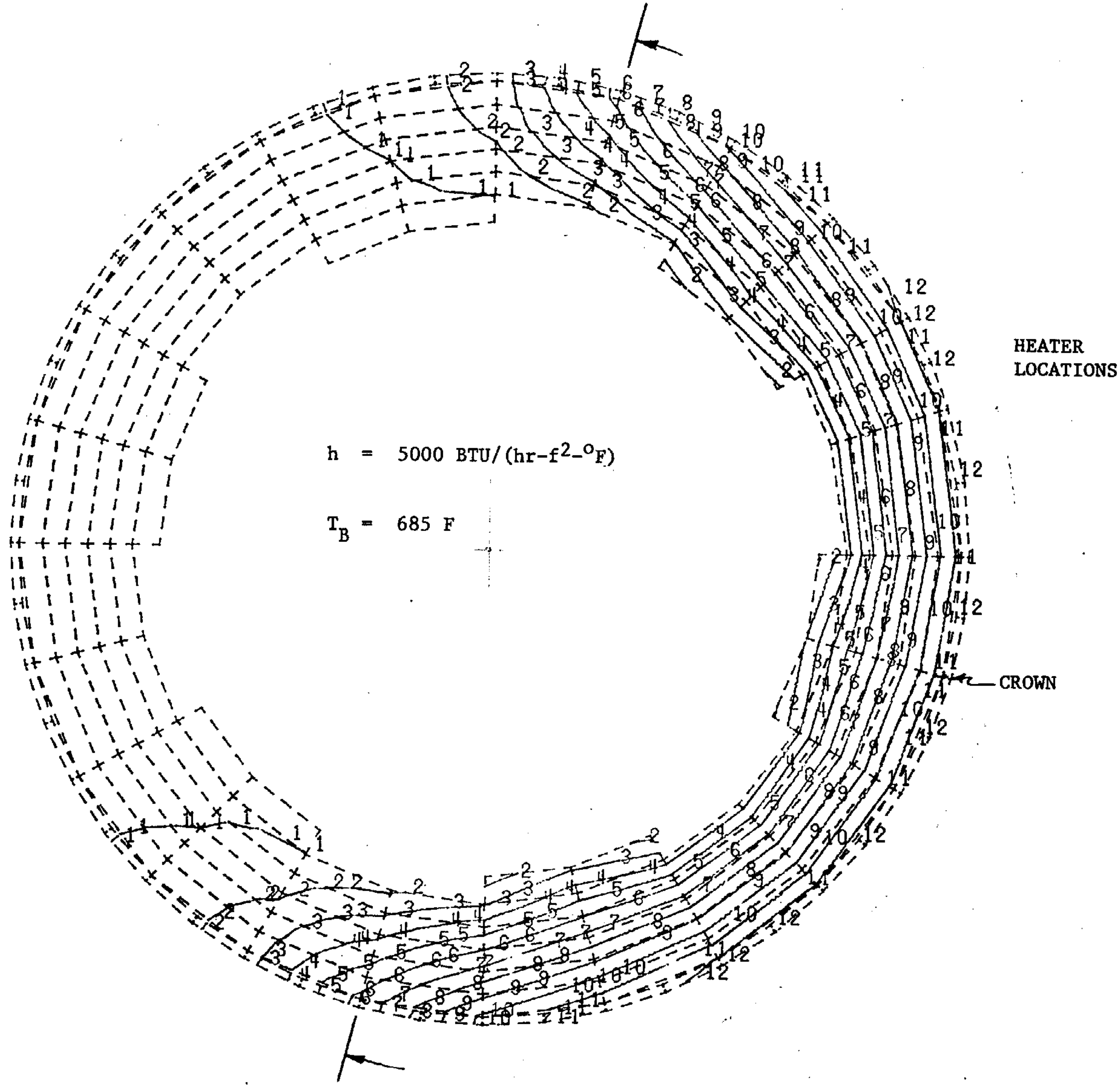

FIGURE 7.29 ISOTHERMS FOR CASE 5

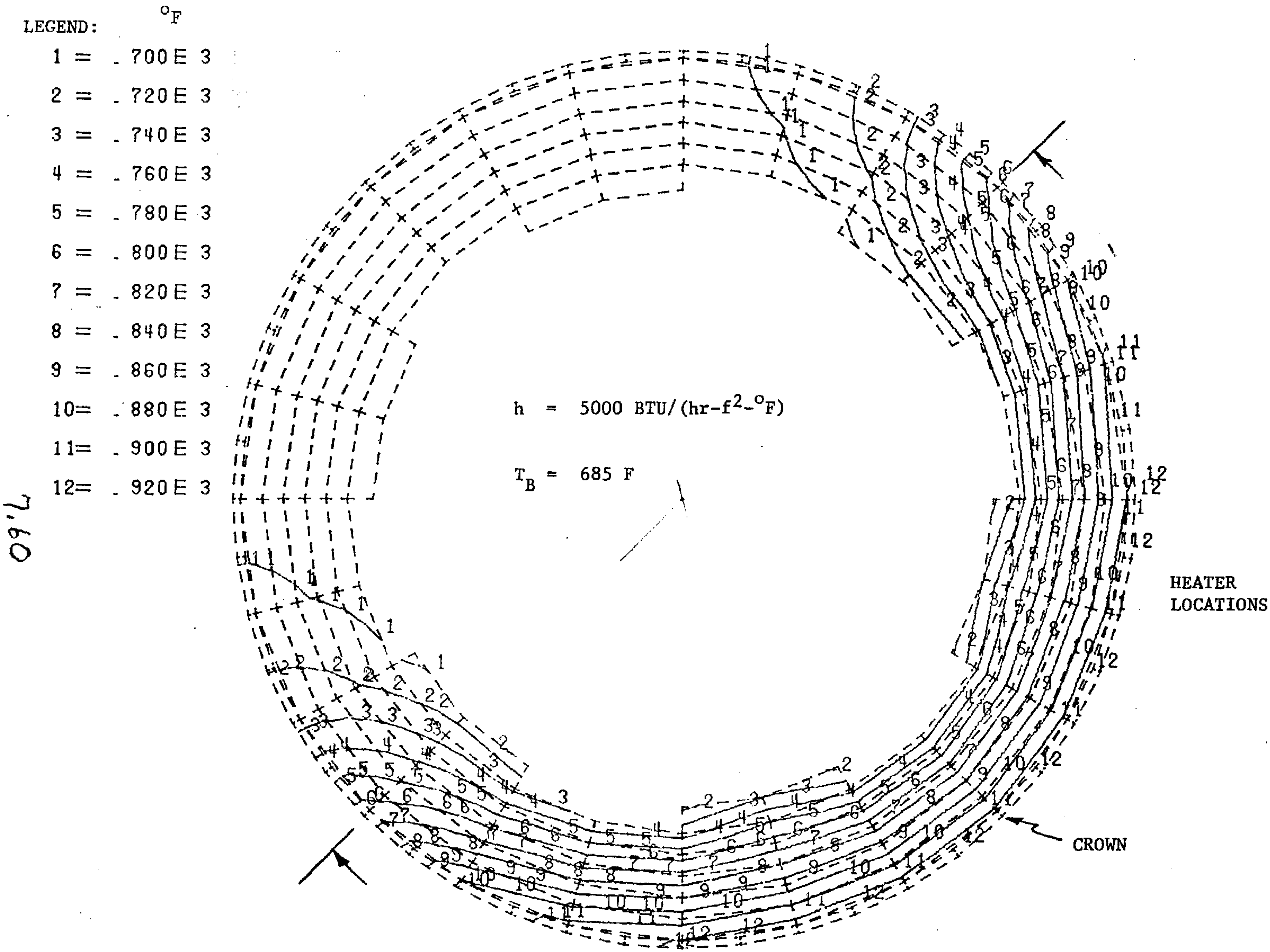

FIGURE 7.30 ISOTHERM FOR CASE 6

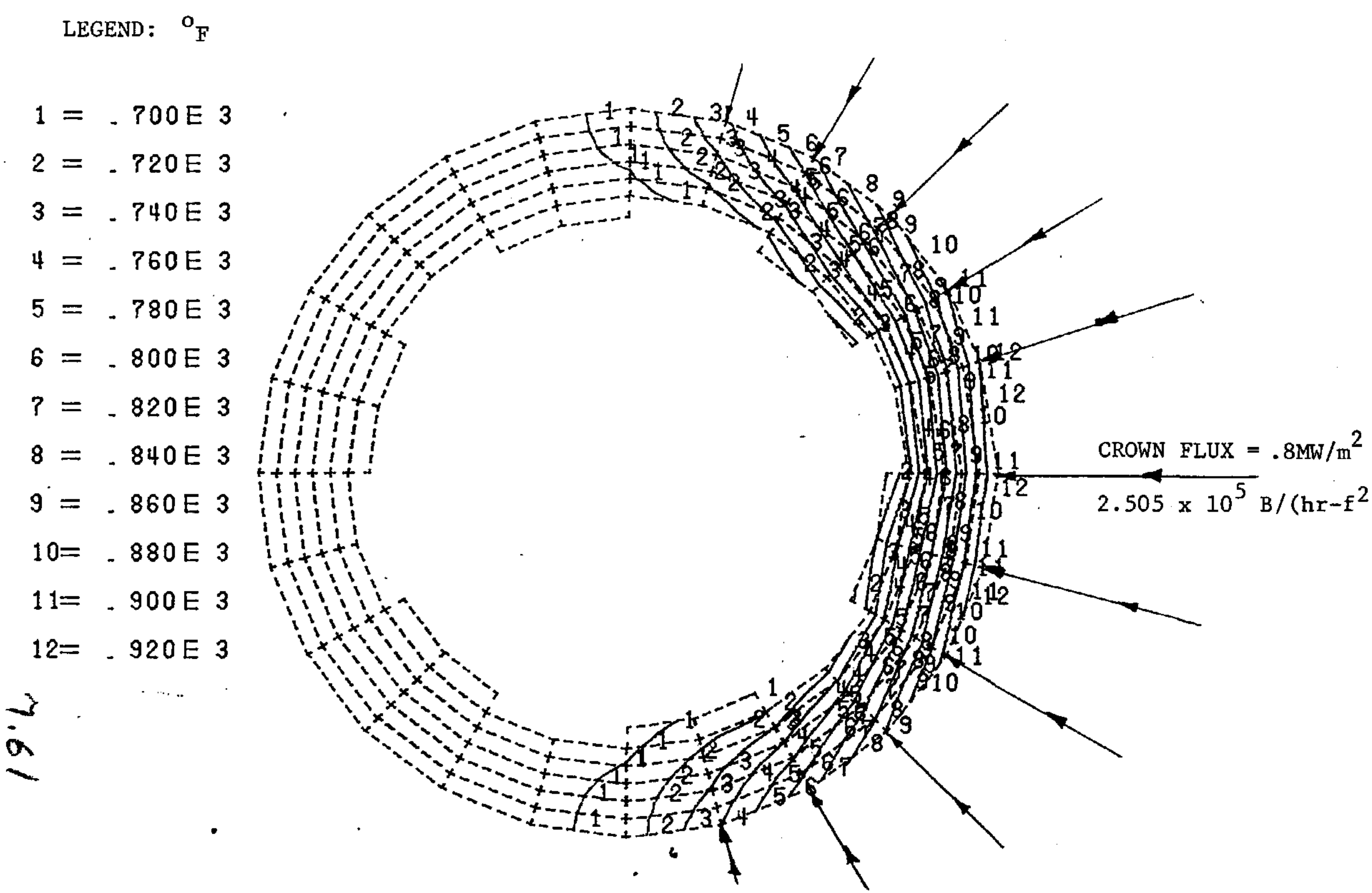

RIFLED TUBE - COSINE FLUX INPUT

Figure 7.31
INSIDE HEAT FLUX DISTRIBUTION

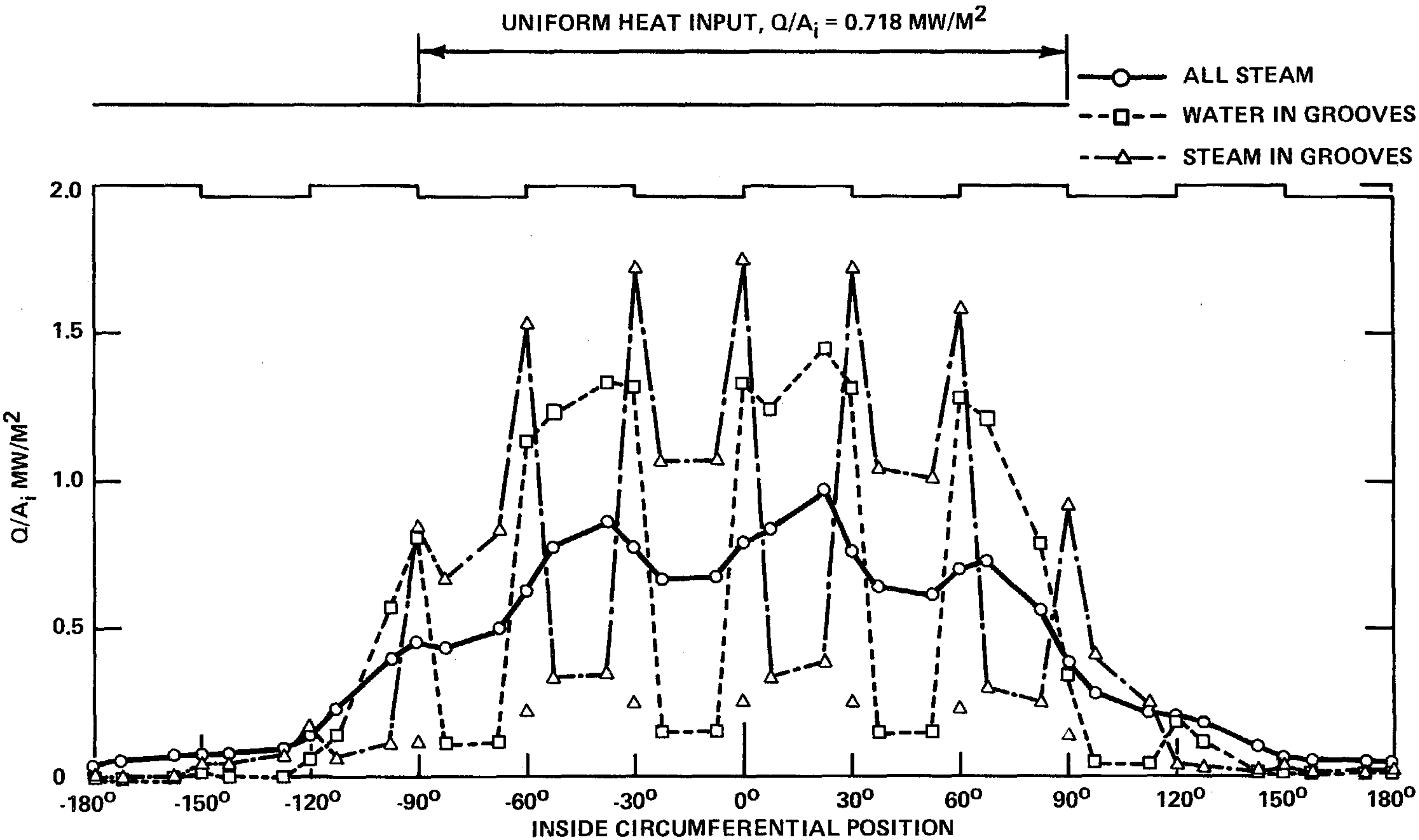

FIGURE 7.32 UNIFORM FILM ISOTHERMS

°F

1 = .700 E 3
2 = .750 E 3
3 = .800 E 3
4 = .850 E 3
5 = .900 E 3
6 = .950 E 3
7 = .100 E 4
8 = .105 E 4
9 = .110 E 4
10= .115 E 4
11= .120 E 4
12= .125 E 4
13= .130 E 4
14= .135 E 4

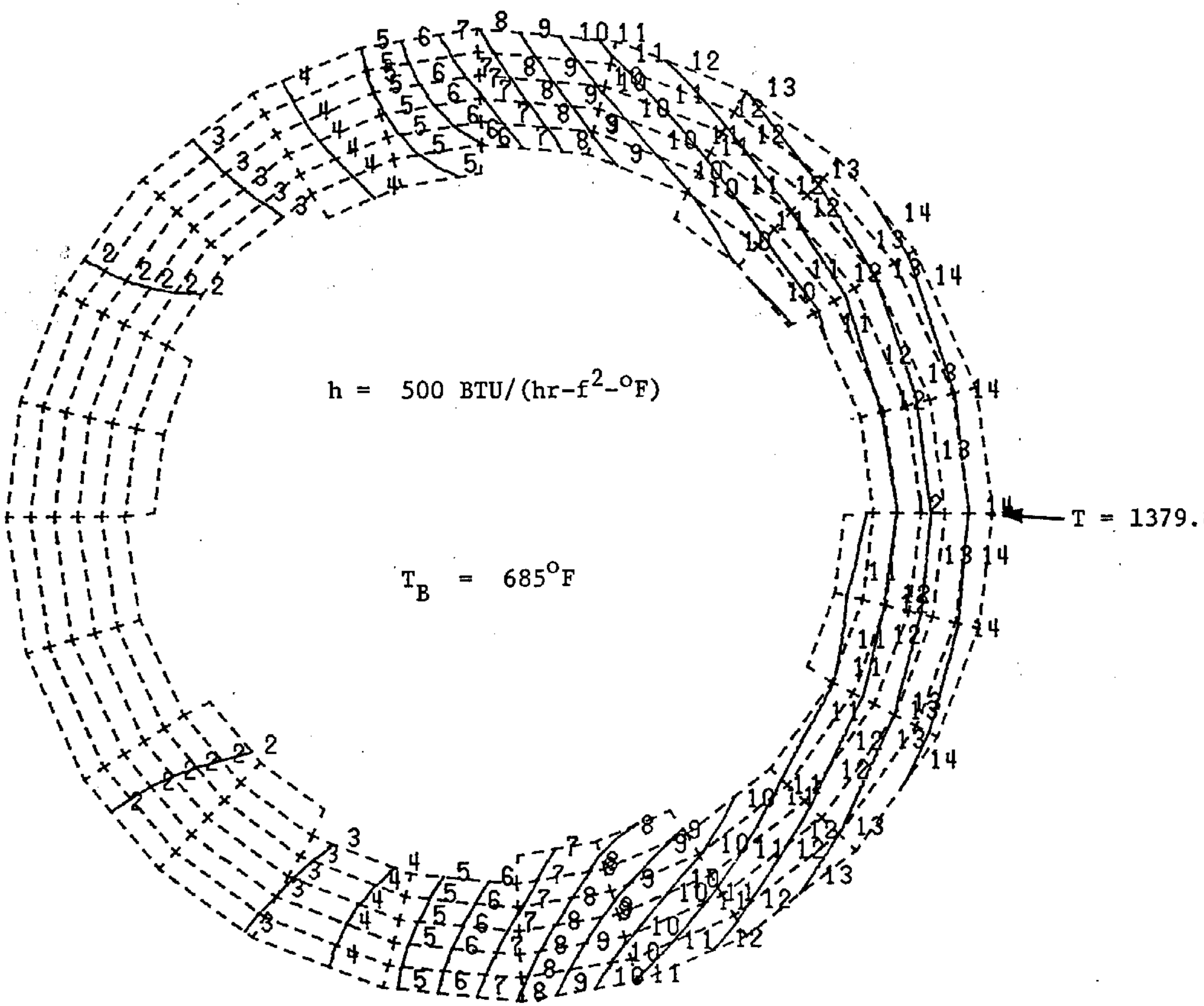

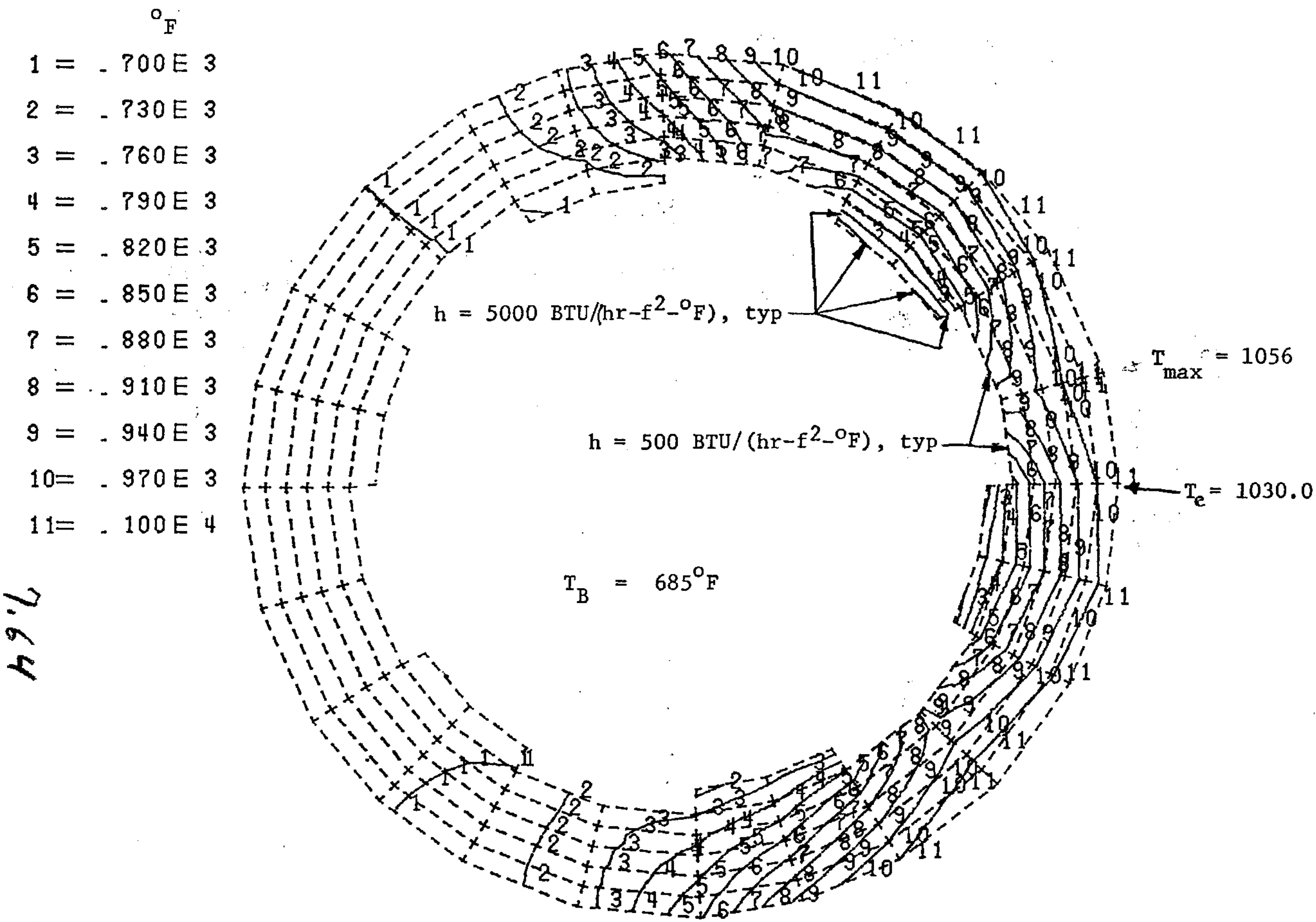

°F
1 = .700E 3
2 = .730E 3
3 = .760E 3
4 = .790E 3
5 = .820E 3
6 = .850E 3
7 = .880E 3
8 = .910E 3
9 = .940E 3
10= .970E 3
11= .100E 4
h = 5000 BTU/(hr-f²-°F), typ
h = 500 BTU/(hr-f²-°F), typ
T_max = 1056
T_e = 1030.0
T_B = 685°F

FIGURE 7.34 VARIED FILM ISOTHERMS II

^oF	
1 =	.700 E 3
2 =	.720 E 3
3 =	.740 E 3
4 =	.760 E 3
5 =	.780 E 3
6 =	.800 E 3
7 =	.820 E 3
8 =	.840 E 3
9 =	.860 E 3
10=	.880 E 3
11=	.900 E 3
12=	.920 E 3

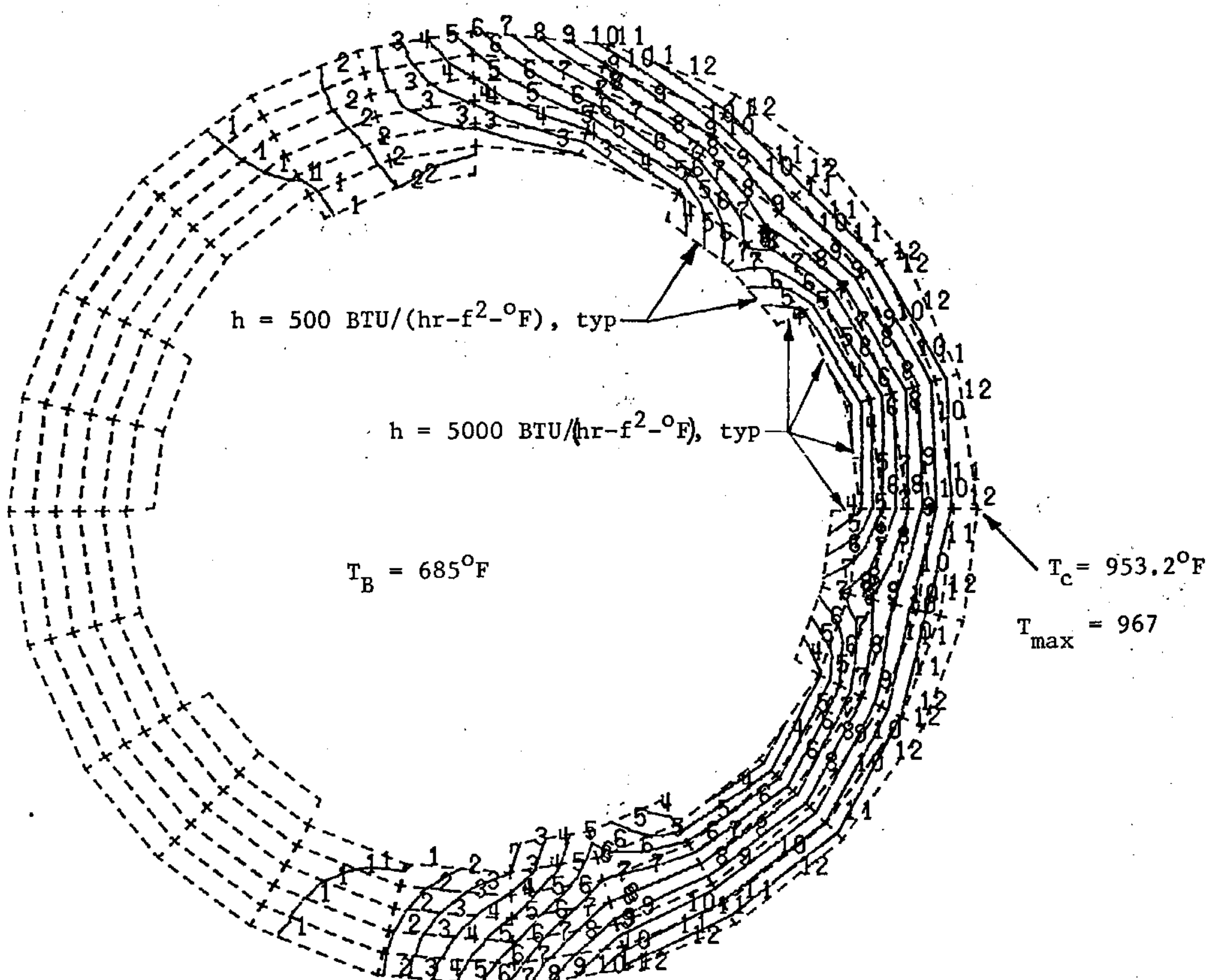

A definite effect was evident depending on where the steam vs. water boundary was located. Reversing the water/steam distribution caused a change in crown temperature from 512°C (953°F) to 554°C (1030°F); a ΔT of 42.8°C (77°F). The large change, 554°C (1030°F) to 749°C (1380°F), occurred when steam filled the entire tube, as would be expected in a minimum film boiling situation.

8. References

1. "A Description and Assessment of Large Solar Power Systems Technology," Sandia Laboratories Report SAND 79-8015, August, 1979.

2. "Central Receiver Solar Thermal Power System, Phase 1," Semi-Annual Review, MDAC, CDRL ITEM10, August, 1977.

3. "MDAC/Rocketdyne Solar Receiver Design Review," Sandia Laboratories Report SAND 79-8188, November, 1978.

4. "Department of Energy Large Solar Central Power Systems Semi-Annual Review," Sandia Laboratories Report SAND 79-8505, May, 1979.

APPENDIX A

SOLAR THERMAL PERFORMANCE PROGRAM

Introduction

The Solar Thermal Performance program described herein performs, as its name implies, a basic engineering performance analysis of an external solar central receiver. Given boiler size (tube size and number), certain heat transfer constants, inlet water conditions and incident solar heat flux, the program calculates requested mass flow for specified outlet conditions. The program can evaluate economizer, evaporator and superheater units. It can also evaluate a once thru steam generator configuration. Details of the program, its input requirements, output and computational options are provided in this manual.

Program Description

The solar panel thermal performance is determined by a mass and energy balance made on an incremental length of tube summed along the total tube length.

The heat conduction equations are written for the axisymmetric flow at the tube crown. The incident heat flux is assumed normal to the tube at this point. A correction factor is incorporated into the one-dimensional, axisymmetrical case to correct the crown temperature for the effect of 2-D heat flux and heat flow. The pressure drop is calculated assuming the homogeneous model.

The flow of the program is as follows: After reading input, initializing parameters and calculating fluid properties* and solar insolation, the program determines the inside convective heat transfer film coefficient in the incremental section of tube being evaluated. The correlation used in calculating this value of hi is dependent on the fluid state existing in that particular tube section. The criteria and corresponding correlations are:

* Fluid properties obtained using STABL[3], SPHT, VISCOS & COND.

1. Single phase, liquid and vapor: (Dittus-Boelter)

$$\frac{hD}{K} = .023\ Re^{.8}\ \ Pr^{.4}$$

2. Two-phase, nucleate boiling region:

$hi = 10{,}000$ Btu/hr ft^2 ^oF

3. Film boiling region: (Groeneveld Correlation)

4. Transitional boiling region (From DNB point to point of h_{min})

   A linear interpolation is made between h_i = 10000 and $h_i = h_{min}$, from the Groeneveld Film Boiling Correlation.

5. Supercritical Region:

   Uses C-E's Supercritical Film Coefficient correlation.

The Groeneveld Film Boiling Correlation noted above is defined as follows:

$$h = a\,\frac{Kg}{D}\left[Reg\ \left(x + \frac{\rho g}{\rho 1}\,(1-x)\right)\right]^b\ Pr_w^c\ \ Y^d\ \ \emptyset^e$$

where h = film coefficient, BTU/hr ft^2 ^oF

$a = 1.85 \times 10^{-4}$, const.

Kg = sat. steam conductivity, BTU/hr ft^2 ^oF

D = tube diameter, feet

Reg = Reynolds Number at sat. steam condition

x = local quality

ρg = density sat. steam

$\rho 1$ = density sat. liquid

b = 1.0, const.

Pr_w = Prandtl Number evaluated at wall temperature

c = 1.57, const.

Y = see below

d = -1.12, const.

$\emptyset$ = heat flux, BTU/hr ft^2, inside surface

e = .131, const.

$$Y = 1 - .1 \left(\frac{\rho l}{\rho g - 1} \right)^{.4} (1 - x)^{.4}$$

and $X_{h_{min}}$ is given by

$$(X_{h_{min}} - X_{DNB}) = .045 + \frac{.048}{2.3 - .01\, p}$$

where: p = pressure, is in bars

X_{DNB} = Quality at DNB point

$X_{h_{min}}$ = Quality at the location of minimum h

The program then calculates the absorbed heat flux and tube crown temperature.

The absorbed crown heat flux is given by:

$$\dot{q}_{abs} = \dot{q}_{inc} \cdot \alpha_s - \sigma\varepsilon(T_{sl}^{\ 4} - T_o^{\ 4}) - h_{ext}\,(T_{si} - T_o)$$

where $\dot{q}_{abs}$ = absorbed heat flux, BTU/hr ft^2

$\dot{q}_{inc}$ = incident solar flux, BTU/hr ft^2

α_s = solar absorptance

σ = Stefan-Boltzmann Constant

ε = infrared emittance

h_{ext} = external convection coefficient

T_{sl} = absolute surface temperature ^oR

T_{so} = absolute ambient temperature ^oR

Also, by: $\dot{q}_{abs} = (T_{sl} - T_f) \;/\; \left[D = \Psi/h_i \;\; D_i \; + (Do/2K)\; \mathrm{Ln}\; \left(\frac{Do}{Di} \;\; \Psi\right)\right]$

where: $\dot{q}_{abs}$ = crown absorbed heat flux, BTU/hr ft^2

T_{sl} = absolute surface temperature ^oR (Tube Crown temperature)

T_f = absolute fluid bulk temperature ^oR

Do = tube outside diameter, inches

Di = tube inside diameter, inches

h_i = inside film convection coefficient, BTU/hr ft^2 ^oF

K = tube conductivity BTU in/hr ft^2 ^oF

Ψ = correction factor for 2-D heat flow.

These 2 equations can be combined into a quartic equation in T_{s1}. This is then solved by formula from a standard math reference:

$$T_{si}^{4} + \left\{ h_{ext}/\sigma\varepsilon + 1/\sigma\varepsilon \left[Do\ \Psi/h_i Di + (Do/2K)\ Ln\ (Do\ \Psi/Di) \right] \right\} T_{s1}$$

$$- \left\{ \dot{q}_{ine}\ \ \alpha_s/\sigma\varepsilon + h_{ext}\ \ To/\sigma\varepsilon + To^4 + T_f/\sigma\varepsilon \left[Do\ \Psi/h_i Di + (Do/2K)\ Ln\ (Do\ \Psi/Di) \right] \right\} = 0$$

The 2-D correlation, Ψ, is calculated by an equation of the form:

$$\Psi = B1 + B2\ (BIOT)^{B3}$$

where: B1, B2, B3 are constants that depend on the diameter ratio.

$$BIOT = \frac{HT}{K}$$

where: H = inside film conductance

T = tube thickness

K = tube conductivity

The incremental increase in fluid enthalpy is then calculated from the absorbed heat flux based on the following energy balance:

$$\dot{q}_{net\ in} = \frac{M \cdot \Delta h_f}{\Delta A}$$

where M = mass flow rate

Δh_f = change in enthalpy

ΔA = incremental area of the element

The program then calculates fluid quality. If this quality lies between 0 and 1, the critical heat flux (Thompson - Mac Beth Correlation) or the Critical Quality (C-E Critical Quality Correlation) is determined and compared to calculated fluid properties as an indicator of the point at which DNB occurs.

Though the correlation to be used must be specified, the criteria for use is:

Thompson - Mac Beth Correlation for $P \leq 2000$ psia

C-E Correlation for $P > 2000$ psia

The C-E Critical Quality Correlation is confidential for company use.

The Thompson - Mac Beth Correlation is described as follows:

I. The low velocity correlation for $G \overline{<} .03 \times 10^6$ lbm/hr ft^2:

$$\frac{q_{crit}}{10^6} = .00633\, H_{fg}\, D^{-.1} \left(\frac{G}{10^6}\right)^{.51} \quad (1-x)$$

where q_{crit} = critical heat flux (BTU/hr ft^2) (inside surface)

H_{fg} = heat of evaporation (BTU/lbm)

D = tube I.D. (in.)

G = mass flux (LBM/hr ft^2)

x = critical quality

II. The high velocity correlation for $G > 0.3 \times 10^6$ lbm/hr ft^2:

$$\frac{q_{crit}}{10^6} = \frac{A^1 - 1/4D\ (G \times 10^{-6})\ x\ H_{fg}}{C^1}$$

where: A^1 and C^1 contain Y constants based on pressure ranges.

Constants (Y) were determined at 1550 psia

$$\therefore A^1 = 36D^{.509} \ (Gx10^{-6})^{-.109} \left[1 - .19D + 0.24(Gx10^{-6}) + .463D\ (Gx10^{-6})\right]$$

$$\text{and } C^1 = 41.7D^{.053} (G \times 10^{-6})^{.0109} \left[1 + .231D + .0656(Gx10^{-6}) + .117D(Gx10^{-6})\right]$$

In the program, a linear interpolation is made between 1150 psia and 2000 psia for the above (Y) constants.

Finally, the pressure drop (ΔP) through the increment of tube length is determined as a function of frictional, momentum, and gravitational components. The details of this calculation are as follows:

$$f = 0.46/Re^{.2}$$

where: f = friction factor

Re = Reynold's Number

$$\Delta P_{friction} = 4 \times 10^{-10} f \frac{\Delta l}{Di} v G^2$$

where Δl = incremental tube length

Di = inside tube diameter

v = average specific volume in increment

G = mass flow rate per unit area per tube.

$$\Delta P_{momentum} = 1.667 \times 10^{-11} (v_2 - v_1) G^2$$

where v_2 = element outlet sp. vol.

v_1 = element inlet sp. vol.

$$\Delta P_{gravity} = \frac{\Delta l}{144 v}$$

$$\Delta P_{total} = \Delta P_{friction} + \Delta P_{momentum} + \Delta P_{gravity}$$

Pressure at the increment's exit is then simply:

$$P = P_{in} - \Delta P_{total}$$

Brake Horsepower is calculated as

$$BHP = 8.551 \times 10^{-5} \Delta P \overline{V} M$$

where ΔP = pressure drop (psi)

$\overline{V}$ = specific volume (ft^3/lb)

M = mass flow rate (lb/hr)

The program recalculates the above variables for each increment of the tube length. If desired, the program will test the final increment output for proper outlet temperature or quality. The program will then automatically adjust the flow rate and recalculate the above parameters until the desired steam temperature or quality is achieved. In these instances of iterating for specified fluid outlet properties, the program will correct flow to obtain a temperature within 5°F of the specified TDESN or .01 of the specified quality. Mass flow rate is adjusted as follows:

For Temperature:

$$M = M * \frac{\text{Enthalpy Out - Enthalpy In}}{\text{(Enthalpy at TDESN - Enthalpy In)}}$$

For Quality:

$$M = M * \frac{\text{Outlet Quality}}{\text{Specified Design Quality}}$$

Once the final solution is obtained the program calculates panel efficiency as follows:

$$N = \frac{M^* \ (H_{out} - H_{in})}{\text{Q absorbed* Absorption Area}}$$

where N = panel efficiency

H_{out} = panel outlet enthalpy (BTU/lb)

H_{in} = panel inlet enthalpy (BTU/lb)

Q absorbed is calculated as the area under the trapazoidal solar insolation flux curve.

$$Q_{abs} = \frac{1}{2} \ (1 - \frac{L1}{LT} + \frac{L2}{LT}) \ X \ Q_{max}$$

Q_{max} = Maximum Solar Insolation

LT = Overall tube length

L1&L2 = Trapazoid's inflection points

The Absorption Area is defined as the panels projected tube area.

$$A = NT * Do * LT$$

where Do = tube outside diamter

NT = number of tubes/panel

Lastly the program writes the output and checks for more cases.

Solar Program General

Flow Chart

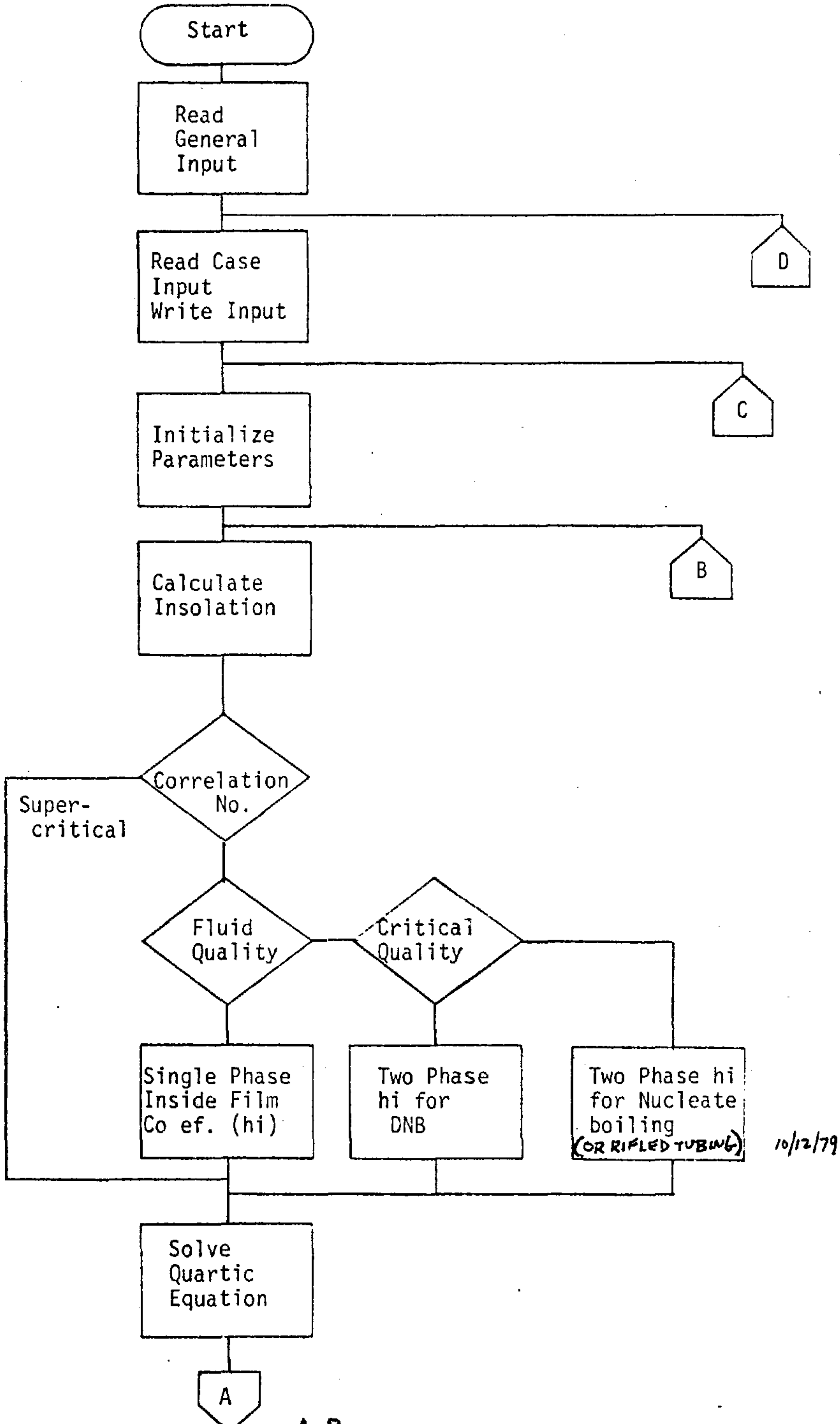

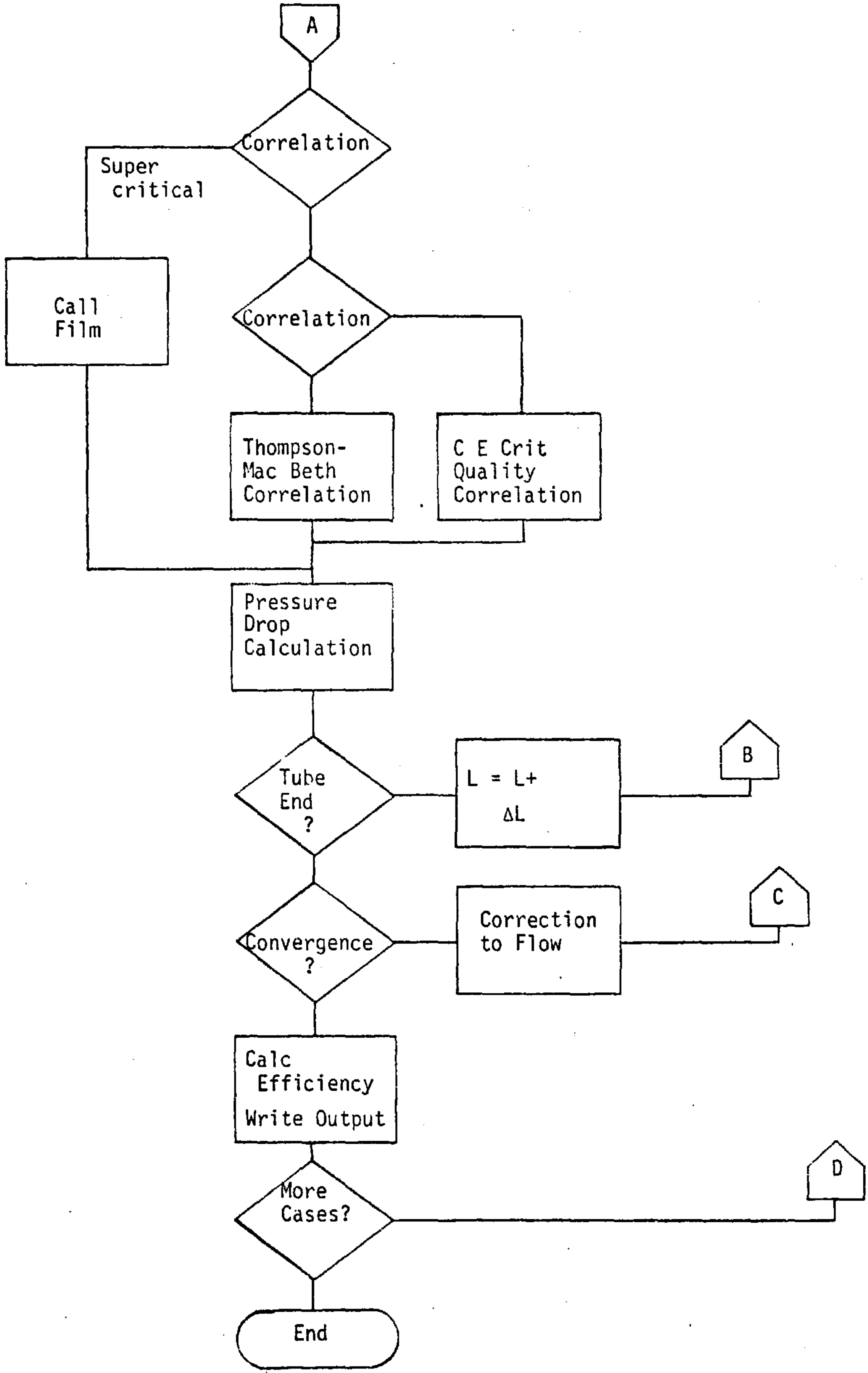
A
Correlation
Super critical
Call Film
Correlation
Thompson-Mac Beth Correlation
C E Crit Quality Correlation
Pressure Drop Calculation
Tube End ?
L = L+ ΔL
B
Convergence ?
Correction to Flow
C
Calc Efficiency
Write Output
More Cases?
D
End

APPENDIX B

STPP TYPICAL COMPUTER PRINTOUTS

BOILER PANEL NO. 1
(USING THOMPSON-MACBETH CORRELATION)

EVAPORATOR PANEL

PRESS PSIA	TEMP F	ENTHALPY BTU/LB	L1 FT	L2 FT*	NO.TUBES	TUBE OD IN	*TUBE ID IN	TUBE LGTH FT	INCREMENT FT
2270.	6[illegible]7.	627.	5.6	37.4	62	1.25	.98	66.	1.0

CONDUCTIVITY B-IN/H-SF-F	EXT.COEFF B/H-SF-F	EMISSIVITY *	ABSORPTANCE	*AMB.TEMP F	MAX.SOLAR FLUX BTU/HR-SQFT
21.	3.	.89	0.95	1[illegible].	27[illegible].

TUBE LGTH FT	PRESS PSIA	BULK TEMP F	ENTHALPY BTU/LB	INSIDE FILM COEF B/H-SF-F	OUTSIDE HEAT FLUX B/H-SF	TUBE *CROWN TEMP F	BULK QUAL	CRIT QUAL	CUMULATIVE PRESSURE DROP FRICTION PSI	MOMENTUM PSI	GRAVITY PSI
1.00	2269.7	610.	628.	2237.	35690.	654.	-.18	0.0	0.0257	0.0003	0.2939
2.00	2269.4	611.	631.	2239.	74099.	694.	-.18	0.0	0.0517	0.0011	.5871
3.00	2269.1	613.	632.	2242.	112416.	739.	-.17	0.0	0.0759	0.0023	.8793
4.00	2268.7	615.	636.	2247.	150811.	784.	-.16	0.0	.1012	0.0039	1.1712
5.00	2268.4	616.	640.	2255.	188661.	829.	-.15	0.0	.1254	0.0058	1.4593
6.00	2268.1	622.	646.	2265.	226643.	875.	-.14	0.0	0.1508	0.0083	1.7461
7.00	2267.8	625.	651.	2278.	249727.	903.	-.13	0.0	0.1764	.0111	2.0314
8.00	2267.5	629.	657.	2293.	249725.	906.	-.11	0.0	0.2022	0.0139	2.3119
9.00	2267.2	632.	663.	2310.	249573.	909.	-.10	0.0	0.2282	0.0170	2.5906
10.00	2266.9	636.	669.	2326.	249612.	912.	-.08	0.0	0.2544	0.0201	2.8655
11.00	2266.6	639.	675.	2348.	249653.	914.	-.07	0.0	0.2808	0.0233	3.1395
12.00	2266.3	642.	681.	2371.	249708.	916.	-.05	0.0	0.3074	0.0268	3.4093
13.00	2266.0	645.	687.	2396.	249448.	918.	-.04	0.0	0.3343	0.0304	3.6764
14.00	2265.7	648.	692.	2423.	249619.	920.	-.03	0.0	0.3615	0.0349	3.9413
15.00	2265.4	651.	698.	2455.	249394.	922.	-.01	0.0	0.3889	0.0381	4.2019
16.00	2265.1	654.	704.	2497.	249344.	923.	0.00	0.00	0.4168	0.0449	4.4573
17.00	2264.8	654.	710.	1[illegible].	251201.	849.	0.02	0.02	0.4458	0.0667	4.7027
18.00	2264.5	654.	716.	1[illegible].	251225.	849.	0.03	0.03	0.4768	.0886	4.9331
19.00	2264.2	654.	722.	1[illegible].	251250.	849.	0.05	0.05	0.5097	0.1105	5.1532
20.00	2264.0	654.	728.	1[illegible].	251273.	849.	0.06	0.06	0.5445	0.1324	5.3555
21.00	2263.7	654.	734.	1[illegible].	251296.	849.	0.07	0.07	0.5811	.1543	5.5572
22.00	2263.5	654.	740.	1[illegible].	251316.	849.	0.09	0.09	0.6197	.1762	5.7354
23.00	2263.2	654.	745.	1[illegible].	251339.	849.	0.10	0.10	0.6601	.1981	5.9119
24.00	2263.0	654.	751.	1[illegible].	251359.	849.	0.12	0.12	0.7024	.2201	6.0[illegible]5
25.00	2262.8	654.	757.	1[illegible].	251379.	849.	0.13	0.13	0.7467	.2420	6.2419
26.00	2262.5	653.	763.	1[illegible].	251398.	849.	0.15	0.15	.7928	0.2639	6.3955
27.00	2262.3	653.	769.	1[illegible].	251417.	849.	.16	0.16	0.8408	0.2858	6.5453
28.00	2262.1	653.	775.	1[illegible].	251435.	849.	0.17	0.17	0.8907	0.3078	6.6853
29.00	2261.9	653.	781.	1[illegible].	251454.	849.	0.19	0.19	.9425	0.3297	6.8261
30.00	2261.7	653.	787.	1[illegible].	251471.	849.	0.20	0.20	0.9962	0.3516	6.959
31.00	2261.5	653.	793.	1[illegible].	251489.	849.	0.22	0.22	1.0518	0.3735	7.0874
32.00	2261.3	653.	799.	1[illegible].	2515[illegible].	849.	0.23	0.23	1.1093	.3955	7.2116
33.00	2261.1	653.	804.	1[illegible].	251523.	849.	0.25	.25	1.1687	.4175	7.3318
34.00	2260.9	653.	810.	1[illegible].	251540.	849.	0.26	0.26	1.2299	0.4394	7.4483
35.00	2260.7	653.	816.	1[illegible].	251557.	849.	0.27	0.27	1.2931	0.4614	7.5513
36.00	2260.5	653.	822.	1[illegible].	251573.	849.	0.29	0.29	1.3582	.4833	7.6711
37.00	2260.3	653.	828.	1[illegible].	25159[illegible].	849.	0.3	0.3	1.4252	.5053	7.7775
38.00	2260.1	653.	834.	1[illegible].	245583.	845.	0.32	0.32	1.4941	0.5268	7.8812
39.00	2259.9	653.	839.	1[illegible].	237659.	838.	0.33	0.33	1.5647	0.5475	7.9822
40.00	2259.7	653.	845.	1[illegible].	228662.	831.	0.34	0.34	1.6371	.5675	8.0816
41.00	2259.5	653.	850.	1[illegible].	221037.	824.	0.36	0.36	1.7112	0.5867	8.1771
42.00	2259.3	653.	855.	1[illegible].	211478.	818.	.37	0.37	1.787	0.6051	8.2713
43.00	2259.1	653.	860.	1[illegible].	202767.	811.	0.38	0.38	1.8643	0.6229	8.3637
44.00	2259.0	653.	864.	1[illegible].	194749.	805.	0.39	0.39	1.9432	.6399	8.4542
45.00	2258.8	653.	869.	1[illegible].	185695.	798.	0.40	0.40	2.0234	0.6561	8.5432
46.00	2258.6	653.	873.	1[illegible].	176946.	791.	0.41	0.41	2.1051	0.6716	8.6315

[illegible]	[illegible]	[illegible]	[illegible]	[illegible]	[illegible]	[illegible]	[illegible]	[illegible]	1.[illegible]	[illegible]	[illegible]
45.	22[illegible].8	[illegible]	[illegible]	1[illegible]	185[illegible].	798.	.4	.4	2.[illegible]234	.[illegible]561	8.5432
46.[illegible]	225[illegible].6	653.	873.	1[illegible]	176945.	791.	.41	.41	2.1[illegible]51	.6716	8.63[illegible]6
47.[illegible]	22[illegible].4	653.	877.	1[illegible]	168687.	784.	.42	.42	2.188	.6963	8.7157
48.[illegible]	22[illegible].2	653.	[illegible]	1[illegible]	16[illegible]277.	778.	.43	.43	2.2722	.7[illegible]3	[illegible].[illegible]15
49.[illegible]	22[illegible]	653.	884.	1[illegible]	151[illegible]89.	771.	.44	.44	2.3576	.7135	8.[illegible]851
50.[illegible]	2257.9	653.	887.	1[illegible]	142538.	764.	.45	.45	2.4441	.726[illegible]	8.9576
51.[illegible]	2257.7	653.	891.	1[illegible]	133887.	757.	.45	.45	2.5316	.7377	9.[illegible]492
52.[illegible]	2257.5	653.	893.	1[illegible]	124595.	75[illegible].	.46	.46	2.62[illegible]1	.7486	9.1095
53.[illegible]	2257.3	653.	896.	1[illegible]	117[illegible]93.	744.	.47	.47	2.7[illegible]96	.75[illegible]	9.2[illegible]
54.[illegible]	2257.1	653.	899.	1[illegible]	1[illegible]	737.	.47	.47	2.7[illegible]9	.7683	9.2[illegible]87
55.[illegible]	2257.[illegible]	653.	9[illegible]1.	1[illegible]	99865.	731.	.48	.48	2.[illegible]	.777	9.3571
56.[illegible]	2256.8	653.	9[illegible]3.	1[illegible]	91682.	724.	.48	.48	2.9828	.7849	9.4448
57.[illegible]	2256.6	653.	9[illegible]5.	1[illegible]	82241.	717.	.49	.49	3.[illegible]753	.7921	9.522
58.[illegible]	2256.4	653.	9[illegible]7.	1[illegible]	73875.	711.	.49	.49	3.1674	.7[illegible]	9.[illegible]37
59.[illegible]	225[illegible].3	653.	9[illegible]8.	1[illegible]	65225.	7[illegible]4.	.5[illegible]	.5[illegible]	3.242[illegible]	.8[illegible]43	9.675
60.[illegible]	225[illegible].1	653.	91[illegible].	1[illegible]	56493.	697.	.5	.5	3.35[illegible]	.8[illegible]92	9.75[illegible]
61.[illegible]	2255.9	653.	911.	1[illegible]	47686.	69[illegible].	.5	.5	3.45[illegible]5	.8134	9.8255
62.[illegible]	2255.7	653.	912.	1[illegible]	38[illegible]48.	68[illegible].	.51	.51	3.5464	.8166	[illegible].[illegible]1[illegible]
63.[illegible]	2255.6	653.	912.	1[illegible]	3[illegible]563.	677.	.51	.51	3.64[illegible]4	.8194	9.9756
64.[illegible]	2255.4	653.	913.	1[illegible]	21[illegible]	67[illegible].	.51	.51	3.7367	.8213	1[illegible].[illegible]518
65.[illegible]	2255.2	653.	913.	1[illegible]	1322[illegible].	663.	.51	.51	3.8312	.8225	1[illegible].1266
66.[illegible]	2255.1	653.	913.	1[illegible]	4844.	657.	.51	.51	3.9267	.8229	1[illegible].2[illegible]13

MASS FLOW =0.2751E 06LB/HR   G =0.847[illegible]E 06LB/HR-SQ FT   PANEL DELTA P= 1[illegible]. PSI   BHP= 6.3HP   ERROR CODE=

HMIN = [illegible] B/HR-SF-F   PANEL EFF = [illegible].934   ABSORBED Q =0.7879E 06BTU/HR   G FACTOR = [illegible].733

INPUT CARD DECK DATA:

NT	62
K1	1
NKASE	1
NCORR	[illegible]
P1	227[illegible].[illegible]
TF1	[illegible]7.[illegible]
H1	627.[illegible]
DO	1.25
DI	[illegible].98
DELL	1.[illegible]
TDESN	[illegible].[illegible]
HIDESN	1[illegible].[illegible]
HEXT	3.
EMIS	.89
ALPS	.95
TO	1[illegible].[illegible]
K	21[illegible].[illegible]
L1	[illegible].[illegible]
L2	37.[illegible]
LT	6[illegible].[illegible]
NPAN	1
KTEST	[illegible]
KRIFLE	1
M	25[illegible].[illegible]
SOLMAX	27[illegible].[illegible]
SLIP	.5

BOILER PANEL NO. 5
(USING THOMPSON-MACBETH CORRELATION)

PRESS PSIA	TEMP F	ENTHALPY BTU/LB	L1 FT	L2 FT*	NO.TUBES	TUBE OD IN	*TUBE ID IN	TUBE LGTH FT	INCREMENT FT
2345.	462.	444.	5.6	37.4	63	1.00	0.73	66.	1.00

PREHEAT PANEL

CONDUCTIVITY B-IN/H-SF-F	EXT.COEFF B/H-SF-F	EMISSIVITY	ABSORPTANCE*	AMB.TEMP F	MAX.SOLAR FLUX BTU/HR-SQFT
325.	3.	.83	.95	1[illegible].	217[illegible].

TUBE LGTH FT	PRESS PSIA	BULK TEMP F	ENTHALPY BTU/LB	INSIDE FILM COEF B/H-SF-F	OUTSIDE HEAT FLUX B/H-SF	TUBE *CROWN TEMP F	BULK QUAL	CRIT QUAL	CUMULATIVE PRESSURE DROP FRICTION PSI	MOMENTUM PSI	GRAVITY PSI
1.0	2344.5	461.	444.	4713.	21516.	499.	-.68	0.0	0.1693	0.0004	0.3524
2.0	2344.[illegible]	461.	445.	4712.	63167.	516.	-.67	0.0	0.3383	0.0011	0.7048
3.0	2343.4	462.	446.	4713.	93626.	533.	-.67	0.0	0.5[illegible]7	0.0021	1.0571
4.0	2342.9	462.	447.	4713.	124783.	551.	-.67	0.0	.6760	0.0033	1.4093
5.0	2342.4	462.	449.	4715.	154681.	568.	-.66	0.0	0.8451	0.0047	1.7613
6.0	2341.9	463.	451.	4716.	186464.	586.	-.66	0.0	1.0142	0.0063	2.1132
7.0	2341.3	464.	453.	4719.	2[illegible]4381.	597.	-.65	0.0	1.1834	0.0081	2.4648
8.0	234[illegible].8	465.	455.	4722.	2[illegible]5476.	598.	-.65	0.0	1.3527	0.0098	2.8159
9.0	234[illegible].3	466.	458.	4724.	2[illegible]4332.	599.	-.64	0.0	1.5220	0.0115	3.1673
10.0	2339.8	467.	45[illegible].	4727.	2[illegible]5287.	60[illegible].	-.63	0.0	1.6915	0.0133	3.5177
11.0	233[illegible].3	468.	462.	473[illegible].	2[illegible]559[illegible].	6[illegible]1.	-.63	0.0	1.8610	0.0151	3.8683
12.0	233[illegible].7	469.	464.	4733.	2.5625.	6[illegible]2.	-.62	0.0	2.[illegible]3[illegible]6	0.0170	4.2180
13.0	233[illegible].2	4[illegible].	464.	4736.	2[illegible]4252.	6[illegible]2.	-.62	0.0	2.2[illegible]3	0.0188	4.5677
14.0	2337.7	4[illegible]1.	469.	4739.	2[illegible]4[illegible]79.	6[illegible]3.	-.61	0.0	2.37[illegible]	0.02[illegible]6	4.9173
15.0	233[illegible].2	4[illegible]2.	471.	4743.	2[illegible]4665.	6[illegible]4.	-.6[illegible]	0.0	2.5399	0.0225	5.2660
16.0	233[illegible].7	493.	473.	4746.	2.5628.	6[illegible]6.	-.6[illegible]	0.0	2.7[illegible]99	0.0244	5.6147
17.0	233[illegible].1	4[illegible]4.	475.	4749.	2.5681.	6[illegible]7.	-.59	0.0	2.88[illegible]	0.0263	5.9630
18.0	233[illegible].6	495.	477.	4753.	2[illegible]565[illegible].	6[illegible]8.	-.59	0.0	3.05[illegible]1	0.0282	6.31[illegible]9
19.0	233[illegible].1	496.	48[illegible].	4756.	2.4742.	6[illegible]8.	-.58	0.0	3.22[illegible]4	0.03[illegible]2	6.6585
20.0	2334.6	497.	482.	47[illegible].	2.5236.	61[illegible].	-.58	0.0	3.39[illegible]8	0.0322	7.[illegible]56
21.0	2334.1	498.	484.	4763.	2[illegible]545[illegible].	611.	-.57	0.0	3.5613	0.0342	7.3524
22.0	233[illegible].5	499.	486.	4767.	2[illegible]5[illegible]18.	612.	-.56	0.0	3.7319	0.0362	7.6988
23.0	233[illegible].	501.	488.	477[illegible].	2[illegible]4[illegible]38.	613.	-.56	0.0	3.9[illegible]26	0.0389	8.0447
24.0	233[illegible].5	503.	491.	4775.	2[illegible]3943.	614.	-.55	0.0	4.0735	0.0425	8.39[illegible]
25.0	233[illegible].	505.	493.	4781.	2[illegible]4917.	615.	-.55	0.0	4.2446	0.0461	8.7346
26.0	233[illegible].5	506.	495.	4786.	2[illegible]4184.	618.	-.54	0.0	4.4160	0.0497	9.0784
27.0	23[illegible].9	508.	497.	4792.	2[illegible]5457.	62[illegible].	-.53	0.0	4.5876	0.0533	9.4216
28.0	23[illegible].4	51[illegible].	499.	4798.	2[illegible]5476.	622.	-.53	0.0	4.7593	0.0570	9.7640
29.0	233[illegible].9	512.	5[illegible]2.	48[illegible]4.	2[illegible]5126.	624.	-.52	0.0	4.9314	0.0607	10.1057
30.0	233[illegible].4	514.	5[illegible]4.	48[illegible]9.	2[illegible]4881.	626.	-.52	0.0	5.1[illegible]36	0.0645	10.4467
31.0	23[illegible].9	516.	5[illegible]6.	481[illegible].	2[illegible]5643.	628.	-.51	0.0	5.2761	0.0682	10.7870
32.0	23[illegible].4	518.	5[illegible]8.	482[illegible].	2[illegible]4229.	629.	-.51	0.0	5.4488	0.0721	11.1265
33.0	2327.8	52[illegible].	51[illegible].	4826.	2[illegible]4682.	631.	-.5[illegible]	0.0	5.6218	0.0757	11.4653
34.0	2327.3	522.	513.	4831.	2[illegible]5523.	633.	-.49	0.0	5.7959	0.0797	11.8034
35.0	23[illegible].8	523.	515.	4837.	2.4985.	635.	-.49	0.0	5.9684	0.0837	12.14[illegible]8
36.0	23[illegible].3	525.	517.	4842.	2[illegible]4463.	636.	-.48	0.0	6.1422	0.0877	12.4773
37.0	23[illegible].8	527.	519.	4849.	2[illegible]4517.	638.	-.48	0.0	6.3162	0.0917	12.8132
38.0	23[illegible].3	[illegible]	521.	4853.	2[illegible]447.	638.	-.47	0.0	6.49[illegible]4	0.0956	13.1482
39.0	2324.[illegible]	531.	523.	4858.	19[illegible].	636.	-.47	0.0	6.6649	0.0994	13.4826
40.0	23[illegible].2	532.	525.	4863.	185811.	633.	-.46	0.0	6.8397	0.1032	13.8163
41.0	23[illegible].7	534.	527.	4868.	179334.	631.	-.46	0.0	7.0147	0.1[illegible]68	14.1492
42.0	23[illegible].2	535.	529.	4873.	172[illegible]18.	629.	-.45	0.0	7.1899	0.11[illegible]2	14.4816
43.0	23[illegible].7	537.	531.	4877.	165267.	626.	-.45	0.0	7.3654	0.1135	14.8133
44.0	23[illegible].2	538.	533.	4881.	1[illegible]8922.	624.	-.44	0.0	7.5411	0.1167	15.1444
45.0	23[illegible].7	54[illegible].	534.	4885.	15[illegible]562.	621.	-.44	0.0	7.7179	0.1197	15.4750
46.0	23[illegible].2	541.	536.	48[illegible].	144266.	619.	-.43	0.0	7.8931	0.1227	15.8050
47.0	23[illegible].7	542.	537.	4893.	13776[illegible].	617.	-.43	0.0	8.0694	0.1257	16.1344
48.0	[illegible]	543.	539.	489[illegible].	13[illegible].	614.	-.43	0.0	8.2459	0.1284	16.4634

B-4

B-3

[illegible]	[illegible]	[illegible]	[illegible]	[illegible]	[illegible]	[illegible]	-.4[illegible]	[illegible]	[illegible]	[illegible]	[illegible]
47.	[illegible]	[illegible]	537.	[illegible]	13776.	617.	-.43	[illegible]	8.[illegible]54	.1257	16.1344
48.	[illegible]	543.	539.	[illegible]	[illegible]	614.	-.43	[illegible]	8.2459	.1284	16.4634
49.	231[illegible].7	544.	54[illegible].	49[illegible].	1[illegible]3595.	611.	-.42	[illegible]	8.4226	.1311	16.7916
5[illegible].	231[illegible].1	545.	541.	49[illegible]3.	1[illegible]43[illegible]1.	[illegible]8.	-.42	[illegible]	8.5995	.1335	17.1198
51.	231[illegible].6	546.	542.	49[illegible]6.	1[illegible]5119.	6[illegible]5.	-.42	[illegible]	8.7765	.1358	17.4474
52.	231[illegible].1	547.	544.	49[illegible]8.	1[illegible]1563.	6[illegible]2.	-.41	[illegible]	8.9537	.1380	17.7746
53.	[illegible]17.6	548.	545.	4911.	[illegible]5909.	6[illegible].	-.41	[illegible]	9.1311	.14[illegible]	18.1[illegible]14
54.	2317.1	549.	546.	4913.	[illegible]9[illegible]82.	597.	-.41	[illegible]	9.3[illegible]85	.1419	18.4279
55.	231[illegible].6	5[illegible].	546.	4916.	8189.	594.	-.4[illegible]	[illegible]	9.4861	.1437	18.754[illegible]
56.	231[illegible].1	55[illegible].	547.	491[illegible].	7441.	59[illegible].	-.4[illegible]	[illegible]	9.6639	.1453	19.[illegible]796
57.	231[illegible].6	551.	548.	49[illegible].	[illegible]7123.	587.	-.4[illegible]	[illegible]	9.8417	.1468	19.4[illegible]54
58.	231[illegible].1	551.	549.	4921.	61195.	584.	-.4	[illegible]	1[illegible].0196	.1482	19.73[illegible]7
59.	231[illegible].6	552.	549.	4923.	53486.	581.	-.4[illegible]	[illegible]	1[illegible].1977	.1494	2[illegible].[illegible]558
6[illegible].	231[illegible].1	552.	55[illegible].	4924.	47127.	578.	-.4[illegible]	[illegible]	1[illegible].3758	.15[illegible]5	2[illegible].38[illegible]6
61.	231[illegible].6	552.	55[illegible].	4925.	[illegible]9391.	574.	-.39	[illegible]	1[illegible].554[illegible]	.1514	2[illegible].7[illegible]53
62.	231[illegible].1	553.	55[illegible].	4926.	[illegible]2458.	57[illegible].	-.39	[illegible]	1[illegible].7322	.1521	21.[illegible]299
63.	231[illegible].6	553.	551.	4927.	25232.	567.	-.39	[illegible]	1[illegible].91[illegible]5	.1527	21.3543
64.	231[illegible].1	553.	551.	4928.	19[illegible]45.	563.	-.39	[illegible]	11.[illegible]889	.1531	21.6787
65.	2311.6	553.	551.	4928.	[illegible]2[illegible]2.	56[illegible].	-.39	[illegible]	11.2673	.1534	22.[illegible]29
66.	231[illegible].1	553.	551.	4929.	5325.	556.	-.39	[illegible]	11.4456	.1535	22.3272

MASS FLOW =[illegible].6444E [illegible]ELB/HR G =[illegible].22[illegible]E [illegible]7LB/HR-SQ FT PANEL DELTA P= 33.9PSI BHP= 36.8HP ERROR CODE= 0

HMIN = [illegible].9 B/HR-SF-F PANEL EFF = [illegible].95 ABSORBED Q =[illegible].65[illegible]4E 08BTU/HR Q FACTOR = 0.733

INPUT CARD DECK DATA:

NT	83
KI	1
NPHASE	[illegible]
NCORR	1
PI	234[illegible].
TF1	462.
HI	444.
D[illegible]	1.
DI	.79
DCLL	1.
TDESN	[illegible]53.
HIDESN	1[illegible].
HEXT	3.
EMIS	.[illegible]9
ALPS	.95
T[illegible]	1[illegible].
K	32[illegible].
L1	[illegible].6
L2	37.4
LT	66.
NPAN	[illegible]
KTEST	[illegible]
KRIFLE	[illegible]
M	5[illegible].
SOLMAX	217[illegible].
GLIM	.

BOILER PANEL NO. 7
(USING THOMPSON-MACBETH CORRELATION)

SUPERHEATER PANEL

PRESS PSIA	TEMP F	ENTHALPY BTU/LB	L1 FT	L2 FT*	NO.TUBES	TUBE OD IN	*TUBE ID IN	TUBE LGTH FT	INCREMENT FT
2150.	699.	1222.	6.6	37.4	150	0.50	0.39	66.	1.00

CONDUCTIVITY B-IN/H-SF-F	EXT.COEFF B/H-SF-F	EMISSIVITY *	ABSORPTANCE	*AMB.TEMP F	MAX.SOLAR FLUX BTU/HR-SQFT
160.	3.	0.89	0.95	100.	161000.

TUBE LGTH FT	PRESS PSIA	BULK TEMP F	ENTHALPY BTU/LB	INSIDE FILM COEF B/H-SF-F	OUTSIDE HEAT FLUX B/H-SF	TUBE *CROWN TEMP F	BULK QUAL	CRIT QUAL	CUMULATIVE PRESSURE DROP FRICTION PSI	MOMENTUM PSI	GRAVITY PSI
1.00	2149.1	699.	1223.	1772.	19633.	717.	1.22	0.0	0.8900	0.0088	0.0314
2.00	2148.1	701.	1225.	1766.	42310.	739.	1.23	0.0	1.7836	0.0288	0.0627
3.00	2147.2	703.	1228.	1753.	65248.	762.	1.23	0.0	2.6835	0.0603	0.0938
4.00	2146.2	706.	1232.	1734.	88402.	786.	1.24	0.0	3.5918	0.1054	0.1246
5.00	2145.2	710.	1237.	1711.	111869.	811.	1.25	0.0	4.5110	0.1635	0.1550
6.00	2144.1	715.	1243.	1681.	133849.	838.	1.27	0.0	5.4435	0.2334	0.1850
7.00	2143.1	720.	1250.	1647.	147340.	858.	1.28	0.0	6.3924	0.3107	0.2146
8.00	2142.0	726.	1257.	1611.	147240.	865.	1.30	0.0	7.3576	0.3853	0.2436
9.00	2140.9	732.	1263.	1578.	147115.	872.	1.31	0.0	8.3393	0.4628	0.2722
10.00	2139.8	739.	1270.	1548.	146673.	880.	1.33	0.0	9.3376	0.5402	0.3003
11.00	2138.7	745.	1277.	1519.	146488.	888.	1.34	0.0	10.3529	0.6164	0.3280
12.00	2137.6	752.	1283.	1493.	146592.	896.	1.36	0.0	11.3851	0.6943	0.3553
13.00	2136.4	759.	1290.	1468.	146435.	904.	1.37	0.0	12.4344	0.7724	0.3821
14.00	2135.2	766.	1297.	1445.	146134.	912.	1.39	0.0	13.5011	0.8495	0.4085
15.00	2134.1	773.	1303.	1424.	146138.	920.	1.40	0.0	14.5850	0.9279	0.4345
16.00	2132.8	780.	1310.	1405.	145876.	928.	1.41	0.0	15.6864	1.0062	0.4601
17.00	2131.6	788.	1317.	1386.	145716.	937.	1.43	0.0	16.8055	1.0837	0.4853
18.00	2130.4	795.	1323.	1370.	145463.	945.	1.44	0.0	17.9422	1.1622	0.5102
19.00	2129.1	803.	1330.	1354.	145445.	954.	1.46	0.0	19.0966	1.2409	0.5347
20.00	2127.9	811.	1337.	1340.	145254.	963.	1.47	0.0	20.2695	1.3196	0.5589
21.00	2126.6	819.	1343.	1327.	144898.	971.	1.49	0.0	21.4594	1.3982	0.5827
22.00	2125.2	828.	1350.	1315.	144833.	980.	1.50	0.0	22.6678	1.4765	0.6062
23.00	2123.9	836.	1357.	1304.	144720.	989.	1.52	0.0	23.8945	1.5552	0.6294
24.00	2122.6	845.	1363.	1294.	144371.	998.	1.53	0.0	25.1393	1.6337	0.6523
25.00	2121.2	853.	1370.	1284.	144310.	1007.	1.55	0.0	26.4025	1.7124	0.6748
26.00	2119.8	862.	1376.	1275.	144025.	1016.	1.56	0.0	27.6840	1.7910	0.6971
27.00	2118.4	871.	1383.	1268.	143779.	1025.	1.57	0.0	28.9841	1.8694	0.7193
28.00	2117.0	880.	1389.	1260.	143612.	1035.	1.59	0.0	30.3026	1.9479	0.7407
29.00	2115.6	889.	1396.	1254.	143297.	1044.	1.60	0.0	31.6398	2.0259	0.7621
30.00	2114.1	898.	1403.	1248.	143033.	1053.	1.62	0.0	32.9955	2.1040	0.7633
31.00	2112.6	908.	1409.	1242.	142760.	1063.	1.63	0.0	34.3699	2.1816	0.8042
32.00	2111.2	917.	1416.	1237.	142667.	1072.	1.64	0.0	35.7631	2.2593	0.8248
33.00	2109.6	927.	1422.	1233.	142345.	1082.	1.66	0.0	37.1750	2.3370	0.8452
34.00	2108.1	936.	1429.	1229.	142181.	1091.	1.67	0.0	38.6058	2.4145	0.8653
35.00	2106.6	946.	1435.	1225.	141867.	1101.	1.69	0.0	40.0553	2.4920	0.8852
36.00	2105.0	955.	1442.	1222.	141570.	1110.	1.70	0.0	41.5238	2.5691	0.9049
37.00	2103.4	965.	1448.	1219.	141363.	1120.	1.71	0.0	43.0112	2.6458	0.9243
38.00	2101.8	975.	1454.	1217.	137999.	1126.	1.73	0.0	44.5172	2.7207	0.9436
39.00	2100.2	984.	1460.	1215.	132807.	1130.	1.74	0.0	46.0415	2.7929	0.9626
40.00	2098.6	993.	1466.	1213.	127403.	1133.	1.75	0.0	47.5834	2.8623	0.9814
41.00	2096.9	1001.	1472.	1212.	122182.	1136.	1.76	0.0	49.1424	2.9287	1.0000
42.00	2095.3	1010.	1477.	1211.	116981.	1138.	1.77	0.0	50.7178	2.9917	1.0185
43.00	2093.6	1018.	1482.	1210.	111684.	1140.	1.78	0.0	52.3091	3.0518	1.0368
44.00	2091.9	1025.	1487.	1210.	106420.	1142.	1.79	0.0	53.9155	3.1092	1.0550
45.00	2090.2	1033.	1492.	1209.	101128.	1144.	1.80	0.0	55.5365	3.1638	1.0730

43.	[illegible]	[illegible]	1482.	121[illegible].	111684.	114[illegible].	1.78	0.0	52.3[illegible]91	3.0518	1.0368
44.00	2091.9	1025.	1487.	1210.	106420.	1142.	1.79	0.0	53.9155	3.1092	1.0559
45.00	2090.2	1033.	1492.	1209.	101128.	1144.	1.80	0.0	55.5365	3.1638	1.0730
46.00	2088.5	1039.	1496.	1209.	95972.	1145.	1.81	0.0	57.1715	3.2155	1.0908
47.00	2086.8	1046.	1500.	1209.	90583.	1146.	1.82	0.0	58.8197	3.2644	1.1086
48.00	2085.1	1052.	1504.	1209.	85467.	1146.	1.83	0.0	60.4897	3.3104	1.1262
49.00	2083.3	1058.	1508.	1208.	80158.	1146.	1.84	0.0	62.1536	3.3531	1.1437
50.00	2081.6	1063.	1511.	1209.	75205.	1146.	1.84	0.0	63.8378	3.3932	1.1611
51.00	2079.9	1068.	1514.	1209.	69766.	1145.	1.85	0.0	65.5327	3.4304	1.1783
52.00	2078.1	1073.	1517.	1209.	64683.	1144.	1.85	0.0	67.2377	3.4649	1.1955
53.00	2076.3	1077.	1520.	1209.	59615.	1143.	1.86	0.0	68.9521	3.4967	1.2127
54.00	2074.6	1081.	1523.	1209.	54285.	1141.	1.86	0.0	70.6753	3.5257	1.2297
55.00	2072.8	1085.	1525.	1209.	49179.	1139.	1.87	0.0	72.4066	3.5519	1.2467
56.00	2071.0	1088.	1527.	1209.	44130.	1136.	1.87	0.0	74.1454	3.5754	1.2636
57.00	2069.2	1091.	1529.	1209.	38954.	1134.	1.88	0.0	75.8911	3.5962	1.2804
58.00	2067.4	1093.	1530.	1209.	33955.	1131.	1.88	0.0	77.6429	3.6142	1.2972
59.00	2065.7	1095.	1532.	1209.	28716.	1127.	1.88	0.0	79.4[illegible]73	3.6295	1.3139
60.00	2063.9	1097.	1533.	1210.	23717.	1123.	1.88	0.0	81.1625	3.6420	1.3306
61.00	2062.1	1098.	1533.	1210.	16611.	1119.	1.88	0.0	82.9296	3.6518	1.3473
62.00	2060.3	1099.	1534.	1209.	13478.	1114.	1.88	0.0	84.6991	3.6587	1.3639
63.00	2058.5	1100.	1534.	1209.	8538.	1109.	1.88	0.0	86.4721	3.6629	1.3805
64.00	2056.7	1100.	1535.	1209.	3491.	1104.	1.88	0.0	88.2474	3.6642	1.3971
65.00	2054.9	1100.	1535.	1209.	-1724.	1098.	1.88	0.0	90.0242	3.6628	1.4136
66.00	2053.1	1099.	1534.	1209.	-6824.	1092.	1.88	0.0	91.8020	3.6586	1.4302

MASS FLOW =0.1367E 06LB/HR   G =0.1099E 07LB/HR-SQ FT   PANEL DELTA P= 96.9PSI   BHP= 250.1HP   ERROR CODE= 0

HMIN = 0.0 B/HR-SF-F   PANEL EFF = 0.877   ABSORBED Q =0.4269E 08BTU/HR   Q FACTOR = 0.733

INPUT CARD DECK DATA:

NT	150
K1	1
NKASE	1
NCORR	1
P1	2150.00
TF1	699.00
H1	1222.00
DO	0.50
DI	0.39
DELL	1.00
TDESN	1100.00
HIDESN	10[illegible]0.00
HEXT	3.00
EMIS	0.89
ALPS	0.95
TO	100.00
K	160.00
L1	6.60
L2	37.40
LT	66.00
NPAN	7
KTEST	0
KRIFLE	0
M	140000.00
SOLMAX	161000.00
QLIM	0.0

APPENDIX C

DERIVATION OF GENERALIZED PRESSURE DROP EQUATION:

The single phase frictional pressure drop through a single tube can be expressed by the Darcy-Weisbach equation as:

$$\Delta P = f\left(\frac{L}{d_i}\right) \rho \frac{V^2}{2g} \qquad (1)$$

$$\Delta P = \frac{16f}{\pi^2} \left(\frac{L}{d_i}\right) \frac{\dot{m}^2}{d_i^4} \times \frac{1}{2g\rho} \qquad (2)$$

The mass flow rate through any tube in a receiver panel can be derived from any energy balance on the tube:

$$\dot{m}\Delta h = \eta I A_t = \eta I \, (d_o L) \qquad (3)$$

Therefore,

$$\dot{m} = \frac{\eta I d_o L}{\Delta h} \qquad (4)$$

Substituting Equation 4 into Equation 2 and rearranging yields:

$$\Delta P = \frac{16f\eta^2}{\pi^2} \left(\frac{L}{d_i}\right)^3 \left(\frac{d_o}{d_i}\right)^2 \left(\frac{I}{\Delta h}\right)^2 \times \frac{1}{2g\rho} \qquad (5)$$

By defining the receiver aspect ratio R = L/D, Equation 5 can equivalently be expressed as:

$$\Delta P = \frac{16f\eta^2}{\pi^2} \left(\frac{D}{d_i}\right)^3 \left(\frac{d_o}{d_i}\right)^2 \left(\frac{I}{\Delta h}\right)^2 \times \frac{R^3}{2g\rho} \qquad (6)$$

An energy balance on the receiver can be used to relate the receiver dimensions to the thermal output of the receiver:

$$Q = \bar{\eta}\cdot\bar{I}\cdot A = \bar{\eta}\cdot\bar{I}\cdot A = \bar{\eta}\cdot\bar{I}\cdot\pi\cdot R\cdot D^2 \qquad (7)$$

Defining $\alpha = \bar{I}/I$ and rearranging Equation 7 to solve for I:

$$I = \frac{Q}{\alpha \bar{\eta} \pi R D^2} \tag{8}$$

Equation 8 relates the thermal output of the receiver and the receiver dimensions (R and D) to the local incident flux on any tube. Equation 8 can be substituted into Equation 6 to yield:

$$\Delta P = \frac{16f}{\alpha^2 \pi^4} \left(\frac{\eta}{\bar{\eta}}\right)^2 \left(\frac{d_o}{d_i}\right)^2 \left(\frac{D}{d_i}\right)^3 \left(\frac{L}{D}\right) \left(\frac{Q}{\Delta h D^2}\right)^2 \times \frac{1}{2g\rho} \tag{9}$$

Equation 9 can be expressed in non-dimensional form as:

$$\Delta P \times 2g\rho \left(\frac{\Delta h D^2}{Q}\right)^2 = \frac{16f}{\alpha^2 \pi^4} \left(\frac{\eta}{\bar{\eta}}\right)^2 \left(\frac{d_o}{d_i}\right)^2 \left(\frac{D}{d_i}\right)^3 \left(\frac{L}{D}\right) \tag{10}$$

Equations 9 and 10 can be used to calculate the frictional pressure drop through any tube in the receiver based on the local flux (α) and the design thermal output and physical configuration of the receiver.

NOMENCLATURE

Variable	Definition
α	Ratio of average flux to local flux ($\bar{I}/I$)
A	Overall receiver surface area.
A_t	Nominal surface area of single tube
d_i	Tube inner diameter
d_o	Tube outer diameter
D	Receiver diameter
f	Moody friction factor
g	Gravitational constant
Δh	Enthalpy rise of fluid through the receiver
I	Local flux on tube
$\bar{I}$	Average flux on the receiver
L	Receiver or tube length
$\dot{m}$	Mass flow through single tube
η	Local absorption efficiency on tube.
$\bar{\eta}$	Average absorption efficiency on the receiver
Q	Overall thermal output of receiver
ρ	Average fluid density in tube.
R	Receiver aspect ratio (L/D)
V	Fluid velocity in single tube.

APPENDIX D

RECEIVER CIRCULATION PUMP SELECTIONS

GENERAL - A

Proposal Reference: 9014-2228

Project: Solar Boiler BCP's

Concept A

Date: January 9, 1989

Number of Pumps Required per Boiler: 2

Number of Boilers: 1

Pump Type: Boiler Circulating Pump

Motor Type: 7/4 6V 110-416

SPECIFICATION REQUIREMENTS - B

Fluid Handled: Boiler Water at Specific Gravity: --				
Design Pressure:		MPa	--	PSIG
Fluid Temperature:		C	651	F
Pump Inlet Pressure:		MPa	2876	PSIG
Hydrotest Pressure:		MPa	--	PSIG
NPSHA:		m	2410	ft.
Inlet Pipe Diameter O.D.:		mm	--	in.
Outlet Pipe Diameter O.D.:		mm	--	in.

Voltage/Phase/Frequency: -- Volts 3 Phase 60 Hz

D-2

D-1

PUMP DATA - C

SINGLE PUMP PERFORMANCE

	Two Pumps Operating				One Pump Operating			
Flowrate:	2191	m^3/h	9640	GPM		m^3/h		GPM
Total head:	154.8	m	508	Feet		m		Feet
NPSH Required:	17.7	m	58	Feet		m		Feet
Power Shaft - Hot:	--	HP				HP		
Power Shaft - Cold:	1545	HP				HP		
Design Pressure:	21.6	MPa	3130	psi				
Design Temperature:	374	C	705	F				
Hydrotest Pressure:	32.3	MPa	4690	psi				

MOTOR DATA - D

Motor Design: 4 pole, wet squirrel cage, 60 Hertz

Service Factor: 1.15

Starting Current: 960 A

Speed: ☒ 1760 rpm

☐ 1170 rpm

	RATED	Maximum Power Required % of Rated
Power Output	1500 HP	115
Current	208 A	
Voltage	4160 Volts	

CE-KSB PUMP CO. INC.
NEWINGTON, N.H. 03801

PROPOSAL DATA SHEET
BOILER CIRCULATING PUMP

BCP-023-79A

Proposal Reference: BCP-023-79A
Project: Solar BCP Selection

*DIMENSIONS NOT TO BE USED FOR CONSTRUCTION PURPOSES

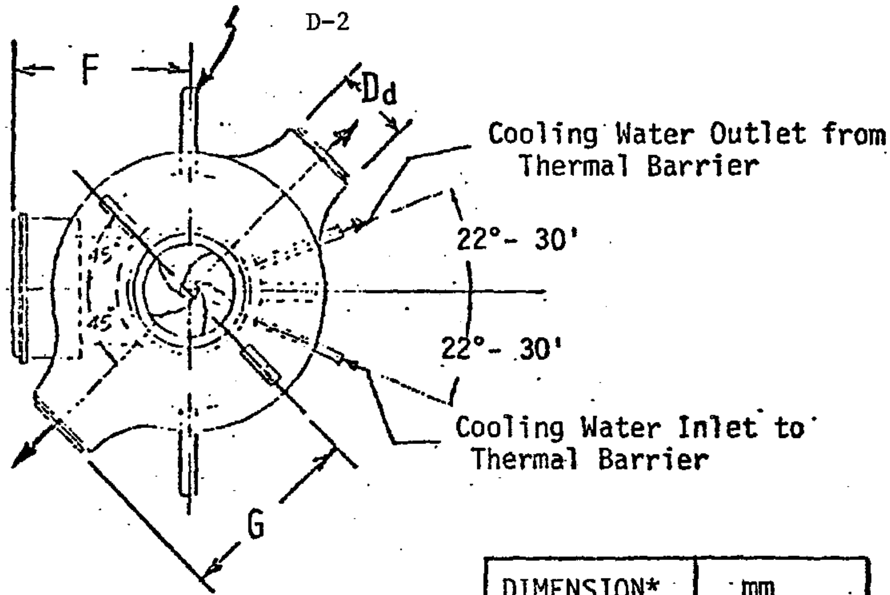

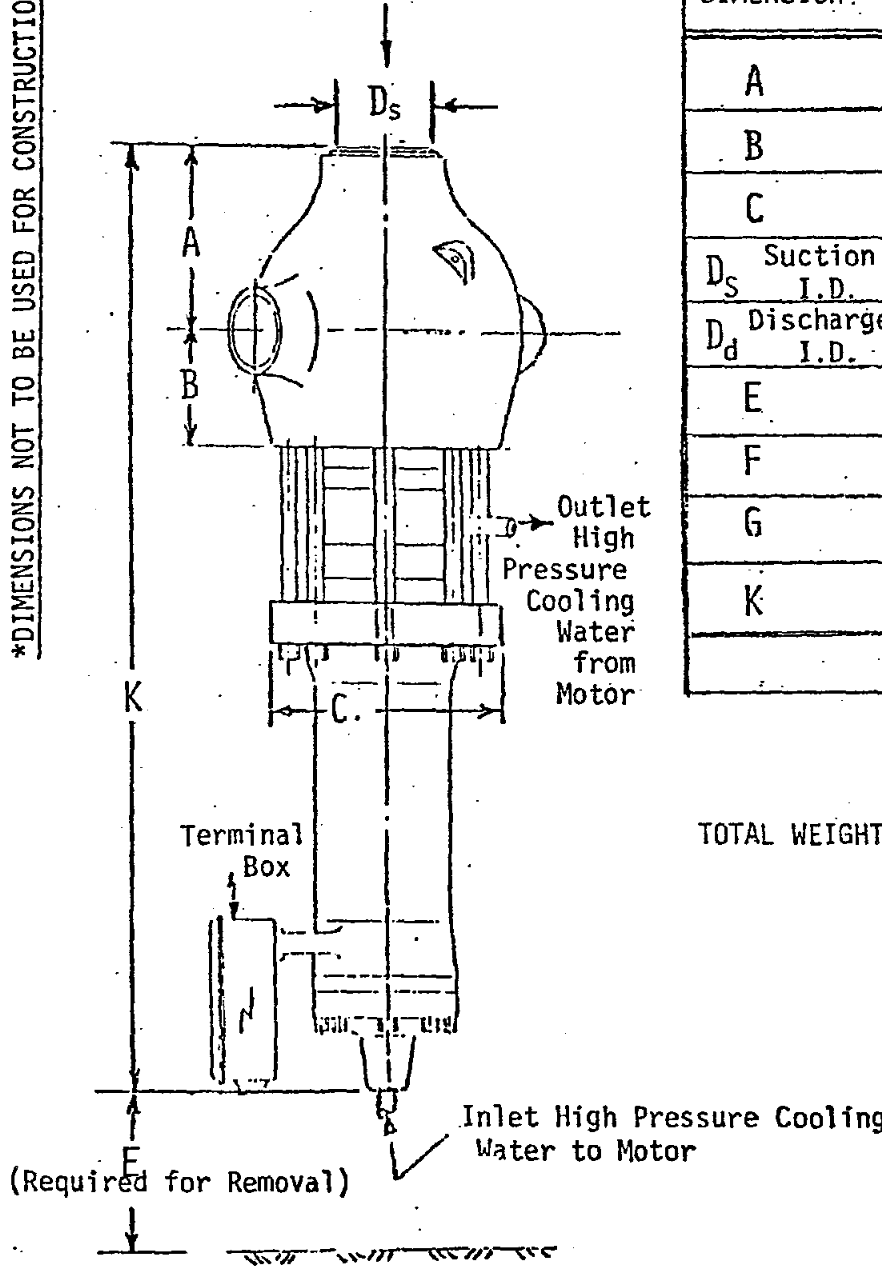

DIMENSION*	mm
A	950
B	530
C	1300
D_s Suction I.D.	500
D_d Discharge I.D.	350
E	2200
F	920
G	1000
K	4910

TOTAL WEIGHT = 27,500 LB.

PROPOSAL DATA SHEET
BOILER CIRCULATING PUMP

CE-KSB PUMP CO. INC.
NEWINGTON, N.H. 03801

BCP-023-79A

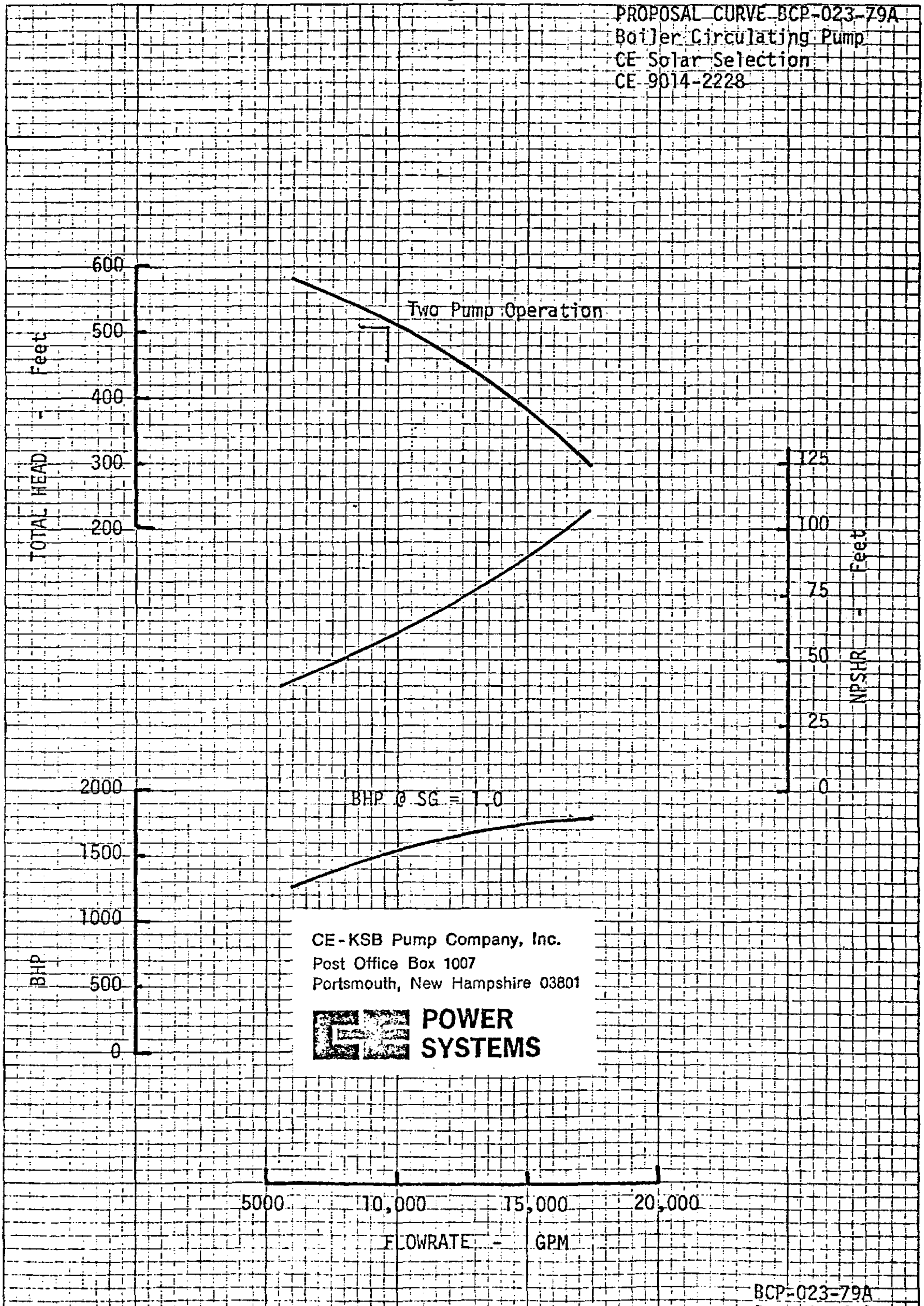

PROPOSAL CURVE BCP-023-79A
Boiler Circulating Pump
CE Solar Selection
CE 9014-2228
Two Pump Operation
TOTAL HEAD - Feet
600
500
400
300
200
125
100
75
50
25
0
NPSHR - Feet
BHP @ SG = 1.0
2000
1500
1000
500
0
BHP
CE-KSB Pump Company, Inc.
Post Office Box 1007
Portsmouth, New Hampshire 03801
POWER
SYSTEMS
5000
10,000
15,000
20,000
FLOWRATE - GPM

GENERAL - A

Proposal Reference: 9014-2228

Project: Solar Boiler BCP's Concept B

Date: January 10, 1980

Number of Pumps Required per Boiler: 2

Number of Boilers: 1

Pump Type: Boiler Circulating Pump

Motor Type: 6/4 FQ-50-416

SPECIFICATION REQUIREMENTS - B

Fluid Handled: Boiler Water at Specific Gravity: ---

Design Pressure:		MPa	---	PSIG
Fluid Temperature:		C	651	F
Pump Inlet Pressure:		MPa	2867	PSIG
Hydrotest Pressure:		MPa	---	PSIG
NPSHA:		m	2380	ft.
Inlet Pipe Diameter O.D.:		mm	---	in.
Outlet Pipe Diameter O.D.:		mm	---	in.

Voltage/Phase/Frequency: -- Volts 3 Phase 60 Hz

PUMP DATA - C

SINGLE PUMP PERFORMANCE

	Two Pumps Operating				One Pump Operating			
Flowrate:	1460	m^3/h	6425	GPM		m^3/h		GPM
Total head:	95.1	m	312	Feet		m		Feet
NPSH Required:	16.2	m	53	Feet		m		Feet
Power Shaft - Hot:	--	HP				HP		
Power Shaft - Cold:	625	HP				HP		
Design Pressure:	21.6	MPa	3130	psi				
Design Temperature:	374	C	705	F				
Hydrotest Pressure:	32.3	MPa	4690	psi				

MOTOR DATA - D

Motor Design: 4 pole, wet squirrel cage, 60 Hertz

Service Factor: 1.15

Starting Current: 539 A

Speed: [x] 1760 rpm

[ ] 1170 rpm

	RATED	Maximum Power Required % of Rated
Power Output	670 HP	115
Current	98 A	
Voltage	4160 Volts	

D-4

5-Q

CE-KSB PUMP CO. INC.
NEWINGTON, N.H. 03801

PROPOSAL DATA SHEET
BOILER CIRCULATING PUMP

BCP-023-79B

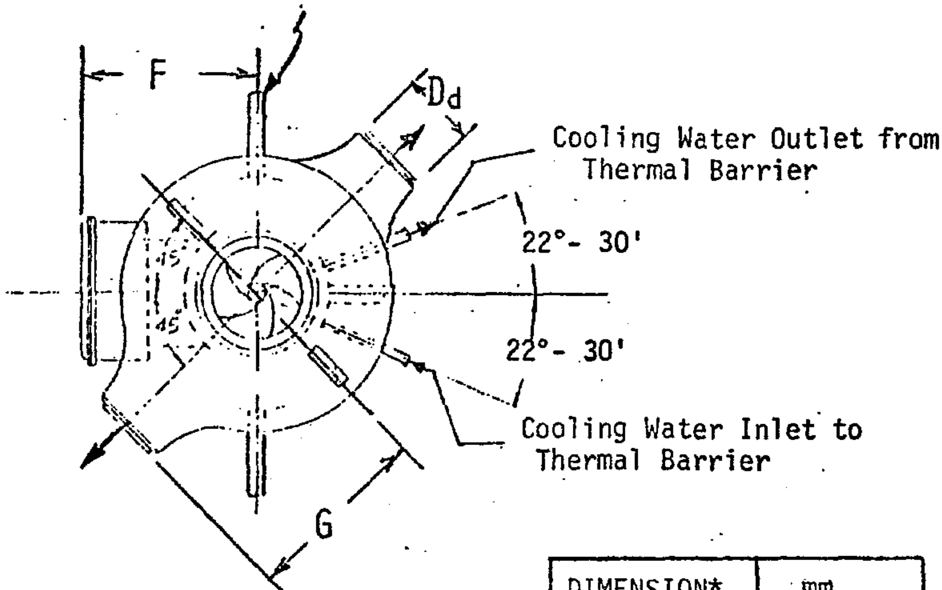

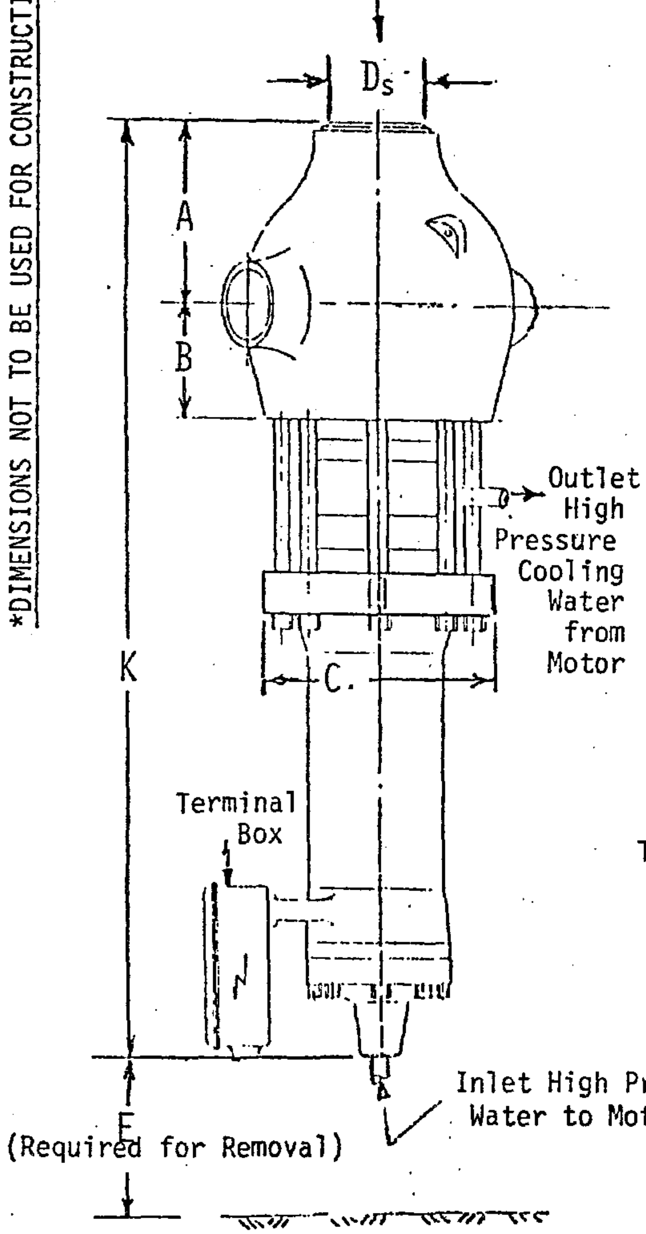

DIMENSION*	mm
A	900
B	530
C	1200
D_S Suction I.D.	500
D_d Discharge I.D.	300
E	1900
F	920
G	950
K	4310

TOTAL WEIGHT = 26,400 LB

Proposal Reference: BCP-023-79B
Project: Solar BCP Selection

*DIMENSIONS NOT TO BE USED FOR CONSTRUCTION PURPOSES

PROPOSAL DATA SHEET
BOILER CIRCULATING PUMP

CE–KSB PUMP CO. INC.
NEWINGTON, N.H. 03801

PROPOSAL CURVE BCP-023-79B
Boiler Circulating Pumps
CE Soalr Selection
CE 9014-2228

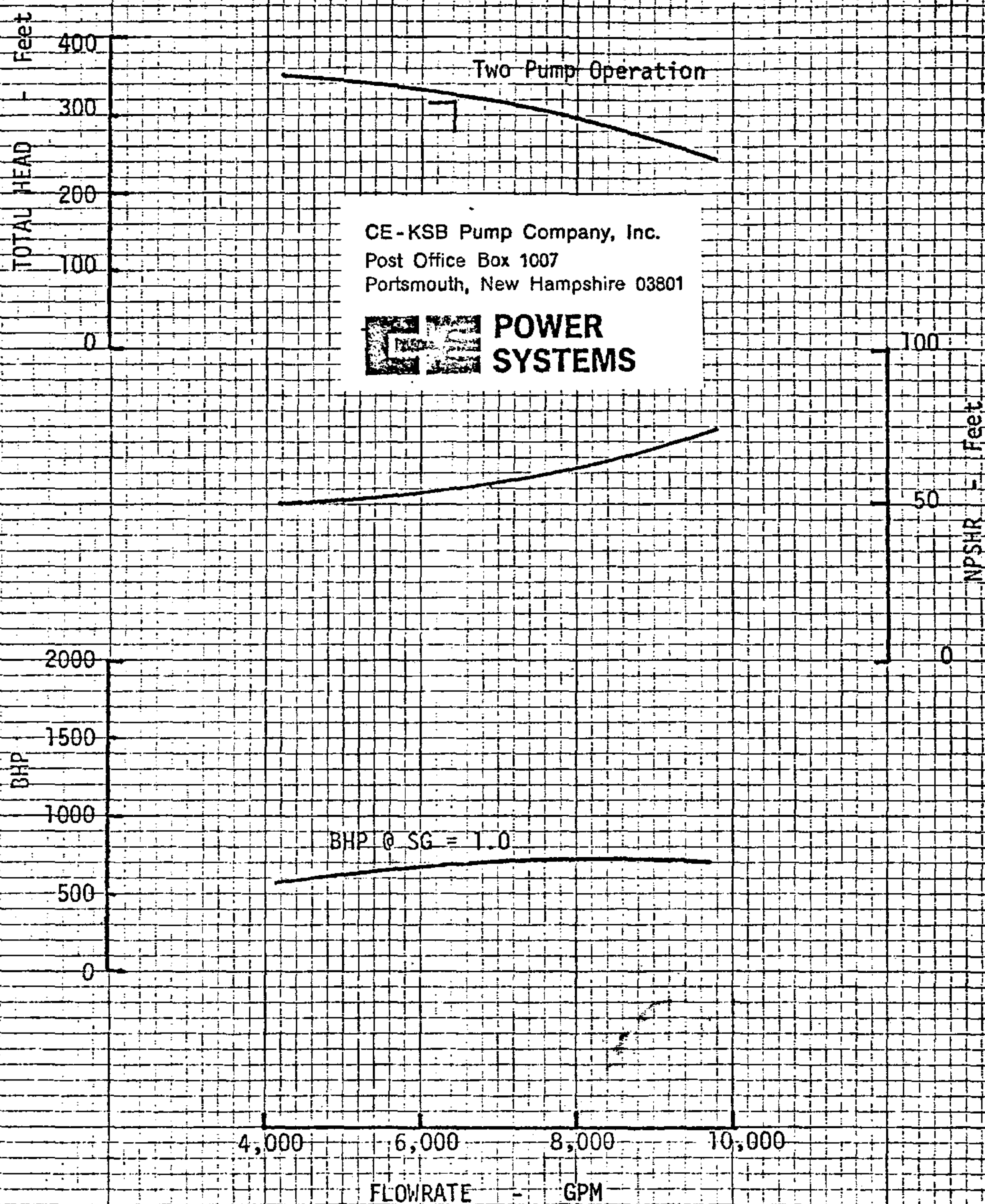

D-8

D-7

GENERAL - A

Proposal Reference: 9014-2228

Date: January 10,1980

Project: Solar Boiler BCP's

Concept C

Number of Pumps Required per Boiler: 2

Number of Boilers: 1

Pump Type: Boiler Circulating Pump

Motor Type: 5/4 EQ25-416

SPECIFICATION REQUIREMENTS - B

Fluid Handled: Boiler Water at Specific Gravity: ---

Design Pressure:		MPa	--	PSIG
Fluid Temperature:		C	610	F
Pump Inlet Pressure:		MPa	2268	PSIG
Hydrotest Pressure:		MPa	--	PSIG
NPSHA:		m	2060	ft.
Inlet Pipe Diameter O.D.:		mm	--	in.
Outlet Pipe Diameter O.D.:		mm	--	in.

Voltage/Phase/Frequency: -- Volts 3 Phase 60 Hz

PUMP DATA - C

SINGLE PUMP PERFORMANCE

	Two Pumps Operating				One Pump Operating			
Flowrate:	1359	m^3/h	5980	GPM		m^3/h		GPM
Total Head:	47	m	155	Feet		m		Feet
NPSH Required:	16.2	m	53	Feet		m		Feet
Power Shaft - Hot:	--	HP				HP		
Power Shaft - Cold:	290	HP				HP		
Design Pressure:	21.6	MPa	3130	psi				
Design Temperature:	374	C	705	F				
Hydrotest Pressure:	32.3	MPa	4690	psi				

MOTOR DATA - D

Motor Design: 4 pole, wet squirrel cage, 60 Hertz

Service Factor: 1.15

Starting Current: 285 A

Speed: ☒ 1760 rpm

☐ 1170 rpm

	RATED	
Power Output	335	HP
Current	50	A
Voltage	4160	Volts

Maximum Power Required

% of Rated

115

CE-KSB PUMP CO. INC.
NEWINGTON, N.H. 03801

PROPOSAL DATA SHEET
BOILER CIRCULATING PUMP

BCP-023-79C

Proposal Reference: BCP-023-79C
Project: Solar BCP Selection

*DIMENSIONS NOT TO BE USED FOR CONSTRUCTION PURPOSES

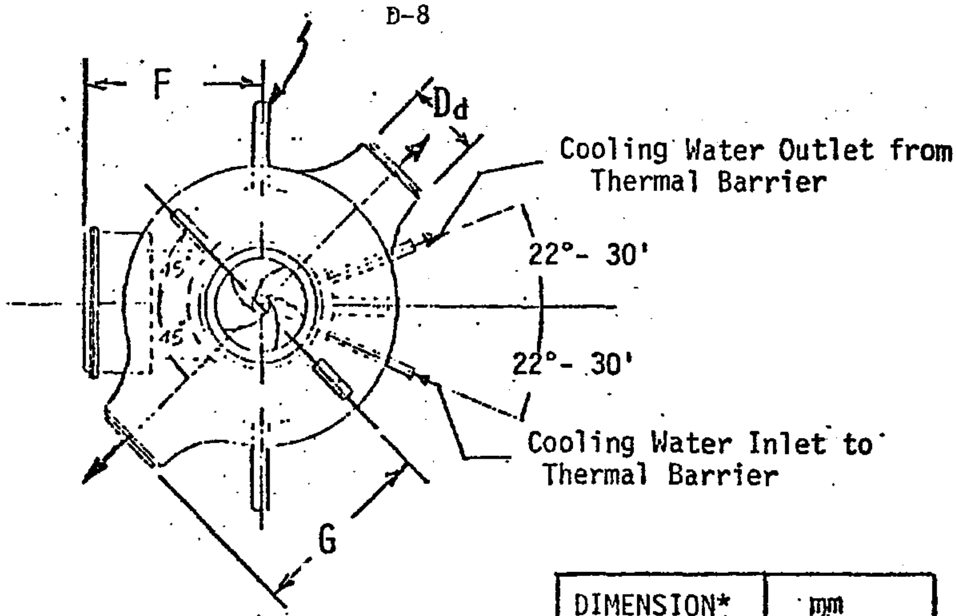

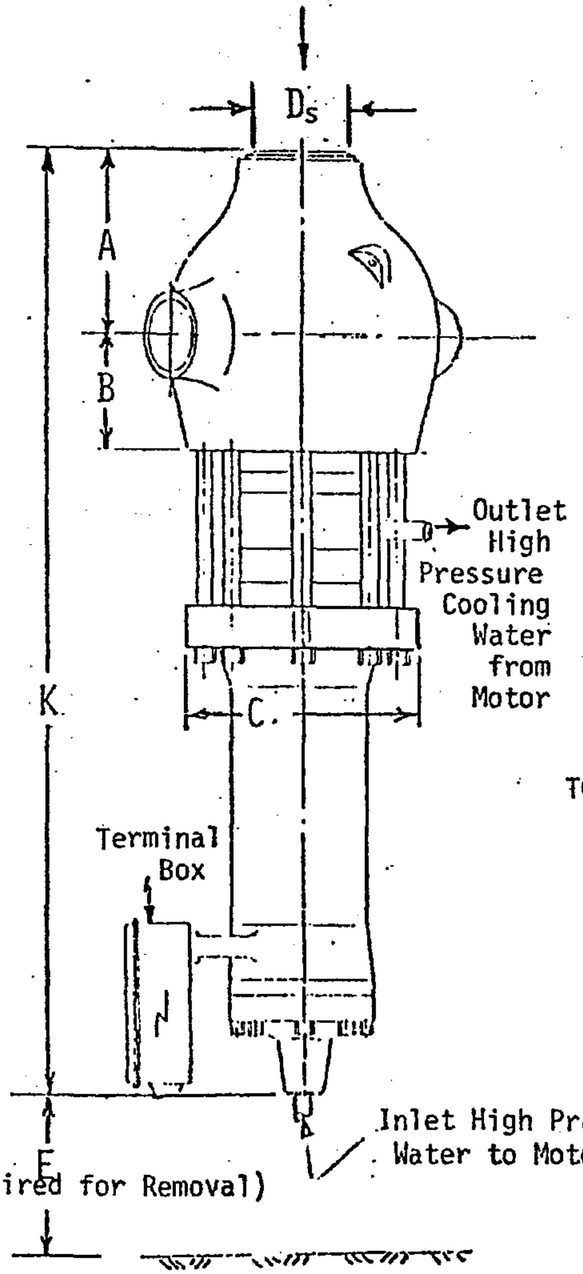

DIMENSION*	mm
A	850
B	510
C	1100
D_s Suction I.D.	450
D_d Discharge I.D.	300
E	1900
F	920
G	900
K	4240

TOTAL WEIGHT = 25,900 LB

PROPOSAL DATA SHEET
BOILER CIRCULATING PUMP

CE-KSB PUMP CO. INC.
NEWINGTON, N.H. 03801

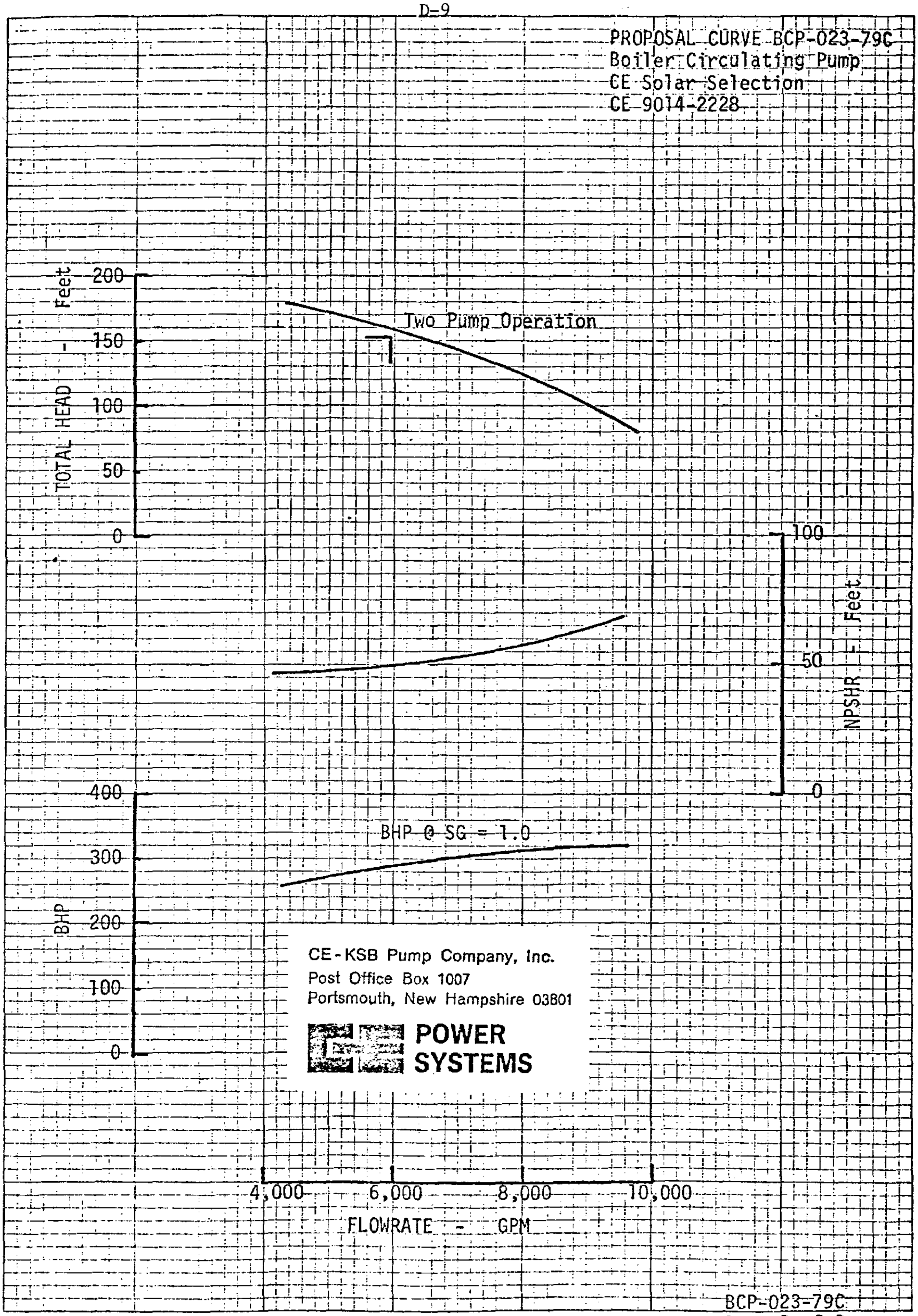
PROPOSAL CURVE BCP-023-79C
Boiler Circulating Pump
CE Solar Selection
CE 9014-2228
TOTAL HEAD - Feet
200
150
100
50
0
Two Pump Operation
NPSHR - Feet
100
50
0
BHP
400
300
200
100
0
BHP @ SG = 1.0
CE-KSB Pump Company, Inc.
Post Office Box 1007
Portsmouth, New Hampshire 03801
POWER
SYSTEMS
4,000
6,000
8,000
10,000
FLOWRATE - GPM
BCP-023-79C
Page 3 of 3

APPENDIX E

Solar Transient Receiver Analysis

A numerical model of the thermal transient response of a large central solar receiver has been developed. The model receives inputs of mass flow, temperature, and solar heat flux and calculates final steam and metal temperatures. The differential equations describing the model response with time are solved by the DARE-P computer program. The program produces listed and graphic data printouts, samples of which are included.

The four heat absorption sections of the steam generator have each been divided into sub-sections whose characteristics have been "lumped" in a simple first order system. In this way the simplicity of a lumped model has been kept, while the use of several sub-sections can help approach continuous system performance. The economizer and evaporator sections have been divided into four sub-sections, the primary and finishing superheaters into three each. The steam drum has been modeled separately as one lumped component. Delays caused by the long flow lengths of the components and connecting lines are simulated by the DELAY function of the DARE-P program.

The economizer and superheater sections are modeled as simple heat exchangers with known heat input. The state variable (representing energy storage in the system) is the exchanger metal temperature, thus

$$\frac{dTEX}{dt} = \frac{UA}{(MCP)_{EX}} \left[\frac{QR}{UA} + \frac{TFO - TFI}{2} - TEX \right]$$

and

$$TFO = \left[TEX + TFI \left[\frac{(MCP)_F}{UA} - 1/2 \right] \right] \Big/ \left[\frac{(MCP)_F}{UA} + 1/2 \right]$$

where

QR = Heat input

UA = Overall heat transfer factor

TFO = Fluid exit temperature

TFI = Fluid inlet temperature

TEX = Heat exchanger metal temperature

MCP_{EX} = Heat exchanger heat capacitance

MCP_{F} = Fluid heat capacitance

The evaporator operates at fairly constant (saturation) fluid temperature with most heat absorption taking place in the phase change to steam. The evaporator has therefore been modeled to calculate fluid enthalpy change rather than temperature change. The equations for the evaporator are:

$$\frac{dTEVAP}{dt} = \frac{UA}{MCP_{EV}} \qquad \frac{QEV}{UA} + TBOIL - TEVAP$$

and

$$HEXIT = \frac{UA}{MREC} \qquad TEVAP - TBOIL \qquad + HIN$$

where

TEVAP = Evaporator metal temperature

UA = Overall heat transfer factor

MCP_{EV} = Evaporator heat capacitance

QEV = Heat input

TBOIL = Saturation temperature in evaporator

HEXIT = Outlet fluid enthalpy

HIN = Inlet fluid enthalpy

MREC = Fluid flow through evaporator

For the drum,

$$\frac{dTDRUM}{dt} = \frac{UA_{DRUM}}{MDP_{DRUM}} \qquad TSAT - TDRUM$$

The model equations were coded for solution and are presented in the following printout. Two runs were performed, one showing the uncontrolled response of the model to a reduction in heat input, and one with controls on feedwater and desuperheater flow rate.

Due to the shift in program emphasis, further work in this area has been postponed. The data and results presented here are purely preliminary and were not intended to reflect an actual design or operation situation.

The model appears to respond as anticipated and could be a valuable tool in examining the magnitude of the WSR control problem.

The program was run twice, with the following results. Figure E-2 and E-6 show the "open-loop" response of the model to an arbitrary change in the heat input to various sections. Heat input was reduced 50% to the economizer, evaporator, finishing superheater and #1 superheater in that order. The heat input was not intended to represent an actual cloud situation but merely to test out the computer model and response times of the various sections.

Figure E-2 plots the outlet temperatures of the economizer and superheater sections. Steam temperatures from the superheaters increase due to the drop in steam generation that occurs when evaporator heat input is cut. Without control the steam temperatures are seen to rise quickly to unacceptable temperatures.

Figure E-3 shows final steam flow rate decreasing slowly as first the economizer heat input is reduced and then more rapidly as the evaporator heat input is cut. Although the evaporator heat input rate drops by only 50%, steam generation is seen to fall over 70%.

Figures E-4 and E-5 show superheater metal temperatures rising as steam flow falls. Final outlet superheater tubes could approach 1100C (2000F) under these conditions.

Figure E-6 shows the section heat inputs graphed against time.

Figures E-7 to E-10 represent the "controlled loop" response to the same heat inputs described above. Two simple controls were added, one to control feedwater flow to the economizer to balance the steam generation rate in the economizer, and another to add desuperheating water to the steam circuit before the finishing superheater. Neither control was optimized in any way.

As can be seen from Figure E-7, the desuperheater control acted to keep final steam outlet temperature close to the 600C (1100F) set-point. Outlet steam from #1 superheater, however, rose to nearly 760C (1400F) with peak metal temperature nearly 700C (1300F) as in Figure E-8.

Figure E-9 shows the influence of the desuperheater on the finishing superheater temperature. No portion of the superheater varys more than 200F during the excursion, but the change is very rapid, particularly in the inlet section.

Figure E-10 shows the need for rapid desuperheater control if final steam temperature is to be held constant. Both the final steam and feedwater flows are shown.

Further work in the area of transient solar modeling is definitely indicated by even this shortened investigation. Standard steam cycle controls may be inadequate to cope with the potential load swings which a central solar receiver may face. Based on these results it may be necessary to investigate alternate methods of cycle control such as multiple desuperheaters or mirror defocus if unreasonable metal temperature changes are to be avoided.

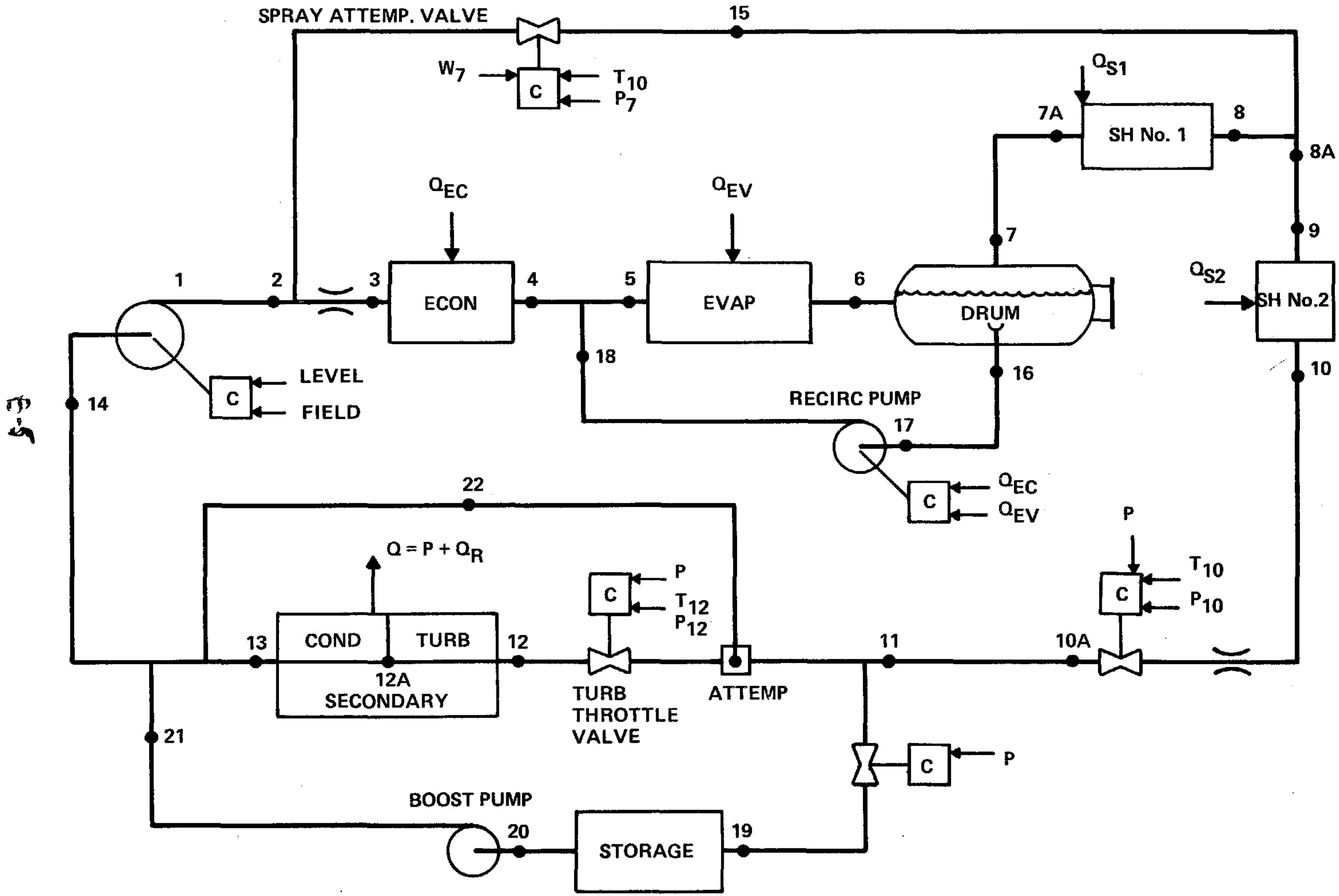

SOLAR TRANSIENT MODEL

FIGURE E-1

E-2

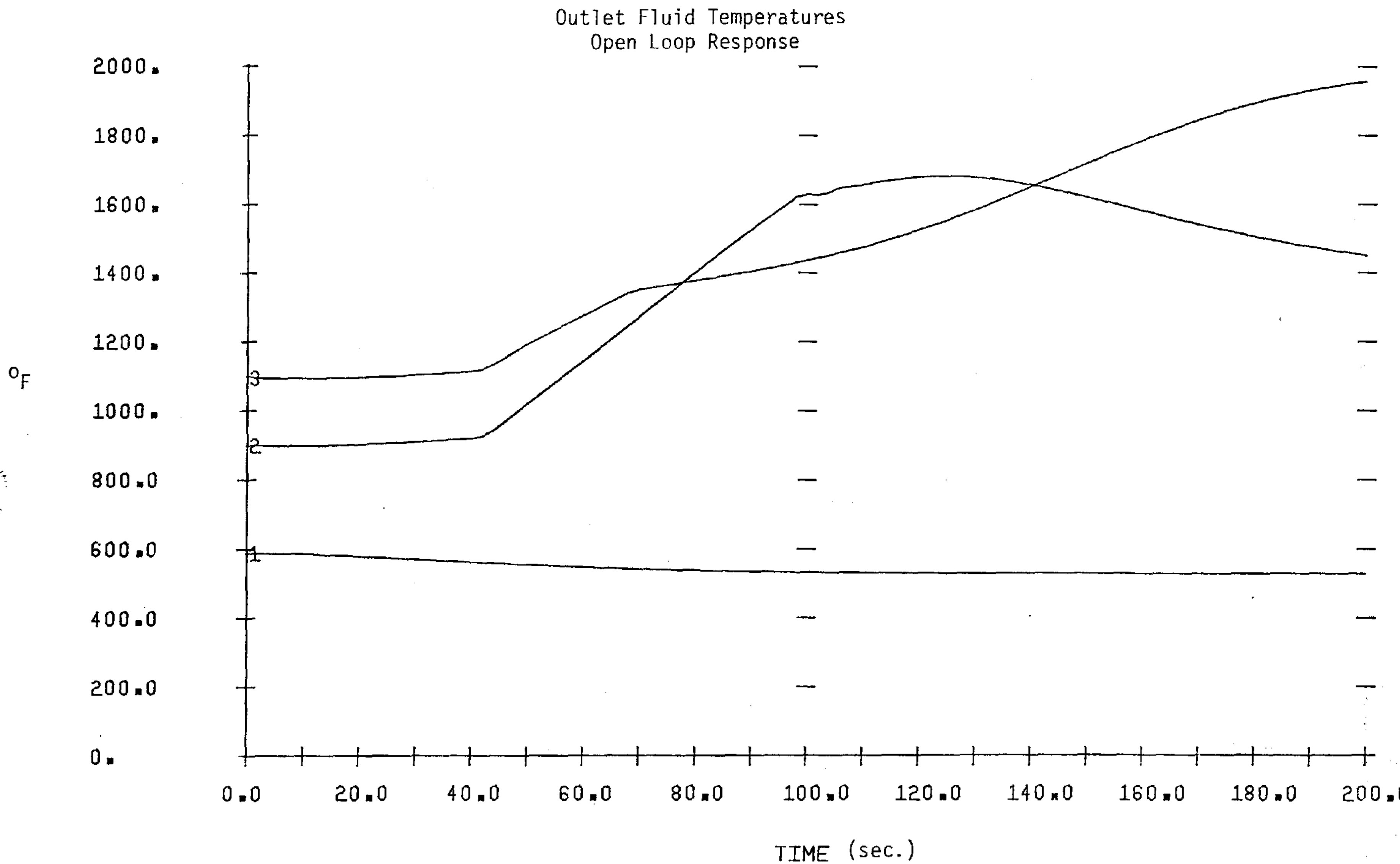

PLOTTER SYMBOL- 1 2 3
Outlet Fluid Temperature: Economizer #1 S.H. Finishing S.H.

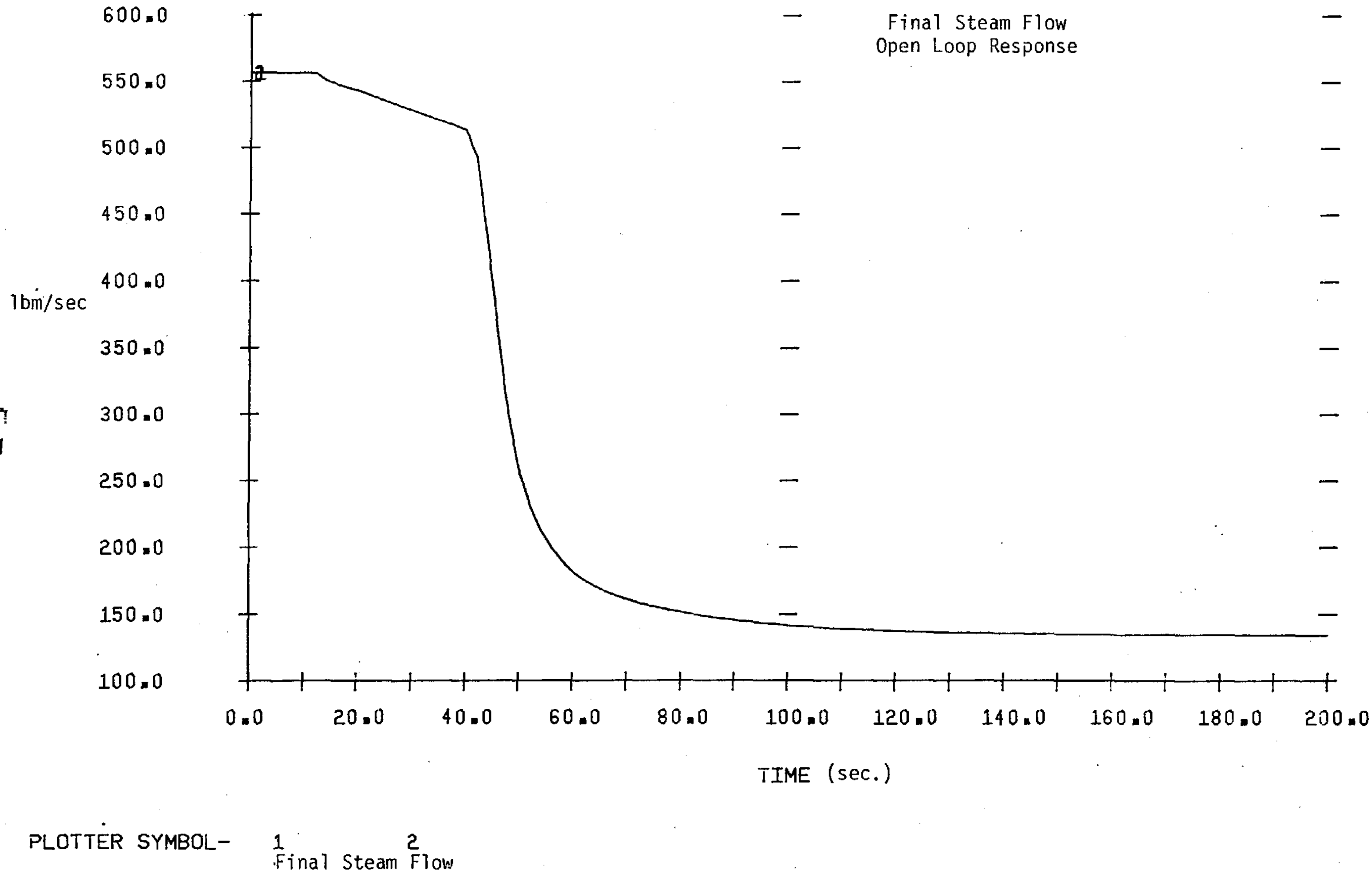
Final Steam Flow
Open Loop Response
lbm/sec
600.0
550.0
500.0
450.0
400.0
350.0
300.0
250.0
200.0
150.0
100.0
0.0
20.0
40.0
60.0
80.0
100.0
120.0
140.0
160.0
180.0
200.0
TIME (sec.)
PLOTTER SYMBOL- 1 2
Final Steam Flow

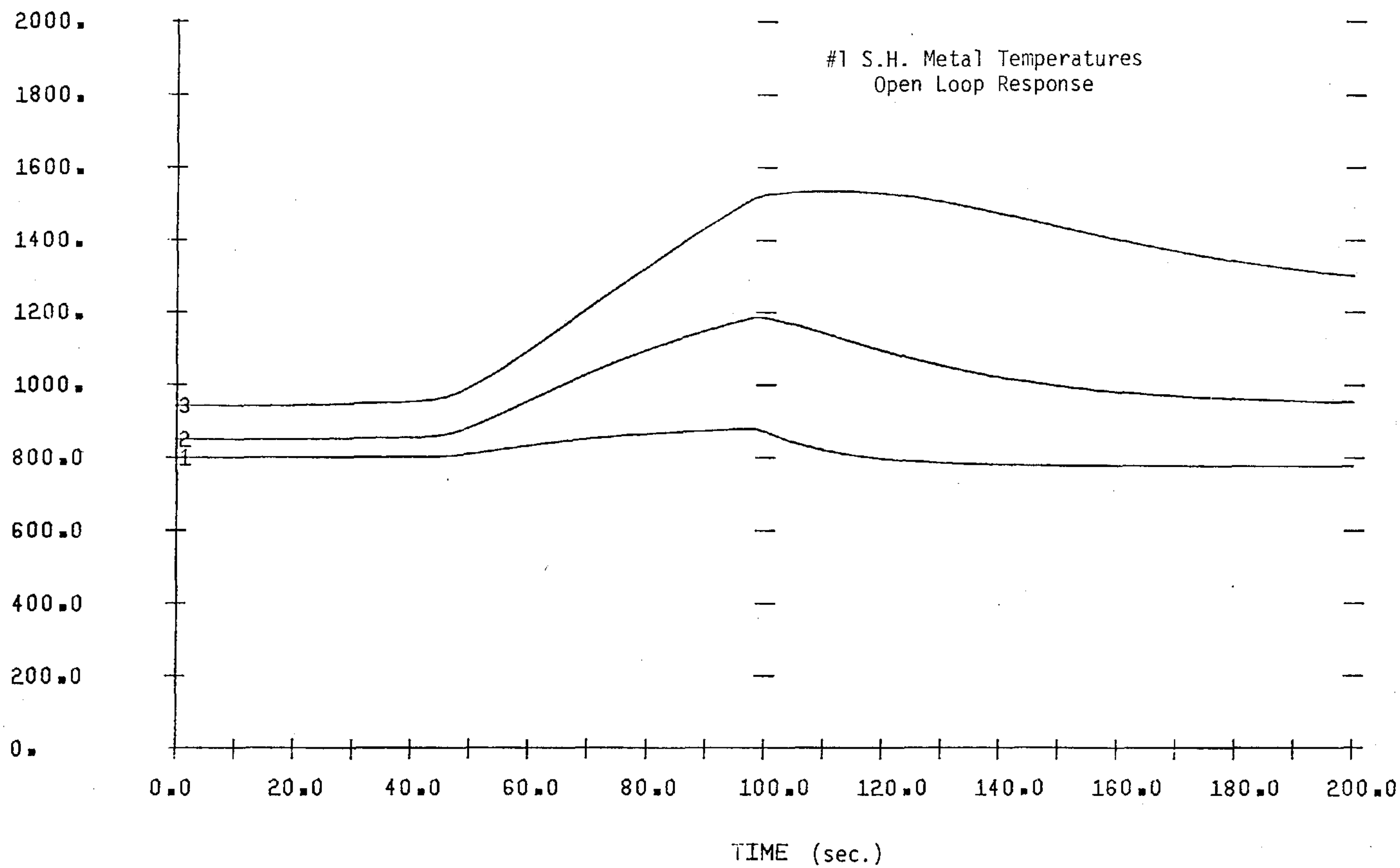

PLOTTER SYMBOL- 1 2 3
Location - Inlet Center Outlet

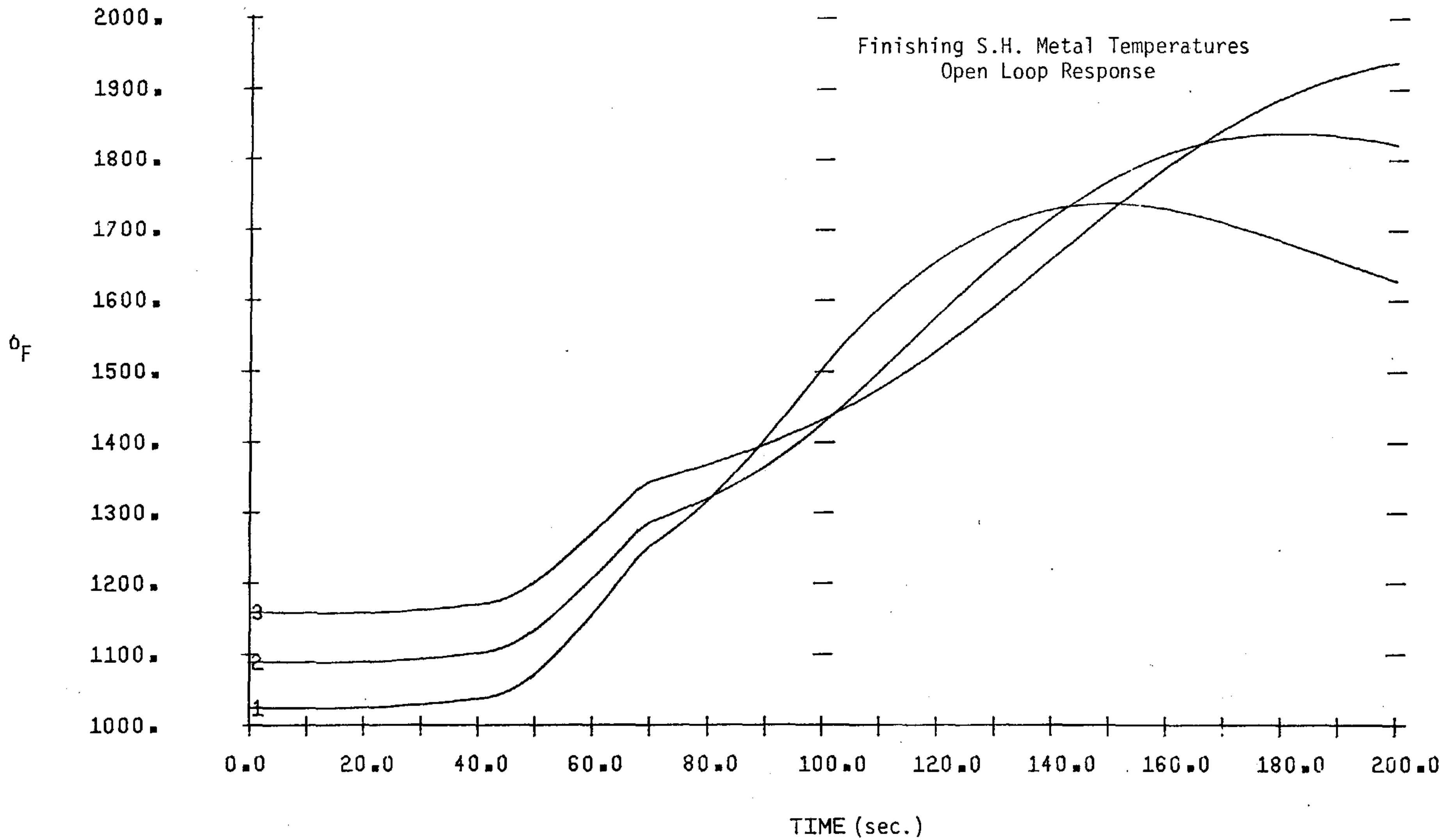

PLOTTER SYMBOL- 1 2 3
Location - Inlet Center Outlet

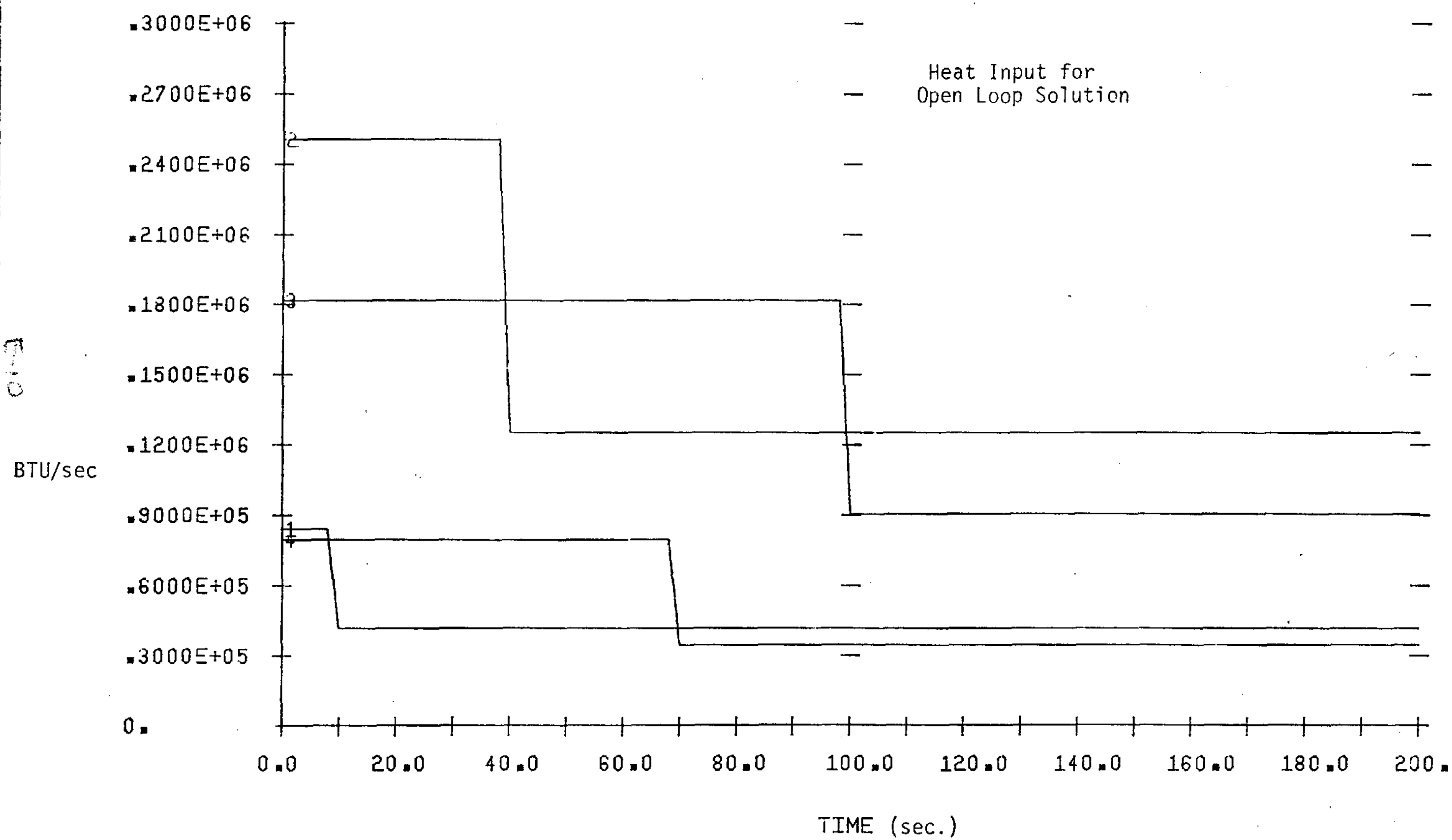

PLOTTER SYMBOL- 1 2 3 4
Section Economizer Evaporator #1 S.H. Finishing S.H.

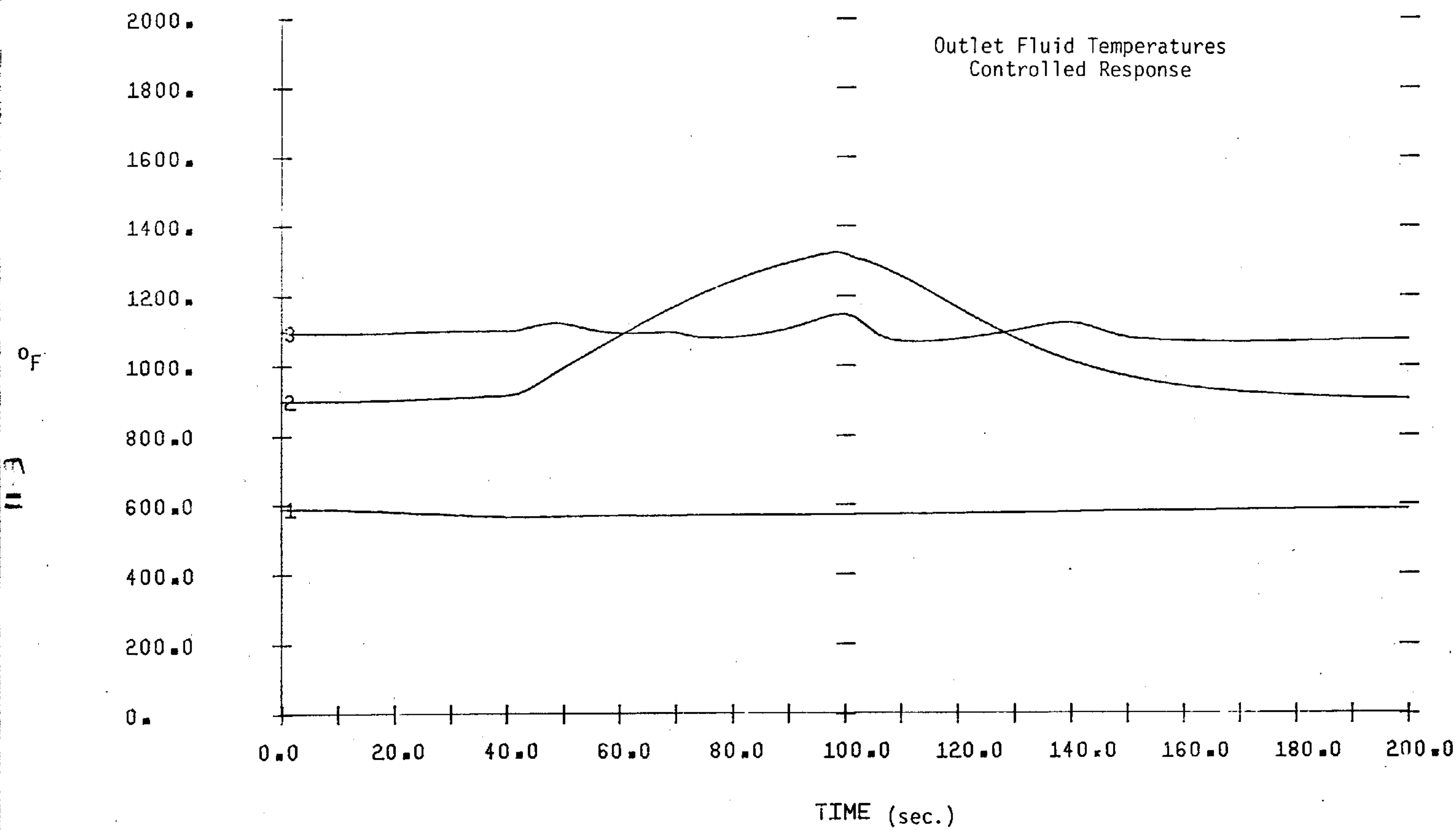

PLOTTER SYMBOL- 1 2 3

Outlet Fluid Temperature — Economizer, #1 S.H., Finishing S.H.

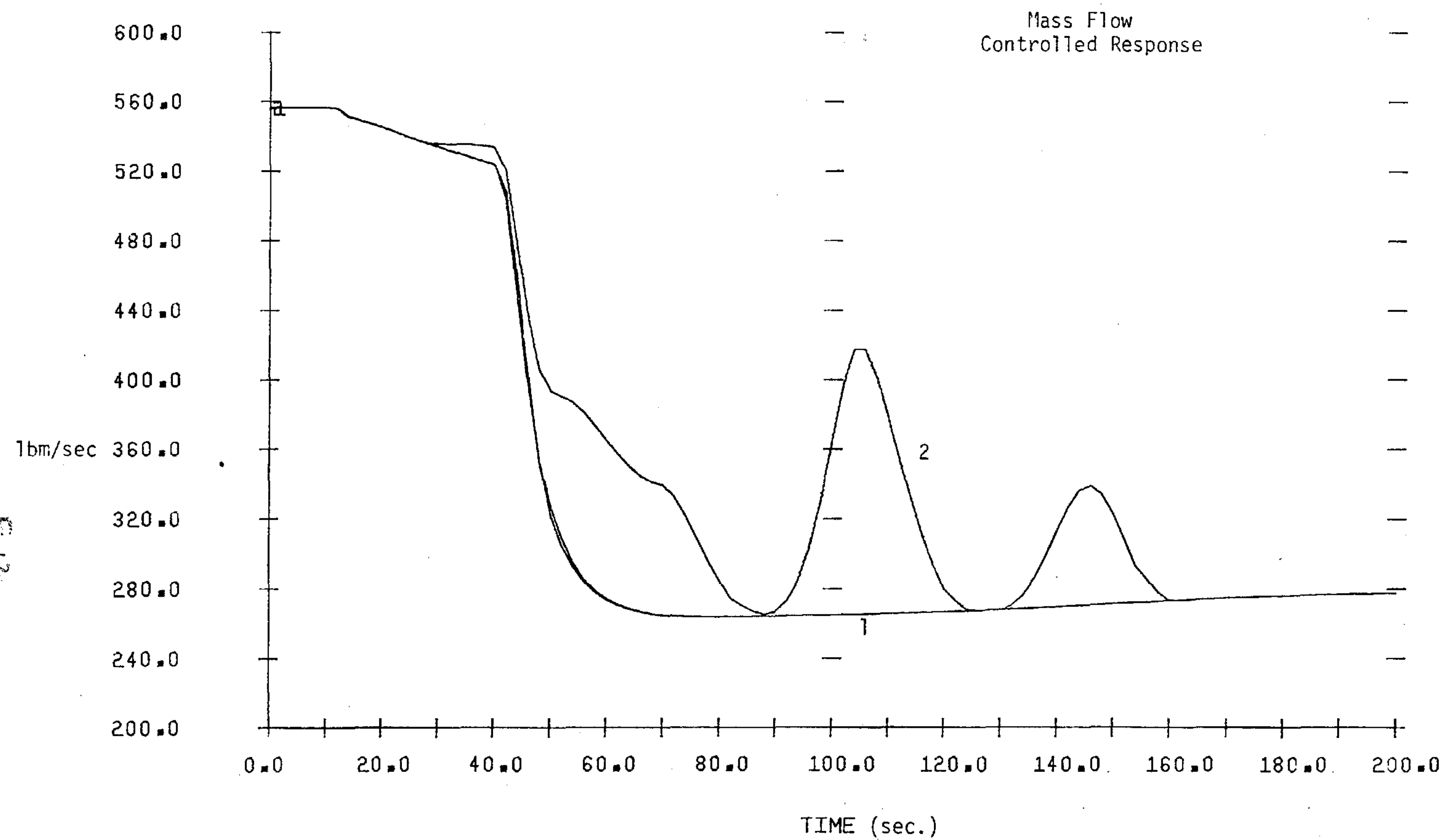

PLOTTER SYMBOL- 1 2
Mass Flow Feedwater Final Steam

#1 S.H. Metal Temperatures #
Controlled Responses

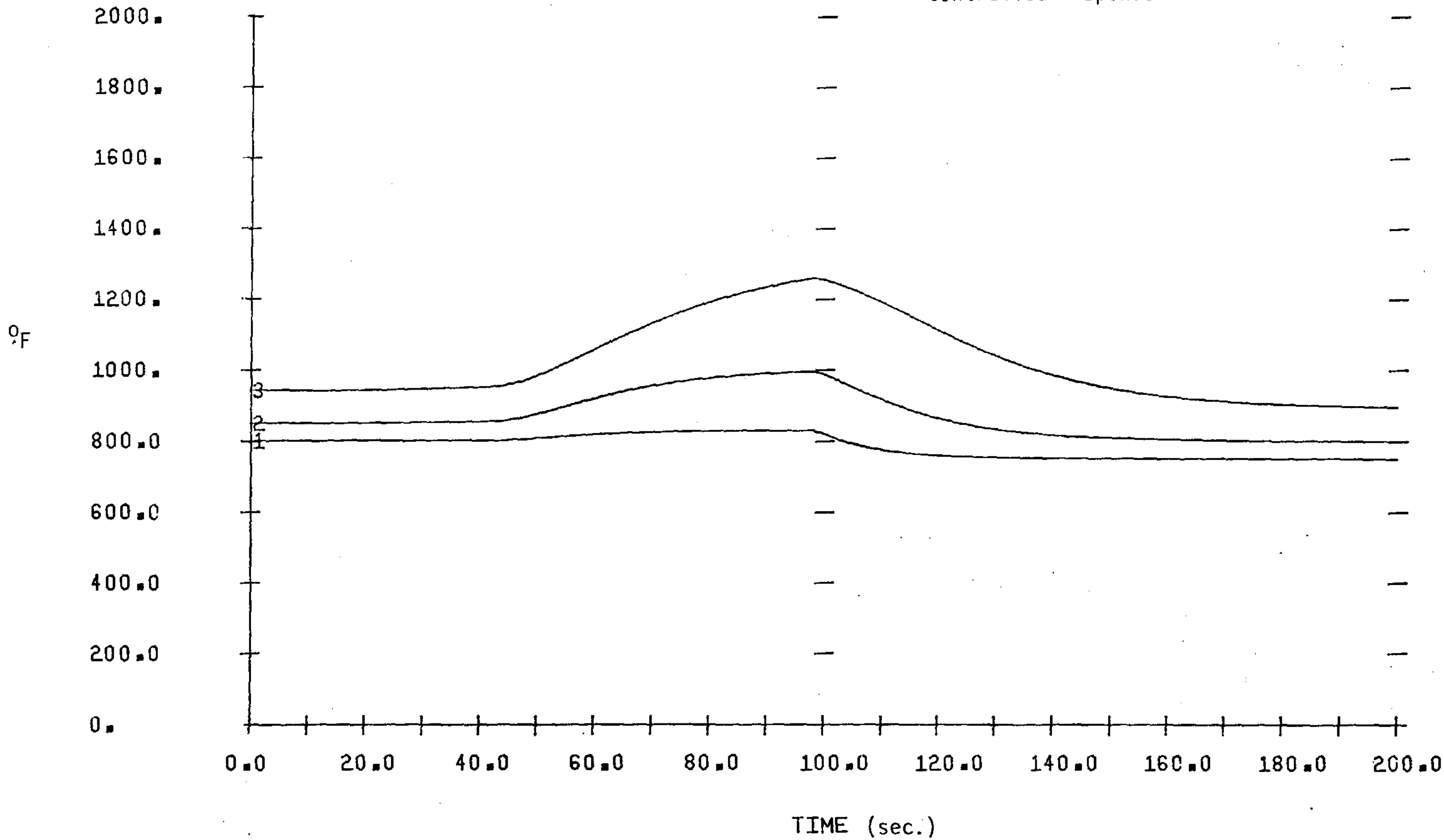

E-13

PLOTTER SYMBOL- 1 2 3
Location Inlet Center Outlet

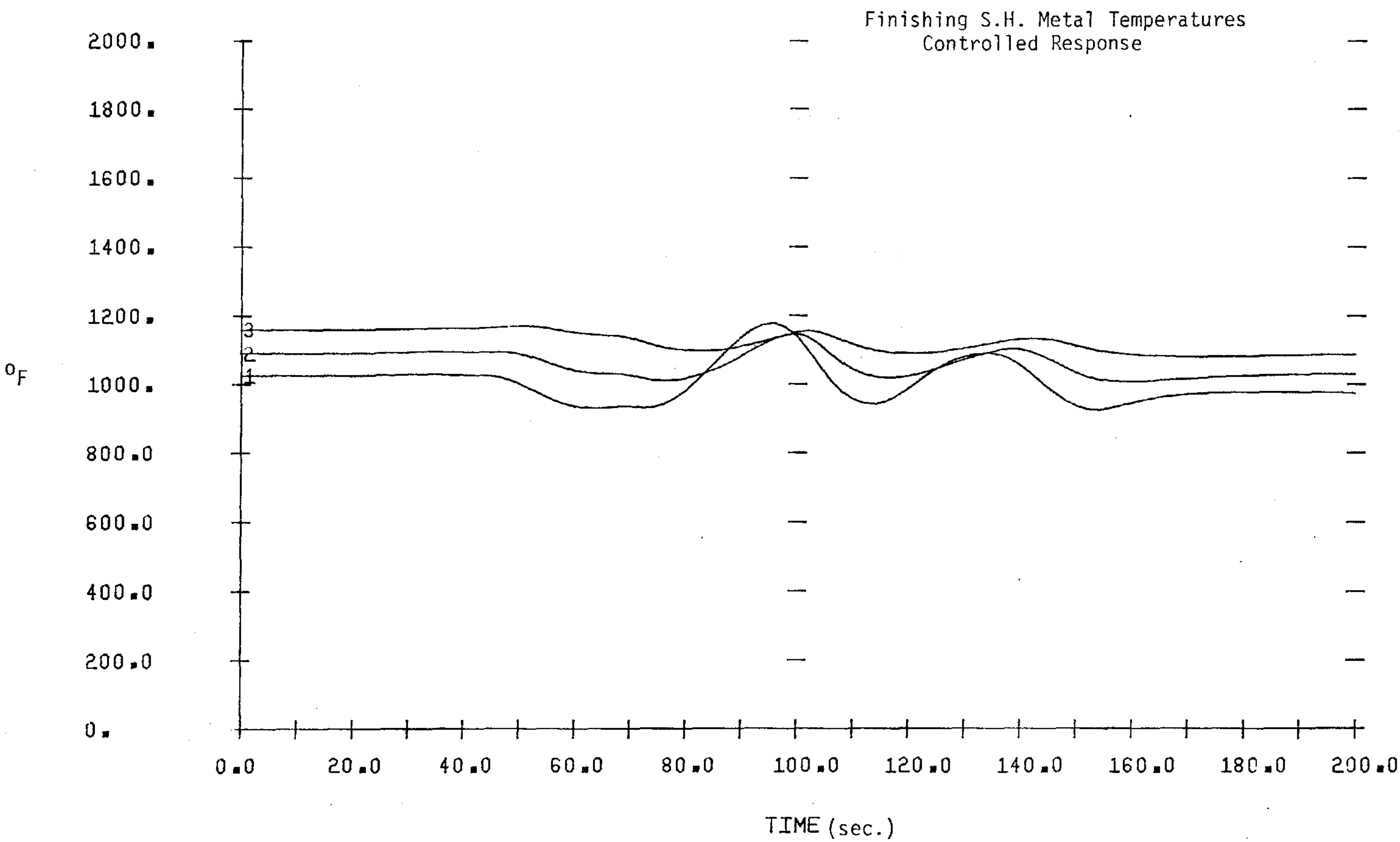

PLOTTER SYMBOL- 1 2 3
Location Inlet Center Outlet

DARE PORTABLE (VERSION 2.2)

FIGURE E-11
COMPUTER MODEL INPUT SOLAR
TRANSIENT PROBLEM

```
EXPERIMENTAL VERSION...
IF PROBLEMS ARE ENCOUNTERED, CONTACT...
ENGINEERING SCIENCE DEPARTMENT...
BUILDING 22, WINDSOR


        $01
         PROCED WDESTM = WFIN,H2SH03,HSET,HFW,WDES ,WSTM,HINT,HOUT,DIFH
         WDESTM =(WDES-(WFIN*(HSET-H2SH03+HOUT)-WSTM*HINT)/HFW)*1.0   0.5
      C      ****  ****  DIFFERENTIAL DAMPING
           $      + 0.8 1.0 + (DIFH*WFIN)/(H2SH03-HFW)
              IF(WDES.LT.0.) GO TO 20
              IF(WDES.GT.(-WDESTM)) GO TO 10
          20 WDES = 0.
             WDESTM = 0.
          10 CONTINUE
        ENDPRO
         PROCED DIFH = H2SH03
              DLYSH2 = DELAY(H2SH03,2.,DT,16,H2SH03)
              DIFH = (H2SH03-DLYSH2)/2.
        ENDPRO
         PROCED HSET = P2SH
      C     ********     CALCULATE ENTHALPY SET-POINT
           HSET = HSHEAT(1150.,P2SH,CP)
         ENDPRO
                WDES. = WDESTM
      C     ******  CALCULATE RATE OF CHANGE FOR FEEDWATER FLOW
              WFW. = (WSTM-WFW) + 0.3*(18780.-WSL)
         PROCED QEC,QEV,Q2SH,Q1SH
      C    ******   VARIATION FO HEAT INLUT WITH TIME
             IF(T.GE.10.) QEC = 42192.
             IF(T.GE.40.) QEV = 125350.
             IF (T.GE.70.) Q2SH = 35000.
             IF(T.GE.100.) Q1SH = 98900.
        ENDPRO
      C    *****    RATE OF CHANGE OF ECONOMIZER
             TEC1. = UAEC/EMCPEC*(QEC/4./UAEC+(TEC01+TFW   )/2.-TEC1)
             TEC2. = UAEC/EMCPEC*(QEC/4./UAEC+(TEC02+TECE2)/2.-TEC2)
             TEC3. = UAEC/EMCPEC*(QEC/4./UAEC+(TEC03+TECE3)/2.-TEC3)
             TEC4. = UAEC/EMCPEC*(QEC/4./UAEC+(TEC04+TECE4)/2.-TEC4)
             FEC   = WFW*CPFW/UAEC
      C     ******   FLUID TEMPERATURES THROUGH ECONOMIZER
             TEC01 =(TEC1+TFW   *(FEC-.5))/(FEC+.5)
             TEC02 =(TEC2+TECE2*(FEC-.5))/(FEC+.5)
             TEC03 =(TEC3+TECE3*(FEC-.5))/(FEC+.5)
             TEC04 =(TEC4+TECE4*(FEC-.5))/(FEC+.5)
      C     ********   DRUM TEMPERATURE CHANGE
             TDRUM.=UADRUM/EMCPDM*(TSAT-TDRUM)
      C    *******    ENTHALPY ENTERING DRUM
             HDM = (WREC*HIN + WFW*HECON)/(WREC+WFW)
      C    *****    - STEAM QUALITY
             GL = (HDM-HSL)/HFG
      C    *****    MASS RATE OF CHANGE IN DRUM
             WSL.    = (WREC+WFW)*(1.-GL)-WREC
             WSLTEM  = (WREC+WFW)*(1.-GL)-WREC
             WSS. =-VSL*WSLTEM/VSS
             WSSTEM=-VSL*WSLTEM/VSS
      C    ****    STEAM FOLW FROM DRUM
             WSTM = GL*(WREC+WFW)-WSSTEM
      C    *****   PRIMATY SUPERHEATER METAL TEMPERATURES
             T1SH1. = UA1SH/ECF1SH*(Q1SH/3./UA1SH+(T1SH  +T1SHE1)/2.-T1SH1)
```

```
      T1SH3.= UA1S/ECP1SH*(Q1SH/3./UA1SH+(T1SH03+T1SHE3)/2.-T1SH3)
C  ***********  CALUCALATIONS OF SPECIFIC HEATS AND OUTLET TEMPERATURES
C    PERHEATERS
PROCED CP1SH1,   T1SH01=T1SHE1,T1SH1,WSTM,UA1SH,P1SH
      CALL TEMPX(T1SH01,T1SHE1,T1SH1,WSTM,UA1SH,P1SH,CP1SH1)
ENDPRO
PROCED CP1SH2,   T1SH02=T1SHE2,T1SH2,WSTM,UA1SH,P1SH
      CALL TEMPX(T1SH02,T1SHE2,T1SH2,WSTM,UA1SH,P1SH,CP1SH2)
ENDPRO
PROCED CP1SH3,   T1SH03=T1SHE3,T1SH3,WSTM,UA1SH,P1SH
      CALL TEMPX(T1SH03,T1SHE3,T1SH3,WSTM,UA1SH,P1SH,CP1SH3)
  ENDPRO
PROCED CP2SH1,   T2SH01=T2SHE1,T2SH1,WFIN,UA2SH,P2SH
      CALL TEMPX(T2SH01,T2SHE1,T2SH1,WFIN,UA2SH,P2SH,CP2SH1)
ENDPRO
PROCED CP2SH2,   T2SH02=T2SHE2,T2SH2,WFIN,UA2SH,P2SH
      CALL TEMPX(T2SH02,T2SHE2,T2SH2,WFIN,UA2SH,P2SH,CP2SH2)
ENDPRO
PROCED CP2SH3,   T2SH03=T2SHE3,T2SH3,WFIN,UA2SH,P2SH
      CALL TEMPX(T2SH03,T2SHE3,T2SH3,WFIN,UA2SH,P2SH,CP2SH3)
ENDPRO
C    *********  DESUPERHEATER COLCULATIONS
      WFIN  = WDES + WSTM
      HOUT  = (WDES* HFW + WSTM*HINT)/WFIN
C    ***  FINISHING SUPERHEATER METAL TEMPERATURES
      T2SH1.=UA2SH/ECP2SH*(Q2SH/3./UA2SH+(T2SH01+T2SHE1)/2.-T2SH1)
      T2SH2.=UA2SH/ECP2SH*(Q2SH/3./UA2SH+(T2SH02+T2SHE2)/2.-T2SH2)
      T2SH3.=UA2SH/ECP2SH*(Q2SH/3./UA2SH+(T2SH03+T2SHE3)/2.-T2SH3)
C     *******   DELAYS IN ECONOMIZER
  PROCED  TECE2=TEC01,DELEC
           TECE2= DELAY(TEC01,DELEC,DT,1 ,TEC01)
  ENDPRO
  PROCED  TECE3=TEC02,DELEC
           TECE3= DELAY(TEC02,DELEC,DT,2 ,TEC02)
  ENDPRO
      DELEC = 8.825*555.56/WFW
      DELER = 1.77*555.56/WFW
  PROCED  TECE4=TEC03,DELEC
           TECE4=DELAY(TEC03,DELEC,DT,3 ,TEC03)
  ENDPRO
C  *******  CALCULATE SH DELAYS
      DELD1S  = .33*555.56/WSTM
      DEL1SH  = .8*555.56/WSTM
      DELS12  = .33*555.56/WFIN
C  *******  DELAY IN SUPERHAETERS
  PROCED T1SHE1=TDRUM,DELD1S
         T1SHE1=DELAY(TDRUM,DELD1S,DT,4 ,TDRUM)
  ENDPRO
  PROCED T1SHE2=T1SH01,DEL1SH
         T1SHE2=DELAY(T1SH01,DEL1SH,DT,5 ,T1SH01)
  ENDPRO
  PROCED T1SHE3=T1SH02,DEL1SH
         T1SHE3=DELAY(T1SH02,DEL1SH,DT,6 ,T1SH02)
  ENDPRO
      DEL2SH = .3*555.56/WFIN
  PROCED T2SHE2=T2SH01,DEL2SH
         T2SHE2=DELAY(T2SH01,DEL2SH,DT,7 ,T2SH01)
  ENDPRO
  PROCED T2SHE3=T2SH02,DEL2SH
         T2SHE3=DELAY(T2SH02,DEL2SH,DT,8 ,1033.)
  ENDPRO
C   ******  CALCULATE EVAPORATOR METAL TEMPERAUREE RATE OF CHANGE
      TEV1. =UAEV/EMCPEV*(QEV/4./UAEV+TBOIL-TEV1)
      TEV2. =UAEV/EMCPEV*(QEV/4./UAEV+TBOIL-TEV2)
```

```
      HEV02 =UAEV/WREC *(TEV2 - TBOIL) + HEVE2
      HEV03 =UAEV/WREC *(TEV3 - TBOIL) + HEVE3
      HEV04 =UAEV/WREC *(TEV4 - TBOIL) + HEVE4
C **** E DELAYS IN EVAPORATOR CIRCUIT
  PROCED HIN=HEV04,DELBD
         HIN=DELAY(HEV04,DELBD,DT,9 ,HEV 4)
  ENDPRO
  PROCED HEVE4=HEV03,DELBLR
         HEVE4=DELAY(HEV03,DELBLR,DT,10,HEV03)
  ENDPRO
  PROCED HEVE3=HEV02,DELBLR
         HEVE3=DELAY(HEV02,DELBLR,DT,11,HEV02)
  ENDPRO
  PROCED HEVE2=HEV01,DELBLR
         HEVE2=DELAY(HEV01,DELBLR,DT,12,HEV01)
  ENDPRO
  PROCED HEVE1=HSL,DELDB
         HEVE1=DELAY(HSL,DELDB,DT,13,HSL)
  ENDPRO
      DELBLR = 1.425*1111.1/WREC
      DELBD= 1.36*1111.1/WREC
      DELDB = 7.46*1111.1/WREC
C ******* STEAM PROPERITIES
  PROCED HSL,HSS,VSL,VSS=TDRUM
         HSL= ENSATL(TDRUM)
         HSS= ENSATS(TDRUM)
         VSL= VESATL(TDRUM)
         VSS= VESATS(TDRUM)
  ENDPRO
  PROCED HINT=H1SH03,DELS12
         HINT=DELAY(H1SH03,DELS12,DT,14,H1SH03)
  ENDPRO
         HFG = HSS-HSL
         TBOIL = TSAT
  PROCED TSAT=PDRUM
         TSAT=EXP(.22151*ALOG(PDRUM) + 4.77123)
  ENDPRO
 PROCED H1SH03=P1SH,T1SH03
        H1SH03= HSHEAT(T1SH03,P1SH,CP)
 ENDPRO
 PROCED T2SHE1=HOUT   ,P2SH
        T2SHE1= TSHEAT(HOUT   ,P2SH,CP)
 ENDPRO
 PROCED H2SH03=T2SH03,P2SH
        H2SH03=HSHEAT(T2SH03,P2SH,CP)
 ENDPRO
 PROCED HEC04=TEC04
C ********    CORRECTION OFOR PRESSURE
        HEC04=ENSATL(TEC04)     - 5.6
 ENDPRO
 PROCED HECON=HEC04,DELEB
        HECON= DELAY(HEC04,DELEB,DT,15,HEC04)
 ENDPRO
 PROCED HFW=TFW
C ********    CORRECTION OFOR PRESSURE
        HFW= ENSATL(TFW)      - 5.6
 ENDPRO
 $F
       FUNCTION ENSATL(TEI)
C  *********   ENTHALPY OF SATURATED LIQUID
        PRI=0.
        ENI=0.
        VOI=0.
```

```
      CALL STEP(3,PRI,ENI,TEI,VOI,XWD,S,AMDA,CP,ETA)
      ENSATL=ENI
      RETURN
      END
      FUNCTION ENSATS(TEI)
C ********** ENTHALPY OF STAURATED SHTEAM
      PRI=0.
      ENI=0.
      VOI=0.
      XWD=1.
      CALL STEP(3,PRI,ENI,TEI,VOI,XWD,S,AMDA,CP,ETA)
      ENSATS=ENI
      RETURN
      END
      FUNCTION VESATL(TEI)
C ***** SPECIFIC VOLUME OF STTURATED LIQUID
      PRI=0.
      ENI=0.
      VOI=0.
      XWD=0.00001
      CALL STEP(3,PRI,ENI,TEI,VOI,XWD,S,AMDA,CP,ETA)
      VESATL=VOI
      RETURN
      END
      FUNCTION VESATS(TEI)
C ***** SPECIFIC VOLUME OF STTURATED STEAM
      PRI=0.
      ENI=0.
      VOI=0.
      XWD=1.
      CALL  STEP(3,PRI,ENI,TEI,VOI,XWD,S,AMDA,CP,ETA)
      VESATS=VOI
      RETURN
      END
      FUNCTION TSHEAT(ENI,PRI,CP)
C     ***TEMPERTURE OF SUPERHEATED STEAM
      VOI=0.
      XWD=0.
      TEI=0.
C *** IF TOO HOT , APPLY BAND-AID AND CONTINUE
      IF(ENI.GT.HSHEAT(1200.,PRI,CPDUM)) GO TO 1
      CALL STEP(3,PRI,ENI,TEI,VOI,XWD,S,AMDA,CP,ETA)
      TSHEAT= TEI
      IF(CP.EQ.0.) CP=.01
      RETURN
 10   HLIM = HSHEAT(1200.,PRI,CP)
      HDUM = HSHEAT(1201.,PRI,CP)
      TSHEAT = 1200. +(ENI-HLIM)/CP
      RETURN
      END
      FUNCTION  HSHEAT(TEI,PRI,CP)
C  ******* ENTHALPY OF SUPERHEATED STEAM
      ENI=0.
      VOI=0.
      XWD=0.
C *** IF TOO HOT , APPLY BAND-AID AND CONTINUE
      IF(TEI.GT.1200.) GO TO 10
      CALL STEP(3,PRI,ENI,TEI,VOI,XWD,S,AMDA,CF,ETA)
      HSHEAT= ENI
      RETURN
 10   CP = .621
      CALL STEP(3,PRI,ENI,1200.,VOI,XWD,S,AMDA,CPDUM,ETA)
      HSHEAT = CP*(TEI-1200.)+ENI
      RETURN
      END
```

E-48

```
      20  F=W*CP/U
          TOUT=(TEX+TIN*(F-.5))/(F+.5)
          DELT = (TOUT-TIN)*.25
          T2 = TIN+DELT
          T3 = T2 + DELT
          T4 = T3 + DELT
C   ***** INTEGRATE SPECIFIC HEAT OFVER TEMPERATURE RANGE
          ENI = HSHEAT(TIN,P,CP1)
          ENI = HSHEAT(T2,P,CP2)
          ENI = HSHEAT(T3,P,CP3)
          ENI = HSHEAT(T4   ,P,CP4)
          ENI = HSHEAT(TOUT,P,CP5)
          CPTEST = (CP1+2.*CP2+2.*CP3+CP4*2. + CP5)* 0.125
C   ***** ITERATE UNTIL VALUE CONVERGES
          IF(ABS(CP-CPTEST).LT.0.002)GOTO10
          CP=CPTEST
          GO TO 20
      10  CP = CPTEST
          RETURN
          END
 $L
          CALL RUN
C   *************    INITIAL CONDITIONS
 END
         TMAX = 200.
            DT = 2.
          TFW =473.8
          PDRUM = 2850.
          PFW = 2950.
WARNING - UNKNOWN NAME OR DOUBLE INITIAL CONDITION
          WDES = 0.
          P1SH = 2850.
          P2SH = 2750.
          WSL =18780.
          WSS = 6120.
          QEC    = 84383
QEC
WARNING - INITIAL CONDITION GIVEN FOR DEFINED VARIABLE
          QEV    = 250750.
QEV
WARNING - INITIAL CONDITION GIVEN FOR DEFINED VARIABLE
          WREC = 1111.1
          WFW = 555.56
          T1SH1 = 802.
          T1SH2 = 851.2
          T1SH3 = 943.4
          T2SH1 = 1025.7
          T2SH2 = 1090.4
          T2SH3 = 1159.6
          Q1SH = 181890.
Q1SH
WARNING - INITIAL CONDITION GIVEN FOR DEFINED VARIABLE
          Q2SH = 79833.
Q2SH
WARNING - INITIAL CONDITION GIVEN FOR DEFINED VARIABLE
          LAEC = 843.89
          TEC1 = 513.3
          TEC2 = 541.8
          TEC3 = 570.3
          TEC4 = 598.8
          CPFW = 1.3324
          TECE2 = 502.5
TECE2
```

```
                TECE3 = 531.
TECE3
WARNING - INITIAL CONDITION GIVEN FOR DEFINED VARIABLE
                TECE4 = 559.5
TECE4
WARNING - INITIAL CONDITION GIVEN FOR DEFINED VARIABLE
                TDRUM = 688.
                UA1SH = 606.4
                UA2SH = 266.11
                UALV = 1250.
                HEVE1 = 777.
HEVE1
WARNING - INITIAL CONDITION GIVEN FOR DEFINED VARIABLE
                HEVE2 = 833.6
HEVE2
WARNING - INITIAL CONDITION GIVEN FOR DEFINED VARIABLE
                HEVE3 = 890.3
HEVE3
WARNING - INITIAL CONDITION GIVEN FOR DEFINED VARIABLE
                HEVE4 = 946.9
HEVE4
WARNING - INITIAL CONDITION GIVEN FOR DEFINED VARIABLE
                TEV1 = 737.854
                TEV2 = 737.854
                TEV3 = 737.854
                TEV4 = 737.854
                UADRUM = 45.56
                EMCPEC = 7240.
                EMCPDM = 44900.
                ECP1SH = 3570.
                ECP2SH = 2400.
                EMCPEV = 6577.
           END
                LIST,WSTM,T1SH01,T1SH02,T1SH03,WSL
             LIST, T1SH01,T1SH02,T1SH03
              LIST, T1SH1,T1SH2,T1SH3,H1SH01,H1SH02,H1SH03
            LIST, T2SH1,T2SH2,T2SH3,H2SH01,H2SH02,H2SH03
                PLOT,TEC04,T1SH03,T2SH03
                PLOT(,,,   )  WSTM,WFW,     WFIN
                PLOT(,,,   )  T1SH1,T1SH2,T1SH3
                PLOT(,,,   )  T2SH1,T2SH2,T2SH3
                PLOT(,,,   )  QEC,QEV,Q1SH,Q2SH
           END

USAGE..  IBLOCK     NAMES    ITABLE
        2344/8000  319/2100  287/2000
```

TABLE E-1

LIST OF VARIABLES

CPFW	Specific heat of feedwater (BTU/lbm)
CP1SH1	Specific heat of steam, 1st superheater section (BTU/lbm)
CP1SH2	" " " " " " " "
CP1SH3	" " " " " " " "
CP2SH1	" " " " 2nd " " "
CP2SH2	" " " " " " " "
CP2SH3	" " " " " " " "
DELBD	Time of flow lag between EVAPORATOR and Drum (sec)
DELBLR	Time " " " in EVAPORATOR
DELDB	" " " " between Drum and Evaporator
DELDIS	" " " " " Drum and 1st Superheater
DELEB	" " " " " Economizer and Drum
DELEC	" " " " in Economizer
DELS12	" " " " between 1st and 2nd (Finishing) Superheaters
DEL1SH	" " " " in 1st Superheater
DEL2SH	" " " " in 2nd Superheater
D1FH	Rate of change of final steam outlet enthalpy (BTU/sec)
DT	Time step (sec)
ECP1SH	Heat capacity, 1st superheater (BTU/F)
ECP2SH	" " , 2nd " "
EMCPDM	" " , steam drum "
EMCPEC	" " , Economizer "
EMCPEV	" " , Evaporator "
FEC	Temporary variable
HDM	Enthalpy into steam drum (evaporator, economizer flows) (BTU/lbm)
HECON	Enthalpy entering drum from economizer (BTU/lbm)
HECO4	Enthalpy exiting economizer (BTU/lbm)

HEVE1	Enthalpy entering evaporator sections (BTU/lbm)
HEVE2	" " " " "
HEVE3	" " " " "
HEVE4	" " " " "
HEVO1	Enthalpy exiting evaporator sections (BTU/lbm)
HEVO2	" " " " "
HEVO3	" " " " "
HEVO4	" " " " "
HFG	Heat of vaporization at drum pressure (BTU/lbm)
HFW	Enthalpy of feedwater (BTU/lbm)
HIN	Enthalpy entering drum from evaporator (BTU/lbm)
HINT	Enthalpy of steam entering desuperheater (BTU/lbm)
HOUT	Desuperheater outlet enthalpy (BTU/lbm)
HSET	Desired final outlet enthalpy (BTU/lbm)
HSL	Enthalpy of saturated liquid in drum
HSS	" " " vapor " "
H1SH03	Outlet enthalpy, 1st superheater (BTU/lbm)
H2SH03	Outlet enthalpy, 2nd superheater (BTU/lbm)
PDRUM	Drum pressure (psia)
P1SH	1st superheater entering pressure (psia)
P2SH	2nd superheater entering pressure (psia)
QEC	Economizer heat input (BTU/sec)
QEV	Evaporator heat input (BTU/sec)
QL	Quality entering drum (M_{steam}/M_{total})
Q1SH	1st superheater heat input (BTU/sec)
Q2SH	2nd superheater heat input (BTU/sec)
T	Time (sec)
TBOIL	Saturation temperature in evaporator (F)

TDRUM	Bulk drum temperature (F)
TEC1	Economizer section metal temperature (F)
TEC2	" " " " "
TEC3	" " " " "
TEC4	" " " " "
TECE1	Economizer section inlet temperature (F)
TECE2	" " " " "
TECE3	" " " " "
TECE4	" " " " "
TECO1	Economizer section outlet temperature (F)
TECO2	" " " " "
TECO3	" " " " "
TECO4	" " " " "
TEV1	Evaporator section metal temperature (F)
TEV2	" " " " "
TEV3	" " " " "
TEV4	" " " " "
TFW	Feedwater temperature (F)
TSAT	Saturation temperature in Drum (F)
TMAX	Maximum time for this simulation (F)
T1SH1	1st superheater section metal temperature (F)
T1SH2	" " " " " "
T1SH3	" " " " " "
T1SHE1	1st superheater section inlet temperature (F)
T1SHE2	" " " " " "
T1SHE3	" " " " " "
T1SHO1	1st superheater section outlet temperature (F)
T1SHO2	" " " " " "
T1SHO3	" " " " " "

T2SH1	2nd superheater section metal temperature (F)
T2SH2	" " " " "
T2SH3	" " " " "
T2SHE1	2nd superheater section inlet temperature (F)
T2SHE2	" " " " " "
T2SHE3	" " " " " "
T2SHO1	2nd superheater section outlet temperature (F)
T2SHO2	" " " " " "
T2SHO3	" " " " " "
UADRUM	Drum overall heat transfer factor (BTU/F)
UAEC	Economizer overall heat transfer factor (BTU/F)
UAEV	Evaporator " " " " "
UA1SH	1st superheater overall heat transfer factor (BTU/F)
UA2SH	2nd superheater " " " " "
VSL	Specific volume saturated liquid
VSS	Specific volume saturated steam
WDES	Flow rate, desuperheating water (lbm/sec)
WDESTM	Temporary valve storage
WFIN	Final steam mass flow (lbm/sec)
WFW	Feedwater to economizer flow rate (lbm/sec)
WREC	Recirculation flow rate (lbm/sec)
WSL	Mass saturated liquid in drum (lbm)
WSS	Mass saturated steam in drum (lbm)
WSSTEM	Temporary value storage
WSTM	Steam flow from drum (lbm/sec)

APPENDIX F

Data Reduction Program Listing (HTLRFD1)

General

A listing of the data reduction program is given in this appendix.

Average instrument readings are designated as R(I) in millivolts. (I being the instrument index number.) That is, R(I) corresponds to the reading of instrument No. I. The instrument output in psid, psig, ^{o}F, etc. is designated as V(I). The measurement errors of the instrument readings and instrument readings and instrument outputs are designated as SR(I) and SV(I). In general, any variable with an S prefix is an error term used in the accuracy analysis. This is used as an aid to distinguish between calculation of average values and the calculation of errors of the average values.

Read Conversion Constants and Zero Data File

This section reads the constants used to reduce instrument millivolt readings to desired outputs of PSI, ^{o}F, etc.

Read Instrument Index Numbers

The first section reads the instrument index numbers for Chromel-Alumel thermocouples, pressure cells, differential pressure cells, resistance temperature devices and watt transducers.

Read Conversion Constants

This section reads the conversion constants to convert millivolts to psi, ^{o}F, etc. This section also reads the instrument calibration error as the 6th value of the constants for each instrument. These constants are listed in the instrument constant file (TAPE88).

Read Orifice Dimensions

This section reads the orifice pipe diameter, orifice diameter, and the measurement error of each value for all the orifice meters. These values are contained in the instrument constant file (TAPE88).

Read Zero Data

This section reads the daily or periodic zero reference readings of each cell for use in converting instrument millivolt readings to the desired output. These values are contained in the instrument constant file. As a matter of convenience, these are stored in the constant file as millivolts. The zeros are subtracted from the average value from the data scanner. The span values of line 1280 are read last. They are also in millivolts.

Read Test Data

Read Manual Scanner Data

Certain data cannot be easily converted to a voltage for recording by the data scanner. This data is entered manually into the data scanner via teletype terminal keyboard and is stored as the first items on the data scanner output tape. This data is then stored in the data file (TAPE1).

The manual data is as follows: A test point identification number, test time, and test date. This is followed by three index numbers of 1 or 0 which indicate whether there is flow (index number = 1) or not (index number = 0). Three flows are circulating water A flow, circulating water B flow and steam flow, in this order. Next, the barometric pressure in mmHg and barometer temperature in ^{o}C are given for use in calculating the barometric pressure. Finally, the number of thermocouples on which DNB occurred, and corresponding instrument numbers of the thermocouples are read. If no DNB occurs; then 1, 10 is given.

Read Scanner Instrument Data

The data recorded by the data scanner is next read. The first data is the time at which each data scan was recorded with the first scan being time zero.

The instrument data is next read for instruments Nos. 0 - 80. Instrument No. 0 is a channel on the data scanner which is shorted and gives a zero input voltage to the data scanner digital voltmeter. This zero voltage reading is used as a reference value to be subtracted from all other readings to account for zero drift of the voltmeter.

Two sums are next calculated for each instrument. S1(J) is the "sum of the readings" of each instrument for all scans. S2(J) is the "sum of the readings squared" of each instrument for all scans. These sums are used later to calculate the average value of readings for each instrument and to calculate the standard error or scatter of the readings around the average.

The sum S1(J) is also used to subtract the digital voltmeter zero reference and each instrument zero from the readings for later conversion to the desired output.

Calculate Average and Deviation of Readings

The average reading value of all the scans R(J) is calculated for each instrument. Also, the standard error of the readings or scatter SR(J) for all the instruments is calculated.

Instrument Conversion

The following sections describe the data reduction procedures for each type of instrument.

Barometric Pressure Conversion

The barometric pressure is converted from mm Hg to psia in this section. The barometer temperature is used to correct for mercury density changes and scale expansion. Also, a gravitational correction is made.

Thermocouple Data Conversion

Thermocouple emf readings are converted to temperatures using a routine obtained from the IPTS-68 standards. These routines have been modified to determine the error of each temperature calculated as follows.

The average reading R(K) is used to calculate the average temperatures V(K) for each thermocouple. The standard reading error SR(K) is added to the average reading R(K) for each thermocouple and a second temperature is calculated for this total. The standard error, SV(K), of the temperature is then calculated for each thermocouple as the difference between the first and second calculated temperatures. This temperature error is then added to the calibration error to obtain the total temperature error. For this test, the calibration error is $2^{o}F$ as recommended in the IPTS-68 tables.

RTD Conversion

Temperatures are calculated for each Resistance Temperature Device (RTD) in this section. The average temperature is calculated from a quadratic equation of the average RTD reading.

The temperature error is calculated by adding the reading error to the average reading; calculating the resulting temperature; and subtracting the average temperature from this temperature. This error is then added to the calibration error C(6,K) to obtain the total temperature error.

Pressure Cell Conversion

Pressures are calculated for each pressure cell in this section. A cold leg density V1 is calculated for use with the constant C(1,K) to correct for elevation differences between the pressure cell and pressure tap. The average pressure is calculated as linear function between the zero and span voltage reading with a sinusoidal nonlinear term added to the linear function. The elevation correction and the barometric pressure is then added to each pressure to obtain the absolute pressure in psia.

The pressure errors are calculated for each pressure cell as follows. The reading error is added to the average reading and a second pressure is calculated. The average pressure is subtracted from this value. This resulting difference is added to the calibration error to obtain the total accuracy for each pressure cell.

Differential Pressure Cell Conversion

Differential pressures from tap to tap are calculated in this section. The cold density, V1, calculated for pressure cell conversion is used to correct for elevation differences in the tubing connecting the taps to the differential pressure cell (dp cell). The differential pressure measured by the dp cell is calculated as a linear function of the average dp cell reading. The dp cells used for this test are not sensitive to static case pressure.

The dp cell tolerences are calculated by adding the reading error to the average reading, calculating a differential pressure from this value, and subtracting the average differential pressure to obtain the error due to reading error.
The calibration error is then added to the reading error to obtain the total error.

Watt Transducer Conversion

Power input from the SCR to test section is calculated in this section. For this conversion, also a quadratic equation of the average Watt transducer reading is used to calculate the power input.

Calculate Mass Flow

Total flow rate of the circulating water A flow, B flow, and steam flow is calculated using subroutine FLOW. This subroutine calculates the flow rate for ASME Thin Plate Flange Tap orifice meters in accordance with standard ASME procedures.

Each flow is calculated independently and summed later. If flow index is 0 the calculation of that flow is skipped. Calculations of circulating water A flow, B flow and steam flow are done using the output from differential pressure cells. For low steam flow, if the output from high-flow DP cell is less than 1.0 mV, then the output from the low-flow DP Cell is used.

The FLOW subroutine has been expanded to also calculate the enthalpy of the fluid flowing through the orifice. The 1967 ASME Steam Table routines used with an input pressure, temperature, and steam-water index are used for this calculation.

The FLOW subroutine also calculates the flow rate accuracy and the enthalpy accuracy from the errors of various measurements used to determine the flow and enthalpy.

Calculate Outlet Pressure and Saturation Temperature

Test section outlet pressure is obtained by subtracting total pressure drop in the test section from the inlet pressure.

Saturation temperature of the test section is then obtained with above pressure, using the steam table function TSL.

Calculate Heat Loss

In this section, both preheater and test section heat losses are calculated. To determine a heat loss coeficient, some heat loss tests were conducted. Heat loss is calculated by multiplying the heat loss coeficient and temperature difference. For preheaters (A and B), temperature difference means the difference between an average of preheater inlet and outlet temperatures and ambient temperature. And for each test section, temperature difference is defined as difference between the average heater element temperature and ambient temperature. Heat loss coefficient and when it is applied to each test section is divided by four, i.e. the number of test sections. Thermocouples (see Figure 7.3) are used to measure the heater element surface temperature.

Calculate Total Power and Preheat Power

Total power input is calculated as the summation of the inputs of total A bus, total B bus and total NM bus watt transducers. The preheat power is calculated from power input from SCRs A1, A2, B1 and B2.

Calculate Enthalpy

In this section the fluid enthalpy in the preheater and various parts of the test section is calculated. The preheater inlet enthalpy is obtained from the water flow measurement orifices at the inlet of the preheater. The preheater exit quality is calculated with the inlet enthalpy, fluid flow rate, and preheat electric input power minus the preheat heat loss.

The test section inlet enthalpy is equal to the preheat outlet enthalpy. Fluid enthalpies at various points in the test section are calculated with the inlet enthalpy, fluid flow rate, and cummulative test section electric heat input to that point minus the heat loss.

Calculate Test Section Properties

In this section various test section properties are calculated to characterize DNB.

Calculate Test Section Power and Heat Flux

Heat transfer area is calculated for each test section using inner diameter. To simulate the 180^{o} actual heat input, heat transfer area is defined as a half of inner surface area. For rifled tube sections, major or rib root diameter is used. Also, the nominal heated length (48 in) of the heating elements is used. The unit is also converted from square inch to square feet.

Each test section piece has different power source as shown in Figure . Each power input is decreased by heat loss and, divided by the heat transfer area converted from KW/ft^2 to BTU/ft^2hr.

Calculate Quality

Quality is defined as a ratio of enthalpy of fluid minus saturated liquid enthalpy divided by the enthalpy difference between saturated vapor and saturated liquid at the test section outlet pressure. Qualities at various points in the test section are calculated in this section using this relation and enthalpies obtained in the previous section.

Calculate Fluid Properties (Test Section Outlet)

In this section, fluid properties are calculated based on test section outlet conditions through subroutines and functions used to formulate the 1967 ASME Steam Tables. Those fluid properties are specific volumes of saturated steam and water, viscosities of steam and water, surface tension, both steam and water thermal conductivities and saturated enthalpies.

Printing Results

The print statements along with format specifications are listed in this section to produce the output data sheet described above.

Writing Results to Storage File (TAPE49)

In addition to the results printed on the output data sheet selected values are written into file TAPE49 and stored permanently in the computer for later data analysis. The selected values enable all results to be calculated from those stored while minimizing the duplication of data stored. The data stored in file TAPE49 does not contain any of the accuracy values. The accuracy values are evaluated manually during data analysis using values from the printout sheets.

Subroutines

The subroutines are listed in this section.

Subroutine FLOW

This subroutine calculates flow rates using the procedures for ASME Thin Plate Flange Tap orifices. Inputs and outputs of the routine follow ;

DP - orifice differential pressure (psid)

P - orifice fluid pressure (psia)

T - orifice fluid temperature (^{o}F)

D - orifice pipe diameter (in)

DO - orifice diameter (in)

I - fluid index 1 = water, 2 = steam

W - the calculated flow rate (lb/hr)

FH - the calculated fluid enthalpy (BTU/lb)

SDP - differential pressure error (psid)

SP - pressure error (psia)

ST - temperature error (^{o}F)

SD - pipe diameter error (in)

SDO - orifice diameter error (in)

SW - flow accuracy (lb/hr)

SFH - enthalpy accuracy (BTU/lb)

Subroutine SRSORT

This subroutine calculates properties of superheated steam and subcooled water.

P - pressure (psia)

R - temperature (^{o}F)

V - the calculated specific volume (ft^3/lb)

H - the calculated enthalpy (BTU/lb)

ISAT - index; 1 for non-saturation point, 2 for saturation point VG - the calculated specific volume of saturated vapor, if ISAT=2.

HG - the calculated enthalpy of saturated vapor, if ISAT=2

Also, if ISAT=2, V and H are specific volume and enthalpy of saturated liquid, respectively.

Subroutine SATUR

This subroutine calculates properties of saturated steam and water.

P - pressure (psia)
T - temperature (^{o}F)
one or other input, the other will be returned

VF - the calculated specific volume of saturated liquid (ft^3/16)

HF - the calculated enthalpy of saturated liquid (BTU/lb)

VG - the calculated specific volume of saturated vapor (ft^3/lb)

HG - the calculated enthalpy of saturated vapor (BTU/lb)

K - index, indicates whether pressure or temperature input

1-pressure, 2-temperature, 3-both.

Subroutine TENS

This subroutine calculates the surface tension of saturated liquid.

TIN - temperature (^{o}F)

S - the calculated surface tension (lb/ft)

Error Analysis

The uncertainty for each output from the data reduction program is calculated as follows.

First, for each instrument output an uncertainty is calculated based on two components--the calibration uncertainty and the drift during the data scan. Calibration uncertainty for each instrument is measured during the pre and post-test instrument calibrations and was found not to change significantly throughout the test program. The values for each instrument are stored in computer file TAPE88 as described above. The uncertainty due to the drift of the measured quantities during the test scan is calculated by comparint the five readings taken during the data scan for each instrument. By assuming a normal distribution and calculating a mean value from the five readings, an uncertainty can be determined from the equation.

$$\sigma_{x_{drift}} = \sqrt{\frac{\Sigma x^2 - \frac{(\Sigma x)^2}{5}}{4}}$$

The instrument standard error for a particular data run is then calculated by combining the calibration error with the uncertainty due to drift:

$$\sigma_{reading} = \sqrt{\sigma^2_{cal} + \sigma^2_{drift}}$$

(The σ used here for uncertainty is equivalent to the standard deviation used in statistical analysis. For a measurement with normally distributed errors, approximately 63% of all the measurements of a particular quantity will fall within one standard deviation of the actual value.)

For derived values and functions based on the measured quantities the error in the evaluated function is evaluated by combining the instrument errors based on their relative influence upon the final value.

For a function F with variables $X_1, X_2, X_3 \ldots X_n$

with uncertainties $\sigma_1, \sigma_2, \sigma_3 \ldots \sigma_n$

The uncertainty σ_F is given by:

$$\sigma_F = \left[\left(\frac{\partial F}{\partial x_1}\sigma_1\right)^2 + \left(\frac{\partial F}{\partial x_2}\sigma_2\right)^2 + \left(\frac{\partial F}{\partial x_3}\sigma_3\right)^2 + \left(\frac{\partial F}{\partial x_n}\sigma_n\right)^2\right]^{\frac{1}{2}}$$

These uncertainties are calculated by the data reduction program for each measured and evaluated value for every test point. The calculated uncertainties are printed on the computer output next to the primary value. Errors due to drifting pressure or flow can be recognized quickly by the operators and the test repeated if necessary.

```
*P*
CHTL
      PROGRAM HTLRED1(INPUT,OUTPUT,TAPE88,TAPE6=OUTPUT,TAPE1,TAPE49)
      DIMENSION PAC(9),R(80),S1(80),S2(80),S3(80),SR(80)
      DIMENSION Z(80),KCA(80),KP(5),KDP(80),KRTD(5)
      DIMENSION KKW(80),ODT(10),SODT(10),CLOS(6)
      DIMENSION D(5),DO(5),SDO(5),SD(5),II(80)
      DIMENSION C(6,80),SV(80),V(80)
      DIMENSION H(10,10),SH(10,10)
      DIMENSION KCM(10),NSCR(10),KSCR(10,10),KE(10),ET(8,8),ETT(10)
      DIMENSION DI(10),SDI(10),CK(10),NTC(10),KTC(10,10)
      DIMENSION TKW(10),STKW(10),QA(10),SQA(10),X(10,10),SX(10,10)
      DIMENSION DX(10),SDX(10)
      DATA IBL,IDNB/3H   ,3HDNB/
C
      READ(1,119)IRUN
  119 FORMAT(I2)
      DO 2001 ITST=1,IRUN
C     INITIALIZE VARIABLES
      DO 10 I=1,80
      Z(I)=0.
      S1(I)=0.
      S2(I)=0.
   10 CONTINUE
C
C     READ CONVERSION CONSTANTS AND ZERO DATA
      REWIND 88
      READ(88,105)
      READ(88,120)DATE98
      READ(88,105)
  105 FORMAT(A10)
      READ(88,*) NI
      READ(88,*)NCA,(KCA(I),I=1,NCA)
      READ(88,*)NP,(KP(I),I=1,NP)
      READ(88,*)NDP,(KDP(I),I=1,NDP)
      READ(88,*)NRTD,(KRTD(I),I=1,NRTD)
      READ(88,*)NKW,(KKW(I),I=1,NKW)
      READ(88,*) NCM,(KCM(I),I=1,NCM)
C
C     READ TEST SECTION PROPERTIES
      READ(88,105)
      READ(88,*) NTS
      DO 80 N=1,NTS
      READ(88,*) NSCR(N) $ L=NSCR(N)
      READ(88,*) (KSCR(N,I),I=1,L)
   80 CONTINUE
      DO 70 N=1,NTS
      READ(88,*) KE(N) $ L=KE(N)
      READ(88,*) (ET(N,I),I=1,L)
70    CONTINUE
      READ(88,*) NTS,(ODT(N),N=1,NTS)
      READ(88,*) NTS,(SODT(N),N=1,NTS)
      READ(88,*) NTS,(DI(N),N=1,NTS)
      READ(88,*)NTS,(SDI(N),N=1,NTS)
      READ(88,*)NTS,(CK(N),N=1,NTS)
      SET=0.25 $ SETT=SQRT(2.*(SET*SET))
      DO 92 N=1,NTS
      READ(88,*) NTC(N) $ L=NTC(N)
92    READ(88,*) (KTC(N,I),I=1,L)
      READ(88,*)TK0,TK1
```

```
      READ(88,*) (CLOS(N),N=1,6)
C
C     READ CONVERSION CONSTANTS
      READ(88,106) IFLA
  106 FORMAT(I1)
      DO 200 I=1,NI
      READ(88,*)(C(J,I),J=1,6)
      IF(IFLA .EQ. 9) PRINT *,"C(J,I)",I,(C(J,I),J=1,6)
200   CONTINUE
C
C    READ ORIFICE DIMENSIONS
      READ(88,105)
      NDO=3
      DO 205 I=1,NDO
205   READ(88,*)D(I),DO(I),SD(I),SDO(I)
C
C     READ ZERO DATA
      READ(88,105)
      DO 207 I=1,NP
  207 READ(88,*) Z(KP(I))
      DO 210 I=1,NDP
      READ(88,*) Z(KDP(I))
      IF(IFLA .EQ. 9) PRINT*,"Z(DP)",KDP(I),Z(KDP(I))
210   CONTINUE
C
C     P CELL SPAN READINGS
      READ(88,105)
      READ(88,*)(C(5,KP(I)),I=1,NP)
      IF(IFLA .EQ. 9) PRINT*,"KP",(C(5,KP(I)),I=1,NP)
C
C     READ MANUAL SCANNER DATA
      READ(1,120)TEST
      READ(1,120) TTIME
      READ(1,120) DDATE
120   FORMAT(A10)
      READ(1,*)IFLA,IFLB,IFLS
      READ(1,*)PABS,TBAR
      READ(1,*)NB,(II(I),I=1,NB)
      READ(1,132)
 132  FORMAT(A40)
      NS=5
C
      IF(IFLA.EQ.9) PRINT *,680
C     READ SCANNER INSTRUMENT DATA
      DO 300 I=1,NS
      READ(1,130)
130   FORMAT(A40)
      READ(1,131)
 131  FORMAT(A40)
      READ(1,195) ZO,R(1),R(2),R(3),R(4)
      IF(IFLA.EQ.9) PRINT *,731,ZO,R(1),R(2),R(3),R(4)
      ZO=ZO+.0001*(I-3)
      N=-1
  135 N=N+5
      IF(N+5 .GE. NI) GO TO 140
      READ(1,195) (R(N+K),K=1,5)
      GO TO 135
  140 N=N+1
      READ(1,195) (R(K),K=N,NI)
195   FORMAT(5F10.3)
```

F.15

```fortran
      DO 280 J=1,NI
      S1(J)=S1(J)+(R(J)-Z0-Z(J))
      S2(J)=S2(J)+(R(J)-Z0-Z(J))**2
280   CONTINUE
300   CONTINUE
      IF(IFLA.EQ.9) PRINT *,860
C
C     CALCULATE AVERAGE AND DEVIATION OF READINGS
      DO 270 J=1,NI
      S3(J)=S1(J)/NS
      SR(J)=SQRT((S2(J)-S1(J)*S1(J)/NS)/(NS-1))
      IF(IFLA.EQ.9) PRINT *,920,S3(J),SR(J)
270   CONTINUE
      DO 250 J=1,NI
      R(J)=S3(J)
250   CONTINUE
      IF(IFLA.EQ.9) PRINT *,970
C INSTRUMENT CONVERSION
C
C     BAROMETRIC PRESSURE CALCULATION
      SPABS=.05/PABS
      PABS=(1-.000622*(TBAR-22))*PABS
      PABS=PABS*(.9999924-1.811241E-4*TBAR+2.075103E-8*TBAR*TBAR)
      PABS=PABS-.2
      PABS=.0193367617*PABS
      SPABS=SPABS*PABS
C
      IF(IFLA.EQ.9) PRINT *,1080
C THERMOUCOUPLE DATA CONVERSION
      DATA PAC/-1.8533063273E+1,3.8918344612E+1,1.6645154356E-2,
     *-7.870237448E-5,2.2835785557E-7,-3.5700231258E-10,
     *2.9932909136E-13,-1.2849848798E-16,2.2239974336E-20/
      DO 396 I=1,NCA
      K=KCA(I)
      IF(R(K).LT.-2.65)GO TO 396
      IF(R(K).GT.40.)GO TO 396
      R(K)=R(K)+SR(K)
      SV(K)=0.
      DO 395 L=1,2
      EI=1000.*(R(K)+2.6621)
      V(K)=.0242*EI
370   T=1.
      EL=0.
      DO 383 J=1,9
      EL=EL+PAC(J)*T
      T=T*V(K)
383   CONTINUE
      EL=EL+125.*EXP(-.5*((((V(K)-127.)/65.)**2)))
      IF(ABS(EI-EL).LT.1.)GO TO 390
      V(K)=V(K)+.0242*(EI-EL)
      GO TO 370
390   CONTINUE
      V(K)=((V(K)*9.)/5.)+32.
      V(K)=V(K)+C(2,K)*R(K)
      SV(K)=SV(K)+V(K)*((-1)**L)
      R(K)=R(K)-SR(K)
      IF(R(K).GT.40.)GO TO 395
      IF(R(K).LT.(-2.65)) GO TO 395
395   CONTINUE
      R(K)=R(K)+SR(K)
```

```
      SV(K)=SQRT(C(6,K)*C(6,K)+SV(K)*SV(K))
396   CONTINUE
C
      IF(1FLA.EQ.9) PRINT *,1440
C RTD CONVERSION
      DO 400 I=1,NRTD
      K=KRTD(I)
      R(K)=R(K)-C(4,K)
      V(K)=C(1,K)+C(2,K)*R(K)+C(3,K)*R(K)*R(K)
      R(K)=R(K)+SR(K)
      SV(K)=C(1,K)+C(2,K)*R(K)+C(3,K)*R(K)*R(K)-V(K)
      SV(K)=SQRT(C(6,K)*C(6,K)+SV(K)*SV(K))
      R(K)=R(K)-SR(K)
      IF(IFLA .EQ. 9) PRINT*,"RTD",K,V(K),SV(K)
400   CONTINUE
C
      IF(IFLA.EQ.9) PRINT *,1550
C PRESSURE CELL CONVERSION
      DO 445 I=1,NP
      K=KP(I)
      CALL SRSORT(700.,V(40),V1,H1,ISAT,V2,H2)
      V1=1./(1728*V1)
      V(K)=C(1,K)*V1+C(3,K)*R(K)/(C(5,K)-Z(K))
      V(K)=V(K)+C(4,K)*SIN(3.14159*R(K)/(C(5,K)-Z(K)))
      CALL SRSORT(V(K),V(40),V1,H1,ISAT,V2,H2)
      V1=1./(1728.*V1)
      V(K)=C(1,K)*V1+C(3,K)*R(K)/(C(5,K)-Z(K))
      V(K)=V(K)+C(4,K)*SIN(3.14159*R(K)/(C(5,K)-Z(K)))
      R(K)=R(K)+SR(K)
      SV(K)=C(1,K)*V1+C(3,K)*R(K)/(C(5,K)-Z(K))
      SV(K)=SV(K)+C(4,K)*SIN(3.14159*R(K)/(C(5,K)-Z(K)))-V(K)
      SV(K)=SQRT(C(6,K)*C(6,K)+SV(K)*SV(K))
      V(K)=V(K)+PABS
      R(K)=R(K)-SR(K)
      IF(IFLA .EQ. 9) PRINT*,"P",K,V(K),SV(K)
445   CONTINUE
      CALL SRSORT(V(14),V(40)+.5,SV1T,H1,ISAT,V2,H2)
      SV1T=1./(1728.*SV1T)-V1
      CALL SRSORT(V(14)+SV(14),V(40),SV1P,H1,ISAT,V2,H2)
      SV1P=1./(1728.*SV1P)-V1
      SV1=SQRT(SV1T*SV1T+SV1P*SV1P)
      IF(IFLA .EQ. 9) PRINT*,"V1",V1,SV1,V(40),SV(40)
C
      IF(IFLA.EQ.9) PRINT *,1810
C DIFFERENTIAL PRESSURE CELL CONVERSION
      DO 505 I=1,NDP
      K=KDP(I)
      V(K)=C(1,K)*V1+(C(2,K)+C(4,K)*V(14))+(C(3,K)+C(5,K)*V(14))*R(K)
      R(K)=R(K)+SR(K)
      SV(K)=C(1,K)*V1+(C(2,K)+C(4,K)*V(14))+(C(3,K)+C(5,K)*V(14))*R(K)
      SV(K)=SV(K)-V(K)
      SV(K)=SQRT(C(6,K)*C(6,K)+SV(K)*SV(K))
      R(K)=R(K)-SR(K)
      IF(IFLA .EQ. 9) PRINT*,"DP",K,V(K),SV(K),V1
505   CONTINUE
      IF(R(15).LT.0.0) V(15)=0.0
       IF(R(16).LT.0.0) V(16)=0.0
C
      IF(IFLA.EQ.9) PRINT *,1930
C      WATTS TRANSDUCER CONVERSION
```

```
      DO 600 I=1,NKW
      K=KKW(I)
      V(K)=C(1,K)*(C(2,K)+C(3,K)*R(K)+C(4,K)*R(K)*R(K))
      R(K)=R(K)+SR(K)
      SV(K)=C(1,K)*(C(2;K)+C(3,K)*R(K)+C(4,K)*R(K)*R(K))-V(K)
      SV(K)=SQRT(C(6,K)*C(6,K)+SV(K)*SV(K))
      R(K)=R(K)-SR(K)
      IF(IFLA .EQ. 9) PRINT*,"KW",K,V(K),SV(K)
600   CONTINUE
      IF(IFLA.EQ.9) PRINT *,2100
C
C     CALCULATE MASS FLOW
      WA=WB=WS=HSO=0.
      SWA=SWB=SWS=SHSO=0.
      IF(IFLA.EQ.0)GO TO 610
      DPA=V(7)  $  IF(DPA .LT. 1.0) DPA=V(8)
      SDPA=SV(7)  $  IF(DPA .LT. 1.0) SDPA=SV(8)
      CALL FLOW(DPA,V(5),V(6),D(1),DO(1),1,WA,HPD,SDPA,
     1 SV(5),SV(6),SD(1),SDO(1),SWA,SHPD,IFLA)
610   CONTINUE
      IF(IFLB.EQ.0)GO TO 620
      DPB=V(9)  $  IF(DPB .LT. 1.0) DPB=V(10)
      SDPB=SV(9)  $  IF(DPB .LT. 1.0) SDPB=SV(10)
      CALL FLOW(DPB,V(5),V(6),D(2),DO(2),1,WB,HPD,SDPB,
     1 SV(5),SV(6),SD(2),SDO(2),SWB,SHPD,IFLA)
620   CONTINUE
      IF(IFLS.EQ.0)GO TO 622
      DPS=V(3) $ IF(V(3).LT.3.5) DPS=V(4)
      SDPS=SV(3) $ IF(V(3).LT.3.5) SDPS=SV(4)
      CALL FLOW(DPS,V(1),V(2),D(3),DO(3),2,WS,HSO,SDPS,SV(1),SV(2),SD
     &,SDO(3),SWS,SHSO,IFLA)
622   CONTINUE
      WAB=WA+WB
      WT=WA+WB+WS
      SWAB=SQRT(SWA**2+SWB**2)
      SWT=SQRT(SWA*SWA+SWB*SWB+SWS*SWS)
      GWTR=WT*4.*144./(3.14159*DI(4)*DI(4))
      SGWTR=SWT*GWTR/WT
      IF(IFLA.EQ.9) PRINT *,2270,WA,WB,WS,WAB,WT,HPD,HSO
C
C     CALCULATE INLET PRESSURE
      PI=V(14)+V(15)  $  PO=V(14)  $  SPO=SV(14)  $  POD=PO+SPO
      SPI=SQRT(SV(14)*SV(14) + SV(15)*SV(15))
      IC1=1
      CALL SATUR (PI,TI,VF,HF,VG,HG,IC1)
C
C     OUTLET SAT TEMP
      TSAT=TSL(PO)
      STSAT=TSAT-TSL(PO-SPO)
      TSATD=TSAT + STSAT
      IF(IFLA.EQ.9) PRINT *,2340
C
C     CALCULATE HEAT LOSS
C
C     TEST SECTION HEAT LOSS
      DO 690 N=1,NTS
      TLOS1=(V(41+2*N)+V(42+2*N))*0.5 - V(40)
      STLOS1=SQRT(0.5*(SV(41+2*N)**2)+0.5*(SV(42+2*N)**2)
     1          +SV(40)*SV(40))
      TKW(N)=(CLOS(1)+CLOS(2)*TLOS1)/4.
```

```
      IF(IFLA .EQ. 9) PRINT *,"TKW ",TKW(N)
  690 STKW(N)=SQRT((0.25*CLOS(2)*STLOS1)**2     +CLOS(3)*CLOS(3))
C
C     PREHEAT POWER LOSS
      TLOS2=(V(6)+V(17))*0.5 - V(40)
      STLOS2=SQRT(0.5*(SV(6)*SV(6))+0.5*(SV(17)*SV(17))+SV(40)*SV(40))
      PHP=CLOS(4) + CLOS(5)*TLOS2
      IF(IFLA .EQ.9) PRINT *,"PHPLOSS ",PHP
      SPHP=SQRT((CLOS(5)*STLOS2)**2  +CLOS(6)*CLOS(6))
C
C  CALCULATE PREHEAT POWER
      PHP=V(20)+V(21)+V(22)+V(23) + PHP
      SPHP=SQRT(SV(20)*SV(20) + SV(21)*SV(21) + SV(22)*SV(22)
     1      + SV(23)*SV(23) + SPHP*SPHP)
C
C     PREHEAT OUTLET ENTHALPY
      HPHO=HPD + 3410.*PHP/WAB
      SHPHO=3410.*PHP/WAB * SQRT((SPHP/PHP)**2 + (SWAB/WAB)**2)
      SHPHO=SQRT(SHPD*SHPD + SHPHO*SHPHO)
C
C     TEST SECTION INLET ENTHALPY
      HTSI=(WAB*HPHO + WS*HSO)/WT
      SHTS1=SQRT((SWAB/WAB)**2 + (SHPHO/HPHO)**2) * WAB*HPHO
      SHTS2=0.
      IF(IFLS.NE.0) SHTS2=SQRT((SWS/WS)**2 + (SHSO/HSO)**2) * WS*HSO
      SHTSI=SQRT(SHTS1*SHTS1 + SHTS2*SHTS2)
      SHTSI=SQRT((SHTSI/WT/HTSI)**2 + (SWT/WT)**2) * HTSI
      IF(IFLA .EQ. 9) PRINT *,HPHO,SHPHO,HTSI,SHTSI
C
C
C     CALCULATE TEST SECTION PROPERTIES
C
C     CALCULATE TEST SECTION POWER AND HEAT FLUX
      DO 700 N=1,NTS
      L=NSCR(N)
      DO 710 I=1,L
      TKW(N)=TKW(N)+V(KSCR(N,I))
      IF(IFLA .EQ. 9) PRINT *,TKW(N)
      STKW(N)=STKW(N)+(SV(KSCR(N,I)))**2
  710 CONTINUE
      STKW(N)=SQRT(STKW(N))
      ETT(N)=ET(N,KE(N)-1)-ET(N,2)
      QA(N)=3410*TKW(N)/(3.14159*CK(N)*DI(N)*ETT(N)/144)
      SQA(N)=(STKW(N)/TKW(N))**2+(SDI(N)/DI(N))**2
      SQA(N)=SQA(N)+(SETT/ETT(N))**2
      SQA(N)=QA(N)*SQRT(SQA(N))
      IF(IFLA .EQ. 9) PRINT *,N,ETT(N),TKW(N),QA(N)
  700 CONTINUE
C
C     CALCULATE QUALITY
      IC1=1
      CALL SATUR(V(14),TSLO,VF,HF,VG,HG,IC1)
      IF(IFLA.EQ.9) PRINT *,2645,V(14),TSLO,HF,HG
      IC1=1
      CALL SATUR(V(14)+SV(14),STSLO,SVF,SHF,SVG,SHG,IC1)
      SVF=SVF-VF $ SVG=VG-SVG $ STSLO=STSLO-TSLO
      SHF=SHF-HF $ SHG=HG-SHG $ SHFSAT=SHF $ SHGSAT=SHG
      VGSAT=VG   $ VFSAT=VF    $ HFSAT=HF    $ HGSAT=HG
      HFG=HG-HF  $ SHFG=SQRT(SHG*SHG+SHF*SHF)
      X(1,2)=((HTSI-HF)/HFG)*100.
```

```
      IF(IFLA.EQ.9) PRINT *,2695,HFD,HFG
      SX(1,2)=SQRT(SHTSI**2+SHF**2)
      SX(1,2)=X(1,2)*SQRT((SX(1,2)/(HTSI-HF))**2+(SHFG/HFG)**2)
      IF(IFLA .EQ. 9) PRINT *,X(1,2),SX(1,2)
      DO 800 N=1,NTS
      IF(IFLA.EQ.9) PRINT *,2715,N,X(N,2)
      DX(N)=(TKW(N)*3410/(WT*HFG))*100.
      IF(IFLA.EQ.9) PRINT *,2725,TKW(N),WT,HFG
      SDX(N)=DX(N)*SQRT((STKW(N)/TKW(N))**2+(SWT/WT)**2+(SHFG/HFG)**2)
      L=KE(N)-1
      DO 810 I=3,L
      X(N,I)=X(N,I-1)+DX(N)*(ET(N,I)-ET(N,I-1))/ETT
      IF(IFLA.EQ.9) PRINT *,2765,X(N,I),X(N,I-1),DX(N),ET(N,I),ET(N,I-
      IF(IFLA.EQ.9) PRINT *,2765,ET(N,KE(N)),N,I
      SX(N,I)=SETT
      SX(N,I)=(X(N,I)-X(N,I-1))*SQRT((SDX(N)/DX(N))**2 +
     1 (SX(N,I)/(ET(N,I)-ET(N,I-1)))**2 + (SETT/ETT)**2)
      SX(N,I)=SQRT(SX(N,I-1)*SX(N,I-1) + SX(N,I)*SX(N,I))
  810 CONTINUE
       X(N+1,2)= X(N,KE(N)-1)
      SX(N+1,2)=SX(N,KE(N)-1)
      IF(IFLA.EQ.9) PRINT *,2807,X(N+1,2)
  800 CONTINUE
      IF(IFLA.EQ.9) PRINT *,2825
C
C     CALCULATE THERMAL FILM COEFFICIENT
      DO 820 N=1,NTS
      L=NTC(N)
      DO 830 I=1,L
      TK=TK0+TK1*V(KTC(N,I))
      STK=TK0+TK1*(V(KTC(N,I))+SV(KTC(N,I)))-TK
      IF(IFLA .EQ. 9) PRINT *," TK,STK ",TK,STK
      H(N,I)=(V(KTC(N,I))-TSLO)/QA(N)
      SH(N,I)=SQRT(SV(KTC(N,I))**2+STSLO**2)
      SH(N,I)=SQRT((SH(N,I)*QA(N)/H(N,I))**2+(SQA(N)/QA(N))**2)
      SH(N,I)=SH(N,I)*H(N,I)
      H1=(DI(N)/2)*ALOG(ODT(N)/DI(N))/TK
      IF(IFLA.EQ.9) PRINT *,2940,H1
      SH1=(ALOG((DI(N)+SDI(N))/DI(N))/ALOG(1.5/DI(N)))**2
      SH1=SQRT(SH1+(SDI(N)/DI(N))**2+(STK/TK)**2)*H1
      H(N,I)=H(N,I)-H1
      SH(N,I)=SQRT(SH(N,I)**2+SH1**2)
      SH(N,I)=SH(N,I)*H(N,I)*H(N,I)
      IF(IFLA .EQ. 9) PRINT *,H1,SH1,H(N,I),SH(N,I)
  830 CONTINUE
      IF(IFLA.EQ.9) PRINT *,3015,KTC(N,L),H(N,L)
  820 CONTINUE
      IF(IFLA.EQ.9) PRINT *,3030
C
C     CALCULATE FLUID PROPERTIES (TEST SECTION OUTLET)
C
C     VISCOSITY
      VISG=3600.*VISV(PO,TSAT)
      SVISG=3600.*VISV(POD,TSATD)-VISG
      VISF=3600.*VISL(PO,TSAT)
      SVISF=VISF-3600.*VISL(POD,TSATD)
C
C     SURFACE TENSION
      CALL TENS(TSAT,TEN)
      CALL TENS(TSATD,STEN)
```

```
      STEN=TEN-STEN
C
C     CONDUCTIVITY
      CONG=CONDV(PO,TSAT)
      SCONG=CONDV(POD,TSATD)-CONG
      CONF=CONDL(PO,TSAT)
      SCONF=CONF-CONDL(POD,TSATD)
C
      IF(IFLA.EQ.9) PRINT *,3770
C     DO 960 I=1,3
C 960 PRINT 950
C 950 FORMAT(///)
      PRINT 970,NI
970   FORMAT(/ *    INSTRUMENT READING - MV - #0-*,I2)
      PRINT 195,ZO,(R(I)+Z(I),I=1,NI)
      PRINT 980,NI
980   FORMAT(/ *    INSTRUMENT OUTPUT        #0-*,I2)
      PRINT 195,ZO,(V(I),I=1,NI)
      PRINT 990,NI
990   FORMAT(/ *    INSTRUMENT STD ERROR     #0-*,I2)
      PRINT 195,ZO,(SV(I),I=1,NI)
      PRINT 995
995   FORMAT(/ *   TEST LOOP ENTHALPIES*)
      IF(IFLA.EQ.9) PRINT 195,V(14),V(5),PO,V(2),V(6),V(17),V(18)
      CALL SRSORT(V(1),V(2),V1,HPDSTM,ISAT,VG,HG)
      CALL SRSORT(V(5),V(6),V1,HPHSTM,ISAT,VG,HG)
      CALL SRSORT(PO,V(18),V1,HTSOST,ISAT,VG,HG)
      CALL SRSORT(PO+V(15),V(17),V1,HTINL,ISAT,VG,HG)
      PRINT 195,HPDSTM,HPHSTM,HTSOST,HTINL,HFSAT,HGSAT
      PRINT 195,PI,TI,PO,TSLO,WA,WB,WS
      IF(IFLA.EQ.9) PRINT 195,V(1),V(5),PO,V(2),V(6),V(17),V(18)
C
C     PRINT HEADINGS
      PRINT 1000
 1000 FORMAT(//////// *    C E KREISINGER DEVELOPMENT LABORATORY*)
      PRINT 1010
 1010 FORMAT( *     PROJECT #900255  SANDIA SOLAR RECEIVER RIFLED TUBE
     1B TEST*)
      PRINT 1020,TEST,TTIME,DDATE
 1020 FORMAT( *      TEST #  *,A10,*    TIME  *,A10,*    DATE  *,A10)
C
C     PRINT TEST SECTION CONDITIONS
      PRINT 1030
 1030 FORMAT(/ *    TEST SECTION CONDITIONS*)
      PRINT 1040,PO,SPO
 1040 FORMAT( *     OUTLET PRESSURE*,14X,F7.1,*   +/- *,F6.1,4X,*PSIA*
      PRINT 1050,WT,SWT
 1050 FORMAT( *     TOTAL FLOW      *,11X,E11.4,* +/- *,E9.2,
     &* LB/HR*)
      PRINT 1054,GWTR,SGWTR
 1054 FORMAT( *     RIFLED MASS FLOW *,10X,E11.4,* +/- *,E9.2,
     &* LB/HR-FT2*)
      PRINT 1060
 1060 FORMAT( /*        TC#  ELEV  TEMP  HEAT FLUX  AT  TC  QUALITY AT
     &C   DNB*)
      PRINT 1070
 1070 FORMAT( *          (IN)        (1000 BTU/HR-FT2)        (PCT)*)
      DO 1110 I=1,NTS
      K=NTS+1-I
      KI=NTC(K)
```

```
      FLXTC=QA(K)/1000.
      SFLXT=SQA(K)/1000.
      DO 1090 L=1,K1
      ICD=IBL
      L1=K1+1-L
      DO 1075 J=1,NB
      IF(KTC(K,L1) .EQ. II(J)) ICD=IDNB
 1075 CONTINUE
 1090 PRINT 1080,KTC(K,L1),ET(K,L1+2),V(KTC(K,L1)),FLXTC,SFLXT,X(K,L1+2
     1   ,SX(K,L1+2),ICD
 1080 FORMAT(8X,I2,2F6.0,3X,F7.1,* +/-*,F4.1,4X,F5.1,* +/-*,F4.1,
     1 3X,A3)
 1110 CONTINUE
C
C     PRINT PRESSURE DROPS
      PRINT 1120
 1120 FORMAT(//,5X,*PRESSURE DROPS*)
      PRINT 1130
 1130 FORMAT(7X,*LOCATION*,12X,*INLET  QUALITY  OUTLET QUALITY*,
     &4X,*PRESSURE DROP*)
      PRINT 1140
 1140 FORMAT(31X,*(PCT)*,11X,*(PCT)*,13X,*(PSID)*)
      PRINT 1160,X(1,2),SX(1,2),X(4,7),SX(4,7),V(15),SV(15)
 1160 FORMAT(7X,*TOTAL TEST SECTION*,2X,F5.1,* +/- *,F4.1,2X,F5.1,
     &* +/- *,F4.1,3X,F5.2,* +/- *,F5.2)
      PRINT 1170,X(3,2),SX(3,2),X(4,7),SX(4,7),V(16),SV(16)
 1170 FORMAT(7X,*UPPER TEST SECTION*,2X,F5.1,* +/- *,F4.1,2X,F5.1,
     &* +/- *,F4.1,3X,F5.2,* +/- *,F5.2)
      PRINT 1175,V(68),(V(I),I=74,79)
 1175 FORMAT(/,5X,*RIB TEMPERATURE PROFILE*,/,4X,7F8.1)
C
C     PRINT TEST SECTION OUTLET FLUID PROPERIES
      PRINT 1180
 1180 FORMAT(//,5X,*TEST SECTION OUTLET FLUID PROPERTIES*)
      PRINT 1190,TSAT,STSAT
 1190 FORMAT(7X,*SAT TEMPERATURE*,15X,F6.1,* +/- *,F4.1,6X,*F*)
      PRINT 1200,VGSAT,SVG
 1200 FORMAT(7X,*STEAM SPEC VOL*,14X,F8.5,* +/- *,F8.5,2X,*FT3/LB*)
      PRINT 1210,VFSAT,SVF
 1210 FORMAT(7X,*WATER SPEC VOL*,14X,F8.5,* +/- *,F8.5,2X,*FT3/LB*)
      PRINT 1220,VISG,SVISG
 1220 FORMAT(7X,*STEAM VISCOSITY*,13X,F8.5,* +/- *,F8.5,2X,*LB/FT-HR*)
      PRINT 1230,VISF,SVISF
 1230 FORMAT(7X,*WATER VISCOSITY*,13X,F8.5,* +/- *,F8.5,2X,*LB/FT-HR*)
      PRINT 1240,TEN,STEN
 1240 FORMAT(7X,*SURFACE TENSION*,12X,F9.6,* +/- *,F9.6,* LB/FT*)
      PRINT 1250,CONG,SCONG
 1250 FORMAT(7X,*STEAM THERM CONDUCTIVITY*,5X,F7.4,* +/- *,F7.4,3
     &X,*BTU/HR-FT-F*)
      PRINT 1260,CONF,SCONF
 1260 FORMAT(7X,*WATER THERM CONDUCTIVITY*,6X,F6.4,* +/- *,F7.4,3X,
     &*BTU/HR-FT-F*)
      PRINT 1270,HGSAT,SHGSAT
 1270 FORMAT(7X,*STEAM SAT ENTHALPY*,10X,F8.2,* +/- *,F5.2,5X
     &,*BTU/LB*)
      PRINT 1280,HFSAT,SHFSAT
 1280 FORMAT(7X,*WATER SAT ENTHALPY*,10X,F8.2,* +/- *,F5.2,5X,
     &*BTU/LB*)
      CALL TIME(TT) $ CALL DATE(DD)
      PRINT 1290,DATE98,TT,DD
```

Fi22

```
 1290 FORMAT(//,5X,*CONST FILE DATE *,A10,7X,*DATA REDUCED*,A10,2X,
     &A10)
      PRINT 1300
 1300 FORMAT(/,5X,*KDL PROJ LEADER .  .  .  .  .  .  .  DATE . ./ . /. .*
      PRINT 1320
 1320 FORMAT(/////)
C
C     PRINT ON TAPE49
      WRITE(49,1500) TEST,TTIME,DDATE
 1500 FORMAT(5X,3A10)
      WRITE(49,1510) PO,WT
 1510 FORMAT(4X,F7.1,4X,E11.4)
C
C  SET DNB PRINT FLAG
C       0=FULL TEST SECTION PRINT
C       1=DNB LEVELS ONLY
C
      IDNBP=1
      IF(IDNBP .EQ. 1) WRITE(49,1520) NB
 1520 FORMAT(5X,I2)
      DO 1540 I=1,NTS
      K=NTS+1-I
      K1=NTC(K)
      FLXTC=QA(K)/1000.
      DO 1540 L=1,K1
      ICD=IBL
      L1=K1+1-L
      DO 1525 J=1,NB
      IF(KTC(K,L1) .EQ. II(J)) ICD=IDNB
 1525 CONTINUE
      IF(IDNBP.EQ.0 .OR. (IDNBP.EQ.1 .AND. ICD.EQ.IDNB)) WRITE(49,1530
     1 KTC(K,L1),V(KTC(K,L1)),FLXTC,X(K,L1+2),ICD
 1540 CONTINUE
 1530 FORMAT(5X,I2,3X,F5.0,5X,E11.4,5X,F5.1,5X,A3)
      WRITE(49,1550)
 1550 FORMAT(/)
      WRITE(49,1560) X(1,2),X(4,7),V(15)
      WRITE(49,1560) X(3,2),X(4,7),V(16)
 1560 FORMAT(4X,F5.1,4X,F5.1,4X,F5.2)
      WRITE(49,1580) TSAT,VGSAT,VFSAT,VISG,VISF,TEN
 1580 FORMAT(/,4X,F5.0,2X,F8.5,2X,F8.5,2X,F8.5,2X,F8.5,2X,F9.6)
      WRITE(49,1590) CONG,CONF,HGSAT,HFSAT
 1590 FORMAT(4X,F7.4,2X,F6.4,2X,F8.2,2X,F8.2)
 2001 CONTINUE
      END
--EOR--
CFLOW
      SUBROUTINE FLOW(DP,P,T,D,DO,I,W,FH,SDP,SP,ST,SD,SDO,SW,SFH,IFLA)
3020  REAL K,K1,K2,K3,K4,K9
3021  REAL K8
      IF (IFLA.EQ.9) PRINT *,"FLOW ROUTINE"
      IF(IFLA.EQ.9) PRINT *,DP,P,T,D,DO
3025  IF(DP .LT. .0) GO TO 7320
      T1=TSAT=T
      IF(P .LE. 3208.23474) TSAT=TSL(P)
3030  IF(1.EQ.2) GO TO 3070
      IF(T1 .GT. TSAT) T1=TSAT
      CALL SRSORT(P,T1,V,FH,ISAT,VG,HG)
      CALL SRSORT(P+SP,T1,VP,FHP,ISAT,VG,HG)
      CALL SRSORT(P,T1-ST,VT,FHT,ISAT,VG,HG)
```

```
      VIS=3600.*VISL(P,T1)
      Y=1.
      SY=0.
      GO TO 3090
3070  CONTINUE
      IF(T1 .LT. TSAT) T1=TSAT
      CALL SRSORT(P,T1,V,FH,ISAT,VG,HG)
      IF(ISAT .EQ. 1) GO TO 3071
      V=VG
      FH=HG
 3071 CONTINUE
      CALL SRSORT(P-SP,T1,VP,FHP,ISAT,VG,HG)
      CALL SRSORT(P,T1+ST,VT,FHT,ISAT,VG,HG)
      IF(IFLA.EQ.9) PRINT *,5325,P,T1,V,FH,FHP,FHT,VG,HG
      VIS=3600.*VISV(P,T1)
      Y=1.-(.41+.35*((DO/D)**4.))*DP/(1.26*P)
      YD=1.-(.41+.35*((DO/(D+SD))**4.))*DP/(1.26*P)
      YDO=1.-(.41+.35*(((DO+SDO)/D)**4.))*DP/(1.26*P)
      YDP=1.-(.41+.35*((DO/D)**4.))*(DP+SDP)/(1.26*P)
      YP=1.-(.41+.35*((DO/D)**4.))*DP/(1.26*(P+SP))
      SY=SQRT((YD-Y)**2+(YDO-Y)**2+(YDP-Y)**2+(YP-Y)**2)
3090  SV=SQRT((VP-V)*(VP-V)+(VT-V)*(VT-V))
      IF(IFLA.EQ.9) PRINT *,V,VIS,Y
      SFH=SQRT((FHP-FH)*(FHP-FH)+(FHT-FH)*(FHT-FH))
3100  FA=.998721+1.78502E-5*T1+2.39695E-9*T1*T1
      FAT=.998721+1.78502E-5*(T1+ST)+2.39695E-9*(T1+ST)*(T1+ST)
      SFA=FAT-FA
3110  B=DO/D
      IF(IFLA.EQ.9) PRINT *,B
3120  K9=.6
      K=.6
3150  K1=0.
      K2=0.
      K3=0.
      K4=0.
3160  K1=(.5993+.007/D)+(.364+.076/(D**.5))*(B**4.)
3170  IF((.07+.5/D-B).LE..0) GO TO 3190
3180  K2=.4*((1.6-1./D)**5.)*((.07+.5/D-B)**2.5)
3190  IF((.5-B).LE..0) GO TO 3210
3200  K3=-(.009+.034/D)*((.5-B)**1.5)
3210  IF ((B-.7).LE..0) GO TO 3230
3220  K4=(65./(D*D)+3.)*((B-.7)**2.5)
3230  A=DO*(830.-5000.*B+9000.*B*B-4200.*B*B*B+530./SQRT(D))
3240  RO=1.E6*DO/15.
3242  K8=(K1+K2+K3+K4)/(1.+A/RO)
3244  W=1890.*K9*DO*DO*FA*Y*SQRT(DP/V)
3246  R=15.28*W/(VIS*DO)
3248  IF(R.LT.1000.) R=1000.
3250  K=K8*(1.+A/R)
       PRINT *,K,A,R
3260  IF((ABS(K-K9)).LT..0001)GO TO 3290
      IF(IFLA.EQ.9) PRINT *,K,A,R,W
3270  K9=K
      XK9=K9
3280  GO TO 3244
3290  XK9=K9
      SW=.0001+(2*SDO/DO)**2+(SFA/FA)**2
      SW=SW+(SY/Y)**2+(.5*SDP/DP)**2+(.5*SV/V)**2
      SW=SQRT(SW)*W
7320  CONTINUE
```

```
      IF(IFLA.EQ.9) PRINT *,K,R,W,A
      PRINT 9990,K,R,W,A
9990   FORMAT(2X,4F10.3)
      RETURN
3295  END
--EOR--
CSRSORT
      SUBROUTINE SRSORT(P,T,V,H,ISAT,VG,HG)
      ISAT=1
      IF(T.GT.705.47)GO TO 10
      T1=T
      PSAT=PSL(T1)
      IF(ABS(P-PSAT) .LE. 1.E-8) GO TO 60
      IF(T.LE.662.0)GO TO 30
      IF(P.GT.PSAT)GO TO 52
10    P23=P23T(T)
      IF(P.GT.P23)GO TO 50
20    V=VPT2(P,T)
      H=H2E(DMY)
      RETURN
30    IF(T.LT.25.0)GO TO 70
      IF(P.LT.PSAT)GO TO 20
40    V=VPT1(P,T)
      H=H1E(DMY)
      RETURN
50    V=VPT3D(P,T)
51    H=HVT3(V,T)
      RETURN
52    V=VPT3L(P,T)
      GO TO 51
60    ISAT=2
      K=3
      CALL SATUR(P,T,V,H,VG,HG,K)
      RETURN
70    ISAT=3
      RETURN
      END
--EOR--
CSATUR
      SUBROUTINE SATUR(P,T,VF,HF,VG,HG,K)
      GO TO(10,20,30),K
10    T=TSL(P)
      GO TO 30
20    T1=T
      P=PSL(T1)
30    IF(T.LE.662.0)GO TO 40
      VF=VPTF3(P,T)
      HF=HVT3(VF,T)
      VG=VPTG3(P,T)
      HG=HVT3(VG,T)
      RETURN
40    VF=VPT1(P,T)
      HF=H1E(DMY)
      VG=VPT2(P,T)
      HG=H2E(DMY)
      RETURN
      END
--EOR--
CTENS
      SUBROUTINE TENS(TIN,S)
```

```
       DIMENSION AS(6)
       DATA AS/1.1609368E-1,1.12140468E-3,-5.75280518E-6,
      C1.28627465E-8,-1.14971929E-11,.83/
       TK=647.3-(TIN+459.67)/1.8
       S=AS(1)*(TK**2)/(1.+AS(6)*TK)
       DO 590 1=2,5
   590 S=S+AS(I)*(TK**I)
       S=6.85217526E-5*S
       RETURN
       END
END OF FILE
\?
```

APPENDIX 'G'

Advanced Water/Steam Receiver
Superheater Panel Stress Analysis

By

M. J. Davidson

ESD-80-6

January 1980

Introduction

A heat transfer and an elastic stress analysis was performed for the 3.0×10^6 lb/hr solar receiver design. Loading conditions for the superheat panel were analyzed. Fatigue lives of the receiver using 316 SS and Incoloy 800 were assessed.

Problem Set-Up

A finite element model was generated using tube OD .625 inches, and ID .46 inches and constraint conditions based on Rockwell International Corporation drawing AP77-084. An eight-noded isoparametric element was used. Material properties for Incoloy 800 and 316 SS were obtained from Code Case 1592. Figures 1 and 2 show the geometry. Tables 1, 2, and 3 shown material properties. Table 4 shows the loading conditions imposed on the model.

Analysis Procedure

The overall procedure consisted of inputting the heat flux loading into MARC Heat and generating steady-state temperature distribution across the model for each flux loading. These temperature distributions were then input into MARC stress via a post tape. An elastic stress analysis was done for each case using the appropriate boundary conditions, pressure loading, and material properties. Using the results of these stress runs, fatigue life was calculated.

A. Heat Transfer

The flux loading condition analyzed was based on maximum crown temperature in the superheat panel. The flux distribution was input on the tubes using a tube shading program. The model temperatures were put on tape to be input into the stress program.

B. Stress Analysis and Boundary Conditions

The generated temperature distributions, pressure loads, and boundary conditons were input into MARC stress. The panel geometry and the large front-to-back temperature loading necessitated the use of a generalized plane strain finite element. This element allowed the element to grow axiall (strained $\propto T_{MEAN}$) without constraint while still calculating the thermal strains due to the difference in temperature from front to back.

The boundary conditions placed on the model are illustrated in Figure 3. Symmetry between horizontal slide locations cause the middle to be placed on rollers in the y direction. The horizontal slide weld point allows only x direction movement and symmetry forces the center line of tube to move the same amount. The tube rotation is fixed to zero in the z direction due to axial constraints.

C. Fatigue Life Assessment

An assessment of the fatigue life for each metal was made. Since an elastic analysis was performed, cyclic life had to be determined by using the calculated elastic strains. However, fatigue life based on high elastic strains is very conservative. To fully evaluate the fatigue life of a highly stressed component, an inelastic analysis is required to determine the inelastic strain range. However, the scope of this design evaluation prevents this type of analysis.

Due to the high elastic strains calculated, it was necessary to modify the elastic strains. J. L. Houtman in the Westinghouse report "Structural Evaluation of the In-Vessel FFTF Plant Unit Instrument Tree", presented a method to approximate inelastic strain using elastic analysis.

The procedure is as follows:

Step 1 Calculate the elastic stress.

Step 2 Calculate the elastic Von Mises effective strain range.

Step 3 Determine the inelastic strain from the elastic strain by multiplying by the appropriate strain correction factor K from Figure 4.

Step 4 Using the determined inelastic effective strain and the appropriate fatigue design curve (Figures 5 and 6) fatigue damage is evaluated.

The maximum elastic effective stress calculated was 36,600 psi for the 316 SS and 36,500 psi for the Incoloy 800. The corresponding strain ranges were 1.22×10^{-3} and 1.24×10^{-3}.

Using the above method, the fatigue life of the two cases were:

316 SS	'Plastic' Strain Range	1.8×10^{-3}	Cycles	30,000
Incoloy 800		1.94×10^{-3}		20,000

This technique calculates the first cycle strain range. Relaxation of this stress with time has not been taken into account. This method produces a conservative fatigue life.

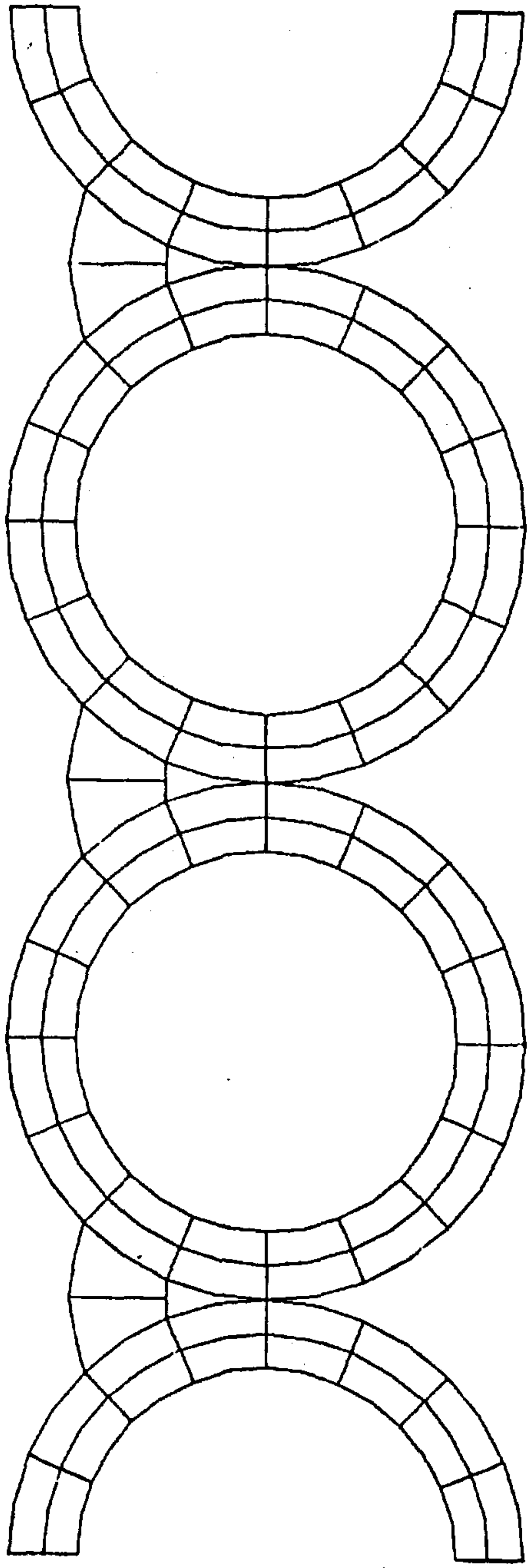

FIGURE 1

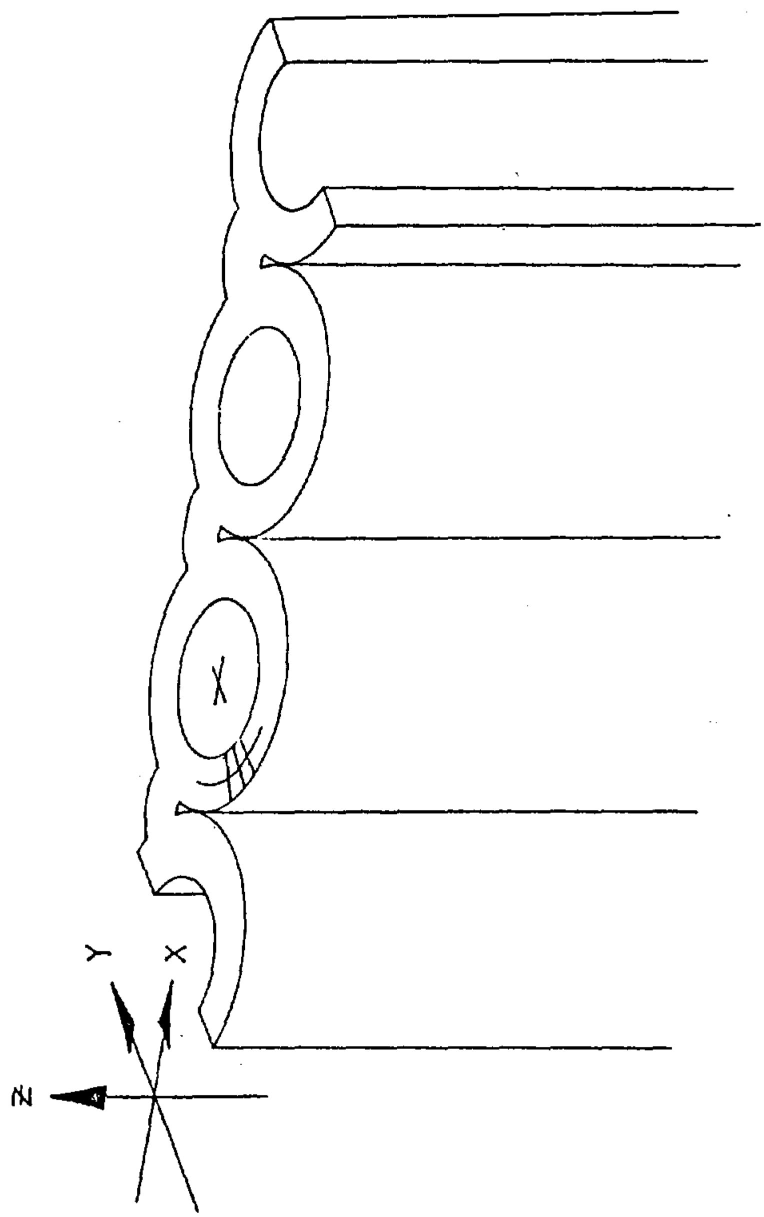

COORDINATE SYSTEM

FIGURE 2

G-7

Instantaneous Coefficient of Thermal Expansion vs. Temperature

Temp., °F	Instantaneous Coefficient of Thermal Expansion, in./in.-°F X 10⁶			
	304 SS and 316 SS	Ni-Fe-Cr Alloy 800H	2¼ Cr - 1 Mo	Ni-Cr-Fe-Cb Alloy 718
70	9.11	–	–	–
100	9.21	–	6.6	6.91
200	9.50	8.8	6.9	7.43
300	9.73	8.9	7.35	7.77
400	9.96	9.0	7.65	7.97
500	10.20	9.1	7.9	8.09
600	10.43	9.2	8.1	8.17
700	10.66	9.3	8.25	8.26
750	10.81	–	–	–
800	10.90	9.5	8.4	8.42
850	11.00	9.65	–	–
900	11.11	9.8	8.5	8.69
950	11.23	10.0	–	–
1000	11.35	10.2	8.6	9.13
1050	11.46	10.4	–	9.46
1100	11.58	10.6	8.65	
1150	11.70	10.8	–	
1200	11.81	11.0	8.7	
1250	11.93	11.2		
1300	12.04	11.4		
1350	12.16	11.55		
1400	12.28	11.7		
1450	12.39	11.8		
1500	12.50	11.9		
1550		12.0		
1600		12.1		

TABLE 1

Modulus of Elasticity vs. Temperature

Temp., °F	(Static) Modulus of Elasticity, psi × 10^{-6}			
	304 SS and 316 SS	Ni-Fe-Cr Alloy 800H	2¼ Cr – 1 Mo	Ni-Cr-Fe-Cb Alloy 718
70	28.3*	28.5	29.9*	–
100	–	–	–	29.0
200	27.7	27.8	29.5*	28.38
300	27.1	27.3	29.0	27.93
400	26.6	26.8	28.6*	27.51
500	26.1	26.3	28.0	27.10
600	25.4	25.7	27.4	26.69
700	24.8	25.2	26.6	26.26
750	–	–	–	–
800	24.1	24.6	25.7	25.82
850	23.7	24.4	–	–
900	23.3	24.1	24.5	25.35
950	22.9	23.8	–	–
1000	22.5	23.5	23.0	24.84
1050	22.1	23.3	–	24.56
1100	21.7	22.9	20.4	
1150	21.3	22.7	–	
1200	20.9	22.4	15.6	
1250	20.5	22.1		
1300	20.1	21.7		
1350	19.7	21.4		
1400	19.2	21.1		
1450	18.7	20.7		
1500	18.3	20.3		
1550		19.8		
1600		19.2		

TABLE 2

Expected Minimum Yield Strength vs. Temperature

Temp., °F	304 SS	316 SS	Ni-Fe-Cr Alloy 800H	2¼ Cr-1 Mo	Ni-Cr-Fe-Cb Alloy 718
			(Stresses in ksi Units)		
RT	30.0	30.0	25.0	30.0	150.0
100	28.8	29.2	24.3	29.4	148.4
200	25.0	25.8	22.5	27.8	143.9
300	22.5	23.3	21.1	26.8	140.7
400	20.7	21.4	20.0	26.6	138.3
500	19.4	19.9	19.0	26.5	136.7
600	18.2	18.8	18.3	26.5	135.4
700	17.7	18.1	17.5	26.5	134.3
750	17.3	17.8	17.2	26.5	133.7
800	16.8	17.6	16.8	26.5	133.1
850	16.5	17.4	16.5	26.3	132.4
900	16.2	17.3	16.3	25.6	131.5
950	15.9	17.1	16.1	24.7	130.5
1000	15.6	17.0	15.8	23.6	129.4
1050	15.2	16.7	15.6	22.1	128.0
1100	14.7	16.5	15.3	20.4	
1150	14.4	16.4	15.0	18.4	
1200	14.1	16.2	14.8	16.1	
1250	13.7	15.8	14.5		
1300	13.2	15.3	14.3		
1350	12.5	14.9	14.0		
1400	11.6	14.4	13.7		
1450	10.6	13.8	13.4		
1500	9.5	13.1	13.0		
1550			12.3		
1600			11.0		

TABLE 3

TABLE 4: LOADING CONDITIONS

Tube Geometry	.625" OD; .46" ID
Tube Material	316 SS, Incoloy 800
Maximum Heat Flux	76,756 BTU/hr-ft^2
Internal Tube Pressure	2750 lb/in^2
Fluid Temperature	1069°F
Inside Film Coefficient	2642 BTU/hr-ft^2-$^\circ$F

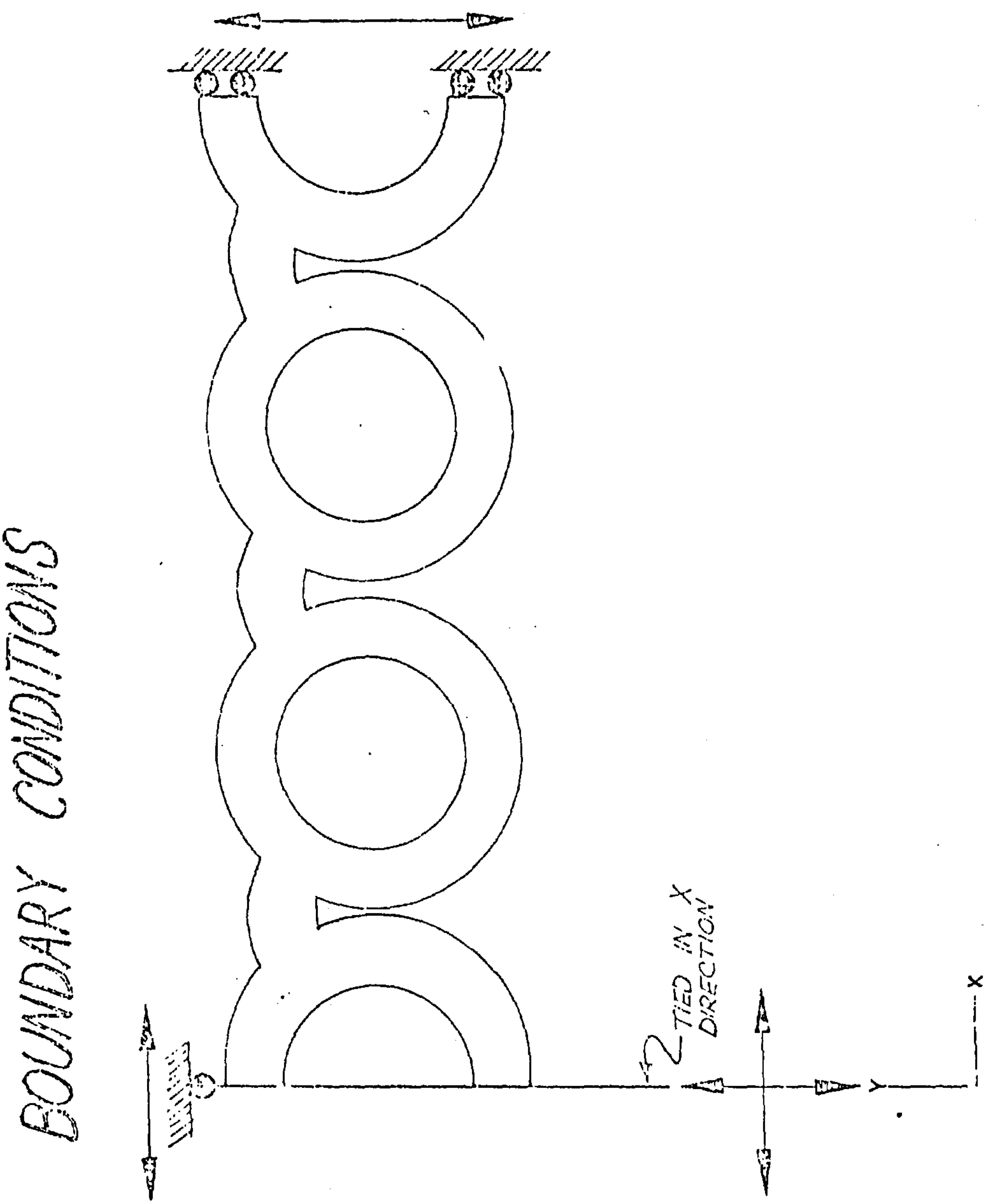

FIGURE 3

STRAIN CORRECTION FACTOR

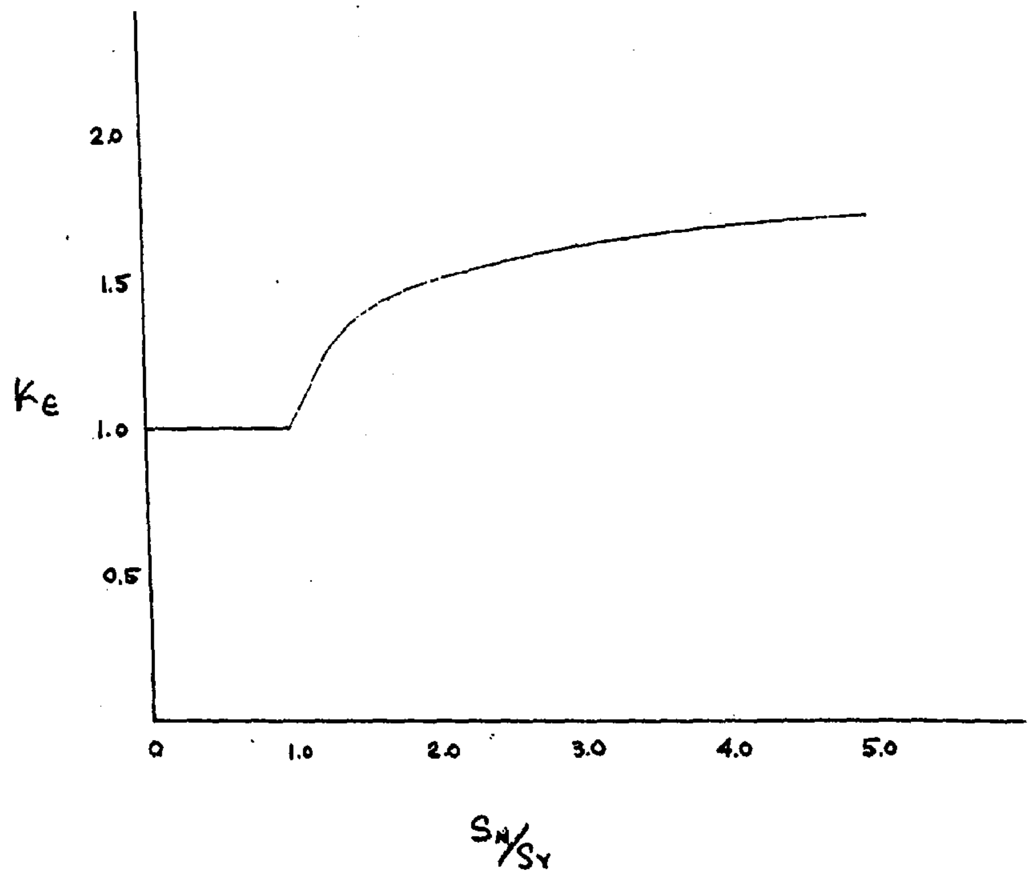

S_N - ELASTIC STRESS

S_Y - YEILD STRESS (SEE TABLE 5)

FIGURE 4

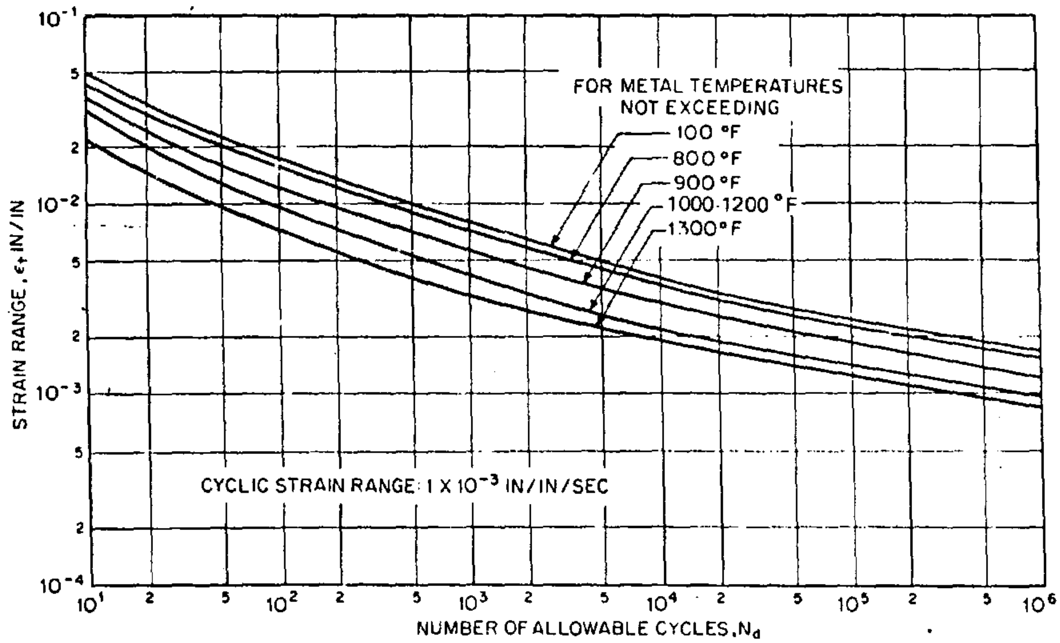

Design fatigue strain range, ϵ_t, for 304 SS and 316 SS

Design Fatigue Strain Range, ϵ_t, for 304 SS and 316 SS

N_d Number of Cycles*	ϵ_t, Strain Range (in./in.) at Temperature 100 F	800 F	900 F	1000-1200 F	1300 F
10^1	.0507	.0438	.0378	.0318	.0214
2×10^1	.0357	.0318	.0251	.0208	.0149
4×10^1	.026	.0233	.0181	.0148	.0105
10^2	.0177	.0159	.0123	.00974	.00711
2×10^2	.0139	.0125	.00961	.00744	.00551
4×10^2	.0110	.00956	.00761	.00574	.00431
10^3	.00818	.00716	.00571	.00424	.00328
2×10^3	.00643	.00581	.00466	.00339	.00268
4×10^3	.00518	.00476	.00381	.00279	.00226
10^4	.00403	.00376	.00301	.00221	.00186
2×10^4	.00343	.00316	.00256	.00186	.00162
4×10^4	.00293	.00273	.00221	.00161	.00144
10^5	.00245	.00226	.00182	.00136	.00121
2×10^5	.00213	.00196	.00159	.00121	.00108
4×10^5	.00188	.00173	.00139	.00109	.000954
10^6	.00163	.00151	.00118	.000963	.000834

*Cyclic strain rate : 1×10^{-3} in./in./sec.

FIGURE 5

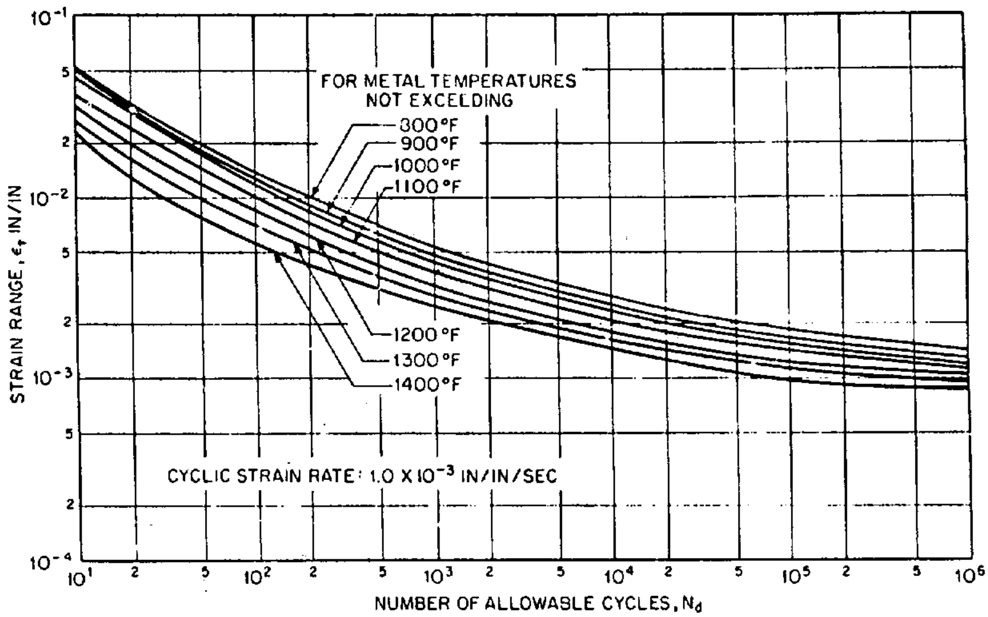

Design fatigue strain range, ϵ_t, for Ni-Fe-Cr Alloy 800H

Design Fatigue Strain Range, ϵ_t, for Ni-Fe-Cr Alloy 800H

N_d Number of Cycles*	ϵ_t, Strain Range (in./in.) at Temperature						
	800 F	900 F	1000 F	1100 F	1200F	1300 F	1400 F
10^1	.0513	.0498	.0468	.0378	.0308	.0263	.0231
2×10^1	.0328	.0313	.0298	.0243	.0198	.0168	.0129
4×10^1	.0218	.0208	.0190	.0163	.0130	.0113	.00866
10^2	.0139	.0129	.0119	.01	.00823	.00725	.00566
2×10^2	.0103	.00939	.00861	.00722	.00603	.00535	.00426
4×10^2	.00777	.00699	.00641	.00542	.00463	.00405	.00331
10^3	.00537	.00489	.00441	.00392	.00328	.00285	.00254
2×10^3	.00427	.00379	.00351	.00312	.00261	.0023	.00209
4×10^3	.00347	.00314	.00291	.00259	.00213	.00195	.00176
10^4	.00277	.00249	.00233	.0021	.00174	.00159	.00143
2×10^4	.00242	.00219	.00201	.00182	.00155	.00142	.00125
4×10^4	.00215	.00193	.0018	.00162	.0014	.00127	.00109
10^5	.00187	.00164	.00151	.00139	.00122	.00115	.000959
2×10^5	.00169	.00149	.00141	.00128	.00113	.00105	.000919
4×10^5	.00157	.00139	.00129	.00121	.00108	.000987	.000889
10^6	.00139	.00129	.00119	.00112	.00103	.000937	.000869

*Cyclic strain rate: 1×10^{-3} in./in./sec.

FIGURE 6

INITIAL DISTRIBUTION

G. W. Braun
Division of Solar Thermal Energy Systems
U. S. Department of Energy
600 E Street, NW
Washington, DC 20585

Division of Solar Thermal Energy Systems (3)
U. S. Department of Energy
600 E Street, NW
Washington, DC 20585
Attn: W. W. Auer
L. Melamed
J. E. Rannels

U. S. Department of Energy (5)
Division of Solar Technology
San Francisco Operations Office
1333 Broadway
Oakland, CA 94612
Attn: S. Cherian
F. Corona
S. D. Elliott
R. W. Hughey
L. Prince

R. N. Schweinberg
DOE/STMPO
Suite 210
9550 Flair Drive
El Monte, CA 91731

P. Mathur
Aerospace Corporation
P. O. Box 92957
Los Angeles, CA 90009

O. W. Durrant
Babcock and Wilcox
20 S. Van Buren Avenue
Barberton, OH 44203

Bechtel Corporation
P. O. Box 3965
San Francisco, CA 94119
Attn: J. Darnell
E. Lam

Black and Veatch
1500 Meadow Lake Parkway
P. O. Box 8405
Kansas City, MO 64114
Attn: J. E. Harder
S. L. Levy
M. L. Wolf

R. D. Zentner
Boeing Engineering & Construction
P. O. Box 3707
Seattle, WA 98124

H. Payne
Advanced Systems Analysis
C-E Power Systems
Combustion Engineering, Inc.
1000 Prospect Hill Road
Windsor, CT 06095

J. E. Brown
El Paso Electric
P. O. Box 982
El Paso, TX 79960

E. R. Elzinga
Exxon
P. O. Box 251
Florham Park, NJ 07932

Exxon
Advanced Energy Systems Lab
Linden, N.J. 07036

Foster Wheeler Development Corporation
12 Peach Tree Hill Road
Livingston, NJ 07039
Attn: A. Robertson
W. Wolowodiuk

J. J. Jimenez
Gibbs & Hill
393 7th Avenue
New York, NY 10001

General Atomic Company
P. O. Box 80608
10955 John Jay Hopkins Drive
San Diego, CA 92138
Attn: H. D. Chiger
A. J. Kelly
M. Lasarev

J. Elsner, ESPD
General Electric Company
1 River Road
Bldg. 6, Room 633
Schenectady, NY 12345

D. Stahlfield
Gulf Research & Development
P. O. Drawer 2038
Pittsburg, PA 15230

T. Heaton
Martin Marietta
P. O. Box 179
Denver, CO 80201

McDonnell Douglas
5301 Balsa Avenue
Huntington Beach, CA 92647
Attn: R. P. Dawson
L. W. Glover

Nielsen Engineering & Research, Inc.
510 Clyde Avenue
Mountain View, CA 94043
Attn: J. N. Nielsen
R. G. Schwind

W. R. Wagner
Rocketdyne Corporation
6633 Canoga Avenue
Canoga Park, CA 91304

Rockwell International
P. O. Box 1449
8900 De Soto Avenue
Canoga Park, CA 91304
Attn: J. J. Auleta
J. B. Brukiewa
E. M. Mouradian
T. S. Springer

F. Kreith
Solar Energy Research Institute
1617 Cole Boulevard
Golden, CO 80401

Mechanical Engineering Department
Stanford University
Stanford, CA 94305
Attn: J. P. Johnston
R. J. Moffat
K. M. Price, 333 Durand Bldg.

R. Kuhr
Stone and Webster
P. O. Box 5406
Denver, CO 80217

R. Schwing
Townsend & Bottum
P. O. Box 366
Daggett, CA 92327

R. Greif
Mechanical Engineering Department
University of California
Berkeley, CA 94720

S. Dasgupta
Energy Laboratory
University of Houston
4800 Calhoun
Houston, TX 77004

L. E. Van Bibber
Westinghouse Electric Corporation
Advanced Energy Systems Division
811 Route 51 South
Large, PA 15025

B. W. Marshall, 4713
T. A. Dellin, 4723
T. B. Cook, 8000; Attn: W. J. Spencer, 8100
A. N. Blackwell, 8200
B. F. Murphey, 8300
L. Gutierrez, 8400
R. C. Wayne, 8450
P. J. Eicker, 8451
A. C. Skinrood, 8452
W. G. Wilson, 8453 (15)
Publications Division, 8265, for TIC (27)
Publications Division, 8265/Technical Library Processes & Systems Division, 3141
Technical Library Processes and Systems Division, 3141 (2)
Library and Security Classification Division, 8266-2 (3)